



IMPERIAL INSTITUTE
OF
AGRICULTURAL RESEARCH, PUSA

PROCEEDINGS
OF THE
ROYAL SOCIETY OF LONDON

SERIES A

CONTAINING PAPERS OF A MATHEMATICAL AND
PHYSICAL CHARACTER

VOL. CXVIII
. . . .

314732
■■■■■■■■■■
IARI

LONDON
PRINTED FOR THE ROYAL SOCIETY AND SOLD BY
HARRISON AND SONS, LTD, 51 MARTINS LANE
PRINTERS IN ORDINARY TO HIS MAJESTY

APRIL, 1928

LONDON

HARRISON AND SONS LTD, PRINTERS IN ORDINARY TO HIS MAJESTY
ST MARTIN'S LANE.

CONTENTS.

SERIES A VOL CXVIII

Minutes of Meetings of January 26, February 2, 9, 16, 23, March 1, 15 1928

No A 779—March 1, 1928

	PAGE
The Deformation of Crystals of β Brass By G I Taylor, F R S	1
Wave Resistance By T H Havelock, F R S	24
The Arc Spectrum of Carbon By A Fowler, F R S, and E W H Selwyn	34
The Chemical Constant of Hydrogen Vapour and the failure of Nernst's Heat Theorem By R H. Fowler, F R S	52
Oscillations in a Bridge caused by the Passage of a Locomotive By C E Inglis Communicated by Sir Alfred Ewing, F R S (Plate 1)	60
Tribo-electricity and Friction II—Glass and Solid Elements By P E Shaw and C S Jex Communicated by Sir William Hardy, F R S	97
Tribo-electricity and Friction III—Solid Elements and Textiles By P E Shaw and C S Jex Communicated by Sir William Hardy, F R S	108
The Effect of Compressibility on the Lift of an Aerofoil By H Glaucert Com municated by G I Taylor, F R S	113
The Alkaline Earth Halide Spectra and their Origin By O H Walters and S Barratt Communicated by T R Merton, F R S (Plate 2)	120
On the Measurement of the Variation of the Specific Heat of Aniline with Temperature, using the Continuous Flow Electric Method By H R Lang Communicated by H L Callendar, F R S	138
The Structure of the Band Spectrum of Helium—IV By W E Curtis Com municated by Prof T H Havelock, F R S	157
The Kinetics of the Combination of Hydrogen and Oxygen By C N Hinshelwood and H W Thompson Communicated by Sir Harold Hartley, F R S	170
On Electrostatics in a Gravitational Field By E T Copson Communicated by E T Whittaker, F R S	184
Some Cases of Instability in Fluid Motion By H Jeffreys, F R S	195
Studies in Adhesion—II By Sir William Hardy, F R S, and M Nottage (Plate 3)	209

	PAGE
The Photo Electric Threshold Frequency and the Thermionic Work Function By R H Fowler, F R S	229
The Polarity of Thunderclouds By B F J Schonland Communicated by C T R Wilson, F R S (Plates 4 and 5)	237
The Interchange of Electricity between Thunderclouds and the Earth By B F J Schonland Communicated by C T R Wilson F R S (Plate 6, upper figure)	252
Note on the Explanation of a so-called "Intertraction" Phenomenon By N K Adam (Communicated by G I Taylor, F R S (Plate 6 lower figure)	262
Examples of the Zeeman Effect at Intermediate Strengths of Magnetic Field By K Darwin Communicated by Prof C G Darwin, F R S	264
The Analysis of the Absorption Spectrum of Cobalt Chloride in Concentrated Hydro- chloric Acid By W R Brode Communicated by E C C Baly, F R S (Plate 7)	286
The Distribution of Intensity in the Band Spectrum of Helium the Band at λ 4650 By W H J Childs Communicated by O W Richardson, F R S	296
The Heating Effects of Thorium and Radium Products By S W Watson and M C Henderson Communicated by Prof Sir E Rutherford F R S	318
An Investigation into the Existence of Zero Point Energy in the Rock Salt Lattice by an X Ray Diffraction Method By R W James I Waller and D R Hartree Communicated by W L Bragg, F R S	334
The Quantum Theory of the Flexatron -- Part II By P A M Dirac Communicated by R H Fowler F R S	351

No A 780--April 2, 1928

The Emission of Light by Flames containing Sodium and the Absorption of Light by Mercury Vapour By H A Wilson, F R S	362
The Hexahydrated Double Sulphates containing Thallium By A E H Tutton, F R S	367
The Hexahydrated Double Selenates containing Thallium By A E H Tutton, F R S	393
The Bending of a Centrally Loaded Isotropic Rectangular Plate Supported at Two Opposite Edges By A E H Love, F R S	427
Relativity and Wave Mechanics By W Wilson, F R S	441
An X-Ray Study of some Simple Derivatives of Ethane --Part I By K Yardley Communicated by Sir William Bragg, F R S	449
An X-Ray Study of some Simple Derivatives of Ethane --Part II By K Yardley Communicated by Sir William Bragg, F R S	485

	PAGE
The Behaviour of a Single Crystal of α Iron subjected to Alternating Torsional Stresses By H Gough Communicated by Sir Thomas Stanton, F R S	498
Some Physical Properties of Gas freed Sulphur By C C Farr and D B Macleod Communicated by C Chree, F R S	534
The Solution of the Wave Equation for the Scattering of Particles by a Coulombian Centre of Force By N F Mott Communicated by R H Fowler, F R S	542
A Redetermination of the Velocities of α Particles from Radium C, Thorium C and C" By G H Briggs Communicated by Sir Ernest Rutherford, P R S	549
Commutative Ordinary Differential Operators By J L Burchnall and T W Chaundy Communicated by A L Dixon, F R S	557
Note on "Commutative Ordinary Differential Operators, by J L Burchnall and T W Chaundy" By H F Baker, F R S	584
The Thermal Conductivities of Oxygen and Nitrogen By H Gregory and S Marshall Communicated by H L Callendar, F R S	594
Studies in Adhesion III—Mixtures of two Lubricants By M Nottage Com- municated by Sir William Hardy, F R S (Plates 14 16)	607
A Generalised Spheroidal Wave Equation By A H Wilson Communicated by R H Fowler, F R S	617
The Ionised Hydrogen Molecule By A H Wilson Communicated by R H Fowler, F R S	636
The Band Spectrum of Water Vapour—II By D Jack Communicated by O W Richardson, F R S	647
The Wave Equations of the Electron By C G Darwin, F R S	654
Fluid Resistance to Moving Spheres By R G Lunnion Communicated by T H Havelock, F R S	680
Studies in the Behaviour of Hydrogen and Mercury at the Electrode Surfaces of Spectrum Tubes By M C Johnson Communicated by S W J Smith, F R S	685
An X Ray Investigation of the Structure of some Naphthalene Derivatives By J M Robertson Communicated by Sir William Bragg, F R S (Plate 17)	709

OBITUARY NOTICES

Albin Haller	i
Francis Robert Japp (with portrait)	iii
Index	vii

PROCEEDINGS OF THE ROYAL SOCIETY.

SECTION A—MATHEMATICAL AND PHYSICAL SCIENCES

The Deformation of Crystals of β -Brass

By Prof G I TAYLOR, FRS

(Received December 23 1927)

It is shown that β brass, which has a crystal structure similar to that of α -iron, behaves in a similar, though not identical, manner when distorted

The peculiar feature of the distortion of iron crystals, namely, the fact that slip does not occur on a definite crystallographic plane, is repeated in β -brass within a certain range of orientations of the crystal axes in the specimen. On the other hand, in another range of orientation slip occurs on a definite crystal plane of type $\{110\}$. The conditions which determine which of these types of distortion will occur in any given case are investigated, and it is shown that the determining cause is the variation in resistance to shear which occurs as the plane of slip rotates about the direction of slip. This variation is calculated from the experimental results within the range to which they apply, and it is shown that resistance to shear is least when the plane of slip coincides with a crystal plane of type $\{110\}$. On either side of this position shear stress increases linearly, there being a discontinuity in the rate of change of shear strength with orientation of plane of slip. This peculiar property is also possessed by the model consisting of hexagonal rods proposed by the author and Miss Elam, and by Mr Hume Rothery's model, which, from this point of view, is identical with the model of hexagonal rods.

The assumptions made in a recent paper by Mr Hume Rothery are discussed, and it is shown that in a body centred cubic structure like α -iron they lead, when analysed, to the conclusion that slipping should always take place parallel to a crystal plane of type $\{110\}$, and not, as he stated, to the conclusion that slip should occur on the non crystallographic planes which were actually found.

It is shown also that in β brass resistance to slipping in one direction on a given plane of slip is not the same as resistance offered to slipping in the opposite direction. Such a difference is to be expected from crystallographic symmetry, but was not observed in α -iron.

In a recent paper* it has been shown that the behaviour of single crystals of iron when deformed by external pressures or tension is different from that of single crystals of any other metal which had been examined up to that time. In all other metals the material distorts in such a way that planes of particles

* "The Distortion of Iron Crystals," 'Roy Soc Proc.' A, vol 112, p 337 (1926)

parallel to definite crystal planes remain undistorted while they slip over one another parallel to some definite crystallographic direction in that plane

In the case of iron there is no such plane. The particles of the material appear to cling together in lines or rods instead of in planes. These rods, which are in the direction in which the atoms of the crystal are closest together, are capable of sliding over one another. In any uniform distortion due to slipping of this type it is a geometrical necessity that there must be one set of parallel planes, containing the direction of the axes of the rods, which remains unstretched and undistorted, and in this sense the material has a plane of slipping, but it is not a definite crystal plane, being differently orientated with respect to the crystal axes in different specimens.

It seemed probable that this peculiarity in the nature of the distortion of iron is connected with the crystal structure. Metals which crystallise in face-centred cubes such as aluminium, copper, silver and gold all behave in the same way when distorted. The question therefore naturally arises as to whether other metals besides iron which crystallise in body-centred cubes would behave like iron in distortion, or whether the peculiar behaviour of iron is connected with some peculiarity in the atom of iron itself. The metals which crystallise in body-centred cubes are, however, mostly unsuitable for experiments of the kind previously carried out with face centred cubic metallic crystals. Tungsten, for instance, seems at present to be unobtainable in the form of large ductile crystals, and its hardness would in any case make compression experiments difficult to carry out.

On the other hand it was pointed out to me by Miss Elam that the alloy β -brass which crystallises in a body centred lattice, has recently been obtained in the form of large crystals by Dr Tamura working with Prof Carpenter. This alloy consists of almost equal numbers of copper and zinc atoms. Its structure was determined recently by Owen and Preston and independently by Phragmen and Westgren, who agreed in showing that the lattice of β -brass is a body-centred cube in which atoms of zinc are situated on one simple cube lattice while the atoms of copper are situated on an identical lattice which interpenetrates the first. The structure is therefore identical with that of iron except that in the one case the two interpenetrating lattices contain atoms of the same metal while in the other they contain different kinds of atoms.

It seemed desirable therefore to carry out distortion measurements with β -brass, and I was able to do so through the kindness of Miss Elam who procured for me two strips of β -brass containing about eight crystals large enough to cut into specimens suitable for carrying out distortion measurements.

These strips were prepared by Dr Tamura who treated them by the method of Carpenter and Elam so that some of the crystals grew large. The dimensions of the strips were 10 cm long \times 11 mm wide \times 3 mm thick and some of the larger crystals occupied as much as 5 cm of their length. An analysis, for which I have to thank Miss Elam, showed that the brass used contained 51.3 per cent copper atoms and 48.7 per cent zinc atoms in some specimens and 53 per cent copper in others. The method adopted was in most cases first to determine by means of X-rays the orientation of the crystal axes of one of the crystals relative to the surface and edge of the strip. Both compression and tensile tests were carried out. The compression specimens were prepared by cutting out circular discs. In some cases their flat surfaces were parallel to the two faces of the original strip, but in others the flat faces were ground in definite orientations with respect to the crystal axes by means of a crystallographer's tripod grinding machine kindly lent to me by Prof A. Hutchinson, FRS. The tensile specimens were rectangular, approximately square, in section, but they had enlarged ends which were bored to take a steel pin which fitted a holder arranged to give a central load. They were arranged in such a way that the central portion was cut from a single crystal. The relationship between the tensile specimens and the original strip is represented in fig. 1 where the

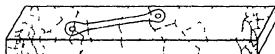


FIG. 1

boundaries of the crystals are represented by dotted lines. Marks were made on the specimen before cutting and grinding in order to preserve a knowledge of the orientation of the crystal axes, but in every case this orientation was redetermined with reference to the marks used in making the distortion measurement.

In preparing both types of specimen a layer about 0.7 mm thick was ground off each face of the original strip, and before ruling the scratches necessary for observing the distortion they were lightly etched to make sure that they contained no small crystals inserted in the main crystal.

The specimens were then marked with systems of marks previously described*. The compression specimens were compressed between polished and greased

* For compression specimens see Taylor and Farren, "Distortion of Aluminium Crystals under Compression," 'Roy Soc Proc,' A, vol 111, p 533 (1926). For tensile specimens see Taylor and Elam "Distortion of Iron Crystals," 'Roy Soc Proc,' A, vol 112, p 337 (1926).

steel plates* till the thickness was reduced by 5 to 15 per cent, and the tension specimens were stretched a corresponding amount. It was found as in the case of aluminium and iron crystals that in general the distortion was uniform, ruled lines on the surface remaining straight after compression. The specimen was then measured and the equation to the unstretched cone calculated.

Ten cases in all were analysed, namely seven compression and three tensile tests. In three of them, numbered β 4 1, β 2 1 and T β 1, the orientation of the crystal axes was determined only after distortion. In those cases the second or distorted position of the unstretched cone† was determined, while in the remaining cases the orientation of the axes was determined before distortion and the first position of the cone was calculated. The unstretched cones were marked on a stereographic figure in a manner previously described‡. Two typical specimens of these diagrams are shown in figs 2 and 3. It will be seen that in each case the cone very nearly coincides with the two great circles which are represented by two arcs of circles. The distortion might be due to slipping parallel to either of the two planes represented by these two great circles. The two possible directions of slip being represented by the points S and S' (fig. 2) at right angles to the line of intersection of the two planes.

Orientation of Crystal Axes

In each case the orientation of the crystal axes with reference to the ruled scratches on the surface of the specimen was determined by Müller's Method using a spectroscope previously described§. The K_{α} and K_{β} reflections from an iron anticathode were used. Using the value of the lattice constant given by Owen and Preston and also by Westgren and Phragmen|| the reflecting angle for the K_{α} radiation from planes of type {110} is $27^{\circ} 40'$. For the K_{β} radiation it is $24^{\circ} 50'$.

To determine the orientation of the crystal axes reflections were obtained from two planes of type {110} which were perpendicular to one another, or from three planes mutually at 60° and not intersecting in one line. In each case the

* See "Compression," p. 531.

† For definition of unstretched cone see "Distortion of an Aluminium Crystal during a Tensile Test," 'Roy Soc. Proc. A,' vol. 102, p. 650 (1923).

‡ "Distortion of Aluminium Crystals under Compression," p. 537, and "Distortion of Iron Crystals," p. 339.

§ *Ibid.*, p. 540.

|| Owen and Preston using β -brass containing 48.3 per cent Zn give the side of unit cube as 2.946 \AA . Westgren and Phragmen using β brass containing 46.9 per cent Zn give it 2.945 \AA .

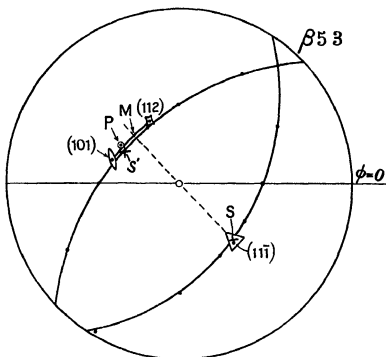


FIG 2 —Unstretched Cone and Crystal Axes for Compression Specimen β 5 1

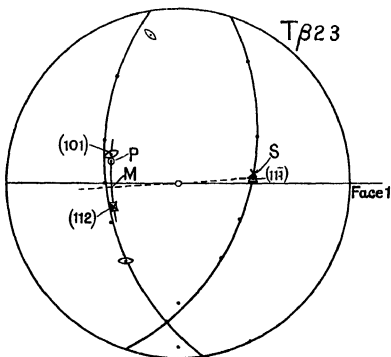


FIG 3 —Unstretched Cone and Crystal Axes for Tensile Test piece T β 2 3

positions of the directions actually determined by X-rays were marked in a stereographic diagram on tracing paper and certain other directions deduced from them, such as those of type $\{111\}$, were also marked on the diagrams

The tracing paper containing the projection of the crystal axes was then laid over the projection of the unextended cone. It was found in each case that one of the two possible directions of slip (which are either of them capable of producing the measured change in shape of the specimen) very nearly coincided with a direction of type $\{111\}$ (i.e., the normal to the plane $\{111\}$).

These directions are marked in figs. 2 and 3 by the symbol Δ and the direction of slip determined by distortion measurements by a cross X. Table I gives the co-ordinates of the direction of slip determined from external measurements and the nearest $\{111\}$ direction. It will be seen that the direction of slip is, as in the case of iron, parallel to the normal to a plane of type $\{111\}$.

Table I - Results of Distortion Measurements

	Direction of slip		Normal to $\{111\}$ plane	
	θ	ϕ	θ	ϕ
T β 1	36	97	35	96
T β 2 3	47½	6	47½	1
T β 2 4	50	224	49	224
β 2 1	59	342½	58	338
β 4 1	64	78½	65½	79½
β 5 1	61	343	60	347
β 5 2	58½	1	59	4½
β 5 3	48½	313½	49	313
β 3 2	48	208	50	208½
β 6 2	50	4	52	6½

The pole of the plane of slip determined by external measurements lies therefore in a crystal plane of type $\{111\}$. This plane contains three directions of type $\{110\}$ and three of type $\{211\}$. It was found that in some cases the pole of the plane of slip coincided with a direction of type $\{110\}$ while in others it did not coincide with either of these crystal directions, but lay at some intermediate position which differed in different specimens. In no case did it coincide with a direction of type $\{211\}$.

Comparison with Iron Crystals

It will be seen that the results are similar to those obtained with iron crystals in that the direction of slip is a crystal direction of type $\{111\}$ while the plane

of slip varies according to the orientation of the crystal axes relative to the direction of the principal stress. On the other hand, the relationship between the orientation of the crystal axes relative to the direction of principal stress, and the orientation of the plane of slip among all the possible planes passing through the given direction of slip is quite different from that found for iron. This difference was first noticed owing to the occurrence of specimens of β -brass in which the plane of slip coincided with a plane of type $\{110\}$. The simplest way to represent the difference seems to be to mark on each stereographic diagram the point M, figs 2 and 3, where the pole of the plane of slip would be if the resistance to shear on all possible planes passing through the given direction of slip were the same. To do this it is only necessary to draw a straight line (dotted line SM, figs 2 and 3) through S and the centre of the diagram. The point M is where this line cuts the circle whose pole is S. In the case of iron crystals it was shown* that P, the pole of the observed plane of slip, was close to M, but that in compression specimens, at any rate, there was a small though distinct tendency to deviate towards the nearest direction of type (211). In the case of tension specimens there seemed to be a slight tendency the other way.

In the case of β -brass it was found that P deviated more from M than it did in the case of iron crystals, but in the opposite direction, that is towards the nearest pole of type (110). This will be seen in figs 2 and 3 where the positions of the poles (101) and (112) are marked. These are the nearest poles of the required type to M, the position where the pole of the slip plane would be if the resistance to shear on all planes passing through the direction of slip (111) were the same.

It was found that if the orientation of the crystal axes is such that M falls near the pole (101) then the plane of slip coincides with the plane (101), but if it falls more than, say, 15 degrees away from (101), then P lies at some point intermediate between M and (101). It may safely be deduced therefore that among all possible planes through a given direction of slip of type (111), the resistance to shear is least when the plane of slip coincides with one of type (101), but this question will now be examined systematically.

Choice of direction of slip

In order to make a complete exploration of all possible orientations of the direction of principal stress in relation to the crystal axes the point representing the position of the normal to the flat surfaces of the compression disc was marked

* "Dislocation of Iron Crystals," p. 352

in each case on a diagram representing the cubic axes of the crystal. It has already been shown* that by a proper choice of one of the three cubic axes as the centre of the projection this point can always be made to lie in one particular spherical triangle. The points representing the axes of all the specimens measured are shown in fig. 4. It will be seen that they are fairly

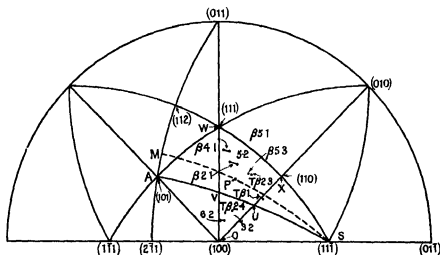


FIG. 4.—Positions of Axes of Specimens relative to Crystal Axes

well distributed over a greater part of the area of the triangle whose points are (111), (110), (100). One specimen, however, $\beta 5 1$, is represented just outside this triangle. Using another choice of axes it could have been made practically to coincide with $\beta 5 2$, but for reasons to be given later it is projected outside the triangle. In every case where the point representing the axis was in the triangle whose points are (111), (110) and (100) it was found that the direction of slip was the line (11 $\bar{1}$) which is represented by the point S in fig. 4.

Representation of Results

It seems unnecessary to give the details of the X-ray measurements from which these points were found, but sufficient data are given in Table II to enable a reader to reconstruct the fig. 4. In column 1 the number of the specimen is given, column 2 contains the angle ξ between the axis of specimen† and the direction of slip (11 $\bar{1}$).

* Taylor and Elam, "Plastic Extension of Crystals," 'Roy Soc Proc,' A, vol 108, p 28 (1925).

† Direction of principle stress, ϵ , normal to plane face in case of compression discs or longitudinal axis in the case of tension specimens.

Table II

	ξ°	χ°	ψ°
$\beta 2\ 1$	59	+18	+11
$\beta 4\ 1$	65	+22	+17
$\beta 5\ 1$	58½	+36	+43
$\beta 5\ 2$	59½	+23	+17
$\beta 5\ 3$	48½	+17½	+9
$\beta 3\ 2$	50	-11	0
$\beta 6\ 2$	52½	-16	-2
T $\beta 2\ 3$	47½	+18	+3
T $\beta 1$	36	+7	0
T $\beta 2\ 4$	50	-8	½

ξ is inclination of axis of specimen to direction of slip

χ is the angle between the normal to the crystal plane {111} and the plane containing the direction of slip and the axis of the specimen

ψ is the angle between plane of slip and crystal plane {111}

As a second co-ordinate the azimuth λ of the plane containing the axis of the specimen and the direction of slip is given in column 3. λ is measured from the direction (101) (marked as A in fig. 4) so that if M is the point of intersection of the azimuth circle SM with the plane {111}, λ is the arc AM. λ is reckoned as positive when M lies between (101) and (011) and negative when it lies between (101) and (211). The values of ξ and χ given in Table II are sufficient for the construction of fig. 4. The points M and S correspond with those similarly marked in figs. 2 and 3.

The results of all the distortion measurements are given in column 4 of Table II which contains the angle ψ between the direction (101) and the pole of the plane of slip (which lies in the plane {111}).

In previous work on aluminium for which the slipping is confined to a given crystal plane the orientation of the plane and direction of slip were defined by co-ordinates θ and η . If the axis of the specimen is supposed vertical, θ was the slope of the slip plane to the horizontal and η was the angle between the direction of slip and the line of greatest slope on the slip plane. θ and η are connected with ξ and $\chi - \psi$ by the equations

$$\text{and } \left. \begin{aligned} \sin \theta \cos \eta &= \cos \xi \\ \cos \theta &= \sin \xi \cos (\chi - \psi) \end{aligned} \right\} \quad (1)$$

If P is the total pressure on a compression specimen of area a or the total pull in a tension specimen of cross section a , then the component of shearing force parallel to the direction of slip is $F = (P/a) \cos \theta \sin \theta \cos \eta$. From (1) it will be seen that

$$F = (P/a) \cos \xi \sin \xi \cos (\chi - \psi) \quad (2)$$

Analysis of Results

The results of all the distortion measurements and X-ray analysis which are summed up in Table II are illustrated graphically in fig 5. In that diagram

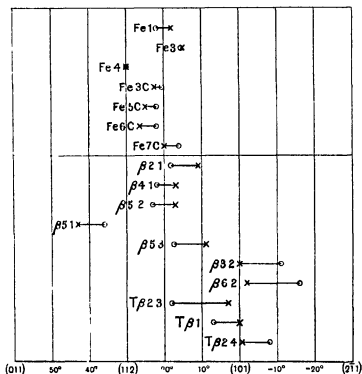


FIG. 5.—Relative positions of M (○) and Pole of Slip Plane (×)

the abscissæ represent directions on the plane $\{11\bar{1}\}$, the point M being represented by a circle (○), and the pole of the slip plane by a cross (×). The angle $\chi - \psi$ is represented by the line connecting the circle and the cross. The vertical lines represent 10° intervals, and the principal crystal directions (011), (112), (101), $(2\bar{1}1)$ which occur at intervals of 30° round the plane $\{11\bar{1}\}$ are marked at the bottom of the figure.

It will be seen that in all 10 cases, namely, 7 compression specimens, $\beta 2\ 1$, $\beta 4\ 1$, $\beta 5\ 1$, $\beta 5\ 2$, $\beta 5\ 3$, $\beta 3\ 2$, $\beta 6\ 2$, and 3 tension specimens T $\beta 1$, T $\beta 2\ 3$, T $\beta 2\ 4$, the pole of the slip plane lies away from the point M in the direction of the nearest pole of type (101). From equation (2) it will be seen that if F , the resistance to shear, were equal on all planes through the given direction of slip, then P would be least when $\chi = \psi$ so that the pole of the slip plane would coincide with M. The fact that the pole of the plane of slip lies away from M

towards the nearest pole of type (101) must therefore mean that of all possible planes through the direction of slip (11 $\bar{1}$), the resistance to shear is least when it coincides with a crystal plane of type (110). For purposes of comparison the corresponding points for the iron crystals previously examined are put at the top of the diagram, fig. 5

Experiments with Compression Discs β 5 1 and β 5 2

Since the resistance to shear is a minimum when the plane of slip coincides with a crystal plane of type {110} it seems probable that the resistance would be a maximum when it coincides with one of the crystal planes of type {112} which lies midway between the planes of type (110). To test this, a crystal, β 5, was chosen for which the normal to its flat surface was close to a plane of type {110}. Two compression discs β 5 1 and β 5 2 were ground from it in such a way that when the point representing the normal to the flat face of β 5 2 was projected on to the diagram of fig. 4, so as to be just inside the triangle whose vertices are (111), (110) and (100), then the point representing β 5 1 fell just outside this triangle when the same cubic axis was turned into the centre of the figure. By turning another cubic axis into the centre the point representing β 5 1 could have been made to lie inside the triangle, but for the purpose of the present experiment it was more convenient to project it in the manner stated above.

Referring to fig. 5 it will be seen that for β 5 2, M was 7° to the right of the pole (112) while the pole of the plane of slip was 13° to the right, for β 5 1, M was 6° to the left of (112) while the pole of the plane of slip was 13° to the left of (112). This seems to indicate a maximum of resistance to shear in the neighbourhood of planes of type (112).

Calculation of Resistance to Shear

It has been shown in the case of aluminium and some other metal that at any given temperature the resistance to shear depends only on the amount of distortion, and not on the component of force normal to the plane of slip, or on the component of shear parallel to the plane of slip and transverse to the direction of slip. If it is assumed that this is a general law governing distortion of metallic crystals, then F , the resistance to shear, would be a function of the amount of distortion and of the angle ψ . It will be seen later that experimental evidence on this point is furnished by the results of these experiments. The actual value ψ for any given value of ξ and χ would be determined by the

condition that P is a minimum as ψ varies, thus from (2), $\frac{F}{\cos(\chi - \psi) \cos \xi \sin \xi}$ is a minimum, so that if F is regarded as a known function of ψ and independent of ξ , the equation for determining χ may be written

$$\frac{1}{F} \frac{dF}{d\psi} = + \tan(\chi - \psi) \quad (3)$$

Conversely if the relationship between χ and ψ is known (3) may be used for determining the relationship between F and ψ . Accordingly we proceed to examine how far these experiments give us the relationship between χ and ψ .

In fig 6 the abscissae represent values of ψ and the ordinates the corresponding values of χ . The numerical magnitudes only are set out, the signs being for

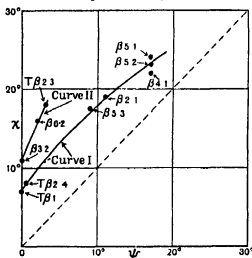


FIG 6

the moment disregarded, and the results of both tension and compression experiments are shown. It will be seen that the points in fig 6 lie very nearly on the two smooth curves which are distinguished by the numbers I and II. Both these curves cut the axis of χ so that for a range of $\chi = 0$ to $\chi = 7^\circ$ in one case and from $\chi = 0$ to $\chi = 11^\circ$ in the other the slip plane is actually the crystal plane (101).

Influence of the Sense of the Direction of Slip

The question naturally arises what is the difference between the two curves? It will be seen that the upper curve, II, contains the points corresponding to the tension specimen T β 2 3, and the compression specimens β 3 2 and β 6 2. The lower curve, I, contains the tension specimen T β 2 4 and the compression specimens β 5 1, β 5 2, β 5 3, β 4 1, β 2 1. The point corresponding

to T β 1 might belong to either curve because it is on the axis $\psi = 0$ and below both the points where these curves cut this axis

An inspection of fig 4 shows that the triangle WXO may be divided into two parts XUVW and UOV by the great circle joining the direction of slip, (11 $\bar{1}$), with (101) XUVW contains the points representing compression specimens which give points on curve I and tension specimens which give points on curve II UOV contains all the points representing tension specimens which give

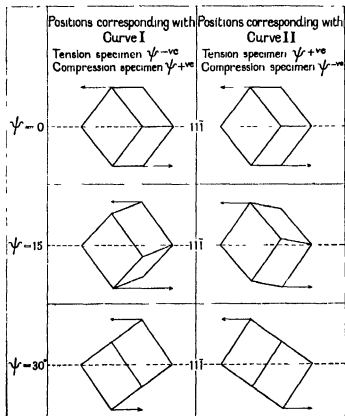


FIG 7—Diagram illustrating Crystallographic Difference between Shearing in Opposite Directions

points on curve I and compression specimens which give points on curve II This is exactly what we should expect if the resistance to shear on a given plane differs according to the *sense* of the direction of slip Consider for instance two compression specimens C_1 and C_2 and suppose that the representative point for C_1 lies in XUVW and that for C_2 lies in UOV Suppose further that the angle ψ for C_1 is Ψ and that the value of ψ for C_2 is $-\Psi$ From the point of view of crystallographic symmetry the *distortion* in the case of C_1 is identical

with that of C_2 except that the *senses* of the direction of slip are opposite in the two cases. On the other hand consider two *tension* specimens T_1 and T_2 , the representative points for which lie in XUVW and UOV respectively, the values of ψ are Ψ and $-\Psi$. The distortion for T_1 is, from the point of view of crystallographic symmetry, identical with that for C_2 , while that for T_2 is identical with that for C_1 .

In order to illustrate the difference the diagrams shown in fig 7 have been prepared to represent a unit cube of the crystal structure viewed perpendicular to the direction of slip and with the eye looking along the plane of slip. The arrows pointing in opposite directions above and below the plane of slip indicate the direction and sense of the slipping motion. The three cubes on the left represent distortions corresponding with points on curve I, fig 6, while the three cubes on the right represent distortions corresponding with points on curve II.

Variations of Resistance to Shear with Orientation of Plane of Slip

(One may infer from the fact that for a given value of ψ curve II lies above curve I in fig 6, that the resistance to shear is greater for specimens corresponding with points on curve II than for points on curve I. To calculate the resistance to shear for various orientations of the plane of slip round the given direction of slip, equation (3) may be used, and here it may be remarked that the curves in fig 6 confirm the assumption made in deducing that equation, that the resistance to shear is independent of the component of force normal to the plane of slip. The ratio of the component normal to the plane of slip to the component of shearing force in the direction of slip is $\frac{\cos \theta}{\sin \theta \cos \theta \cos \gamma}$ and from equation (2) this is equal numerically to $\sec \xi$, but it is positive for compression specimens and negative for tension specimens.)

The value of ξ varies from 36° to 65° , but in spite of this variation the curves of fig 6 show that the value of χ depends only on ψ and not on ξ , so that the assumption used in equation (3) seems to be justified. If F_0 represents the value of the resistance to shear when the slipping is on the plane (101) then on integrating (3) it will be found that

$$\log_e (F/F_0) = \int_0^\psi \tan (\chi - \psi) d\psi \quad (4)$$

Taking the values of χ from curve I or II one can determine graphically the values of $\int_0^\psi \tan (\chi - \psi) d\psi$ for the range of values of ψ covered by the experi-

ments The results of this operation are shown in fig 8 where the ratio F/F_0 is given for a series of values of ψ It will be seen that as the plane of slip passes

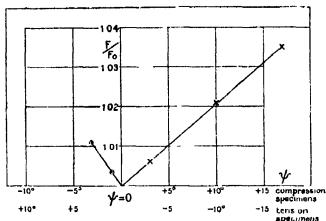


FIG 8—Curve showing Variations in Resistance to Shear in β brass as ψ varies

through the crystal plane $\psi = 0$, i.e., $\{101\}$, the resistance to slipping passes through a minimum and $dF/d\psi$ changes abruptly both its sign and its magnitude. The resistance increases linearly at a rate of 0.2 per cent for 1° change in ψ over the range $\psi = 0$ to $\psi = 17^\circ$. In the range $\psi = 0$ to $\psi = -3^\circ$ the resistance increases linearly by 0.37 per cent per degree increase in $-\psi$.

Comparison with Results of Direct Measurements of Force

The consistency of the experimental results affords good evidence that we are really measuring changes in resistance to shear with changes in the orientation of the plane of slip round the given crystallographic direction of slip. Unfortunately it is not possible to verify the results by direct measurement of the shearing force in several specimens, the crystal axes of which are in different orientations. Measurements of shearing force at different stages of the tests were in fact made, and they are discussed below. The shearing force depends to a small extent, as we have seen, on ψ , but it depends very much more on the value of s , the amount of shear. Each compression specimen gives us a curve connecting F the resistance to shear, and s for a given value of ψ . At first sight one might suppose that if we obtain a series of such curves for different values of ψ , the variation of F with s might be found by comparing the values of F for a given value of s . This is not the case, however, for there is no reason to suppose when a series of different crystals are compared after having sheared through the same amount, s , but parallel to planes having different values of

ψ , that they will have the same properties. It will not be possible to discuss the meaning of direct observations of shearing force until some adequate theory can be advanced to explain quantitatively the "hardening" or strengthening of a metal with increase in distortion. On the other hand the consistency of the observations giving a "one to one" connection between ψ and χ , among specimens covering a large range of values of s and ξ , seems to show that the variations of F with ψ is the same whether a large or a small amount of slip has taken place. For this reason there seems some hope that it may be possible to account for the connection between F and ψ from a knowledge of the properties of the crystal lattice itself, apart from any knowledge of the way in which F depends on s .

Direct Measurement of Shearing Force

Each of the seven compression discs here described was compressed in several stages. The total compressive load was measured at each stage and methods described in a previous paper were used to find S the component of shear stress parallel to the plane of slip, and s the amount of shear. These results are given in Table III and are exhibited graphically in fig. 9. Inspection of that figure shows that the curves for different specimens are not the same. The difference may be due to slight differences in the material. There might, for instance, be small included crystals in some specimens and not in others. This possibility, though always present, is unlikely to be the cause of the difference between specimens $\beta 5 1$, $\beta 5 2$ and $\beta 5 3$, because they were all cut from the same

Table III—Results of Measurements of Compressive Force S is shear strength parallel to slip plane in lbs per square inch

$\beta 5 1$	S	9100	13700	17800	22000	26000				
	s	0 027	0 058	0 083	0 136	0 189				
$\beta 5 2$	S	7100	13000	20400	28700					
	s	0 027	0 075	0 131	0 199					
$\beta 5 3$	S	3250	6350	9200	10100					
	s	0 014	0 060	0 133	0 149					
$\beta 2 1$	S	2300	4580	6900	9000	11100	13200	15200	17300	19200
	s	0 0104	0 0182	0 0270	0 0465	0 0688	0 0933	0 122	0 149	0 164
$\beta 4 1$	S	3500	6900	10300	13500	16600	19600	22400	25340	
	s	0 007	0 031	0 049	0 077	0 119	0 164	0 196	0 232	
$\beta 3 2$	S	3100	6900	9100	11800	14800				
	s	0 028	0 056	0 066	0 139	0 182				
$\beta 6 2$	S	3100	6050	8800						
	s	0 010	0 070	0 131						

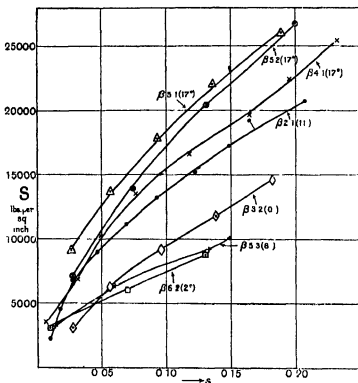


FIG 9—Shear Strength S in lbs per square inch of the Slip Plane for different values of the amount of shear

crystal $\beta 5 1$ and $\beta 5 2$ were cut so that their planes of slip were crystallographically similar though their shapes and sizes were not the same. It will be seen that the corresponding curves in fig 8 are nearly coincident. Specimen $\beta 5 3$ on the other hand was cut in a different orientation so that $\psi = 8\frac{1}{2}^\circ$. It will be seen that its resistance to shear is very much less than that of $\beta 5 1$ or $\beta 5 2$. It will be seen that specimens $\beta 5 1$, $\beta 5 2$, $\beta 4 1$ and $\beta 2 1$ for which the planes of slip have the higher values of ψ have also the higher resistance to shear. Specimens $\beta 3 2$, $\beta 6 2$ and $\beta 5 3$ which have slipped on planes near the crystal plane of type $\{110\}$ have a low resistance to shear. The values of ψ are given in brackets in fig 9.

These direct force measurements are given here because they appear fairly consistent, but it is necessary to state that the shearing force was deduced from the total pressure on the specimen making the assumption that the friction of the specimen on the greased surfaces of the polished steel plates produced only a negligible effect on the shear stress. In the case of aluminium specimens

somewhat elaborate experiments were made to find out whether this assumption is true and it was found to be so. The method used in the case of specimens of β -brass was the same as that used in the case of aluminium, but it must be remembered that pressures in the former case were considerably greater than they were in the latter. On the other hand the observed uniformity of the distortion is strong evidence that the friction has no appreciable effect.

Slip Lines

Though I made repeated efforts I was unable to see slip lines, so I cannot say whether they are of the same type as those of α iron or not. Attempts by metallurgists skilled in polishing also failed to reveal them.

Connection between Choice of Plane of Slip and Crystal Structure

At the present time one of the models for representing crystal structure in pure metals, which is most in favour among metallurgists, seems to be that of a pile of similar ionised atoms mutually repelling one another but held together by a kind of "glue" of electrons moving about in the spaces between them. This is the type of model used for instance by Frenkel in discussing the properties of metals. Recently Mr Hume Rothery* has proposed alternatively that the electrons instead of moving about occupy definite positions between the atoms, though he does not explain how they can maintain those positions.

In seeking to predict from such a model which of the crystal planes would afford least resistance to slipping, the principle which has commonly been adopted is to imagine a close packed pile of spheres whose centres are at the lattice points of the crystal structure. Slipping parallel to various crystal planes is then contemplated. In order that the spheres may move over one another it is necessary for the two portions into which the material is divided by the plane of slip to move apart, thus doing work against the attractions of the electrons moving between the atoms, and it is supposed that the condition which determines which among the crystallographic planes shall be a plane of slip is that this distance of separation shall be a minimum.

Another method which has been used gives a similar result. The spheres are imagined to contract in radius, their centres remaining fixed. At first it is not possible to place any plane in such a position that it misses all the spheres. At a certain stage of the contraction it becomes possible to place a sheet parallel to one of the crystallographic planes in such a position that it does not cut any

* 'Phil Mag.', vol 4, p 1017 (1927)

of the spheres. As the contraction proceeds it becomes possible to place sheets parallel to other crystallographic planes, but the plane of slip is the first of those "ways through" to appear. It is obvious that purely geometrical conceptions of this kind are not capable of explaining distortion of metals, but, as has frequently been pointed out, they give the right result in the case of face-centred cubic metals like aluminium.

In the case of a body-centred structure like iron the first "ways through" which appear as the spheres are contracted towards their centres are not a series of parallel planes as they are in the case of face-centred cubic structures, but they are the faces of a pile of hexagonal rods. The view looking down the lines of atoms which are the centres of these hexagonal rods at the stage when the "ways through" first appear is shown in fig 10. The "ways through" are

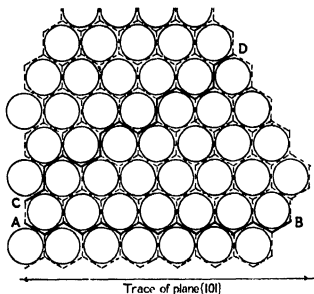


FIG 10—Diagram illustrating Crystal Structure of body-centre Cubic Crystals, when viewed along a cube diagonal

shown dotted. In our paper on the "Distortion of Iron Crystals" Miss Elam and I described the deformation in terms of these hexagonal rods, but for reasons which will shortly be explained we made no reference to the piles of atoms lying along them. Other metallurgists however, placed the ions in position along our hexagonal rods, and concluded from data which were purely geometrical that the type of distortion which we observed for iron could be explained without any detailed reference to the forces between the atoms of the structure. Shortly after our paper appeared, for instance, a distinguished metallurgist

wrote to me that he had been inclined to doubt our experimental results till it had occurred to him that in a body-centred pile of spheres the first "ways through" seen as the spheres contract towards their centres consist of a network of hexagonal prisms instead of the set of parallel planes which first appear in the case of face-centred piles. More recently a similar idea has been put forward by Mr Hume Rothery*.

The reason why we did not put forward ideas of this kind, though they were in our minds when we put forward the "hexagonal rod" description of distortion, was that if pursued to their logical conclusion they led to the wrong result. Assuming for the moment that the direction of slip is along the lines where the atoms are closest together, namely, one of the directions of type {111}, the choice of the plane of slip must depend on the relative amounts of the resistances to shear parallel to the various planes which pass through the given direction of slip. In order to predict therefore which of these various planes will be the plane of slip we must first predict the way in which resistance to shear varies as the plane of slip rotates round the direction of slip.

To do this it is necessary to make some assumption as to the cause of the resistance to shear, or, in other words, the cause of the dissipation of energy which occurs when a metal crystal is distorted. The simplest assumption that can be made is that the energy is lost when one pile of atoms moves relative to its immediate neighbours. If it is supposed that a certain definite amount of energy is dissipated between each pair of piles when the two move through a given distance relatively to one another, then the resistance to shear will be the same as that of a pile of hexagonal rods when they are placed so that their sides are parallel to planes of type {112} provided that the friction at every interface is the same. This assumption of equal friction between any neighbouring pair of piles of ions is necessarily implied, though it is not specifically stated, in Mr Hume Rothery's work, for in order to distinguish between different types of slipping he takes as his criterion that the resistance to slipping will be least when the depth to which the ions of one pile penetrate during a slipping motion into the spheres of repulsion of those in the neighbouring pile is least. This necessarily implies that when the depths of penetration in two cases are the same, the resistance to slipping between the piles is the same.

Making this assumption we can now work out the resistance to shear of any plane of slip which passes through the direction of slip. Let ψ be the angle between any plane of slip and the plane {101}.

Let F be the magnitude of the shear stress which will just cause slip on the

* 'Phil Mag,' vol 4, p 1035 (1927)

plane ψ , and let f be the resistance to slipping experienced by unit length of each pile of ions as it slips past its neighbour. Let $a\sqrt{3}$ be the distance between the central lines of two neighbouring piles of ions, so that a is the breadth of a face of one of the hexagonal rods. It is required to find F in terms of f , a and ψ . Consider a length l of the trace of the slip plane on a plane perpendicular to the direction of slip. This trace, though a straight line from the point of view of an observer who cannot see the individual atoms, may be regarded as consisting of microscopic elements which are the sides of the hexagons. In fig. 10 the section of a slip plane parallel to $\{101\}$ is shown at AB . The section of a slip plane parallel to $\{112\}$ is shown at CD . There are three types of these elements inclined at 30° , -30° and 90° respectively to the plane $\{101\}$. Suppose that ψ lies in the range 0 to 30° and that in the breadth l of the slip plane there are n_1 elements of the first type, n_2 of the second, and n_3 of the third.

We then have the following relationships which can easily be verified by looking at fig. 10

$$\left. \begin{aligned} n_1 - n_2 &= n_3 \\ (n_1 + n_2) a \cos 30^\circ &= l \cos \psi \\ (n_1 - n_2) a \sin 30^\circ + an_3 &= l \sin \psi \\ (n_1 + n_2 + n_3) f &= Fl \end{aligned} \right\} \quad (5)$$

Eliminating n_1 , n_2 and n_3 from these equations it is found that

$$F = \frac{4}{3} \frac{f}{a} \cos(\psi - 30^\circ)$$

If F_0 is the value of F when $\psi = 0$

$$F/F_0 = \frac{1}{2} \sqrt{3} \cos(\psi - 30^\circ), \quad (6)$$

when the angle ψ is between 0 and -30°

$$F/F_0 = \frac{1}{2} \sqrt{3} \cos(\psi + 30^\circ)$$

Now let us apply the condition given in equation (3) which determines the value of ψ when χ is given and the relationship between F/F_0 and ψ is known.

It is

$$\frac{1}{F} \frac{dF}{d\psi} = \tan(\chi - \psi)$$

differentiating (6) it will be found that

$$\frac{1}{F} \frac{dF}{d\psi} = -\tan(\psi - 30^\circ)$$

When χ has any positive value less than 30° there is no possible positive value of ψ less than 30° for which $\tan(\chi - \psi) = -\tan(30^\circ - \psi)$. In fact, for all orientations of the crystal axes except special symmetrical ones for which $\chi = 30^\circ$ (i.e., ones for which the axis of the specimen lies in a crystal plane of type $\{110\}$) the plane of slip would be a crystal plane of type $\{110\}$. This conclusion follows directly from an analysis of the effect of Mr Hume Rothery's hypothesis, no other hypothesis than that necessarily implied in his discussion being employed. Since in the case of iron crystals the plane of slip is not in general a plane of type $\{110\}$, it follows that the hypothesis that the conditions of slipping are determined by the geometrical considerations put forward by Mr Hume Rothery is unsound.

Comparison between Slipping in β -brass and Model of Hexagonal Rods

Though we cannot hope to explain the choice of slip planes in metal crystals in the manner of Mr Hume Rothery, using only simple geometrical data, yet there is one very remarkable feature of the slip phenomena in crystals of β -brass which is reproduced in our model in which we represented piles of ions by hexagonal rods (and from this point of view our model complies with the requirements of Mr Hume Rothery's hypothesis). The rate of variation of resistance to shear with the angle ψ is discontinuous at the point $\psi = 0$ both in the model and in β -brass. This can be seen by comparing fig 11 which represents F/F_0 for the model, with fig 8 which represents a limited range of values

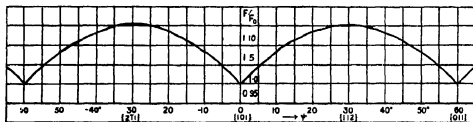


FIG 11.—Theoretical Curve showing Variation in Shear Strength, as Plane of Slip rotates about the Direction of Slip

of the same quantity deduced from distortion and X-ray measurements of β -brass

In view of this point of similarity it is of interest to enquire why the model shows this peculiar feature. Referring to fig 10 it will be seen that when the slip plane coincides with the crystal plane $\{101\}$, i.e., when $\psi = 0$, all the elements composing the plane of slip are at angles of $\pm 30^\circ$ to its general direction. A small change $\delta\psi$ in ψ introduces elements of the slip plane at

right angles to its general direction, the number of them being proportional to the absolute value of $\delta\psi$ irrespective of whether $\delta\psi$ is positive or negative

On the other hand when the slip plane is at $\psi = 30^\circ$ so that it coincides with the crystal plane $\{112\}$ as in CD, fig 10, the three types of element composing the whole slip plane make angles of 0 and $\pm 60^\circ$ with the general direction. A small change $\delta\psi$ in ψ does not change the number of elements at angle 0° . If $\delta\psi$ is positive there is an increase proportional to $\delta\psi$ in the number of elements at $+60^\circ$ together with an equal decrease in the number at -60° . Small changes in $\delta\psi$ therefore leave the total number of elements unaltered so that the rate of change in resistance to shear is zero when the plane of slip coincides with a crystal plane of type $\{112\}$.

It will be seen that in the case of β -brass there is not only a sudden change of sign in the rate of increase in F/F_0 with ψ at $\psi = 0$, but there is also a sudden change in its absolute magnitude. This corresponds presumably with a difference in the resistance to slipping between neighbouring hexagonal prisms or piles of atoms, according to the direction of motion. That such a difference is to be expected from the point of view of crystallographic symmetry has already been pointed out. Fig 12 shows a pair of neighbouring piles of ions AB and CD. Regarding CD as fixed it will be seen that the motion of AB from A to B is crystallographically different from that from B to A. It should be noticed however that the hypothesis that the resistance to relative motion between two piles of ions depends only on the direction of motion does not account for the asymmetry of the curve of resistance as shown in fig 8, for it is a geometrical necessity that among the elements which make up the slip plane the direction of slip across half of them must be the type illustrated in fig 12.

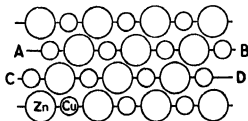


FIG 12—Atomic Spacing in neighbouring Lanes of Atoms parallel to the Cube Diagonal

when the pile AB moves from A to B while the other half is of the opposite kind typified by a motion from B to A.

It seems to me that it is useless to put forward hypotheses about the manner in which slip will occur in a metal crystal until some theory is put forward which

will account, in a quantitative manner, for the way in which energy is lost during the process of distortion. So far no progress whatever has been made in this direction.

In conclusion I should like to express my thanks to Sir Ernest Rutherford for permission to carry out the work in the Cavendish Laboratory, and to Miss Elam, Prof. Carpenter and Dr. Tamura for the material with which these experiments were carried out.

Wave Resistance

By T H HAVELOCK, F R S

(Received December 15, 1927)

Introduction

1 The object of this paper is to give more direct proofs of certain expressions for wave resistance which have been used in previous calculations, further, in view of other possible applications, the expressions are generalised so that one can obtain the wave resistance for any set of doublets in any positions or directions in a uniform stream, or for any continuous distribution of doublets or equivalent sources and sinks. The only limitation is the usual one that the additional velocities at the surface are small compared with the velocity of the stream. One might take a simple source as the unit, but to avoid certain minor difficulties it would be necessary to assume an equal sink at some other point. The possible applications are to bodies either wholly, or with certain limitations partially, submerged. The image system in such a case consists of a distribution of sources and sinks of zero aggregate strength, and so may be replaced by an equivalent distribution of doublets. Hence it is simpler to use the doublet as the unit from the beginning.

The wave resistance of a submerged sphere was obtained previously both by direct calculation of pressures on the sphere and by an analogy with the effect of a certain surface distribution of pressure. The latter method was then generalised to give the wave resistance of any distribution of horizontal doublets in a vertical plane parallel to the direction of the stream. In a recent paper Lamb* has supplied a method for calculating wave resistance which avoids the

* H Lamb, 'Roy Soc Proc.,' A, vol 111, p 14 (1926)

comparison with an equivalent surface pressure, it consists in calculating the rate of dissipation of energy by a certain integral taken over the free surface when, as is usual in these problems, a small frictional force has been introduced into the equations of motion of the fluid. Lamb, however, deals only with a single doublet, to which a submerged body is equivalent to a first approximation, and so does not obtain the interference effects which arise from an extended distribution of doublets, further, he carries out the necessary calculation by analysing first the surface distribution of velocity potential, or in effect analysing the wave pattern. In the following paper it is shown that this intermediate analysis may be avoided by a direct application of the Fourier double integral theorem in two dimensions. This step simplifies the extension of the calculation to any distribution of doublets in any positions and directions, various cases, which it is hoped to use later, are given in some detail for deep water, and one case of a single doublet in a stream of finite depth.

Two-dimensional Motion

2 The results for a two-dimensional doublet are well-known, but there are one or two points of interest in the calculation. We shall suppose the liquid to be at rest, and the doublet to be moving with uniform velocity c . Let the doublet be of moment M , with its axis horizontal, at a depth f . Take the origin in the free surface, with Ox in the direction of motion and Oz vertically upwards. If ζ is the surface elevation, and if there is a frictional force proportional to velocity, the pressure condition at the free surface gives

$$\frac{\partial \phi}{\partial t} - g\zeta + \mu' \phi = \text{constant}, \quad (1)$$

ϕ being the velocity potential. Since, at the free surface $\partial \zeta / \partial t = -\partial \phi / \partial z$, we have for the steady motion relative to the moving axes,

$$\frac{\partial^2 \phi}{\partial x^2} + \kappa_0 \frac{\partial \phi}{\partial z} - \mu \frac{\partial \phi}{\partial x} = 0, \quad (2)$$

to be satisfied at $z = 0$, with $\kappa_0 = g/c^2$ and $\mu = \mu'/c$. The conditions of the problem are satisfied by

$$\phi = \frac{M}{x + i(z + f)} - \frac{M}{x + i(z - f)} + 2i\kappa_0 M \int_0^\infty \frac{e^{kx - \kappa(z - f)}}{\kappa - \kappa_0 + i\mu} d\kappa, \quad (3)$$

where the real part is to be taken

If R is the equivalent wave resistance, Rc is equal to the rate of dissipation of energy, this gives, following Lamb,

$$R = - \frac{\rho'}{c} \int \phi \frac{\partial \phi}{\partial n} dS, \quad (4)$$

taken over the free surface. Thus in the two-dimensional case we have

$$R = \lim_{\mu \rightarrow 0} \mu \rho \int_{-\infty}^{\infty} \phi \frac{\partial \phi}{\partial z} dx, \quad (5)$$

with $z = 0$

The surface values of ϕ and $\partial \phi / \partial z$ can be obtained from (3), after applying well-known transformations we obtain, at $z = 0$,

$$\phi = 2\kappa_0 M \int_0^{\infty} \frac{(m + \mu) \sin mf + \kappa_0 \cos mf}{(m + \mu)^2 + \kappa_0^2} e^{-mx} dm,$$

$$\frac{\partial \phi}{\partial z} = - \frac{4Mxf}{(x^2 + f^2)^2} - 2\kappa_0 M \int_0^{\infty} \frac{(m + \mu) \cos mf - \kappa_0 \sin mf}{(m + \mu)^2 + \kappa_0^2} m e^{-mx} dm,$$

for $x > 0$, and

$$\begin{aligned} \phi &= 4\pi\kappa_0 M e^{\mu x - \kappa_0 f} \cos(\kappa_0 x + \mu f) \\ &\quad - 2\kappa_0 M \int_0^{\infty} \frac{(m - \mu) \sin mf - \kappa_0 \cos mf}{(m - \mu)^2 + \kappa_0^2} e^{mx} dm, \\ \frac{\partial \phi}{\partial z} &= 4\pi\kappa_0 M e^{\mu x - \kappa_0 f} \{\kappa_0 \cos(\kappa_0 x + \mu f) + \mu \sin(\kappa_0 x + \mu f)\} \\ &\quad - \frac{4Mxf}{(x^2 + f^2)^2} + 2\kappa_0 M \int_0^{\infty} \frac{(m - \mu) \cos mf - \kappa_0 \sin mf}{(m - \mu)^2 + \kappa_0^2} m e^{mx} dm, \end{aligned} \quad (6)$$

for $x < 0$

These expressions are continuous at $x = 0$. It is easily seen that the only terms which give any contribution to (5) in the limit are the first terms in the expressions for ϕ and $\partial \phi / \partial z$ when x is negative. These are the terms which arise from the train of regular waves established in the rear of the moving doublet and so this method is connected with the alternative calculation of wave resistance by means of group velocity. The dissipation of energy when there is a frictional term is represented in the limit, when μ is made zero, by the propagation of energy away from the system in the train of regular waves. To complete the calculation from (5) and (6) we have

$$\begin{aligned} R &= \lim_{\mu \rightarrow 0} \mu \rho \int_{-\infty}^0 16\pi^2 \kappa_0^3 M^2 e^{2\mu x - 2\kappa_0 f} \cos^2 \kappa_0 x dx \\ &\quad - 4\pi^2 \rho \kappa_0^3 M^2 e^{-2\kappa_0 f} \end{aligned} \quad (7)$$

We may obtain this result without analysing the expressions for ϕ and $\partial\phi/\partial z$. We obtain from (3) the following complete expressions in real terms, at $z = 0$,

$$\phi = 2\kappa_0 M \int_0^\infty \frac{\mu \cos \kappa x - (\kappa - \kappa_0) \sin \kappa x}{(\kappa - \kappa_0)^2 + \mu^2} e^{-\mu f} d\kappa, \quad (8)$$

$$\frac{\partial\phi}{\partial z} = 2M \int_0^\infty \frac{\mu\kappa_0 \cos \kappa x - \{\kappa(\kappa - \kappa_0) + \mu^2\} \sin \kappa x}{(\kappa - \kappa_0)^2 + \mu^2} e^{-\mu f} d\kappa \quad (9)$$

To carry out the integration of the product over the surface, we use the following theorem if

$$f(x) = \int_0^\infty (A_1 \cos \kappa x + B_1 \sin \kappa x) d\kappa,$$

$$\psi(x) = \int_0^\infty (A_2 \cos \kappa x + B_2 \sin \kappa x) d\kappa,$$

where A_1, A_2, B_1, B_2 are functions of κ , then

$$\int_{-\infty}^\infty f(x) \psi(x) dx = \pi \int_0^\infty (A_1 A_2 + B_1 B_2) d\kappa \quad (10)$$

This theorem is derived from the Fourier double integral

$$\phi(x) = \frac{1}{\pi} \int_0^\infty d\kappa \int_{-\infty}^\infty \phi(\alpha) \cos \kappa(x - \alpha) d\alpha, \quad (11)$$

and is subject to the same conditions

In the present case, comparing (8) and (11) we have

$$\begin{aligned} \int_{-\infty}^\infty \phi(\alpha) \cos \kappa \alpha d\alpha &= \frac{2\pi\kappa_0 M \mu e^{-\mu f}}{(\kappa - \kappa_0)^2 + \mu^2}, \\ \int_{-\infty}^\infty \phi(\alpha) \sin \kappa \alpha d\alpha &= -\frac{2\pi\kappa_0 M (\kappa - \kappa_0) e^{-\mu f}}{(\kappa - \kappa_0)^2 + \mu^2} \end{aligned} \quad (12)$$

Hence we have

$$\begin{aligned} \int_{-\infty}^\infty \phi \frac{\partial\phi}{\partial z} dx &= 4\pi\kappa_0 M^2 \int_0^\infty \frac{\kappa^2 e^{-2\mu f}}{(\kappa - \kappa_0)^2 + \mu^2} d\kappa, \\ R &= \lim_{\mu \rightarrow 0} 4\pi\kappa_0 M^2 \rho \mu \int_0^\infty \frac{\kappa^2 e^{-2\mu f}}{(\kappa - \kappa_0)^2 + \mu^2} d\kappa \\ &= 4\pi^2 \rho \kappa_0^3 M^2 e^{-2\kappa_0 f} \end{aligned} \quad (13)$$

Horizontal Doublet

3 To consider three-dimensional fluid motion, take first a horizontal doublet of moment M at the point $(0, 0, -f)$. Assume that the velocity potential can be expressed in the form

$$\phi = -\frac{iM}{2\pi} \int_{-\pi}^{\pi} \int_0^{\infty} \kappa e^{-\kappa(z+f) + i\kappa(x \cos \theta + y \sin \theta)} \cos \theta \, d\theta \, d\kappa \\ + \int_{-\pi}^{\pi} \int_0^{\infty} \kappa F(\theta, \kappa) e^{-\kappa(f-z) + i\kappa(x \cos \theta + y \sin \theta)} \cos \theta \, d\theta \, d\kappa, \quad (14)$$

where real parts are to be taken, and where the first term is the velocity potential of the given doublet in a form valid for $z+f > 0$.

The surface condition is equation (2) as before, applying this, we obtain

$$F(\theta, \kappa) = \frac{iM}{2\pi} \frac{\kappa + \kappa_0 \sec^2 \theta + i\mu \sec \theta}{\kappa - \kappa_0 \sec^2 \theta + i\mu \sec \theta} \quad (15)$$

Hence from (14) and (15) the surface values of ϕ and $\partial\phi/\partial z$ are

$$\phi = \frac{i\kappa_0 M}{\pi} \int_{-\pi}^{\pi} \int_0^{\infty} \frac{e^{-\kappa f + i\kappa(x \cos \theta + y \sin \theta)}}{\kappa - \kappa_0 \sec^2 \theta + i\mu \sec \theta} \kappa \sec \theta \, d\theta \, d\kappa, \quad (16)$$

$$\frac{\partial\phi}{\partial z} = \frac{iM}{\pi} \int_{-\pi}^{\pi} \int_0^{\infty} \frac{e^{-\kappa f + i\kappa(x \cos \theta + y \sin \theta)}}{\kappa - \kappa_0 \sec^2 \theta + i\mu \sec \theta} \kappa^2 (\kappa + i\mu \sec \theta) \cos \theta \, d\theta \, d\kappa \quad (17)$$

Taking real parts of these expressions we obtain

$$\phi = \int_{-\pi}^{\pi} \int_0^{\infty} \{F_1(\theta, \kappa) \cos(\kappa x \cos \theta) \cos(\kappa y \sin \theta) \\ + F_2(\theta, \kappa) \sin(\kappa x \cos \theta) \cos(\kappa y \sin \theta)\} \kappa \, d\kappa \, d\theta, \quad (18)$$

and a similar form for $\partial\phi/\partial z$ with G instead of F , with

$$F_1 = M\kappa_0 \mu e^{-\kappa f} \sec^2 \theta / D \\ F_2 = -M\kappa_0 (\kappa - \kappa_0 \sec^2 \theta) e^{-\kappa f} \sec \theta / D \\ G_1 = M\mu \kappa_0 \kappa e^{-\kappa f} \sec^2 \theta / D \\ G_2 = -M \{ \kappa (\kappa - \kappa_0 \sec^2 \theta) + \mu^2 \sec^2 \theta \} \kappa e^{-\kappa f} \cos \theta / D \\ D = \tau \{ (\kappa - \kappa_0 \sec^2 \theta)^2 + \mu^2 \sec^2 \theta \} \quad (19)$$

We now apply a theorem in two dimensions corresponding to that given in (10). The Fourier integral theorem is

$$F(x, y) = \frac{1}{4\pi^2} \int_{-\infty}^{\infty} du \int_{-\infty}^{\infty} dv \int_{-\infty}^{\infty} \int_{-\infty}^{\infty} F(s, t) \cos u(x-s) \cos v(y-t) \, ds \, dt$$

Putting $u = \kappa \cos \theta$, $v = \kappa \sin \theta$, this may be written

$$\begin{aligned} F(x, y) = & \int_{-\pi}^{\pi} d\theta \int_0^{\infty} \{F_1 \cos(\kappa x \cos \theta) \cos(\kappa y \sin \theta) \\ & + F_2 \sin(\kappa x \cos \theta) \cos(\kappa y \sin \theta) + F_3 \cos(\kappa x \cos \theta) \sin(\kappa y \sin \theta) \\ & + F_4 \sin(\kappa x \cos \theta) \sin(\kappa y \sin \theta)\} \kappa d\kappa, \end{aligned} \quad (20)$$

where

$$F_1 = \frac{1}{4\pi^2} \int_{-\infty}^{\infty} \int_{-\infty}^{\infty} F(s, t) \cos(\kappa s \cos \theta) \cos(\kappa t \sin \theta) ds dt, \quad (21)$$

with similar expressions for F_2, F_3, F_4

If $G(x, y)$ is another function given as a double integral in the form (20), it follows as in the one-dimensional case that

$$\int_{-\infty}^{\infty} \int_{-\infty}^{\infty} F(x, y) G(x, y) dx dy = 4\pi^2 \int_{-\pi}^{\pi} d\theta \int_0^{\infty} (F_1 G_1 + F_2 G_2 + F_3 G_3 + F_4 G_4) \kappa d\kappa \quad (22)$$

It is assumed that the various integrals are convergent

For the particular case given in (18) and (19), we find that $F_1 G_1 + F_2 G_2$ reduces to a simple expression, and we obtain

$$\begin{aligned} R &= \lim_{\mu \rightarrow 0} \mu \rho \int_{-\infty}^{\infty} \int_{-\infty}^{\infty} \phi \frac{\partial \phi}{\partial z} dx dy \\ &= \lim_{\mu \rightarrow 0} 16\rho\kappa_0 M^2 \mu \int_0^{\pi/2} \int_0^{\pi} \frac{\kappa^3 e^{-2\kappa f} d\kappa}{(\kappa - \kappa_0 \sec^2 \theta)^2 + \mu^2 \sec^2 \theta} \\ &= 16\rho\kappa_0^4 M^2 \int_0^{\pi/2} \sec^5 \theta \phi e^{-2\kappa_0 f \sec^2 \theta} d\theta \\ &= 4\pi\rho\kappa_0^4 M^2 e^{-\kappa_0 f} \left\{ K_0(\kappa_0 f) + \left(1 + \frac{1}{2\kappa_0 f}\right) K_1(\kappa_0 f) \right\}, \end{aligned} \quad (23)$$

where K_n is the Bessel Function defined by

$$K_n(x) = \int_0^{\infty} e^{-x \cosh u} \cosh nu du$$

Horizontal Doublets in Vertical Plane

4 This method allows easily an extension to any distribution of doublets. Consider first two horizontal doublets M and M' at the points $(h, 0, -f)$ and $(h', 0, -f')$ respectively. The surface value of ϕ is now given by (16) with

$x - h$ instead of x , together with a similar expression in M' and $x - h'$. Taking the real part we have

$$\phi = \frac{\kappa_0}{\pi} \int_{-\pi}^{\pi} \sec \theta \, d\theta \int_0^{\infty} \frac{\cos(\kappa y \sin \theta)}{(\kappa - \kappa_0 \sec^2 \theta)^2 + \mu^2 \sec^2 \theta} P \kappa \, d\kappa,$$

$$\begin{aligned} P = & \mu \sec \theta [M e^{-\kappa f} \cos \{\kappa (x - h) \cos \theta\} + M' e^{-\kappa f} \cos \{\kappa (x - h') \cos \theta\}] \\ & - (\kappa - \kappa_0 \sec^2 \theta) [M e^{-\kappa f} \sin \{\kappa (x - h) \cos \theta\} + M' e^{-\kappa f} \sin \{\kappa (x - h') \cos \theta\}] \end{aligned} \quad (24)$$

There is a similar expression for the surface value of $\partial \phi / \partial z$. We now write both these in the form (18), omitting terms which from symmetry give zero when integrated with respect to θ . We find again that we have only to form the quantity $F_1 G_1 + F_2 G_2$ and that this simplifies considerably, the wave resistance, after this reduction, is given by

$$\begin{aligned} R = & \lim_{\mu \rightarrow 0} 16\pi \kappa_0 \mu \int_0^{\pi/2} d\theta \int_0^{\infty} \frac{M^2 e^{-2\kappa f} + M'^2 e^{-2\kappa f} + 2MM' e^{-\kappa(f+f)} \cos \{\kappa (h - h') \cos \theta\}}{(\kappa - \kappa_0 \sec^2 \theta)^2 + \mu^2 \sec^2 \theta} \kappa^2 \, d\kappa \\ = & 16\pi \rho \kappa_0^4 \int_0^{\pi/2} [M^2 e^{-2\kappa_0 f \sec^2 \theta} + M'^2 e^{-2\kappa_0 f \sec^2 \theta} \\ & + 2MM' e^{-\kappa_0(f+f) \sec^2 \theta} \cos \{\kappa_0 (h - h') \sec \theta\}] \sec^5 \theta \, d\theta \end{aligned} \quad (25)$$

The first two terms give the resistance due to the two doublets separately, while the third term represents the interference effects. This expression was obtained formerly from the analogy between the waves produced by a submerged sphere and those due to a certain surface distribution of pressure, it was then generalised for any distribution of horizontal doublets in the vertical plane $y = 0$.* The method given here can also obviously be extended by integration for any such continuous distribution, and confirms the general expression used in previous calculations, if $M(h, f)$ is the moment per unit area at the point $(h, 0, -f)$, then (25) generalises to give

$$\begin{aligned} R = & 16\pi \rho \kappa_0^4 \int_0^{\infty} df \int_0^{\infty} df' \int_{-\infty}^{\infty} dh \int_{-\infty}^{\infty} dh' \int_0^{\pi/2} M(h, f) M(h', f') \times \\ & e^{-\kappa_0(f+f') \sec^2 \theta} \cos \{\kappa_0 (h - h') \sec \theta\} \sec^5 \theta \, d\theta \end{aligned} \quad (26)$$

General Distribution

5 We can use the same method for doublets with their axes in any directions, for we can always obtain the surface values of ϕ and $\partial \phi / \partial z$ in the form (20) and so can integrate over the surface by means of (24). Beginning with a single

* 'Roy Soc Proc,' A, vol 95, p 363 (1919), also A, vol 108, p 78 (1925)

doublet at the point $(0, 0, -f)$, let the direction cosines of its axis be (l, m, n) . By the same process as for the horizontal doublet in (16) and (17), the surface values of ϕ and $\partial\phi/\partial z$ are found to be

$$\begin{aligned}\phi &= \frac{\kappa_0 M}{\pi} \int_{-\pi}^{\pi} d\theta \int_0^{\infty} \frac{(l \cos \theta + m \sin \theta - n) \sec^2 \theta}{\kappa - \kappa_0 \sec^2 \theta + i\mu \sec \theta} Q \kappa d\kappa, \\ \frac{\partial\phi}{\partial z} &= \frac{M}{\pi} \int_{-\pi}^{\pi} d\theta \int_0^{\infty} \frac{\kappa (l \cos \theta + m \sin \theta - n) (\kappa + i\mu \sec \theta)}{\kappa - \kappa_0 \sec^2 \theta + i\mu \sec \theta} Q \kappa d\kappa, \quad (27)\end{aligned}$$

with $Q = e^{-\kappa f + i\kappa (x \cos \theta + y \sin \theta)}$

With the same notation as before,

$$\begin{aligned}F_1 &= \kappa_0 \{ \mu l - n (\kappa - \kappa_0 \sec^2 \theta) \} D \sec^3 \theta, \\ F_2 &= -\kappa_0 \{ \mu n \sec \theta + l (\kappa - \kappa_0 \sec^2 \theta) \cos \theta \} D \sec^3 \theta, \\ F_3 &= -\kappa_0 m (\kappa - \kappa_0 \sec^2 \theta) D \sin \theta \sec^3 \theta, \\ F_4 &= -\kappa_0 \mu m D \sin \theta \sec^3 \theta, \\ G_1 &= \kappa [\mu \kappa_0 l \sec^3 \theta - n \{ \kappa (\kappa - \kappa_0 \sec^2 \theta) + \mu^2 \sec^3 \theta \}] D, \\ G_2 &= -\kappa [l \{ \kappa (\kappa - \kappa_0 \sec^2 \theta) + \mu^2 \sec^3 \theta \} \cos \theta + \mu n \kappa_0 \sec^3 \theta] D, \\ G_3 &= -\kappa m \{ \kappa (\kappa - \kappa_0 \sec^2 \theta) + \mu^2 \sec^3 \theta \} D \sin \theta, \\ G_4 &= -\mu m \kappa_0 D \sin \theta \sec^3 \theta, \\ D &= (M/\pi) e^{-\kappa f} / \{ (\kappa - \kappa_0 \sec^2 \theta)^2 + \mu^2 \sec^2 \theta \} \quad (28)\end{aligned}$$

We find that ΣFG simplifies very much even if we take the expressions as they stand, since we are only concerned ultimately with μ zero, we could further simplify the work by omitting superfluous terms. The expression for R reduces to the limit of an integral of the same type as in (23), and the result is

$$\begin{aligned}R &= 16\pi\rho\kappa_0^4 M^2 \int_0^{\pi/2} (l^2 \cos^2 \theta + m^2 \sin^2 \theta + n^2) e^{-2\kappa_0 f \sec^2 \theta} \sec^7 \theta d\theta \\ &= 4\pi\rho\kappa_0^4 M^2 e^{-\alpha} \left[l^2 \left\{ K_0(\alpha) + \left(1 + \frac{1}{2\alpha}\right) K_1(\alpha) \right\} \right. \\ &\quad \left. + \frac{m^2}{4\alpha} \left\{ K_0(\alpha) + \left(1 + \frac{2}{\alpha}\right) K_1(\alpha) \right\} \right. \\ &\quad \left. + n^2 \left\{ \left(1 + \frac{1}{4\alpha}\right) K_0(\alpha) + \left(1 + \frac{3}{4\alpha} + \frac{1}{2\alpha^2}\right) K_1(\alpha) \right\} \right], \quad (29)\end{aligned}$$

where $\alpha = \kappa_0 f = qf/c^2$

6 The only further stage to which we need carry the calculation is for two doublets in any positions M at the point $(h, k, -f)$ with its axis in the direction

(l, m, n), and M' at ($h', k', -f'$) in the direction (l', m', n') We have simply to put the surface values of ϕ and $\partial\phi/\partial z$ in the standard form, and evaluate the quantity ΣFG The reduction need not be reproduced here, omitting terms in μ which make no contribution in the limit, we obtain

$$\begin{aligned} & \pi^2 \Sigma FG \{(\kappa - \kappa_0 \sec^2 \theta)^2 + \mu^2 \sec^2 \theta\} / \kappa_0 \kappa^2 \sec^3 \theta \\ &= [(l \cos \theta \sin P \cos Q + m \sin \theta \cos P \sin Q - n \cos P \cos Q) M e^{-\kappa f} \\ &+ (l' \cos \theta \sin P' \cos Q' + m' \sin \theta \cos P' \sin Q' - n \cos P' \cos Q') M' e^{-\kappa' f}]^2 \\ &+ [(l \cos \theta \cos P \cos Q - m \sin \theta \sin P \sin Q + n \sin P \cos Q) M e^{-\kappa f} \\ &+ (l' \cos \theta \cos P' \cos Q' - m' \sin \theta \sin P' \sin Q' + n' \sin P' \cos Q') M' e^{-\kappa' f}]^2 \\ &+ [(l \cos \theta \sin P \sin Q - m \sin \theta \sin \theta \cos P \cos Q - n \cos P \sin Q) M e^{-\kappa f} \\ &+ (l' \cos \theta \sin P' \sin Q' - m' \sin \theta \cos P' \cos Q' - n' \cos P' \sin Q') M' e^{-\kappa' f}]^2 \\ &+ [(l \cos \theta \cos P \sin Q + m \sin \theta \sin P \cos Q + n \sin P \sin Q) M e^{-\kappa f} \\ &+ (l' \cos \theta \cos P' \sin Q' + m' \sin \theta \sin P' \cos Q' + n' \sin P' \sin Q') M' e^{-\kappa' f}]^2, \end{aligned} \quad (30)$$

where $P = \kappa h \cos \theta$, $Q = \kappa l \sin \theta$, and similarly P' and Q' Carrying out the rest of the calculation for R , the wave resistance is given by

$$\begin{aligned} R &= 16\pi\rho\kappa_0^4 \int_0^{\pi/2} \left[(l^2 \cos^2 \theta + m^2 \sin^2 \theta + n^2) M^2 e^{-2\kappa_0 f \sec^2 \theta} \right. \\ &+ (l'^2 \cos^2 \theta + m'^2 \sin^2 \theta + n'^2) M'^2 e^{-2\kappa_0' f \sec^2 \theta} \\ &+ 2 \{ (ll' \cos^2 \theta + mm' \sin^2 \theta + nn') \cos A \cos B \\ &- (lm' + l'm) \sin \theta \cos \theta \sin A \sin B + (nm' - n'm) \sin \theta \cos A \sin B \\ &\left. + (nl' - n'l) \cos \theta \sin A \cos B \} MM' e^{-\kappa_0 (\kappa + \kappa') f \sec^2 \theta} \right] \sec^7 \theta d\theta, \end{aligned} \quad (31)$$

where $A = \kappa_0 (h - h') \sec \theta$, $B = \kappa_0 (k - k') \sin \theta \sec^2 \theta$ The various terms represent the contributions of the three components of each doublet and their mutual interference in pairs

Water of Finite Depth

7 For water of finite depth h , we shall consider only the simplest case of a horizontal doublet of moment M at depth f It is clear that the same surface integral can be used for evaluating the wave resistance

We now assume the velocity potential in the form

$$\begin{aligned} \phi &= -\frac{iM}{2\pi} \int_{-\pi}^{\pi} \cos \theta d\theta \int_0^{\infty} \{e^{-\kappa f} + e^{-\kappa(2h-f)}\} e^{-\kappa z + i\kappa(x \cos \theta + y \sin \theta)} \kappa d\kappa \\ &+ \frac{iM}{2\pi} \int_{-\pi}^{\pi} \cos \theta d\theta \int_0^{\infty} F(\theta, \kappa) \cosh \kappa(z+h) e^{i\kappa(x \cos \theta + y \sin \theta)} \kappa d\kappa \end{aligned} \quad (32)$$

This satisfies the condition $\partial\phi/\partial z = 0$ at $z = -h$, we note that the first term represents the original doublet and its image in the bed in an analytical form valid for $z + f > 0$, and therefore suitable for applying the boundary condition (2) at the free surface. This yields

$$F(\theta, \kappa) = \frac{2e^{-\kappa h} \cosh \kappa(h-f)}{\cosh \kappa h} \frac{\kappa + \kappa_0 \sec^2 \theta + i\mu \sec \theta}{\kappa - \kappa_0 \sec^2 \theta \tanh \kappa h + i\mu \sec \theta}, \quad (33)$$

consequently the required surface values are given by the real parts of

$$\phi = \frac{2i\kappa_0 M}{\pi} \int_{-\pi}^{\pi} \sec \theta d\theta \int_0^{\infty} \frac{e^{-\kappa h} \cosh \{\kappa(h-f)\} \tanh \kappa h}{\kappa - \kappa_0 \sec^2 \theta \tanh \kappa h + i\mu \sec \theta} e^{i\kappa x} \kappa d\kappa, \\ \frac{\partial\phi}{\partial z} = \frac{iM}{\pi} \int_{-\pi}^{\pi} \cos \theta d\theta \int_0^{\infty} \frac{e^{-\kappa h} \cosh \{\kappa(h-f)\} (1 + \tanh \kappa h) (\kappa + i\mu \sec \theta)}{\kappa - \kappa_0 \sec^2 \theta \tanh \kappa h + i\mu \sec \theta} e^{i\kappa x} \kappa^2 d\kappa, \quad (34)$$

where $x = x \cos \theta + y \sin \theta$

Comparing these with the corresponding values for deep water given in (16) and (17), we can write down the expression for the wave resistance as

$$R = \lim_{\mu \rightarrow 0} 32\rho\kappa_0 M^2 \mu \int_0^{\pi/2} d\theta \int_0^{\infty} \frac{\kappa^3 e^{-2\kappa h} \cosh^2 \{\kappa(h-f)\} \tanh \kappa h (1 + \tanh \kappa h)}{(\kappa - \kappa_0 \sec^2 \theta \tanh \kappa h)^2 + \mu^2 \sec^2 \theta} d\kappa \quad (35)$$

There are two points to notice in evaluating this limit. The result is only different from zero when

$$\kappa - \kappa_0 \sec^2 \theta \tanh \kappa h = 0 \quad (36)$$

has a real positive root, and this occurs only for $\kappa_0 h \sec^2 \theta > 1$. Further we must introduce in the denominator $d(\kappa - \kappa_0 \sec^2 \theta \tanh \kappa h)/d\kappa$. We may sum up the result in this form

$$R = 32\pi\rho\kappa_0 M^2 \int_{\theta_0}^{\pi/2} \frac{\kappa^3 e^{-2\kappa h} \cosh^2 \{\kappa(h-f)\} \tanh \kappa h (1 + \tanh \kappa h)}{1 - \kappa_0 h \sec^2 \theta \tanh^2 \kappa h} \cos \theta d\theta, \quad (37)$$

where κ is the positive root of (36), further, the lower limit θ_0 is given by

$$\theta_0 = 0, \quad \text{for } \kappa_0 h > 1, \quad \text{or } c^2 < gh, \\ \theta_0 = \arccos \sqrt{(\kappa_0 h)}, \quad \text{for } c^2 > gh$$

We may note that the change in the lower limit occurs at the so-called critical velocity \sqrt{gh} for the given depth. From (37), R may be graphed as a function of the velocity for various ratios of f to h , the calculations may be carried out by numerical and graphical methods. A similar expression in the case of a certain distribution of surface pressure was examined in detail in a previous paper,* and it may be anticipated that (37) would give somewhat similar curves

* 'Roy Soc. Proc., A, vol. 100, p. 503 (1922)

The Arc Spectrum of Carbon.

By A FOWLER, D Sc, F R S, Yarrow Research Professor of the Royal Society,
and E W H SFLWYN, B Sc, Imperial College, South Kensington

(Received January 4, 1928)

Introductory

It is well known that in the region of observation extending from the red to λ 2000 the spectrum of an ordinary carbon arc shows only a single line, λ 2478. Merton and Johnson, however, have observed a considerable number of lines which they have attributed to the neutral atom of carbon in the spectrum of a vacuum tube containing a trace of an oxide of carbon in helium at 20 to 30 mm pressure*. Another method of developing the lines of C I, in this case almost perfectly free from lines of C II, has recently been described by J W Ryde†. In these experiments, a carbon arc was fed with currents up to 250 amperes, the potential drop across the arc being 60 to 80 volts. Many of the lines assigned to C I by Merton and Johnson then appeared with great intensity, together with lines of N I, O I, and A I from the atmospheric gases, the lines in question being localised in a region near the negative pole of the arc.

With additional observations made during the present investigation, the spectrum of neutral carbon is now sufficiently well known to justify an attempt to extend the analysis of the spectrum, which has already been partially elucidated by Bowen‡ from lines observed in the extreme ultra-violet.

Experimental

Photographs of the spectrum of an oxide of carbon in helium, as in Merton and Johnson's experiments, have been taken with the vacuum grating spectrograph, covering the region λ 1250 to λ 2760 in the first order and λ 1250 to λ 1380 in the second order. Some of the lines have also been photographed in higher orders with other sources. The effect of admixture with helium is to emphasise the known lines of C I with respect to those of C II which appear in company with them, and to introduce additional lines, of which many are probably due to C I. The lines which remain after eliminating bands of

* 'Roy Soc Proc,' A, vol 103, p 384 (1923), vol 108, p 343 (1925)

† 'Roy Soc Proc,' A, vol 117, p 164 (1927)

‡ 'Phys Rev' vol 29, p 238 (1927)

carbon* and lines of oxygen, mercury, nitrogen, and ionised carbon, and omitting those which appear in the list of classified lines (Table VI), are shown in Table I

Table I—Unclassified Lines in Helium-Carbon

Merton and Johnson	λ ν		λ ν		λ ν	
	λ	ν	λ	ν	λ	ν
	2865 24 (0n)	37509	2385 85 (1)	41901	1961 27 (1)	73461
	2864 48 (0n)	37520	2268 50 (2)	44068	1359 42 (1)	73561
	2863 04 (1)	37540	2042 24 (2)	48950	1357 21 (1)	73681
2861 7 (0)	2861 90 (1)	37556	2005 0 (0)	49859	1331 83 (1)	75085
2860 3 (1)	2860 33 (1)	37578	λ vac		1321 77 (1)	75656
	2658 50 (0)	37904	1993 65 (2)	50159	1313 50 (1)	76132
	2639 42 (0)	37876	1765 4 (0)	56644	1311 36 (2)	76257
	2602 90 (0)	38407	1764 0 (0)	56689	1283 11 (1)	77936
	2592 30 (0n)	38564	1481 75 (5)	67487	1280 75 (2)	78079
2382 9 (2)	2582 85 (1)	38705	1472 3 (0)	67920	1280 33 (3)	78105
2567 7 (0)	2567 78 (0)	38932	1470 20 (1)	68018	1279 85 (1)	78134
2515 15 (1)		39747	1468 5 (0)	68097	1279 17 (2)	78176
2499 6 (0)		40978	1467 48 (3)	68144		
2413 9 (0)		41414	1364 20 (2)	73303		

Several of the brighter lines of C I in Merton and Johnson's list were noted as rather feeble lines in the spectra of ordinary carbon dioxide vacuum tubes photographed some years ago. It has since been found that these lines can be obtained quite prominently, and comparable in intensity with many of the lines of C II, by merely raising the pressure of the gas to about 20 mm. All but the very faint lines of Merton and Johnson's list in the region λ 4740– λ 6600 have been observed by this method. The C I spectrum under these conditions would seem to resemble that obtained by Ryde's high-current arc more closely than that given by the helium-carbon vacuum tube, as, for example, in the absence of the lines $\lambda\lambda$ 4758 78 and 4757 59.

Results similar to those of Ryde, but excluding some of the fainter lines, have been obtained with currents much smaller than those employed by him. Thus, it was found that while the lines in question could not be seen at all with the ordinary currents of 5 to 10 amperes on a 110-volt circuit, they appeared with considerable intensity in the neighbourhood of the negative pole when the current was increased to 15 or 20 amperes. The lines so obtained are in excellent agreement with those tabulated by Ryde. By the use of the valuable neocyanine plates of the Eastman-Kodak Company, this method has been utilised.

* Some of these carbon bands could only be distinguished from lines by comparison with other plates in which the band spectrum was more strongly developed (*cf* Jevons, 'Phil Mag,' vol 47, p 586 (1924)).

to extend the observations as far as λ 10120 in the near infra-red, and the lines which have been observed, other than those listed by Ryde, are shown in Table II. As the dispersion employed was about 100 Å per millimetre, no great accuracy can be claimed for the tabulated wave-lengths.

Table II—Infra-Red Lines of Carbon Arc

λ	ν	Remarks
10119 (0)	9880	Possibly C I See Table V
9661 (0)	10348	} $\Delta\nu$ suggests C I See Table IV
9623 (0)	10389	
9407 (2)	10627	Probably C I See Table V
9394 (0)	10642	
9264 7 (0)	10790 7	O I (Paschen)
9190 6	10877 7	
9170 2	10901 9	} $\Delta\nu$ suggests N I
9142 1	10935 4	
9111 4	10972 2	
9094 5	10992 7	} C I multiplet See Table IV
9088 5	10999 9	
9078 1	11012 5	
9061 8	11032 3	
*8336 4	11992 3	Carbon line

* Occurs in Ryde's list of lines of unknown origin. Other lines of nitrogen and oxygen fall between λ 9061 and λ 8336.

The conspicuous multiplet beginning with λ 9111 and the singlet λ 8336 have been proved to be due to carbon by their observation in the spectrum of carbon dioxide and their absence from the spectrum of oxygen. The origins of other lines are somewhat uncertain, as the vacuum-tube observations were not successful beyond λ 9111. It is possible, however, that the pair of lines $\lambda\lambda$ 9661, 9623 and the lines $\lambda\lambda$ 10119, 9407 are due to C I, as they yield values of the order expected for terms of this spectrum.

The poles used in the experiments on the arc spectrum were rods of Acheson graphite, and were practically free from impurities. It was found convenient to use thin or sharply pointed carbon poles in order to localise the stream in which the C I lines appeared.

In connection with the foregoing observations, it is important to note that the spectrum of the ordinary carbon arc, with small current, in so far as it is represented by an arc in an atmosphere of nitrogen, has been found to show the principal lines of C I in the region more refrangible than λ 2000, including the strong line at λ 1931. These lines also occur, together with lines of C II, in the spectra of the carbon vacuum arc, vacuum tubes containing carbon compounds, and the "hot spark" of carbon investigated by Millikan and Bowen.

It thus appears that all the ordinary sources yield lines of C I which arise from combinations of the deeper terms of the spectrum, and that special methods only become necessary for the excitation of lines due to combinations of terms representing higher energy levels. The observations of the arc recall those of A. S. King,* who similarly found that in metallic arcs with currents of about 1000 amperes there was an increased development of lines of the neutral atom due to higher terms, while lines due to ionised atoms were not notably modified.

Predicted Terms

The terms of C I predicted by the Heisenberg-Hund theory are similar to those for N II† and O III‡ and are shown in Table III. The notation is on the system adopted for O III, terms in each row being prefixed by the n_1 designation of the corresponding orbit of the series electron. Under ordinary circumstances, combinations between terms on different rows are regulated by the familiar rules, applicable in this notation to the *electron* symbols, and by the rule for inner quantum numbers as applied to the *term* symbols. Dashes are applicable to the electron symbols alone, and only become necessary when there is more than one family of terms. In the case of C I the need for distinguishing terms of similar type on the same row does not arise. Other singlet, triplet and quintet terms appear when one of the three $2s$ electrons represented in the last row of the table is removed to successively higher orbits.

Table III—Predicted Terms of C I

K	L	M	N	Electrons in unclosed groups	Terms	
1_1	$2_1, 2_2$	$3_1, 3_2, 3_3$	$4_1, 4_2, 4_3$			
2	2 2	1 1 1		$s^2 p^2$	2p	$^1P, ^1D, ^1S,$
2	2 1			$s^2 p \ s$	3s	$^1P, ^1P_1$
2	2 1			$s^2 p \ p$	3p	$^1D, ^1P, ^1S, ^1D_2, ^1P_1, ^1S_0,$
2	2 1			$s^2 p \ d$	3d	$^1F, ^1D, ^1P, ^1F_3, ^1D_2, ^1P_1$
2	2 1		1	$s^2 p \ s$	4s	$^1P, ^1P$
2	2 1		1	$s^2 p \ p$	4p	$^1D, ^1P, ^1S, ^1D_2, ^1P_1, ^1S_0,$
2	2 1		1	$s^2 p \ d$	4d	$^1F, ^1D, ^1P$
2	1 3			$s p^3$	2p'	$^3S, ^3D, ^3P, ^3S, ^1D_2, ^1P_1$

* 'Astrophys. J.', vol 62 p 238 (1925)

† A. Fowler and L. J. Freeman, 'Roy. Soc. Proc.,' A, vol 114, p 672 (1927)

‡ A. Fowler, 'Roy. Soc. Proc.,' A, vol 117, p 317 (1928)

Combinations involving some of the deeper terms have already been identified by Bowen, namely, $2p^3P - 2p'^3P$, $2p^3P - 2p'^3D$, $2p^3P - 3s^3P$. In addition, he has suggested that a partially resolved line at $\lambda 1277$ represents $2p^3P - 3d^3D$, and, by assuming that $3d^3D$ has one-quarter of its value for N II, finds a probable value of 91300 for $2p^3P$. Bowen has found confirmation of the two pp' combinations in the fact that they follow the irregular doublet law when compared with corresponding combinations of N II, O III and F IV. Comparison with O III and N II (Table VII) also shows that the magnitudes of the p' terms are inappropriate for the main family of terms.

Triplet Combinations

The four triplet combinations identified by Bowen, with one addition, are shown in the first part of Table IV. The $2p^3P - 3d^3D$ multiplet has been resolved into two components, and the table indicates a provisional attempt to show the structure of this group, the separation $^3D_1 - ^3D_2$ being merely estimated. A similar attempt has been made to represent the structure of the other multiplets.

The second part of Table IV shows the probable combinations with the second deepest triplet term, $3s^3P$. These include all the $3p$ and $4p$ triplet terms except $3p^3D$, which probably gives a group of lines in the infra-red just beyond the limit of the present photographs. Two lines observed in this region at $\lambda 9661$ and $\lambda 9623$, approximately, have been taken to represent the first two lines of the triplet $3s^3P - 3p^3S$, they have only been photographed in the high-current arc in air, and there is no independent evidence of their carbon origin. The resulting value of $3p^3S$, however, is of the magnitude expected.

It is of interest to note that the $3d^3P$ term is inverted, exactly as the corresponding terms of O III and N II. It may also be remarked that Merton and Johnson's lines, $\lambda\lambda 4758$ and 4757 , which were not found by Ryde, do not form part of the multiplet $3s^3P - 4p^3P$.

Three p^3P terms are available for the calculation of triplet term values. The computed formula for these is

$$p^3P_0 = R/[m + 0.719265 - 0.616474/m]^2 \quad R = 109737, \quad m = 1, 2, 3,$$

giving $2p^3P_0 = 90230$, $3p^3P_0 = 18878$, $4p^3P_0 = 8888$. The correcting term, however, is so large that the formula cannot be relied upon to give closely approximate values. The formula for the sequence of three singlet p^3D terms, on the other hand, involves a very small correcting term, and the calculated values are much more likely to be near the true values. A similar result was

Table IV—Triplet Combinations

	$2p\ ^3P_1$ 90975 0	27 5	$2p\ ^3P_1$ 91002 5	14 8	$2p\ ^3P_0$ 91017 3
$3s\ ^3P_0 = 30686\ 0$ 20 0			60316 5 (2) 20 1		
$3s\ ^3P_1 = 30686\ 0$ 40 1	60308 9 (2) 40 8	27 7	60336 6 (2) 40 0	13 1	*60349 7 (3)
$3s\ ^3P_2 = 30625\ 9$	*60349 7 (3)	26 9	60376 6 (2)		
$2p'\ ^3D_2 = 26929\ 1$ -2 1	64045 9 (5)				
$2p'\ ^3D_1 = 26927\ 0$ -1 3	[64048 0]		64075 5 (4)		
$2p'\ ^3D_1 = 26925\ 7$	[64049 3]		[64076 8]		64091 6 (3)
$2p'\ ^3P_{110} = 15763\ 5$	75211 6 (4)	27 3	75238 9 (4)	14 8	75253 7 (3)
$3d\ ^3D_1 = [12714\ 5]$ [5 0]	[78260]		[78286]		[78303]
$3d\ ^3D_2 = 12709\ 5$ 9 5	[78265]		78293 (1)		
$3d\ ^3D_2 = 12700\ 0$	78275 (2)				
$3d\ ^3P_2 = 11709$ -10	79260 (2)		[79293]		
$3d\ ^3P_1 = 11699$ [-5]	[79276]		79303 (1)	15	79318 (0)
$3d\ ^3P_0 = [11694]$			[79308]		
	$3s\ ^3P_2$ 30625 9	40 0	$3s\ ^3P_1$ 30666 0	20 0	$3s\ ^3P_0$ 30686 0
$3p\ ^3D$	Out of range				
$3p\ ^3S_1 = 20278\ ?$	10348	41	10389		
$3p\ ^3P_0 = 19686\ 1$ 12 5			10999 9 (1) 12 6		
$3p\ ^3P_1 = 19653\ 6$ 20 4	10972 2 (1) 20 5	40 3	11012 5 (1) 19 8	19 8	*11032 3 (4)
$3p\ ^3P_2 = 19633\ 2$	10992 7 (4)	40 1	*11032 3 (4)		
$4p\ ^3D_1 = 10833\ 5$ 7 0	[19792 5]		[19832 5]		19832 5 (0)
$4p\ ^3D_2 = 10826\ 5$ 29 8	[19799 5]		19839 5 (3)		
$4p\ ^3D_1 = 10796\ 7$	19829 2 (3)				
$4p\ ^3S_1 = 9913\ 7$	20712 2 (1)	40 4	20752 6 (1)	19 4	†20772 0 (1)
$4p\ ^3P_0 = 9707\ 5$ 14 5			20958 5 (2) 14 8		
$4p\ ^3P_1 = 9683\ 0$ 18 0	20932 7 (3) 18 2	40 6	20973 3 (2) 18 6	18 6	*20991 9 (4)
$4p\ ^3P_2 = 9675\ 0$	20950 9 (4)	41 0	*20991 9 (4)		

* Used twice

† Occurs in Ryde's list of unknown lines

found for the corresponding terms of O III, and the calculated singlet terms have accordingly been adopted. Since no intercombinations of singlets and triplets have yet been recognised, the triplet terms have been adjusted so as to give triplet and singlet terms in the same order as in O III and N II. From the comparative list of term values in Table VII, it will be seen that the $3d$ terms of each type show only small variations in the three spectra, and the value 12700 assigned to $3d^3D_3$ (or 12714.5 to $3d^3D_1$) cannot be greatly in error. It is to be understood, however, that the triplet and singlet terms have not yet been brought into exact relation with each other.

Numbers enclosed in square brackets represent calculated wave-numbers of lines forming parts of multiplets, or term values which have merely been estimated.

Singlets

The classification of singlets in C I presents considerable difficulties, because there are no extended series and many of the expected lines must occur either in the near infra-red or in the Schumann region. Some of the lines, however, can be classified with considerable certainty from a general consideration of the predicted terms in relation to the already known terms of N II and O III. Thus, there can be no doubt that the strong lines $\lambda 2478$ and $\lambda 1931^*$ represent $2p^1S_0 - 3s^1P_1$ and $2p^1D_2 - 3s^1P_1$ respectively, since these combinations should give the strongest of all the singlets. The three brightest lines in the visible spectrum, $\lambda\lambda 5380, 5052, 4932$, can also be classified with almost equal certainty. Again, the interval between the lines $\lambda 1751$ and $\lambda 1459$ appears to be the same as that between $2p^1D_2$ and $2p^1S_0$ and would seem to justify the identification of the common combining term as $3d^1P_1$.

The terms $2p^1D_2$ and $4p^1D_2$ having been determined from some of these lines, an approximate value for $3p^1D_2$ could be derived by interpolation. This suggested the line $\lambda 9407$ ($\nu = 10627$) as $3p^1D_2 - 3d^1P_1$, and assuming this to be correct, a sequence of three p^1D_2 terms became available for a more precise determination of singlet term values, to replace those which had been provisionally adopted. The calculated formula is

$$p^1D_2 = R/[m + 0.168835 - 0.007117/m]^2 \quad R = 109737, \quad m = 1, 2, 3$$

This gives $2p^1D_2 = 81311.5$, and other singlet terms have been determined,

* Millikan and Bowen have assigned $\lambda 1931$ to C III ('Phys. Rev.', vol 26, p 316 (1925)), but this is altogether in contradiction with the experimental evidence, since this line occurs in the ordinary arc in air, where neither C II nor C III lines are present. There is another line, however, at $\lambda 1923$ which appears under strong discharges, and is doubtless the C III line anticipated by Millikan and Bowen.

with this as a basis, from the combinations shown in Table V. The more doubtful term identifications are distinguished by a ? mark.

Table V—Singlets of C I

	$2p^1D_2$ 81312	11452	$2p^1S_0$ 69860	$3s^1P_1$ 20526	$3p^1D_2$ 23406 ?	$3p^1S_0$?	$3p^1P_1$ 19646 ?
$3s^1P_1 = 29526$	51786 (10)	11452	40334 (10)		° °	° °	° 9840 °
$3d^1F_3 = 12979?$	68333 (5)		—				
$3d^1P_1 = 12779$	68533 (3)	11452	57081 (5)		† 10627 (3)	° °	° °
$3d^1D_2 = 11414?$			—		‡ 11992 (3)	—	
$4s^1P_1$							
$4p^1D_2 = 10045$				18581 (8)			
$4p^1S_0 = 9738$				19788 (6)			
$4p^1P_1 = 9256$	—		—	20270 (5)	—	—	—
$4d^1F_5$							
$4d^1P_1 = 7475?$	73837 (1)		62379 (3)				
$4d^1D_2$			—				

† Used for calculation of $3p^1D_2$

‡ Used for calculation of $3p^1P_1$

§ Used for calculation of $3d^1D_2$

° ° Out of range

— Not expected

As will appear from the blank spaces where lines might be expected, further progress in the identification of terms must depend largely upon the possibility of extending the observations farther into the infra-red, and of obtaining more complete development of the C I lines in the Schumann region.

List of Classified Lines

The lines which have been classified, in some cases merely tentatively, are included in Table VI. In view of the disturbances of wave-lengths in the high-current arc, Merton and Johnson's vacuum-tube wave-lengths have been adopted in preference to those of Ryde for the region λ 5380 to λ 2478. The wave-lengths for which no authorities are quoted in the footnotes have been determined in the course of the present investigation.

Table VI—Classified Lines of C I

λ air	ν	Classification	λ vac	ν	Classification
10119	9880	$3s^1P_1-3p^1P_1$?			
9661	10348	$3s^1P_1-3p^1S_1$?	†1931 027 (10)	51785 9	$2p^1D_2-3s^1P_1$
9623	10389	$3s^1P_1-3p^1S_1$ *	1751 80 (5)	57080 9	$2p^1S_2-3d^1P_1$
9407	10627	$3p^1D_2-3d^1P_1$			
9111 4 (2)	10972 2	$3s^1P_1-3p^1P_1$	‡1658 13 (2)	60308 9	$2p^1P_1-3s^1P_1$
9094 5 (5)	10992 7	$3s^1P_1-3p^1P_1$	‡1657 92 (2)	60316 5	$3p^1P_1-3s^1P_1$
9088 5 (1)	10999 9	$3s^1P_1-3p^1P_1$	‡1657 37 (2)	60336 6	$2p^1P_1-3s^1P_1$
9078 1 (1)	11012 5	$3s^1P_1-3p^1P_1$	‡1657 01 (3)	60349 7	$2p^1P_1-3s^1P_1$
9061 8 (4)	11032 3	$3s^1P_1-3p^1P_1$ $3s^1P_1-3p^1P_1$	‡1656 27 (2)	60376 6	$2p^1P_1-3s^1P_1$
8336 4 (5)	11992 3	$1p^1D_2-3d^1D_2$ *			
*5380 242 (8)	18581 37	$3s^1P_1-4p^1D_2$	1803 10 (3)	62379 1	$2p^1S_2-4d^1P_1$?
*5052 123 (6)	19788 16	$3s^1P_1-4p^1S_2$	‡1561 381 (5)	64045 9	$2p^1P_1-2p^1D_2$
*5041 06 (3)	19829 2	$3s^1P_1-4p^1D_2$	‡1560 660 (4)	64075 5	$2p^1P_1-2p^1D_2$
*5039 05 (3)	19839 5	$3s^1P_1-4p^1D_2$	‡1560 267 (3)	64091 6	$2p^1P_1-2p^1D_2$
*5035 75 (0)	19852 5	$3s^1P_1-4p^1D_2$			
*4932 00 (5)	20270 1	$3s^1P_1-1p^1P_1$	1463 43 (5)	68332 6	$2p^1D_2-3d^1P_1$?
*4826 73 (1)	20712 2	$3s^1P_1-4p^1P_1$	1459 15 (3)	68533 0	$2p^1D_2-3d^1P_1$
*4817 33 (1)	20752 6	$3s^1P_1-4p^1P_1$	1354 34 (1)	73836 7	$2p^1D_2-4d^1P_1$?
†4812 84 (1)	20772 0	$3s^1P_1-4p^1P_1$	‡1329 583 (4)	75211 6	$2p^1P_1-2p^1P_1$
*4775 87 (3)	20932 7	$3s^1P_1-4p^1P_1$	‡1329 100 (4)	75238 9	$2p^1P_1-2p^1P_1$
*4771 72 (4)	20950 9	$3s^1P_1-4p^1P_1$	‡1328 839 (3)	75253 7	$2p^1P_1-2p^1P_1$
*4770 00 (2)	20958 5	$3s^1P_1-4p^1P_1$	1277 54 (3)	78275	$2p^1P_1-3d^1D_2$
*4766 62 (2)	20973 3	$3s^1P_1-4p^1P_1$	1277 26 (2)	78293	$2p^1P_1-3d^1D_2$
*4762 41 (4)	20991 9	$3s^1P_1-4p^1P_1$ $3s^1P_1-4p^1P_1$	1261 57 (2)	79266	$2p^1P_1-3d^1P_1$
*2478 525 (10)	40334 39	$2p^1S_2-3s^1P_1$	1260 99 (1)	79303	$2p^1P_1-3d^1P_1$
			1260 75 (0)	79318	$2p^1P_1-3d^1P_1$

* λ Merton and Johnson† λ Ryde, not in Merton and Johnson's list‡ λ Bowen and Ingram ('Phys. Rev.', vol. 28, p. 445 (1926))§ λ Bowen ('Phys. Rev.', vol. 29, p. 238 (1927))*Comparison with N II and O III*

A close similarity between the spectra of C I, N II and O III is to be expected from the general theory, since the three atoms are similarly constituted. Each has six external electrons, but the nuclear charge is 6 for C I, 7 for N II and 8 for O III. A general comparison of the terms of the three spectra is given in Table VII, those of O III having been divided by 9 and those of N II by 4. The triplet separations of O III and N II have been similarly reduced for easier comparison with those of C I.

Table VII —Terms of O III, N II and C I

	O III/9	$\Delta\nu/9$	N II/4	$\Delta\nu/4$	C I	Δ_i
$2p\ ^3P_0$	49406 8		59712 25		91017 3	
$\quad\quad\quad\ ^3P_1$	49393 9	12 7	59690 7	12 55	91002 5	14 8
$\quad\quad\quad\ ^3P_2$	49372 1	21 8	59678 7	21 0	90975 0	27 5
$2p\ ^1D_2$	47153 9		55882 7		81312	
$2p\ ^1S_0$	44008 0		*[36779 7]		69860	
$3s\ ^3P_0$	19704 0		22484 3		30686 0	
$\quad\quad\quad\ ^3P_1$	19690 9	13 1	22476 4	7 9	30666 0	20 0
$\quad\quad\quad\ ^3P_2$	19662 3	28 6	22442 3	34 1	30625 9	40 1
$3s\ ^1P_1$	19057 0		22414 5		29526	
$3p\ ^1D_2$	17070 8		18558 8		23406	
$3p\ ^3D_1$	16747 6		18081 0		} Out of range	
$\quad\quad\quad\ ^3D_2$	16732 4	15 2	18065 6	15 4		
$\quad\quad\quad\ ^3D_3$	16708 0	24 4	18041 8	23 8		
$3p\ ^3S_1$	16337 3		17489		20746 †	
$3p\ ^1S_0$	16253 1		*[15143 1]			
$3p\ ^3P_0$	16040 6		17068 3		19666 1	
$\quad\quad\quad\ ^3P_1$	16031 5	9 1	17059 5	8 8	19653 6	12 5
$\quad\quad\quad\ ^3P_2$	16017 0	14 5	17044 9	14 0	19633 2	20 4
$3p\ ^1P_1$	13421 4 †		16158 4			
$3d\ ^1F_3$	13348 0		13042 0		12979 †	
$3d\ ^3F_2$	13347 9		13083 6			
$\quad\quad\quad\ ^3F_3$	13326 1	21 8	13068 7	14 9		
$\quad\quad\quad\ ^3F_4$	13306 3	19 8	13048 3	20 4		
$3d\ ^1P_1$	13317 7		12938 6		12779	
$3d\ ^3D_1$	13040 0		12852 1		†[12715]	
$\quad\quad\quad\ ^3D_2$	13035 1	5 5	12846 1	6 0	12710	[5 0]
$\quad\quad\quad\ ^3D_3$	13027 0	8 1	12838 5	7 6	12700	10 0

* Identifications somewhat doubtful

† Estimated by probable $\Delta\nu$

Table VII—(continued)

	O III/9	$\Delta\nu/9$	N II/4	$\Delta\nu/4$	Cl	$\Delta\nu$
3d ³ P ₁	12791 7		12497 2		11709	
³ P ₁	12779 1	-12 6	12484 2	-13 0	11699	-10 0
³ P ₀	12772 2	-6 9	12477 2	-7 0	*[11694]	[-5 0]
3d ¹ D ₂	12424 0		12181 4		11414 †	
4s ³ P ₂	†		10576 4			
³ P ₁			10563 5	12 9		
³ P ₀			10533 6	29 9		
4s ¹ P ₁	10190 2 †		10246 9			
4p ¹ D ₂	8763 3		9201 †		10945	
4p ³ D ₁	8678 5		9032 9		10833 5	
³ D ₂	8666 6	11 0	9020 2	12 7	10826 5	7 0
³ D ₃	8643 6	23 0	8996 2	24 0	10796 7	29 8
4p ³ S ₁	8515 7		8828 5		9913 7	
4p ¹ S ₀	8332 5 †				9738	
4p ³ P ₀	8251 9		8258 9		9707 5	
³ P ₁	8242 0	9 0	8251 2	7 7	9693 0	14 5
³ P ₂	8229 9	12 1	8239 2	12 0	9675 0	18 0
4p ¹ P ₁	8109 †				9256	
2p' ³ D ₂	36070		36652		26731	
2p' ³ P _{1,2}	33596		32408		15565	
2p' ¹ P ₁						
2p' ¹ D ₂						
2p' ³ S ₁	20930		27508			

* Estimated by probable $\Delta\nu$

† Previous identification in O III considered doubtful

A perfect correlation of the terms is scarcely possible, because for each spectrum the values have been obtained by the use of a formula which is only

approximate The term values for O III and C I have been determined from a sequence of three singlet p^1D terms in each case, and those for N II from a sequence of three s^3P terms A recomputation for N II, using a third p^1D term which has since been identified, merely increases all the term values by about 18 units, which may be considered negligible In all these formulæ, however, the correcting terms to the Rydberg formula are very small, so that the tabulated values for the three spectra are unlikely to be much in error relatively to each other

A regular progression in most of the term values in passing from O III to C I is clearly shown in the table In particular it will be observed that the $3d$ terms vary very slightly in the three spectra and that this fact justifies the adoption of 12700 as an approximate value for $3d^3D_3$ in C I, on which the values of the remaining triplet terms of this spectrum have been based This value clearly cannot be much in error, but since intercombinations of triplets and singlets have not been identified in C I, the triplet and singlet term values are not necessarily correct with respect to each other in this spectrum The adoption of this value, however, results in giving the terms of C I in the same order of magnitude as those of the other two spectra

The p^1S_0 terms of N II, as already noted in a previous comparison with O III,* are very discordant Interpolation of $2p^1S_0$ between O III and C I, with the aid of the "irregular doublet" law, suggests a value of about 206000 (= 51500 when divided by 4), but no support for this can be found in the observations of N II This term should combine strongly with $3s^1P_1$, and produce a line near λ 862, but no line has been observed in this position At the same time, the $3s^1P_1$ term may be considered to be well established, because it combines with $2p^1D_2$, as deduced from the nebular spectrum, to give a line at λ 746.9, and the adopted value of $2p^1D_2$ is itself supported by an observed combination with $3d^1D_2$, as determined from the laboratory spectrum Thus, adopting Bowen's suggestion that the separation of two red nebular lines is identical with $2p^3P_1 - 2p^3P_2$ of N II, and identifying these lines as $2p^4P_{21} - 2p^1D_2$, we have

From laboratory observations	Nebular lines		Supposed combinations
	λ	ν	
$2p^4P_0 = 238849$			
$2p^3P_1 = 238799$	6548.1	15267.4	$2p^3P_1 - 2p^1D_2$
$2p^3P_2 = 238715$	6585.6	15184.8	$2p^3P_2 - 2p^1D_2$
therefore $2p^1D_2 = 223531$			

* 'Roy Soc Proc.' A, vol 117, p 317 (1928)

The value of $2p^1D_2$ thus determined is strongly supported by the following combinations —

$2p^1D_2 = 223531$	$2p^1D_2 = 223531$
(Lab) $3s^1P_1 = 89658$	(Lab) $3d^1D_2 = 51754$
Calc line = <u>133873</u>	Calc line = <u>171777</u>
= $\lambda 746\ 98$	= $\lambda 582\ 15$
Obs line = $\lambda 746\ 97$	Obs line = $\lambda 582\ 16$

Thus, there can be little doubt that the $3s^1P_1$ term of N II has been correctly determined, and, for the present, the $2p^1S_0$ and $3p^1S_0$ terms of this spectrum must be regarded as anomalous. The corresponding terms of O III and C I, however, appear to be normal.

Another way of comparing the terms of the three spectra, which is more useful in some respects, is by the application of the "irregular doublet" law, which has been so successfully utilised by Millikan and Bowen for the identification of lines observed by them in the extreme ultra-violet. For similarly constituted atoms this law takes the form, for spectroscopic terms,

$$\sqrt{T/R} = \frac{1}{n} (Z - s),$$

where T represents a term, R the Rydberg constant, n the principal quantum number, Z the atomic number, and s the screening constant, which is not very different for corresponding terms of the three spectra. It follows that $\sqrt{T/R}$ and Z should show an approximately linear relationship for terms of the same type which have the same principal quantum number. The linear law accordingly provides a valuable test of the identifications of the three sets of terms.

In the first place it will be instructive to compare the triplet terms, for the reason that these have been identified with greater certainty than the singlets, and the nature of the regularity to be expected in the singlets will be more clearly indicated.

Table VIII shows the values of $\sqrt{T/R}$ for the three sets of terms and the differences between them. The near equality of the differences on the same row may be taken as an indication that the terms have been correctly identified. The three C I terms which have not yet been identified yield lines in the infra-red, but approximate values for them may be found by interpolation if desired. The screening constants may be derived from the tabulated values of $\sqrt{T/R}$ by multiplying these values by the appropriate principal quantum numbers and subtracting the results from the atomic numbers. Thus, for the $2p^3P_0$,

Table VIII—Values of $\sqrt{T/R}$ for Triplet Terms

	O III	Difference	N II	Difference	C I
$2p^3P_0$	2 011	0 538	1 475	0 564	0 911
$3s^3P_0$	1 272	0 366	0 906	0 377	0 529
$3p^3D_1$	1 172	0 360	0 812		
$3p^3S_1$	1 157	0 359	0 798	0 363	0 495?
$3p^3P_0$	1 147	0 358	0 789	0 366	0 423?
$3d^3F_3$	1 046	0 356	0 690		
$3d^3D_1$	1 034	0 350	0 684	0 344	0 340
$3d^3P_0$	1 024	0 349	0 675	0 348	0 327
$4s^3P_0$	0 928	0 307	0 621		
$4p^3D_1$	0 844	0 270	0 574	0 260	0 314
$4p^3S_1$	0 836	0 269	0 567	0 266	0 301
$4p^3P_0$	0 823	0 271	0 549*	0 251	0 298

* Identified since paper on N II was published

terms the screening constants are 3.97 (O III), 4.05 (N II) and 4.18 (C I). The reduction in screening with increase of atomic number is presumably accounted for by the greater relative distance of the orbit from the core of the atom.

The values of $\sqrt{T/R}$ for the singlet terms are shown in Table IX.

Table IX—Values of $\sqrt{T/R}$ for Singlet Terms

	O III	Difference	N II	Difference	C I
$2p^1D_2$	1 966	0 539	1 427	0 566	0 861
$2p^1S_0$	1 913				0 798
$3s^1P_1$	1 250	0 346	0 904	0 355	0 519
$3p^1D_2$	1 183	0 361	0 822	0 360	0 462
$3p^1S_0$	1 157				
$3p^1P_1$	1 049?	0 282?	0 767	0 341	0 423?
$3d^1F_3$	1 046	0 356	0 690	0 346	0 344
$3d^1P_1$	1 045	0 358	0 687	0 346	0 341
$3d^1D_2$	1 009	0 343	0 666	0 311	0 322?
$4s^1P_1$	0 911	0 303	0 611		
$4p^1D_2$	0 848	0 267	0 581	0 265	0 316
$4p^1S_0$	0 827				
$4p^1P_1$	0 816?	0 272?	0 514	0 253	0 291

* Identified since paper on N II was published

Apart from the p^1S_0 terms, which have already been considered, most of the identifications of the singlet terms appear to be justified by the progressive values of the differences shown in the table. The $3p^1P_1$ and $4p^1P_1$ terms were already considered doubtful in O III, and the above comparison suggests that the provisional identification of $3p^1P_1$, at least, is improbable.

The above equation for $\sqrt{T/R}$ may be extended to combinations between terms with principal quantum numbers n_1 and n_2 , as follows —

$$\frac{T_1}{R} - \frac{T_2}{R} = \frac{\nu}{R} = \frac{(Z - s_1)^2}{n_1^2} - \frac{(Z - s_2)^2}{n_2^2}$$

$$= [(n_2^2 - n_1^2) Z^2 - 2(n_2^2 s_1 - n_1^2 s_2) Z + n_2^2 s_1^2 - n_1^2 s_2^2] / n_1^2 n_2^2,$$

which shows that an approximately linear relationship is to be expected between Z and the wave-numbers of lines, when both terms involved have the same principal quantum numbers. This is illustrated in Table X.

Table X—Linear Relations between Corresponding Lines

Line	CI	Difference	N II	Difference	O III	Difference	F IV
$3s^1P_1 - 3p^1P_1$	10903	10597	21590	11218	32808		
$3p^1D_2 - 3d^1P_1$	10627	11854	22481	11297	33778		
$2p^1P_1 - 2p'^1D_1$	64018	28072	92120	27627	119747	27487	147234
$2p^1P_1 - 2p'^1P_1$	75212	33875	19087	32988	142075	32552	174627

Milikan and Bowen have shown* that although a linear relationship should not exist for lines whose terms have different principal quantum numbers, such a relation is to be expected for numbers obtained by reducing the wave-numbers of these lines by the formula

$$\nu' = \nu - (Z - A)^2 (n_2^2 - n_1^2) / n_1^2 n_2^2,$$

where A is a number whose value is chosen convenient for calculation. Assigning a value of 5 to A , this procedure has been adopted for corresponding lines of the three spectra, as shown in Table XI.

It will be seen that the approximate linear relations shown in Tables X and XI justify the classification of the lines in question, with the possible exception of $2p^1D_2 - 3s^1P_1$. The identifications of these lines in the three spectra, however, appear to be well founded.

* Phys. Rev., vol 26, p 314 (1925)

Table XI—Further Linear Relations between Corresponding Lines

Line		ν	ν	Difference
$2p^1D_2-3s^1P_1$	C I	51786	36545	36364
	N II	133874	72909	42768
	O III	252892	115067	
$2p^3P-3s^3P_2$	C I	60350	15109	42880
	N II	148943	87989	42011
	O III	267165	130000	
$2p^1D-3d^1P_1$	C I	68533	53202	57531
	N II	171778	110813	57584
	O III	304562	167497	
$2p^3P_2-3d^3D_2$	C I	78275	63034	63433
	N II	187431	126467	63486
	O III	327118	189973	
$2p^3P_2-3d^3P_2$	C I	79266	61025	63727
	N II	*[189716]	127752	64355
	O III	329272	192107	

* Calculated line

Triplet Separations

As regards the separations of the triplet terms indicated in Table VII, it will be observed that $\Delta\nu/9$ for O III and $\Delta\nu/4$ for N II are nearly equal for most of the corresponding terms. In N II the $3s^3P$ separations are somewhat anomalous, but the sum of the two separations is practically identical with the corresponding sum in O III. The $3d^3F$ separations in the two spectra are also slightly discordant.

The most notable feature of the separations in C I is that they are generally greater than the reduced separations in the other two spectra.

Sommerfeld's "regular doublet" law, which Millikan and Bowen have found to be applicable to many optical spectra of similarly constituted atoms, does

not appear to hold for the spectra under consideration, with the exception of the $2p\ ^3P$ terms. This law takes the form

$$\Delta\nu = \frac{R\alpha^2 (Z - s)^4}{n^3 k (k - 1)},$$

where R is the Rydberg constant, α the relativity constant ($\alpha^2 = 5.31 \times 10^{-6}$), Z the atomic number, s a screening constant, n the principal quantum number, and k has its usual values, 2 for P, 3 for D terms, and so on. $R\alpha^2 = 5.83$, and it is thus found that $R\alpha^2/n^3 k (k - 1)$ is 0.365 for 2P, 0.108 for 3P and 0.0456 for 4P. Some of the results for the spectra in question are as follows —

	$2p\ ^3P_0 - 2p\ ^3P_1$ $\Delta\nu\ \sqrt[4]{\Delta\nu/0.365} \quad ,$			$3p\ ^3P_0 - 3p\ ^3P_1$ $\Delta\nu\ \sqrt[4]{\Delta\nu/0.108} \quad s$			$4p\ ^3P_0 - 4p\ ^3P_1$ $\Delta\nu\ \sqrt[4]{\Delta\nu/0.0456} \quad s$		
C I	42	3 275	2 725	33	4 181	1 819	33	5 166	0 834
N II	134	4 377	2 623	94	5 433	1 567	78	6 431	0 569
O III	309	5 394	2 606	213	6 665	1 335	197	8 108	-0 108
F IV	637*	6 404	2 536						

* I S Bowen, 'Phys. Rev.' vol 29, p 242 (1927)

It will be observed that while the calculated values of s are consistent in each case, they show a diminution, in place of the expected increase, towards a maximum of 5, in passing from $2p\ ^3P$ to $4p\ ^3P$.

Landé's modified formula† also leads to unexpected results. This may be written in the form

$$\Delta\nu = \frac{R\alpha^2 C^2 (Z - s)^2}{(n^*)^3 k (k - 1)},$$

where n^* is the Rydberg denominator [$C^2 R / (n^*)^2 = \nu$], $C = 1$ for neutral atoms, 2 for singly ionised atoms, and so on, and s is a screening constant. The formula may also be written

$$\Delta n^* = \frac{\alpha^2}{2k(k-1)} (Z - s)^2$$

The application of this formula gives the following results for some of the terms in question —

† 'Z f Physik,' vol 25, p 49 (1924)

	$2p^3P_0 - 2p^3P_1$				$3p^3P_0 - 3p^3P_1$			
	$\Delta\nu$	$\Delta n^* \times 10^4$	$Z-s$	s	$\Delta\nu$	$\Delta n^* \times 10^4$	$Z-s$	s
C I	42	253	4.366	1.634	73	1979	12.21	
N II	134	381	5.357	1.643	94	1738	11.44	
O III	309	524	6.283	1.717	211	1925	12.04	

The results for $2p^3P$ are in close agreement, but for $3s^3P$, $3p^4P$ and $4p^3P$ the calculated values of $Z-s$ are greater than Z itself, and the formula is clearly not applicable to the determination of s from these spectra

Summary

Further observations of the arc spectrum of carbon (C I) have been made, and the classification of the lines has been considerably extended. The deepest term is a triplet P_0 , the value of which is estimated at 91017, corresponding to an ionisation potential of 11.2 volts. Comparisons are made with the spectra of N II and O III, the atoms of which are similarly constituted, but differ in nuclear charge.

The authors desire to express their thanks to the Department of Scientific and Industrial Research for a grant which has enabled one of them (E. W. H. S.) to take part in the foregoing investigation.

The Chemical Constant of Hydrogen Vapour and the Failure of Nernst's Heat Theorem

By R H FOWLER, FRS

(Received January 10 1928)

§ 1 *Introduction* -The recent successful explanation of the specific heats of hydrogen gas at low temperatures by Dennison* leaves little doubt that at all low and ordinary temperatures hydrogen must be regarded as a mixture of two sets of molecules, effectively distinct. One of these sets may be called the antisymmetrical molecules, because for these the rotational quantum number is *odd* and the rotational wave function *antisymmetrical* in the nuclei. The other set may be called the symmetrical molecules because for these the rotational quantum number is *even* and the wave function *symmetrical* in the nuclei. When account is taken of the orientations of the nuclei the complete wave function is antisymmetrical in the nuclei in all cases. At the temperatures mentioned the rate of change from one of these forms to the other is very slow† though not zero, and any changes that actually occur in any experiment as ordinarily conducted will be so few that they can be neglected altogether.

In view of what we have said it is natural to discuss the results of any experiment at these temperatures as if the hydrogen gas were a mixture of two absolutely distinct sets of molecules. In this case the laws of classical thermodynamics of course apply and control the equilibrium properties of the mixture. From the point of view of the actual hydrogen gas this equilibrium is a false or metastable one. Provided however, that the false equilibrium is attained rapidly compared with the neglected rate of change the thermodynamic properties of the ideal mixture must be true of the actual gas, and we shall assume this in the following discussion.

It is natural to follow up Dennison's work by applying it to a study of the vapour-pressure equation of hydrogen and of its chemical constant as determined by gaseous equilibria. We shall find that the vapour-pressure equation can be satisfactorily accounted for if both antisymmetrical and symmetrical molecules are present indifferently in the vapour and condensed phases. As a

* Dennison, 'Roy Soc Proc,' A, vol 115, p 483 (1927)

† The rate of change can be estimated theoretically, though with considerable uncertainty at present. I understand that it might be so great that the mean life of a molecule of either set before changing into one of the other set could be about 10 days, but that this is an upper limit for the rate and lower limit for the mean life.

result of this it follows, however, that the weight of the hydrogen molecule in the crystal form cannot be unity (with the usual convention) but must be 9 and 1 for the lowest states of the antisymmetrical and symmetrical molecules respectively. The constant in the vapour-pressure equation is therefore not the chemical constant of gaseous hydrogen but is smaller than that constant by $\frac{1}{2} \log 3$. This result fits in qualitatively with a suggestion made by Eucken* as long ago as 1924, after an exhaustive analysis of all the observational material. It appears to be a definite example of a failure of Nernst's heat theorem even in its most restricted enunciation, but a failure due, of course, to the fact that the theory and observations are concerned rather with a metastable equilibrium than with the true equilibrium state of the hydrogen concerned.

§ 2 *Known Properties of Hydrogen*—We must now record what we may regard as known with certainty about hydrogen gas. As taken over from higher temperatures it is a mixture of antisymmetrical and symmetrical molecules in the ratio 3 : 1. [This particular ratio arises from the weights of the nuclear orientations. There are three symmetrical orientations and one antisymmetrical.] The rotational partition functions are respectively

$$f_a(\Theta) = 3 \sum_{j=1,3,5} (2j+1) \Theta^{j(j+1)h^2/8\pi^2 A}$$

$$f_s(\Theta) = \sum_{j=0,2,4} (2j+1) \Theta^{j(j+1)h^2/8\pi^2 A}$$

The external factor 3 is for the nuclear orientations. The moment of inertia A is 4.67×10^{-41} gm. cm². The specific heat curve at low temperatures is characteristic of a constant 3 : 1 mixture of two sets of molecules with these partition functions.

At very low temperatures hydrogen vapour in equilibrium with the condensed form has a well defined vapour pressure, and the constant in the vapour pressure equation is that characteristic of a monatomic gas whose structural units have the same weight in the crystal and vapour phases.

These facts must be carefully analysed, for if they were based on sufficiently varied experiments they would have important consequences. Suppose we start with the 3 : 1 mixture, cool it down and condense it (the normal process). If the remaining vapour is not in the constant 3 : 1 proportion at all temperatures we could remove it at any convenient stage, and on heating it up should find that it had no longer the usual specific heat. This experiment has probably never been performed. For this discussion we shall assume that it shows no

* Eucken, 'Z f Physik,' vol 29, p 12 (1924) and the next following paper (with collaborators)

change in the specific heat curve, and therefore that in the vapour-solid equilibrium the two components are always present in either phase in the constant 3:1 proportion. On general grounds this seems to be the most probable state of affairs.

We can now carry this analysis a little further. It is evident without calculation that the constant 3:1 proportion can only be preserved if the work of removing one molecule of either sort from the condensed form to the gas is exactly the same at all temperatures. It follows that molecules of either sort must be indifferently present in the condensed phase with the same rotational partition function as they possess in the vapour phase, and a work of evaporation at the absolute zero the same for both types. Only the absolute values of the weights can differ in the two phases, and as we shall see this last difference is ruled out by the observed value of the chemical constant. Of course at the low temperatures at which the condensed forms actually can exist we are really only concerned with molecules of either type in their respective lowest rotational states.

We now pass on to a formal presentation of this argument. It is in this connection a matter of indifference whether we use classical statistics or the modified form required by the new quantum mechanics*. We shall, therefore, cast the discussion into the classical form, to avoid an appearance of unfamiliarity in non-essentials.

§ 3 *Mixed Crystals*.—It is necessary to contemplate a rather more general assembly than any commonly discussed,† which contains a mixed crystal of two components and the corresponding vapours. This is easy enough in a formal way in the general case. If $\kappa_{P, P'}(z)$ is the partition function for all possible states of the crystal composed of P molecules of one type and P' of the other, we have then only to form the function

$$K(x, x', z) = \sum_{P, P' \geq 0} x^P x'^{P'} \kappa_{P, P'}(z), \quad (1)$$

and the total number C of weighted complexions of the assembly is, in the usual notation,

$$C = \frac{X! X'!}{(2\pi i)^2} \iiint \frac{dx dx' dz}{x^{X+1} x'^{X'+1} z^{R+1}} K(x, x', z) \exp \{xg(z) + x'g'(z)\} \quad (2)$$

* For the statistics of hydrogen molecules (or any neutral atom or molecule) the modified form is probably that of Bose and Einstein which may only use wave functions symmetrical in all the molecules. If the wave functions are to be *antisymmetrical* in all the electrons and all the protons they will necessarily be *symmetrical* in neutral combinations. This is pointed out by Born and Heisenberg in their report to the Solvay Conference (1927).

† See, for example, Darwin and Fowler, 'Proc. Camb. Phil. Soc.', vol. 21, p. 730 (1923).

In this expression X and X' are the total numbers of molecules of the two types E is the total energy of the assembly and $g(z)$ and $g'(z)$ are the partition functions for the two types of molecule in the vapour phase. From equation (2) all the usual mean values of importance can be derived formally, but the formal expressions are of little value unless $K(x, x', z)$ can be evaluated at least approximately.

The form of K has hitherto only been evaluated properly for a crystal of one component ($P' \equiv 0$). But there is another case, sufficiently representative of what we require here, in which explicit evaluation is possible, the case in which the two components are so much alike that the partition functions $\kappa_P, \kappa_{P'}$ are practically independent of the relative arrangements of the molecules of the two components. The number of such arrangements is $(P + P')! / P! P'!$, so that in this case $\kappa_{PP'}(z)$ takes the approximate form

$$[f(z)]^P [f'(z)]^{P'} (P + P')! [\kappa(z)]^{P+P'} / (P! P'!) \quad (3)$$

The factors $f(x), f'(x)$ are retained to represent the rotational partition functions of the two components in the crystal, and $[\kappa(z)]^{P+P'}$ is the ordinary approximate partition function for the crystal of $P + P'$ units constructed by analysis of the normal modes. With the use of (3) in (1) we now find

$$K(x, x', z) = \frac{1}{1 - \{x f(z) + x' f'(z)\} \kappa(z)} \quad (4)$$

We can now use all the ordinary arguments. If \bar{N}, \bar{N}' are the average numbers of molecules of the two types in the vapour,

$$\bar{N} = \xi g(\mathfrak{z}), \bar{N}' = \xi' g'(\mathfrak{z}) \quad (5)$$

The average numbers \bar{P}, \bar{P}' in the crystal are

$$\bar{P} = \frac{\xi f(\mathfrak{z}) \kappa(\mathfrak{z})}{1 - \{\xi f(\mathfrak{z}) + \xi' f'(\mathfrak{z})\} \kappa(\mathfrak{z})} \quad \bar{P}' = \frac{\xi' f'(\mathfrak{z}) \kappa(\mathfrak{z})}{1 - \{\xi f(\mathfrak{z}) + \xi' f'(\mathfrak{z})\} \kappa(\mathfrak{z})} \quad (6)$$

The parameters ξ, ξ' and \mathfrak{z} , the partial potentials and the temperature, are determined by the unique position of the saddle-point of the integrand of C , given by the vanishing of its three partial differential coefficients. In addition to these equations we have, of course,

$$\bar{N} + \bar{P} = X, \quad \bar{N}' + \bar{P}' = X' \quad (7)$$

Finally since most of the molecules of both sorts will be in the crystal \bar{P} and \bar{P}' must both be very large, so that

$$\{\xi f(\mathfrak{z}) + \xi' f'(\mathfrak{z})\} \kappa(\mathfrak{z}) = 1 \quad (8)$$

In our problem we have a given relation between X and X' of the type

$$X = nX', \quad (9)$$

and we assert that we know that we must have $\bar{N} = n\bar{N}'$ for all temperatures. Therefore $\bar{P} = n\bar{P}'$ also. These conditions are satisfied if and only if

$$\frac{\xi g}{\xi' g'} = \frac{\xi f}{\xi' f'} = \frac{n}{1} \quad (10)$$

The equality $g/g' = f/f'$ means (i) that the work of evaporation at the absolute zero is the same for both types of molecule, (ii) that the ratio of the ordinary rotational partition functions is the same in both phases, (iii) as a consequence of (ii) the only reasonable difference remaining in the separate partition functions is that all the weights in both functions in the vapour phase should differ by a constant factor α from those in the solid phase. On general grounds any value of α other than unity is inadmissible.

From (8) and (10) it follows that

$$\xi = \frac{n}{n+1} \frac{1}{f(\vartheta) \kappa(\vartheta)}, \quad \xi' = \frac{1}{n+1} \frac{1}{f'(\vartheta) \kappa(\vartheta)} \quad (11)$$

Therefore

$$\begin{aligned} \bar{N} &= \frac{n}{n+1} \frac{g(\vartheta)}{f(\vartheta) \kappa(\vartheta)}, & \bar{N}' &= \frac{1}{n+1} \frac{g'(\vartheta)}{f'(\vartheta) \kappa(\vartheta)}, \\ \bar{N} + \bar{N}' &= \frac{g(\vartheta)}{f(\vartheta) \kappa(\vartheta)} = \frac{g'(\vartheta)}{f'(\vartheta) \kappa(\vartheta)} \end{aligned} \quad (12)$$

§ 4 *Application to Hydrogen at Low Temperatures*—The application to hydrogen at low temperatures is immediate. Let χ be the work of evaporation of one molecule of either type at the absolute zero. If the energy zeros are suitably chosen, then

$$\kappa(\vartheta) \sim \kappa(0) = 1 \quad (\vartheta \rightarrow 0),$$

and $\kappa(\vartheta)$ is a partition function which may be chosen to reproduce exactly the specific heat of the condensed phase. Further, retaining only (for these temperatures) the first terms in f_s and f_v , we have

$$f(\vartheta) = 9\vartheta^{3\tau}, \quad f'(\vartheta) = 1, \quad \left(\tau = \frac{\hbar^2}{8\pi^2 A} \right),$$

$$g(\vartheta) = \frac{(2\pi m)^{3/2} V \vartheta^{3\tau}}{\hbar^3 (\log 1/\vartheta)^{1/2}} \alpha f(\vartheta),$$

where V is the volume accessible to the vapour phase. If v is the vapour density

of the hydrogen as a whole at temperature T ($\mathfrak{Z} = e^{-1/kT}$) we find on ignoring the specific heat of the crystal that

$$\nu = \alpha \frac{(2\pi mkT)^{1/2}}{h^3} e^{-\kappa/kT}, \quad (13)$$

or

$$\log p = -\frac{\chi}{kT} + \frac{1}{2} \log T + \log \left\{ \alpha \frac{(2\pi m)^{1/2} k^{1/2}}{h^3} \right\} \quad (14)$$

This is the standard result for monatomic vapours of the same weight in both phases, and agrees with the observed result for hydrogen at very low temperatures, if $\alpha = 1$

This analysis of the known facts seems reasonable in itself and carries the facts without strain. There seems to be no other obvious alternative.

We must observe, however, that this success requires a solid phase for which the complete partition function cannot have unit weight for its lowest possible state. For the complete partition function for the normal crystal, a 3:1 mixture of the two types, will be

$$\{f(\mathfrak{Z})\}^{\bar{P}} \{f'(\mathfrak{Z})\}^{\bar{P}} \{\kappa(\mathfrak{Z})\}^{\bar{P} + \bar{P}'} \quad (\bar{P} = 3\bar{P}'),$$

and as $\mathfrak{Z} \rightarrow 0$ the asymptotic form of this is

$$[9\frac{1}{2} \mathfrak{Z} \frac{1}{2} \tau]^{\bar{P} + \bar{P}'}$$

If therefore we treat all the hydrogen together we have a crystal partition function $\kappa^*(\mathfrak{Z})$ satisfying

$$\kappa^*(\mathfrak{Z}) \sim 9^{\frac{1}{2}} \quad (15)$$

The various factors contributing to this result should be distinguished. It has long been recognised† that supercooled liquids and mixed crystals need not obey Nernst's Heat Theorem in the form which asserts that these entropy differences necessarily tend to zero with the temperature. Though we are formally dealing with a mixed crystal of two sorts of hydrogen the case here dealt with is not an example of this recognised exception, for we should assign the same value to $[\kappa^*(\mathfrak{Z})]^{\bar{P} + \bar{P}'}$ if the two sorts of hydrogen were present permanently as distinct crystals, the antisymmetrical and the symmetrical. Again the 9 itself is really built up of two separate factors 3 arising from distinct sources. One comes from the pair of orientations of each nucleus, and the other from the three antisymmetrical rotational wave functions for the molecule as a whole. The former of these factors 3 is due to a source which must persist through all combinations into which the hydrogen atom enters, and *might* equally affect

† See particularly Lewis and Randall, 'Thermodynamics' (1924), especially chap. 31.

them all, though this is not likely. The other factor 3, due to the non-interchanging property of the two sorts of the hydrogen molecule itself, might be peculiar to this combination.

The same result is, of course, true of the vapour. If we treat the vapour mixture as a whole then its energy and specific heat correspond exactly to the partition function

$$g^*(\mathfrak{z}) = \{f_a^2(\mathfrak{z}) f_s(\mathfrak{z})\}^{\frac{1}{2}} \frac{(2\pi m)^{\frac{3}{2}} V \mathfrak{z}^3}{h^3 (\log 1/\mathfrak{z})^{\frac{1}{2}}}, \quad (16)$$

and the equation for the equilibrium density of the vapour is now

$$\bar{N}^* = \bar{N} + \bar{N}' = \frac{g^*(\mathfrak{z})}{\kappa^*(\mathfrak{z})} \quad (17)$$

The only effect on these formulæ due to the evanescent rate of change between the antisymmetrical and the symmetrical molecules is that we have to use $\{f_a^2(\mathfrak{z}) f_s(\mathfrak{z})\}^{\frac{1}{2}}$ instead of $\{f_a(\mathfrak{z}) + f_s(\mathfrak{z})\}$.

§ 5 *Hydrogen at Ordinary Temperatures*.—Once we have accounted for the value of the chemical constant at low temperatures, there is nothing more to do. For thermodynamical arguments give us the relation (if the vapour phase is a perfect gas)

$$\log p = -\frac{\lambda_0}{RT} + \int^T \frac{dT'}{RT'^2} \int^1 \{(C_p)_{\text{vap}} - (C_p)_{\text{sol}}\} dT'' + A, \quad (18)$$

where λ_0 and A are constants, R is the ordinary gram-molecular gas constant and C the specific heat of the specified phase. $(C_p)_{\text{sol}}$ must include the latent heats of melting or any other transition of form. Any form of the quantum theory allows us to particularise this to

$$\log p = -\frac{\lambda_0}{RT} + \frac{1}{2} \log T + \int_0^T \frac{dT'}{RT'^2} \int_0^T \{(C_p')_{\text{vap}} - (C_p)_{\text{sol}}\} dT'' + \mathfrak{s} \quad (19)$$

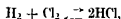
In (19) $(C_p')_{\text{vap}}$ is the specific heat of the internal motions (vibrations and rotations) of the molecules in the vapour phase and \mathfrak{s} the chemical constant which we have just been studying. If, as is constantly done for convenience in a suitable range of temperatures, we break up $(C_p')_{\text{vap}}$ into $nR + (C_p'')_{\text{vap}}$ with n constant, equation (19) can be replaced by

$$\log p = -\frac{\lambda_0}{RT} + \left(\frac{1}{2} + n\right) \log T + \int_0^T \frac{dT'}{RT'^2} \int_0^T \{(C_p'')_{\text{vap}} - (C_p)_{\text{sol}}\} dT'' + \mathfrak{s}', \quad (20)$$

where \mathfrak{s}' is another constant, also called the chemical constant for this range. The difference of \mathfrak{s} and \mathfrak{s}' depends only on the specific heat of the vapour molecules. A theory which gives \mathfrak{s} correctly and correct specific heats, will

automatically give the correct value of ϵ' , which need not therefore be further discussed

§ 6 *The Position of Nernst's Heat Theorem*—In its most restricted and least exceptionable form Nernst's Heat Theorem asserts that the entropy change in any reaction between pure crystalline substances tends to zero as the temperature tends to zero. No question arises as to the validity of the assertion that such an entropy change tends to a finite limit as $T \rightarrow 0$, the only question is whether this finite limit is always zero. General statistical theory indicates that this finite limit is always zero if and only if the weights of the lowest states of all the crystalline forms concerned can be taken to be unity. It is, of course, not necessary that they should be so taken, any weight whatever can be assigned to the lowest state of any atom provided that it carries that weight with it as a factor into every combination. For example, the orientations of the hydrogen nuclei add a weight factor 2 to all the states of the hydrogen atom and 4 to all the states of the molecule (apart from questions of the possibility of intercombination). If they also add 2 to the weight of the normal HCl molecule, they will be without effect on the equilibrium constant of the reaction



and so on in general

The foregoing investigation of hydrogen throws grave doubts, however, on this persistence of the weight factors. Once it is clear that the simple convention of unit weight for any state of a simple non-degenerate system obeying the laws of quantum mechanics does not lead naturally to unit weight for the normal state of a crystal built up out of the particular systems, hydrogen molecules, the whole argument from simplicity falls to the ground and we have no longer any theoretical reason to expect Nernst's theorem to be true. Whether it fails or not in actual cases we are not yet in a position to predict from the theory of molecular structure alone. We should require for this a knowledge of all the normal molecules concerned in any gas reaction as precise as we possess for hydrogen. It is therefore hardly possible at present to do more than note that the evidence collected by Eucken already mentioned is very difficult to reconcile with the general validity of Nernst's Heat Theorem. In fact, Eucken makes the interesting observation that apparently the hydrogen molecule is the worst culprit, and that the greater part of the discrepancies can be removed by increasing its chemical constant by 0.3 ($\log_{10} 2$) above the value derived from the vapour-pressure equation on the assumption $\kappa^*(3) \sim 1$. If we might ignore the nuclear weights and simply take hydrogen as a mixture in which $\frac{1}{2}$ of the molecules have a lowest state of weight 3 we could suggest that the chemical

constant of hydrogen ought to be increased by $\frac{3}{4} \log_{10} 3$ or 0.36 which fits Eucken's figures still better than 0.3. There is, however, no proper justification for such a procedure. We can only conclude, but this is amply justified, that both theory and observation suggest that Nernst's Heat Theorem should not hold for reactions in which hydrogen plays a part.

It is of some importance to note that the theoretical reasons for expecting this failure depend eventually on the fact that hydrogen must be treated as a metastable mixture. If the whole process is conducted so slowly that the hydrogen is in its true equilibrium state then the exact theory gives a unit weight for the lowest state of the normal molecule both in the vapour and the solid, and all basis for suspecting failure disappears. It may therefore be preferred to say that Nernst's Heat Theorem is inapplicable to hydrogen reactions as ordinarily conducted, though it might be true, or probably is true, of such reactions if they were conducted at extravagantly slow rates. But the quasi-equilibrium properties of hydrogen ordinarily recorded, its vapour pressure, reaction constants and specific heats, do not refer (or at least do not all refer) to this true series of equilibrium states at all.

Oscillations in a Bridge caused by the Passage of a Locomotive

By Prof C E INGLIS

(Communicated by Sir Alfred Ewing, F R S —Received October 11, 1927)

[PLATE I]

For purposes of bridge design it is all important to be able to predict with a reasonable degree of accuracy the state of oscillation which will be set up when a given locomotive crosses a bridge at any specified speed. A large amount of experimental data relating to impact effects on bridges has been accumulated, but in default of an underlying theory sufficiently comprehensive in character to account for the phenomena observed, the conclusions emerging from experimental results have been somewhat disappointing and vague.

The problem is one which most essentially calls for the closest possible co-operation between mathematical analysis and practical experiment. At the present stage experiment has outrun theory, and it was with the object of redressing, in some measure, this lack of balance that the following theoretical investigation was undertaken.

In March, 1923, a Committee under the chairmanship of Sir Alfred Ewing, K C B, F R S, was appointed by the Department for Scientific and Industrial Research to investigate stresses in railway bridges with special reference to impact effects. The author of this paper has been privileged to serve on this Committee, and in the process of evolving the following mathematical analysis he has consequently enjoyed the exceptional advantage of having the guidance of practical experiment to point the way and to check predictions deduced by theory.

Through the courtesy of the Bridge Stress Committee it has been possible to reproduce some of their experimental records, and to give thereby an indication of the degree of accuracy which can be attained in predicting practical results by means of the mathematical methods developed in this paper.

Fundamental Assumptions

Locomotives and bridges are complicated structures, and to reduce the problem to manageable proportions some process of simplification and idealisation is a necessity. This preliminary process demands careful consideration guided by experiment, otherwise there is a danger that, in seeking for simplicity, factors which are of first-rate importance may be idealised out of existence. As an example of the necessity of experimental guidance to prevent mathematical analysis running off the rails, it may be mentioned that the experiments of the Bridge Stress Committee had reached an advanced stage before it was fully realised that the friction in the spring movements of locomotives played a most important part in limiting the oscillations in bridges of moderate span. A mathematical analysis which leaves this factor out of account, though applicable to certain types of bridges, will in other cases lead to results which have no resemblance to reality.

For a bridge of fairly long span whose natural period of vibration is comparatively sluggish, the oscillations set up by the passage of a locomotive are not sufficiently large or rapid to overcome spring friction. In such a case the whole mass of the locomotive behaves as though it was unsprung and damping action due to spring friction does not occur. This is the state of affairs to which mathematical analysis will be directed in the first instance, and the locomotive will be idealised as a concentrated mass moving across the bridge. Associated with this concentrated mass a pulsating force will be taken into account. This force has its origin in the weights attached to the driving wheels, to neutralise the inertia forces set up by reciprocating parts of the locomotive. These balance weights give rise to an alternating pressure between the wheels and the

rails which varies as the square of the speed, and it is this action which is mainly responsible for the oscillations generated in a bridge by the passage of a locomotive

In the case of electric locomotives, where such balance weights are not required, their passage across a bridge sets up little or no oscillation, and the deflection at all speeds is practically identical with the "crawl deflection," that is, the deflection produced by the locomotive moving at a very slow speed

The most important bridge characteristics which have to be taken into account are its total mass and its natural period of vibration. Provided that these two factors are left unchanged, then for purposes of calculating bridge oscillations the structure can, without serious loss of accuracy, be treated as uniform in mass and section

Damping influences in the bridge itself must be taken into account. The effect of damping when residual vibrations are dying out may appear insignificant, but in checking the growth of a synchronous oscillation it plays a most important part, and a theory which fails to take account of this influence will predict in certain cases a state of oscillation far in excess of that actually observed. This damping arises partly from a lack of perfect elasticity in the structure, augmented by the somewhat inelastic character of the permanent way, and partly from friction in the supports at the piers

In bridges of long span no great error is introduced if the locomotive is treated as a concentrated mass, and, provided that the oscillations do not become sufficiently violent to induce spring movement, their general character can be ascertained by a mathematical investigation of the comparatively simple case depicted in fig 1, the moving mass there shown being the total mass of the locomotive

Throughout the analysis it will be assumed that the speed v is constant and that the supports do not in any way constrain the directions of the ends of the girder

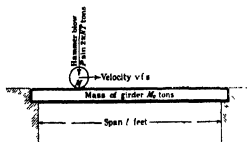


FIG 1.

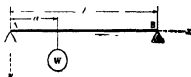


FIG 2.

Deflection of a Girder expressed in the form of a Harmonic Series

Consider the case shown in fig 2, in which a girder AB of uniform section, freely supported at its extremities, is deflected by a load W concentrated at a section defined by $x = a$. The concentrated load can be represented by the harmonic series

$$\frac{2W}{l} \left[\sin \frac{\pi a}{l} \sin \frac{\pi x}{l} + \sin \frac{2\pi a}{l} \sin \frac{2\pi x}{l} + \text{etc} \right],$$

and the deflection (y) at any point (x) on the centre line of the girder is given by

$$EI \frac{d^4 y}{dx^4} = \frac{2W}{l} \left[\sin \frac{\pi a}{l} \sin \frac{\pi x}{l} + \sin \frac{2\pi a}{l} \sin \frac{2\pi x}{l} + \text{etc} \right],$$

where I is the moment of inertia of its cross section

Hence

$$y = \frac{2Wl^3}{\pi^4 EI} \left[\sin \frac{\pi a}{l} \sin \frac{\pi x}{l} + \frac{1}{2^4} \sin \frac{2\pi a}{l} \sin \frac{2\pi x}{l} + \text{etc} \right]$$

gives the deflection expressed in a harmonic series

The form of this series indicates that the first harmonic component of the load is the predominant cause of deflection, and, unless a high degree of accuracy is required, contributions made by the other harmonic components can be ignored. This is particularly true if the calculations relate to the determination of the central deflection, since the contribution made by the second harmonic component is then necessarily zero. Before extending this treatment to the case of moving and pulsating loads, it is desirable to study the natural period of vibration of a girder when unloaded and also when it is carrying a concentrated mass

Natural Periods of Vibration for an Unloaded Girder freely supported at its Ends

Let m be the mass of the girder per unit length

For a free undamped oscillation, the equation of motion is

$$EI \frac{d^4 y}{dx^4} + m \frac{d^2 y}{dt^2} = 0$$

A solution of this which satisfies the condition that $y = 0$ and $d^2y/dx^2 = 0$ at both ends is

$$y = A_1 \sin \frac{\pi x}{l} \sin 2\pi n_0 t,$$

where

$$2\pi n_0 = \frac{\pi^2}{l^2} \sqrt{\frac{EI}{m}} = \frac{\pi}{l^2} \sqrt{\frac{EI}{M_1}} \quad (A)$$

This is the fundamental mode of vibration

Higher frequency modes are given by

$$y = A_2 \sin \frac{2\pi x}{l} \sin 8\pi n_0 t,$$

$$y = A_3 \sin \frac{3\pi x}{l} \sin 18\pi n_0 t,$$

etc, etc

It should be noted that a close approximation to the central deflection D produced by a steady central load W is given by

$$D = \frac{W}{2\pi^2 n_0^2 M_G} \quad (B)$$

Natural Periods of Vibration for a Girder carrying a Mass M concentrated at Section $x = a$

Let h be the deflection at $x = a$. The mass M concentrated at this section applies to the girder a downward force $-M(d^2h/dt^2)$

Replacing this concentrated force by its equivalent series of sinusoidal load distributions, the equation of motion for a free undamped vibration take the form

$$EI \frac{d^4 y}{dx^4} + m \frac{d^2 y}{dt^2} = -\frac{M}{l} \frac{d^2 h}{dt^2} \left[\sin \frac{\pi a}{l} \sin \frac{\pi x}{l} + \sin \frac{2\pi a}{l} \sin \frac{2\pi x}{l} + \text{etc} \right]$$

Consider a solution in the form

$$y = A \sin 2\pi n t \left[\frac{\sin \frac{\pi a}{l} \sin \frac{\pi x}{l}}{1 - \frac{n^2}{n_0^2}} + \frac{\sin \frac{2\pi a}{l} \sin \frac{2\pi x}{l}}{2^2 - \frac{n^2}{n_0^2}} + \text{etc} \right]$$

This will satisfy the equation provided that

$$\begin{aligned} \frac{\pi^4}{l^4} EI & \left[\frac{\sin \frac{\pi a}{l} \sin \frac{\pi x}{l}}{1 - \frac{n^2}{n_0^2}} + \frac{2^4 \sin \frac{2\pi a}{l} \sin \frac{2\pi x}{l}}{2^4 - \frac{n^2}{n_0^2}} + \text{etc} \right] \\ & - 4\pi^2 n^2 m \left[\frac{\sin \frac{\pi a}{l} \sin \frac{\pi x}{l}}{1 - \frac{n^2}{n_0^2}} + \frac{\sin \frac{2\pi a}{l} \sin \frac{2\pi x}{l}}{2^4 - \frac{n^2}{n_0^2}} + \text{etc} \right] \\ & = \frac{2M}{l} 4\pi^2 n_1^2 \left[\frac{\sin^2 \frac{\pi a}{l}}{1 - \frac{n^2}{n_0^2}} + \frac{\sin^2 \frac{2\pi a}{l}}{2^4 - \frac{n^2}{n_0^2}} + \text{etc} \right] \\ & \quad \times \left[\sin \frac{\pi a}{l} \sin \frac{\pi x}{l} + \sin \frac{2\pi a}{l} \sin \frac{2\pi x}{l} + \text{etc} \right] \end{aligned}$$

That is, if

$$\begin{aligned} n_0^4 M_G & \left[\sin \frac{\pi a}{l} \sin \frac{\pi x}{l} + \sin \frac{2\pi a}{l} \sin \frac{2\pi x}{l} + \text{etc} \right] \\ & - 2n^2 M \left[\frac{\sin^2 \frac{\pi a}{l}}{1 - \frac{n^2}{n_0^2}} + \frac{\sin^2 \frac{2\pi a}{l}}{2^4 - \frac{n^2}{n_0^2}} + \text{etc} \right] \\ & \quad \times \left[\sin \frac{\pi a}{l} \sin \frac{\pi x}{l} + \sin \frac{2\pi a}{l} \sin \frac{2\pi x}{l} + \text{etc} \right] \end{aligned}$$

That is, if

$$1 = \frac{2M}{M_G} \frac{n_1^2}{n_0^2} \left[\frac{\sin^2 \frac{\pi a}{l}}{1 - \frac{n^2}{n_0^2}} + \frac{\sin^2 \frac{2\pi a}{l}}{2^4 - \frac{n^2}{n_0^2}} + \text{etc} \right]$$

From this condition a series of values of n can be determined specifying the various frequencies and modes of vibration

The fundamental frequency (n_1) is given approximately by

$$1 = \frac{2M}{M_G} \frac{n_1^2}{n_0^2} \frac{\sin^2 \frac{\pi a}{l}}{1 - \frac{n_1^2}{n_0^2}},$$

or

$$\frac{n_1^2}{n_0^2} = \frac{M_G}{M_G + 2M \sin^2 \frac{\pi a}{l}},$$

and the fundamental mode of vibration is approximately defined by

$$y = A_1 \sin 2\pi n_1 t \sin \frac{\pi x}{l},$$

where

$$2\pi n_1 = \frac{\pi^2}{l^2} \sqrt{\frac{EI}{M_0 + 2M \sin^2 \frac{\pi a}{l}}} \quad (C)$$

The second mode of vibration is likewise approximately defined by

$$y = A_2 \sin 2\pi n_2 t \sin \frac{2\pi x}{l},$$

where

$$2\pi n_2 = \frac{2^2 \pi^2}{l^2} \sqrt{\frac{EI}{M_0 + 2M \sin^2 \frac{2\pi a}{l}}}$$

As previously mentioned, the primary cause of oscillations in a bridge is the "hammer-blow" effect of the balance weights of locomotives. The frequency of the blows can range up to a maximum of about 6 per second, 6 revolutions per second being about the maximum attainable in the case of a steam locomotive. Except for short spans, this range of frequency will include the fundamental frequency of the loaded bridge, but it is usually well below the frequency of the higher modes of vibration of the structure. In consequence, these higher modes of vibration cannot be developed to any considerable extent, and the bridge oscillations approximate in form to a simple sine curve. A maximum state of oscillation is to be anticipated when the engine speed is such that the hammer-blows synchronise as closely as possible with the fundamental frequency of the bridge. Exact synchronism can, however, be only momentarily attained, since the natural period of the loaded structure is changing constantly as the mass moves along the bridge, and it is this change of natural frequency combined with the influence of damping that shields a railway bridge from the

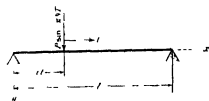


FIG 3

excessive state of oscillation which would inevitably occur if a condition of exact resonance could be maintained over a prolonged period, unchecked by damping. For bridges of long span the dead load of the structure is so great that, in comparison, the mass of a locomotive becomes

insignificant. Accordingly, the case of a long-span bridge can be studied with a fair approach to reality by reducing the problem to that depicted in fig 3,

in which the mass of the moving load is ignored and the girder is merely subjected to a periodic force $P \sin 2\pi Nt$ moving forward at a uniform speed v

Oscillation produced by a Concentrated Pulsating Force moving at Uniform Speed along a Girder

The applied moving force can be represented by the harmonic series

$$\frac{2P}{l} \sin 2\pi Nt \left[\sin \frac{\pi vt}{l} \sin \frac{\pi x}{l} + \sin \frac{2\pi vt}{l} \sin \frac{2\pi x}{l} + \text{etc} \right],$$

or

$$\frac{2P}{l} \sin 2\pi Nt \left[\sin 2\pi nt \sin \frac{\pi x}{l} + \sin 4\pi nt \sin \frac{2\pi x}{l} + \text{etc} \right],$$

where

$$n = \frac{v}{2l}$$

Retaining, in the first instance, only the primary component of this series, and neglecting the effect of damping, the equation of motion for the girder is

$$EI \frac{d^4 y}{dx^4} + m \frac{d^2 y}{dt^2} = \frac{2P}{l} \sin 2\pi Nt \sin 2\pi nt \sin \frac{\pi x}{l},$$

or

$$EI \frac{d^4 y}{dx^4} + m \frac{d^2 y}{dt^2} = \frac{P}{l} \left[\cos 2\pi (N - n)t - \cos 2\pi (N + n)t \right] \sin \frac{\pi x}{l}$$

Using results already established, viz ,

$$2\pi n_0 = \frac{\pi^2}{l^2} \sqrt{\frac{EI}{m}} \quad \text{and} \quad D = \frac{P}{2\pi^2 n_0^2 M},$$

where D is the central deflection due to a steady central load P , a particular integral of the above equation can be obtained in the form

$$y = \frac{D}{2} \left[\frac{\cos 2\pi (N - n)t}{1 - \left(\frac{N - n}{n_0}\right)^2} - \frac{\cos 2\pi (N + n)t}{1 - \left(\frac{N + n}{n_0}\right)^2} \right] \sin \frac{\pi x}{l}$$

To satisfy the starting conditions that $y = 0$ and $dy/dt = 0$ initially, it is necessary to superpose upon this forced oscillation a free oscillation of the type

$$y = B_0 \cos 2\pi n_0 t \sin \frac{\pi x}{l}$$

Making this adjustment, the state of oscillation which satisfies the general differential equation and also satisfies the starting conditions is obtained in the form

$$y = \frac{D}{2} \left[\frac{\cos 2\pi (N - n)t - \cos 2\pi n_0 t}{1 - \left(\frac{N - n}{n_0}\right)^2} - \frac{\cos 2\pi (N + n)t - \cos 2\pi n_0 t}{1 - \left(\frac{N + n}{n_0}\right)^2} \right] \sin \frac{\pi x}{l} \quad (D)$$

The higher harmonic components of the applied force will each give rise to corresponding harmonic deflections of the girder which can separately be determined without difficulty. For instance, the state of oscillation generated by the p th harmonic component of the applied force is given by

$$y = \frac{D}{2p^4} \left[\frac{\cos 2\pi (N-pn) t - \cos 2p^2\pi n_0 t}{1 - \left(\frac{N-pn}{p^2 n_0}\right)^2} - \frac{\cos 2\pi (N+pn) t - \cos 2p^2\pi n_0 t}{1 - \left(\frac{N+pn}{p^2 n_0}\right)^2} \right] \sin \frac{p\pi x}{l}$$

These higher harmonic components are usually small in comparison with the primary component, and in practical calculations relating to the central deflections of bridges it is hardly necessary to take into account more than the first harmonic component, that is to say, the effect produced by the primary harmonic component of the applied force.

In a brief article communicated by Prof S P Timoshenko to the 'Philosophical Magazine,' vol 43 (1922), this same harmonic series was established and the exact solution from which the harmonic series emanates is given in a paper contributed by the present writer to the 'Proceedings of the Institution of Civil Engineers,' May 18, 1924. The numerical manipulation of this exact solution, which involves hyperbolic functions, is, however, a somewhat laborious process, and, unless an exceptionally high degree of accuracy is required, it is preferable and justifiable to adopt the approximation given by formula (D), which results from retaining only the first harmonic component of the exact solution.

As mentioned previously, the most violent state of oscillation is to be anticipated when the frequency of the applied force synchronises with the fundamental frequency of the girder, that is to say, when $N = n_0$. Under these circumstances the oscillations are cumulative in character, and, in the absence of damping, they will mount up continuously until the instant at which the force leaves the bridge.

By putting $vt = l$, that is, $nt = \frac{1}{2}$ in formula (D), this culminating state of oscillation is defined by

$$y = D \cos 2\pi Nt \left[\frac{1}{1 - \left(1 + \frac{n}{N}\right)^2} - \frac{1}{1 - \left(1 - \frac{n}{N}\right)^2} \right] \sin \frac{\pi x}{l}$$

Now

$$\frac{n}{N} = \frac{\text{Circumference of driving wheel}}{\text{Twice span of bridge}},$$

and consequently for long-span bridges, to which the application of this theory is confined, n/N is a small fraction. For example, if the span is 250 feet, n/N

is unlikely to exceed $\frac{1}{15}$, and for numerical calculations it is legitimate to neglect π^4/N^4 in comparison with $4\pi^2/N^2$

Employing this approximation, the above expression takes the form

$$y = 2NTD \cos 2\pi Nt \sin \frac{\pi x}{l},$$

where T is the time taken for the load to traverse the bridge. The extent of the oscillations when the pulsating force is just leaving the bridge is accordingly the deflection due to the force steadily applied at the centre, magnified by twice the number of alternations the force makes during its passage along the bridge.

Up to this stage no consideration has been given to the fact that in addition to the alternating force the girder will be subjected to a constant gravity force W arising from the weight of the moving load.

The equation for the deflection so produced is

$$EI \frac{d^4 y}{dx^4} + m \frac{d^2 y}{dt^2} = \frac{2W}{l} \left[\sin \frac{\pi vt}{l} \sin \frac{\pi x}{l} + \sin \frac{2\pi vt}{l} \sin \frac{2\pi x}{l} + \text{etc} \right],$$

and the corresponding forced oscillation is

$$y = \frac{2Wl^3}{\pi^4 EI} \left[\frac{\sin \frac{\pi vt}{l} \sin \frac{\pi x}{l}}{1 - \left(\frac{v}{2ln_0}\right)^2} + \frac{\sin \frac{2\pi vt}{l} \sin \frac{2\pi x}{l}}{2^4 \left\{1 - \left(\frac{v}{4ln_0}\right)^2\right\}} + \frac{\sin \frac{3\pi vt}{l} \sin \frac{3\pi x}{l}}{3^4 \left\{1 - \left(\frac{v}{6ln_0}\right)^2\right\}} + \text{etc} \right]$$

In a long-span bridge even at the highest practicable speed $\left(\frac{v}{2ln_0}\right)^2$ can hardly exceed $1/100$. Consequently, a very close approximation to the forced oscillation is given by

$$y = \frac{2Wl^3}{\pi^4 EI} \left[\sin \frac{\pi vt}{l} \sin \frac{\pi x}{l} + \frac{1}{2^4} \sin \frac{2\pi vt}{l} \sin \frac{2\pi x}{l} + \frac{1}{3^4} \sin \frac{3\pi vt}{l} \sin \frac{3\pi x}{l} + \text{etc} \right]$$

To this close degree of approximation the deflection of the girder undergoes no dynamic magnification and the forced oscillation due to a gravity force may, for all practicable speeds, be treated as identical with the crawl deflection, that is to say, the deflection produced when the steady force is moving very slowly along the bridge. This agreement holds true when instead of a single gravity force the girder is acted upon by a number of separate forces such as occur in the case of an actual locomotive.

It must not, however, be assumed that the gravity forces of moving loads are incapable of setting up oscillations. The approximate expression given

above for the forced oscillation satisfies the condition that the girder is initially without deflection, but it does not satisfy the condition that the girder is initially at rest. The adjustment of this starting condition calls for the superposition of a free period oscillation, and the complete state of motion set up by a steady moving force is very accurately defined by

$$y = \delta \left[\left(\sin \frac{\pi vt}{l} - \frac{v}{2ln_0} \sin 2\pi n_0 t \right) \sin \frac{\pi x}{l} + \frac{1}{2^4} \left(\sin \frac{2\pi vt}{l} - \frac{v}{4ln_0} \sin 8\pi n_0 t \right) \sin \frac{2\pi x}{l} + \text{etc} \right], \quad (E)$$

where δ is the central deflection produced by the load W when placed at the centre

In spans of a sufficient length to justify neglecting the inertia effects of the moving mass, $v/2ln_0$ is a small fraction, and the state of oscillation included in formula (E) can hardly add 10 per cent to the crawl deflection. Accordingly, this theory tends to confirm a statement made earlier in this paper that smooth-running locomotives produce but little vibration in a bridge, the deflection at all practicable speeds being nearly identical with the crawl deflection.

The result of applying the foregoing theory is illustrated by fig. 4, which gives the deflection at the centre of the girder plotted to a base which represents the position of the load. In order to draw a comparison with experimental records given later, the bridge characteristics taken in the calculation agree with those of Newark Dyke Bridge, a single-track bridge on the main line of the London and North Eastern Railway. The span is 262.5 feet, the total mass is 460 tons, and the unloaded frequency is 2.88 oscillations per second. For the locomotive the hammer blow is 0.576 ton at one revolution per second, the circumference of the driving wheels is 14.0625 feet and the total weight is 107.65 tons.

In the calculation the locomotive is treated as a concentrated load, and the central deflection produced by this load placed at the centre is 0.55 inch. When the locomotive is at the centre of the bridge the frequency of the structure is reduced to 2.4 oscillations per second. The engine speed is taken as 2.4 revolutions per second or approximately 23 miles per hour, and the calculation is based upon the somewhat inaccurate assumption that during the passage of the locomotive the frequency of the girder has the constant value 2.4, so that the condition of synchronism is realised in its fullest possible form. It will be seen that the oscillations continue to mount up until the load leaves the bridge and the maximum deflection exceeds the crawl deflection by 75 per cent.

The violence of these oscillations is greatly in excess of those actually observed.

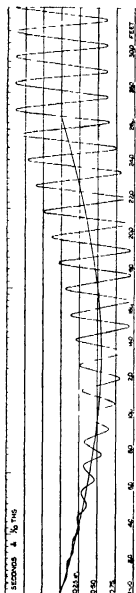


FIG 4.—Undamped Synchronous Oscillation.



FIG 5.—Damped Synchronous Oscillation.



FIG 7.—Oscillation due to a Moving Mass, Hammer blow, zero Speed 75 m p.h.

in Newark Dyke Bridge, and this lack of agreement between experiment and theory is due to the fact that in the latter neither the change in natural frequency due to the passage of the moving mass nor the influence of damping have been taken into account

Effect of Damping

Consider again the case represented by fig 3. The damping is assumed to be a distribution of force along the bridge which varies with the velocity of the vertical movement. For convenience this load distribution per unit length will be represented by $4\pi n_b m \frac{dy}{dt}$, where n_b is a damping coefficient which has the dimension of a frequency. Taking into account only the primary harmonic component of the applied alternating force, the state of oscillation it sets up is given by the equation

$$EI \frac{d^4 y}{dx^4} + 4\pi n_b m \frac{dy}{dt} + m \frac{d^2 y}{dt^2} = \frac{2P}{l} \sin 2\pi Nt \sin 2\pi nt \sin \frac{\pi x}{l},$$

and a particular integral of this equation is

$$y = \frac{D}{2} \left[\frac{\cos \{2\pi (N - n) t - \phi\}}{\left[\left\{ 1 - \left(\frac{N - n}{n_0} \right)^2 \right\}^2 + \left\{ \frac{n_b (N - n)}{n_0^2} \right\}^2 \right]^{\frac{1}{2}}} - \frac{\cos \{2\pi (N + n) t - \psi\}}{\left[\left\{ 1 - \left(\frac{N + n}{n_0} \right)^2 \right\}^2 + \left\{ \frac{n_b (N + n)}{n_0^2} \right\}^2 \right]^{\frac{1}{2}}} \right] \sin \frac{\pi x}{l}, \quad (F)$$

where

$$\tan \phi = \frac{n_b (N - n)}{n_0^2 - (N - n)^2} \quad \text{and} \quad \tan \psi = \frac{n_b (N + n)}{n_0^2 - (N + n)^2}$$

The free oscillations of the girder are given by

$$EI \frac{d^4 y}{dx^4} + 4\pi n_b m \frac{dy}{dt} + m \frac{d^2 y}{dt^2} = 0,$$

and provided that n_b is less than n_0 , this yields a fundamental mode of vibration of the form

$$y = e^{-\alpha t} [A \sin \beta t + B \cos \beta t] \sin \frac{\pi x}{l},$$

where

$$\pi = 2\pi n_b \quad \text{and} \quad \beta = 2\pi \sqrt{n_0^2 - n_b^2}$$

In any practical case relating to a bridge oscillation, n_b^2 is negligible in comparison with n_0^2 , the fundamental frequency is hardly affected by damping, and a sufficiently accurate representation of the fundamental mode of vibration is given by

$$y = e^{-2\pi n_b t} [A \sin 2\pi n_0 t + B \cos 2\pi n_0 t] \sin \frac{\pi x}{l} \quad (G)$$

The form of this equation indicates that free oscillations die out in geometric progression. For long span bridges this decrease as indicated by the subsidence of residual vibrations is not very rapid. A ratio of 0.85 for successive oscillations is fair average estimate and the value of n_b will not in general exceed 1/10.

The complete expression for the oscillation set up by the alternating force must satisfy the conditions that $y = 0$ and $dy/dt = 0$ when $t = 0$. These starting conditions are adjusted by superposing upon the forced oscillation given by formula (F) a free oscillation of the character defined by formula (G), the constants A and B being selected so as to satisfy the two conditions.

As in the previous case of the undamped girder, the forced oscillation due to the gravity force is indistinguishable from the crawl deflection, but in order to smooth away the abrupt commencement of this deflection, another free oscillation has to be brought into existence. The result of applying this full process is depicted in fig. 5 (p. 71).

The case is the same as that which gave rise to fig. 4, the only difference being the introduction of damping. The value of n_b is taken as 0.075, which causes free oscillations to die out in a geometric progression having a common ratio 0.82. A comparison of figs. 4 and 5 reveals the fact that a small amount of damping can exert a powerful effect in subduing the oscillations generated under conditions of resonance, and by taking this influence into account theoretical predictions relating to actual bridges assume some semblance to reality.

If the value of n_b as deduced from the subsidence of the residual vibrations in the bridge is employed, the state of oscillation predicted in the case of resonance is still appreciably greater than that recorded by experiment. The agreement, however, is sufficiently good to suggest that analysis is proceeding in the right direction, and with some degree of confidence we now pass on to the more complete theory in which the inertia of the moving load is taken into account.

Impact Effects due to Hammer-Blow, taking into account the Mass of the Moving Load and Bridge Damping

The problem to be investigated is illustrated by fig. 6

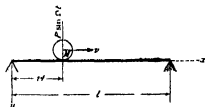


FIG. 6

Most of the symbols involved have already been defined, but for convenience they are now re-stated in the following table —

M_G is the total mass of the girder ,

m is the mass of the girder per unit length ,

l is the length of span ,

I is the moment of inertia of the cross section ,

$\omega_0 = 2\pi n_0 = \frac{\pi^2}{l^2} \sqrt{\frac{EI}{M_G}}$, defines the natural frequency of the girder ,

$1\pi n_b m \frac{dy}{dt}$ is the distribution of force which produces damping ,

M is the moving mass ,

v is the velocity of the mass along the girder ,

$P \sin 2\pi Nt$ is the hammer blow associated with the moving load ,

$\omega = 2\pi n = \frac{\pi v}{l}$,

$\Omega = 2\pi N$,

$\omega_b = 2\pi n_b$

Adopting the approximation which has been justified in previous cases, it will be assumed that the state of oscillation owes its existence almost entirely to the primary component of the reaction between the moving load and the girder and that the higher harmonic components of this reaction can be neglected.

On this assumption, and leaving out of account the effect of gravity, the equation of motion for the girder takes the form

$$EI \frac{d^4 y}{dx^4} + 2\omega_b m \frac{dy}{dt} + m \frac{d^2 y}{dt^2} - \frac{2}{l} \left[P \sin \Omega t - M \frac{d^2 h}{dt^2} \right] \sin \omega t \sin \frac{\pi x}{l},$$

where h is the depth of M below its mean level

A solution of this equation is obtained in the form $y = f(t) \sin \frac{\pi x}{l}$, consequently $h = f(t) \sin \omega t$ and

$$\frac{d^2 h}{dt^2} = \sin \omega t \frac{d^2 f}{dt^2} + 2\omega \cos \omega t \frac{df}{dt} - \omega^2 \sin \omega t f(t)$$

To determine $f(t)$ we have the differential equation

$$\begin{aligned} \frac{\pi^4}{l^4} f(t) + 2\omega_b m \frac{df}{dt} + m \frac{d^2 f}{dt^2} + \frac{2M}{l} \left[\sin^2 \omega t \frac{d^2 f}{dt^2} + \omega \sin 2\omega t \frac{df}{dt} - \omega^2 \sin^2 \omega t f(t) \right] \\ = \frac{2P}{l} \sin \Omega t \sin \omega t, \end{aligned}$$

and this reduces to

$$f(t) \left[\omega_0^2 - \frac{M\omega^2}{M_G} (1 - \cos 2\omega t) \right] + \frac{df}{dt} \left[2\omega_0 + \frac{2M}{M_G} \omega \sin 2\omega t \right] + \frac{d^2f}{dt^2} \left[1 + \frac{M}{M_G} (1 - \cos 2\omega t) \right] = \frac{P}{M_G} [\cos (\Omega - \omega) t - \cos (\Omega + \omega) t] \quad (\text{II})$$

An exact solution can hardly be expected for this somewhat complicated differential equation, but two alternative methods are available for deducing numerical results. The first and least laborious method is limited in its application to cases in which the varying frequency of the girder due to the passage of the moving load does not at any instant synchronise with the constant frequency of the applied alternating force.

In the second method of attack the solution is obtained in the form of a convergent series. The numerical work involved is distinctly laborious, but it is free from the limitation restricting the application of the other more concise method.

Approximate Solution applicable to Non-Synchronous Cases

Consider the solution of the equation

$$f(t) \left[\omega_0^2 - \frac{2M}{M_G} \omega^2 \sin^2 \omega t \right] + 2 \frac{df}{dt} \left[\omega_0 + \frac{M}{M_G} \sin 2\omega t \right] + \frac{d^2f}{dt^2} \left[1 + \frac{2M}{M_G} \sin^2 \omega t \right] = \frac{P}{M_G} \cos \Omega_1 t, \quad \text{where } \Omega_1 = \Omega - \omega$$

Let

$$f(t) = \cos \Omega_1 t \phi(t) + \sin \Omega_1 t \psi(t)$$

Unless a state of synchronism occurs at some stage in the passage of the moving and pulsating load, it will be found that the time variations of $\phi(t)$ and $\psi(t)$ are always small in comparison with those of $\cos \Omega_1 t$ and $\sin \Omega_1 t$.

Consequently

$$\frac{df}{dt} = \Omega_1 [-\sin \Omega_1 t \phi(t) + \cos \Omega_1 t \psi(t)] \text{ approximately,}$$

and

$$\frac{d^2f}{dt^2} = -\Omega_1^2 [\cos \Omega_1 t \phi(t) + \sin \Omega_1 t \psi(t)] \text{ approximately}$$

Hence, by substituting these approximate values in the original equation

$$\begin{aligned} \cos \Omega_1 t \left\{ \left(\omega_0^2 - \frac{2M}{M_G} \omega^2 \sin^2 \omega t \right) \phi(t) + 2 \left(\omega_b + \frac{M}{M_G} \omega \sin 2\omega t \right) \Omega_1 \psi(t) \right. \\ \left. - \left(1 + \frac{2M}{M_G} \sin^2 \omega t \right) \Omega_1^2 \phi(t) \right\} \\ + \sin \Omega_1 t \left\{ \left(\omega_0^2 - \frac{2M}{M_G} \omega^2 \sin^2 \omega t \right) \psi(t) - 2 \left(\omega_b + \frac{M}{M_G} \omega \sin 2\omega t \right) \Omega_1 \phi(t) \right. \\ \left. - \left(1 + \frac{2M}{M_G} \sin^2 \omega t \right) \Omega_1^2 \psi(t) \right\} \\ = \frac{P}{M_G} \cos \Omega_1 t \end{aligned}$$

Equating coefficients of $\cos \Omega_1 t$ and $\sin \Omega_1 t$

$$\begin{aligned} \left\{ \omega_0^2 - \Omega_1^2 - \frac{2M}{M_G} (\Omega_1^2 + \omega^2) \sin^2 \omega t \right\} \phi(t) \\ + 2\Omega_1 \left\{ \omega_b + \frac{M}{M_G} \omega \sin 2\omega t \right\} \psi(t) = \frac{P}{M_G}, \end{aligned}$$

and

$$\begin{aligned} \left\{ \omega_0^2 - \Omega_1^2 - \frac{2M}{M_G} (\Omega_1^2 + \omega^2) \sin^2 \omega t \right\} \psi(t) \\ - 2\Omega_1 \left\{ \omega_b + \frac{M}{M_G} \omega \sin 2\omega t \right\} \phi(t) = 0 \end{aligned}$$

Hence

$$\phi(t) = \frac{P}{M_G} \frac{\omega_0^2 - \Omega_1^2 - \frac{2M}{M_G} (\Omega_1^2 + \omega^2) \sin^2 \omega t}{\Omega_1^2 \left[2\omega_b + \frac{2M}{M_G} \omega \sin 2\omega t \right]^2 + \left[\omega_0^2 - \Omega_1^2 - \frac{2M}{M_G} (\Omega_1^2 + \omega^2) \sin^2 \omega t \right]^2},$$

and

$$\psi(t) = \frac{P}{M_G} \frac{\Omega_1 \left[2\omega_b + \frac{2M}{M_G} \omega \sin 2\omega t \right]}{\Omega_1^2 \left[2\omega_b + \frac{2M}{M_G} \omega \sin 2\omega t \right]^2 + \left[\omega_0^2 - \Omega_1^2 - \frac{2M}{M_G} (\Omega_1^2 + \omega^2) \sin^2 \omega t \right]^2}.$$

If D is the central deflection produced by a steady central force P ,

$$\frac{P}{M_G} = \frac{D}{2} \omega_0^2 = \frac{D}{2} [4\pi^2 n_0^2]$$

Let $\Omega_1 = 2\pi N_1$

Then using the notation

$$\omega_b = 2\pi n_b, \quad \omega = 2\pi \frac{v}{2l},$$

and dividing through by $4\pi^2$

$$\phi(t) = \frac{D}{2} n_0^2 \frac{n_0^2 - N_1^2 - \frac{2M}{M_G} \left(N_1^2 + \frac{v^2}{4l^2} \right) \sin^2 \frac{\pi v t}{l}}{N_1^2 \left[2n_b + \frac{M}{M_G} \frac{v}{l} \sin \frac{2\pi v t}{l} \right]^2 + \left[n_0^2 - N_1^2 - \frac{2M}{M_G} \left(N_1^2 + \frac{v^2}{4l^2} \right) \sin^2 \frac{\pi v t}{l} \right]^2}$$

$$\psi(t) = \frac{D}{2} n_0^2 \frac{N_1 \left[2n_b + \frac{M}{M_G} \frac{v}{l} \sin \frac{2\pi v t}{l} \right]}{N_1^2 \left[2n_b + \frac{M}{M_G} \frac{v}{l} \sin \frac{2\pi v t}{l} \right]^2 + \left[n_0^2 - N_1^2 - \frac{2M}{M_G} \left(N_1^2 + \frac{v^2}{4l^2} \right) \sin^2 \frac{\pi v t}{l} \right]^2}$$

Abrupt variations in $\phi(t)$ and $\psi(t)$ only occur when the expression

$$n_0^2 - N_1^2 - \frac{2M}{M_G} \left(N_1^2 + \frac{v^2}{4l^2} \right) \sin^2 \frac{\pi v t}{l}$$

passes through a zero value, the variations due to the other term in the denominators which is numerically small being relatively unimportant

Owing to the smallness of $v^2/4l^2$ in comparison with N_1^2 , this zero condition in effect states an equivalence between N_1 and the loaded frequency of this bridge. As long as this equivalence is avoided by an ample margin, the assumption that the variations in $\phi(t)$ and $\psi(t)$ are small in comparison with those of $\sin \Omega t$ and $\cos \Omega t$ is justifiable, and the state of forced oscillation can be expressed in the form

$$y = \frac{D}{2} n_0^2 \left[\frac{\phi_1 \cos 2\pi N_1 t + \psi_1 \sin 2\pi N_1 t}{\phi_1^2 + \psi_1^2} - \frac{\phi_2 \cos 2\pi N_2 t + \psi_2 \sin 2\pi N_2 t}{\phi_2^2 + \psi_2^2} \right] \sin \frac{\pi v t}{l},$$

where

$$N_1 = N - \frac{v}{2l}, \quad N_2 = N + \frac{v}{2l},$$

$$\phi_1 = n_0^2 - N_1^2 - \frac{2M}{M_G} \left(N_1^2 + \frac{v^2}{4l^2} \right) \sin^2 \frac{\pi v t}{l},$$

$$\psi_1 = N_1 \left[2n_b + \frac{M}{M_G} \frac{v}{l} \sin \frac{2\pi v t}{l} \right],$$

$$\phi_2 = n_0^2 - N_2^2 - \frac{2M}{M_G} \left(N_2^2 + \frac{v^2}{4l^2} \right) \sin^2 \frac{\pi v t}{l},$$

$$\psi_2 = N_2 \left[2n_b + \frac{M}{M_G} \frac{v}{l} \sin \frac{2\pi v t}{l} \right]$$

In practice it is convenient to express the oscillations in terms of the maximum crawl deflection, since this measurement is always recorded in an actual bridge test. Let δ denote this quantity, which in the idealised case under consideration is the central deflection produced by a steadily applied central load M . Let P_1 be the hammer blow at one revolution per second. The hammer blow at N revolutions is $P_1 N^2$, and this steadily applied at the centre has been taken to give a central deflection D .

Consequently

$$D = \delta \frac{P_1 N^2}{M},$$

and the expression for forced oscillation takes the form

$$y = \frac{P_1 N^2 n_0^2}{2M} \delta \left[\begin{aligned} & \sin 2\pi Nt \left\{ \left(\frac{\phi_1}{\phi_1^2 + \psi_1^2} + \frac{\phi_2}{\phi_2^2 + \psi_2^2} \right) \sin \frac{\pi vt}{l} \right. \\ & \quad \left. + \left(\frac{\psi_1}{\phi_1^2 + \psi_1^2} - \frac{\psi_2}{\phi_2^2 + \psi_2^2} \right) \cos \frac{\pi vt}{l} \right\} \\ & + \cos 2\pi Nt \left\{ \left(\frac{\phi_1}{\phi_1^2 + \psi_1^2} - \frac{\phi_2}{\phi_2^2 + \psi_2^2} \right) \cos \frac{\pi vt}{l} \right. \\ & \quad \left. - \left(\frac{\psi_1}{\phi_1^2 + \psi_1^2} + \frac{\psi_2}{\phi_2^2 + \psi_2^2} \right) \sin \frac{\pi vt}{l} \right\} \end{aligned} \right] \sin \frac{\pi x}{l} \quad (J)$$

For non-synchronous cases to which this formula is restricted, the maximum state of oscillation is to be expected when the load is at the centre, that is to say, when $\pi x/l = \pi/2$. This maximum state of oscillation is accordingly defined by

$$y = \frac{P_1 N^2 n_0^2}{2M} \delta \left\{ \sin 2\pi Nt \left(\frac{\phi_1}{\phi_1^2 + \psi_1^2} + \frac{\phi_2}{\phi_2^2 + \psi_2^2} \right) - \cos 2\pi Nt \left(\frac{\psi_1}{\phi_1^2 + \psi_1^2} + \frac{\psi_2}{\phi_2^2 + \psi_2^2} \right) \right\} \sin \frac{\pi x}{l},$$

where $\phi_1, \phi_2, \psi_1, \psi_2$ have the particular values consequent on putting $\pi x/l = \pi/2$.

Series Method of solving the Equation

$$\begin{aligned} f(t) \left[\omega_0^2 - \frac{M}{M_G} \omega^2 (1 - \cos 2\omega t) \right] + \frac{df}{dt} \left[2\omega_0 + \frac{2M}{M_G} \omega \sin 2\omega t \right] \\ + \frac{d^2 f}{dt^2} \left[1 + \frac{M}{M_G} (1 - \cos 2\omega t) \right] = \frac{P}{M_G} [\cos (\Omega - \omega) t - \cos (\Omega + \omega) t] \quad (H) \end{aligned}$$

This method is applicable to all cases, but is particularly suitable for those in which synchronism occurs.

Let

$$f(t) = \sum_{r=-\infty}^{+\infty} [A_r \cos(\Omega + r\omega)t + B_r \sin(\Omega + r\omega)t]$$

where r is any odd number positive or negative

By substitution it appears that the coefficient of $\cos(\Omega + r\omega)t$ for the left-hand side of the equation is

$$A_r \left[\omega_0^2 - (\Omega + r\omega)^2 - \frac{M}{M_G} \{ \omega^2 + (\Omega + r\omega)^2 \} \right] + B_r 2\omega_0 (\Omega + r\omega) \\ + A_{r-2} \frac{M}{2M_G} (\Omega + r-1\omega)^2 + A_{r+2} \frac{M}{2M_G} (\Omega + r+1\omega)^2,$$

and the coefficient of $\sin(\Omega + r\omega)t$ is

$$B_r \left[\omega_0^2 - (\Omega + r\omega)^2 - \frac{M}{M_G} \{ \omega^2 + (\Omega + r\omega)^2 \} \right] - A_r 2\omega_0 (\Omega + r\omega) \\ + B_{r-2} \frac{M}{2M_G} (\Omega + r-1\omega)^2 + B_{r+2} \frac{M}{2M_G} (\Omega + r+1\omega)^2$$

The right-hand side of equation (H) can be expressed in the form

$$\frac{D}{2} \omega_0^2 [\cos(\Omega - \omega)t - \cos(\Omega + \omega)t],$$

where D is the central deflection produced by a steady central load P

Abbreviating the notation by writing

$$n_0^2 = \frac{M}{M_G} n^2 - p_0^2,$$

$$N + rn = q_r,$$

and equating the coefficients of $\cos(\Omega + r\omega)t$ and $\sin(\Omega + r\omega)t$ on both sides of the equation, the following relations are established —

$$A_r \left[p_0^2 - \frac{M + M_G}{M_G} q_r^2 \right] + B_r 2n_0 q_r + A_{r-2} \frac{M}{2M_G} q_{r-1}^2 + A_{r+2} \frac{M}{2M_G} q_{r+1}^2$$

$$\text{has the value } \frac{D}{2} n_0^2 \text{ when } r = -1,$$

$$\text{has the value } -\frac{D}{2} n_0^2 \text{ when } r = +1,$$

$$\text{has the value zero for all other values of } r$$

$$B_r \left[p_0^2 - \frac{M + M_G}{M_G} q_r^2 \right] - A_r 2n_0 q_r + B_{r-2} \frac{M}{2M_G} q_{r-1}^2 + B_{r+2} \frac{M}{2M_G} q_{r+1}^2$$

is zero for all values of r

From these equations the coefficients in the series

$$\sum [A_r \cos (\Omega + r\omega) t + B_r \sin (\Omega + r\omega) t]$$

can be determined to any degree of accuracy which may be desired

If the solution only extends, say, from $r = -11$ to $r = +11$, there will be a lack of balance represented by small terms of the character $\cos (\Omega + 13\omega) t$, $\sin (\Omega + 13\omega) t$, $\cos (\Omega - 13\omega) t$, $\sin (\Omega - 13\omega) t$. These can be regarded as small forces, and their neglect is justified if the period of these forces is either much above or much below the range of frequency of the loaded structure. The series must, in fact, be extended in both directions until it passes right outside this range, and this method of solution is particularly applicable to a case in which the frequency of the hammer-blow is well inside the range of frequency of the loaded structure, because, under these conditions, the series does not have to be carried far in either direction.

For a non-synchronous case, the series in one direction is apt to be divergent before it ultimately becomes convergent, and to such a case it is preferable to apply the approximate method of solution established previously.

Since the forced oscillation does not in general satisfy the condition that the girder is initially at rest with zero velocity, it is necessary to superpose another state of oscillation obtained by solving the equation

$$f(t) \left[\omega_0^2 - \frac{2M}{M_0} \omega^2 \sin^2 \omega t \right] + 2 \frac{df}{dt} \left[\omega_0 + \frac{M}{M_0} \sin 2\omega t \right] + \frac{d^2 f}{dt^2} \left[1 + \frac{2M}{M_0} \sin^2 \omega t \right] = 0 \quad (K)$$

A solution of this can be effected in the form

$$f(t) = e^{-\alpha t} \sum_{r=-\infty}^{+\infty} [A_r \cos (\beta + r\omega) t + B_r \sin (\beta + r\omega) t],$$

where r is any even number, positive, negative or zero

By substituting and equating separately to zero the coefficients of $\cos (\beta + r\omega) t$, $\sin (\beta + r\omega) t$, two general relations between A_{r+2} , B_{r+2} , A_r , B_r , A_{r-2} , B_{r-2} can be established. If a limit is put to the extension of the series in both directions, the "A" coefficient can all be expressed in terms of A_0 , α and β , and the "B" coefficient can all be expressed in terms of B_0 , α and β . Finally, equating to zero the coefficients of $\cos \beta t$ and $\sin \beta t$, two equations are obtained from which values of α and β can be determined. If a high degree of accuracy is desired, it is attainable by this process, but in practical bridge calculations the accuracy required hardly justifies the laborious computations involved in this

method The state of oscillation under examination is one which soon dies down to insignificance It is only concerned with the early stages in the growth of the bridge oscillations, and for its determination the approximate method, which follows, is sufficiently accurate for all practical purposes

Approximate Method for determining the State of Free Oscillation in a Girder when traversed by a Concentrated Mass and subjected to Damping

Consider a solution of equation (K) of the form $f(t) = e^{-\alpha t} \sin \beta t$, where α and β are function of t , or the position of the load on the girder These variations of α and β over a limited period of time, say, the period of one free oscillation, are hardly appreciable, and over such a period α and β can, without serious loss of accuracy, be treated as constants.

On this assumption

$$\frac{df}{dt} = -\alpha e^{-\alpha t} \sin \beta t + \beta e^{-\alpha t} \cos \beta t,$$

and

$$\frac{d^2f}{dt^2} = (\alpha^2 - \beta^2) e^{-\alpha t} \sin \beta t - 2\alpha\beta e^{-\alpha t} \cos \beta t$$

Substituting in the equation for $f(t)$, and equating separately to zero the coefficients of $\cos \beta t$, $\sin \beta t$, the values of α and β for the particular period under consideration are given by

$$\alpha = \frac{\omega_0 + \frac{M}{M_G} \omega \sin 2\omega t}{1 + \frac{2M}{M_G} \sin^2 \omega t},$$

$$\beta^2 = \frac{\omega_0^2 - \frac{2M}{M_G} \omega^2 \sin^2 \omega t}{1 + \frac{2M}{M_G} \sin^2 \omega t} - \left[\frac{\omega_0 + \frac{M}{M_G} \omega \sin 2\omega t}{1 + \frac{2M}{M_G} \sin^2 \omega t} \right]^2$$

Another way of arriving at this same conclusion is to assume that over a limited period of time the coefficients of $f(t)$, df/dt and d^2f/dt^2 in the differential equation for $f(t)$ can be treated as constants Neglecting, in the expression for β , certain terms which have no numerical importance, values for α and β which

can be employed when the load has advanced a distance x along the bridge are given by

$$\alpha = \frac{2\pi \left[n_0 + \frac{M}{M_G} \frac{v}{2l} \sin \frac{2\pi x}{l} \right]}{1 + \frac{2M}{M_G} \sin^2 \frac{\pi x}{l}},$$

$$\beta = \frac{2\pi n_0}{1 + \frac{2M}{M_G} \sin^2 \frac{\pi x}{l}}$$

When $t = 0$ the state of free oscillation is

$$y = e^{-2\pi n_0 t} [A \sin 2\pi n_0 t + B \cos 2\pi n_0 t],$$

and by a suitable choice of A and B this free oscillation can be adjusted to satisfy the starting conditions. By dividing the girder into a number of short lengths and applying to each length in turn the approximate method just explained, the manner in which the superposed free oscillation dies out can be predicted with an accuracy quite sufficient for all practical purposes. If hammer blow does not exist, the deflection produced by the moving mass is merely the crawl deflection combined with a state of free oscillation which smooths off the abrupt commencement and termination of the crawl deflection.

One result of applying this foregoing general analysis to the case of Newark Dyke Bridge is shown in fig 7 (p 71). The data for the bridge have already been given. The locomotive is treated as a concentrated mass of 107.65 tons, and, in the case illustrated, it is taken to be running smoothly without hammer blow at a speed of $57\frac{1}{2}$ miles per hour.

It will be seen that the dynamic effect of the load is quite small, and if it were possible to dispense with balance weights in steam locomotives, impact allowances for railway bridges would shrink into insignificance.

This problem of the dynamic effect of a smooth-running load was investigated by Sir G. G. Stokes as far back as 1849*. His treatment was mainly restricted to cases in which the mass of the bridge was neglected. Its unloaded frequency in consequence was infinitely high, and this, added to the fact that damping was not taken into account, led to results which, though interesting from a mathematical standpoint, can hardly be applied to predict the behaviour of actual bridges. Further results of applying the general analysis to the case of Newark Dyke Bridge are shown in fig 8.

Eleven different engine frequencies have been examined, the locomotives in

* 'Proc Camb Phil Soc,' vol. 1, p 83 (1849)

each case developing a hammer blow having the value of 0.576 ton at one revolution per second

For the two lowest and the three highest engine frequencies the approximate method of analysis was employed. For the six intermediate cases, conditions of synchronism necessitated the series method of solution. The experimental records actually observed by the Bridge Stress Committee when a locomotive having the same characteristics traversed the bridge at various speeds are shown in fig. 9. In both diagrams the curves give the deflection at the centre plotted to a base which represents the position of the locomotive. In the experiments some difficulty was experienced in maintaining a constant speed for the locomotive. The periodicities recorded represent fairly accurately the frequency of the hammer blows when the locomotive was at the centre, but in some of the records, particularly the case defined by $N = 2.4$, there is evidence that the engine speed was increased during the latter part of the run.

Making allowance for some small uncertainty in the specification of the hammer-blow frequencies, the agreement between theory and experiment is sufficiently close to justify the belief that the foregoing mathematical analysis, which takes into account the inertia of the moving load and the damping in the bridge, is capable of predicting oscillations with an accuracy sufficiently good to form the basis for the calculation of bridge impact allowance.

Owing to the distributed character of the load, it will be observed that in the experimental records the crawl deflection does not start down abruptly as it does when the locomotive is idealised into a concentrated load. On this account in constructing the theoretical diagrams, the state of free oscillation necessary to eliminate the initial slope of the crawl deflection has not been included, since, for the purpose of comparison, its introduction would constitute a departure from reality.

Theory and experiment agree in demonstrating that the most violent state of oscillation occurs when $N = 2.4$, that is, when synchronism occurs as the locomotive passes over the centre of the bridge. The residual oscillations recorded for this case are considerably greater than those predicted by theory, but this can be accounted for by a speeding up of the locomotive as it approached the end of the bridge.

The maximum deflections show a good agreement between predicted and recorded results throughout the whole range of speeds, and the rapid diminution of the impact effects predicted by theory when the engine frequency passes outside the range of frequency of the bridge is well confirmed by the experimental records. At the highest speed ($N = 6$), amounting to $57\frac{1}{2}$ miles per hour,

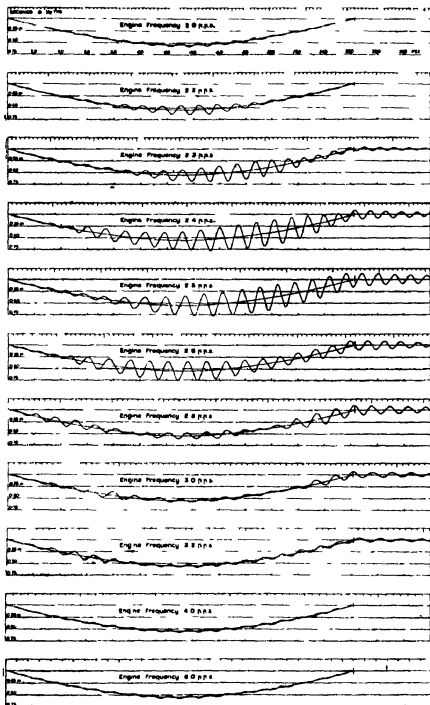
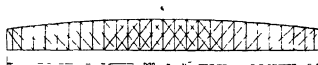


FIG 8—Theoretical Deflection Curves. Newark Dyke.

SPAN N° 2

NEWARK DYKE



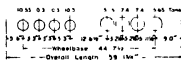
Loaded Frequency of Bridge 3.4 cps
 Unloaded Frequency of Bridge 6.0 cps



TEST LOAD

LOCOMOTIVE

Total Weight 107.65 T



Clearance of Driver 14.05m

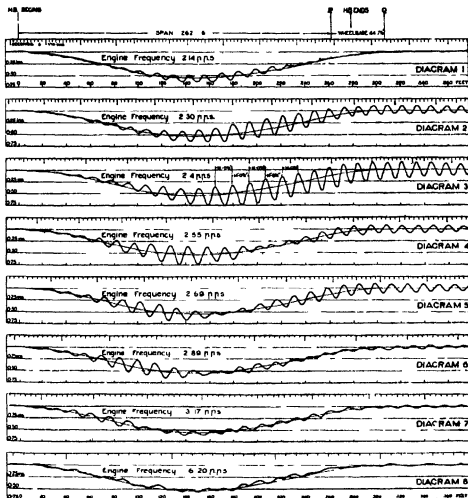


FIG 9—Deflection Curves.

although the hammer blow is nearly 21 tons, its frequency so greatly exceeds that of the bridge that its capability of producing oscillations is reduced to insignificance. For engine speeds lying within the range of the bridge frequency, that is, for cases between $N = 2.4$ and $N = 2.9$, the passage through a condition of resonance is likely to produce the phenomenon of "beats." This expectation is fulfilled, and beats can be detected in both the theoretical and the experimental records.

A further check on the validity of the mathematical analysis has been provided by experiments on a model bridge performed at the Cambridge Engineering Laboratory.

Fig. 10 (Plate 1) is a photograph of the apparatus.

The bridge consists of two parallel rectangular steel bars giving a span of 12 feet. To eliminate damping, the bars rest on fixed knife edges at one end and on rocking knife edges at the other. The moving load is a two-wheeled truck stabilised by a small trailing wheel which runs on a centre rail supported independently of the bridge. The hammer-blow effect is produced by motor-driven wheels rotating in opposite directions and carrying balance weights. The frequency of the hammer blows and their magnitude can accordingly be altered at will and independently of the velocity of the truck. The truck in its approach run is accelerated by a falling weight, but it crosses the bridge at a constant speed. The central deflection is recorded directly by a needle on a moving celluloid film. In computing bridge oscillations, apart from damping, the quantities which have to be known are n_0 , M/M_0 , v/l , P/M and N . If these data are the same for two bridges, the state of oscillation will be the same.

The model bridge is designed so that $n_0 = 5.7$ and $M/M_0 = 2/5$, and these characteristics correspond to those of a bridge of about 120 feet span. Consequently, the behaviour of a locomotive on such a bridge can be deduced by experiment if the speed of the truck is made one-tenth the speed of the locomotive and its hammer blow is that of the locomotive reduced in the ratio of the mass of the truck to the mass of the locomotive. If it is desired to introduce damping, this can be done by locking the rocking knife edge and regulating the friction thus created until the free oscillations of the model bridge die out at the desired rate. Experiments with this model confirm theoretical predictions in a satisfactory manner. The degree of accuracy attained is illustrated by fig. 11. The full line represents the deflection computed by the series method of analysis and the dotted curve is the deflection obtained by experiment. The periodicity of the hammer blows was 4.4 periods per second and the speed was 12 feet per second.



FIG. 10

Up to this stage the analysis developed is only applicable to cases in which the whole mass of the locomotive can be regarded as unsprung. This con-

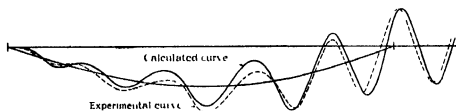


FIG 11 —Deflection Diagrams for Model Bridge.

dition is satisfied in long-span bridges such as Newark Dyke. An examination of the deflection records of that bridge reveals a maximum acceleration of 5.14 feet per second. The unsprung mass of the locomotive excluding the tender is about 45 tons, and to give this mass an acceleration of 5.14 feet per second calls for a force of 7.32 tons. Experimental evidence derived from an analysis of numerous bridge records leads to the belief that, in the case of this particular locomotive, it requires a force of at least 8 tons to overcome spring friction, and consequently in its passage across Newark Dyke Bridge no spring movement is likely to occur.

For short span bridges of, say, less than 30 feet, the frequency of the bridge even when loaded is so high in comparison with that of the hammer blows that the effect of these in producing deflection is almost purely statical.

This point is brought out by fig 12, which is an actual deflection record

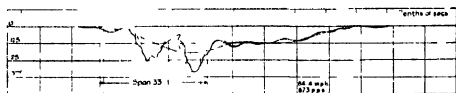


FIG 12.

taken by the Committee on a bridge of 33 feet span at Lancaster. The full line is the record obtained by experiment and the dotted line is the curve of deflection obtained by treating the hammer blows as if they were statical forces.

For bridges of intermediate length, say from 40 to 200 feet span, spring movement at high engine speeds is likely to occur. This movement has a profound effect on the state of oscillation generated by hammer blows, and a theory which fails to take this effect into account may be very misleading when applied

to bridges of moderate span. The motion of the sprung part of the locomotive modifies the apparent free periodicity of the bridge, and the friction in the spring movement exercises a powerful braking action which limits the extent to which the bridge oscillations can be developed.

The general effect which spring movement has on bridge oscillations can be studied by reference to fig 13, which represents a typical amplitude frequency curve for a bridge of moderate length, say 200 feet. The diagram shows how the maximum amplitude of the oscillation varies with the frequency of the hammer blow.

If the springs were locked, the amplitude frequency variation would follow the full-line curve. If spring movement occurs when the vertical acceleration exceeds a definite value, the amplitude frequency variation follows the dotted line.

Up to the frequency $N = 2.0$ the locomotive behaves as though it was without springs. The acceleration of the body of the locomotive then becomes more than spring friction can provide, spring movement is induced and provides a damping influence which rounds off the resonance peak which would occur if the springs had remained completely locked.

Spring movement ceases again when $N = 2.5$ and does not recommence until $N = 5$.

At this comparatively high frequency, although the amplitude of the motion is small, its acceleration is sufficient once again to break down spring friction, and from this point onwards in the range of frequencies spring movement will continue. The natural frequency of the locomotive on its springs is considerably less than 5, and as the oscillations of the bridge increase in frequency beyond this figure, the motion of the spring-borne part of the locomotive tends to become antiphased to the motion of the bridge.

The spring-borne part of the locomotive then in effect makes a negative mass contribution to the bridge, and the net inertia effect of the whole locomotive may be an increase rather than a decrease in the apparent natural frequency of the loaded structure.

Owing to this, a condition of resonance at a high frequency of hammer blow is established, and this resonance gives rise to the peak which occurs in fig 13, when $N = 6.35$.

If the engine frequency is limited to 6, for spans approaching 200 feet in length, this second peak is off the picture, and even if it was practically attainable, its height would be found to be less than that of the low frequency peak.

Fig 14 represents a typical amplitude frequency curve for a moderate span of,

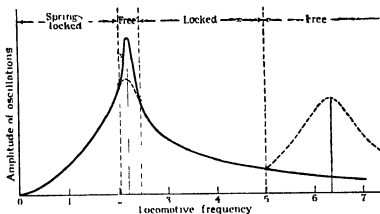


FIG 13.—Typical Amplitude Frequency Curve for a Bridge of 200 feet span.

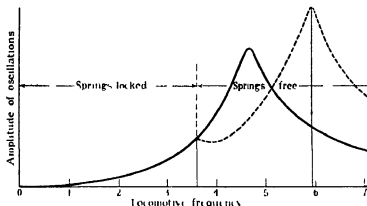


FIG 14.—Typical Amplitude Frequency Curve for a Bridge of 120-foot span.

say, 120 feet It differs from fig 13 in that there is no intermediate range of frequencies for which the springs become locked, and the second peak in this case is considerably higher than the first

Fig 15 gives a number of amplitude frequency results recorded by the Committee in experiments on Langport Bridge, having a span of 120 feet Though somewhat erratic, the records can be seen to group themselves along a curve which has the general character of the dotted curve in fig 14 The amplitudes first of all increase with the frequency This growth then receives a check, but at yet higher frequencies a more vigorous growth leading up to a high frequency condition of resonance is indicated, though owing to practical considerations relating to engine speeds this condition of resonance could not be fully attained

During the passage of a locomotive across a bridge the springs may be locked for parts of the run and free at other stages This consideration discourages

the application of mathematical analysis to predict the state of oscillation throughout a complete run, but in calculating impact allowances it is only

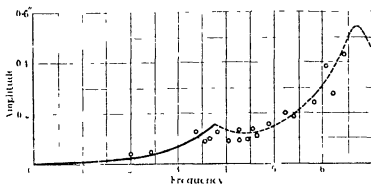


FIG 15—Langport Bridge Deflection Records.

essential to determine the maximum state of oscillation which will be developed, and a value for this which at any rate is not an underestimate can be obtained in the following manner —

Imagine a locomotive standing at the centre of the bridge and suppose that when the throttle is opened it starts skidding its driving wheels at a constant speed. A state of oscillation will thereby be generated which sets a superior limit to the maximum oscillation developed when the locomotive traverses the bridge at the same wheel speed.

This simplification of the problem does not introduce any great error, because, owing to the heavy damping introduced by spring movement, the oscillations reach their maximum in a space of time so short that it is only a fraction of the time taken by a locomotive in crossing a bridge of moderate span. In a long-span bridge, where the comparatively small amount of bridge damping alone exists to limit the oscillations, the full state of oscillation takes longer to develop, but as a compensation the period during which the locomotive is approximately at the centre of the bridge is extended. The kind of error introduced by predicting the maximum state of oscillation on the assumption that the locomotive remains stationary at the centre of the bridge is indicated by fig 16, which gives the maximum deflection curves, actual (with a moving locomotive) and predicted (on the assumption of a stationary oscillator) for Newark Dyke Bridge.

The calculation gives a value about 10 per cent in excess of the maximum recorded deflection, and this error at least has the merit of being on the safe side.

The analysis for deducing impact allowances based on the assumption that the

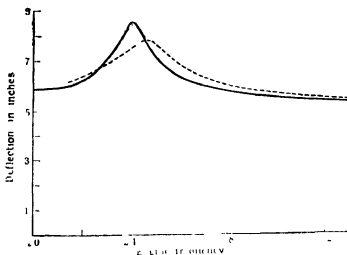


FIG 16

— Deflection produced by Central Oscillator
 ---- Deflection produced by Moving Locomotive.

bridge must be capable of withstanding the oscillating effect of a locomotive stationary at the centre of the bridge will now be considered

Oscillations due to a Locomotive situated at the Centre of a Bridge

The locomotive is supposed to be stationary but its driving wheels to be rotating N times per second

The bridge oscillator situated at the centre of the span, which for purposes of analysis replaces the actual locomotive, is represented by fig 17

M_s is the mass of the sprung load

M_1 is the mass of the unsprung load

M_0 is the total mass of the girder, l is its length and m its mass per unit length

$P \sin \Omega t$ is the alternating force action on M_1

$2\pi n_0 = \omega_0$ defines the unloaded frequency of the girder

$2\pi n_1 = \omega_1$ defines the frequency of the girder when carrying a mass M_1 at the centre

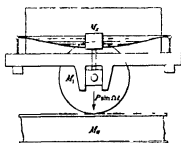


FIG 17 — Bridge Oscillator

$2\pi n_2 = \omega_2$ defines the frequency of the girder when carrying a mass $M_1 + M_2$ at the centre

$$\omega_0^2 = \frac{\pi^4 EI}{l^3 M_G}, \quad \omega_1^2 = \frac{\pi^4 EI}{l^3 [M_G + 2M_1]}, \quad \omega_2^2 = \frac{\pi^4 EI}{l^3 [M_G + 2M_1 + 2M_2]}.$$

Let h denote the depth of M_1 below its mean level

Let z denote the depth of M_2 below its mean level

Let $\mu(z - h)$ be the extra thrust in the springs due to the extra compression $(z - h)$

Let the damping effect due to resistances in the spring movement amount to a force $k \frac{d}{dt}(z - h)$ acting downwards on M_1 and upwards on M_2

Let $2\pi n_3 m \frac{dy}{dt}$ be an upward distribution of force representing the effect of damping in the girder

The equation of motion for the girder, assuming that concentrated forces are represented by their first harmonic component, is

$$\begin{aligned} EI \frac{d^4 y}{dx^4} + 2\pi n_3 m \frac{dy}{dt} + m \frac{d^2 y}{dt^2} \\ = \frac{2}{l} \left[P \sin \Omega t - M_1 \frac{d^2 h}{dt^2} + \mu(z - h) + \kappa \frac{d}{dt}(z - h) \right] \sin \frac{\pi x}{l} \quad (L) \end{aligned}$$

Obtaining a solution for this in the form $y = f(t) \sin \frac{\pi x}{l}$, $h = f(t)$ and the equation for $f(t)$ is

$$[M_G \omega_0^2 + 2\mu] f(t) + [2\pi n_3 M_G + 2\kappa] \frac{df}{dt} + M_G \frac{d^2 f}{dt^2} = 2P \sin \Omega t + 2\mu z + 2\kappa \frac{dz}{dt} \quad (M)$$

For the motion of M_1 ,

$$-M_1 \frac{d^2 z}{dt^2} = \mu(z - h) + \kappa \frac{d}{dt}(z - h)$$

or

$$M_1 \frac{d^2 z}{dt^2} + \kappa \frac{dz}{dt} + \mu z = \mu f(t) + \kappa \frac{df}{dt}. \quad (N)$$

For a free undamped oscillation of M_2 on its springs

$$M_2 \frac{d^2 z}{dt^2} + \mu z = 0,$$

and the oscillation is given by

$$z = A \sin 2\pi n_2 t,$$

where

$$4\pi^2 M_s^2 = \omega_s^2 = \frac{\mu}{M_s}$$

For a damped free oscillation

$$M_s \frac{d^2 z}{dt^2} + \kappa \frac{dz}{dt} + \mu z = 0,$$

and provided that $\kappa < 2M_s n_s$, the damped oscillation is given by

$$z = e^{-\frac{\kappa}{2M_s} t} \sin 2\pi \sqrt{n_s^2 - n_d^2} t,$$

where

$$2\pi n_d = \omega_d = \frac{\kappa}{2M_s}$$

Eliminating z between equations (M) and (N) and substituting $\frac{\kappa}{2M_s} = \omega_d$,

$\frac{\mu}{M_s} = \omega_s^2$, the equation for $f(t)$ can be reduced to the form

$$\begin{aligned} \frac{d^4 f}{dt^4} + \left[2 \frac{n_1^2}{n_2^2} \omega_d + \frac{2n_1^2}{n_0^2} \omega_b \right] \frac{d^3 f}{dt^3} + \left[\omega_1^2 + \frac{n_1^2}{n_2^2} \omega_s^2 + \frac{4n_1^2}{n_0^2} \omega_d \omega_b \right] \frac{d^2 f}{dt^2} \\ + \left[\frac{2n_1^2}{n_0^2} \omega_s^2 \omega_b + 2\omega_1^2 \omega_d \right] \frac{df}{dt} + \omega_1^2 \omega_s^2 f(t) \\ = -2 \frac{\Omega^2 - \omega_s^2}{M_T} P \sin \Omega t + \frac{4\Omega \omega_d}{M_T} P \cos \Omega t, \end{aligned}$$

where $M_T = M_G + 2M_1$

Solving the equation it is found that

$$f(t) = \frac{2P}{M_T} \frac{[(\Omega^2 - \omega_s^2)^2 + (2\Omega \omega_d)^2]^{\frac{1}{2}} \sin(\Omega t - \alpha)}{\left[\left\{ \Omega^4 - \Omega^2 \left(\omega_1^2 + \frac{n_1^2}{n_2^2} \omega_s^2 + \frac{4n_1^2}{n_0^2} \omega_d \omega_b \right) + \omega_1^2 \omega_s^2 \right\}^2 + \left\{ \left(2\omega_1^2 \omega_d + \frac{2n_1^2}{n_0^2} \omega_s^2 \omega_b \right) \Omega - \left(\frac{2n_1^2}{n_2^2} \omega_d + \frac{2n_1^2}{n_0^2} \omega_b \right) \Omega^2 \right\}^2 \right]^{\frac{1}{2}}}$$

The central deflection for a steady central load P is

$$\frac{2P}{M_G \omega_0^2} = \frac{2P}{M_T \omega_1^2} = D,$$

and under the action of the oscillator shown in fig 15 the centre of the girder

risks and falls periodically above and below its mean position by amount $D \times K$, where K , the dynamic magnification, has the value

$$K = \left\{ \frac{\psi_1^2 + \psi_2^2}{\phi_1^2 + \phi_2^2} \right\}^{\frac{1}{2}} n_1^2, \quad (P)$$

and

$$\begin{aligned} \psi_1 &= N^2 - n_s^2, \\ \psi_2 &= 2Nn_d, \\ \phi_1 &= N^4 - N^2n_1^2 \left(1 + \frac{4n_b n_d}{n_0^2} + \frac{n_s^2}{n_2^2} \right) + n_1^2 n_s^2, \\ \phi_2 &= 2Nn_1^2 \left(\frac{n_s^2 - N^2}{n_2^2} n_d + \frac{n_s^2 - N^2}{n_0^2} n_b \right) \end{aligned}$$

The particular case of the springless load is obtained by putting $z = h$ in equation (L). The value of the dynamic magnification thus deduced is

$$\frac{1}{\left\{ \left(1 - \frac{N^2}{n_1^2} \right)^2 + \left(\frac{2n_b N^2}{n_0^2} \right)^2 \right\}^{\frac{1}{2}}},$$

where n_1 is the frequency of the girder when carrying the full load at the centre.

This result can also be derived by putting n_d and n_s zero in the general formula (P). In that formula the dominating factor is ϕ_1 and when this function is zero the dynamic magnification becomes large.

There are two distinct values of N which makes $\phi_1 = 0$. These are the roots of the equation

$$N^4 - N^2 n_1^2 \left[1 + \frac{n_0^2}{n_2^2} + \frac{4n_b n_d}{n_0^2} \right] + n_1^2 n_s^2 = 0,$$

and the existence of these high and low critical frequencies accounts for the double peak formation of the amplitude frequency curves shown in figs 12 and 13.

Amplitude frequency curves for given bridges can be predicted by formula (P) and the class of agreement attained between theory and experiment is indicated by fig 15. The points recorded are those obtained by experiments on Langport Bridge, and the full and dotted lines are the amplitude frequency curves deduced by formula (P).

The accuracy of theoretical predictions is necessarily limited by the precision with which numerical values can be ascribed to the various bridge and locomotive characteristics entering into the composition of formula (P). There are six of these characteristics, viz., n_0 , n_1 , n_2 , n_b , n_s , n_d , and their numerical

determination presents no difficulty, with the exception of n_d and to a lesser extent n_s .

n_s is given by $4\pi^2 n_s = \mu/M_s$. Its evaluation demands a knowledge of the strength of the locomotive springs, and information on this point is apt to be somewhat vague.

The determination of n_d is by no means straightforward.

This coefficient specifies a force opposing spring movement and it owes its existence partly to the friction between the leaves of laminated springs and partly to the friction between the axle boxes and their guides.

If the spring movement defined by $(z - h)$ in equation (N) is given by $(z - h) = a \sin 2\pi(Nt - \alpha)$, then the damping force assumed in the analysis is $\kappa \times 2\pi Na \cos 2\pi(Nt - \alpha)$.

The variation of this is illustrated by the dotted line in fig 18. In any actual locomotive the frictional resistance in the spring movement will conform

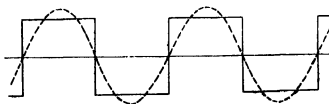


FIG 18

more nearly to the laws of friction between solids, and the variation of the damping force instead of being sinusoidal will approximate to the rectangular form indicated by the full line in fig 18.

If the dotted curve is the first harmonic component of the rectangular graph, the two forces will have almost identical effects in producing oscillations.

Consequently, by making $\kappa \times 2\pi Na = \frac{4}{\pi} f$, where f is the constant frictional force brought into operation by spring movement, the analysis which assumed a fluid friction type of damping is rendered applicable to the case of a locomotive in which the damping is of the dry friction variety.

The fact that κ and consequently n_d cannot be treated as independent of the amplitude of the spring movement introduces a slight complication. To determine κ from the condition just stated (a) must be known, but the determination of (a) by equations (M) and (N) in its turn requires a knowledge of κ . Consequently a "trial and error" method must be employed until an assumed value for κ and the corresponding deduced value for a are found which fit the condition

$\kappa a = 2f/\pi^2 N$ With a little experience this adjustment can be accomplished almost by guesswork

When spring movements occur, the locomotive characteristic f plays an important part in deciding impact allowances. This conclusion cannot be disregarded, though it is to be regretted because the value of f is apt to be somewhat indefinite. It varies considerably with different types of locomotives, and owing to the fact that the balance weights at high speeds introduce large pressures between the axle boxes and their guides, it is not altogether independent of the speed.

The variations which may occur in f are without doubt largely responsible for the inconclusive character of many series of bridge impact experiments performed in the past, and the difficulty which exists in deciding definite numerical values for this quantity constitutes the real and only obstacle in the way of setting the determination of impact allowances on a sound scientific basis.

Experiments can be devised to remove this difficulty, and it is hoped that before long adequate evidence relating to this important locomotive characteristic will be forthcoming to supplement the rather meagre data upon which analysis at present has to rely. The present position may be summed up by saying that whereas mathematical analysis is on sure ground when predicting impact effects for long or short bridges, in its application to bridges of medium span it is somewhat starved owing to an insufficiency of experimental data relating to the springing of locomotives.

At the commencement of this paper it was stated that in bridge impact researches experiment had tended to outrun theory, but the conclusions arrived at in the course of this present theoretical investigation suggest that, in one direction at any rate, mathematical analysis is pointing the way for a further experimental advance.

The theoretical researches dealt with in this paper have extended over a period of three years, and during that time much valuable and enthusiastic assistance has been received from students at the Cambridge Engineering Department. To mention them all by name would necessitate a lengthy list, and accordingly at this stage the author can only express his indebtedness to these numerous individuals collectively and anonymously.

Tribo-electricity and Friction 11—*Glass and Solid Elements*

By Prof P E SHAW, M A, D Sc, and C S FOX, B Sc, University College,
Nottingham

(Communicated by Sir William Hardy F R S —Received November 3, 1927)

1 Experience teaches us that the arrangement of solids in a tribo-electric series is fallacious. We shall show in the next paper that in the case of three solids (A, B, C) A may be positive to B, and B to C, and yet C be positive to A. This may occur when the bodies are of different classes, say, metal, textile, glass, which have different physical and chemical characteristics. In the case of one material, one characteristic predominates, in another, another may be paramount. The true arrangement may prove ultimately to be in branching or parallel lines rather than in one continuous line or series.

The problem is to obtain reliable data of sign and amount of charge when two *standard* solids are rubbed together. The only hope of progress lies in the use of material of known composition and—even more important—of definite surface cleanliness and physical structure. Further, to obtain quantitative results the rubbing should be performed, not by hand, but in some regulated machine to insure consistency of action.

Our plan is to divide the principal solids into several families. (1) Glasses, (2) Metals, (3) Textiles, (4) Other organic materials, such as waxes, celluloid, caoutchouc, (5) Solids which crystallize, especially when a single crystal is obtainable. The members of one family are rubbed with those of another in identical ways so that, varying one factor only, at a time, we may obtain comparable results. The simpler the materials and the more easy their surfaces are to clean, the easier it is to draw theoretical conclusions from the charges found. For these reasons the combination glass/elements is ideal.

We have already dealt with glass/textiles*.

Work on glass/metals has been done by Coehn and Lotz† and Coehn and Curs‡. They found that the noble metals Cu, Ag, Au, Pt, Hg are positive, and the baser metals Fe, Sn, Cd, Zn, Na, K, negative to glass. Their results are, however, qualitative.

2 In our experiments care is taken first to free the glass rod surfaces of organic or other defilement, as well as of strain, by boiling in chromic or nitric

* 'Roy Soc Proc,' A, vol 111, p 339 (1926)

† 'Z f Physik,' vol 5, p 242 (1921)

‡ 'Z f Physik,' vol 29, p 186 (1924)

acid, and then to treat it exhaustively with boiling water to remove residual acid. Chromic acid should be used for 15 minutes, nitric acid for 1 hour. The water treatment for chromic and nitric acids, respectively, should last for 8 hours and half an hour. The glass surfaces thus prepared we call "well-washed." If the washing is less thorough, residual acid remains and the surface is called "standard," as in the former paper. Another method of cleansing the glass is to fuse it and draw it out so as to produce a fresh surface. The elements employed are the purest we can obtain, but our experience is that commercial metals act for the present purpose like pure ones. Just before each rub the surfaces are scraped by a steel blade recently cleansed in a Bunsen flame. Other elements are commercial products which in such cases as Au, Pt, Ag, Pb are also very pure.

We wish to thank the Metallurgical Department, National Physical Laboratory, for the gift of specially pure elements.*

3 To commence with the experiments in air. Fig 1 shows a glass rod, A, mounted on ebonite pillars, EE. The inductor I, which consists of a metal plate, bent so as to lie below and beside the glass rod A, is insulated from the table and is joined as shown to the Hankel electroscope (see former paper, *loc cit*, the sensitiveness of the electroscope is of the same order as in that paper). Another glass rod C carrying the element B to be rubbed on A is clamped in brass block D. This is attached to the bar ZZ which moves freely in the collars GG.

A small amount of radium is enclosed in a lead box S. By the rod KK attached to it the radium can be drawn out of its box over A to discharge it. By the glass tube LL provided with a number of small holes as shown we can allow dry or moist hot air to flood the rod A during an experiment. The apparatus is enclosed in a wooden box, earthed.

To perform an experiment the operator pulls the rod ZZ and rotates it till B touches A. On letting go, a weight, attached to the rod ZZ by a string over a

* The purity of these elements and of the glasses used are certified by analysis to be —

	Per cent	" Soda " Glass		" Lead " Glass	
			Per cent		Per cent
Zn	99.95	SiO ₂	70.71	SiO ₂	52.91
Sn	99.99	Al ₂ O ₃	3.44	Sb ₂ O ₃	0.58
Al	99.96	CaO	6.86	PbO	34.37
Fe	99.99	MgO	0.17	Al ₂ O ₃	0.43
Ni	99.84	Na ₂ O	10.54	K ₂ O	11.81
Cr	100.00	K ₂ O	7.70		
Cd.	100.00	SO ₃	0.33		
Sb	99.7				

Vitreous silica is 100 per cent SiO₂

pulley, causes B to slide over A and then by a guide II to rise clear of it. During the rub the two surfaces are pressed together with a definite force by the weight W, and rub over a definite length. This process is repeated a number of times.

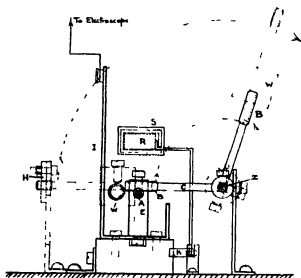
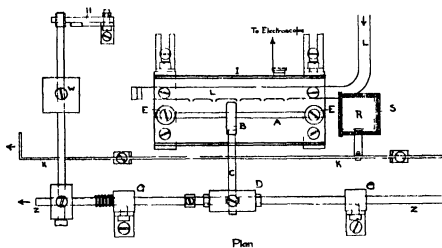


FIG 1

After each rub the deflection of the electroscope is noted, then A and B are earthed. Thus we can obtain comparable quantitative results using one element after another on a range of variously prepared glass surfaces. In addition to the method described we made experiments of another kind a

horizontal metal sheet is insulated and connected to the electroscope. A standard glass rod with a sharp end is then struck on the sheet with a glancing blow. The point of the glass plunges into the metal and so passes through surface oxide and other films. We thus obtain the true, glass/element, effect. The results are shown in curves 7, figs 2 and 3, where we see that those "negative" elements tested all acquire negative, and the positive elements

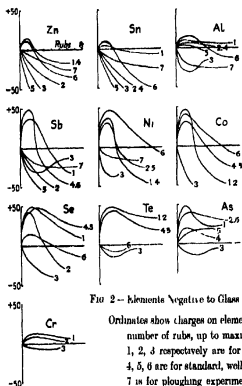


FIG. 2 - Elements Negative to Glass

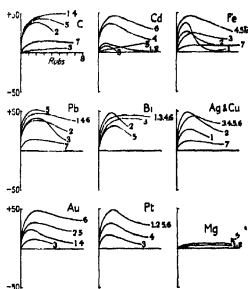


FIG. 3 - Elements Positive to Glass

Ordinates show charges on element to maximum ± 50 scale divisions. Abscissae stand for number of rubs, up to maximum 8, on the same glass surface.

1, 2, 3 respectively are for standard, well washed and recently fused glass.

4, 5, 6 are for standard, well washed and heated vitreous silica.

7 is for ploughing experiments of glass on the elements.

positive, charges. This confirms our view that the initial positive charges in fig. 2 are due to (presumably acid) films and that the true charge for metal/glass is negative. A variant of this method is to have the end of the glass rod rounded by fusion. The impact is performed in the same manner as before. Here again the impact is so violent that the glass passes through all films and gives effects identical with those of curves 7.

Tribo-electric experiments *in vacuo* have the advantage that atmospheric oxygen, moisture or other adventitious materials can be eliminated. But quantitative results are difficult to obtain and a systematic investigation is

vacuo with determinate forces and identical surfaces is well nigh impossible Coehn and Curs (*loc cit*) worked with high *vacua* but obtained only qualitative results

In order to make a direct comparison between vacuum and plenum experiments we set up a vacuum apparatus of a simple form a wide soda glass tube is cleaned, dried and filled with hydrogen and into it is introduced a heavy brass block provided with feet of the metal to be tested against the glass The tube is heated to 120° C and exhausted for half an hour till the actual surface moisture is eliminated (The moisture remaining in pores does not concern us) After sealing the vacuum the block is allowed to slide in the tube and the charges measured in the inductor The typical elements tested in this way were Zn, Sb, Cd, Cu These behaved exactly as in the open air experiments (see figs 2 and 3)

Films of oxide and moisture are likely to be troublesome when soft materials are used, but for two hard surfaces like glass and metal, which cut through the films, their influence, at least for warm glass, is of small account For this reason we think that our open-air experiments, between surfaces newly cleaned and kept warm, are quite reliable

4 The curves in figs 2 and 3 show the rounded mean results deduced from a vast number of repeated tests for 20 of the commoner elements on glass Those which acquire a negative sign are in fig 2, they have one feature in common, viz, the initial negative charge they attain when rubbed on recently fused glass Two other elements Thallium and Sulphur acquire a very small negative charge Fig 3 includes elements which always become positive, and never, even with fused glass, become negative on glass Tungsten is in the same class but its positive charges are very small Other elements used but giving small charges of uncertain sign are Mn, Li, Na, K

Mercury being liquid cannot be treated like the other metals We prepare it by long continued passage of air through mercury to oxidise residual zinc or other metals It is then shaken up with chromic acid, well washed and then distilled *in vacuo* The distillate is sealed off *in vacuo* in a standard soda glass tube On rolling the mercury along the tube it shows positive charges which remain steady however often the rolling be repeated On letting air into the tube, the mercury commences positive but each roll produces less charge until finally the mercury becomes negative The negative charge seems to be due to water adsorbed on the glass, for the positive always appears again when heat is applied The conclusion is that mercury is to be ranked among the positive elements, but by the action of adsorbed water becomes temporarily

negative In short, the behaviour of mercury is remarkable and calls for special treatment *

We find little difference in degree and none in sign between the behaviour of soda glass and lead glass (see composition in footnote, section 2) so that results for soda glass only are given

The initial positive charge, where occurring (as in curves 1) in the elements of fig 2, we attribute to the slight acid effect residual on the glass It is well known that acidic surfaces of glass have this positive effect due to their yield of $+$ (H) ions, just as alkaline surfaces have a negative effect due to giving up $-$ (OH) ions In the rubbing this residual acid is attacked or rubbed away quickly by the oxidisable metals Zn, Sn, less quickly by Ni and Co, and not at all by the metalloids Se and As Thus do we interpret curves 1, 2, 4, 5

As acidic, alkaline and aqueous films play such an important part in triboelectric experiments, we give curves in fig 4 to show that small amounts of

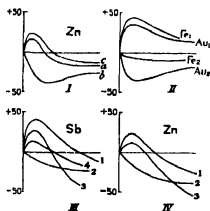


FIG. 4—Tests of the Effect of Acid, Alkali or Moisture

acid or alkali and small deposition of moisture may completely change the nature of the charging These facts of themselves reveal the futility of seeking data from solid surfaces of uncertain composition or surface purity The curves in fig 4 are as follows —

I Acid

Zinc rubbed on (a) standard glass, (b) well-washed glass, (c) well-washed glass with trace of acid

II Alkali

Fe₁, Au₁ are curves for these metals rubbed on well-washed glass

Fe₂, Au₂ are curves for these metals rubbed on slightly alkaline glass

* See Buhl, 'Ann d Physik,' vol. 80, p 137 (1926)

III *Moisture*

Charges found on Sb (1) when rubbed on warm glass, (2) when rubbed on glass left 1 hour in air, (3) (4) when rubbed after first warming and then leaving in air

IV *Moisture*

Charge on Zn (1) when glass is warm, (2) after blowing water-saturated air on the glass, (3) after blowing dry air on the glass

III and IV show that moisture on the glass has a negative influence on the elements

The falling off of charge seen in so many curves is in part due to the formation of a metal streak on the glass. Soft metals like Al, Zn, Cd produce a dense streak. It must be discontinuous (in fact a low power microscope shows it to be so) or the charge would always fall to zero, on account of recombination of the charges on the two surfaces.

On referring to section 1, it will be seen that substantially our grouping into positive and negative agrees with that of Coehn and Curs, though in opposition to them we rank the metals Fe, Cd as positive.

The discrepancy between our work and that of Coehn and Curs was particularly examined by us, and our final decision to rank Fe among the positive elements is based on the curves shown in the figs 2 and 3. On reference to these it will be seen that our full classification is --

- + Fe, Bi, Cu, Ag, Pb, Mg, Cd, C, Au, Pt
- Al, Zn, Sn, Ni, Co, Sb, As, Se, Te, Cr

We tested all these materials repeatedly, and the curves in the figures show a distinct difference between the positive and negative elements, with Fe decidedly among the former.

5 It is interesting to compare the classification of the elements from the above process with the corresponding combined list derived from the Volta-effect, the photo-electric effect, and from thermionics.

Langmuir's* list is —

- (a) (+ Al, Zn, Fe, Sn, Bi, Cu, Ag, C, Pt —)

Our classification is —

- (b) (+ Fe, Bi, Cu, Ag, C, Pt)
- (— Al, Zn, Sn)

Comparison between these two groups shows that, in general, the noble metals

* 'Trans Amer Elec Soc,' vol 29 (1916)

and the base metals are separated from one another. But whereas in group (a) the base metals are at the positive end, in series (b) they are at the negative end. It will be shown in a later paper that if the elements are rubbed on filter paper, instead of glass, this reversal does not occur, but that the base metals are at the positive end as in group (a). We do not think this marked difference in behaviour can be attributed to the different action of adsorbed water films on the glass and the paper, for our experiments include cold surfaces, hot surfaces and surfaces rubbed after being dried by prolonged heating in a vacuum and there is no difference in characteristics in these various cases.

This subject will be discussed in the paper following.

b) *Theories*.—Riecke* has investigated a case like ours, where a conductor rubs an insulator. He obtained the expression for charge on rubbed body

$$\int_0^s r ds = x \cdot u/q \cdot \delta \{1 - \exp(-qs/u)\},$$

where q = surface density of charge, s = length of stroke, δ = area of rubber used, u = speed, x, q are parameters depending on the nature of the two surfaces, x concerns charging and q recombinations. The width of the rubber is taken to be unity.

According to this formula our curves should be of simple form, for we discharge between each rub and thus the successive charges should be equal. But in figs 2 and 3, above, we find that, in general, the charges decrease, and even reverse, as the rubbing continues. Clearly then, since all the other factors are constant, the terms x, q change during the experiment corresponding to physical or chemical changes brought about by the rubbing, and the above expression needs modification.

The present bewilderment on the subject of frictional electricity may be gauged by the number of theories in the field.

The followers of Helmholtz† regard the effects for insulators as merely akin to the Peltier P.D. between metals. If this be so, rubbing is not essential: contact between unlike solids should suffice for production of charges, and rubbing merely serves to increase the area of contact and therefore the charges. But though it is true that impact between solids does generate charge,‡ it cannot be inferred that the charges are due to the contact alone, since impact involves both contact and rupture.

In the past many attempts have been made to find a contact P.D. with

* 'Wied. Ann.' vol 3, p 414 (1878)

† 'Wied. Ann.' vol 7, p 337 (1879)

‡ See Richards, 'Phys. Rev.' vol 16, p 290 (1920)

insulators The evidence is conflicting. It is useless to look for the effect between two insulators, since any electric charges separated at the interface must be so intimately associated that they constitute molecular doublets, with no external field. But by using an insulator in contact with a metal, some investigators, Christiansen* and Pernucca,† concluded that the effect exists, while Morris Owen‡ and Richards (*loc cit*) failed to find it. Hoorweg,§ by an indirect method decided that the effect exists, and that temperature affects the electric separation as in the Seebeck effect.

We have shown in section 5 that the tribo-electric series does not always agree with the Peltier effect series.

The simple contact theory ignores several principles which have been discovered since the time of Helmholtz: (a) The very powerful influence of acid, alkaline or adsorbed water films on the sign of the charge, (b) the effect on the electron surrender of the temperature changes brought about by friction, which changes are intense and in general different for the two solids, (c) the strains produced on the solids by rubbing, (d) the effect of rupture which proceeds continuously as the solids slide over one another.

To take these in turn —

(a) The rôle of adsorbed films has been demonstrated by many investigators ||. We ourselves have found that water films greatly affect the charges in amount and sign (see fig. 4). When a water film is broken the main body of the water is charged positive and the escaping ions are negative. This is Leonard's "Water-fall" effect.

Further, Nernst's theory is that metals go into solution when brought into contact with liquid films, each metal having its own solution pressure and receiving a corresponding greater or less negative charge. Coehn¶ goes a step farther by supposing that insulators like glass are merely bad electrolytes, so that even for these solid contacts the Nernst principle holds good.

Again, Freundlich** regards the rubbing of two solids (each with its own film) as bringing four interfaces into action, one solid/solid, two solid/liquid and one liquid/liquid, so we should have a set of four interfaces each capable

* 'Wied Ann,' vol 53, p. 401 (1894)

† 'N. Cimento,' June, 1925

‡ 'Phil. Mag,' vol 17, p. 457 (1909)

§ 'Wied Ann,' vol 11, p. 133 (1880)

|| Fröhen, 'Phys. Rev,' vol 9, p. 151 (1917). Vieweg, 'J. Phys. Chem.' vol 30, p. 865 (1926)

¶ 'Wied Ann,' vol 66, p. 119 (1898)

** 'Colloid and Capillary Chemistry' (Methuen)

of producing electric separation. An important distinction between solid and liquid is that the latter, but not the former, possesses a double electric layer. In particular, when a liquid rubs a solid we should have the electrokinetic phenomenon of "stream potential," the converse of electro-osmosis, whereby the solid would become charged according to Helmholtz's formula (see Freundlich, *loc cit*).

It has been shown by various writers, notably Knoblauch* that an acid surface has itself a negative, and an alkaline one has a positive, tendency. In the first case the surface loses $+$ (H) ions, in the latter $-$ (OH) ions. As surfaces are commonly acidic or alkaline, this is an important factor in tribo-electricity. The curves in fig. 4 emphasise the point.

(b) According to the electron theory of matter the interface P D varies as the absolute temperature, yet little account has been taken by theorists of the intense temperature changes, caused by friction at the rubbing faces of insulators whereby the properties of the two solids must be fundamentally changed. Fusion and evaporation must frequently occur at the interface of bad conductors like ebonite. This principle is emphasised by Melander †.

(c) One of us (P E S) has shown‡ that a solid surface may by rubbing or pressure undergo such great physical changes that its tribo-electric properties are permanently and greatly affected. Two surfaces originally identical may by mere friction be changed in different degrees. They then behave like two unlike solids and acquire unlike charges as rubbing continues.

(d) To the presence of the "double electric layer" at a liquid/air interface is attributed the production of ballo-electricity and waterfall electricity. There can be no such double layer in the case of a purely solid/solid interface. But just as charges are generated by the rupture of the liquid/air face so something of a like nature may occur when a solid/solid face is broken. We know that when crystals are cleaved charges are found: we have found such charges for calcite, selenite, mica, fluor spar, gypsum. See also Vieweg §.

We suppose that when two solids come into "contact" they invariably cohere. Interlinking, i.e., exchange, or sharing, of electrons, causes a fusion of the surfaces. It is not yet established that a P D exists across the interface as the Helmholtz school suppose (see above). When, however, the solids are again separated after contact, the rupture at the interface causes elective attachment

* 'Z f Phys. Chem.', vol 39, p 225 (1902)

† 'Phys. Z.', vol 8, p 700 (1907)

‡ 'Roy Soc. Proc.' A, vol 94, p 16 (1917), 'Proc. Phys. Soc.', vol 39, p 449 (1927)

§ Vieweg, 'Journ. Phys. Chem.', XXX, No 7

of electrons to one or other solid, and we now have a P D *in evidence*. There is no doubt about this charge between solids after rupture.

To sum up the foregoing principles tribo-electricity cannot be a purely statical effect, the kinetic effects must be important and may be paramount. The above many conflicting influences are, in general, in operation simultaneously in the present experiments. It is not known what function the resulting potential is of each factor. (For instance, each factor is sure to be a complex, but different, function of temperature.) In the absence of this knowledge we can still bring the terms together by writing the net potential as the algebraic sum of all effects operating under the special conditions of the experiment, so that, allowing for the positive or negative influence of each, acting independently —

$$V = E - P \pm S - M \pm A - T,$$

where

E = Electron surrender causing a P D akin to the Peltier P D

P = Solution pressure (Nernst)

S = Strain effect (Shaw)

M = Moisture effect (French, Vieweg)

A = Acid effect (positive)
Alkaline effect (negative) } of glass (Knoblauch)

T = Effect due to rise in temperature of the "rubber"

For any particular combination of solids one or the other factor may be absent, when the rub occurs *in vacuo* (M) is eliminated, when the surfaces are strictly neutral (A) vanishes.

Our gratitude is due to friends who have contributed valuable technical advice or pure materials. Mr S L Archbutt, Metallurgical Department, National Physical Laboratory, has kindly prepared purest attainable iron, nickel, tin, cadmium, chromium, zinc, aluminium, antimony. Prof W E S Turner, Sheffield, has given us freely of his special knowledge on glass. One of us (C S J) has had the great benefit of a maintenance grant from the Department of Scientific and Industrial Research while the work has proceeded.

Summary

1 Various prepared glass rods are rubbed by various solid elements in an apparatus designed to give constant conditions of pressure and surface. Curves are given showing the resultant charges.

2 Some elements never, with any type of glass surface tried, show negative charge. These are C, Cd, Fe, Pb, Bi, Ag, Cu, Au, Pt, Mg, W.

Other elements show ultimate negative charge These are Zn, Sn, Al, Sb, Ni, Co, Se, Te, As, Cr, Ti, S

3 Evidence is given of the predominating influence on the charging, of residual acid, alkali, or water, films, on the glass

4 Rubbing *in vacuo* yields results similar to those found in the open air, at least in the typical cases tried

5 An attempt is made to apportion to each recognised source of charge its own weight in the various experiments

Tribo-electricity and Friction III —*Solid Elements and Textiles*

By Prof P E SHAW, M A, D Sc, and C S JEX, B Sc,
University College, Nottingham

(Communicated by Sir William Hardy F R S —Received November 3, 1927)

1 No systematic investigation on this subject has yet been attempted The efforts made to group these materials in a series according to the charges generated when they are rubbed two at a time are of uncertain value because of (1) impurities of substance and surface, (2) indeterminate initial surface strains Moreover, the general practice has been to rub the solids when held, one in each hand A more reliable method is to mount the bodies in a mechanism which ensures that the same parts of them come into contact at each fresh stroke

In the present research, the elements, mostly metals, are those specified in the preceding paper The textiles are made and cleansed as described in an earlier paper* Silk, cotton and linen in our experience behave reliably when fully cleaned The other great textile material, wool, is more oily and cannot be readily cleansed, so is less trustworthy We therefore at present confine ourselves to one animal and one vegetable textile, choosing the pure samples of silk and cotton specified in the above paper Also filter paper, another convenient fabric, is used after being boiled in several lots of distilled water As the silk and cotton are treated with boiling chloroform, we tried exhausting the filter paper in this solvent to see if such treatment affected the cellulose in any way, but no effect on the properties of the paper could be found

2 The apparatus and methods used are just as described in the preceding

* 'Roy Soc Proc,' A, vol 111, p 339 (1926)

paper, with the modification that the element is rubbed, not on glass, but on the textile wrapped round glass rods

The results for silk, cotton, and filter paper are placed (fig 1) beside those

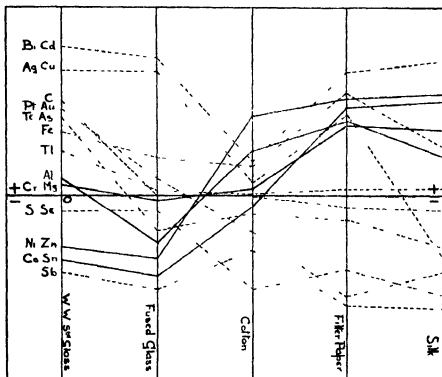


FIG 1 - W W Glass signifies well washed glass (Section 2, former paper)

for well-washed and fused glass (see preceding paper) There are five vertical columns, one for each material on which the elements are rubbed Elements above the zero line are charged positive, those below negative, to the rubbed surface, which itself occupies the zero position 0 The position above or below zero depends on the amount of charge obtained on the element after one rub To elucidate the figure take the case of aluminium It is positive to W W Glass, Cotton, Filter Paper and Silk, but negative to Fused Glass

Joining one column to the next are full and dotted lines These show how the charges on the elements vary according to the material they rub In some cases the connecting lines cross the horizontal line The significance of this will appear later in fig 2 The dotted lines are for elements which behave normally and occupy one definite position in the tribo-electric series (fig 2) The full lines are for Zn, Sn, Ni, Co, Al, Mg, Cr, whose anomalous behaviour is shown in fig 2

3 If the five compounds, silk, filter paper, cotton, fused glass, well-washed glass, be rubbed together in pairs their order is found to be as shown in the

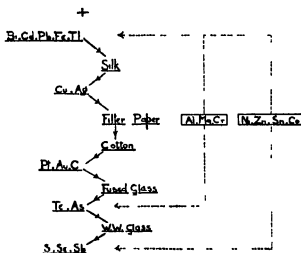


FIG 2

central column (fig 2), silk being most positive, well-washed glass most negative. Then from the data in fig 1 all the elements except the seven mentioned can be arranged in series with the compounds as in the figure. But each of these seven has two positions, one above silk and another below glass.

It thus becomes manifest that it is impossible—as stated in the preceding paper—to devise a *simple* tribo-electric series of one column to include all solids, although from the time of Wilcke (1759) to the present day many attempts to do so have been made. To illustrate this point it will be seen from the figure that the five materials zinc, silk, filter paper, cotton, glass are related in a continuous ring as in the figure, the arrow in each case pointing from positive to negative.

In the preceding paper (section 6) is a statement of the various sources of tribo-electric charge. We must look to one or more of these in the present problem of the anomalous metals.

Consider throughout the case of zinc. The net positive charge on it due to silk might be attributed to —

(E), Electron surrender to the silk

(P), Solution pressure from metal to silk (if any)

- (S) and (M), Strain and moisture effect These should not appear for zinc rather than other metals, *e g*, Pb, Cd, so we must rule these factors out
 (A), Acid action of the silk, in which case the zinc would be given + H ions But we have no evidence of any such effect
 (T), Temperature effects should be alike for zinc and the normal metals

The net negative charge on the zinc due to well washed glass might be due to —

- (E'), Electron surrender to glass, E' being greater than E , since silk is itself positive to glass, with electron surrender e
 (P'), Solution pressure which according to Coehn exists from zinc to glass This would make the zinc negative
 (S') and (M'), There seems no reason to suppose strain or moisture effects for zinc rather for other metals, *e g*, Ag, Pb
 (A'), No doubt fused and well-washed glass are slightly alkaline and hence would yield — (OH) ions to zinc
 (T'), Temperature effects should not influence the results If this reasoning be true the solution pressure (P') and alkaline effect (A') exceed the electron surrender ($E + e$) acting from the susceptible metals Zn, Sn, Ni, Co, Cr, Al, Mg, to glass, and cause them to be negative, whereas the normal position for these electro-positive elements is above silk
 If V_1 , V_2 be the potentials of one of these metals to silk and glass respectively, we have —

$$V_1 = E$$

$$V_2 = - P' - A' + E + e$$

Fig 2 of this paper epitomises the work of our three papers in tribo-electricity, I, Glass and Textiles, II, Glass and Elements, III, Elements and Textiles It will be seen that the elements in this figure are associated according to well-known chemical qualities Electro-positive elements at the top, the +ve end, electro-negative and non metallic elements at the bottom, the —ve end Kindred elements are found grouped together, *e g*, Pt and Au, Ag and Cu

In the case of some congeners we find slight divergence in character by these methods, *e g*, Se and Te, Ni and Co, Zn and Cd Thus the purely physical processes of tribo-electricity enable us to sort the elements into groups without employing chemical methods, depending on combination

Greater care has been taken in the present set of researches than in the earlier one (*loc cit*) to eliminate the influences of surface impurities and moisture, and initial strains The results are, roughly, quantitative and have

been repeated frequently and with great variation of temperature and other atmospheric conditions. The conditions of material and procedure have been standardised so that the results can be repeated in any further work.

[*Added January 2, 1928* — The foregoing results are at variance with those found in the text-books, and even in modern researches, so that some further comment is due to the reader. The key to the matter lies in two papers by one of us ('Roy Soc Proc,' vol 94 (1917), and 'Proc Phys Soc,' vol 39 (1927)). It is shown in the former that there is no *fixed* place for any solid in the tribo-electric series, but that the same material, variously prepared as to surface, will assume various places in the series.

In order to make the idea clear, consider the case of glass. This has, by tradition, a high place, say, above silk and cotton, but in reality, its true place is below them, for when all these materials are cleansed, or even if the glass is heated to 245°, the order—silk, cotton, glass—is obtained, the other order—glass, silk, cotton—appearing when the materials have been well rubbed together.

This rule applies to a smooth glass surface, whereas one rendered matt by abrasion, or one deeply eaten away by solvent, as in standardising, is very intractable, and after prolonged rubbing by silk may remain negative to it (see, 'Roy Soc Proc,' A, vol 111, p 346).

In 1917 I had found these effects, but their cause emerged only in 1926, it is a question of strain of surface produced by rubbing, and removed either by dissolving off the strained particles or by orienting them by heat into the annealed condition.

Not perceiving this principle when writing the first paper the terms "normal" and "abnormal" were used in wrong sense, and should have been "strained" and "unstrained" respectively, for clearly the normal state is the annealed one.

To lend further support to this "strain" principle the reader is referred to column 5 of the earlier paper. This is headed P H denoting "Pressed Hot". Materials were found to be permanently more affected by rubbing when hot than when cold. This we should anticipate on the strain theory, since the hotter the surface the more easily and completely is it strained by force.

It should have been obvious to those who worked on this subject (especially after Sir George Beilby's work on surface flow and the contrasted crystalline and vitreous states of surfaces) that, when surfaces are violently rubbed, several distinct, but related, processes operate simultaneously. (1) electric separation at the interface due to constitutional differences of the materials, (2) surface

flow and consequent permanent strain caused by the rubbing, (3) temperature changes affecting both (1) and (2)

The second (1926) paper establishes (2) and, more significant, proves that the tribo-electric charges depend on the amount of strain]

Summary

1 Commercial textile material is unsuitable for precise tribo-electric experiments, on account of natural and artificial impurities. Well-cleansed material acts consistently on the various solid elements

2 The arrangement of the different elements according as they charge textiles and glass, is found to correspond closely to their chemical qualities

3 Anomalies are found in the case of some strongly electro-positive elements which appear in two places in the tribo-electric series. An attempt is made to apportion to each known source of charge its own weight in these phenomena

The Effect of Compressibility on the Lift of an Aerofoil

By H. GLAUERT, M.A.

(Communicated by G. I. TAYLOR, F.R.S.—Received November 24, 1927)

1 Introduction

At ordinary aeroplane speeds the effect of the compressibility of the air is very small, and there is complete justification for the usual assumption that the air may be regarded effectively as an incompressible medium. This assumption, however, ceases to be valid in the case of high tip-speed airscrews and is not really satisfactory even when the tip speed is no greater than 800 f.p.s. It is important, therefore, to examine, both theoretically and experimentally, the effect of compressibility at high speed on the characteristics of an aerofoil. Experimental investigations are in progress at the Royal Aircraft Establishment in which the aerofoil characteristics are derived by analysing the observed behaviour of high-speed model airscrews, but owing to the complexity both of the experiments and of the analysis it is impossible that the results should have the same accuracy as those obtained from direct tests of an aerofoil at low speed.

An attempt has now been made to estimate theoretically the effect of com-

compressibility on the lift of an aerofoil in two-dimensional motion and to indicate the nature of the variation which may be anticipated in the curve of lift coefficient against angle of incidence. It is unfortunately impossible at the present state of knowledge to make any similar calculation for the drag of the aerofoil, but on general grounds we may anticipate that the drag coefficient will rise at an increasing rate until the velocity of sound is reached, and that above this speed the drag coefficient will decrease again, remaining, however, higher than at low speeds.

2 Circulation in a Compressible Fluid

The irrotational motion of a compressible fluid, expressed in polar co-ordinates, is governed by the following equations. The condition for irrotational motion is

$$\frac{\partial(rv)}{\partial r} - \frac{\partial u}{\partial \theta} = 0, \quad (1)$$

where u and v are respectively the radial and circumferential components of the resultant velocity q . The equation of continuity is

$$\frac{\partial(rvu)}{\partial r} + \frac{\partial(rv)}{\partial \theta} = 0,$$

or

$$\frac{\partial(ru)}{\partial r} + \frac{\partial v}{\partial \theta} + \frac{ru}{\rho} \frac{\partial \rho}{\partial r} + \frac{v}{\rho} \frac{\partial \rho}{\partial \theta} = 0, \quad (2)$$

and the relationship between pressure and velocity is determined by Bernoulli's equation

$$\int \frac{dp}{\rho} + \frac{1}{2} q^2 = \text{constant}$$

For adiabatic expansion p is proportional to ρ^γ and the velocity of sound a in the undisturbed fluid is

$$a = \sqrt{\gamma p_0/\rho_0}$$

Assuming V to be the velocity of the undisturbed stream, Bernoulli's equation becomes

$$\frac{\gamma}{\gamma-1} \frac{p}{\rho} + \frac{1}{2} q^2 = \frac{\gamma}{\gamma-1} \frac{p_0}{\rho_0} + \frac{1}{2} V^2,$$

and hence finally

$$\left(\frac{p}{p_0}\right)^{\frac{\gamma-1}{\gamma}} = \left(\frac{\rho}{\rho_0}\right)^{\gamma-1} = 1 - \frac{\gamma-1}{2a^2} (q^2 - V^2) \quad (3)$$

Consider now the flow past a body round which there is a circulation K in the clockwise sense. Then for any circle enclosing the body we have the two integral relationships

$$\int_0^{2\pi} u r d\theta = -K, \quad (4)$$

and

$$\int_0^{2\pi} \rho u r d\theta = 0 \quad (5)$$

The lift and drag experienced by the body can also be determined by evaluating the integrals

$$\left. \begin{aligned} L &= - \int_0^{2\pi} \{ p \sin \theta + \rho u (u \sin \theta + v \cos \theta) \} r d\theta \\ D &= - \int_0^{2\pi} \{ p \cos \theta + \rho u (u \cos \theta - v \sin \theta) \} r d\theta \end{aligned} \right\} \quad (6)$$

All these integrals may be taken round any circle enclosing the body, but it is convenient to consider a circle of very large radius. The body is then equivalent to a point vortex of strength K at the origin and the velocity components u and v may be expanded in the series

$$\left. \begin{aligned} u &= V (\cos \theta + \sum A_n/r^n) \\ v &= -V (\sin \theta + \sum B_n/r^n) \end{aligned} \right\}, \quad (7)$$

where A_n and B_n are functions of θ . Moreover, to evaluate the integrals over the large circle, it is sufficient to retain only the first terms of each power series, and on this basis we have simply

$$\left. \begin{aligned} u &= V (\cos \theta + A/r) \\ v &= -V (\sin \theta + B/r) \end{aligned} \right\} \quad (8)$$

To this order

$$q^2/V^2 = 1 + 2(A \cos \theta + B \sin \theta)/r$$

and writing

$$\lambda = V^2/a^2 \quad (9)$$

equation (3) gives

$$\left. \begin{aligned} p &= p_0 - \rho_0 V^2 (A \cos \theta + B \sin \theta)/r \\ \rho/\rho_0 &= 1 - \lambda (A \cos \theta + B \sin \theta)/r \\ \frac{r}{\rho} \frac{\partial \rho}{\partial r} &= \frac{\lambda}{r} (A \cos \theta + B \sin \theta) \\ \frac{1}{\rho} \frac{\partial \rho}{\partial \theta} &= \frac{\lambda}{r} (A \sin \theta - B \cos \theta - \frac{dA}{d\theta} \cos \theta - \frac{dB}{d\theta} \sin \theta) \end{aligned} \right\} \quad (10)$$

The solution is now obtained by inserting these expressions in the fundamental equations. The condition for irrotational motion (1) requires that A shall be a constant, and the equation of continuity (2) gives

$$\frac{dB}{d\theta} (1 - \lambda \sin^2 \theta) = \lambda (A \cos 2\theta + B \sin 2\theta), \quad (11)$$

while the integral equations (4) and (5) become respectively

$$\int_0^{2\pi} B d\theta = \frac{K}{V} \quad (12)$$

and

$$\frac{1}{2}\lambda \int_0^{2\pi} B \sin 2\theta d\theta = 2\pi A (1 - \frac{1}{2}\lambda) \quad (13)$$

It is now possible to determine the lift and drag of the body by means of these relationships, without proceeding to the actual determination of A and B , for equations (6) lead quite simply to the values

$$\left. \begin{aligned} L &= \rho_0 V K \\ D &= 0 \end{aligned} \right\} \quad (14)$$

The integration of equation (11) gives

$$B (1 - \lambda \sin^2 \theta) = C + \frac{1}{2}\lambda A \sin 2\theta,$$

where C is a constant, and on inserting this expression in the integral equation (13) it is found that the value of A must be zero. Finally the value of C is determined from equation (12) as

$$C = K\sqrt{1 - \lambda/2\pi V}$$

and the expressions (8) for the velocity components then become

$$\left. \begin{aligned} u &= V \cos \theta \\ v &= -V \sin \theta - \frac{K}{2\pi r} \frac{\sqrt{1 - \lambda}}{1 - \lambda \sin^2 \theta} \end{aligned} \right\} \quad (15)$$

It appears, therefore, that the effect of the compressibility, at a considerable distance from the body, is simply to modify the expression $K/2\pi r$ for the velocity due to the circulation by the addition of a factor depending on λ or $(V/a)^2$. The solution is clearly valid only when λ is less than unity, i.e., for speeds below that of sound. When the speed exceeds this value, compression waves arise in the fluid and the flow is no longer of the type considered in the analysis.

3 The Lift of an Aerofoil

A thin aerofoil in two-dimensional motion may be regarded approximately as a line distribution of point vortices whose strength is such that the component of the velocity due to those vortices at each point of the aerofoil normal to its surface exactly balances the normal component of the velocity V . If the preceding analysis can be applied to this case in spite of the small distances involved, it would appear that in a compressible fluid the induced velocity receives the factor

$$\sqrt{1 - \lambda}/(1 - \lambda \sin^2 \theta),$$

and for points on the aerofoil, which is inclined at a small angle to the direction of the velocity V , this factor is sensibly equal to

$$\sqrt{1 - \lambda}$$

In order to obtain the correct induced velocity at the surface of the aerofoil, it is therefore necessary to increase the strength of all the elementary vortices by the factor

$$(1 - \lambda)^{-1} \quad (16)$$

and by virtue of equation (14) the lift at a given angle of incidence will rise by the same factor,* the lift distribution along the chord remaining unaltered.

Some insight into the assumptions involved in applying the analysis for points distant from a vortex to the induced velocity at the surface of an aerofoil is obtained by considering the problem in an alternative manner. In Cartesian co-ordinates the fundamental equations for the irrotational flow of a compressible fluid may be expressed in the form

$$\begin{aligned} \frac{\partial v}{\partial x} - \frac{\partial u}{\partial y} &= 0 \\ \frac{\partial u}{\partial x} + \frac{\partial v}{\partial y} + \frac{1}{\rho} \left(u \frac{\partial \rho}{\partial x} + v \frac{\partial \rho}{\partial y} \right) &= 0 \\ \left(\frac{\rho}{\rho_0} \right)^{\gamma-1} &= 1 - \frac{\gamma-1}{2a^2} (q^2 - V^2) \end{aligned}$$

Hence

$$\begin{aligned} \left(\frac{\rho}{\rho_0} \right)^{\gamma-1} \frac{1}{\rho} \frac{\partial \rho}{\partial x} &= -\frac{1}{a^2} \left(u \frac{\partial u}{\partial x} + v \frac{\partial v}{\partial x} \right) \\ \left(\frac{\rho}{\rho_0} \right)^{\gamma-1} \frac{1}{\rho} \frac{\partial \rho}{\partial y} &= -\frac{1}{a^2} \left(u \frac{\partial u}{\partial y} + v \frac{\partial v}{\partial y} \right) \end{aligned}$$

* This result is quoted without proof by Ackert in the 'Handbuch der Physik,' vol. 7, p. 340 (1927), as given by Prandtl in his lectures at Göttingen in 1922

and the equation of continuity becomes

$$\left\{1 - \frac{\gamma - 1}{2a^2} (q^2 - V^2)\right\} \left(\frac{\partial u}{\partial x} + \frac{\partial v}{\partial y}\right) = \frac{u}{a^2} \left(u \frac{\partial u}{\partial x} + v \frac{\partial v}{\partial x}\right) + \frac{v}{a^2} \left(u \frac{\partial u}{\partial y} + v \frac{\partial v}{\partial y}\right).$$

Now let the aerofoil be part of the x axis, to which the velocity V is inclined at a small angle α . Then on the surface of the aerofoil v is zero, and the equation of continuity becomes

$$\left\{1 - \frac{\gamma - 1}{2a^2} (u^2 - V^2)\right\} \left(\frac{\partial u}{\partial x} + \frac{\partial v}{\partial y}\right) = \frac{u^2}{a^2} \frac{\partial u}{\partial x},$$

which may be written in the form

$$(1 - k) \frac{\partial u}{\partial x} + \frac{\partial v}{\partial y} = 0,$$

where

$$k = \frac{u^2}{a^2} \left\{1 - \frac{\gamma - 1}{2a^2} (u^2 - V^2)\right\}$$

The assumption is now made that the velocity u does not differ appreciably from the undisturbed velocity V , and then the value of k becomes $(V/a)^2$ or λ , as previously defined. Now let

$$\begin{aligned} u' &= u \sqrt{1 - \lambda} \\ x &= x' \sqrt{1 - \lambda} \end{aligned}$$

and then the equations of irrotational motion and continuity become

$$\begin{aligned} \frac{\partial v}{\partial x'} - \frac{\partial u'}{\partial y} &= 0 \\ \frac{\partial u'}{\partial x'} + \frac{\partial v}{\partial y} &= 0, \end{aligned}$$

which represent a corresponding perfect fluid solution in which x' is greater than x . This distortion of the system is necessary near the aerofoil, but the flow at infinity is unaltered and hence the lift is the same in both cases. The chord of the aerofoil in the compressible fluid, however, is less than in the perfect fluid, and hence for a given aerofoil the lift in a compressible fluid is increased by the factor $(1 - \lambda)^{-1}$.

In view of this discussion it would appear that the validity of the result (16) depends on the assumption that the velocity at the surface of the aerofoil does not differ appreciably from the undisturbed velocity V . High velocity occur

over the shoulder of an aerofoil, but for aerofoils of medium thickness working at moderate lift coefficients the maximum velocity is not greater than $2V$. The theoretical formula may, therefore, be expected to give a good indication of the effect of compressibility on the lift of an aerofoil as the speed increases, but to breakdown before the velocity of sound is attained, and the breakdown of the formula, due to the local velocity over an appreciable part of the aerofoil rising to a high value, may be expected to show itself first at high lift coefficients.

These theoretical predictions are confirmed qualitatively by the experimental tests of high-speed airscrews, and the table below gives the comparison between the observed and calculated slopes of the lift curve for a thin biconvex section*. The no-lift angle remained constant at $-3\frac{1}{2}^\circ$ for the range $V = 0.4a$ to $0.7a$ and then fell to zero for $V = a$. The slope of the lift curve began to fall off above $0.6a$, but the critical drop of lift occurred at a slightly higher speed. Owing to the necessity of obtaining the experimental results from the analysis of tests of an airscrew, these results are a surprisingly good confirmation of the theory.

Slope of Lift Curve

V/a	0	0.4	0.6	0.7	1.0
Observed	—	0.060	0.075	0.060	0.058
Calculated	0.055	0.060	0.060	0.077	—

The general conclusions, which should apply to any aerofoil, may now be stated as follows —

(1) As the speed increases from zero to $0.6a$, the slope of the lift curve increases according to the factor $(1 - V^2/a^2)^{-\frac{1}{2}}$, and the no-lift angle is unaltered. The increase at $V = 0.6a$ is therefore 25 per cent.

(2) Between $V = 0.6a$ and $V = a$ the lift decreases, but the critical speed at which the lift begins to fall rapidly depends on the shape of the aerofoil. The rapid decrease probably shows itself first at the higher lift coefficients.

* 'The Characteristics of Biconvex No. 2 Aerofoil Section at High Speeds,' by G. P. Douglas and W. G. A. Perring (Aeronautical Research Committee, R. & M. 1115)

The Alkaline Earth Halide Spectra and their Origin

By O H WALTERS, B Sc., and S BARRATT, B A., University College
London

(Communicated by T R Merton, F R S —Received November 25, 1927)

[PLATE 2]

It has been known since the early days of spectroscopy that there is a group of band spectra associated with the halogen salts of the alkaline earths. Probably the first distinction between the oxide and chloride bands of these elements was made by Lecoq de Boisbaudran* when he observed relative intensity fluctuations between two band systems on introducing hydrochloric acid vapour into a flame charged with calcium chloride. The system intensified by the acid vapour he attributed to the chloride. The other halides were also found to yield characteristic spectra. Since their discovery they have been the subject of only one publication of any real note. Olmsted† made a careful study of these spectra as they are found under flame excitation, and his catalogue of bands contains the only reliable data concerning these spectra which is available. An exception must be made of the fluoride spectra, which have been closely studied by Dufour, Datta, and others.

The origin of the present investigation of these bands was the discovery that it is possible to observe them, very conveniently, in absorption against a continuous background spectrum. In the course of attempts to find band spectra of the alkaline earth metals (corresponding to those of the alkali metals) a pair of bands at about λ 6200 was observed in the absorption spectrum of a column of calcium vapour at temperatures of 900° C and upwards. On measurement, these bands, which are reproduced in Plate 2, figs 1, 2 and 5, were found to coincide with two prominent calcium chloride bands. Ordinary commercial calcium had been used for the experiments, and on analysis approximately 0.05 per cent of chloride was found in it‡. It seemed evident that the development of the bands was due to this impurity in the metal, and the matter was clinched by adding a trace of bromide to the metal before heating, when the calcium bromide bands in the red also appeared prominently in absorption.

* 'Compt. Rend.', vol. 69, p. 445 (1869).

† 'Z. Wiss. Photographie,' vol. 4, p. 255 (1906).

‡ Eagle ('Astrophys. J.', vol. 30, p. 231 (1909)) observed the chloride bands in the arc spectrum of commercial calcium, and attributed them to chloride present as impurity.

We have since found that this method (of heating excess of the metal with the halogen salt) is a general one for obtaining all the members of this class of spectra in absorption—from magnesium, calcium, strontium, and barium, in combination with fluorine, chlorine, bromine or iodine. The method has obvious advantages over the previous practice of obtaining the bands in emission. Such emission sources are usually faint, and the photographic exposures required are excessive, while if the absorption method is employed the exposure can be made as short as may be desired merely by increasing the intensity of the continuous background. Another great advantage is that the spectra are obtained free from the oxide bands, or from any other interfering spectra. The bands, and especially the fainter ones, can thus be ascribed to their respective molecules with much more certainty than has previously been possible. We have therefore re-examined each of these spectra in absorption, with results that will be found in the catalogue of band heads given later in the paper. It is of interest that Liveing and Dewar* recorded the appearance of the green bands of barium chloride in absorption, when the salt was heated with reducing agents to high temperatures. The observation was only incidental, and they did not pursue the matter any further.

The observation that these bands can be obtained in absorption in this manner is of importance in other directions, as it throws light upon the nature of the "carriers" of the spectra. The only explanation, as we shall see, of the absorption phenomenon, is that the bands originate not from the normal halide molecules such as CaCl_2 or BaI_2 , but from subhalide molecules (CaCl , BaI , etc.). Molecules of this type must persist in the vapour state at the temperature of the experiments. On the chemical side, there have already been several reported preparations of these subsalts in the solid state, and these statements have been followed by some polemical discussion. The claims for the existence of such compounds are completely vindicated, we believe, by the present observations.

It will be more convenient to discuss these conclusions fully, subsequent to an account of the experimental methods employed.

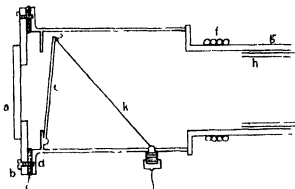
Experimental

Apparatus—The absorption spectra observed were those of a column of vapour about a foot long, maintained in a steel tube of $1\frac{1}{4}$ inch diameter. The tube was heated in a nichrome wound electric furnace, and the temperatures found to be necessary in practice were as high as can be obtained with such a

* 'Collected Papers,' p 22

winding— 1,000° to 1200° C The bands appear at lower temperatures, say 900° C, but they are not then sufficiently intense for satisfactory photography The ends of the steel tube projected several inches from the furnace and were water-cooled by copper spirals, so that quartz windows could be affixed For convenience the windows were first attached to brass plates, and these were screwed to flanges soldered on the ends of the furnace tube, a washer of greased rubber making an airtight joint between the plate and the flange A side tube was also let into the furnace tube near one end, for the removal or admission of gases

Modifications were made in this simple system to smooth the running of the experiments The charge of metal, etc., was not placed directly into the furnace tube but into an inner iron sheath which was withdrawn and cleaned each time This addition prolonged the life of the main tube and kept it in much better condition One of the chief experimental difficulties, and one which caused much delay, was the gradual distillation of the charge from the heated portion of the tube on to the end windows These frequently became too opaque for observation just at the critical part of an experiment This trouble was removed entirely by arranging behind each window an internal shutter which was only pulled down during exposures The disposition of these shutters and of the rest of the apparatus will be evident from the diagram



a, Quartz window, *b* Brass plate, *c*, Rubber washer, *d*, Flange, *e*, Internal shutter, *f*, Copper spiral, *g*, Furnace tube, *h*, Inner sheath, *k*, Operating wire for shutter

The shutter was hinged at one end, and a wire attached to the other, passing out through a packing gland Normally the shutter closed the tube, and was kept in place by a spring On pulling the wire the shutter was lowered, and the system was ready for observations

The continuous background spectrum was provided by a 500-c p "Pointo-

lite" lamp, down to λ 3800 (and with long exposures to λ 3100) For shorter wave-lengths the positive crater of a carbon arc was used as a source, enabling us to photograph down to λ 2300 or λ 2200, and this was the limit of the observations The spectrographs were a constant deviation instrument for the visible region, and a Hilger "E₃" quartz spectrograph for the ultra-violet

Preparation of Sub-halide Vapours—In studying the calcium spectra, the sub-halide vapours were invariably obtained by heating a mixture of calcium turnings and a powdered and dehydrated calcium halide salt This was the obvious procedure in view of the original observations, and it was found to work very well The magnesium halide spectra were obtained in an analogous manner It had been anticipated that to prepare the sub-halide vapours of strontium and barium it would be necessary to isolate the metals themselves, and then to mix them with the normal salts, but this proved to be superfluous The vapours of these salts can be obtained quite readily by heating a mixture of calcium metal and the strontium or barium normal halides The various calcium halide bands, of course, also appear in the absorption spectrum of the vapour, but these can easily be identified after a little experience Further, by regulating the temperature it is possible to minimise the admixture of calcium subhalide vapour with the others, as the strontium and barium compounds seem to be more volatile One slight difficulty arises from the hygroscopic nature of the normal salts The water they soon absorb from the atmosphere is sufficient to cover the surface of the admixed metal with an oxide layer, through which it is most difficult to distil the underlying metal at the temperatures employed It was sometimes found preferable therefore to heat the metal alone in the tube until it was volatilising freely, and then to admit free halogen in small quantity through the side tube, so that the subhalide was prepared *in situ*

Some of the experiments were carried out with the tube evacuated, but more usually an atmosphere of dry hydrogen or argon was introduced, to slow up distillation of the charge to the cooler ends of the tube Evacuation had no visible effect on the appearance of the spectra, with one important exception—the CaF band at λ 5292 The behaviour of this band is fully described in another section Perhaps owing to some chemical reaction, a hydrogen atmosphere had a distinct influence in making the spectra—and presumably the subhalides themselves—difficult to obtain Argon was therefore always used when it was available It may be mentioned that Guntz* states that hydrogen reduces the subsalts when these are in the solid state We are also

* 'Bull Soc Chim,' vol 35 (6), p 709 (1924)

in agreement with his observations that the ease of preparation of these salts increases with the atomic weight of the halogen component. The fluorides proved to be by far the most difficult vapours to obtain, and required a higher temperature than any of the others.

The Origin of the Alkaline Earth Halide Bands

We may now consider the bearing of these experiments upon the origin of the spectra. There can be no doubt from the conditions under which the bands can be excited that they originate from molecules containing both alkaline earth and halogen atoms. The point upon which no experimental evidence has previously borne is whether these molecules are those of the normal halides, such as CaCl_2 , or of a subhalide such as CaCl , or—just possibly— Ca_2Cl_2 . The present observations eliminate two of these possibilities with some degree of certainty, and show that the carriers of the spectra are subhalide molecules of the simple type MX , where M stands for an alkaline earth and X for a halogen atom.

We have made many attempts to observe the spectra by heating the normal halides alone in the furnace, but always with a negative result, even on reaching furnace temperatures well in excess of those normally employed. Further it must be remembered that many of the normal salts are very involatile and have quite negligible vapour pressures at 1000°C , a temperature which is quite sufficient for the development of the bands when other conditions are satisfactory. We can therefore rule out the possibility that the normal halides themselves can show the absorption phenomena which we have recorded. The metal vapours by themselves have no band absorption spectra in the wavelength region under examination, but only a line absorption, details of which we have given elsewhere*. Commercial calcium, it is true, always gives the chloride bands on heating, but this can be traced to chloride present as an impurity, and the bromide, etc., bands are invariably absent from its absorption spectrum. It is only when the two materials, free metal and normal salt are present in the charge that the bands are developed, and so long as this condition is satisfied they always appear. The only explanation of this fact is that these two constituents of the charge must react to give a new type of halide molecule which contains a greater proportion of metal than the original normal salt, and which is also more volatile.

On theoretical grounds, both chemical and spectroscopic, by far the most

* Walters and Barratt, 'Phil. Mag.' (3), p. 991 (1927)

probable formula for these molecules is the simple MX type. The foregoing experiments by themselves do not rule out such molecules as M_2X or M_2X_2 , but other experimental facts render such possibilities quite negligible. We have carried out many trials in which several alkaline earths and halogens were present together in the tube, and we have always found that the spectra were strictly additive—that is to say, there has never been any suspicion of spectra due to such mixed molecules as $CaSrCl$, or Ca_2ClBr , which might be expected if the carriers of the spectra were other than the simple diatomic molecules of the MX type.

These conclusions are in gratifying agreement with the theoretical predictions of R. S. Mulliken* on the origin of these and similar spectra. Such bands, it is held, would not be expected from a "complete" molecule such as $CaCl_2$, but are much more likely to be due to a molecule $CaCl$, containing an unsatisfied valency electron.

Further experiments may now be mentioned which, taken by themselves, would not present a very cogent argument for the subhalide origin of the spectra, but which receive a ready explanation in terms of it. It is well known that if chloroform or other vapour of high chlorine content or chlorine itself is introduced into a flame tinged with the familiar sodium yellow this colouration is immediately destroyed. The generally accepted explanation is that the excess of chlorine combines with the free sodium atoms, and therefore prevents the emission of the D lines. We have found that calcium, strontium, etc., flames can be made to exhibit similar, but rather more complex changes. A flame fed with a spray of a solution of any calcium salt is tinged with the usual calcium reddish colour, and this on examination with the spectroscope is seen to be due to the oxide bands in the red and green. If cotton wool soaked in chloroform is brought moderately near the air inlet of the burner, the colour of the flame changes slightly, and at the same time the oxide bands become extremely faint, and are replaced by the chloride bands in the orange. Finally, when even more chlorine is introduced into the flame by the near approach of the chloroform, the flame becomes "colourless" and neither oxide nor chloride bands can be distinguished. Parallel observations can be made by introducing bromine, or a volatile iodine compound such as ethyl iodide, into the flame. On the subhalide theory the explanation is as follows. The oxide bands show so long as no halogen, or only a little, is present, with more, the chances of a CaX molecule being formed become greater, and the halide bands appear. With excess of halogen present most of the calcium atoms are present

* 'Phys. Rev.', vol 26, pp 29-32 (1926)

as normal halide molecules, and the flame ceases to radiate either oxide or halide bands

Wave-lengths, etc., of the Alkaline Earth Halide Bands

The bands are likely to be of some theoretical interest now that they are known to be associated with an unusually simple type of molecule. Molecules of the type MX, according to current views of atomic structure, must contain a 'completed' halogen atom, bound to an alkaline earth atom which still possesses one free "valency" electron. It has already been pointed out by Mulliken (*loc cit*) and by R. Mecke* that such a system resembles in some respects an atom of an alkali metal. It is not surprising that the resemblance extends to the spectra and that doublet bands are a characteristic of the halide spectra, just as doublet principal series are found with the alkali metals. In the early stages of this work we had some hope that the resemblance might extend further, and that a careful examination of the visible and ultra-violet bands of any one of these molecules might reveal a number of heads arranged according to the Rydberg series spectrum law. Such regularities would not have been new in kind, as they have already been found in the helium band spectrum by Fowler and in the secondary spectrum of hydrogen by Richardson. No such bands could be traced from the older emission data, but it was hoped that the higher members of such a band series, if it existed, would be more prominent in absorption than in emission as are, for example, the higher members of the sodium principal series. In the event, the greater sensitivity of the absorption method certainly asserted itself by enabling us to detect new groups of bands in the ultra-violet, but these do not appear to be arranged according to the series law. We therefore conclude that the various groups of bands in each of these spectra do not correspond to successive members of a single atomic line series, but rather to the first members only of several such series.

All these molecules, except the magnesium halides, have band groups in the visible region. In general, the group of longest wave-lengths in each spectrum consists of bands degraded to the short wave-length side. The next group—usually in the near ultra-violet—is degraded to the long wave-length side. When other groups were found in absorption the direction of degradation alternated from one group to the next. The barium halide bands appear to be exceptional, but in all probability the first group of bands belonging to these molecules lies in the infra red, out of the range of observation. In all cases the first, or visible,

* 'Naturwiss,' vol 13, p 755 (1925), and 'Z f Physik,' vol 42, p 390 (1927)

group was found to be of far greater intensity than the others, some of which were only observed with difficulty, and with unusually dense vapour in the absorbing column. In the accompanying plate, several of the absorption spectra have been reproduced.

With the object of simplifying future work on this subject, in which instruments of higher dispersion than ours will probably be used, we have re-examined all these band spectra by the new absorption method, and we have catalogued below the band heads which can safely be ascribed to each of the various molecules. The possible wave-length accuracy of the measurements is not high, and in most cases we have given the wave-lengths only to the nearest Angstrom unit. Visual intensity estimates have been given for each group of bands, and the degradation to the "long" or "short" wave-length side is indicated. A few bands had no definite degradation. Some of the bands which were exceptionally weak, and others, with ill-defined heads, could not be measured satisfactorily. These are marked with an asterisk. It has not been thought necessary to give a bibliography of each spectrum, as these are available in Kayser's "Handbuch."

The wave-length limit of observation was curtailed for certain spectra by the inveterate appearance of clouds in the absorbing column, and we have therefore given this limit for each spectrum individually.

CaF Bands

Limit of observations, λ 2250 (See Plate 2, fig 5)

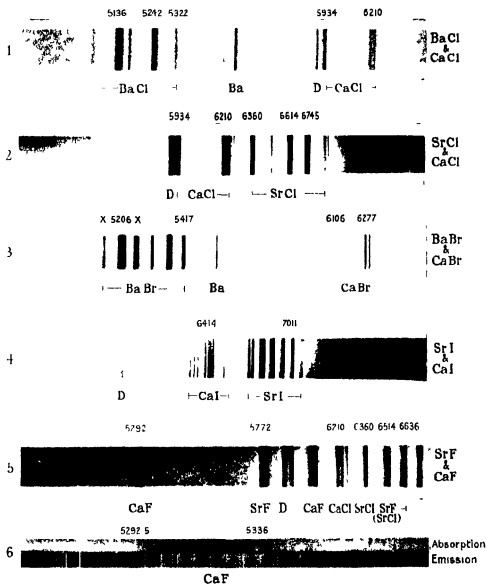
λ Air	ν Vac	Int	Degr
6064 3	16485	8	Long
6051 0	16522	5	"
6035 8	16566	8	"
5861	17086	0	"
*5835	17133	0	"
5292	18891	10	"

A group of bands were noticed at λ 2330, near the observation limit, but they were not developed suitably for measurement. A discussion of the behaviour of the λ 5292 band, and measurements on it with higher dispersion, will be found in a later paragraph.

CaCl Bands

Limit of observations, λ 2500 (See Plate 2, figs. 1, 2, 5)

λ Air	ν Vac	Int	Degr
{ 6350	15743	0	Short
6310	15843	0	"
{ 6210	10098	10	"
6191	16148	5	"
{ 6183	16169	10	"
{ 6075	16456	2	"
6068	16475	2	"
{ 6045	16538	2	"
{ 5934	16847	7	"
5810	17207	1	"
3994	25030	0	Long
3985	25087	0	"
3969	25188	0	"
3948	25322	0	"
3937	25393	0	"
3923	25483	0	"
3907	25588	1	"
3896	25660	1	"
{ 3889	25706	3	"
3877	25786	5	"
{ 3827	26123	3	"
3821	26164	2	"
{ 3816	26191	9	"
{ 3774	26489	3	"
3768	26532	2	"
{ 3763	26567	10	"
{ 3727	26823	3	"
3722	26859	2	"
{ 3717	26896	8	"
3694	27063	2	"
3683	27144	2	"
3671	17233	2	"
3238	30874	0	Short
3220	31047	0	"
3186	31378	0	"
3182	31477	0	"
2918	34260	0	"



CaBr Bands

Limit of observations, λ 2200 (See Plate 2, fig 3)

λ Air	ν Vac	Int	Degr
{ 6390 6	15643	0	Short
{ 6363 8	15709	0	"
{ 6285 0	15906	0	"
{ 6277 5	15925	10	"
{ 6258 0	15975	0	"
{ 6252 7	15988	10	"
6211 6	16094	0	"
6168 5	16207	0	"
6145 6	16267	0	"
6106 6	16371	5	"
6004 3	16651	0	"
3996	25018	0	Long
3960	25245	0	"
3950	25309	4	"
3917	25522	4	"
3910	25568	0	"
2967	33694	0	Short
2952	33865	0	"
2945	33946	0	"
2910	34354	0	"
2890	34592	0	"

We believe a further group of bands exists at about λ 2300, but these were always too indistinct for measurement

CaI Bands.

Limit of observations, λ 2900 (See Plate 2, fig 4)

λ Air	ν Vac	Int	Degr
{ 6609*	15126	0	Short
{ 6578*	15198	0	"
{ 6557*	15246	0	"
{ 6509 3	15358	1	
{ 6486 9	15411	1	"
{ 6460 1	15475	1	"
{ 6411 3	15586	10	"
{ 6390 3	15645	10	"
{ 6363 6	15711	6	"
{ 6314 6	15934	8	"
{ 6291 0	15861	6	"
{ 6268 4	15949	8	"
4334	23097	1	Long
4289	23309	5	"
4255	23405	1	"
4244	23534	0	"
4211	23740	2	"
3266	30600	0	Short
3215	31095	3	
3186	31378	1	
3158	31656	1	
3127	31970	1	

SrF Bands

Limit of observations, λ 2950 (See Plate 2, fig 5)

λ Air	ν Vac	Int	Degr
6635 7	15066	10	Short
6514 9	15345	10	"
5772 8	17318	7	Long

A very faint band was registered on some plates at λ 3646

SrCl Bands

Limit of observations, λ 2300 (See Plate 2, fig 2)

λ Air	ν Vac	Int	Degr
6879	14533	3	Short
6745	14822	10	"
6614	15115	10	"
6478	15432	3	"
6360	15719	10	"
6237	16029	2	"
6220	16072	2	"
4006	24955	2	Long
3982	25106	2	"
3959	25252	10	"
3935	25406	10	"
3916	25529	0	"
3892	25686	0	"

SrBr Bands

Limit of observations, λ 3000

λ Air	ν Vac	Int	Degr
6924	14438	0	Short
6800 2	14701	10	"
6666 6	14996	10	"
6514 7	15345	5	"
4186*	23882	0	Long
4146	24113	4	"
4129	24212	1	"
4108	24336	9	"
4090	24443	3	"
4073	24545	2	"
4053	24666	10	"
4019	24875	2	"
3992*	25043	0	"
3945	25341	5	"
3909	25575	5	"

SrI Bands

Limit of observations, λ 2400

λ Air	ν Vac	Int	Degr
7094 0	14092	2	Short
7011 0	14259	10	"
6930 2	14425	10	"
6847 7	14599	10	"
6767 8	14772	10	"
6691 5	14941	8	"
6602 3	15005	8	"
6177 3	16184	4	"
4482	22305	0	Long
4447	22481	4	"
4412	22659	10	"
4381	22819	1	"
4339	23040	2	"
4307	23211	6	"
4276	23380	1	"
3439*	29070	0	Short
3406*	29351	0	"
3378*	29595	0	"

BaF Bands

Limit of observations, λ 2800

λ Air	ν Vac	Int	Degr
7358	13587	10	Long
7117	14047	10	"
6911	14486	10	"
5119*	19529	0	"
4995 4	20013	2	"
4988 3	20041	2	"
4948 5	20202	4	"
4939 9	20237	4	"
3497	28588	0	"
3458	28910	0	"
3419	29240	0	"
3401	29394	0	"
3372	29647	0	"
3365	29709	0	"
3347	29869	0	"
3330	30021	0	"
3311	30193	0	"

BaCl Bands

Limit of observations, λ 2200 (See Plate 2, fig 1)

λ Air	ν Vac	Int	Degr
5322	18785	1	Short
5241 9	19072	10	Long
5213 9	19174	0	Short
5166 6	19350	2	Long
5136 0	19465	10	"
5066 6	19731	0	Short

BaBr Bands

Limit of observations, λ 2600 (See Plate 2, fig 3—The two bands marked * are due to BaCl)

λ Air	ν Vac	Int	Degr
5417	18455	7	No head
5361	18648	10	"
5303	18852	6	"
5261	19002	4	"
5206	19203	10	"
5153	19400	5	"
5101	19598	0	"

BaI Bands

Limit of observations, λ 3000

λ Air	ν Vac	Int	Degr
5609 5	17822	10	Short
5381 7	18576	10	"
5260*	19006	0	?
5160*	19374	0	?
3830	26102	1	Short
3804	26280	2	"
3778	26461	3	"
3756	26616	3	"
3736	26769	1	"

MgF Bands

Limit of observations, λ 2800

λ Air	ν Vac	Int	Degr
3659	27322	3	Long
3637	27487	0	"
3619	27624	3	"
3592	27832	2	"
3563	28058	4	"
3527	28344	4	"
3497	28596	8	"
3478	28744	1	"
3462	28876	10	"
3419	29240	10	"
3401	29395	1	"
3388	29507	0	"
3382	29560	8	"
3364	29718	3	"
3345	29887	6	"
3329	30030	4	"
3314	30166	1	"
3309	30212	3	"
3294	30349	1	"
3270	30516	0	"
3261	30656	0	"

MgCl Bands

Limit of observations, λ 2700

λ Air	ν Vac	Int	Degr
3779	26454	0	?
3776	26475	10	Short
3748	26673	10	"
3708*	26961	0	"
3687*	27114	0	"

The band at λ 3779 was so narrow that it had the appearance of a sharp line

MgBr Bands

Limit of observations, λ 3000

λ Air	ν Vac	Int	Degr
3934*	25412	0	Short
3918*	25516	2	"
3881	25759	10	?
3864	25872	10	Short
3841*	26027	0	"
3821	26164	2	?
3819	26177	2	Short

3881 and 3821 were so narrow as to appear to be sharp line absorptions

MgI Bands

Limit of observations, λ 3000

λ Air	ν Vac	Int	Degr
4110	24324	10	Short
4027	24825	1	"
4001	24987	1	Long
3983	25099	10	Short
3951	25303	10	Long
3927	25457	2	"
3902	25620	2	"
3877	27337	1	Short
3828	27555	1	"
3602	27754	1	"
3432	29129	0	"
3405	29360	0	"
3396	29438	0	"
3380	29577	0	"
3358	29711	0	"

The Structure of the CaF Band, λ 5292, in Absorption

We have compared many of the bands obtained in absorption by the methods described in preceding sections, with the corresponding emission spectra from flames and arcs, and in general we have been unable to detect any differences in their structure or intensity distribution. The calcium fluoride band at λ 5292 provided a notable exception. This band has been fully described by Datta* and observed in emission it has a very simple structure, consisting of a number of doublet lines with a separation of about 2 Å, which conform to a Deslandres formula. It was immediately evident, even under the small dispersion of the constant deviation instrument, that the structure of the absorption band was very different. It covered the same wave-length range, but there were many more lines developed within that range, and the intensity distribution had no relation to that of the emission band. With the very kind assistance of Prof T R Merton we were afterwards able to examine the behaviour of this band under much higher dispersion. Photographs of the spectrum, in emission and absorption were taken in his laboratory with a Littrow spectrograph fitted with a glass prism which gave a dispersion of 5 Å per millimetre in the region of λ 5300. The differences of structure suspected under small dispersion were found to be real. An enlarged reproduction of the band in arc emission and in absorption is given in the Plate 2, fig 6.

The appearance of the band is so changed under the two conditions that

* 'Roy Soc Proc,' A, vol 99, p 436 (1921)

evidence may be required that we are really dealing with the same band, and not merely with a coincidence in the position of two distinct bands of different "carriers" In the first place, the band cannot be obtained in either form unless calcium and fluorine are present Also some of the lines in the emission band (including the two of shortest wave-length) coincide with lines in the absorption band, and finally parallel changes were seen, under small dispersion, in the SrF band at λ 5773, which vastly diminishes the chances of a mere coincidence

The table appended to this section gives the wave-lengths of over 80 absorption lines in this CaF band, and also the wave-lengths of the few emission lines in the same region, calculated from Datta's formula in the paper previously quoted The relative wave-lengths of the absorption lines are probably accurate to a few hundredths of an Angstrom unit, but the absolute errors may be greater, as only one plate was available for measurement

We are unable to assign any certain cause for this radical difference in the structure of the band in emission and absorption The pairs in the emission band presumably correspond to molecular vibrational changes, and the closely packed absorption lines to rotational changes in the same molecule It may be mentioned that, on strong plates the emission spectrum has a faint background of fine structure also, but this does not correspond in any way with the absorption lines The most usual cause of intensity modifications in a band spectrum is a temperature effect, and the conditions of experiment were certainly such as to render operative any influence of this nature The temperature in the absorbing column must have been very much less than that in the arc which produced the emission bands The data we present in this paper are not sufficient to settle this point satisfactorily, but we do not believe that temperature differences—though doubtless these produce some modification—will prove a complete explanation of the changes

There is one consideration which suggests that pressure may have an important bearing on the matter While the absorption spectrum was being examined with the high dispersion spectrograph it was found that the fine structure of the band, here recorded, was only developed when the furnace tube had been evacuated of foreign gas When hydrogen or argon were admitted, the absorption merged into two continuous regions separated by a rift at about λ 5303. Now if a photograph of the emission band is examined it will be found that there is always a weak continuous background in evidence, and that this has the characteristic rift at the same wave-length It therefore seems possible that the fine structure of this CaF band only appears under suitable conditions

of pressure, and that it is usually represented only by a weak continuous spectrum

Absorption Lines in the CaF Band, λ 5292

λ Vac	ν Vac	Int	λ Vac	ν Vac	Int	λ Vac	ν Vac	Int
5292 52	18894 59	1	5310 85	18829 37	1	5325 19	18778 67	1
5294 36	18888 02	2	5311 38	18827 49	1	5325 47	18777 68	1
5296 20	18881 46	0	5311 66	18826 60	1	5325 65	18777 05	1
5296 54	18880 29	1	5311 95	18825 47	1	5325 95	18775 99	1
5296 97	18878 71	2	5312 17	18824 69	1	5326 17	18775 21	2
5297 49	18876 85	2	5313 21	18821 01	3	5326 42	18774 73	1
5297 94	18875 26	3	5313 79	18818 95	1	5326 89	18772 67	8d
5298 84	18872 05	4	5314 16	18817 68	2	5327 52	18770 45	5
5299 60	18869 34	2	5314 73	18815 63	3	5328 19	18768 09	1
5300 12	18867 49	2	5315 32	18813 54	3d	5328 56	18766 79	3
5300 95	18864 54	5d	5316 07	18810 88	2	5329 34	18764 04	2
5302 12	18860 38	5	5316 45	18809 54	0	5329 04	18762 99	1
5302 86	18857 74	4	5316 89	18807 98	2	5329 89	18762 11	1
5303 55	18855 29	6	5317 36	18806 32	1	5330 11	18761 33	1
5304 21	18852 84	4	5318 05	18803 88	7d	5330 39	18760 35	2
5304 68	18851 27	3	5318 58	18802 08	0	5330 92	18758 48	0
5305 10	18849 78	2	5319 31	18799 43	3	5331 16	18757 64	1
5305 74	18847 51	3	5319 60	18798 19	2	5331 90	18755 04	4d
5305 94	18846 80	8	5320 16	18796 42	1	5332 88	18751 59	1
5306 29	18845 55	10	5320 85	18793 98	0	5333 71	18748 67	2
5306 56	18844 59	4	5321 27	18792 50	1	5334 02	18747 58	1
5307 31	18841 93	4	5321 52	18791 62	3	5334 55	18745 72	1
5307 70	18840 55	3	5321 96	18790 06	7	5334 82	18744 77	1
5308 02	18839 41	4	5322 24	18789 08	10	5336 22	18739 85	1
5308 52	18837 64	2	5323 02	18786 32	1	5336 55	18738 60	1
5309 19	18835 26	2	5323 51	18784 59	1	5336 90	18737 46	0
5309 51	18834 12	3	5323 76	18783 71	0	5337 22	18736 34	0
5310 25	18831 50	7	5324 01	18782 83	4			
5310 48	18830 68	7	5324 53	18781 00	0			

Emission Lines in the same Band

5292-5	5298 2	5304 1	5310 1	5316 1	5322 1	5328 1	5334 6
94 4	5300 1	06 0	11 9	17 8	23 9	30 1	36 3

NOTE—The lines marked (d) are unresolved complex lines

Summary

1* Alkaline earth subhalide molecules of the type MX exist in the vapour state at 1000° C in equilibrium with the metal and the normal salts

2 The alkaline earth halide spectra are the resonance spectra of these molecules, and they are readily observed in absorption through a column of the vapour

3 The bands in each halide spectrum have been examined by the absorption methods, and new groups have been found in the ultra-violet.

4 The CaF band, λ 5292, has been examined under a dispersion of 5 Å per millimetre. The structure of the band is very different in emission and absorption. The fine structure of the absorption band only appears at reduced pressures

On the Measurement of the Variation of the Specific Heat of Aniline with Temperature, using the Continuous Flow Electric Method

By H R LANG, Ph D , A Inst P

(Communicated by H L Callendar, F R S—Received November 26, 1927)

1 *Introduction*

These experiments were undertaken in order to obtain reliable data on the variation of the specific heat with temperature of a liquid of low vapour pressure, in the neighbourhood of its freezing point. The employment of a continuous flow method required large quantities of the liquid, and aniline was chosen as it was thought that it could be procured in bulk, pure and dry. Unfortunately, this proved less easy than was anticipated and was one of the chief difficulties encountered. In addition, the viscosity of aniline increases very rapidly below about 10°C which caused some uncertainty below this temperature. Most of the ordinary laboratory materials are slowly attacked by aniline, the earlier apparatus was constructed without rubber, and this necessitated the use of a hermetically sealed calorimeter. Subsequently a good quality rubber was found that withstood the action of aniline, and this greatly simplified the mechanical difficulties.

2 *Outline of Method*

The principle of the method is to allow a stream of the liquid to flow through a fine bore tube, through which passes an electrically heated manganin strip, and to measure the resulting rise in temperature. A very full description and discussion of the method has been given by Prof Callendar and Dr Barnes,* and frequent reference to these papers will be made, which will be indicated by the name and the page.

The elementary theory is as follows

If E is the p.d. between the ends of the heater in volts,

C current in amperes,

Q the rate of flow of the liquid in grams per second,

s specific heat of the liquid,

J the mechanical equivalent of heat,

d rise in temperature in degrees Centigrade,

h rate of loss of heat per degree rise in temperature,

* 'Phil Trans,' A, vol 199, pp 55 and 149 (1902)

then, when conditions are steady, the energy equation per second is

$$EC = JsQ d\theta + h d\theta \quad (1)$$

By changing the watts EC and the rate of flow Q so as to keep the rise $d\theta$ the same, two equations are obtained between which h may be eliminated and so s found. In practice it would take too long to arrange exactly the same rise, so that a value within about 1 per cent is obtained and the equations are reduced, as explained below. It is to be noted that h is here assumed to be independent of Q and $d\theta$, and the necessary conditions for this have been investigated by Callendar (p. 121) and Barnes (p. 225). In these experiments great trouble was taken to ensure that these conditions were fulfilled.

3 Measurements

(a) *Electrical*—The main current to the heater was supplied from two groups of five 40-ampere-hour accumulators in series, the two groups being in parallel. In series with the battery was an ammeter, standard resistance coil, a variable manganin wire resistance, and the heater. The watts supplied to the heater were measured by determining the potential difference between the ends of the heater and the ends of the standard resistance, in terms of Weston-cadmium cells, using a four-dial potentiometer and a high-resistance moving-coil galvanometer. The readings of the various potential differences could be taken in rapid succession by changing over copper connectors between suitably arranged mercury cups. The potentiometer was calibrated against a standard one at the beginning and end of the experiments and found to be correct to 1 part in 10,000. Further, the coils being of manganin no temperature correction was necessary.

The standard resistance was a flat coil of platinum-silver enclosed in a metal casing, made by R. W. Paul, and bearing a Cambridge certificate of 1894. This gives the values in International ohms as

$$1.0000 \text{ at } 16.3^\circ \text{C}$$

$$0.99950 \text{ at } 14.7^\circ \text{C}$$

The temperature coefficient was taken as 3.1×10^{-4} per deg. C. After completion of this work the coil was sent for standardisation to the National Physical Laboratory, and was reported to have the value

$$1.0010, \text{ International ohms at } 20^\circ \text{C},$$

which differs by 1 part in 10,000 from the value used.

The standard cells were hermetically sealed H-type of cadmium cells, and the E M F of each was taken as

$$1.0183 \text{ volts at } 20^{\circ} \text{ C}$$

with a temperature correction given by

$$E_t = E_{20} - 0.0000406 (t - 20),$$

where t is the temperature in degrees Centigrade

A group of six new cells was purchased specially for this work, and on several occasions these were compared with each other, and found to agree among themselves to the accuracy with which the instruments could be read. Two of the cells were sent to the National Physical Laboratory for test, and the following are the values given on the certificates —

Cell No 1—1.0182 volts at 20° C ,

Cell No 2—1.0181 volts at 20° C ,

and both cells showed a decrease of 0.00004 volt per degree Centigrade increase of temperature. These values agree well with the International value used.

(b) *Thermometry*—Two platinum thermometers of the usual type were used differentially. The coils were about 6 mm diameter and 7 cms long, wound on mica crosses, and the heads were small rubber bungs drilled to grip the leads. A detailed description of the method of construction has already been given*. As they were for use differentially, the fundamental intervals were adjusted to be as nearly equal as possible, and the value chosen was 500 bridge units, which is a convenient one for calculations. One bridge unit is equal to 0.01 ohm. Two Callendar-Griffiths bridges of the usual type made by the Cambridge Scientific Instrument Company, with manganin coils, were used in conjunction with an Ayrton-Mather type of galvanometer of resistance 7.40 ohms. The bridges were calibrated on several occasions by the well-known method, in terms of the largest coil, and the corrections found to be very small, the separate calibrations agreed to better than 0.02 bridge units or 0.004° C. The ends of the external leads of the thermometers were soldered to special contact pieces, fitting copper-mercury cups to facilitate rapid change from the differential reading to the direct measurement of the inflow temperature. A movement of the bridge contact through 1 mm of bridge wire was equivalent to 0.02° C and gave a deflection of five scale divisions on reversing the current, and this was tested before each experiment and found remarkably constant.

* 'J. Sci. Inst.', vol 2, p 228 (1926)

No attempt was made to obtain exact balance, the contact being set to the nearest millimetre, the deflection on reversing the current was noted, and the exact balance point was deduced to the nearest 0.01 cm. The fixed points of the thermometers (ice and steam) were determined on several occasions, and the following table gives a summary of the values found. As the temperature rise could be read to 1 part in 5,000 only, it was unnecessary to obtain a much greater accuracy in determining the fundamental intervals.

Table I — Fundamental Intervals of Thermometers

Date	Thermometer A	Thermometer B
1925 December 23	Using bridge No. 2087	500.03 units
		500.04
		500.03
		500.05
		500.10
December 24 December 30		500.01
1926 March 22	499.92 units	
March 23		
March 24		500.10
March 25		500.05
	Using bridge No. 862	
August 26	499.76	499.96
August 27	499.67	499.89
	Mean value used in reduction of results —	
	499.87	500.00

The absolute value of the unit on the two bridges is slightly different, which accounts for the lower value obtained with the second bridge.

By taking "cold" readings, t_c , the differential reading before the heating current was switched on, all other conditions being the same (Barnes, *loc. cit.*, p. 195), several corrections were accurately eliminated. The "hot" readings were those taken when the current had been switched on and conditions had become steady.

Let C be the "cold" bridge reading, and H the corresponding "hot" reading, then if F is the fundamental interval of the thermometer at the outflow end,

$$\text{temperature rise on the platinum scale} = (H - C) 100/F. \quad (2)$$

As the fundamental intervals of the thermometers had been adjusted so nearly equal, a change of a whole degree in the inflow temperature would make a

correction of only 1 part in 25,000 to the temperature rise, and the apparatus was so designed to ensure that it remained constant to within 0.05°C . If there were no conduction losses or heat generated by internal friction in the fine flow tube, the "cold" reading would be zero, but owing to these minor effects it was never quite so. The only conduction effect which is not eliminated by this method is that extra part due to the increase of the outflow end's temperature, but as a great length of this thermometer (25 cms) was inside the vacuum jacket, and the rise used was generally only 8 or 10 degrees, this must have been quite negligible (*cf* Callendar, p 125, and Barnes, p 230). This is further shown to be negligible by the fact that the value of the specific heat came out the same, within the limits of experimental error, whatever rise in temperature was used.

Having obtained the rise in temperature on the platinum scale, it was reduced to the gas scale by applying the well-known formula

$$t - pt = \delta(t)(t - 100), \quad (3)$$

taking the value of δ as 1.5×10^{-4} .

(c) *Determination of Weight*—The outflowing liquid was run into a 500 cc flask which had just previously been weighed. The weight of liquid collected was of the order of 300 or 400 gms and was taken on a chemical balance, using brass weights. These were previously tested, and the errors found to be negligible compared with the accuracy of the other observations. A small correction to reduce the weighings to *vacuo* was applied. On to the end of the apparatus was sealed a specially ground large bore two-way tap, the feature of which was that in the midway position the liquid flowed out of both sides, so that the flow was never actually stopped, and thus steady flow conditions were left undisturbed. A large wooden handle was fixed to the key of the tap and stops on each side arranged in suitable positions.

(d) *Time Determinations*—A Dent's ship chronometer was used and was rated against the Greenwich time signals sent out by the BBC. The rate of gain was sufficiently constant, but was rather larger than was expected, being about 30 seconds a day. This comes to nearly 1 part in 3,000, and being a small systematic correction was applied to the final results as a whole. An experiment usually lasted 10 to 15 minutes, and on the faster flows two determinations were made during this time of the rate of flow. The intervals were started and stopped by counting the last 5 seconds with the tick of the chronometer and rapidly switching over the tap at the given time. It is not likely

that the error made in this way was more than 1/10 second, or on the average about 1 part in 6,000

4 The Calorimeters

In all some six calorimeters were used at various times, but of these only two survived the handling to which they were subjected, these will be referred to as calorimeters A and B. Calorimeter A (fig 1) was similar to those used



FIG 1

by Callendar and Barnes in the original experiments by this method with water, and calorimeter B (fig 2) had the vacuum jacket separate, in place of being

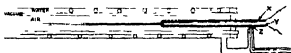


FIG 2

sealed on to the flow tube, the intervening space being filled with air. The idea of this was to be able to use the same vacuum jacket and water jacket with different flow tubes, thereby making replacement in case of breakage more easy, but owing to convection in the air space, calorimeter A proved more satisfactory. At one time the air space in calorimeter B was filled with powdered cork to prevent this convection, but the thermal capacity was so large that it had to be abandoned. The glass work was done by Messrs The National Glass Industry, of London, who also silvered the vacuum jackets, and exhausted them with a Born-Kessel mercury-vapour pump whilst heating them in an oven to about 200° C. They were then sealed off. I should like to testify to the strict attention to details of dimensions which was paid, and which was so important in order that the metal parts should fit tightly.

Calorimeter A had the following dimensions. The fine bore-flow tube CD (fig 1) was 2 mm in diameter, and 50 cms long. It was fused at each end to tubes AC, DE, of 2 cms diameter. The vacuum jacket was fused to these wider tubes at C and D and enclosed 20 cms of the inflow tube DE, and 25 cms of the outflow tube AC. A greater length of the outflow tube was enclosed, as the

heat loss from this end is greater, since at the outflow end the water circulating around the calorimeter is at a different temperature to the liquid, whereas at the inflow end it is at the same temperature. The vacuum jacket was 5 cms in diameter and 95 cms long, and the exhaustion seal was horizontal so as to facilitate the mounting in the water jacket. In fig 1 is shown the calorimeter with the thermometers and other fittings in place. The "heater," which passed through the fine bore-flow tube, was a twisted manganin strip with about one twist per centimetre, and which served to prevent stream-line motion (Barnes, p 234). This was made from a piece of 18-gauge manganin wire rolled between a small pair of steel rollers. It was annealed every third time through the rollers and was finally annealed by passing a current through it, whilst held fixed and twisted, and in this way took up a permanent twist. A portion of suitable length was got into position between copper cylinders in the manner described by Barnes (p 204). On the outside of these cylinders a rubber cord, of square cross-section, was wound, which served to hold them firmly in position and allowed no liquid to pass without being stirred around the cylinder, thereby ensuring the accurate measurement of the mean temperature of the stream. The *vital* importance of this was not at first realised to the fullest extent (*cf* Callendar, p 106), and thereby most of the earlier experiments were spoiled. In trying to avoid the use of rubber, copper wire, wound on the outside of the cylinders was tried, but was a failure. In some cases a screw thread of 0.5 cm pitch and 2.5 mm deep was cut on the outside of the cylinders, and, when carefully ground to fit the tubes, proved satisfactory. On to the ends of the cylinders, four 18-gauge tinned copper wires were soldered, three carried the current and one was a potential lead. The coils of the thermometers were completely covered by the cylinders, which served also to prevent the generation of heat in this neighbourhood. Some difficulty was experienced in closing the ends of the tubes AC, DF (fig 1), but this was finally done as follows. The four wires were painted with collodion acetate and pulled through rubber bungs bored to take the thermometers, and the whole then given several coats of collodion. Small side tubes were sealed into the wider ones for entrance and exit of the liquid into the calorimeter. The inflow tube and calorimeter were wound with rubber spirals to make the jacketing water circulate efficiently, and the copper water jacket was lagged with cotton wool and asbestos.

5 Arrangement of Flow Circuits

Fig 3 shows diagrammatically the liquid flow circuits. Taking first the water circulation, the water tank A was of copper and contained a pump of the screw-propeller type, and thermo-regulation apparatus. The return water from the jacket around the calorimeter was sucked into the base of a wide

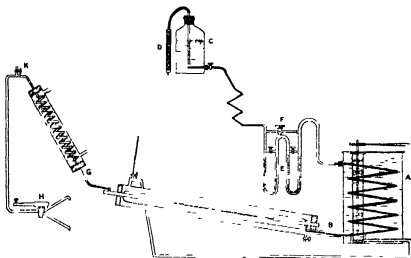


FIG 3

vertical cylinder, and discharged at the top. It then drifted downwards, and re-entered the jacket at B, passing over the liquid inflow tube *en route*, and so returned once again to the tank. The thermo-regulator used was of the type devised by Gouy and described in detail by Barnes (p 209). The aniline was supplied from the glass Mariotte bottle C which was mounted on a platform that could be raised and lowered, thus enabling the replenishing of the reservoir to be readily performed. A central glass tube passed nearly to the bottom of the bottle, and kept the head constant after the manner of an aspirator, a calcium chloride tube D was connected to this so that only dry air could come in contact with the aniline. From here the liquid passed through a flexible composition tube to the capillary throttles E. These controlled the rate of flow, and consisted of a U of 1-2 mm diameter glass capillary, which could be short circuited by a wide-bore tap, fused across the top. There were six of these in series (only two are shown in the figure), and a $\frac{1}{4}$ inch bore tap was fused right across the whole group, so that they could be completely cut out of the flow circuit. They were immersed in a water bath to prevent fluctuations due to change in viscosity with temperature. In order to acquire

the correct inflow temperature, the aniline now passed through some 25 feet of tin tubing immersed in the tank D. The liquid then entered the calorimeter, and became stirred by the spirals round the copper cylinders, and by the twist in the heating strip, until it emerged again to enter the cooler at G. This was a long glass spiral around which tap water was made to circulate. From here it passed out through the special two-way tap already described, and was collected and poured back into the reservoir, thus completing the circuit. At K, the highest point of the flow tubes, an air trap was introduced, and the calorimeter was tilted so as to help the air to travel up to this point. This served to release any air that had accidentally got into the apparatus.

6 *Purification of the Aniline*

As is well known, aniline, if kept, even in closed bottles, turns a dark brown, the cause, apparently, is unknown. Further, it is hygroscopic and it is believed that this accounts largely for the conflicting results found in the literature. According to the results of Bartoli, which are discussed below, 1 per cent of water causes an increase of 2 per cent in the specific heat. It was therefore important to use only dry and freshly distilled aniline, much time was spent in finding suitable means to do this for the large quantities required, and finally Messrs Hopkin and Williams undertook this part of the work. Dr Jackson, of this firm, went to great trouble to deal satisfactorily with this problem, and I wish here to tender my thanks to him. The method adopted to prepare a batch (about 40 lbs) of aniline was as follows. It was left in contact with powdered caustic soda for three days, and distilled from a tin-lined still with a silica condenser and a closed-up glass receiver at atmospheric pressure. When it was delivered it was of a very pale straw yellow colour, and was rapidly transferred to the glass reservoir, after this had been rinsed out two or three times with the fresh liquid. After it had been twice through the apparatus, it was sent back to be dried and again re-distilled. Dr Jackson very kindly determined the freezing point of each batch, using a mercury thermometer, which he lent to me to calibrate against the platinum thermometer which I used later for the same purpose. These corrected values formed the means whereby the water content could be determined. A series of experiments was performed to determine the variation of the freezing point with percentage water, for this purpose some aniline was initially specially dried over calcium chloride for several days and its freezing point determined immediately after re-distillation, using a platinum thermometer and motor-driven stirrer, and supercooling about 1.5°C . The following figures were obtained —

Freezing point	Percentage water by weight
- 6 05	0 00
- 7 03	0 48
- 8 61	0 97
- 9 58	1 46
-10 36	1 95

These agree very well with the values given by Appleby and Davies,* and both sets are plotted in fig 4, which was the curve used in the reduction of the

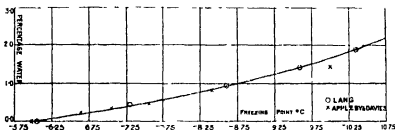


FIG 4

results The aniline used, with one exception, had freezing points between -5.9 and -6.3°C , corresponding to zero and to 0.1 per cent water. On three occasions aniline which had been kept in tightly stoppered bottles in the dark was used, and though now a pale brown colour gave a specific heat agreeing with the value given by the freshly distilled liquid, these results are given in the tables below. It seems probable, therefore, that the darkening does not affect the specific heat.

7 *Modus Operandi*

The water in the jacket around the calorimeter and that in the tank had first to acquire the required inflow temperature. For the lowest temperature used, the tank was filled with ice chippings and water, and the thermo-regulator device removed. The tank was continually replenished with fresh ice, and during one experiment about $1\frac{1}{2}$ cwt. was used, remarkably constant conditions could be obtained in this way.

Some experiments were also tried with the thermo-regulator, and an additional spiral in the tank, through which ran a stream of water, previously cooled in an ice bath, but steady conditions were never obtained in this way, and so the results were rendered very uncertain. A tap-water circulation was also

* *J Chem Soc*, vol 127, p 1839 (1925)

used, and in this case the temperature slowly crept up during the day, but was sufficiently constant over one experiment. For points in the neighbourhood of 20°C the laboratory temperature was used, and to do this the thermo-regulator was put out of action, and the water just circulated around the calorimeter. Points above this were taken using the thermo-regulator, and those above 30°C required a small gas flame to aid the heating lamp, the latter acting only as a fine adjustment over and above the heat supplied by the gas flame, and thus compensating for fluctuations in the gas pressure.

The rate of flow was next fixed by adjusting the capillary throttles, and when conditions had become steady (about half an hour), the "cold" readings were taken over a period of about 10 minutes. In the case of the lowest points a measurement of the rate of flow was taken in order to find the change with the current on and off, and so correct the "cold" readings to the rate of flow actually used in the experiment.

The current was next adjusted to a suitable value and its rough value read from the ammeter. After about half an hour conditions had become sufficiently steady for the readings to be commenced. Meanwhile the empty flasks were weighed, and the approximate values of the bridge and potentiometer balances were found.

A "run" was commenced with the determination of the potentiometer balance of the standard cells, and a reading of their temperature and then the inflow temperature. The flow was now switched into a weighed flask, at a definite time by the chronometer, and immediately afterwards a reading of the rise in temperature taken. Following this, the potential difference across the standard resistance and its temperature, and then the rise again, followed by the potential difference across the heater, and the rise again, the cycle of readings was then repeated. The rise was read in this way every minute and the potential differences every two minutes. The times of all observations were noted to the nearest half-minute, in order to assist in tracing possible errors. Two "runs" were taken on the faster flow, and then the current and the rate of flow reduced to give the same rise of temperature to within 1 per cent as in the faster flow, and two more "runs" taken when conditions had again become steady. At the end of each "run" the inflow temperature and the standard cell readings were again taken. The current was now switched off and the apparatus allowed to cool down to the inflow temperature, when the "cold" readings for the slower rate of flow were taken.

It will be seen from the summarised tables of observations that two "runs" agree to 1 part in 1,000 and often better than this. On some occasions three

or, four different rates of flow were taken in order to test whether the heat loss was independent of the rate of flow as required by the theory of the method

8 Method of Reduction of Results

In reducing the results, the watts per gramme per degree were first calculated, i.e.,

$$X = EC/Q d\theta$$

This is the value of the specific heat in work units, uncorrected for the heat loss. Taking, then, the mean of the two "runs" on the same rate of flow, and using this in equation (1) in conjunction with the mean of two "runs" on the other rate of flow, by eliminating h the following equation is obtained —

$$\text{Specific heat} = (Q_1 X_1 - Q_2 X_2) / J (Q_1 - Q_2)$$

By substituting back the value of h was found. For the mechanical equivalent of heat (J) the value 4.180 joules/calorie was used (Callendar, p. 132)

9 The "X Test" on the Calorimeters

The elementary theory of the method assumes that h in equation (1) is independent of the rate of flow, and it was considered necessary to test this point experimentally. In order to do this three or four different rates of flow were used on various occasions, and the values of X plotted against $1/Q$, in fig. 5. Equation (1) may be written

$$X = EC/Q d\theta = Js + h/Q \quad (4)$$

If h is independent of Q throughout the range, then the graph should be a straight line, of which the slope would be equal to h and the intercept on the ordinate axis the value of the specific heat in work units. In fig. 5 the mean

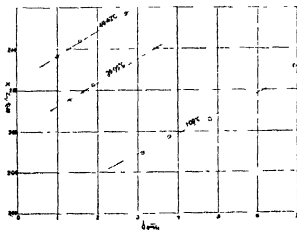


FIG. 5

temperature of the experiment is written along the lines, and it will be seen that, leaving the low temperature point (1.09°C) for later consideration, equation (4) is true to at least 1 part in 2,000 over the range, and all the curves show a very slight curvature in the same direction, this means that there is a very small term, varying inversely as Q , to be added to equation (1). The cause of the existence of this term and its magnitude are discussed below. As regards the determinations at the lowest temperatures, it was most important here to try the X test, as the viscosity is so great, and varies so rapidly with temperature in this region, that it was uncertain whether the necessary conditions were fulfilled for the theory of the method to hold. The X test shows a rather more marked curvature than at higher temperatures, the point representing the smallest rate of flow is here assumed to be in error, owing to the great experimental difficulties in measuring such a small rate of flow and so small a rise of temperature to this high degree of accuracy. At these low temperatures, then, where the viscosity plays such an important part, the accuracy of the experiments must be considerably less than at higher temperatures.

It has been shown by Barnes (p. 231) that the heat loss per degree rise \dot{h} is independent of the rise of temperature $d\theta$. Further, as \dot{h} was actually found in each case for two different rates of flow but the same rise, it would not matter if it were somewhat dependent on $d\theta$, as the value for those conditions was measured and used in each case. The value of \dot{h} was found to be nearly proportional to the mean temperature of the experiment and to depend to some extent on the previous history of the calorimeter. The reason for the latter is, no doubt, the release of occluded gas from the silvered walls of the vacuum jacket. Thus, after a low temperature point, on returning to about 30°C the heat loss had slightly decreased, and similarly after the calorimeter had been at a high temperature and was then used at a much lower one, the heat loss increased from the value expected at this point. Although curves were plotted showing the relation between \dot{h} and the mean temperature of the experiment, it serves no purpose in reproducing them here, as the value of \dot{h} is actually measured in each case, and therefore its variation with temperature does not affect the calculated values of the specific heat.

10 Corrections

In the published papers on the applications of the method of continuous flow calorimetry (Callendar and Barnes, *loc. cit.*) will be found a full discussion

of the possible sources of errors and the corrections applicable, and it is not proposed, therefore, to deal with them here in detail

There is a correction for the variation of the gradient in the fine flow tube (Callendar, p. 121) and also for the conduction from the outflow tube due to the rise in temperature. This requires the addition of a small term, varying inversely as Q , to be added to equation (1), and it is this term that accounts for the slight deviation of the plot of equation (4) from a straight line. A calculation of this correction, based on the reasoning given by Callendar, showed it to be of the order of 1 part in 5,000, and in the case of the lowest temperatures and slowest flows, where it was largest, about 1 part in 1,000.

Correction for Water Content. The water content of each batch of aniline was determined in each case from the freezing point in the manner described above, and then, using Bartoli's figures, which are sufficiently accurate for this very small correction, the value of the specific heat found was reduced to that for perfectly dry aniline. The correction was of the order of 1 part in 500 and in many cases zero.

11 Summary of Observations

The following tables give a summary of the observations taken with calorimeter A. Column I gives the date of the experiment for purposes of reference to the original books of observations, column II gives the inflow temperature reduced to the gas scale, and is the mean of the value at the beginning and end of a "run". Column III contains the mean temperature rise, reduced to the gas scale, and is the mean of readings taken every minute during an experiment of 10–15 minutes. Column IV gives the watts supplied to the heater, and is the mean of readings every two minutes. Column V contains the value of the rate of flow of the liquid in grammes per second, and in most cases is the mean of two independent observations. The calculated values of X or $EC/Q \, d\theta$ are given in column VI, and the remarkable agreement for successive "runs" on the same rate of flow shows how accurately the results could be reproduced. In calculating the results the mean value of X has been used in each case. Column VII gives the mean temperature of the experiment, and column VIII the value of the specific heat in calories per gramme degree Centigrade, calculated by the elementary theory. The value of h is also tabulated in column VIII. The final values, corrected for water content, are tabulated in the last column in Table II.

Table II—Calorimeter A

I	II	III	IV	V	VI	VII	VIII	IX
1926								
Nov 23	21 74 21 74 21 78 21 76 21 78	8 598 8 606 8 542 8 602 8 490	13 881 13 871 6 443 6 438 9 419	0 7048 0 7038 0 7518 0 3487 0 5220	2 1110 2 1102 2 1441 2 1463 2 1252	26 06	$s = 0.4977$ $h = 0.0225$	0 4977
Nov 24	9 723 9 731 9 717 9 723	10 552 10 534 10 599 10 603	12 883 12 885 7 016 7 009	0 5812 0 5815 0 3110 0 3108	2 1004 2 1002 2 1285 2 1284	15 00	$s = 0.4945$ $h = 0.0188$	0 4945
Nov 30	0 209 0 209 0 260 0 256	7 899 7 892 7 891 7 885	6 510 6 498 4 656 4 651	0 3937 0 3937 0 2795 0 2795	2 0932 2 0913 2 1111 2 1105	4 18	$s = 0.4895$ $h = 0.0178$	0 4895
Dec 1	0 225 0 219 0 256 0 238	3 953 3 955 3 943 3 958	3 009 3 006 2 157 2 456	0 3649 0 3641 0 2970 0 2960	2 0800 2 0871 2 0984 2 0966	2 21	$s = 0.4876$ $h = 0.0174$	0 4876
Dec 14	45 41 45 36 45 40 45 40 45 40	8 015 8 009 7 963 8 053 8 119	17 338 17 312 6 407 6 489 11 079	1 0053 0 9925 0 3667 0 3674 0 6290	2 1518 2 1547 2 1943 2 1933 2 1675	19 42	$s = 0.5091$ $h = 0.0238$	0 5091
Dec 20	54 420 54 134 54 109 54 105	9 197 9 273 9 172 9 156	20 981 20 986 7 466 7 443	1 0518 1 0414 0 3661 0 3668	2 1692 2 1711 2 2156 2 2163	58 87	$s = 0.5131$ $h = 0.0257$	0 5131
Dec 21	0 203 0 222 0 224 0 242	1 735 1 739 1 727 1 759	1 1487 0 7587 0 9159 0 5439	0 3210 0 2086 0 2639 0 1443	2 0587 2 0915 2 0754 2 1430	1 08 1 10	$s = 0.4778$ $h = 0.0195$ $s = 0.4768$ $h = 0.0209$	0 4778 0 4768
1927								
Feb 15	26 277 26 261 26 255 26 253	9 960 10 036 10 067 10 125	6 999 6 991 17 087 17 086	0 3247 0 3222 0 8019 0 7957	2 1576 2 1619 2 1166 2 1172	31 29	$s = 0.4993$ $h = 0.0240$	0 4993
Feb 16	31 578 31 572 31 550 31 558	8 270 8 254 8 334 8 302	5 960 5 953 15 112 15 098	0 3323 0 3328 0 8542 0 8499	2 1688 2 1673 2 1229 2 1244	35 71	$s = 0.5010$ $h = 0.0243$	0 5000
April 3	39 103 39 051 39 093 39 089	7 979 8 039 7 993 7 980	14 994 14 982 5 756 5 752	0 8807 0 8721 0 3301 0 3299	2 1338 2 1370 2 1815 2 1825	43 09	$s = 0.5040$ $h = 0.0245$	0 5030
April 5	30 108 30 110 30 108 30 114	9 775 9 755 9 801 9 823	7 226 7 214 17 473 17 451	0 3422 0 3423 0 8394 0 4369	2 1602 2 1604 2 1238 2 1228	35 00	$s = 0.5016$ $h = 0.0215$	0 5006

[Note added December 1927—The results obtained with calorimeter B showed an almost constant difference of nearly 1 per cent from those of A, and eventually the cause was traced to convection in the air space between the flow tube and the double walled vacuum jacket (fig 2). The correction calculated for this raised the curve as a whole, and reconciled very closely the results from the two calorimeters, but it involved a constant which made the results not strictly independent of those from calorimeter A. Since the convection taking place was of a complicated nature, there is some uncertainty as to the theory of this correction. The tabular results of the series of the 13 complete experiments made with calorimeter B have therefore been omitted, but the general agreement of the shape of the curve with that obtained from the experiments with the other calorimeter is shown in fig 6.]

Using calorimeter A, some values were obtained with aniline that had been standing for six weeks in dark glass bottles, which were closed with tightly fitting ground glass stoppers. When used, the liquid was a light brown colour. The following figures were obtained —

Temperature	Specific heat	
	Observed	Calculated
° C		
39.34	0.5011	0.5021
18.79	0.5021	0.5019
29.10	0.4972	0.4978

The calculated values are from the mean curve for the freshly distilled liquid. It appears, therefore, that the darkening does not affect the specific heat.

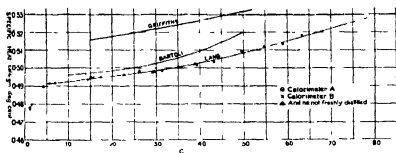


FIG. 6

The final results have been plotted in fig. 6 against the mean temperature, and a smooth curve drawn through the points. Between 5° and 60° C the specific heat is represented in terms of the 20-degree calorie per gramme degree Centigrade by the following formula —

$$s = 0.4951 + 0.000287(t - 20) + 0.0000027(t - 20)^2 + 0.00000061(t - 20)^3$$

The following table gives the results read off from the curve, and the close agreement of the above equation over the range 5° to 60° C is shown —

Table III

Temperature	Observed from curve	Calculated from formula
° C		
5	0 4912	0 4912
10	0 4923	0 4924
15	0 4937	0 4936
20	0 4951	0 4951
25	0 4967	0 4968
30	0 4982	0 4981
35	0 5003	0 5002
40	0 5024	0 5024
45	0 5050	0 5050
50	0 5080	0 5079
55	0 5112	0 5111
60	0 5148	0 5148
65	0 5183	(0 5189)
70	0 5218	(0 5234)
75	0 5253	(0 5292)

No attempt has been made to draw a curve through the points below 5° C, as owing to the high viscosity of aniline in this region the results, as pointed out above, are less certain

12 *Comparison of the Results with the Work of other Observers*

Bartoli* used a method of "heating" which is in reality the same as the well known method of cooling, but in this case the temperature of the jacket is above that of the liquid instead of below. Great care was exercised to use pure aniline, and two samples were used, one prepared from the sulphate and another from acetanilide. The unit used was the 15° calorie and the results have been reduced for comparison purposes to the 20° calorie, in terms of which my results are given. The reduced results for the aniline prepared from the sulphate are plotted in fig 6. The difference between the specific heat for the two samples is 0 0019 at 10° C, increases to 0 0034 at 30° C and decreases again to 0 0004 at 50° C, and the increments are not consistent. If the difference were due to slight impurities present, the difference would be very nearly constant over the range used, and if it did change, would show a regular variation. It seems therefore more probable that the discrepancies are due to inaccuracies in the experiments. The method employed is not susceptible of great accuracy, owing to the difficulty of reproducing identical conditions for the experiments with the comparison liquid and the liquid

* 'Rend R Inst Lombardo,' vol 28, p 1032 (1894)

under investigation, the assumptions involved in the theory of the method are open to doubt*. Finally, it was necessary for Bartoli to read his thermometer on a moving meniscus, which renders the readings uncertain. For these reasons it would seem that his results are only accurate to about 1 per cent. Bartoli also carried out some experiments on the change in the specific heat due to small percentages of water in solution. His results for 20° C are as follows:

Aniline containing	0 per cent	1 per cent	2 per cent	3 per cent	4 per cent water
Specific heat	0.5005	0.5104	0.5200	0.5302	0.5408

Perrot† also observed an increase of specific heat if small amounts of water were present.

E. H. Griffiths‡ carried out a very careful series of experiments, but unfortunately paid no attention to the dryness or purity of the aniline. He used an electrical method and the same calorimeter as was used in his experiments on water§. It would serve no purpose to discuss the possible sources of error in his method, as this has been done both by himself and others in connection with his work on water, and his results are for impure aniline. It must be stated here, however, that the variation of the water equivalent of the calorimeter with temperature was of the order of 20 per cent. of the total variation, and the corrections were large, by the methods adopted in reducing the results Griffiths claims to have eliminated these errors. When the aniline was taken out at the end of the series of experiments, it "had darkened considerably," which is a sure indication of impurities, and particularly water. His results, reduced to the 20-degree calorie, are plotted in fig. 6. As the calorimeter was closed, the water content of the aniline would remain constant throughout the series of experiments, and if it be assumed that 2.3 per cent. of water was present, and the results corrected accordingly, they then agree with my values to 1 part in 500 over the whole range. This large percentage is quite possible in view of the hygroscopic nature of aniline. Experiments have also been carried out by others, but are not of such a high degree of

* Callendar, 'Ency. Brit.,' Art. "Calorimetry."

† 'Arch. Soc. Phys.,' vol. 32, p. 145 (1894).

‡ 'Proc. Phys. Soc.,' vol. 13, p. 234 (1894).

§ 'Phil. Trans.,' A, vol. 184, p. 361 (1893).

accuracy, or are over too large a range of temperature to merit a discussion of their results here

13 *Experiments using a Dewar Flask as Calorimeter*

In order to confirm the above results, and to re-investigate the specific heat below 5°C , some experiments were performed using a Dewar flask and a manganin heating coil. These preliminary experiments soon showed, however, the impossibility of obtaining accurate data by this method. The calorimeter had a large water equivalent, which could not be kept constant, and which, in addition, rapidly increased with temperature. In fact, the variation of water equivalent was of the same order as the variation to be measured, and while the continuous flow method is free from this defect, no suitable method has yet been found for such a highly viscous liquid as aniline is at these temperatures.

The experiments were carried out in the Physics Department of the Imperial College of Science under the direction of Prof. Callendar, to whom I wish to express my indebtedness for continual advice and encouragement. I desire also to express my thanks to many colleagues for advice and assistance at various times, and particularly to Mr. W. J. Colebrook, the director of the physics workshop, for assistance in the construction of the apparatus.

14 *Summary*

New measurements have been made on the specific heat of aniline by the continuous flow electric method, over short ranges of temperature between 5° and 75°C . The rate of change of the specific heat with temperature over this range was found to increase with rising temperature. Some values have also been obtained below 5°C , but owing to the high viscosity of aniline at these temperatures the results are less certain. Great care was exercised to use only pure dry aniline, and the minute water content was determined in each case.

The Structure of the Band Spectrum of Helium —IV

By Prof W E CURTIS, D Sc, Armstrong College, Newcastle-upon-Tyne

(Communicated by Professor T H Havelock, F R S - Received December 1, 1927)

1 *Introductory*

Since the publication of the last paper in this series* some important contributions to the interpretation of the spectrum have been made, notably by Mulliken † In extension of his work on other bands he has proposed electronic term designations for all the helium bands published up to the present, and has shown that these designations provide an explanation of several characteristic features of the bands, such as the absence of certain branches in some of them, and the number of "missing lines" in the neighbourhood of the null line of each band The identification of the electronic levels renders it possible to calculate the positions of certain other bands which should occur, and one of these ($5S \rightarrow 2P$, ortho-helium family) has since been found by Weizel and Fuchtbauer ‡ They have also recorded a number of bands involving the first vibration state of the molecule

In the present paper it is intended to give details of three new bands which have the same final electronic state ($2P$) as the three which were first investigated, to discuss their relationships and interpretation, and to derive molecular constants for all six bands Before proceeding with this it is desirable briefly to outline the changes in notation which are necessitated by the recent advances mentioned above The most radical of these is the re-numbering of the lines according to Mecke's suggestion§ that alternate members of all branches are missing As this view is now generally accepted by workers in this field, no more than a brief summary need be given of the evidence on which it is based This is as follows —

(1) Analogy with other symmetrical molecules, where alternating intensities are actually observed (*e.g.* N_2^+)

(2) The molecular constants are brought into better accordance with those derived for other molecules In particular, the old value of 0.5 \AA for the nuclear separation seems remarkably small for such an unstable molecule

* Curtis, 'Roy Soc Proc,' A, vol 101, p 38 (1922), vol 103, p 38 (1923), and vol 108, p 513 (1925)

† 'Proc Nat Acad Sci,' vol 12, p 158 (1926), 'Phys Rev,' vol 28, p 1202 (1926)

‡ 'Z f Physik,' vol 44, p 431 (1927)

§ 'Phys Zeitschr,' vol 26, p 227 (1925)

(3) Assuming that alternate lines are missing, Mulliken has been able to account quite simply and naturally for the absent lines of low quantum number in each band

(4) Vibration frequencies as actually observed by Weizel and Fuchtbauer are in good agreement with those calculated from the rotation structure, provided that alternate lines are supposed missing. The previously calculated values are double the observed

It is thus clearly necessary to renumber the lines in accordance with the new interpretation. This has the further advantage of converting the $\frac{1}{2}$ values previously found for ϵ into $\frac{1}{2}$ values, in agreement with many other band spectra

A further complication which exists in this spectrum is the doubling of the rotation states for all electron levels except the S. These are designated A and B after Mulliken, and are alternately suppressed. The following scheme shows which are actually observed —

$$\begin{array}{l} \text{S levels, B states only, } j = 1, 3, 5, \\ \text{P levels } \left\{ \begin{array}{l} \text{A states only, } j = 1, 3, 5, \\ \text{B states only, } j = 2, 4, 6, \end{array} \right. \\ \text{D levels } \left\{ \begin{array}{l} \text{A states only, } j = 2, 4, 6, \\ \text{B states only, } j = -, 3, 5, \end{array} \right. \end{array}$$

The rotational quantum changes responsible for the emission of the various branches are as follows, in the convenient notation of Weizel and Fuchtbauer for bands of the subordinate series type —

Sharp series, $mS \rightarrow 2P$, $e g$, $\lambda\lambda$ 6400, 4546

$$P'(j) = s(j) - p_b(j+1)$$

$$R(j) = s(j+1) - p_b(j)$$

$$Q(j) = s(j) - p_a(j)$$

Diffuse series, $mD \rightarrow 2P$, $e g$, λ 5730

$$P'(j) = d_b(j) - p_b(j+1) \quad P(j) = d_a(j) - p_a(j+1)$$

$$R(j) = d_b(j+1) - p_b(j) \quad R'(j) = d_a(j+1) - p_a(j)$$

$$Q_1(j) = d_b(j) - p_a(j) \quad Q_2(j) = d_a(j) - p_b(j)$$

In these formulæ small letters have been used for the electron term symbols, since P is already in general use to denote the rotational transition $j \rightarrow j+1$, and the rotational substances are distinguished by suffixes a, b , in order to avoid confusion with the B which occurs in the rotation term formula. But capital letters will hereafter be used when no confusion is likely to arise

It is convenient to retain the symbols P' , R' used in previous papers to denote branches which extrapolate approximately to the head of the Q branch. The lines of the P and R branches fall nearly midway between those of the P' and R' branches for small values of the rotational quantum numbers.

The rotation terms may be evaluated in the usual way by forming suitable combination differences, as shown below.

Sharp series

Initial term differences	Final term differences
$R(j) - P'(j-1)$	$R(j-1) - P'(j)$
$= s(j+1) - s(j-1)$	$= p_b(j+1) - p_b(j-1)$
	$Q(j) - P'(j)$
	$= p_b(j+1) - p_a(j)$

Diffuse series

Initial term differences	Final term differences
$R(j) - P'(j-1)$	$R(j-1) - P'(j)$
$= d_b(j+1) - d_b(j-1)$	$= p_b(j+1) - p_b(j-1)$
	$Q_1(j) - P'(j)$
	$= p_b(j+1) - p_a(j)$
$R'(j) - P(j-1)$	$R'(j-1) - P(j)$
$= d_a(j+1) - d_a(j-1)$	$= p_a(j+1) - p_a(j-1)$
	$Q_2(j) - P(j)$
	$= p_a(j+1) - p_b(j)$

2 The New Bands

In Table I below the details of the three new bands are given. Those of the three already published are not repeated, but their numeration may be converted to the new system according to the following scheme, which shows the old and new designations of the first observed line in each branch. The old numeration proceeds by successive integers and the new by alternate integers.

	Sharp			Diffuse					
Old	P'1	Q1	R2	P2	P'2	Q ₁ 1	Q ₂ 1	R2	R'1
New	P'1	Q1	R2	P2	P'3	Q ₁ 3	Q ₂ 2	R2	R'1

Table II shows the combination differences upon which the interpretation is based.

J	P' branch			Q branch			R branch		
	Int	λ (air) Å	ν (vac)	Int	λ (air) Å	ν (vac)	Int	λ (air) Å	ν (vac)
1	00	4564.23	21903.38	—	—	(21931.5)			
2									
3	1	70.49	873.38	1	4558.78	21929.57			
4							00	4544.72	21997.41
5	1+	76.96	842.46	1	59.45	26.34			
6							00	39.86	22020.95
7	1	83.71	810.30	2	60.51	31.25			
8							00	35.47	042.27
9	1	90.69	777.14	1+	61.88	14.66			
10									
11	2	97.89	743.04	1	63.60	06.40			
13				1-	65.68	896.42			

Table I—(continued)
(c) Band near λ 5885

J	P branch			Q branch			R' branch		
	Int	λ (air) Å	ν (vac)	Int	λ (air) Å	ν (vac)	Int	λ (air) Å	ν (vac)
1				Absent			1*	5876 78	17011 41
2	6+	5902 18	16938 21				6*	70 26	30 32
3							9*	65 77	43 36
4	9+	16 00	898 63				6	63 13	51 02
5		31 75	853 77				6	62 12	53 96
6	10	49 23	804 26				4	62 68	52 14
7		68 27	750 65				4*	64 64	46 03
8	8+	88 62	693 72				5*	67 84	37 32
9		6010 16	633 90				1*	72 35	24 24
10	4	32 70	571 75				1*	77 97	07 97
11		56 19	507 48						
12	2+								
13	1+								
14	1-								
15									
16									
17									
18	0								
19									

Wave numbers in brackets are calculated values for lines which fall under strong lines of the neighbouring bands. Intensities marked * in (c) are unreliable owing to the proximity of the helium D₂ line, λ 5876, which is heavily overexposed and accompanied by much fogging. In (a) and (b) the P' branches have already been published as constituents of the bands $\lambda\lambda$ 6400 and 4546 respectively. Since that time it has become apparent that they do not belong to these bands. Wenzel and Fichtlsauer record many of the lines of (b) with the exception of the R branch, but their numbering of the Q branch is incorrect.

Table II—Combination Differences for New Bands

J	$R(J-1) - P'(J) = p_s(J+1) - p_s(J-1)$		$Q(J) - P'(J) = p_s(J+1) - p_s(J)$	
	Band (a)	Band (b)	Band (a)	Band (b)
3			56 26	56 19
5	155 28	154 95	83 93	83 88
7	211 04	210 65	111 04	110 95
9	268 10	265 13	137 75	137 52

J	$R'(J-1) - P(J) = p_s(J+1) - p_s(J-1)$	
	Band (c)	Band λ 5730
2	73 20	73 34
4	131 09	131 64
6	189 59	189 53
8	246 76	246 69
10	303 31	303 20
12	358 62	358 61
14	412 73	412 86
16	465 57	465 57

3 Interpretation of the New Bands

(a) and (b) — It is evident from the similarity of structure that these must be closely associated with the neighbouring strong bands $\lambda\lambda$ 6400 (3S \rightarrow 2P) and 4546 (4S \rightarrow 2P), yet the absence of combination relationships with these shows that they have no state in common with them. It seemed probable that in each case the weak band was due to the vibration transition $1 \rightarrow 1$, the strong band arising from the vibrationless molecule, as already concluded by me. This view was supported by the relations between the molecular constants (see below) derived from the term differences for each band,* and has recently been confirmed by the recognition by Weizel and Fichtbauer of a number of other weak $1 \rightarrow 1$ bands similarly situated with respect to the $0 \rightarrow 0$ bands arising from the same electron transition. For convenience of description we may thus designate the bands (a) and (b) as 3S (1) \rightarrow 2P (1) and 4S (1) \rightarrow 2P (1) respectively, the bracketed figures indicating vibrational quantum numbers (apart from the $\frac{1}{2}$ which should probably be added to each according to the latest theoretical developments).

(c) — The combination result indicates that the final state is identical with that of the R'P branches of λ 5730, ϵ , 2P_A (0). In view of the strength of the band the initial state must also be vibrationless, but its electronic designation is uncertain at present. The evidence derived from the molecular constants is discussed later. It should be mentioned that the absence of a Q branch renders it impossible to determine directly whether the two branches should be designated R'P or RP'. The former view is probably the correct one, as will appear later.

4 The Molecular Constants

From an analysis of the rotational structure of a band we may derive the moments of inertia of the molecule in its initial and final states, and also, if the measurements are sufficiently accurate and extensive, corresponding values of the vibration frequency. But the precise values obtained depend upon the formula employed, and it is not quite certain which of the various types is to be preferred. In III it was shown that the terms could be represented with great accuracy by the expression, due to Kratzer,† $B(m - \epsilon)^2 - \beta(m - \epsilon)^4$. For the main (principal) series of doublet bands the value of ϵ appeared to be exactly $\frac{1}{2}$ for the common final (2S) state and for the initial (3P to 10P) A states,

* The results were not published at the time, but were communicated privately to Prof Birge and included in the 'Report of Molecular Spectra in Gases' (p. 207).

† 'Z f Physik,' vol. 3, p. 280 (1920).

for the initial B states it showed a marked decrease in going from $3P$ ($\epsilon = \frac{1}{2}$) to $8P$ ($\epsilon = 0.14$). Similar calculations were carried through by least square methods for the present bands, including $\lambda\lambda$ 6400, 4546, 5730, the term values of which had not previously been obtained except approximately by Kratzer *. It was found that $\epsilon = \frac{1}{2}$ for the common final states $2P_A$ and $2P_B$ and for the $3S$ initial state, for the other initial states appreciable deviations from $\frac{1}{2}$ existed. The actual values obtained for B , β and ϵ are given in Table III.

Table III —Term Constants for Bands having Common Final State $2P$

	State	B	β	ϵ
$n = 0$	$2P_A$	29 3418	0 008122	$+\frac{1}{2}$
	$2P_B$	29 2441	0 008200	$-\frac{1}{2}$
	$3S$	28 9225	0 008459	$+\frac{1}{2}$
	$4S$	28 7462	0 009509	$+\frac{1}{2}$ 2641
	$3D_A$	29 9916	0 012092	-0 2635
	$3D_B$	30 5593	0 011557	$+0$ 2727
	3Σ	26 4940	0 003277	-0 2381
$n = 1$	$2P_A$	28 6693	0 011093	$+0$ 2655
	$2P_B$	28 7709	0 007781	-0 2475
	$3S$	28 145	0 010313	$+0$ 2604
	$4S$	27 8107	0 012004	$+0$ 2594

$\lambda\lambda$ denotes the initial state of band (ϵ), λ 5885

According to the new interpretation and notation ($m \pm \frac{1}{2}$) is to be replaced by ($j + \frac{1}{2}$), where odd values of j correspond to $-\frac{1}{2}$ and even values to $+\frac{1}{2}$. The term values may be represented by means of an expression of the form

$$B \{(j + \frac{1}{2} - \rho)^2 - \sigma^2\} - \beta \{(j + \frac{1}{2} - \rho)^2 - \sigma^2\}^2$$

Here ρ is only required when ϵ departs appreciably from the exact $\frac{1}{2}$ value, and is always small for the bands considered here. σ represents the component ($\sigma\hbar/2\pi$) of electronic angular momentum parallel to the internuclear axis, and takes the values 0 for 1S states, 1 for 1P states and 2 for 1D states. B and β have the same significance as before, but will be respectively about $\frac{1}{4}$ and $\frac{1}{16}$ as large as before. To evaluate them with the utmost attainable accuracy it would have been necessary to carry through a completely fresh set of calculations. In view of the labour involved in this the new constants were derived from the old by means of the relations $\beta = \bar{\beta}/16$ and $B = \bar{B}/4 - 2\bar{\beta}\sigma^2$, where \bar{B} and $\bar{\beta}$ are the old values. Also the approximate ρ values are $(2\epsilon - \frac{1}{2})$ for ϵ positive and $(2\epsilon + \frac{1}{2})$ for ϵ negative. The results for B and r_0 (the inter-nuclear distance) are probably accurate to within 0.1 per cent or so, but ρ and β are

* *Ibid*, vol 16, p 353 (1924)

more difficult to determine, and may be considerably in error for the more excited states, since their evaluation depends upon the magnitude of a small deviation from the quadratic term formula. Hence the values of $\omega_0 (2\sqrt{B^3/\beta})$ are also somewhat uncertain in these cases.

The constants relating to the electronic states 2S, 3P, 4P are recalculations by Mulliken from the values published by me in 1925. The remainder are new.

Table IV —Molecular Constants for "Orthohelium Bands"

	State	B_A	B_B	ρ_A	ρ_B	$\beta_A \times 10^4$	$\beta_B \times 10^4$	ω_0	r_0 (A U)	
									A	B
$n = 0$	2S		7 589		0		5 52	1790		1 050
	3S		7 231		0		5 29	1692		1 074
	4S		7 187		1 0 0282		5 94	1580		1 077
	2P	7 334	7 310	0	0	5 201	5 125	1744	1 066	1 068
	3P	7 175	7 102	0 003	0	5 17	5 01	1690	1 081	1 086
	4P	7 140	6 906	0 005	0	5 32	4 48	1700	1 084	1 098
	3D	7 491	7 633	-0 0270	+0 0484	8 12	7 22	1505	1 055	1 045
$n = 1$	3X	6 623		+0 0238		2 05		2382	1 122	
	3S		7 036		+0 0208		6 45	1473		1 089
	4S		6 953		+0 0188		7 88	1308		1 095
	2P	7 166	7 094	+0 0310	+0 0050	6 93	4 86	1585	1 079	1 084

5 Discussion of Results

The constants show in the main the kind of variation to be expected. For example, in each sequence the nuclear separation r_0 increases with the degree of excitation, whilst at the same time the vibration frequency ω_0 diminishes, indicating a diminution in the strength of the binding. A similar effect on the molecule is produced by the development of nuclear vibration. Thus the increase in r_0 due to vibration is 0 013, 0 015, 0 015 and 0 018 A U for the 2P_A, 2P_B, 3S and 4S states respectively. In the non-vibrating 3S and 3P states there is little difference in r_0 and ω_0 , but in the 3D state r_0 is distinctly smaller, whilst ω_0 is considerably smaller. It is true that the latter value is somewhat uncertain owing to the presence of a ρ , but the small value of r_0 is quite definitely established, and is responsible for the fact that $\lambda 5730$ is degraded in the opposite direction to that of all the other bands.

It has been mentioned that the tabulated values of ω_0 are somewhat uncertain, particularly when a ρ exists. More reliable values may probably be obtained,

by making use of the separation of the (0, 0) and (1, 1) bands arising from the same electron transition. Denoting the respective values of ν_0 by ν_0 and ν_1 , we have

$$\text{for } \lambda 6400, \nu_0 = -3S + 2P,$$

$$\text{and for } (a), \nu_1 = -3S + \omega_s + 2P - \omega_p \text{ approximately,}$$

where ω_s and ω_p are the vibration frequencies in the 3S and 2P states. Hence $\nu_0 - \nu_1 = \omega_p - \omega_s$.

Now ω_p is probably better determined than ω_s , since it is derived from many more observations involving three separate bands and both A and B sub-states, whereas ω_s is derived from only one band and involves only B sub-states. We shall therefore take the tabulated value of ω_0 for the 2P state, *i.e.* 1744, as our starting point. The values of ν_0 and ν_1 are as follows* —

ν_0	3S (0) \rightarrow 2P (0), 15621	4S (0) \rightarrow 2P (0), 21994
ν_1	3S (1) \rightarrow 2P (1), 15581	4S (1) \rightarrow 2P (1), 21932

$$\text{Whence } \omega_p - \omega_s = \frac{43}{62}$$

and therefore $\omega_0 = 1701$ for 3S and 1682 for 4S.

These values inspire more confidence than those tabulated, for they correspond much more closely with the ν_0 values. They also obtain support from the fact that they yield an almost constant value of ω_0/B for the 2S, 3S and 4S states, namely, 234.5, 235.2 and 234.0 respectively. This corresponds to the approximate constancy of $I\omega_0$ for molecules of similar constitution, first noted by Mecke (see 'Report,' p. 233) but is much more nearly exact. It is therefore of interest to see whether a similar relation holds for the P sequence. The ω_0 values for 3P, 4P etc., were determined directly by Weizel and Fichtbauer, but they made no observations relating to the 2P state. By comparison of their values for 3P and 2S (1643 and 1732) with the calculated ones given in Table IV (1690 and 1780) it appears that the latter are respectively 47 and 48 too high. In order to get a 2P value comparable with theirs we may accordingly subtract 48 from the calculated value 1744, which gives 1696. The results are then as follows —

State	ω_0	ω_0/B
2P	1696	231.6
3P	1643	230.1
4P	1628	230.8
6P	1624	234.7
7P	1622	235.8

* Omitting Muliken's $B\sigma^2$ term, which would not affect this result

The agreement is not particularly good, but it should be noted that a complication exists here, in that the P states are all double, each having two B values. B_n decreases much more rapidly than B_A as the electronic quantum number increases, but the average of the two has been used above. It appears from the manner in which Weizel and Fichtbauer derive ω_0 that it must refer to the B states, but the difference between the A and B values is not likely to be appreciable. On the whole the evidence does not point to an exact proportionality between ω_0 and B for the P sequence.

Taking $\omega_{0/B}$ as about 235 we obtain for the product $l\omega_0$ the value 6500×10^{-40} , which is of the order of magnitude characteristic of the hydride group of molecules (cf. AlH, 6080, CuH, 6800, AgH, 7120, AuH, 8410). This affords further support to Lenz's suggestion* that the structure of the helium molecule is generally similar to that of the hydrogen molecule. In this connection it is worthy of note that Richardson has shown† that the electronic states of the hydrogen molecule run closely parallel to those of the helium atom, whilst Mulliken has established a similar correspondence between the helium molecule and atom, so that again we are led to the recognition of an essential similarity of structure in the case of these two molecules.

The rotational doubling does not affect only the rotation terms, but may have an influence also on the electronic terms, as is particularly clear in the case of the initial state 3D of the band $\lambda 5730$. The six branches yield two distinct values of ν_0 , as will be seen by reference to Table V, which gives the values derived from each line by using the term values calculated from the constants of Table III. At the same time the figures will serve to indicate the order of accuracy to which the experimental results are capable of representation by these formulae.

The six mean values of ν_0 clearly fall into two sets, one derived from the P'Q₁R branches and having a mean value 17438.21 and the other from the PQ₂R' branches and having a mean value 17435.98. The P'Q₁R branches have the initial state D_n in common and the PQ₂R' the initial state D_A, so that we conclude that the electron term for the 3D_A state exceeds that for the 3D_n state by about 2.23 cm^{-1} . There is no such marked similarity of the values associated with the same final state,‡ so that the separation of the A and B values of ν_0 must be inappreciable in the 2P state. But a similar difference

* 'Verh. d. D. Phys. Ges.', vol. 21, p. 632 (1919).

† 'Roy. Soc. Proc.', A, vol. 113, p. 400 (1926).

‡ But there is perhaps an indication of a similar effect in the fact that the values associated with the P_n state are all higher than those associated with the P_A state.

Table V—Values of ν_0 derived from each Line of Band λ 5730

j		1	2	3	4	5	6	7	8	9	10	11	12	13	Mean
P	174			38 17		38 20		38 21		38 20		38 34		38 45	38 26
Q ₁				38 00		38 16		38 10		38 05*		38 44*		38 11	38 16
R			38 00		38 23		38 14		38 13		38 22		38 45		38 21
P			35 89		35 84		35 91		36 17		36 08		35 97		35 97
Q ₂			35 76		35 82		36 02		36 10		36 23		36 07		36 01
R		35 95*		35 84		35 90		36 01		36 06		35 99		36 05	35 97

* Denotes that the line is a blend
The B α term is again neglected here

makes its appearance for higher terms of the P sequence, as has been established in III (p 530) from a study of the "main" (principal) series of doublets. Here again the electronic term is larger for the A state, the difference ranging from 0.14 for 3P to 4.14 for 8P. It thus appears probable that in general an electronic energy difference between the A and B sub-states develops with increase of excitation.

The precise significance of the duplication of the rotation levels is at present obscure, although we may surmise that it refers to the two opposite senses of the electronic angular momentum. The rules of combination for the rotation terms are most conveniently summarised, as Weizel and Fuchtbauer have suggested, by assigning quantum numbers s to them, such that $s_1 - s_2 = \pm 1$. The observed branches are then represented by the condition that $\Delta j + \Delta s = \pm 1$. This means that P and R branches result from $A \rightarrow A$ or $B \rightarrow B$ transitions and Q from $A \rightarrow B$ or $B \rightarrow A$ (so-called crossing-over property of Q branches). On this notation the j values which actually occur are as stated in Section 1. The scheme there given is rather a complex one, and it is natural to enquire whether it could be simplified by changing the notation. This is in fact the case, for if we were to interchange the A and B labels in the P states we should be able to say that only the even A sub-states and the odd B sub-states are present. This would, of course, involve a restatement of the combination rule, thus —

A \rightarrow A or B \rightarrow B transitions give Q branches, and

A \rightarrow B or B \rightarrow A transitions give P and R branches

Apart from evidence to be obtained from other spectra, there is internal evidence against such an interpretation, since it would render permissible the occurrence of S \rightarrow S and P \rightarrow P electron transitions, which are impossible on the first scheme and which are not in fact observed. There might, of course,

be some other cause inhibiting them, but so far as the evidence goes it certainly points to the essential correctness of Mulliken's scheme. At the same time it should be remarked that this rests on a somewhat arbitrary basis in the case of the helium bands, since the criterion he employs, namely, that $F_A(j) > F_B(j)$, lacks definiteness for the 3D (0) and 2P (1) levels, the two term sequences crossing over as shown by the figures below —

3D rotation terms, calculated values

<i>j</i>	2	4	6	8	10	12	14
A	47 84	153 32	317 94	540 87	820 92	1156 51	1546 11
B	46 00	151 21	317 02	542 34	826 33	1167 52	1564 57

2P (1) rotation terms calculated values

<i>j</i>	3	5	7	9
A	86 15	213 76	397 69	637 08
B	86 59	213 79	397 02	635 37

The criterion suggested is thus not satisfactory, although in all the vibrationless P states $F_A(j)$ is consistently larger than $F_B(j)$. It is probable that a more satisfactory method of distinguishing the two states could be based on the effects upon them of increasing excitation, viz —

(1) The electronic term value becomes greater for A than for B, as mentioned above, and

(2) The moment of inertia for the A state remains almost constant, whilst that for the B state increases rather rapidly. If further terms of the D sequence can be observed, it should be possible to reach a pretty definite conclusion on this point. The next band, 4D \rightarrow 2P, ought to be quite strong enough to be detected on the author's grating plates, but its expected position, about λ 4400, falls in a complex region, so that it is not easily recognisable. A systematic analysis of the whole band spectrum is now in progress, and should lead to its identification.

In conclusion, the question of the electron transition associated with the band (c), λ 5885, calls for some consideration. As mentioned previously, the two observed branches may be interpreted as R'P or RP', according to whether the 2P electron state is regarded as the final or initial state respectively. The former assumption leads to an effective initial quantum number 2.96 and the latter to an effective final quantum number 1.54. Having regard to the effective quantum numbers derived from the other electron terms of this spectrum, which all have approximately integral values, it seems much more likely that

the former interpretation is the correct one. We may thus designate the band as $3X \rightarrow 2P$, and since the final states are $2P_A$ the initial states are presumably $3X_A$, accepting the convention that RP branches do not "cross over". The absence of the X_B levels suggests that the initial state is of the S type (but with B levels suppressed instead of A as usually), but the absence of the Q branch, $3X_A \rightarrow 2P_B$ remains unexplained. The nature of the hypothetical new S level is also obscure, since there is no place for such a level in Mulliken's term scheme. It is close to the $3P$ initial level of the "parhelium" band $\lambda 5130$, but is not identical with it, since the initial term differences are not in agreement. The $3S$ "parhelium" term (of the band spectrum) has not yet been isolated, but the effective quantum number of $2S$ is 1.853, so that it is very unlikely that for $3S$ it could be so high as 2.96. We may hope that further evidence will be forthcoming as the result of a search for the next member $4X \rightarrow 2P$, but this again will probably fall in a region rich in lines (about $\lambda 4440$) and will not be easy to disentangle. Apart from its electronic configuration the $3X$ state is somewhat remarkable in comparison with the S, P and D, in that the nuclear vibration frequency comes out abnormally large, whilst the nuclear separation is also large, whereas these two quantities usually vary in an inverse sense. In other words, the product $1/\omega_0$ (9900) for this state is considerably greater than for the other states (6500), indicating that we have to do with a distinctly different molecular structure.

Summary

Details are given of three new helium bands which have the final electronic level $2P$ in common. Two of them are due to the vibrational transition $1 \rightarrow 1$, the initial electronic levels being $3S$ and $4S$. The other has an initial electronic level of effective quantum number 2.96, but its term type is uncertain, as it does not appear to fit into the general scheme of electronic levels. The rotation terms have been accurately evaluated for the three new bands and for three others previously described which also have the final level $2P$. The molecular constants are thence determined and their relations considered. New evidence is presented which favours the view that the helium and hydrogen molecules are structurally similar. The question of a suitable criterion for distinguishing between the A and B rotational sub-states is discussed in the light of the new data.

The Kinetics of the Combination of Hydrogen and Oxygen

By C. N. HINSHLWOOD, and H. W. THOMPSON

(Communicated by Sir Harold Hartley, F.R.S. —Received December 1, 1927)

Introduction

Although there are few gaseous reactions of more fundamental interest than the union of hydrogen and oxygen, it can hardly be said that the kinetics of this combination are at all completely understood. Many investigations have been made of the catalytic reaction which occurs in contact with various surfaces, and of the phenomena accompanying the production of flame or explosion in the gas. Little is known about the conditions governing the rate of the actual chemical change in the gas phase, because although flames and explosions depend very much upon these they are determined by a great many other factors as well.

In 1899 Bodenstein,* following up some work initiated by Victor Meyer, made a long series of experiments by streaming mixtures of the two gases through porcelain vessels, heated to a constant temperature, and then analysing the products. He came to the conclusion that the reaction is of the third order, following the equation $d[\text{H}_2\text{O}]/dt = k[\text{H}_2]^2[\text{O}_2]$. Since the rate of combination was very different in different vessels, he inferred that the reaction was taking place almost entirely on the surface of the vessel.

Bone and Wheeler,† by circulating the gases at lower temperatures for long periods, measured the rate of slow surface combination in contact with various materials, including porcelain, and found that under these conditions the reaction was of the first order.

Comparing these results with those of Bodenstein, the natural conclusion would be that at the lower temperatures the porcelain surface is relatively thickly covered with adsorbed molecules, so that pressure has a comparatively small effect on the reaction, thus giving an apparent order of unity. With increasing temperature the adsorption diminishes and ultimately becomes small enough for the chance that two molecules of hydrogen and one of oxygen should find themselves in juxtaposition on the surface to be proportional to the concentration product $[\text{H}_2]^2[\text{O}_2]$ in the gas phase.

* 'Z. physikal. Chem.', vol. 29, p. 665 (1899).

† 'Phil. Trans.', A, vol. 206, p. 1 (1906).

Rowe,* however, suggested that Bodenstein's third order reaction really took place more in the gas phase than Bodenstein had supposed. He carried out experiments of a similar kind, but diluted the gases with steam and worked over a wider range of temperature. He concluded that the constants of a third-order velocity equation became more regular with increasing temperature, but under no circumstances were the constants satisfactory.

Neither Rowe nor Bodenstein refer to any influence of the concentration of the steam on the course of the reaction. With regard to this point, Baker showed that dried hydrogen and oxygen were less ready to explode than the moist gases, although catalytic combination on the surface of a heated silver wire proceeded rapidly whether the gases were initially dry or not. H. B. Dixon† showed, however, that the dried gases would always explode if heated rapidly, the failure to explode when a silver wire was slowly heated in the gases being due to the secondary cause that the wire became entirely surrounded by steam from the catalytic reaction before it was hot enough to initiate the explosion.

It is difficult from experiments on explosions to derive very definite conclusions about the kinetics of the isothermal chemical change. Experiments made at constant temperature by the streaming method suffer from the disadvantage that the whole course of the reaction cannot be followed in a given experiment. This is a particularly serious drawback when rather erratic catalytic influences are involved. In the particular reaction with which we are dealing, the streaming method turns out to be exceptionally unsuitable for a reason which will become apparent when the results of the present investigation have been described.

We hoped to obtain more definite information about the gaseous reaction between hydrogen and oxygen by using a static method, and examining the whole course of the reaction at constant temperature and volume, and carrying out the experiments over a range of temperature from the region where the reaction is undoubtedly a heterogeneous surface reaction up as nearly as possible to the explosion point, where there can be no question that changes in the gas phase occur. Results of great interest are found in the last 40 degrees of this range.

Experimental Method

The apparatus was essentially that described in former papers on the rate

* 'Z. physikal. Chem.', vol. 59, p. 41 (1907).

† 'J. Chem. Soc.', vol. 97, p. 661 (1910).

of gaseous reactions * The reaction chamber was a silica bulb of about 200 c.c. capacity, connected by capillary tubes to gas holders containing pure hydrogen and pure oxygen, and to a high vacuum pump The bulb was heated by an electric furnace the temperature of which was measured by a platinum-rhodium thermocouple, and could be kept constant to within a degree The progress of the reaction was indicated by the rise of mercury in a capillary manometer The silica part of the apparatus was attached to the rest by means of a finely ground flange clamped to a similar glass flange In order to prevent condensation of water in the parts of the apparatus projecting from the furnace, the capillaries and flanges were kept at 80°–90° C by electrically heated wire Some means of lubricating the flanges had to be found, and the use of sealing wax proved very satisfactory, since at 80° it is soft without running A thin layer of it round the outer edges of the flanges ensured that the joint held a vacuum perfectly for days

Long experience with this type of apparatus has shown that definite, reproducible rate measurements can be made with reactions which are over in periods as short as 30 seconds It should be mentioned that thermal equilibrium between the bulb and a cold gas admitted to it is established in less and possibly much less than 2 seconds When cold air is let into the red-hot bulb something of the order of five calories are exchanged between the bulb and the gas in less than 2 seconds, in the experiments on the combination of hydrogen and oxygen the rate at which the heat of reaction was liberated never exceeded about a quarter of a calorie per second, even in the fastest We are justified, therefore, in regarding the conditions of the experiments as isothermal

Diffusion of hydrogen through the silica was shown directly to be too small to influence the results in any way

The Low-order Surface Reaction

At temperatures below or not much above 500° C, the reaction was found to be approximately of the first order, in complete agreement with the results of Bone and Wheeler It was very much accelerated by the presence of powdered silica in the bulb, and somewhat retarded by the presence of steam For the present purpose these results are only of importance in so far as they allow the surface reaction in silica vessels to be characterised and thus distinguished from the quite different kind of reaction which supervenes at higher temperatures Some results typical of many are given below

* 'J Chem Soc,' vol 125, p 393 (1924), 'Roy Soc Proc,' A, vol 111, p 245 (1926)

Bulb	Temperature ° C	[H ₂] Mms Hg	[O ₂] Mms Hg	Per cent combined	Time	Order
2	476	400 200 400	200 100 200	10 10 10	41' 49' 40'	1 27
2	503	200 100 200	100 200 100	10 10 10	37' 30' 35' 30"	
2	510	200 400 200	100 200 100	20 20 20	68' 40' 56	
1 (with powdered silica added)	507	320 160 80	200 100 50	50 50 50	<div style="display: inline-block; vertical-align: middle;"> { 19 45" 14' 18" 18' 30" 15 20" 18' 32" 20' 30" </div>	1 15
Cf 1 (empty)	507	320	200	50	400'	

It should be mentioned that, throughout this investigation, whenever the effect of varying any condition was to be determined, the first and third experiments of a series were made under identical conditions and the second under different conditions, the average of the first and third being compared with the second. Alternatively, the experiments of a long series were made in a random order. These precautions were taken to guard against systematic variations in the catalytic activity.

The High-order Gas Reaction

With increasing temperature a remarkable change in the nature of the predominating reaction takes place. The reaction which comes into prominence is characterised by (a) extreme sensitiveness to pressure, that is high order, (b) a marked autocatalysis by steam, (c) greatly diminished dependence on the extent of the surface.

The remarkable influence of pressure is shown by the following results, typical of many.

Bulb	Temperature °C	[H ₂]	[O ₂]	Time for 50 per cent combination
1	507	325	200	1' 46"
		240	150	7' 48"
		230	137	19' 17"
		202	129	30' 35"
		160	101	43' and 44'
		80	51.5	182'
1	547	452	280	5' 51"
		321	204	19' 43"
		162	107	102'
2	554	400	200	3' 10"
		300	150	7' 0"
		200	100	30' 0"

A definite order cannot be assigned to the reaction since the apparent order tends to increase with pressure and with temperature. But on the average the influence of pressure between 540° and 560° is not far removed from that which would be characteristic of a reaction of the fourth order. No other gas reaction is known in which pressure has so marked an influence. To take an extreme case, the first set of results in the above table give, when the logarithms

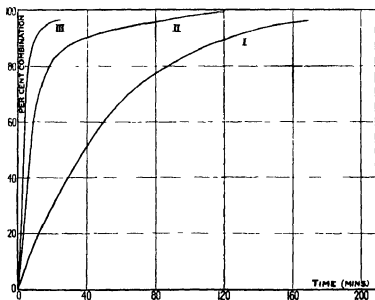


FIG 1—I, 200 mm H₂, 100 mm O₂, II, 300 mm H₂, 150 mm O₂,
III, 400 mm H₂, 200 mm O₂

of the times are plotted against the logarithms of the pressures, a curve to which tangents at the extreme points can be drawn and are found to correspond to an order increasing from 2.6 to 7.1. Here there is still a little of the first order reaction at the lower pressures and possibly a little heating at the highest pressure, which corresponds to the most rapid rate in any experiment made. The three results next quoted give an order varying between 3.0 and 1.5. A similar series, not quoted, gave an average order of 4.4, and the last three results in the table are consistent with an almost constant order of 4.3.

By measuring the initial rate of reaction an attempt was made to find the separate effects of the pressure of hydrogen and of oxygen respectively.

Bulb	Temperature °C	[H]	[O ₂]	Time for 5 mm Hg pressure change at the beginning of the reaction
1	540	300	100	43"
		300	200	10"
		300	100	30"
		200	100	1' 26"
		200	200	45"
		200	100	1' 45"
		200	100	2' 22"
		300	100	52"
		400	100	20"

At this point in the investigation the results tended to be a little erratic as will be seen from some of the duplicates given above, but in spite of this it is quite clear that the rate is roughly proportional to the square of the pressure of the hydrogen and rather less affected by the pressure of the oxygen.

The reaction is strongly autocatalytic as shown by the following detailed results, which give the whole course of the reaction.

Bulb 2 549° C 324 mm H₂, 202 mm O₂

Time <i>t</i>	Total change in pressure <i>z</i>	Time for successive 10 mm changes <i>Δt</i>
0	0	
55"	10	55"
1' 25"	20	30"
1' 55"	30	30"
2' 23"	40	28"
3' 15"	60	2 × 26"
3' 44"	70	29"
4' 15"	80	31"
4' 52"	90	37"
5' 35"	100	43"
6' 40"	110	65"
11' 30"	130	2 × 145"
42' 0"	151	
80' 0"	158	
127' 0"	160	
∞ (calc)	162	

Bulb 1 549° 403 mm H ₂ , 212 mm O ₂			Bulb 2 533° 401 mm H ₂ , 197 mm O ₂		
<i>t</i>	<i>z</i>	<i>Δt</i> (for 5 mm)	<i>t</i>	<i>z</i>	<i>Δt</i> (for 10 mm)
0	0		0	0	
36"	5	36"	4' 55"	10	4' 55"
1' 2"	10	26"	8' 2"	20	3' 7"
1' 27"	15	25"	10' 25"	30	2' 23"
1' 54"	20	27"	12' 50"	40	2' 25"
2' 15"	25	21"	14' 52"	50	2' 2"
2' 38"	30	23"	17' 20"	60	2' 28"
2' 56"	35	18"	19' 13"	70	1' 53"
3' 18"	40	22"	21' 10"	80	1' 57"
3' 35"	45	17"	23' 10"	90	2' 0"
3' 54"	50	19"	26' 5"	100	2' 55"
4' 30"	60	2 × 18"	31' 50"	120	2 × 2' 53"
5' 3"	70	2 × 16 5"	41' 0"	143	
6' 11"	80	4 × 17"	58' 30"	165	
6' 48"	100	2 × 18 5"	107' 0"	185	
7' 70"	110	2 × 21"	120' 0"	190	
8' 19"	120	2 × 24 5"	130' 0"	192	
10' 17"	140	4 × 29 5"	∞ (calc)	197	
11' 50"	150	2 × 46 5"			
13' 55"	160	2 × 62 5"			
17' 18"	170	2 × 1' 41"			
23' 4"	180	2 × 2' 53"			
33' 15"	190	2 × 5' 5"			
∞ (calc)	201 5				

The autocatalysis is very marked, since the rate of reaction actually increases in spite of the very great retarding effect of the diminishing concentrations of hydrogen and oxygen. It is to be noted that the last experiment given above

is quite a slow one. This, and numerous others, show that the autocatalysis is not merely apparent and due to a gradual increase in the temperature of the system resulting from the liberation of the heat of reaction.

The "initial rates" given in an earlier table were taken arbitrarily at the stage of nearly constant speed near the beginning of the reaction. All refer to a constant steam concentration.

To confirm the unavoidable conclusion that the autocatalysis is due to the steam, a number of experiments were made in which steam was present initially. Some typical results are shown in fig. 2.

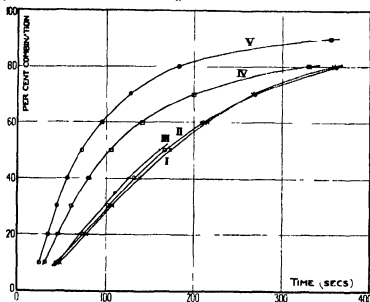


FIG. 2—I, II, III, 200 mm H_2 , 100 mm O_2 ; IV, 200 mm H_2 , 100 mm O_2 , 100 mm H_2O ; V, 200 mm H_2 , 100 mm O_2 , 200 mm H_2O .

The following are two consecutive experiments, one made with steam initially present, the other without.

549° C 200 H_2 , 99 O_2 , 88 mm H_2O initially		549° C 199 H_2 , 97 O_2 , No steam initially	
t	x	t	x
48"	10	2' 5"	5
1' 30"	20	3' 35"	10
2' 25"	30	4' 30"	15
3' 25"	40	5' 45"	20
4' 50"	50	7' 8"	25
6' 55"	60	8' 35"	30
12' 0"	70	10' 15"	35

Influence of the Surface

There can be no doubt that from about 520°–530° a reaction comes into prominence which is of a quite different character from the low temperature heterogeneous reaction. A changed character might result from the gradual thinning out of the layer of adsorbed molecules, whereby the chance of suitable molecular configurations becomes proportional to a high power of the concentration in the gas phase. But the appearance of a marked catalytic effect of steam could not be accounted for in this way. Moreover it is significant that this change in the nature of the reaction only comes about as the explosion temperature is approached. It is much more probable that the new reaction takes place in the gas phase. This supposition is confirmed by a comparison of the effect of added silica powder to the bulb at different temperatures and pressures.

Bulb	Temperature °C	Pressure of H ₂ and O ₂	Ratio of rate with silica to rate without
1	507	325/202	22
		450/280	0.9
		325/200	1.8
	567	180/100	8.5
		325/200	0.5
		240/150	about 1
		180/100	1.3

Nevertheless the reaction does not become quite as independent of the surface as this would at first sight indicate. Even in this region of "homogeneous" combination the rate of reaction varies quite considerably from bulb to bulb, and, in a given bulb, with time and previous treatment. This points to the fact that certain catalytic influences are still at work. A few examples, chosen from a period when the bulb had reached a rather "unsteady" state, will illustrate this.

Order of experiment	Temperature °C	H ₂	O ₂	Time for 50 per cent combinations	Remarks
	547	321 162	204 107	19' 43" 102' 0"	Early experiments
(4)		321	201	3' 20"	
(1)	549	242	151	11' 40"	After long use, several weeks heating at 500°–600°, dismantling and boiling out with chromic acid
(3)		244	147	12' 8"	
(5)		240	149	9' 5"	
(7)		240	153	13' 6"	
(8)		181	108	27' 40"	
(2)		121	81	76' 30"	

This was the most extreme case met with

An explanation of these rather curious facts is provided by a further examination of the influence of powdered silica, which at still higher temperatures actually produces a considerable slowing down in the rate of reaction.

In neither of the two empty bulbs could any experiments be carried out at temperatures much above 575° *. When, however, a bulb was packed about half full of powdered silica it was still possible to carry out experiments at 601° although not at 606° .

Two factors thus appear to be at work—one causing an acceleration of the surface reaction, the other an inhibition of the gas reaction.

Since the conditions inside the bulb containing powdered silica were not very uniform, two special bulbs were procured of about 150 c.c. capacity and completely packed with spherical silica beads about 1 cm. in diameter. In each of these the reaction proceeded with extreme slowness at temperatures far above that at which explosion would have occurred in an empty bulb. The following is an example.

648° C 200 mm H ₂ 129 O ₂		540° C 203 mm H ₂ 108 mm O ₂	
<i>t</i>	Per cent combined	<i>t</i>	Per cent combined
8' 20"	20	2' 50"	5
19' 0"	33	10' 15"	10
29' 0"	46	18' 15"	15
92' 0"	81	34' 30"	20
		66' 0"	30

Even at 700° C under these conditions the high order, autocatalytic reaction did not come into prominence.

* The range of possible measurement was limited in two distinct ways. At higher pressures the mixed gases exploded a second or so after mixing, the rate of evolution of heat in the interior of the mixture being so great that the conditions ceased to be isothermal. At lower pressures, when the reaction velocity in the mixed gases is much smaller, it might be supposed that measurements could still be made. The tendency of a jet of oxygen to inflame at the point where it enters an atmosphere of hydrogen increases as the pressure of hydrogen diminishes (Dixon, 'Mem and Proc Manchester Lit and Phil Soc,' vol 70, p 29 (1926)). This is evidently due to variation in the heat conducting power of the mixture, and places a limit on the low pressure side to the experiments which can be made at high temperatures. Under the conditions of the present investigations measurement at high and low pressures ceased to be possible at about the same temperature. If hydrogen was streamed into oxygen, low pressure experiments became impossible from this cause at a lower temperature than if the mixing were attempted in the reverse order.

The Temperature Coefficient

The temperature coefficient of the surface reaction is low. The following are typical results —

Bulb 2 — Increase in rate for 10°C over the range 470° – 510° 1.32

Bulb 1 (containing powdered silica) — Increase for 10°C over the range 500° – 540° (low pressures) 1.22

The value for the gas reaction is not easy to specify, as it varies somewhat with pressure and temperature, tending to increase with both.

In bulb 1, for example, the temperature coefficient over the range 547° – 567° is 3.3 for 10° for a pressure of 320 mm H_2 and 160 mm O_2 , and is only 1.6 for a pressure of 160/100.

The following are some typical results for bulb 2 —

$^{\circ}\text{C}$	H_2	O_2	Time for 50 per cent combination	Ratio for 10°C
533	200	100	112' 0"	1.7
554	200	100	38' 30"	
533	400	200	14' 0"	2.4
554	400	200	7' 0"	

The figure (3) shows the logarithm of the time of half change for initial pressures 200/100 in bulb 2 plotted against the reciprocal of the absolute temperature in the usual way. In a simple reaction of unchanging character

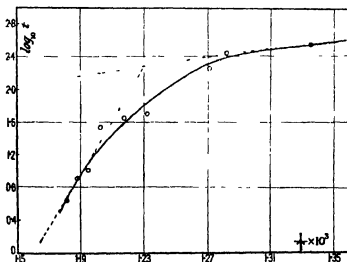


FIG 3

a straight line would be obtained. The slope varies from that corresponding to a temperature coefficient of 1.3 for 10° in the region of surface reaction to that represented by the steeper dotted line at 570° , where the coefficient is 3.2.

Obviously it is not possible to calculate the value of the energy of activation for this reaction since the actual velocity is determined by a process much more complex than the initial activation of the molecules. Taking a tangent to the curve at a given temperature and calculating from this the energy of activation corresponding would for the same reason be an inadmissible procedure.

Discussion

The high-order reaction which comes into prominence within about 50° of the explosion temperature must take place in the gas. The increase in the order alone could be explained by assuming the adsorption of the oxygen and hydrogen to diminish with temperature in a suitable way, but this assumption would require the temperature coefficient of the reaction velocity to become lower rather than higher, and could not explain the autocatalysis by steam nor the disappearance of the positive catalytic effect of the surface.

The influence of the various concentrations suggests that some such complex as $2\text{H}_2 \mid \text{O}_2 \mid \text{H}_2\text{O}$ plays some part in a series of changes, but it is hardly possible to infer its exact composition. Moreover, activated molecules of hydrogen peroxide may be formed and may act catalytically.

Egerton and Gates* have put forward the theory that in the rapid combustion of hydrocarbons autocatalysts are formed, and that these are rapidly destroyed by certain substances, which thus act as negative catalysts for the combustion itself, and behave as "anti knocks" in an exploding mixture.

There is a suggestive similarity between the negative catalysis of hydrocarbon combustion and the retarding action of the surface on the union of hydrogen and oxygen. If the autocatalyst, which for the sake of a definite picture we may provisionally call hydrogen peroxide, is rapidly destroyed by a heterogeneous reaction, the whole course of the combination will be retarded.

Another factor has also to be taken into account. The reaction is a highly exothermic one. Each pair of steam molecules which are formed have between them an excess energy equivalent to well over 100,000 calories, and thus may possibly set up what Christiansen calls a chain reaction by activating fresh molecules which they encounter. Such a chain would be interrupted when any

* 'J. Inst. Petroleum Technol.', vol. 13, p. 281 (1927).

of the highly activated molecules collided with the walls of the vessel, since the time of relaxation in such a collision is extremely small, and molecules rebounding from a solid surface are, in general, in thermal equilibrium with it. The smaller the free space in the reaction bulb the shorter will be the reaction chains, and the much smaller rate in the packed vessel could thus be accounted for.

These two possible explanations are not mutually exclusive, since the autocatalyst, which we have referred to as hydrogen peroxide, is probably only capable of existence in an activated form.

The reaction chain hypothesis has two things in its favour. First, it is consistent with other work* on negative catalysis in general. Secondly, it is inherently probable since the excess energy possessed by the steam molecules is just of the order of magnitude of heats of activation for reactions taking place in the region of 500°-600° C. It has moreover the advantage of giving a picture of a continuous transition from the region of slow reaction to the region of explosion. At the lowest temperatures the reaction is entirely confined to the surface, and we have complete thermal equilibrium. As the temperature increases reaction centres appear in the gas, or at the surface, whence chains pass through the gas. When the gas reaction first becomes appreciable there are probably many unfruitful encounters which may terminate a chain, but the proportion is likely to diminish with increasing temperature. The system ceases to be in thermal equilibrium in the sense that the heat of reaction makes each new steam molecule a potential source of further reaction, but it remains isothermal in the sense that the unreacted gases and all but the freshly generated steam have energies in accordance with Maxwell's law at the temperature of the walls of the reaction chamber. At last a point is reached where the rate of production of energy in the system is so great that even the unreacted gas no longer remains in thermal equilibrium with the vessel, and inflammation occurs. The large and complex variation of the reaction velocity with temperature and pressure is thus understandable.

A more detailed investigation may render possible the determination of the energy of activation, the length of the reaction chains and the fruitfulness of collisions at different temperatures. To this end an examination is being made of the combination of hydrogen and oxygen in a porcelain bulb, with which more accurate results are obtainable. A comparison of the two

* Christiansen, 'J. Physical Chem.', vol. 28, p. 145 (1924); Bäckström, 'J. Amer. Chem. Soc.', vol. 49, p. 1460 (1927).

investigations will probably yield interesting results which it is hoped to communicate in due course

Summary

An examination has been made by a static method of the complete course of the combination of oxygen and hydrogen, at constant temperature and volume, over a range of temperature extending from the region of purely catalytic surface reaction up as nearly as possible to the point where the combination ceases to be isothermal and passes into explosion

In the last 50° of this range a reaction comes into prominence, which is quite different from the low-order, heterogeneous reaction. It is of high but variable order, the influence of pressure being on the average approximately that corresponding to a reaction of the fourth order, it is strongly autocatalysed by steam, and has a high temperature coefficient. At high temperature the normal positive catalytic effect of the walls of the reaction chamber gives place to a negative effect, which may be due to the catalytic destruction of an auto-catalyst for the principal reaction, or the interruption of "reaction-chains," or to both causes. It is concluded that the reaction measured is the true gas reaction between hydrogen and oxygen

On Electrostatics in a Gravitational Field

By E T COPSON, M A., Lecturer in Mathematics in the University of Edinburgh

(Communicated by E T Whittaker, F R S — Received December 1, 1927)

§ 1 Introduction

In a recent paper, Prof Whittaker* has discussed the effect, according to the general theory of relativity, of gravitation on electromagnetic phenomena. In particular, he has discussed electrostatics in gravitational fields of two kinds, namely (i) the field due to a single gravitating mass, in which case space-time has the metric discovered by Schwarzschild, and (ii) a limiting case of this, called a *quasi-uniform* field, in which the gravitational force is, in the neighbourhood of the origin, uniform.

Whittaker's general method, so far as electrostatical problems were concerned, was to solve the partial differential equation satisfied by the electrostatic potential in terms of generalised harmonic functions, and then, from these, to build up other solutions. In this way, he succeeded in finding an algebraic expression which represents the potential of a single electron in the quasi-uniform field, he did not, however obtain a corresponding algebraic expression for the potential of an electron in the Schwarzschild field.

The chief result of the present paper is the solution of the problem which is thus presented, namely, to determine the potential of an electron in the Schwarzschild field in an algebraic form. In order to obtain it, I have departed altogether from Whittaker's method of investigation and have relied instead on Hadamard's theory of "elementary solutions" of partial differential equations. I show first, in § 2, how the solution obtained by Whittaker for the quasi-uniform field may be obtained by the aid of Hadamard's theory, and then show, in § 3, that the same methods yield the solution in an algebraic form (3.6) for the Schwarzschild field. In the last section, the new solution is expanded in terms of generalised harmonic functions, some of the relations obtained in this section are believed to be new properties of the Legendre functions.

The following brief résumé of Hadamard's theory of elementary solutions is given to make the rest of the paper intelligible.

The solution $[(x-a)^2 + (y-b)^2 + (z-c)^2]^{-\frac{1}{2}}$ of Laplace's equation in three dimensions is distinguished from all other solutions by the following properties —

* 'Roy Soc Proc,' A, vol 116, p 720 (1927)

- (1) it is continuous and differentiable as often as we please in any finite region of space, except in the neighbourhood of the singular point (a, b, c) ,
- (2) it becomes infinite, to as low an order as possible* at the singular point and on all the isotropic lines through it

But the isotropic lines are the "bicharacteristics"† of Laplace's equation. This suggests at once the appropriate generalisation

Let $g^{\alpha\beta}$, h^{α} , k be holomorphic functions in a certain domain of real values of the variables (x^1, x^2, \dots, x^m) . Then Hadamard‡ has shown that the partial differential equation

$$\sum_{\alpha, \beta=1}^m g^{\alpha\beta} \frac{\partial^2 u}{\partial x^\alpha \partial x^\beta} + \sum_{\alpha=1}^m h^{\alpha} \frac{\partial u}{\partial x^\alpha} + ku = 0,$$

possesses, when m is odd, a unique solution which is continuous and differentiable as often as we please in the domain where $g^{\alpha\beta}$, h^{α} , k are holomorphic, except in the neighbourhood of one singular point (a^1, a^2, \dots, a^m) and the bicharacteristics through it, in the neighbourhood of the singular point, this solution becomes infinite to as low an order as possible, and may be expanded in the form

$$\Gamma^{-\frac{m-2}{2}} (U_0 + U_1 \Gamma + U_2 \Gamma^2 + \dots)$$

Γ here denotes the square of the geodesic distance from the singular point to (x^1, x^2, \dots, x^m) in the space whose metric is

$$ds^2 = \sum_{\alpha, \beta} g_{\alpha\beta} dx^\alpha dx^\beta,$$

the functions U_0, U_1, U_2, \dots are holomorphic in the given domain. This solution is called the "elementary solution",

$$[(x-a)^2 + (y-b)^2 + (z-c)^2]^{-\frac{1}{2}}$$

is obviously the elementary solution of Laplace's equation. Accordingly we shall assume that *the potential of an electron in a gravitational field is the elementary solution of the partial differential equation of electrostatic potential*

* It is this property which distinguishes $[(x-a)^2 + (y-b)^2 + (z-c)^2]^{-\frac{1}{2}}$ from the solution $(x-a)[(x-a)^2 + (y-b)^2 + (z-c)^2]^{-\frac{1}{2}}$

† On "bicharacteristics," see Hadamard, "Lectures on Cauchy's Problem in Linear Partial Differential Equations" (Yale University Press, 1923), p. 75, *et seq*

‡ *Loc cit*, Book II, chap. 3. We make use here of the tensor notation. Thus $g_{\alpha\beta}$ and $g^{\alpha\beta}$ are corresponding elements in reciprocal determinants. We shall later write $g(x)$ for the value of the determinant $|g_{\alpha\beta}|$ at (x^1, x^2, \dots, x^m)

In the course of his proof of the existence of the elementary solution, Hadamard shows how to construct it, thus the equation

$$U_0 = \sqrt{g(a)} \exp \left[- \int_0^s \left(\sum_{\alpha, \beta} g^{\alpha\beta} \frac{\partial^2 \Gamma}{\partial x^\alpha \partial x^\beta} + \sum_{\alpha} h^\alpha \frac{\partial \Gamma}{\partial x^\alpha} - 2m \right) \frac{ds}{4s} \right]$$

determines U_0 . Here integration is along the geodesic from the singularity to (x^1, x^2, \dots, x^n) , with respect to the arc s of the geodesic. The other functions U_α are given by recurrence relations

§ 2 *Electrostatics in the Quasi-Uniform Gravitational Field*

The electrostatic potential in the quasi-uniform gravitational field satisfies the equation*

$$\left(1 + \frac{2gx}{c^2} \right) \frac{\partial^2 u}{\partial x^2} + \frac{\partial^2 u}{\partial y^2} + \frac{\partial^2 u}{\partial z^2} = 0 \quad (2.1)$$

If we apply the transformation

$$1 + \frac{2gx}{c^2} = (1 + \xi)^2, \quad \frac{gy}{c^2} = \eta, \quad \frac{gz}{c^2} = \zeta, \quad (2.2)$$

this equation becomes

$$\frac{\partial^2 u}{\partial \xi^2} + \frac{\partial^2 u}{\partial \eta^2} + \frac{\partial^2 u}{\partial \zeta^2} - \frac{1}{1 + \xi} \frac{\partial u}{\partial \xi} = 0 \quad \dagger \quad (2.3)$$

In terms of these co-ordinates, the metric of space time is

$$ds^2 = (1 + \xi)^2 dt^2 - \frac{c^2}{g^2} (d\xi^2 + d\eta^2 + d\zeta^2),$$

so that ξ, η, ζ represent actual distance

It is a consequence of Hadamard's theory, that the elementary solution is, if $1 + \xi$ is positive,

$$\Gamma^{-1} [U_0 + U_1 \Gamma + U_2 \Gamma^2 + \dots]$$

where

$$\Gamma = (\xi - \alpha)^2 + (\eta - \beta)^2 + (\zeta - \gamma)^2.$$

The formula for $U_0 \dagger$ is

$$\begin{aligned} U_0 &= \exp \left[- \int_{\alpha}^{\xi} \left\{ \frac{\partial^2 \Gamma}{\partial \xi^2} + \frac{\partial^2 \Gamma}{\partial \eta^2} + \frac{\partial^2 \Gamma}{\partial \zeta^2} - \frac{1}{\xi + 1} \frac{\partial \Gamma}{\partial \xi} - 6 \right\} \frac{d\xi}{4(\xi - \alpha)} \right] \\ &= \exp \int_{\alpha}^{\xi} \frac{d\xi}{2(\xi + 1)} \\ &= \left(\frac{1 + \xi}{1 + \alpha} \right)^{\frac{1}{2}} \end{aligned}$$

* Whittaker, *loc cit*, p. 723 (13)

† This equation would also occur, in classical electrostatics, as the equation of potential when the specific inductive capacity is $(1 + \xi)^{-1}$

‡ Hadamard, *loc cit*, p. 94 (41)

The recurrence relations, from which the functions U_1, U_2, \dots are to be determined, are*

$$U_n = -\frac{U_0}{2(2n-1)(\xi-\alpha)^n} \int_{\alpha}^{\xi} \frac{(\xi-\alpha)^{n-1}}{U_0} \left[\frac{\partial^2 U_{n-1}}{\partial \xi^2} + \frac{\partial^2 U_{n-1}}{\partial \eta^2} + \frac{\partial^2 U_{n-1}}{\partial \zeta^2} - \frac{1}{\xi+1} \frac{\partial U_{n-1}}{\partial \xi} \right] d\xi,$$

where integration is along the straight line from (α, β, γ) to (ξ, η, ζ) . We easily find that

$$U_1 = \frac{3}{2} U_0 (1+\xi)^{-1} (1+\alpha)^{-1}$$

$$U_2 = -\frac{5}{12} U_0 (1+\xi)^{-2} (1+\alpha)^{-2},$$

and, generally, that

$$U_n = k_n U_0 (1+\xi)^{-n} (1+\alpha)^{-n}$$

where

$$\frac{k_n}{k_{n-1}} = -\frac{(2n+1)(2n-3)}{4 \cdot 2n(2n-1)}$$

The constants k_n are therefore the coefficients in the expansion of

$$(1 + \frac{1}{2}x)(1 + \frac{1}{2}x)^{-1}$$

Hence the elementary solution, having singularity at (α, β, γ) , is equal to

$$\left. \begin{aligned} & \frac{U_0}{\Gamma^3} \left[1 + k_1 \frac{\Gamma}{(1+\xi)(1+\alpha)} + k_2 \frac{\Gamma^2}{(1+\xi)^2(1+\alpha)^2} + \dots \right] \\ &= \frac{U_0}{\Gamma^3} \left(1 + \frac{\Gamma}{2(1+\xi)(1+\alpha)} \right) \left(1 + \frac{\Gamma}{4(1+\xi)(1+\alpha)} \right)^{-1} \\ &= \frac{[(\xi-\alpha)^2 + (\eta-\beta)^2 + (\zeta-\gamma)^2 + 2(1+\xi)(1+\alpha)]}{[(\xi-\alpha)^2 + (\eta-\beta)^2 + (\zeta-\gamma)^2 + 4(1+\xi)(1+\alpha)]^{\frac{1}{2}} [(\xi-\alpha)^2 + (\eta-\beta)^2 + (\zeta-\gamma)^2 + (1+\alpha)]^{\frac{1}{2}}} \dagger \end{aligned} \right\} \quad (2.4)$$

If (a, b, c) is the point in the original co-ordinate system corresponding to (α, β, γ) the elementary solution becomes, in terms of x, y, z ,

$$\begin{aligned} & \left[2 + 2\frac{q}{c^2}(x+a) + \frac{q^2}{c^4}\{(y-b)^2 + (z-c)^2\} \right] \\ & \left\{ \left[2 + 2\frac{q}{c^2}(x+a) + \frac{q^2}{c^4}\{(y-b)^2 + (z-c)^2\} \right]^2 - 4 \left(1 + \frac{2qx}{c^2} \right) \left(1 + \frac{2qa}{c^2} \right) \right\}^{\frac{1}{2}} \sqrt{1 + \frac{2qa}{c^2}} \\ &= \frac{1 + \frac{q}{c^2}(x+a) + \frac{q^2}{2c^4}\{(y-b)^2 + (z-c)^2\}}{\frac{q}{c^2} \sqrt{1 + \frac{2qa}{c^2}} \left[(x-a)^2 + (y-b)^2 + (z-c)^2 + \frac{q}{c^2}(x+a)\{(y-b)^2 + (z-c)^2\} + \frac{q^2}{4c^4}\{(y-b)^2 + (z-c)^2\}^2 \right]^{\frac{1}{2}}} \end{aligned}$$

* *Ibid.*, p. 95 (44)

† It will be observed that this has a singularity at the image point of (α, β, γ) in $\xi = -1$. This is not of importance since the region $\xi \leq -1$ is inaccessible in the relativity case. It is of interest when the PDE is regarded as the classical potential equation with $K = (1+\xi)^{-1}$, K becomes infinite for $\xi = -1$.

This is precisely the formula given by Whittaker* for the potential of an electron in the quasi-uniform gravitational field

§ 3 *Electrostatics in the Field due to a Single Gravitating Centre*

The metric of space-time about a single gravitating centre is specified by Schwarzschild's formula

$$ds^2 = \left(1 - \frac{\alpha}{R}\right) dt^2 - \frac{1}{c^2} \left(\frac{dR^2}{1 - \frac{\alpha}{R}} + R^2 d\theta^2 + R^2 \sin^2 \theta d\phi^2 \right),$$

in this field, the equation of electrostatic potential† is

$$\left(1 - \frac{\alpha}{R}\right) \frac{\partial}{\partial R} \left(R^2 \frac{\partial u}{\partial R} \right) + \frac{1}{\sin \theta} \frac{\partial}{\partial \theta} \left(\sin \theta \frac{\partial u}{\partial \theta} \right) + \frac{1}{\sin^2 \theta} \frac{\partial^2 u}{\partial \phi^2} = 0 \quad (3.1)$$

If we transform to the isotropic co-ordinates specified by

$$r = \frac{2R}{\alpha} - 1 + \frac{2}{\alpha} \sqrt{R^2 - \alpha R}, \quad (3.2)$$

the partial differential equation becomes

$$\frac{\partial^2 u}{\partial x^2} + \frac{\partial^2 u}{\partial y^2} + \frac{\partial^2 u}{\partial z^2} + \frac{2-4r}{r^2(r^2-1)} \left(x \frac{\partial u}{\partial x} + y \frac{\partial u}{\partial y} + z \frac{\partial u}{\partial z} \right) = 0 \quad (3.3)$$

where

$$x = r \sin \theta \cos \phi, \quad y = r \sin \theta \sin \phi, \quad z = r \cos \theta$$

In terms of the isotropic co-ordinates, the metric of space-time is‡

$$ds^2 = \left(\frac{r-1}{r+1} \right)^2 dt^2 - \frac{\alpha^2}{16c^2} \left(1 + \frac{1}{r} \right)^4 (dx^2 + dy^2 + dz^2),$$

the transformation conformally represents the spatial part ($R > \alpha$) of Schwarzschild's metric on to the part ($r > 1$) of Euclidean space. In these co-ordinates, $r = 1$ is an inaccessible boundary.

The potential of an electron at $(0, 0, a)$, being the elementary solution of equation (3.3), must have the form

$$\Gamma^{-1} [U_0 + U_1 \Gamma + U_2 \Gamma^2 + \dots] \quad (3.4)$$

where $\Gamma = x^2 + y^2 + (z-a)^2$ and where U_0, U_1, U_2, \dots are holomorphic for $r > 1$.

* *Loc. cit.*, p. 727 (19).

† *Ibid.*, p. 729 (25).

‡ This equation would occur in classical electrostatics if the specific inductive capacity were assumed to be $(r+1)^2/r^2(r-1)$.

§ Cf. de Sitter, 'Amsterdam Akad. Verslagen,' vol. 25, p. 232 (1916), or Eddington, "Mathematical Theory of Relativity," p. 93 (1924).

The Hadamard formula for U_0 is

$$U_0 = \exp \left[- \int_0^r \frac{(1-2r)}{r^2(r^2-1)} (r^2 - az) \frac{ds}{s} \right]$$

where integration is along the straight line specified by

$$x = s \sin \beta \cos \gamma, \quad y = s \sin \beta \sin \gamma, \quad z = a + s \cos \beta,$$

where β and γ are constants. But evidently we have

$$(r^2 - az) \frac{ds}{s} = (s + a \cos \beta) ds = r dr,$$

hence

$$U_0 = \exp \left[\int_a^r \frac{2r-1}{r(r^2-1)} dr \right] = \frac{r(r-1)^{1/2} (a+1)^{3/2}}{a(a-1)^{1/2} (r+1)^{3/2}}$$

Instead of using Hadamard's recurrence relations connecting U_0, U_1, U_2 , we may apply the process by which they were obtained, that is, we may substitute (3.4) in equation (3.3), regarding U_1, U_2 as holomorphic functions of r (> 1). If we do this, we obtain

$$U_1 = \frac{3}{2} \frac{U_0}{(r^2-1)(a^2-1)},$$

$$U_2 = -\frac{5}{8} \frac{U_0}{(r^2-1)^2(a^2-1)^2},$$

and so on. Hence the elementary solution is of the form

$$\frac{r(a+1)^2}{a(r+1)^2} \left[\frac{(r^2-1)}{(a^2-1)\Gamma} \right]^{\frac{1}{2}} \left\{ 1 + \frac{3}{2} \frac{\Gamma}{(r^2-1)(a^2-1)} - \frac{5}{8} \frac{\Gamma^2}{(r^2-1)^2(a^2-1)^2} + \dots \right\}$$

The form of the first three terms in the elementary solution suggests that, instead of determining successively the remaining U_n , we should substitute, in the equation (3.3),

$$u = \frac{r}{(r+1)^2} F(\gamma),$$

where

$$\gamma = \Gamma/(r^2-1)$$

If we do this, we find that $F(\gamma)$ is a solution of

$$2\{\gamma^2 + (a^2-1)\gamma\} \frac{d^2 F}{d\gamma^2} + 3\{2\gamma + a^2-1\} \frac{dF}{d\gamma} = 0,$$

and hence that

$$F(\gamma) = A + B \frac{2\gamma + (a^2-1)}{\{\gamma^2 + \gamma(a^2-1)\}^{\frac{1}{2}}}$$

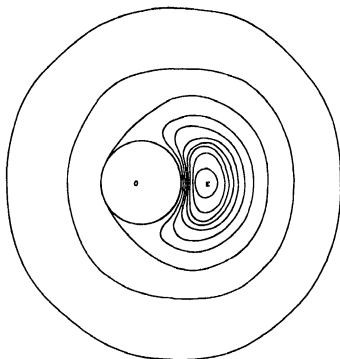
where A and B are arbitrary constants

The elementary solution of equation (3.3) with singularity at $r = a$, $\theta = 0$, is thus seen to be a constant multiple of

$$\frac{r}{(r+1)^2} [2\Gamma + (a^2 - 1)(r^2 - 1)] [\Gamma^2 + \Gamma(a^2 - 1)(r^2 - 1)]^{-1/2} \quad (3.5)$$

$$= \frac{r}{(r+1)^2} \left[\left(\frac{a^2 r^2 + 1 - 2ar \cos \theta}{r^2 + a^2 - 2ar \cos \theta} \right)^{1/2} + \left(\frac{r^2 + a^2 - 2ar \cos \theta}{a^2 r^2 + 1 - 2ar \cos \theta} \right)^{1/2} \right]^\dagger \quad (3.6)$$

When we transform back to the co-ordinates (R, θ, ϕ) , this expression for the potential becomes rather complicated. In any practical application it seems preferable to use the isotropic co-ordinate system. The figure below shows the equipotential surfaces due to an electron E at $R = 1.56a$, $\theta = 0$, corresponding to $a = 4$. With the exception of the two surfaces nearest to the electron, the difference of potential between consecutive surfaces is constant. It will be observed that $R = a$ is always an equipotential surface.



* A comparison of this formula with (2.4) shows that (2.4) is the limiting form of (3.5) when the Schwarzschild metric degenerates into the quasi-uniform metric. This is, of course, what one would expect.

† This shows that there is a singularity at $r = a$, $\theta = 0$, and at its image point in the sphere $r = 1$. In the relativity case, this latter singularity does not concern us, but when we regard (3.3) as the classical electrostatic potential equation with $K = (r+1)^2/r^2(r-1)$ it is of some interest. Cf. footnote †, p. 187.

If we put $\alpha = 1$ in the potential (3.6), we find that it reduces to a constant multiple of R^{-1} , in other words, the potential of an electron on the boundary sphere $R = \alpha$ is independent of its position on the sphere, a rather curious result

§ 4 The Expansion of the Potential in Terms of Generalised Harmonic Functions

It has been shown* that the equation (3.1) possesses the particular solution

$$\frac{2}{(2n)!} \frac{(n-1)! n!}{\alpha^{n-1} (R-\alpha)} P_n'(\rho) P_n^m(\cos \theta) \frac{\cos m\phi}{\sin} \quad (4.1)$$

if $n = 1, 2, 3, \dots$, where $\rho\alpha = 2R - \alpha$, this solution reduces to

$$R^n P_n^m(\cos \theta) \frac{\cos m\phi}{\sin},$$

when α tends to zero. When $n = 0$, the expression (4.1) is meaningless and should be replaced by 1. It may be shown in a similar way that, if $n = 0, 1, 2, \dots$, then

$$-\frac{4}{n!} \frac{(2n+1)!}{(n+1)!} \alpha^{n-2} (R-\alpha) Q_n'(\rho) P_n^m(\cos \theta) \frac{\cos m\phi}{\sin} \quad (4.2)$$

is the particular solution of the second kind, which reduces to

$$R^{-n-1} P_n^m(\cos \theta) \frac{\cos m\phi}{\sin},$$

as α tends to zero, for $n = 0$, the second solution actually is R^{-1} . These functions (4.1) and (4.2) may be called *generalised harmonic functions*. Any solution, algebraic in $\cos \theta$, of the partial differential equation (3.1) must possess expansions in terms of them, which are valid for certain ranges of values of R . We now propose to investigate the expansion of the elementary solution in terms of these functions, incidentally this will show us whether Whittaker's infinite series of generalised harmonic functions† is or is not the elementary solution.

Consider then the elementary solution with singularity at $R = B$, $\theta = 0$, corresponding to $r = b$. If we choose the constant multiplier so that the potential is symmetrical in r and b , it has the form

$$V = \frac{4br}{\sigma (b+1)^2 (r+1)^2} \left[\frac{(r^2 - 2br \cos \theta + b^2)^{\frac{1}{2}}}{(b^2 - 2br \cos \theta + 1)^{\frac{1}{2}}} + \frac{(b^2 r^2 - 2br \cos \theta + 1)^{\frac{1}{2}}}{(r^2 - 2br \cos \theta + b^2)^{\frac{1}{2}}} \right] \quad (4.3)$$

* Whittaker, *loc. cit.*, p. 730 (31)

† *Ibid.*, p. 730 (33)

If $r > b > 1$, the value of this potential on $\theta = 0$ is

$$\begin{aligned} V_0 &= \frac{4br}{\alpha(b+1)^2(r+1)^2} \left[\frac{r-b}{br-1} + \frac{br-1}{r-b} \right] \\ &= \frac{2(R-\alpha)}{\alpha B \sqrt{\rho^2-1}} \frac{r}{r^2-1} \left[\frac{1}{b} \left(1 - \frac{b}{r}\right) \left(1 - \frac{1}{br}\right)^{-1} + b \left(1 - \frac{1}{br}\right) \left(1 - \frac{b}{r}\right)^{-1} \right] \\ &= \frac{2(R-\alpha)}{\alpha B \sqrt{\rho^2-1}} \frac{1}{r} \left[1 + \frac{1}{r^2} + \frac{1}{r^4} + \dots \right] \left[\left(b + \frac{1}{b}\right) + \left(b^2 - 2 + \frac{1}{b^2}\right) \frac{1}{r} + \dots \right] \\ &= \frac{2(R-\alpha)}{\alpha B \sqrt{\rho^2-1}} \left[\left(b + \frac{1}{b}\right) \frac{1}{r} + \left(b^2 - 2 + \frac{1}{b^2}\right) \frac{1}{r^2} + \left(b^3 + \frac{1}{b^3}\right) \frac{1}{r^3} \right. \\ &\quad \left. + \left(b^4 - 2 + \frac{1}{b^4}\right) \frac{1}{r^4} + \dots \right] \end{aligned}$$

Now Schläfli* has shown that

$$\{\rho + \sqrt{\rho^2 - 1}\}^{-n} = -n \sum_{m=0}^{\infty} \frac{2m+n-1}{2\pi} \frac{\Gamma(m-\frac{1}{2}) \Gamma(m+n-\frac{1}{2})}{m! (m+n)!} Q_{2m+n-1}(\rho)$$

Term-by-term differentiation may be easily shown to be valid here, it gives

$$\begin{aligned} \frac{r^{-n}}{\sqrt{\rho^2-1}} &= \frac{\{\rho + \sqrt{\rho^2-1}\}^{-n}}{\sqrt{\rho^2-1}} \\ &= \sum_{m=0}^{\infty} \frac{(2m+n-1)}{2\pi} \frac{\Gamma(m-\frac{1}{2}) \Gamma(m+n-\frac{1}{2})}{m! (m+n)!} Q'_{2m+n-1}(\rho) \end{aligned}$$

If we substitute this series for the various inverse powers of r in the expansion of V_0 , we have

$$\begin{aligned} V_0 &= \frac{2(R-\alpha)}{B\alpha} \left[\sum_{m=0}^{\infty} \sum_{p=0}^{\infty} \left\{ b^{2m+1} + \frac{1}{b^{2m+1}} \right\} \frac{2p+2m+1}{2\pi} \frac{\Gamma(p-\frac{1}{2}) \Gamma(2m+p+\frac{1}{2})}{p! (2m+p+1)!} Q'_{2p+2m}(\rho) \right. \\ &\quad \left. + \sum_{m=0}^{\infty} \sum_{p=0}^{\infty} \left\{ b^{2m+2} - 2 + \frac{1}{b^{2m+2}} \right\} \frac{2p+2m+1}{2\pi} \frac{\Gamma(p-\frac{1}{2}) \Gamma(2m+p+\frac{1}{2})}{p! (2m+p+1)!} Q'_{2p+2m+1}(\rho) \right] \\ &= \frac{2(R-\alpha)}{B\alpha} \left[\sum_{n=0}^{\infty} \sum_{t=0}^{\infty} \left\{ b^{2(n-t+1)} - 2 + \frac{1}{b^{2(n-t+1)}} \right\} \frac{2n+1}{2\pi} \frac{\Gamma(t-\frac{1}{2}) \Gamma(2n-t+\frac{1}{2})}{t! (2n-t+1)!} Q'_{2n+1}(\rho) \right. \\ &\quad \left. + \sum_{n=1}^{\infty} \sum_{t=0}^{\infty} \left\{ b^{2(n-t+1)} + \frac{1}{b^{2(n-t+1)}} \right\} \frac{2n+1}{2\pi} \frac{\Gamma(t-\frac{1}{2}) \Gamma(2n-t+\frac{1}{2})}{t! (2n-t+1)!} Q'_{2n}(\rho) \right. \\ &\quad \left. - \frac{1}{2} \left(b + \frac{1}{b} \right) Q'_0(\rho) \right] \end{aligned}$$

Now by the use of the expansion

$$(1 - kb)^{-3/2} (1 - kb^{-1})^{-3/2} = \sum_0^{\infty} h^2 P'_{n+1} \left(\frac{1}{2} \left(b + \frac{1}{b} \right) \right),$$

* See Whittaker and Watson, 'Modern Analysis' (1920), p 334, ex 31

we can easily show that

$$\begin{aligned} \left(b^2 - 2 + \frac{1}{b^2}\right) P'_n \left(\frac{1}{2} \left(b + \frac{1}{b}\right)\right) \\ = -\frac{2n(2n+1)}{\pi} \sum_{t=0}^{\infty} \left\{ b^{2(n-t+1)} + \frac{1}{b^{2(n-t+1)}} \right\} \frac{\Gamma(t-\frac{1}{2}) \Gamma(2n-t+\frac{1}{2})}{t! (2n-t+1)!}, \\ \left(b^2 - 2 + \frac{1}{b^2}\right) P'_{2n+1} \left(\frac{1}{2} \left(b + \frac{1}{b}\right)\right) \\ = -\frac{(2n+1)(2n+2)}{\pi} \sum_{t=0}^{\infty} \left\{ b^{2(n-t+1)} - 2 + \frac{1}{b^{2(n-t+1)}} \right\} \frac{\Gamma(t-\frac{1}{2}) \Gamma(2n-t+\frac{3}{2})}{t! (2n-t+2)!} \end{aligned}$$

If we use these expansions and write β for $\frac{1}{2} \left(b + \frac{1}{b}\right)$, we find that

$$\begin{aligned} V_0 &= -\frac{(R-\alpha)}{B\alpha} \left[\left(b + \frac{1}{b}\right) Q'_0(\rho) + \frac{1}{2} \sum_{n=1}^{\infty} \frac{(2n+1)}{n(n+1)} \left(b^2 - 2 + \frac{1}{b^2}\right) P'_n(\beta) Q'_n(\rho) \right] \\ &= \frac{2(R-\alpha) Q'_0(\rho)}{B\alpha} - \left[\frac{4}{\alpha^2} (R-\alpha) Q'_0(\rho) \right. \\ &\quad \left. + \frac{8}{\alpha^3} \sum_{n=1}^{\infty} \frac{(2n+1)}{n(n+1)} (R-\alpha) P'_n(\beta) (R-\alpha) Q'_n(\rho) \right] \\ &= -\frac{\alpha}{2BR} + \sum_{n=0}^{\infty} E_n(B, 0) F_n(R, 0), \end{aligned} \quad (4.4)$$

where

$$\begin{aligned} E_n(R, 0) &= \frac{2}{(2n)!} \frac{(n-1)! n!}{\alpha^{n-1}} (R-\alpha) P'_n(\rho) P_n(\cos \theta), \\ F_n(R, 0) &= -\frac{4}{n! (n+1)!} \alpha^{-n-2} (R-\alpha) Q'_n(\rho) P_n(\cos \theta) \end{aligned}$$

Now V , which is given by (4.3), is a solution of the partial differential equation (3.1), is algebraic in $\cos \theta$, and does not involve ϕ . Accordingly, for a certain range of values of R , it is expandable in the form

$$\sum_{n=0}^{\infty} a_n E_n(R, \theta) + \sum_{n=0}^{\infty} b_n F_n(R, \theta),$$

where a_n, b_n do not involve R and θ . But, on $\theta = 0$, V takes the value given by (4.4), if $R > B > \alpha$. Hence, if $R > B > \alpha$,

$$V = -\frac{\alpha}{2BR} + \sum_{n=0}^{\infty} E_n(B, 0) F_n(R, 0) \quad (4.5)$$

Similarly, if $R < B$, we can show that

$$V = -\frac{\alpha}{2BR} + \sum_{n=0}^{\infty} F_n(B, 0) E_n(R, 0). \quad (4.6)$$

We have thus shown that

The electric potential at the point (R, θ, ϕ) due to a unit point-charge at rest at the point $(R = B, \theta = 0)$ in the gravitational field due to a mass at the origin is

$$\frac{4br}{\alpha(b+1)^2(r+1)^2} \left[\left(\frac{r^2 - 2br \cos \theta + b^2}{b^2 r^2 - 2br \cos \theta + 1} \right)^{\frac{1}{2}} + \left(\frac{b^2 r^2 - 2br \cos \theta + 1}{r^2 - 2br \cos \theta + b^2} \right)^{\frac{1}{2}} \right],$$

where

$$\frac{4R}{\alpha} = \frac{(r+1)^2}{r}, \quad \frac{4B}{\alpha} = \frac{(b+1)^2}{b}$$

This potential may be expanded in the form

$$-\frac{\alpha}{2BR} - \frac{4}{\alpha^2}(R-\alpha)Q_0'\left(\frac{2R}{\alpha}-1\right) \\ - \frac{8}{\alpha^3} \sum_{n=1}^{\infty} \frac{(2n+1)}{n(n+1)} (B-\alpha) P_n'\left(\frac{2B}{\alpha}-1\right) (R-\alpha) Q_n'\left(\frac{2R}{\alpha}-1\right) P_n(\cos \theta)$$

if $R > B > \alpha$

When α tends to zero, the series (4.5) and (4.6) reduce to the classical formulæ

$$\sum_{n=0}^{\infty} B^n R^{-n-1} P_n(\cos \theta), \quad \sum_{n=0}^{\infty} B^{-n-1} R^n P_n(\cos \theta),$$

which hold when the mass of the gravitating centre vanishes. Whittaker's infinite series is similar to the series (4.6), and both have the same limit when α tends to zero, they differ in that the constant coefficients are not the same and in the presence of the term $-\alpha/2BR$. It seems unlikely that Whittaker's series can be expressed in terms of algebraic functions.

In conclusion I should like to thank Prof. Whittaker for his kind interest and encouragement during the progress of this work, and for his advice during its preparation for publication.

Some Cases of Instability in Fluid Motion

By HAROLD JEFFREYS, F R S

(Received October 24, 1927)

1 In a recent paper* I obtained a numerical solution of some problems concerning the stability of a layer of incompressible fluid when the temperature decreases upwards. The results depended on the solution of the sixth-order differential equation

$$\left(\frac{d^2}{d\zeta^2} - a^2\right)^3 Z = -\lambda a^2 Z \quad (1)$$

In this solution the co-ordinates were x , y and z , the last being taken vertically. The depth of the fluid is h , and

$$\zeta = z/h \quad (2)$$

Z is the factor of the disturbance of temperature that involves Z . The other factor is supposed to be of the form $\sin kx \sin my$, and

$$a^2 = (l^2 + m^2) h^2 \quad (3)$$

Further

$$\lambda = -g\alpha\beta h^4/\kappa\nu \quad (4)$$

where g is gravity, α the coefficient of expansion of the fluid, β the undisturbed vertical gradient of temperature, κ the coefficient of thermometric conductivity, and ν that of kinematic viscosity. Here ζ , a , and λ are all positive numbers.

The previous solution was obtained by L. F. Richardson's method of finite differences†. An alternative method is to use the principle that the solution of (1) is a combination of exponential functions, and therefore has no singularities for finite values of the argument. Hence it must be expansible for $0 < \zeta < 1$ in a series of sines of multiples of $\pi\zeta$. On assuming such an expansion and substituting in the equation we might expect to be able to equate coefficients of corresponding terms. But the result is obviously that terms of different arguments do not combine at all, and the inference would be that the only solution is one where every term is zero, which is not the case. The reason for the error is that where r is great the coefficients of the terms in the sine-series will ordinarily decrease like r^{-1} or r^{-2} . The trigonometric series obtained by differentiating more than twice are therefore divergent. But the derivatives of the solution, like the solution itself, are linear combinations of exponentials,

* 'Phil Mag.', vol 2, p 833 (1926)

† 'Math Gazette', July, 1925

and have valid expansions in sine-series. In fact the series obtained by differentiating the series for Z term by term are not the correct series for the derivatives of Z , and if we are to substitute in (1) and equate coefficients we must use the correct Fourier expansions.

We can, however, work from the other end. We can assume a trigonometric series for $d^3Z/d\xi^3$, and then obtain forms for lower derivatives and for Z itself by integration. The constants introduced by the integrations give a polynomial of the fifth degree in Z , while the trigonometric portion gives a series converging like r^{-7} or r^{-8} —that is to say, very rapidly. The divergence of the derived series in the former attempt arises from the Fourier series for the polynomial, but in the present method we have the whole of the polynomial in finite terms and can conveniently deal with it separately.

We put then

$$\xi = \pi\zeta = \pi z/h, \quad (5)$$

so that $\xi = 0$ and π at the limits. Put also

$$a = \pi b, \quad \lambda = \mu\pi^4. \quad (6)$$

Then (1) can be written

$$\left\{ \frac{d^2}{d\xi^2} - b^2 \right\}^3 Z + \mu b^2 Z = 0. \quad (7)$$

We now assume

$$\frac{d^2 Z}{d\xi^2} = \sum_{r=1}^{\infty} A_r \sin r\xi \quad (8)$$

whence, on repeated integration

$$\begin{aligned} Z = B_0 + B_1\left(\frac{1}{2}\pi - \xi\right) + \frac{B_2}{2!}\left(\frac{1}{2}\pi - \xi\right)^2 + \frac{B_3}{3!}\left(\frac{1}{2}\pi - \xi\right)^3 + \frac{B_4}{4!}\left(\frac{1}{2}\pi - \xi\right)^4 + \frac{B_5}{5!}\left(\frac{1}{2}\pi - \xi\right)^5 \\ - \sum_{r=1}^{\infty} \frac{A_r}{r^6} \sin r\xi \end{aligned} \quad (9)$$

Let us denote the polynomial by P . Then (7) is equivalent to

$$\Sigma \{ (r^2 + b^2)^3 - \mu b^2 \} \frac{1}{r^6} \sin r\xi + \left\{ \left(\frac{d^2}{d\xi^2} - b^2 \right)^3 + \mu b^2 \right\} P = 0 \quad (10)$$

Put

$$\frac{1}{2}\pi - \xi = \eta \quad (11)$$

$$\sum_{r=1}^{\infty} \lambda_r \sin r\xi = - \left\{ \left(\frac{d^2}{d\xi^2} - b^2 \right)^3 + \mu b^2 \right\} P \quad (12)$$

$$\begin{aligned} &= 3b^2 (B_4 + B_5\eta) - 3b^4 \left(B_2 + B_3\eta + \frac{B_4}{2!}\eta^2 + \frac{B_5}{3!}\eta^3 \right) \\ &\quad + (b^6 - \mu b^2) \left(B_0 + B_1\eta + \frac{B_2}{2!}\eta^2 + \frac{B_3}{3!}\eta^3 + \frac{B_4}{4!}\eta^4 + \frac{B_5}{5!}\eta^5 \right) \\ &= Q, \end{aligned} \quad (13)$$

say Then

$$A_r = \frac{r^2}{(r^2 + b^2)^2 - \mu b^2} \lambda_r \quad (14)$$

where

$$\frac{1}{2}\pi \lambda_r = \int_0^\pi Q \sin r\xi d\xi \quad (15)$$

The A_r thus become determinate functions of the six B 's Also

$$\int_0^\pi \eta^n \sin r\xi d\xi = 0 \quad (16)$$

if n and r both odd or both even, and otherwise

$$\begin{aligned} &= 2 \int_0^\pi \eta^n \sin r\xi d\xi \\ &= \frac{2}{r} \left(\frac{1}{2}\pi\right)^n \left(1 - \frac{n(n-1)}{r^2} \left(\frac{2}{\pi}\right)^2 + \frac{n(n-1)(n-2)(n-3)}{r^4} \left(\frac{2}{\pi}\right)^4 - \dots\right) \quad (17) \end{aligned}$$

Hence

$$\begin{aligned} \frac{1}{2}\pi r \lambda_r &= \{3b^2 B_4 - 3b^4 B_2 + (b^6 - \mu b^2) B_0\} \\ &+ \left(\frac{1}{2}\pi\right)^2 \left\{1 - \frac{2}{r^2} \left(\frac{2}{\pi}\right)^2\right\} \left\{-\frac{3}{2!} b^4 B_4 + (b^6 - \mu b^2) \frac{B_2}{2!}\right\} \\ &+ \left(\frac{1}{2}\pi\right)^4 \left\{1 - \frac{12}{r^2} \left(\frac{2}{\pi}\right)^2 + \frac{24}{r^4} \left(\frac{2}{\pi}\right)^4\right\} (b^6 - \mu b^2) \frac{B_4}{4!}, \quad (18) \end{aligned}$$

when r is odd, and

$$\begin{aligned} \frac{1}{2}\pi r \lambda_r &= \frac{1}{2}\pi \{3b^2 B_0 - 3b^4 B_2 + (b^6 - \mu b^2) B_4\} \\ &+ \left(\frac{1}{2}\pi\right)^3 \left\{1 - \frac{6}{r^2} \left(\frac{2}{\pi}\right)^2\right\} \left\{-\frac{1}{2!} b^4 B_4 + (b^6 - \mu b^2) \frac{B_2}{3!}\right\} \\ &+ \left(\frac{1}{2}\pi\right)^5 \left\{1 - \frac{20}{r^2} \left(\frac{2}{\pi}\right)^2 + \frac{120}{r^4} \left(\frac{2}{\pi}\right)^4\right\} (b^6 - \mu b^2) \frac{B_4}{5!}, \quad (19) \end{aligned}$$

when r is even. From these expressions, together with (9) and (14), we can write down the formal solution of the differential equation. We see, as expected, that when r is great the coefficients in the trigonometric series included in Z decrease like r^{-7} . It also appears from the form of the coefficients that if the boundary conditions are such that the same derivatives of Z are zero at the top and bottom the even and odd B 's enter the solution entirely separately, and the possible solutions break up into two sets, one symmetrical and the other anti-symmetrical about the median plane.

2 *Rayleigh's problem**. In this the boundary conditions were that Z , Z'' , and Z^{iv} vanished at the top and bottom. The trigonometric part

* 'Phil Mag,' vol 32, p 529 (1916)

contributes nothing to any of these derivatives when ξ is 0 or π , and the conditions for the symmetrical solutions are

$$B_0 + \frac{B_2}{2!} \left(\frac{1}{2}\pi\right)^2 + \frac{B_4}{4!} \left(\frac{1}{2}\pi\right)^4 = 0, \quad (1)$$

$$B_2 + \frac{B_4}{2!} \left(\frac{1}{2}\pi\right)^2 = 0, \quad (2)$$

$$B_4 = 0, \quad (3)$$

whence all the B 's, and thence by 1 (18) and (19) all the λ 's are zero. The only possibility of a solution different from zero is therefore that one of the denominators in (14) may vanish, when the solution will reduce to a single trigonometric term. The lowest value of μ is then given by $r = 1$, and we have

$$\mu b^2 = (1 + b^2)^2, \quad (4)$$

which is equivalent to 4 (2) of my previous paper and to equations (42) and (44) of Rayleigh's

3 *Two boundaries where Z , Z'' , and Z''' vanish* — Here 2 (1) and (2) still hold, but (3) is replaced by

$$-\frac{1}{2}\pi B_4 + \sum A_r/r^2 = 0, \quad (1)$$

while

$$B_0 = \frac{5}{16} \left(\frac{1}{2}\pi\right)^4 B_4, \quad B_2 = -\frac{1}{2} \left(\frac{1}{2}\pi\right)^2 B_4. \quad (2)$$

Substituting in 1 (18) and simplifying, we find

$$\frac{1}{4}\pi r \lambda_r = \{3b^2 + 3b^4/r^2 + (b^6 - \mu b^2)/r^4\} B_4, \quad (3)$$

whence

$$A_r = \frac{4r}{\pi} \left(1 - \frac{r^2}{(r^2 + b^2)^2 - \mu b^2}\right) B_4 \quad (4)$$

and our required condition of consistency is

$$-\frac{1}{2}\pi^2 + \sum \frac{1}{r^2} \left(1 - \frac{r^2}{(r^2 + b^2)^2 - \mu b^2}\right) = 0 \quad (5)$$

the summation extending over odd positive values of r . But with this condition

$$\sum 1/r^2 = \frac{1}{6}\pi^2 \quad (6)$$

and we have finally

$$\sum \frac{r^4}{(r^2 + b^2)^2 - \mu b^2} = 0 \quad (7)$$

For a given value of b , the lowest admissible value of μ is evidently larger than in Rayleigh's problem, and will make the first term of (7) negative, but all the

others positive. We can improve the convergence as follows. Restore a and λ , thus obtaining the equation

$$\Sigma \frac{r^4 \pi^4}{(r^2 \pi^2 + a^2)^3} - \lambda a^2 = 0, \quad (8)$$

and use the identity

$$\tanh \frac{1}{2} a = \Sigma \frac{4a}{r^2 \pi^2 + a^2} \quad (9)$$

From the latter we derive the further identity

$$\left(1 + \frac{1}{4} a \frac{d}{da}\right) \left(1 + \frac{1}{2} a \frac{d}{da}\right) \left(\frac{1}{4a} \tanh \frac{1}{2} a\right) = \Sigma \frac{r^4 \pi^4}{(r^2 \pi^2 + a^2)^3} \quad (11)$$

Comparing (8) and (11) we have

$$\lambda a^2 \Sigma \frac{r^4 \pi^4}{(r^2 \pi^2 + a^2)^3 \{(r^2 \pi^2 + a^2)^3 - \lambda a^2\}} = -K, \quad (12)$$

where K denotes the known function on the left of (11). The terms of the series diminish like r^{-8} , and the second is of order 3^{-8} compared with the first. We shall therefore have, very nearly,

$$\frac{\lambda a^2 \pi^4}{(\pi^2 + a^2)^3 \{(\pi^2 + a^2)^3 - \lambda a^2\}} = -K,$$

whence

$$\lambda a^2 = \frac{K(\pi^2 + a^2)^6}{K(\pi^2 + a^2)^3 - \pi^4} = \frac{(\pi^2 + a^2)^3}{1 - \pi^4/(\pi^2 + a^2)^3} K \quad (13)$$

Also

$$64K = \frac{6}{a} \tanh \frac{1}{2} a + 5 \operatorname{sech}^2 \frac{1}{2} a + a \operatorname{sech}^2 \frac{1}{2} a \tanh \frac{1}{2} a \quad (14)$$

Working out the values of λ for a number of values of a , we find

a	2.6	2.8	3.0	3.2
λ	1056	1053	1051	1075

Hence λ has a rather flat minimum in the neighbourhood of $a = 3.0$, and its value is 1051 within at most a few units.

When this problem was treated by the method of finite differences, λ was found to take the values 540, 793 and 928 when the intervals d were $\frac{1}{2}$, $\frac{1}{3}$, $\frac{1}{4}$. Extrapolation to zero on the hypothesis that the error was of the form $Aa^2 + Bd^4$ gave $\lambda = 1140$. But if only $d = \frac{1}{3}$ and $\frac{1}{4}$ are used, extrapolation on the hypothesis that the error varies as d^2 gives $\lambda = 1101$, which is nearer the accurate value.

4 *Two rigid conducting boundaries*—The problem of the previous section was investigated under this title in my former paper, but I overlooked the fact that the full boundary conditions

$$V' = 0, \quad \nabla^2 V' = 0, \quad \frac{\partial}{\partial z} \nabla^2 V' = 0, \quad (1)$$

reduce, when V' is of the form $Z \sin lx \sin my$, to

$$Z = 0, \quad \frac{d^2 Z}{dz^2} = 0, \quad \frac{d^2 Z}{dz^2} - (l^2 + m^2) \frac{dZ}{dz} = 0, \quad (2)$$

and the last of these conditions does not reduce to $Z''' = 0$. If we use the substitutions 1 (2) and (3) it becomes

$$\frac{d^2 Z}{d\zeta^2} - a^2 \frac{dZ}{d\zeta} = 0 \quad (3)$$

and by 1 (6)

$$\frac{d^2 Z}{d\xi^2} - b^2 \frac{dZ}{d\xi} = 0 \quad (4)$$

The solution follows the same lines as in § 3. Equations 3 (2) (3) (4) still hold, but (1) is replaced by

$$-\frac{1}{2}\pi B_1 + b^2 \left\{ \frac{1}{2}\pi B_2 + \left(\frac{1}{2}\pi\right)^2 \frac{B_3}{3} \right\} + \sum_{r=1}^{\infty} \frac{A_r}{r^2} + b^2 \sum_{r=1}^{\infty} \frac{A_r}{r^6} = 0 \quad (5)$$

On substitution for A_r and B_s we find

$$-\frac{1}{2}\pi^2 \left\{ 1 + \frac{1}{3} \left(\frac{1}{2}\pi\right)^2 b^2 \right\} + \sum \frac{1}{r^2} \left(1 + \frac{b^2}{r^2} \right) \left\{ 1 - \frac{r^6}{(r^2 + b^2)^3 - \mu b^2} \right\} = 0 \quad (6)$$

But

$$\sum \frac{1}{r^2} = \frac{1}{2}\pi^2, \quad \sum \frac{1}{r^4} = \frac{1}{6}\pi^4 \quad (7, 8)$$

(only odd values of r arising) and therefore

$$\sum \frac{r^2(r^2 + b^2)}{(r^2 + b^2)^3 - \mu b^2} = 0, \quad (9)$$

which is equivalent to

$$\sum \frac{r^2 \pi^2 (r^2 \pi^2 + a^2)}{(r^2 \pi^2 + a^2)^3 - \lambda a^2} = 0 \quad (10)$$

Now if we write

$$K = \sum \frac{r^2 \pi^2}{(r^2 \pi^2 + a^2)^2} \quad (11)$$

$$= \frac{1}{8} \left(\frac{1}{a} + \frac{d}{da} \right) \tanh \frac{1}{2}a = \frac{1}{8a} \tanh \frac{1}{2}a + \frac{1}{16} \operatorname{sech}^2 \frac{1}{2}a \quad (12)$$

and subtract from (10), we have

$$\frac{\lambda a^2 \pi^2}{(\pi^2 + a^2)^2 \{ \lambda a^2 - (\pi^2 + a^2)^2 \}} = K + \lambda a^2 \sum' \frac{r^2 \pi^2}{(r^2 \pi^2 + a^2)^2 \{ (r^2 \pi^2 + a^2)^2 - \lambda a^2 \}}, \quad (13)$$

where the summation on the right covers the values 3, 5, 7 of r . On account of the high power of r involved these terms are very small for the lowest value of λ that satisfies the equation and we have the approximation

$$\lambda a^3 = (\pi^2 + a^2)^3 \left/ \left\{ 1 - \frac{r^2}{(\pi^2 + a^2)^2 K} \right\} \right., \quad (14)$$

where K is to be found from (12). On proceeding to calculation we find

a	2	3	3.2	3.4	4
λ	2166	1726	1717	1734	1984

By interpolation the least value of λ occurs when $a = 3.17$, and is nearly 1717. We can now obtain a second approximation by substituting in the small terms in (13), and altering (14) accordingly. The new value of λ is 1709.5, the corresponding value of a is hardly changed. Since a is nearly equal to π , the wave-length in a two-dimensional disturbance is nearly $2h$. The cells in a vertical plane, bounded by the solid boundaries and by neighbouring upward and downward currents, are therefore nearly square.

5 *Rigid conducting boundary at base, non-conducting free surface at top* — In the previous paper it was supposed that the conditions of this problem could be realized by taking Z , Z'' , and Z''' zero at $\zeta = 0$, and Z' , Z'' and Z''' zero at $\zeta = 1$. These are not quite correct: the proper conditions are

$$Z = 0, \quad Z'' - a^2 Z = 0, \quad \frac{\partial}{\partial \zeta} (Z'' - a^2 Z) = 0 \quad \text{at } \zeta = 0$$

$$Z' = 0, \quad Z'' - a^2 Z = 0, \quad \frac{\partial^2}{\partial \zeta^2} (Z'' - a^2 Z) = 0 \quad \text{at } \zeta = 1$$

The conditions being dissimilar, the full set of odd and even powers of η is required in the solution, and six constants of integration have to be determined. The former solution is, however, probably not far wrong, and the necessary revision has not yet been undertaken.

6 *Effect of a Current* — A. R. Low* has called attention to the fact that when instability occurs through heating below, but the liquid is already in steady flow, the form of the disturbance generated differs from that when the liquid is originally at rest. In the absence of a current the liquid forms into roughly regular hexagonal or pentagonal cells, rising in the centres and sinking around the edges. A current elongates the cells into strips, the greater dimension being along the stream. The reason for this can be seen easily. When there is no current the factor $\sin kx \sin my$ in the disturbance of the temperature

* 'Nature,' vol 115, pp 299-301 (1925)

affects the differential equation 1 (1) only through the number α , that is, through $l^2 + m^2$. All disturbances with the same value of this quantity should begin to develop at the same time, the ultimate preponderance of the honeycomb structure, with cells as nearly symmetrical as possible, is to be attributed to terms of higher order in the differential equations. The cause making for motion is that an element of fluid hotter than normal tends to rise, and therefore to draw up from the bottom locally a column of warm and light fluid, thus intensifying the differences of pressure over horizontal surfaces. The action is resisted by conduction and viscosity, which tend to spread out the inequalities of temperature and velocity.

When there is a permanent current in the direction of x increasing, on the other hand, the bottom layer of the liquid is at rest, and the remainder is shearing over it. Thus a vertical column of warm fluid is distorted into a curved sloping one, and the possibility of a steady cellular motion disappears. But when the type of disturbance considered is such that the variables u, v, w, V are all independent of x , a shear parallel to x leaves the warm vertical planes unaltered, and the condition for instability is the same as in the absence of a current. To put the matter formally, we notice that in equations (1) to (3) of the previous paper, when a permanent current of velocity U exists, d/dt is equivalent to $\partial/\partial t + U\partial/\partial x$, except in the equation of motion parallel to x , where we have

$$\frac{du}{dt} = \frac{\partial u}{\partial t} + U \frac{\partial u}{\partial x} + w \frac{\partial U}{\partial z} \quad (1)$$

u being now the departure of the x velocity from its mean value U . But if u, v, w, V are independent of x , $\partial/\partial x$ in all cases gives zero. In passing from (6) to (7), again, we formed the divergence of the equations of motion, but in our conditions

$$\frac{\partial}{\partial x} \left(w \frac{\partial U}{\partial z} \right) = 0 \quad (2)$$

so that the terms involving U make no contribution to the further work. The same applies to the boundary conditions. Thus the effect of a steady current is to promote stability for all modes except those with $l = 0$, for these it has no effect. This explains why it causes the convective disturbance to occur in strips instead of in roughly symmetrical cells.

7 Fluid between Two Rotating Cylinders -Prof G I Taylor and Major A R Low have both suggested to me that there should be an analogy between the conditions in a layer of liquid heated below and in a liquid between two coaxial cylinders rotating at different rates. In Taylor's discussion of the latter

problem* the equations of motion are referred to cylindrical co-ordinates r , ϕ , z . The undisturbed velocity is V in the direction of ϕ increasing, where

$$V = Ar + B/r \quad (1)$$

and A and B are constants determined by the rates of rotation of the inner and outer cylinders. Symmetry about the axis is assumed for the disturbed motion.

Taylor takes the components of velocity to be u , $V + v$, w , and assumes

$$u = u_1 \cos \lambda z e^{\sigma t}, \quad (2)$$

$$v = v_1 \cos \lambda z e^{\sigma t}, \quad (3)$$

$$w = w_1 \sin \lambda z e^{\sigma t}, \quad (4)$$

where u_1 , v_1 , and w_1 are functions of r only. The relevant equations reduce to

$$\frac{u_1}{r} + \frac{\partial u_1}{\partial r} + \lambda w_1 = 0, \quad (5)$$

$$v \left(\nabla_1^2 - \frac{1}{r^2} - \lambda^2 - \frac{\sigma}{v} \right) v_1 = 2A u_1, \quad (6)$$

$$\frac{v}{\lambda} \frac{\partial}{\partial r} \left\{ \left(\nabla_1^2 - \lambda^2 - \frac{\sigma}{v} \right) w_1 \right\} = -2 \left(A + \frac{B}{r^2} \right) v_1 - v \left(\nabla_1^2 - \frac{1}{r^2} - \lambda^2 - \frac{\sigma}{v} \right) u_1 \quad (7)$$

Now if we are considering only marginal instability $\sigma = 0$. Also

$$\nabla_1^2 = \frac{\partial^2}{\partial r^2} + \frac{1}{r} \frac{\partial}{\partial r} \quad (8)$$

In all cases fully worked out by Taylor the difference between the radii of the cylinders is a fraction, a quarter to a twentieth, of either radius separately. We can therefore in a first approximation ignore $1/r$ in comparison with $\partial/\partial r$ and reduce the equations to

$$\lambda w_1 + \frac{\partial u_1}{\partial r} = 0, \quad (9)$$

$$2A u_1 = v \left(\frac{\partial^2}{\partial r^2} - \lambda^2 \right) v_1, \quad (10)$$

$$\frac{v}{\lambda} \frac{\partial}{\partial r} \left\{ \left(\frac{\partial^2}{\partial r^2} - \lambda^2 \right) w_1 \right\} = -2 \left(A + \frac{B}{r^2} \right) v_1 - v \left(\frac{\partial^2}{\partial r^2} - \lambda^2 \right) u_1 \quad (11)$$

From (9) and (10) we obtain u_1 and w_1 in terms of v_1 . Substituting in (11) we have on simplification

$$\left(\frac{\partial^2}{\partial r^2} - \lambda^2 \right)^2 v_1 = \frac{4A\lambda^2}{v^2} \left(A + \frac{B}{r^2} \right) v_1 \quad (12)$$

* 'Phil. Trans.' A, vol. 223, p. 280 (1923)

If h be the distance between the inner and outer cylinders we put

$$\lambda h = a, \quad r = h\zeta + \text{const}, \quad (13)$$

and we have

$$\left(\frac{\partial^2}{\partial \zeta^2} - a^2\right)^3 v_1 = \frac{4Aa^2h^4}{\nu^2} \left(A + \frac{B}{r^2}\right) v_1 \quad (14)$$

The components of velocity at the inner and outer boundaries are all prescribed by the motion of the cylinders, and therefore $u_1 = v_1 = w_1 = 0$ there. Hence from (10) $\partial^2 v_1 / \partial r^2 = 0$, and from (9)

$$\frac{\partial}{\partial r} \left(\frac{\partial^2}{\partial r^2} - \lambda^2 \right) v_1 = 0 \quad (15)$$

The conditions are the same as those satisfied by the disturbance of temperature V' in the thermal problem with rigid conducting boundaries at the top and bottom, namely, $V' = 0$, $\nabla^2 V' = 0$, $\frac{\partial}{\partial z} \nabla^2 V' = 0$. But the differential equation (14) is not quite the same. Whereas in the thermal problem the coefficient of V' on the right was a numerical constant $-\lambda a^2$, that of v_1 here involves r . A complete analogy is therefore not to be expected. Nevertheless if $A + B/r^2$ always has the same sign, that is, if the cylinders rotate in the same direction, the comparison indicates that instability should be possible if A and $A + B/r^2$ have opposite signs. This means that rV decreases with r , giving the result that the circulation must decrease outwards for instability. If, on the other hand, $A + B/r^2$ changes sign, A and $A + B/r^2$ have the same sign in an outer region, which is therefore stable, instability arises near the inner cylinder. Thus Taylor's results that the stronger currents occur in the inner region, and that the velocity needed for instability is greater when the cylinders rotate in opposite directions than in the same direction, are in accordance with what we should expect. A general qualitative correspondence therefore exists between the two problems, but quantitative agreement is not to be expected on account of the variability of $A + B/r^2$.

We may recall that Taylor's fundamental equations assume that the disturbed motion has cylindrical symmetry. He does not, however, prove theoretically that the first mode to become unstable will actually be symmetrical, and the question naturally arises why it has this property. A full discussion would have to start from the full equations of viscous motion in cylindrical co-ordinates. But we may notice that

$$\nabla^2 = \frac{1}{r} \frac{\partial}{\partial r} \left(r \frac{\partial}{\partial r} \right) + \frac{1}{r^2} \frac{\partial^2}{\partial \phi^2} + \frac{\partial^2}{\partial z^2}, \quad (16)$$

so that if we neglect $1/r$ in comparison with $\partial/\partial r$ we can take

$$\nabla^2 = \frac{\partial^2}{\partial r^2} + \frac{\partial^2}{r^2 \partial \phi^2} + \frac{\partial^2}{\partial z^2}, \quad (17)$$

which is analogous to the Cartesian form. The correspondence of co-ordinates is

Thermal problem	Taylor's problem
z	r
r	ϕ
y	z

The chief effect of the velocities is to make

$$\frac{d}{dt} \text{ equal to } \frac{\partial}{\partial t} + u \frac{\partial}{\partial r} + \frac{V+v}{r} \frac{\partial}{\partial \phi} + w \frac{\partial}{\partial z},$$

if the quantity operated on is small, this reduces to $\frac{\partial}{\partial t} + \frac{V}{r} \frac{\partial}{\partial \phi}$. The second term corresponds to the extra term $U \partial/\partial x$ in the thermal problem. Taylor's problem is, in fact, not analogous to the thermal problem with the fluid initially at rest, but to that with steady streaming parallel to the axis of x . In the latter, instability first arises for disturbances not involving x , and therefore, by analogy, the first instability in Taylor's problem is for a disturbance independent of ϕ , that is, a symmetrical one.

The analogy could be pushed further if $A + B/r^2$ was nearly constant, with Taylor's notation $\Omega_2/\Omega_1 = \mu$ must be nearly 1. Putting Ω_1 and Ω_2 both equal to Ω we have the condition for marginal instability

$$\frac{4A\lambda^4}{v^2} \Omega = -1709 \quad (18)$$

Taylor's first approximation when μ is nearly 1 is (equations (5.43) and (7.08) of his paper)

$$\frac{2 \Omega_1^2 \lambda^2 R_1^2 (1 - R_2^2 \mu / R_1^2)}{\pi^4 v^2 (R_1 + R_2)} = \frac{1}{0.0571 (1 + \mu)} \quad (19)$$

which is equivalent to

$$\frac{4A\lambda^4}{v^2} \Omega_1 = -\frac{\pi^4}{0.0571} = -1706 \quad (20)$$

This is in good enough agreement with 1709, obtained by the methods of this paper.

A curious result emerges from (14) if the radii of the cylinders are made

very great while h remains the same. The outer radius being R_2 , we take the inner cylinder to be at rest and the outer to have a linear velocity V , so that

$$(R_1 + R_2) hA = R_2 V, \quad (21)$$

while

$$A + B/\mu^2 = Vp/hR_2 \quad (22)$$

where p is the distance from the inner plate. Then the coefficient of $\alpha^2 v_1$ on the right of (14) is

$$\frac{2Vh^4}{h\nu^2} \frac{Vp}{hR_1} = \frac{2V^2 h^2 p}{\nu^2 R_1}, \quad (23)$$

which tends to zero for all values of p when R_1 is made great enough. Thus if the plates are flat the equation (14) takes the same form as for the thermal problem with no gradient of temperature. The system is then thoroughly stable, and we infer that instability cannot arise from the shearing of one flat plate over another.

[*Added January 20, 1928*—This result, like the others of this paper, is to be read in conjunction with the first section of its predecessor, that is, it depends on the postulate that the method of exchange of stabilities is applicable to problems of the types here considered. The postulate is certainly valid for the stability of steady states of holonomic conservative systems, and of many dissipative ones, but it has not been justified universally. The apparent simplicity of the method of the last paragraph, in comparison with the difficult discussions of the stability of steady motion by Orr and others, is therefore somewhat illusory, to prove that the method is valid would probably be as difficult as Orr's work. The justification of the postulate, in fact, lies at present in the general agreement of its results with experiment.]

8 *The Effect of a General Rotation*—Rotation of the solid boundaries about a vertical axis influences the treatment of the consequences of heating a fluid below by introducing terms $-2\omega v$, $+2\omega u$ into the two equations of horizontal motion. It is easy to see that in some cases they will seriously alter the results, since they may be larger than the viscosity terms. In the problem of the burning of porridge, which was used as an illustration in the previous paper, the kinematic viscosity was probably about $1000 \text{ cm}^2/\text{sec}$, and the vertical dimensions a few centimetres. Hence $\nu \partial^2 u / \partial z^2$ was of order $1000u$, while $2\omega u$ is only about $10^{-4}u$, when ω arises from the earth's rotation, and the rotational (or geostrophic) terms are quite unimportant. But in a fluid of depth 10 km with the same rotation the viscosity would have to be about $10^5 \text{ cm}^2/\text{sec}$ to make the viscous terms equal to the rotational ones. Thus rotation may have

an important influence on stability in meteorological phenomena. It is interesting to notice that the critical viscosity is actually comparable with the observed coefficient of eddy-viscosity (though this is only another way of expressing the well-known fact that the effects of surface friction extend up for a kilometre or more)

A qualitative discussion of the effects of rotation appears worth attempting. The tendency to instability in a non-rotating fluid heated below comes, as has been said, from the fact that a local heated mass of fluid tends to rise and draw up a column of new hot fluid from the bottom. Instability occurs when this effect is enough to overcome the tendency of conduction and viscosity to redistribute the temperature and the velocities horizontally. In a rotating fluid, however, we have as a first approximation the equations

$$\rho u = -\frac{1}{2\omega} \frac{\partial p}{\partial y} \quad (1)$$

$$\rho v = \frac{1}{2\omega} \frac{\partial p}{\partial x} \quad (2)$$

whence

$$\frac{\partial}{\partial x}(\rho u) + \frac{\partial}{\partial y}(\rho v) = 0 \quad (3)$$

showing that there is no accumulation of fluid within any vertical column, whatever the pressure distribution may be*. There is no indraught into the heated region, and the cause making for instability has disappeared except for the small amount due to flow across the isobars due to friction at solid boundaries. If the horizontal and vertical scales of the motion remain the same as before, the effects of viscosity and conduction remain much the same. Hence the effect of rotation is to maintain stability.

The vertical scale of the motion is practically fixed by the depth of the fluid, but the horizontal scale may vary. If it becomes so small that the terms like $\frac{\partial^2 u}{\partial x^2} + \frac{\partial^2 u}{\partial y^2}$ become greater than the rotational terms, the theory given for no rotation will again be a useful first approximation, but a much larger gradient of temperature will be needed for instability on account of the increase of α . In air, for instance, with $2\omega = 10^{-4}$ and $\nu = 0.2$, in c.g.s. units, such an approximation would work if the horizontal scale was of the order of 40 cm. But then we shall have

$$a^2 = (l^2 + m^2) h^2 = (h/40 \text{ cm})^2,$$

* This consequence of the geostrophic relation was given by Proudman, 'Roy Soc. Proc.' A, vol. 92, p. 420 (1916), and experimentally verified by G. I. Taylor, 'Proc. Camb. Phil. Soc.', vol. 20, pp. 328-329 (1921), cf. also 'Phil. Mag.', vol. 38, pp. 1-8 (1919).

and if we keep Rayleigh's form as a good enough approximation at the present stage we have nearly

$$\lambda = a^4 \rightarrow (h/40 \text{ cm})^4$$

But with our formula 1 (4) for λ and with values of the constants suitable for air this gives

$$\begin{aligned} -\frac{g\alpha\beta}{\kappa\nu} &= \left(\frac{1}{40}\right)^4 \quad \beta = O(10^{-2} \text{ degrees C/cm}) \\ &= O(1^\circ \text{ C/km}) \end{aligned}$$

The depth of the atmosphere, h , cancels during the work. It appears that even in such a case as this the lapse-rate of temperature does not need to become much greater than the adiabatic to produce instability. The small horizontal dimensions indicated are suggestive of tornadoes, dust devils, and waterspouts but the apparent agreement depends on the initial absence of turbulence from the air before these phenomena develop.

On the other hand, if the air is turbulent and the eddy-conductivity and eddy-viscosity both of order $10^5 \text{ cm}^2/\text{sec}$, rotation is no longer of primary importance, and we shall have roughly

$$\lambda = -\frac{g\alpha\beta h^4}{\kappa\nu} = O(1000),$$

giving

$$\beta = O(10^{-11} \text{ degree C/cm})$$

In presence of rotation, high viscosity and conductivity may actually make instability easier to produce, by preventing the effects of rotation from being dominant. The effect of heating from the bottom an atmosphere originally perfectly stagnant might therefore be to give first disturbances of the nature of tornadoes, but with increasing turbulence these would spread out and give movements on a larger horizontal scale, comparable with the height of the atmosphere, or with tropical cyclones and thunderstorms. Such considerations as these suggest the character of the effect of rotation on the instability though further development will probably require increased knowledge of the factors that determine the amount of the eddy-viscosity

Studies in Adhesion—II.

By SIR WILLIAM HARDY, F.R.S., and MILLICENT NOTTAGE

(Received June 3 1927)

(Report to the Lubrication Research Committee of the Department of Scientific and Industrial Research)

[PLATE 3]

PART I—EXPERIMENTAL.

[In this paper the results of measurements of the tensile strength of a joint between a cylinder and a plate are described. Such measurements are made with difficulty owing to the sensitiveness of the joint to vibrations. It is therefore the more important to state that the values recorded in the following pages are entirely due to my colleague's patience and skill.—W.B.H.]

An admirable summary of previous work on adhesion is given by McBain and Lee* in a paper which breaks new ground, and should be read in conjunction with what follows.

To obtain the measurements a clean metal cylinder was placed upon a clean metal plate in a chamber filled with clean air and warmed above the melting point of the lubricant,† some of which was also placed in the chamber. When the lubricant was melted and the temperature steady, some of the now fluid lubricant was allowed to be drawn under the cylinder by capillary attraction until the space between cylinder and plate was completely filled. Enough lubricant was then added to form a large pool. After a time had elapsed sufficient to permit orientation of the molecules by the attraction fields of the solids to become complete, the lubricant was frozen by allowing the temperature to fall to 18° C. The excess lubricant was then trimmed away from the base of the cylinder, and the plate with the attached cylinder removed from the chamber to a special clamp which could be levelled. A pan was then attached to the end of the cylinder and weights added until the joint broke. This gave the adhesion value B. In other cases the pan was connected with the cylinder as close as possible to the joint and in such a way as to apply the external force tangentially. The tangential pull required to break the joint is the value S.

* 'Roy Soc Proc.,' A, vol 113, p 606 (1927)

† Throughout this series of papers upon friction and adhesion the word "lubricant" has been used to indicate the substance present between the solid faces. It is retained in this study of the tensile strength of a solid joint.

The cylinder had always the same diameter and weight as those used in the previous* paper, namely, 1 cm. and 5.6 grammes, and both cylinder and plate were polished to "optical" surfaces.

If it was desired to vary the load, weights were placed on the top of the cylinder before the fluid lubricant was run underneath.

Up to this stage the procedure exactly resembled that followed in obtaining value A of the last paper—value B and value A refer therefore to mechanically corresponding states.

The temperature fell from 56° to 18° in about 20 minutes, from 84° to 18° in about 40 minutes, and adhesion was measured at any time from 3 to 20 hours after the joint had been made. The effect of errors in the form of the surfaces was tested by comparison between the values taken after prolonged use and immediately after refacing.

The pressure adhesion curve obtained after refacing was more regular and the values for each pressure more concordant, but the difference was not great.

Steel on steel Myristic acid

Pressure varying from 7.1 to 3160 grammes

	Mean values	Mean difference between highest and lowest values for each load
Before repolishing	19120	91 = 0.6 per cent
After repolishing	20260	34 = 0.2 „

The effect of untruthness of the surface was, as might be expected, greater the heavier the load—that is to say, the thinner the layer of lubricant—this appears from the curves fig. 1.

The temperature at which lubrication took place had little or no influence. The following values illustrate this.

Cetyl Alcohol Adhesion (B) in grammes per square centimetre					
Temperature of lubrication	Cylinder	Steel	Copper	Steel	Copper
	Plate	Steel	Steel	Copper	Copper
°					
54		—	—	14550	13480
56		15090	14550	14580	13300
84		15390	14470	14545	12380

* 'Roy Soc. Proc.' A, vol. 112, p. 62 (1926)

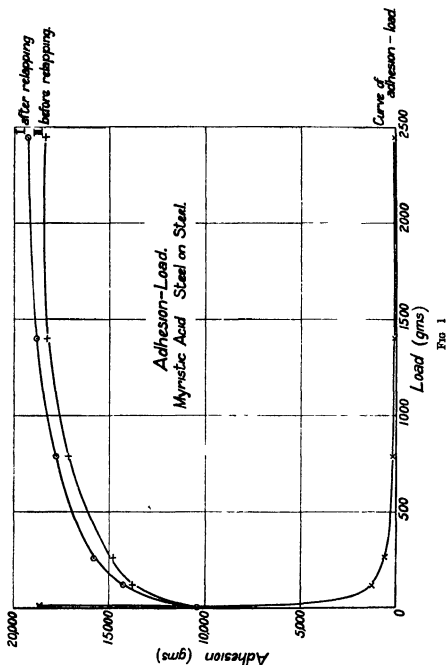


FIG 1

The time occupied in applying the breaking strain varied from 11 to 20 minutes. The variation had no detectable influence on the result.

The latent period is the time taken to reach a steady state. It may be due

either to the cylinder rising or falling in the pool of lubricant to a position of equilibrium, or to the alteration in the structure of the lubricant due to the orientation of the molecules by the attraction of the solids. It has been discussed fully in earlier papers*. In these experiments the age of the *solid* joint had no influence upon adhesion, changes took place only whilst the lubricant was fluid, and the latent period appeared to be due wholly to orientation. This follows from the fact that, though each of the acids gave a latent period of about 60 minutes and the one alcohol available a period of about 30 minutes, the symmetrical paraffins gave no detectable latent period. The following is an example

Palmitic Acid M P, 62°		Temperature of Lubrication, 68°	
Liquid state maintained for—		Adhesion	
		Steel on steel	Copper on steel
minutes			
40		13950	11550
50		14840	13720
60		<u>15880</u>	<u>14980</u>
70		<u>16800</u>	<u>15030</u>

The values underlined are steady values independent of time

Eicosane M P, 36.7°		Temperature of Lubrication, 45°	
Liquid state maintained for—		Steel on steel	
minutes			
5*		<u>8652</u>	
20		8553	
70		<u>8590</u>	

The time value "starred" was the least possible, namely, that taken up by the solidification of the lubricant when the heat was cut off at once

During the latent period the structure of the lubricant is becoming more orderly in the sense that its molecules are moving into positions of equilibrium

* See especially 'Roy Soc Proc,' A, vol 104, p 25 (1923)

with respect to the attraction fields of the solids. Therefore, since adhesion invariably increased when lubricants with polar molecules were maintained in the fluid state long enough to permit the molecules to orient themselves, we may conclude that orderliness as defined above increases adhesion just as it decreases friction.

This conclusion is in conflict with the finding of McBain and Lee (*loc. cit.*), namely, that disorderly structure increases adhesion. The study of the microscopical structure of the plate of lubricant leaves no doubt as to the orderliness of the disposition reached when a critically pure lubricant was allowed to come into equilibrium with the forces acting upon it. All that need be said at this stage is that "order" and "disorder" need careful definition and that no generalisation is yet possible. No exception has been found to the rule that adhesion rises during the latent period when the lubricant is composed of a single pure chemical substance unless this be a paraffin, in which case there is no latent period. When the lubricant is composed of two chemical substances sometimes adhesion falls sometimes rises during the latent period when the structure is becoming more orderly.

Effect of Chance Impurity—On a few occasions the supply of pure air to the chamber failed after the lubricant was in place, but whilst it was still fluid, and on some of these occasions the procedure was carried through in the ordinary way and the adhesion measured. It was always found to be from 60 to 70 per cent. below its value for the pure substance.

The Purity of the Lubricants—Normal paraffins, their related normal acids and one alcohol were tested. In studies of adhesion as in those of friction when the lubricants are critically pure, and the tests made under mechanically corresponding states, orderly results of remarkable simplicity are obtained, the criterion of purity adopted is therefore of great importance in the logical scheme. It was neither more nor less than the attainment of this same orderliness. This may seem to be reasoning in a circle, but the assumption that orderliness is evidence that the number of variables is small and under control is implicit in all tests of chemical purity.

The final stages of purification were carried out by recrystallisation. This was continued until adhesion became constant and the character of the fracture regular.

A few figures are quoted below to illustrate two things: that the adhesion given by impure lubricants was characteristically variable, and that purification raised the value for all the long chain acids used and for the single alcohol, and lowered it for all paraffins. The irregularity in the values is without doubt

related to the irregular character of the surface of break of impure lubricants.

Substance	State	Cylinder Plate	Steel	Copper	Steel	Copper
			Steel	Steel	Copper	Copper
Cetyl alcohol	Impure		14270	12840	12420	11100
	Intermediate state		14510	12600	11800	11730
	Steady values		15860	14540	14540	13380
Lauric acid	Impure		8736	6533	6279	5414
	Intermediate		9563	6606	8085	7977
	Steady values		10660	9872	9924	9096
Palmitic acid	Impure		Figures too erratic to quote			
	Several recrystallisations		8954	—	8013	5740
	Later stages	{	12050	10820	7941	6606
	Steady values		13120	11620	9636	9311
			15860	15030	14960	14190
Eicosane	Impure	{	11610	10740		
			12290	8948		
			8736	7473		
	Nearly pure		8553	7362		

The adhesion of acids and of the alcohol is much greater than that of paraffins, and therefore the effect of impurities is perhaps what might have been expected. The want of concordance in the values obtained at the same stage of purification is owing to the fact that two time values are involved in the changes of state of an impure lubricant, namely, the time occupied by the orientation of the molecules of the lubricant itself, and the time occupied by the positive or negative adsorption of the impurity on to the face of the solids and at interfaces within the layer of lubricant. The layer of lubricant on fracture was always found to be crystalline, and as purification proceeded the crystals became larger. An impurity would condense at the interfaces between crystals, and the small size of the latter was no doubt due to barriers of impurity being set up between centres of crystallisation. The rate of cooling would therefore be likely to have a great influence upon the structure of impure lubricants. The irregularity in the values, the irregularity in the fracture and the small size of the crystals are different aspects of the same phenomenon, namely, the redistribution of two or more components during fluidity and crystallisation.

Structure and Thickness of the Layer of Lubricant—On breaking the joint, a crystalline cake of lubricant was left on either the cylinder or the plate or partly on one and partly on the other. The cake was easily visible to the naked eye

and obviously became thinner as the load was increased As it thinned it showed Newtonian colours

Lubricant, myristic acid

Pressure	Colour	Texture
grammes 71	White	Long narrow plates laid flat and in fan-shaped masses
147	Very faint red	Crystals smaller and narrower
331	Decided red and green	—
1009	Bright blue and yellow	—
1783		
3122		
8756	Uniformly a brownish yellow	Crystals very much smaller and narrower

The character of the break was studied in detail under the microscope When the lubricant was impure the break occurred anywhere and the crystals were small The surface of break therefore was irregular As purification proceeded it became more and more regular until the break occurred, so far as the microscope or the unaided eye could detect, at the interface between solid and lubricant (see Plate 3, figs 2B, 3A) The break actually occurred, however, not at the metal-lubricant interface, but within the lubricant at a distance from the interface so small as to leave behind on the metal a film of totally insensible thickness That the film was there was proved by comparing the friction of the surface of apparently clean steel or copper with that of the clean surface of the plate on which lubricant had not been placed

Cylinder, steel, plate, copper

Lubricant, eicosane

Friction measured with a glass slider

Where the lubricant had been broken away $\mu = 0.176$

Clean part of the same plate $\mu = 0.8$

A plate of chemically pure lubricant which has been frozen *in situ* is therefore composed of a central plate of flat crystals enclosed by two primary layers, one on each of the enclosing solids. Each of these primary layers is possibly one and certainly not more than a few molecules in thickness, and the break under either normal, and, as we shall see later, under tangential stress appears to occur at one or both of the surfaces between the primary film and the plate of crystals

These surfaces mark the limit beyond which the attraction fields of the solids are unable to prevent crystallisation. They do not, of course, mark the limit

to which orientation spreads from the metal face into a *fluid* lubricant. This is fixed by the kinetic energy of the molecules in the fluid state. By X-ray examination Trillat* found stratification and orientation of long chain molecules to persist up to at least $5\ \mu$ from a solid face.

They might mark the limit of the adsorbed layer of an impurity in the lubricant which was more strongly adsorbed by the solids than the latter. The known effect of added impurity, however, does not favour this interpretation (see later).

The position of the surface of break, that is to say, whether it was at one or at both of the surfaces mentioned in the last paragraph but one, was found to depend upon whether cylinder and plate were or were not of the same material.

A diagrammatic section through the layer of lubricant when both solids are the same is given in fig 2. The surface of rupture is *a, b, c, d*. It is shown not

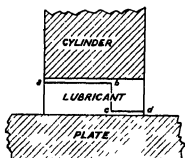


FIG 2

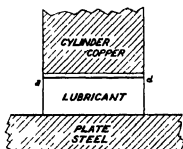


FIG 3

at the interface but at an insensible distance within the lubricant for reasons just given. A break of this kind can be seen in Plate 3, figs 1 and 4.

The process of purification was by its nature asymptotic, and it is legitimate to assume, recollecting the extreme sensitiveness to impurity, that, at the theoretical limit when both solid faces are identical physically and chemically, the lubricant absolutely pure, and the pull perfectly normal, the break would occur simultaneously near both solid faces.

When the solids were different the surface of rupture was near the metal with weaker attraction field, as in fig 3. Plate 3, figs 2 and 3 show that fragments and sometimes a whole crystal were left attached to the copper when the other surface was of steel, but again, at the unattainable limit of experimental precision, it is certain that the surface of break would be close to the copper.

The crystalline structure was apparent in the thinnest films obtained by the

* 'Ann de physique,' vol 10, p 5 (1926)

heaviest loads but, as the load increased, the crystals became smaller (Plate 3, fig 4) The law defining the position of the break stated above held for the thinnest films and for all the lubricants tried Discussion of the significance of this law must be postponed until after the effect of the nature of the solid has been further described

The structure of the plate of lubricant gives objective reality to the conception which has been reached inductively of the presence in colloids of free and bound water, the latter being water so firmly attached to the solute as to be incapable of being frozen * The free and bound portion of the lubricant are sharply divided as the diagrams show, but the freezable portion could not be expected to have the same relations to temperature as the same substance in mass, but would be best described as "capillary" If the solids were moved further apart we should finally have really "free" lubricant between the faces

Effect of Added Impurity—The position of the surface of break could be altered at will by impurity localised at one or other interface To effect this, silk, freed from contaminating substances by prolonged extraction with purest benzene, was lightly rubbed on the contaminant and then lightly rubbed on one or both of the metal faces previously heated to above the melting point of both contaminant and lubricant when the latter was myristic acid (M P 54°), and to a temperature below that of the contaminant and above that of the lubricant when the latter was eicosane (M P 36.7°) The quantity of contaminant conveyed in this way to the surface must have been exceedingly small A pool was then formed of the pure lubricant and adhesion measured in the ordinary way (See Table on p 218)

The figures give the adhesion in grammes per square centimetre

This table merits careful consideration It illuminates vividly the whole subject and has much practical significance The adhesion value of myristic acid is greater than that of eicosane, and of steel greater than that of copper The table shows that an insensible film of contaminant at one interface leads to the following —

- (1) When one surface only is contaminated the break occurs at the contaminated surface when the adhesion of the contaminant is weaker than that of the lubricant, and at the uncontaminated surface when the lubricant is the weaker adhesive

* 'Roy Soc Proc,' A, vol 112, pp 30 and 47 (1926)

Load 5.6 grammes

Lubricant	Cylinder Contaminant Plate	Steel	Copper	Steel	Copper	Position of break
		Steel	Steel	Copper	Copper	
Myristic acid	Eicosane on plate	10360	8845			At plate
	Eicosane on cylinder	10820	7611			At cylinder
	Eicosane on plate			7291	5702	At plate
Eicosane	Myristic acid on plate	9636	8085			At cylinder
	Myristic acid on cylinder	9864	8736			At plate
Myristic acid	Eicosane on both plate and cylinder	9249				At both plate and cylinder
			7578			At the plate
Eicosane	Myristic acid on both plate and cylinder	10540				At both plate and cylinder
			9017			At the cylinder
Myristic acid	None	13260		12440	11680	
Eicosane	None	8644		7416		

- (2) When both surfaces are contaminated the ordinary relation between the position of the break and the adhesion values of the solids is not interfered with
- (3) A weak contaminant lowers the adhesion value and to its own value in one case. A strong contaminant raises the adhesion though the surface of break may not be near the contaminated but near the uncontaminated surface

Therefore, a film of contaminant of the order of one molecule in thickness introduces a surface of weakness *or of strength*, the latter being the more significant theoretically, and imposes its own value on the adhesion of the entire joint, though as relation (2) shows not to the extent of obscuring the characteristic effect of the nature of the solid. The position of the surface of break proves that the contaminant did not diffuse throughout the lubricant.

PART II—STEADY VALUES

The steady value which we call value B is the adhesion per square centimetre. Its relations to the variables are described in this section.

Temperature—A small chamber containing a coil of tubing was built about the clamp and cylinder, and the temperature at which the solid joint was broken controlled by fluid run through the tubing. Manipulation was difficult

and to this may be ascribed the irregularity in the values. In the following table the temperature is that at which the joint was broken.

Load 5.6 grammes, Cylinder and Plate of Steel

Lubricant	Temperature	Adhesion value B
Myristic acid (M.P., 54°)	0	
	4	12970
	8	13190
	18	13280
	38	13710
Palmitic acid (M.P., 62°)	4	15810
	6	15700
	8	15430
	14	15500
	18	15880
	42	15820
	56	15474

Within the limits explored adhesion seems to be independent of temperature. It is remarkable that the value should be the same so near the melting point of the lubricant. This relation proves that the break was uncomplicated by a viscous flow of the lubricant, and the most careful microscopical examination of the lubricant after the joint had been broken failed to reveal any signs of such flow.

The Nature of the Enclosing Solids—Throughout these studies both friction and adhesion have been found to obey what might for convenience be called the mean value rule, which may be stated as follows—

When the enclosing solids are different, being composed of substances M and N, the value of friction or of adhesion is the mean of what it is when both solids are composed of M or both of N. The general equation therefore is

$$X_{MN} = \frac{1}{2}(X_{MM} + X_{NN})$$

As it is important from the theoretical point of view to know whether this equation holds exactly or only as an approximation a series of critical determinations of value B were made with the following results

Load 5 6 grammes, Temperature 18° C

Lubricant	Molecular weight	Steel plate		Copper plate	
		Steel cylinder	Copper cylinder	Steel cylinder	Copper cylinder
Lauroic acid	200	10610 } 10750 } 10690 } 10683	9891 } 9854 } 9872	9981 } 9891 } 9926	9133 } 9061 } 9097
			9899		
Myristic acid	228	13280 } 13340 } 13360	12420 } 12480 } 12450	12420	11550 } 11620 } 11585
			12437		
Palmitic acid	256	15840 } 15990 } 15730 } 15853	15020 } 15050 } 15035	14980	14250 } 14110 } 14180
			15007		
Stearic acid	284	18380 } 18330 } 18480 } 18397	17090 } 17620 } 17655	17580 } 17580 } 17580	16820 } 16710 } 16785
			17617		
Mean values		14546	13753	13727	12917
Mean for steel on steel and copper on copper					13731
Mean for steel on copper and copper on steel ..					13740

The mean value rule seems to hold exactly and the figures for the paraffins confirm this

	Molecular weight	Steel plate			Copper plate		
		Time (mins)	Steel cylinder	Copper cylinder	Time (mins)	Steel cylinder	Copper cylinder
Eicosane $C_{20}H_{42}$	282	10 15	8553 } 8664 } 8608	7362 } 7291 } 7326	10 10	7147	5919 } 5991 } 5955
$C_{21}H_{44}$	310	10 15	9495 } 9387 } 9441	8158 } 8085 } 8121	5 10	8015 } 8121 } 8068	6606 } 6676 } 6641
$C_{22}H_{46}$	422	40 18 9	12810 } 12710 } 12710 } 12743	11370 } 11290 } 11330	10 30	11270 } 11330 } 11300	9819 } 9924 } 9871
Mean values			10284	8882		7489	8876

It was pointed out in an earlier paper on friction that the mean value rule seemed to prove that the influence of the attraction field of each of the enclosing solids extends to the surface of slip. The direct knowledge of the position of the surface of break shows that it extends right through the disc of lubricant.

Consider for example the acids. When both surfaces were of copper the mean adhesion was 12917, and when both were of steel it was 14546. When one surface was of copper and the other of steel the break took place near the copper at a surface removed from the steel by a layer of lubricant at least $4\ \mu$ in thickness. If the influence of the steel had been only of molecular range the adhesion would have been that of copper. Instead it was the mean between that of steel and that of copper.

The effect of contaminants is equally remarkable. When myristic acid was applied to one solid face, both solids being alike and the lubricant being the weaker adhesive eicosane, the break took place in pure eicosane at a surface near the uncontaminated face and removed, say, $3\ \mu$ from the myristic acid. Yet the adhesion was not that of pure eicosane but always something larger than this and between the values for pure eicosane and pure myristic acid.

Molecular Weight—The adhesions in the tables on page 220 are plotted against molecular weight in fig. 4. By an oversight the observed values and not the values per square centimetre were plotted. The relation is linear for

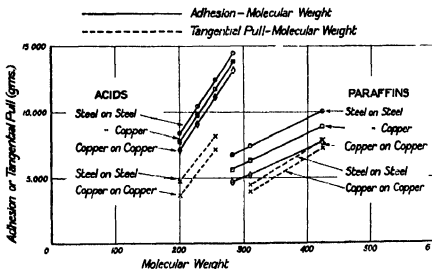


FIG. 4

the acids and paraffins. Owing to the depletion of our stock of pure substances it was not possible to confirm this for the alcohols, but the great body of evidence

accumulated in these papers justifies the statement that for the same chemical series the equation is linear

Pressure —The pressure is the load in grammes divided by the area in square centimetres

Myristic Acid Steel plate and cylinder Temperature 15°			
Load	Pressure	Adhesion	B + Pressure
5 6	7 15	13280 13240 } 13260	1855
115 1	147	18120 18200 } 18160	123 5
259 6	331	20180 20070 } 20130	60 8
792	1008	22740	22 5
1400	1783	24040 23890 } 23965	13 4
2451	3122	24620 24430 } 24525	7 86

The values are plotted in fig 1, curve I Curve II gives the values for the same cylinder and plate but before refacing

The fact that adhesion increases as the layer of lubricant decreases is part of the general experience of mankind and is indeed recorded in the directions how to use any commercial cement, it may therefore be claimed to be a general property of films enclosed by two continuous solids It is not, however, easy to explain, for in the case under consideration the break occurs close to one or other or both faces, and pressure merely varies the thickness of the median plate of crystals

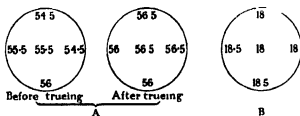
An attempt was made to measure directly the distance between the surfaces of the cylinder and the plate, when the one was resting on the other either loaded or unloaded and with various lubricants For this purpose a spherometer was specially constructed by Messrs Hilger so that the measurements of the distance between the upper surfaces of the cylinder and of the plate could be made in clean air, and the firm also made two pairs of cylinders and plates The first pair, owing to the nature of the steel, were the less perfect Call this pair "A" and the more perfect pair "B"

The first-set of measurements revealed the totally unexpected fact that the distance between cylinder and plate was of the same order when the lubricant

was clean air as it was when some liquid had been allowed to displace the air, indeed, within the limits of accuracy the distance h was found to be independent of the nature of the lubricant whether the pair "A" or the pair "B" was used. This left us with measurements of the variation in value of h , but without the absolute value because we did not know the length of the cylinders.

The Metrology Department of the National Physical Laboratory were good enough to measure these lengths, which they did by wringing the cylinders down on to a plane surface, a standard gauge being used for reference. They discovered on cylinder "A" two minute bosses which were removed before it was measured. They also subjected the spherometer to critical examination and found the screw to be free from periodic error, but to have a total error over the length used of -0.009 mm.

Each value in the following tables is the mean of five measurements taken at different points on the top of the cylinder. To show the variation in these individual readings three diagrams are given. The circle represents the top of the cylinder, and the figures are placed where the measurements were taken and are the readings on the circular scale of the spherometer. Each division of the scale is 2.5μ . The examples were taken at random from the notes.



Save where the contrary is stated once the cylinder was placed on the plate it was not moved until all readings had been taken.

If H be the distance between the upper surfaces of the cylinder and the plate, and L the length of the cylinder, then $H - L$ is equal to h , the distance between the opposed faces. In the following tables h_0 is the value when cylinder and plate were clean and in clean air, and h the value after liquid lubricant had been run in. The procedure was as follows —

H was measured at 18° , the temperature was raised above the melting point of the lubricant, and the melted lubricant then run underneath. The temperature was lowered to 18° , and when it was steady, the lubricant being now solid, H was again measured. In those cases in which the lubricant was fluid at 18° it was simply run underneath and H measured at once.

The first series were made before the cylinders and plates had been sent to

the National Physical Laboratory and therefore before the two bosses had been removed from the lower face of cylinder "A"

	Lubricant	h_0	Lubricant	h	Difference
Series I—Cylinder A (before treatment at the N P L) Steel plate Load 5.6 grammes	Air	mmms		mmms	
		0.0070	Palmitic acid	0.0070	0
		0.0070	Cetyl alcohol	0.0070	0
		0.0070			
		0.0070			
		0.0062			
		0.0065			
		0.0067			
		0.0070			
		0.0067			
		0.0070			
		0.0065			
Mean value		0.0068		0.0070	
Series II—Cylinder A (after treatment at the N P L) Steel plate Load 5.6 grammes	Air	0.0045	Octane	0.0042	Negligible
		0.0038	Caprylic acid	0.0042	Negligible
		0.0037	—	—	
		0.0040	—	—	
		0.0043	Octyl alcohol	0.0040	Negligible
		0.0045	—	—	
		0.0037	—	—	
		0.0040	—	—	
		0.0042	—	—	
		—	—	—	
Mean value		0.0041	—	0.0041	
Series III—Cylinder B (before measurement at N P L) Steel Plate	Air	0.0049	Octyl alcohol	0.0049	0
		0.0044	Caprylic acid	0.0044	0
		0.0039	Octane	0.0036	Negligible
		0.0036	Octyl alcohol	0.0036	0
		0.0049			
		0.0036			
		0.0031			
		0.0041			
		0.0036			
		0.0031			
Mean value		0.0039	—	0.0041	
Series IV—Cylinder B (after measurement at N P L) Steel Plate	Air	0.0041	Octyl alcohol	0.0039	Negligible.
		0.0041	Cetyl alcohol	0.0041	0
		0.0036			
		0.0044	Octane	0.0044	0
		0.0041	Caprylic acid	0.0044	Negligible
		—	—	—	
Mean value		0.0041		0.0042	

If more accurate methods should confirm the figures, the distance h between the cylinder and plate would be the same for a gas as for a liquid and independent of the chemical constitution of the lubricant and of the enclosing solids.

The decrease in the value of h due presumably to the removal of the bosses on cylinder A is remarkable

It was inferred from earlier measurements of friction and adhesion* that when a cylinder or slider was forced down in a pool of lubricant it rose rapidly when the external pressure was removed. This inference was confirmed. The figures give the readings on the circular scale of the spherometer. Each division is equal to 2.5μ .

Cylinder "A" Weight 5.6 grammes.

Lubricant	Unloaded.	After being loaded with 1400 grammes
Air	55.2	55.2
"	55.2	55.2
Octyl Alcohol	55.5	55.5

The load in the case of air was left on for 24 hours. Measurements completed in from 10 to 15 minutes after the load had been removed.

The load (1400 grammes) in the second case was left on for 30 minutes which would allow of only a slight descent in the pool of alcohol.

The effect of a normal pressure upon the value of h was determined as follows. Readings were taken with the clean unloaded cylinder standing on a clean plate in clean air at 18° . The cylinder was then loaded to the required amount and the temperature was then raised to slightly above the melting point of the lubricant. Whilst the load was still on melted lubricant was run underneath and a pool formed in the usual way. The temperature was then lowered to 18° when the lubricant froze. The load was then removed and a second set of readings taken.

In the following table the readings on the circular scale are given, those in the third column being for the unloaded cylinder in air at 18° , and those in the fourth column being for the cylinder at 18° but fixed to the plate by the solid joint which had been formed and frozen under the pressure given in the second column. The difference is the distance the cylinder was forced down by the load and h is this value subtracted from the value of h when the pressure was 7.1 grammes, namely, 0.007 mm.

* 'Roy Soc Proc,' A, vol. 104, p. 27 (1923), *ibid*, A, vol. 112, p. 67 (1926)

Cylinder and Plate "A"

(Readings taken before the bosses were removed)

Lubricant	Pressure	Readings		Difference	h
				mm	μ .
Palmitic acid	331	55.5	56.1	0.0015	5.5
	331	55.4	56.1	0.0017	5.3
	1783	55.3	56.7	0.0035	3.5
	3160	55.2	57.0	0.0045	2.5
	5580	55.3	57.5	0.0035	1.7
	7185	55.2	57.5	0.0057	1.3
	8758	55.4	57.8	0.0060	1.0

In fig 5 h is plotted against the pressure. The curve for adhesion and pressure (fig 1) is of the same form. Both curves tend to become horizontal as pressure increases. When the pressure was 8758 the cake of lubricant was still clearly visible to the naked eye and still showed Newtonian colours.

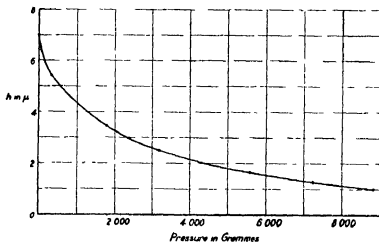


FIG 5

The surfaces of cylinder and plate "B" were of proof plane order of accuracy, and they were used to determine whether the distance h was different for clean and contaminated surfaces. If an adsorbed substance neutralises some fraction of the attraction fields of the metals the Leslie pressure which supports the load should be less for contaminated than for clean faces. The cylinder had to be lifted between the measurements to allow of the application of the film of palmitic acid, but octyl alcohol was applied as vapour, the cylinder being left in position.

Cylinder "B" of Steel

Plate	Clean in clean air	After contamination by—	
Steel	18.3	Palmitic acid	19.2
"	18.5	"	19.2
"	18.7	Octyl alcohol	19.0
"	—	" Grease " adsorbed from air of room	19.7
Glass	18.5	Palmitic acid	19.3
"	18.7	Octyl alcohol	19.2
"	18.7	" Grease " adsorbed from air of room	19.4
Mean	18.6	Difference $0.7 \approx 1.7 \mu$	19.3

Therefore $h_{\text{clean}} - h_{\text{contaminated}} = 1.7 \mu$

These measurements were repeated with cylinder and plate "A" after the former had been trued

	Clean	After contamination by
"A"	56.5	Palmitic acid 57.5
	56.4	Contact with ordinary leather 57.5
"B"	18.4	Palmitic acid 19.6
	18.3	Contact with leather 19.7

Mean difference 1.2

It will be noticed that the differences are all in the same direction, h always being less for contaminated surfaces. When the surfaces were dirty running lubricant under the cylinder produced no detectable change in h .

Surfaces contaminated by contact with ordinary leather—

"A"	57.5	Caprylic acid run under 57.7
"B"	19.7	" " 19.6

Octyl alcohol and palmitic acid were also run under the cylinder when the surfaces of both cylinder and plate were contaminated by contact with the ordinary air of the laboratory and the level was not changed. We therefore seem to have

- (1) h independent of the state or chemical nature of the fluid run underneath whether the surfaces are clean or contaminated, and
- (2) h is less for contaminated surfaces in pure air than for clean surfaces in pure air

The method of measurement was only a rough one but it seems to have established the following facts. The thickness of the air film when the surfaces

were plane and the normal pressure was 7.1 grammes was of the order of 0.004 mm., and this value was not greatly changed by replacing the air by a liquid. The value was, however, decreased when the surfaces were contaminated. A long chain molecule with 20 carbon atoms would be about 2.8×10^{-7} cm in length, therefore 4μ is equal to about 1500 such molecules arranged end to end

PART III—TANGENTIAL PULL.

A few measurements intended merely to determine the relation to molecular weight and the order of magnitude were made of the tangential pull *S* required to break a joint. The external force was applied in the plane of the plate and as low down on the cylinder as was possible

Steel Plate (*S* value in grammes per square centimetres)

Lubricant	Steel cylinder	Copper cylinder
$C_{21}H_{44}$	5743 } 5706 5670 }	5128 } 5055 4963 }
$C_{26}H_{54}$	9965 } 9911 9880 }	9208 } 9235 9244 }
Lauric acid	6030 } 5994 5958 }	4731 } 468 4585 }
Palmitic acid	10400 } 10375 10330 }	9155 } 9063 8990 }

The values in the table are per square centimetre, that is the observed values divided by 0.785. The observed values are plotted against molecular weight in the curve in fig. 4

Under the microscope the fracture was seen to take place at the same surface as it did with a normal force, the surface of break therefore was the same in the two cases. *S* was in each instance much less than *B*. The break away was sudden, the resistance falling apparently instantly to that of simple external friction.

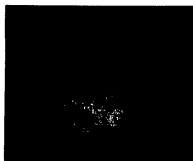
DESCRIPTION OF PLATE 3

FIG. 1.—Lubricant, myristic acid. Cylinder and plate of copper. (a) Cylinder. (b) Plate.

FIG. 2.—Cylinder of copper, plate of steel. (a) Plate. (b) Cylinder.

FIG. 3.—Plate of copper, cylinder of steel. (a) Plate. (b) Cylinder. Load 5.6 grammes (pressure 7.1 grammes) for figs. 1, 2, and 3

FIG. 4.—Cylinder and plate of steel. (a) Plate. (b) Cylinder. Load 259.6 grammes (pressure 331 grammes).



1A



1B



2A



2B



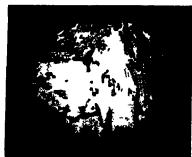
3A



3B



4A



4B

(Facing p. 228)

Summary.

1. The adhesion of and tangential pull required to slide a cylinder attached to a plate by a solid joint are described. The joint was formed by running fluid lubricant between the cylinder and plate and freezing it *in situ*.

2. The disc of lubricant was found to be composed of a plate of crystals with an adsorbed layer on each side.

3. The relation of the value observed to the temperature, pressure, chemical composition of the lubricant and composition of cylinder and plate is discussed.

The Photo-Electric Threshold Frequency and the Thermionic Work Function

By R. H. FOWLER, F.R.S.

(Received January 15, 1928.)

§ 1. Sommerfeld's revived electron theory of metals has already had marked successes, and gives a convincing account of all their equilibrium thermoelectric properties. It is based, of course, on a greatly simplified model of the interior of a metal as a region of uniform potential χ_0/e positive relative to free space, so that the work χ_0 is required to extract an electron from rest in the metal to rest at infinity. The electrons, however, are not all at rest, but form practically a perfect gas—a gas, however, at such a concentration that they are almost tight-packed, and obey the Fermi-Dirac statistics. The theory also yields, as I have shown in a recent note,* the remarkably satisfactory formula for I , the thermionic saturation current at temperature T in amperes per cm^2 ,

$$I = 120(1-r)T^2 e^{-\chi/kT} \quad (1)$$

In this formula r is the fraction of electrons incident on the metal from outside which are reflected at the surface, and χ is the customary thermionic work function. It is related to χ_0 by the formula

$$\chi = \chi_0 - \frac{h^2}{2m} \left(\frac{3\bar{n}}{4\pi g} \right)^{2/3} \quad (2)$$

In formula (2) \bar{n} is the concentration of "free" electrons in the metal—for univalent metals of the order of one per atom—and $g (= 2)$ is the weight of

* Fowler, *supra*, p. 52.

the free electron. The second term in (2) arises from the thermodynamic partial potential of the tight-packed electrons

§ 2 *The Photo-electric Effect*—In a recent very interesting paper† O W Richardson has pointed out that no theory hitherto has been able to explain the existence of a *sharp* photo-electric threshold frequency ν_0 . Admittedly it is not always sharp, but that it ever is so is sufficient to establish the difficulty. He makes suggestions as to the nature of the "free" electrons which provide the requisite sharp threshold. Though these suggestions may be formally correct, they seem to me to be unnecessarily complicated. It follows, as I shall now show, quite generally from the simple theory of Sommerfeld, and independently of any particular assumptions as to the nature of the surface action—

- (i) That there exists a *sharp* photo-electric threshold frequency ν_0 .
- (ii) That the energy corresponding to this threshold frequency is equal to the thermionic work function, that is

$$h\nu_0 = \chi \quad (3)$$

Equation (3) has long been surmised

It follows from Sommerfeld's theory that the electrons are almost tight-packed at temperatures up to 1000–2000° K. At room temperatures therefore the tight-packing may be taken to be absolute, and the \bar{n} electrons in unit volume will be found occupying the \bar{n} smallest energy values, or, if it is preferred, represented by the functions corresponding to the \bar{n} smallest characteristics of Schrodinger's equation for free electrons in the volume containing them.

The characteristics may be enumerated in the usual way‡. If the greatest characteristic required is ϵ^* then

$$\bar{n} = \frac{4\pi g}{3} \left\{ \frac{2m\epsilon^*}{h^2} \right\}^{3/2}, \quad (4)$$

$$\epsilon^* = \frac{h^2}{2m} \left\{ \frac{3\bar{n}}{4\pi g} \right\}^{2/3} \quad (5)$$

Thus it happens that the *maximum* energy of the electrons is equal to the contribution of their partial potential to the work function.

Let us now consider the nature of the photo-electric effect. A quantum of ν -radiation strikes the metal and is absorbed by one of the "free" electrons, of energy ϵ . This is not a possible process for genuine free electrons, but there is nothing to prevent its happening in the metal. However, we are concerned

† O W. Richardson, 'Roy Soc Proc,' A, vol 117, p 719 (1928)

‡ See, for example, in this connection, Dirac, 'Roy Soc Proc,' A, vol. 112, p 661 (1926), Fowler, *ibid*, vol 113, p 432 (1926)

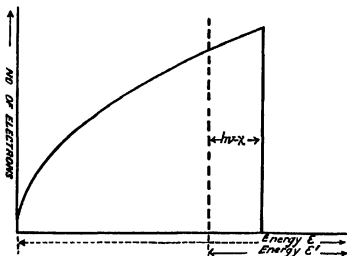
only with the energy account of the process, as long as it is a possible one. The electron has then energy $h\nu + \epsilon$ and can escape from the metal with energy ϵ' , where

$$\epsilon' \leq h\nu + \epsilon - \chi_0 \quad (6)$$

Since $\epsilon < \epsilon^*$, we have $\epsilon' \leq h\nu - (\chi_0 - \epsilon^*)$,

$$= h\nu - \chi \quad (7)$$

This is the relation (3). The sharpness of the edge comes from the almost complete absence of electrons (at these temperatures) with energy greater than ϵ^* , together with the distribution law for the energies of the bound electrons. The number with energies between ϵ and $\epsilon + d\epsilon$, by differentiating (4), can be seen to vary as $\sqrt{\epsilon} d\epsilon$. If electrons of any energy are approximately equally likely to absorb the quantum of ν -radiation, and we ignore energy changes subsequent to absorption, we get a spectrum of emitted electrons with the energy distribution shown in the figure. The fall to zero on the right of $h\nu - \chi$



is actually a violent exponential curve. The sharpness of the observed threshold is amply accounted for.

We have cast this argument into an extreme form, which represents the actual state of affairs more clearly than the exact formula, but a more exact formula for the various numbers of ϵ -electrons at temperature T , and therefore of ϵ' -photo-electrons on the foregoing assumptions, is easily given. It is

$$n(\epsilon') d\epsilon' = 2\pi g \left(\frac{2m}{h^3} \right)^{3/2} \frac{\sqrt{\epsilon} d\epsilon}{1 + e^{(\epsilon' - \epsilon)/kT}} \quad (\epsilon' = \epsilon + h\nu - \chi_0) \quad (8)$$

Since ϵ^* and χ are of the order of 5 volts, ϵ^*/kT is of the order of 200 at room

temperature Thus in the photo-electric current, electrons of energy greater than $h\nu - \chi$ by 1 per cent of χ are infrequent, and greater by 3 per cent 400 times less frequent than the commonest The frequency threshold is equally sharp.

Perhaps I may be permitted to mention in conclusion that Sommerfeld's theory appears to give an equally satisfactory account of the currents extracted from cold metals by intense fields

[*Note added February 9, 1928* — With the help of Nordheim's theory of the reflection coefficient r , it is now possible to take account to a first approximation of this factor, which may be the most important neglected factor concerned in modifying the distribution law $n(\epsilon')$ for the emerging electrons It may be of interest to indicate the nature of the effect Equation (8) puts $n(\epsilon') = n(\epsilon)$ If we still ignore *scattering effects*, that is losses of energy by the future photoelectron in collisions suffered after absorption but before complete escape, we may replace equation (8) by the more exact

$$n(\epsilon') = n(\epsilon) \alpha(\nu, \epsilon) D(\epsilon + h\nu),$$

in which $\alpha(\nu, \epsilon)$ is the fraction of ν -quanta which are picked up by one ϵ -electron, and $D(\epsilon + h\nu)$ is the fraction of $(\epsilon + h\nu)$ electrons which penetrate the boundary field It is unlikely that $\alpha(\nu, \epsilon)$ will vary so fast in the relevant range as to affect the general form of $n(\epsilon')$ Nordheim has calculated $D(\epsilon + h\nu)$ for various simple forms of the boundary potential gradient, and has shown that, for a simple potential step,

$$D(\epsilon + h\nu) \sim 4 \sqrt{\left(\frac{\epsilon + h\nu - \chi_0}{\epsilon + h\nu} \right)} \quad (\epsilon \rightarrow \chi_0 - h\nu)$$

If $\epsilon < \chi_0 - h\nu$ escape is impossible, $D = 0$ The coefficient D should tend to zero in a somewhat similar way for any type of boundary gradient The curve of ϵ' -electrons bounded in the figure by two vertical ordinates will therefore be rounded off on the left into a parabola with a vertical tangent at $\epsilon' = 0$, and on the right into a steep exponential curve To the best of my knowledge this is in excellent qualitative agreement with the observed distribution curves of photoelectrons]

The Polarity of Thunderclouds

By B F J SCHONLAND, M A., Ph D, Senior Lecturer in Physics, University
of Cape Town

(Communicated by C T R Wilson, F R S —Received November 21, 1927)

[PLATES 4 and 5]

§ 1 *Introduction*

In a paper on "The Electric Fields of South African Thunderstorms,"* Mr J Craib and the writer described some observations made at Somerset East during 1926, from which it was concluded that the majority of the storms examined were of positive polarity. The study of these storms has been continued during the present year and a number of fresh points have been examined. In this paper some further evidence as to the polarity of thunderstorms will be discussed.

After the observations had been made, an important paper by Dr G C Simpson† appeared in which the effects to be expected from a cloud of negative polarity, formed according to the breaking-drop theory, were discussed and considered to be in agreement with our 1926 measurements. I hope to be able to show, however, that our original conclusion as to the polarity of the clouds was correct.

§ 2 *Apparatus*

The main equipment of the station has already been described*. In order to obtain more observations of the field-changes due to distant storms, a single horizontal wire aerial was erected. This was 18.0 metres long, 5.0 metres above the ground, and 0.71 mm in diameter, with one end joined to the ball and the other to an ebonite-sulphur insulator attached to a mast, so that the whole arrangement could be quickly dismantled on the approach of a storm. The calculated capacity of the elevated system, including the ball, was 186 cms and a displacement of 1 mm on the photographic records represented a change of 11.3 volts per metre in the potential gradient. With this aerial system the range of observation using the capillary electrometer was extended to storms at a distance of 40 or 50 kms. Some eye observations were made on still more distant storms by joining the aerial to a Wulf quartz fibre electroscope.

* 'Roy Soc. Proc.,' A, vol. 114, p. 229 (1927)

† 'Roy Soc. Proc.,' A, vol. 114, p. 376 (1927)

In order to correlate observations of the appearance of flashes with the field-changes produced by them, the outside observer was provided with a clock synchronised with another inside the hut and used for timing the record. He also had a simple arrangement for determining the azimuth of any special point in the cloud such as the beginning or end of a flash.

§ 3 *Meteorological*

All the storms were moving from west to east with a velocity which ranged from 10 to 40 kms an hour. They could first be seen about 100 kms away to the north-west, some five hours before they came overhead.

Very little rain was discharged by any of them, presumably because they originated in the drought-stricken districts of Aberdeen and Graafreinet. The total rainfall during the months of January and February, 1927, when the observations were made, was 2.02 inches.

The lower surfaces of the clouds were about 2 kms. above the ground and the tops sometimes five times as high. No hail was observed nor did the clouds present the greenish appearance associated with hail.

§ 4 *Tests to Determine the Polarity of a Thundercloud*

Without recapitulating the discussion given in the previous paper of the field-changes and other effects to be expected from thunderclouds at various distances, it is necessary to consider the manner in which these effects may be used as tests to determine the polarity of the cloud. The cloud will be assumed to be of positive polarity, and each effect will be examined to see whether it is peculiar to such a cloud or whether it can also be produced by a cloud of negative polarity, in other words, whether it may serve as a definite criterion of cloud polarity. For the cloud of negative polarity the discussion by Dr Simpson already referred to will be used.

(1) *Field-changes due to Distant Discharges within the Cloud*—A distant cloud of positive polarity may be considered as a positive point charge elevated above a negative one. Except in one special case all discharges within such a cloud should produce negative changes of field, since they involve a downward movement of positive charge. The exception arises when the two poles are not vertically above each other and the lower pole is sufficiently near to the observer for the field due to a positive charge situated at the upper end of the discharge path to be less than that due to the same charge situated at the lower end. An example is afforded by a discharge between a positive pole at a height of 5 kms and a horizontal distance of 20 kms and a negative pole at a height of 3 kms.

and a horizontal distance of 16.8 kms, which would produce a positive change of field

The greater the distance of the storm, the more inclined must the discharge be in order to produce a positive field-change, so that positive field-changes should be rare in the case of discharges within clouds more than 20 kms away

Discharges within a distant cloud of negative polarity, on the other hand, should frequently exhibit positive field-changes due to the neutralisation of the upper negative pole by the lower positive one. It is possible that the lower positive pole may often give rise to negative field-changes by moving downwards as a branched "brush" discharge,* but positive field-changes must necessarily be frequent if the upper negative pole exists

If, therefore, positive changes of field associated with discharges within a distant cloud are found to be rare or absent, the cloud is definitely of positive polarity. If they are found to be frequent, the cloud is equally definitely of negative polarity

(2) *Association of Positive Field-Changes with Discharges to Ground* —Owing to the difficulty of seeing distant discharges within a cloud in daylight, it is not always possible to apply the preceding test. It may, however, still be possible to see flashes between the cloud and the ground, and if it is found that practically every positive change of field is associated with such a flash, this is clear evidence that practically no positive changes are caused by discharges within the cloud, and indicates that the cloud is of positive polarity

A distant cloud of negative polarity, on the other hand, should frequently give rise to positive changes of field which cannot be identified with discharges to ground, because they take place between the poles of the cloud

(3) *Field-Changes due to Discharges taking place to Ground at any Distance* —The sign of the field-change caused by a lightning discharge between cloud and ground at any distance is a definite indication of the sign of the pole which supplies the charge. Since this will generally be the lower pole, observations of this kind might be expected to be of use in determining the polarity of the cloud. Thus a cloud of positive polarity should generally give rise to a positive change of field in such a case, as a result of the disappearance of its lower and negative charge, while a cloud of negative polarity should give rise to a negative change of field

Simpson* has, however, suggested a type of cloud of negative polarity which has a positively charged base in front and a negatively charged base at the rear. With such a cloud, discharges to ground might be expected to produce both

* Simpson, *loc. cit.*

positive and negative field-changes according as the flashes involved the rear or the front of the cloud

(4) *The Reversal of the Sign of the Majority of the Field-Changes with Distance*—In every storm so far examined the flashes in the clouds far outnumber those passing to ground. The ratio of the two types of discharge has been directly determined by outside observation on several occasions and varies from 50/1 to 5/1 with an average value of about 10/1 *

From what has been said it follows that distant storms of positive polarity should exhibit a marked preponderance of sudden negative changes of field due to discharges within the clouds. As the clouds approach, the field-changes due to these discharges will reverse in sign and a marked preponderance of positive changes of field should accompany an overhead storm.

The same type of reversal will, however, be shown by a cloud of negative polarity if the most frequent discharge within the cloud is the downward "brush" discharge of the lower pole already referred to. Thus the reversal effect is not in itself a criterion of cloud polarity †

(5) *The Sign of the Field-Changes from Overhead Storms*—When a cloud of positive polarity comes overhead, the discharges between the poles of the cloud will almost always produce positive changes of field, since they involve a downward movement of positive charge. Discharges between the lower pole and the ground will also give rise to positive field-changes, and negative changes can only be caused by discharges from the upper pole to the ground and by certain exceptional discharges within the cloud which are sufficiently inclined downwards away from the observer. In these cases the field due to a positive charge situated at the upper end of the discharge path must be greater than that due to the same charge when situated at the lower end. An example is the discharge between a positive pole at a height of 6 kms. and a negative pole at a height of 3 kms. which would cause a negative field-change if the horizontal co-ordinates of the two poles were 2 and 5 kms. respectively. Inclined discharges of this type and discharges from the top pole to ground are not likely to occur very often, so that negative changes of field from an overhead storm of positive polarity should be comparatively rare.

On the other hand, in the case of clouds of negative polarity, negative field-changes should be frequent, since they are caused by discharges between the two poles of the cloud as well as from the lower positive pole to the ground.

If, therefore, negative changes of field are found to occur but seldom while a

* 541 flashes in the clouds and 50 flashes to ground.

† Simpson, loc. cit.

storm is overhead, there can be little doubt that the cloud is of positive polarity

(6) *The Steady Fields due to Near and Distant Storms*—The steady field of a thundercloud has been defined* as the field produced just before the passage of a lightning discharge between the poles, when the cloud charges have reached their maximum values. Unless these charges are very different, the steady fields due to near and distant storms should be of the same sign as the charge on the lower and upper poles respectively.

In view of the stipulation as to the relative strengths of the cloud-poles and the difficulty of dissociating the steady field of a distant storm from that due to other charged clouds, this effect does not offer a certain test of the polarity of a thundercloud except in one particular case. This is when the steady field is definitely observed to reverse in sign on approaching the station. For no arrangement of the strengths or positions of the charges in a cloud of negative polarity will enable it to produce both a positive steady field at a distance and a negative steady field when overhead.

Of the effects discussed in this section, numbers (1), (2) and (5) offer a definite decision as to the polarity of the cloud and numbers (3) and (6) promise useful information bearing upon the question. Number (4), while not offering a criterion of cloud polarity, is of considerable interest in other ways.

Numbers (1), (2) and (3) call for the correlation of the field-changes with the appearances of the discharges producing them, and this, besides requiring the special attention of a trained observer, cannot always be carried out in day-time, when the majority of the storms occur, owing to the difficulty of seeing the discharges. Numbers (5) and (6) can only be examined in the case of storms which pass overhead. For these reasons it has not proved possible to apply these tests to every thunderstorm within the range of the station, but only to those for which conditions of visibility or distance were favourable.

§ 5 *Correlation of the Sudden Field-Changes with the Appearance of the Flashes*

In this section an account is given of observations made both in 1926 and 1927 in connection with effects (1), (2) and (3) just discussed.

(1) *Distant Discharges within the Cloud*—The results obtained from a correlation of distant flashes in the cloud with the sign of the corresponding sudden changes of field are shown in the following table, which refers to storms at a

* Schonland and Crab, *loc. cit.*, p. 232.

distance of more than 15 kms. The figures represent the number of field-changes of a particular sign accompanying discharges within the cloud

Table I

Storm	Distance	Field-changes		Remarks
		Positive	Negative	
	kms			
9 } 1926	20	0	118	At night
17 }	20	1	39	
19 }	>50	0	9	At night
20 }	50	(2)*	7	At night *Horizontal
31 }	15	1	5	At night
32 }				
33 }	40	2	222	At night Three storms
34 }				
44 }	30	0	28	
47 }	30	0	64	Two storms
48 }				
50 }	25	0	25	At night
Total		6	517	

The total for the two years shown in the table is 517 negative and 6 positive sudden field-changes associated with discharges taking place within the cloud. This is decisive evidence that most of these twelve storms were of positive polarity. Two more storms, Nos 12 and 15, were examined for this effect in 1926 and gave 77 negative and 4 positive field-changes between them, but they have not been included in the table as they were each at a distance of only 10 kms and inclined discharges easily produce positive field-changes from a cloud of positive polarity at this distance. Storm No 13 of 1926 was previously included in error.*

Storm 20 shows an interesting case of two positive changes associated with flashes in the cloud. Conditions for outside observation were good and sketches of the flashes showed that these two positive field-changes were due to the only two horizontal discharges observed, the other discharges passing downwards and producing negative changes of field. These two flashes thus illustrate the discussion of inclined discharges given in § 4 (1).

An examination of the details of the table shows that in the case of nine of the storms the absence or rarity of positive field-changes definitely indicates that their polarity was positive, and that while the observations upon the remaining three (19, 20 and 31) are insufficient for a definite decision, they are

* The observer's report reads "Flashes in clouds were upwards."

in favour of positive polarity. No evidence has been found of the frequent positive field-changes which must accompany discharges within a cloud of negative polarity at a distance.

(2) *Positive Field-Changes from Distant Storms*—The following table shows the number of positive field-changes found to be due to distant flashes in the clouds and to ground respectively on those occasions on which a test could be made. The storms were all at a distance of more than 15 kms.

Table II

Storm	Distance	Positive field changes		Remarks
		Discharge in cloud	Discharge to ground	
17 (1926)	kms	1	0	* Horizontal
9 (1926)	20	0	12	
20	50	(2)*	0	
27	30	0	1	
31	15	1	2	
32, 33, 34	40	2	20	
44	30	0	1	
47, 48	30	0	5	
49, 50	25	0	7	
Total		6	48	

This table shows that out of 54 positive changes of field due to distant storms, 6 have been found to be associated with discharges taking place within the cloud, and two of these were caused by horizontal discharges. These observations therefore agree with those just considered in showing that positive field-changes due to flashes in the cloud are rare. 13 storms have been examined, and out of 523 flashes within the clouds only 6 produced positive changes of field, two of which at least are easily accounted for, 48 more positive changes were due to discharges between the clouds and the ground.

(3) *The Field-Changes due to Flashes to Ground at any Distance*—The following table shows the numbers of positive and negative field-changes found to be associated with flashes between the cloud and the ground taking place at all distances from the station —

Table III

Storm	Field-changes		Remarks
	Positive	Negative	
2 (1926)	8	1	* From top pole
9 (1928)	12	0	
20	0	(2)*	
25	4	0	
27	1	0	
29 and 30	5	0	
21	2	0	
32, 33, 34	20	2	
38	2	0	
44	1	(1)†	
47, 48	5	(1)‡	† Second part of double flash. ‡ Second part of double flash
49, 50	7	1	
Total	67	4	

Four negative changes have been excluded from the totals, two of these formed the second portions of double flashes and may have come from the top of the cloud, the other two were definitely observed to proceed from the top of the cloud, the flashes having downward forks within the cloud and starting from the highest active portion

These particular cases are instructive in considering the remainder of the observations, for the great majority of these field-changes must be due to discharges between the base of the cloud and the ground. The large preponderance of positive field-changes, which were found in 67 out of 71 such observations, indicate that a flash of this kind almost always involves the negatively charged portion of the cloud and therefore that the part of the cloud base active in producing flashes to ground is negative

While this conclusion offers strong support for the view that the clouds examined were of positive polarity, it has already been said (§ 4 (2)) that it is not a definite criterion of cloud polarity. The results will be referred to again when the observations on the steady fields immediately below thunderclouds have been examined

§ One further point must be emphasised in connection with the observations given above, it will be found in the next section that of the field-changes due to the distant storms examined in 1927, 188 were positive and 1931 negative. The observations of Table II show that 48 of the former were found to be due to discharges to ground, and this number represents 89 per cent of the test

observations which could be made. It is therefore reasonable to suppose that only about 19 of the 188 positive changes were due to flashes within the cloud and incorrect to say that 188 — 48, or 140, can be ascribed to such discharges. I mention this point because our 1926 observations have been interpreted in the latter manner by Sumpson*.

§ 6 *Further Observations upon the Sign of the Sudden Field Changes caused by Lightning Discharges*

The sign of the sudden changes of field produced by lightning discharges at various distances is of interest in connection with the general electrical mechanism of the thundercloud apart from the question of polarity. The work done in 1926 on this subject showed the importance of an accurate knowledge of the distances of the discharges, and special attention was paid to this point in 1927.

For reasons which will appear later, the storms have been divided into three classes, "distant" when more than 15 kms away, "intermediate" when between 15 and 7 kms off, and "near" when within 7 kms.

The results obtained from 19 distant storms in 1927 are shown in Table IV, the arrangement of which is similar to that employed in the previous paper except for the second column, which shows the nature of the observing arrangement. The letters A-E refer to observations made with the aerial system and the Wulf electroscope, A-C to those with the aerial and the capillary electrometer, and B to those with the ball and the capillary electrometer.

The table shows a marked preponderance of negative over positive sudden changes of field, the ratio being 10.3 to 1 (1931/188) and the preponderance holds for every one of the 29 storms. The results are in general agreement with those obtained in 1926, which gave 444 negative and 62 positive changes and so a ratio of 7.2 to 1†. The totals for the two years are 2375 negative and 250 positive changes of field due to distant lightning discharges.

As the 1926 observations were all obtained with the aid of the ball, it is of interest to analyse the figures in the table according to the method of observation employed. The aerial and electroscope were employed to examine storms at an average distance of 50 kms and the value of the numbers of negative and positive field-changes observed in this way was 17.9 to 1 (449/25), the aerial and capillary electrometer were employed on storms at an average distance of 30 kms and gave a ratio of 9.8 to 1 (1299/133), the ball and the electrometer were used for storms at an average distance of about 17 kms and gave a

* *Loc. cit.*, p. 394.

† For distances greater than 14 kms.

Table IV

Storm	Inst	Distance	Sudden field-changes						Remarks
			Visual		Photographic		Combined		
			Pos	Neg	Pos	Neg	Pos	Neg	
		kms							
19	A I	> 50	0	9			0	9	
20	A C	> 40	2	9			2	9	
21	B	20	1	6			1	6	
22	A F	70	2	29			2	29	
23	A F	60	8	189					
24	A C	10	5	26			13	215	
24, 25	A C	20-10	5	29	7	82	12	111	
25	B	15	2	8					
25	A C	20	5	48			7	56	
26	A C	25	6	62			6	62	
27	A F	> 30	0	16					
27	A C	> 20	2	33	1	15	15	204	
28	A C	30	12	63			12	63	
31	B	15			1	18	4	18	
32, 33, 34	A C	> 30	22	224			22	224	
35, 36	A C	> 30	4	90			4	90	
37	B	19	2	8	7	57	9	65	Field = 190 v/m
39	A F	> 10	1	6			1	6	
40, 41	A F	10	9	101					
40, 41	A C	40	3	45			12	140	
41	A C	30	2	22	1	71			
41	B	20	0	16	11	45	16	154	Approaching F +ve increasing
41, 42	A F	> 30	4	68			4	68	
44	A F	40	1	31					
44	A C	30	1	9	1	28	3	68	Approaching F +ve increasing
44, 45	A C	50	0	7	6	25	6	32	
46	A C	35	8	57			8	57	
47	A C	20			0	8			
47	B	20	3	14	0	11	3	33	Approaching F +ve increasing F = + 140 v/m
47, 48	A C	30	2	22	1	56	3	78	Approaching F +ve increasing
48	A C	25	5	17	0	2	5	19	
49, 50	A C	25	2	8	15	91	17	99	Field = - 50 v/m.
51	A C	> 30	1	10			1	10	
			120	1282	68	649	188	1931	

ratio of 6 1 to 1 (183/30). The ball observations are hardly sufficiently numerous to warrant any serious attention being paid to the increase of the ratio from 6 1/1 to 9 8/1 between 17 and 30 kms, but the further rise in this ratio to 17 9/1 when the distance is increased to 50 kms needs explanation. It may only be due to the fact that the positive changes of field from very distant storms were generally very small in comparison with the negative ones and liable to be missed in the eye observations with the electroscope. For this

reason it seems advisable to discard the observations on the electroscope and to take the value of the ratio for 1927 as 9.1 to 1 (1482/163)

The following table contains the results of an examination of the field-changes due to storms at intermediate distances, some or all of whose flashes took place within from 7 to 15 kms of the station, as judged by the lightning-thunder interval either marked upon the records or observed outside the hut

Table V

Storm	Distance	Field	Sudden field changes					
			Visual		Photographic		Combined	
			Pos	Neg	Pos	Neg	Pos	Neg
	kms	v/m						
25	11	-4000		—	30	18	30	18
25	9-15	—	4	17	—	—	4	17
29	7-10	40	—	—	1	7	1	7
30	15-7	-250		—	7	18	7	18
38	15-6	-1100	3	12	—	—	3	12
41	12-9	-300	—	—	7	3	7	3
36	4-10	-8000	—	—	9	8	9	8
							61	83

Although the observations are not very numerous, the totals in this table show no marked preponderance of field-changes of one particular sign. Those storms at the outer limit of the intermediate region show more negative than positive changes and those at the inner limit more positive than negative ones. That the negative field-changes found in the case of the distant storms are changing in sign within this region is clearly shown by the observations on near storms shown in the next table.

This table contains the observation on storms most of whose flashes occurred within a distance of 7 kms as judged by the lightning-thunder interval, although it was not possible, for obvious reasons, to determine this interval in the case of every flash.

It will be seen that these near storms show a very considerable preponderance of sudden positive changes of field, the ratio of the total numbers of positive and negative changes observed being 21/1.

The preponderance of negative field-changes at a distance and of positive ones when near is a definite indication that the most frequent process in every storm examined is a discharge of positive electricity downwards, and the reversal

Table VI

Storm	Distance	Field	Sudden field changes					
			Visual		Photographic		Combined	
			Pos	Neg	Pos	Neg	Pos	Neg
	kms	v/m						
25	3~7	-7000~-5000	25	1	22	2	47	3
30	3~7	-11,000~-8000	30	0	34	2	64	2
34	3~5	-8000	3	0	—	—	3	0
36	2~7	-16,000~-5000	19	0	53	1	72	4
43	7	-16,500~-10,000	1	0	—	—	1	0
41	3~7	-8000	1	0	—	—	1	0
		Total	79	1	109	8	188	9

effect shows that such discharges do not extend to the ground. It has been found necessary to replace the concept of a reversal distance, at which the field-changes due to these discharges pass through zero, by that of an intermediate reversal region, because the two ends of the discharge are not often in the same vertical line and inclined discharges introduce complications.

Take, for example, the field-change due to a discharge of positive electricity from a height of 6 to one of 3 kms. If the discharge path is vertical, this field-change will be zero at a distance of 6.8 kms from the nearest end of the flash. Consequently 6.8 kms is the reversal distance for an ideal cloud of this type, and discharges at greater and smaller distances would be expected to produce negative and positive field-changes respectively. If, however, the upper and lower ends of the discharge had horizontal co-ordinates 11 and 8 kms respectively, the field-change would be found to be positive, though the distance of the flash would be determined as 8.5 kms. Again, if their horizontal co-ordinates were 2 and 5 kms respectively, the field-change would be negative, although the distance would be determined as 5.8 kms.

The effect of these departures from the ideal vertical discharge is to replace the reversal distance, at which the field-changes abruptly change in sign, by an intermediate region in which field-changes of either sign are equally probable. Evidence of this region is afforded by Table V and it probably extends from 7 to 12 kms from the station, though occasional exceptional discharges may occur at any distance.

To decide whether this frequent downward discharge of positive electricity takes place between the poles of a cloud of positive polarity or whether it is

merely a downward movement of the lower pole of a cloud of negative polarity, the discussion given in § 4 (5) may be applied to the results of Table VI. This table shows that when the cloud is overhead, negative field-changes are comparatively rare, occurring only once in every 22 discharges. The observations therefore speak against the view that the clouds examined were of negative polarity, for they imply that upward discharges of positive electricity taking place between the poles of such a cloud are rare. They are in accord with the view that the clouds were of positive polarity, the few negative changes being due to discharges of a special type.

The observations of near storms in 1926 have not been considered here because it is probable that some of the field-changes were due to flashes at a distance of more than 7 kms.

§ 7 *The Steady Fields due to Thunderclouds*

Distant Storms—Few direct observations of the steady fields due to distant storms were made in 1927, because the aerial system was largely used in place of the ball. It was, however, found that approaching storms when studied in this way usually caused a steady movement of the mercury meniscus in such a direction as to indicate an increasing positive field. A good example is afforded by fig. 3. The effect was observed in the case of four storms when no rain was falling and no local clouds were present.

Direct measurements were made by lowering the ball in the case of three distant storms, and these, together with the effects found with the aerial, are shown in the last column of Table IV. Two were positive and greater than the fine weather field of about 50 v/m, while the third (storm 50) was negative. There is other evidence that the polarity of this storm was positive (Tables I and II), and it is described in the next section.

These results support those of 1926 in associating positive fields with distant storms.

Intermediate Storms—Measurements of the steady fields due to 6 storms at distances between 7 and 15 kms from the station are shown in the third column of Table V. In only one case was the storm at what seems to have been a reversal point for its steady field, in the other cases the field within the intermediate region was negative, and smaller if the cloud was approaching than if it was receding.

Near Storms—On approaching still nearer, the small negative field rapidly increased and, as in 1926, the passage of an active storm overhead invariably produced a strong and persistent negative field below it. To the 11 near storms,

whose fields have been given in Table VI, and in Table IV of the previous paper, two others must be added whose fields were determined although records of the field-changes were a failure. These were storms 4 and 38, which gave fields of -7000 and $-12,500$ v/m respectively. Thus 13 active storms have so far been observed to pass close to the station, all of which produced persistent negative fields below them. The maximum field observed was $-16,500$ v/m, in 1927.

Strong positive fields were only observed on two occasions under active storms and only for a few minutes in each case. On two other occasions they were produced for a longer time by mammatiform cloud-residues which did not discharge, but in no case were these fields greater than 6000 v/m. The most careful watch was kept for positive fields. During 1927 negative fields exceeding -5000 v/m were observed for 300 minutes, and positive fields exceeding $+5000$ v/m for 5 minutes, when the storm-centre was within 7 kms. The corresponding figures for inactive cloud residues were 53 and 37 minutes respectively.

While it is perfectly true that "the sign of the field at a single observing point is no criterion even of the polarity of the cloud,"* it is permissible to say that the almost complete absence of positive fields below active thunderclouds is not only in accord with the view that the lower pole is negative, but difficult to reconcile with the opposite view. The persistent negative fields below these clouds must be compared with the fact (§ 5 (3)) that practically every discharge between the base of the cloud and the ground which has been examined has carried a negative charge to the earth.

Positive steady fields have now been found to be associated with 10 out of 11 distant storms examined and negative steady fields with all the 13 storms which passed near to the station. In the case of storms 10, 12 and 41, an actual reversal of the steady field has been observed, showing definitely that these storms were of positive polarity.

§ 8 *Discussion of Results*

Simpson has concluded that our 1926 results can be regarded as supporting his discussion of the nature of a cloud of negative polarity formed according to the breaking-drop theory. It has, however, been pointed out that one step in his interpretation of the observations is not justified, for it has now been established that practically every distant discharge responsible for a positive change of field takes place between the cloud and the earth.

* Simpson, *loc. cit.*, p. 391.

In this connection Simpson has stated* that "If a thundercloud is of positive polarity and it is observed that all the discharges are within the cloud, these discharges can only produce negative field-changes at a distant point. If in such circumstances both positive and negative field-changes are observed, this is clear proof that the polarity of the cloud is not positive." I have shown (§ 4 (1)) that inclined discharges within the cloud can sometimes give rise to exceptions to the above statement. The true criterion of positive polarity is the rarity, not the absence, of positive field-changes due to distant discharges within the cloud.

The observations discussed in this paper may be summed up as follows:

(a) No evidence has been obtained that discharges within a thundercloud, near or distant, ever involve an upward movement of positive charge such as must frequently occur within a cloud of negative polarity. On the contrary, the results indicate that these discharges are invariably downwards, as would be the case if they took place between the poles of a cloud of positive polarity.

(b) Confirmation of the view that these clouds were of positive polarity has been obtained in other ways, the charge carried away by a flash between the base of the cloud and the earth was practically always found to be negative, the strong fields below active clouds were invariably and persistently negative, and the fields due to distant clouds practically always positive, when they could be measured.

Finally, it may be pointed out that since outside observations show that about 1 in every 10 lightning flashes proceeds from the cloud to the ground and since tests have shown that practically every such flash produces a positive change of field, we should expect that about 263 of the 2625 distant flashes described in § 6 should have been discharges between the cloud and the ground and should have produced positive changes of field. The actual number of positive field-changes observed was 250, so that, even allowing for the roughness of the estimate of the relative frequencies of the two kinds of flashes, only a very small percentage of flashes within the clouds could have given rise to positive changes. Such a conclusion implies an absence of upward discharges of positive electricity, and this in its turn means that the negative pole of the cloud was below and not above the positive pole.

§ 9 *Photographic Records*

In this section some photographic records will be described to illustrate the points which have been raised.

* *Loc. cit.*, p. 400

Distant Storms Fig 1 Storms 24 and 25 24/1/27 13 h 39 m to 13 h 47 m. This record shows the field-changes (50 negative and 1 positive) due to two storms at a distance of about 40 kms. It was obtained with the aerial

Fig 2 Storms 24 and 25 Aerial, 14 h 25 m to 14 h 31 m. The two storms of fig 1 have here approached to within a distance of about 30 kms and the record shows 22 negative and 3 positive field-changes

Fig 3 Storms 47 and 48 22/2/27 Aerial, 15 h 21½ m to 15 h 34 m. Two storms were in action, one of which was approaching the station. The record shows a rapidly increasing positive field which caused one mercury meniscus to move out of the field of view and the other to enter it. This positive field was destroyed by a lightning flash at 32½ m which took place within the cloud at a distance of 12.6 kms. This flash caused a field-change of at least 540 v/m, for it displaced the original meniscus below the limits of the record. Seven other flashes have thunder-marks which give their distances as from 23 to 27 kms.

At 28 m the outside observer noted the only flashes to ground during the record and sketched two discharges to earth travelling along different paths. These are represented in the record as a positive field-change followed after 1.1 seconds by a negative one. The remaining 56 negative field-changes occurred within the cloud.

Fig 4 Storm 27 31/1/27 Aerial, 13 h 7.3 m to 13 h 17.3 m. The record shows 39 negative and 2 positive field-changes and the flashes were at distances ranging from 17 to 31 kms. A continuous watch was not kept but the positive field-change at 16.8 m, identified by the shutter-mark immediately following it, was due to a flash to ground from the foremost portion of the base of the cloud. The flashes in the cloud could not be seen owing to daylight.

Fig 5 Storms 49 and 50 22/2/27 Aerial, 19 h 6½ m to 19 h 18 m. Two storms were in progress, the nearer at a distance of 27 kms. The record shows 66 negative and 12 positive sudden field-changes, all except one of the latter being very large. The maximum positive and negative changes were + 170 v/m and - 90 v/m respectively.

No flashes were observed between the clouds and the ground until 9½ m, when the first discharge of this kind occurred and was followed by others at 11½, 13, 14, 15 and 17 m,* accounting for 6 out of the 11 large positive changes. It is quite likely that the remaining 5 were of similar origin, for it was not possible to keep a continuous watch on both clouds. No note was kept of the frequent discharges in the clouds.

* These times are approximate.

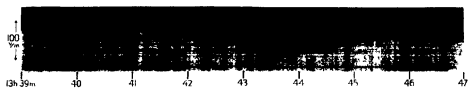


FIG 1

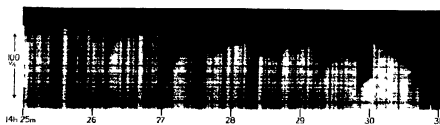


FIG 2

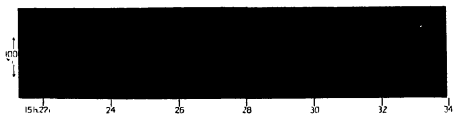


FIG 3



FIG 4



FIG 5

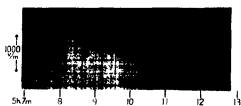


FIG 6

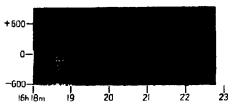


FIG 7

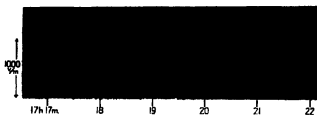


FIG 8

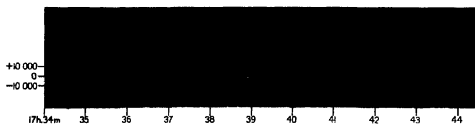


FIG 9

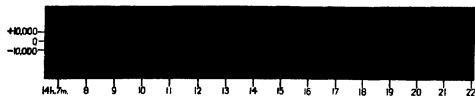


FIG 10

The only three positive changes of field on a record immediately following fig. 5 were definitely due to discharges to ground. One other flash to ground gave a negative field-change, and the remaining 24 negative changes were due to discharges within the cloud. This record, which is not suitable for reproduction, shows also that at 19 h 27½ m the steady field due to the cloud was -50 v/m.

The discharges to ground were of unusual length, determined as 3.5 to 4.0 kms from the angular elevation of the point from which they appeared to start. The rounded top of the cloud was illuminated at intervals and had an elevation of 18.5° , so that it was at a height of 9 kms if at the same horizontal distance as the active portion. The top of the active part of the cloud did not extend to a height of more than 5 kms.

Intermediate Storms—Fig. 6 Storm 25 24/1/27 15 h 7 m to 15 h 12.8 m, about 1½ hours after fig. 1.

This is a portion of a record taken on the ball, which had to be lowered to a height of 1 metre above the ground, owing to the negative field of -4000 v/m prevailing. The following outside observations were made: 7½ m flash in cloud. 8.0 m double flash to ground at 10.4 kms. 8½ m flash in cloud storm getting nearer. 9½ m flash to ground at 5 kms. 10½ m flash in cloud. 12 m flash in cloud at 5 kms. The storm now came overhead and gave a strong negative field of -5000 to $-10,000$ v/m accompanied by heavy rain which conveyed a positive charge to the test-plate. The record shows 22 positive and 16 negative field-changes.

Fig. 7 Storm 41 16/2/27 16 h 18 m to 16 h 23 m. This record was taken on the ball at the usual height. The storm moved over the station at about 30 kms per hour. When distant it gave 7 negative and 3 positive field-changes. During this record it approached from 11.3 kms (flash at 18.8 m) to less than 7 kms (at 20.8 m) and at 26½ m a flash to ground took place at a distance of 2.8 kms. The field, which was -530 v/m at 21.8 m, increased to -6000 v/m as the storm came overhead. The field-changes at 20.8 m and 21.4 m were double, $+680$ and $+1080$ followed by -360 and -760 v/m respectively at intervals of about 0.5 second. The record shows 7 positive and 3 negative field-changes.

Fig. 8 Storm 30 31/1/27. This record was taken on the ball during the approach of the storm and shows 18 negative and 7 positive sudden field-changes. Flashes to ground occurred at 18.4 and 20.4 m which the record shows to have produced positive changes of field.

The ball was lowered to measure the field at 17.3, 19.6 and 21.4 m.

Initially -109 v/m, the field rose to -420 v/m as the storm approached, and later became so strong as to drive the meniscus out of the field of view. At 32 m, after the close of the record, it had reached $-10,000$ v/m, and the next record, which is shown in fig 9, was obtained.

A record made at 17 h 10 m, when the storm was at a distance of 11 kms, showed that the steady field was then $+40$ v/m.

Near Storms—Fig 9 Storm 30 Test-plate, 17 h 34 m to 17 h 44½ m. The distances of 9 of the flashes have been determined from the thunder-marks following the field-changes and lie between 3.0 and 6.4 kms. The test-plate was uncovered at 34½ m and covered for a few seconds at 37, 37½, 40 and 42½ m, the field varying from -8800 to $-10,600$ v/m. The largest sudden change of field, at 35.5 m, amounted to $+11,800$ v/m and was due to a flash in the cloud at a distance of 4.4 kms. It was followed 3 seconds later by a change of -3000 v/m. The other negative change, -2000 v/m, occurred at 39.6 m.

Rain started to fall at 35.5 m, was noted as heavy at 40 m and as very heavy from 41½ m to the end of the record. This is the cause of the upward slope of the record, which indicates an average current of 6.5×10^{-14} amps/sq cm from 34½ m to 42½ m. The peculiar hump at 43½ m is probably due to the heavy rainfall. Flashes to ground occurred at 37.5 m (5.4 kms) and 38.8 m (3.0 kms). The record shows 34 positive and 2 negative field-changes.

Fig 10 Storm 36 9/2/27 Test-plate, 14 h 6.5 m to 14 h 22 m. The distances of 12 of the flashes have been determined and lay between 2.0 and 7.2 kms. The test-plate was covered for a few seconds at 7, 10, 11.7, 13.6, 15.2 and 19.0 m, the field varying from $-11,800$ v/m to $-3,500$ v/m. The largest sudden change of field amounted to $+11,800$ v/m and occurred at 9.4 m, momentarily reducing the field to zero.

Three small negative changes of field occurred at 8.7, 11.3 and 12.2 m, the first two being due to discharges at distances of 5.4 and 11.2 kms respectively. Two larger negative changes occurred at 16.6 m at the end of a half-minute interval during which a positive field of the order of 6000 v/m prevailed. They reduced the field by 14,000 v/m in two jumps of -4700 and -9300 v/m about 1½ seconds apart.

Rain fell at 12 m, becoming heavy at 13 m, and the upward slope of the record indicates that this was positively charged and gave an average current of 4.9×10^{-14} amps/sq cm between 11.7 and 15.2 m.

The full history of this storm is as follows. At 12 h 20 m it was approaching from a distance of 40 kms and gave 90 negative and 4 positive field-changes. At 13 h 12 m it was 6 kms away and gave rise to a field of -7000 v/m which

rose to $-16,000$ v/m at 13 h 41 m and continued to vary from -8000 to $-12,000$ v/m (except for the half-minute of positive field referred to) until 14 h 27 m. During this half-hour the discharges were between 2.0 and 7.2 kms off and 72 positive and 5 negative changes* were observed. Another record was taken at 14 h 27 m, just after fig. 10, when the active centre was reported to be moving away and the flashes were at distances lying between 7 and 10 kms. This record shows 9 positive field-changes followed by 8 negative ones and the sign of the field-changes evidently reversed. The steady field, however, remained between -5500 and -8100 v/m for another 31 minutes.

My thanks are due to Prof. C. T. R. Wilson for his interest in these experiments, to my wife and Mr. J. Linton for assistance with the outside observations, and to the South African Research Grant Board for a grant in aid.

§ 10. *Summary*

A discussion is given of the tests available for determining the polarity of thunderclouds and further observations at Somerset East are described, which appear to support the conclusions of Craib and the writer that the polarity of these storms was positive.

* One of these was outside the reversal distance, at 11.2 kms.

The Interchange of Electricity between Thunderclouds and the Earth

By B F J SCHONLAND, M A , Ph D , Senior Lecturer in Physics,
University of Cape Town

(Communicated by C T R Wilson, F R S—Received November 21, 1927)

[PLATE 6 (Upper figure)]

§ 1 Introduction

Prof C T R Wilson* has suggested that the exchange of electricity between thunderclouds and the ground may be an important factor in the maintenance of the earth's negative charge, the replenishment of which, in view of the fine-weather air-earth current, is an outstanding problem in atmospheric electricity. He has shown† that such an exchange can take place in three ways, by the momentary currents due to lightning discharges between the cloud and the ground, by the convection currents carried by rain, and by the continuous currents carried by ions moving in the powerful electric fields below the cloud. This last effect may be expected to be considerable since such ions will be produced in quantity as a result of point-discharges from trees and bushes below the cloud.

In the present paper an attempt is made to estimate the magnitudes of these three factors in the exchange. Before describing the measurements, it may be recalled that in two studies‡ of the strong electric fields below these clouds, it has been found that negative potential gradients are very much more frequent and considerably stronger than positive ones. Indeed, occasions of strong positive fields below active thunderclouds are so rare as to be negligible, and the predominance of strong negative fields must cause the point-discharge currents to be mainly upwardly directed. The earth must therefore gain a negative charge from this effect.

It has also been found that the great majority of lightning discharges between these clouds and the ground involve only the negatively charged portion of the cloud. This factor in the exchange must therefore also result in a gain of negative charge by the earth.

The rain, on the other hand, may be expected to convey a positive charge

* 'Phil. Trans.,' A, vol. 221, p. 112 (1921).

† Glazebrook's "Dictionary of Applied Physics," vol. 3, p. 100.

‡ Schonland and Craib, 'Roy Soc. Proc.,' A, vol. 114, p. 229 (1927); Schonland, *supra*, p. 233.

to the earth if the point discharge current is large, for the falling drops, whatever their initial condition, will generally intercept enough of the upward-moving positive ions to reach ground with a charge of positive sign *

It is perhaps necessary to point out that the measurements to be described are independent of any discussion concerning the polarity of the thundercloud. The conclusions of Craib and the writer (*loc. cit.*) on this point are only invoked when it is required to generalise from the results obtained by direct measurement.

The observations were made at Somerset East, South Africa, in January and February, 1927.

§ 2 *Apparatus*

The ordinary equipment of the station, which has already been described,† is sufficient for the examination of the first two factors. The sign and the quantity of the electricity discharged from the cloud in a flash to earth, as well as the rate at which such discharges take place, can be found from observations of the field changes produced by distant storms. The sign and quantity of the electricity carried down by rain can be determined by collecting the rain in the earth-filled test plate.

In order to obtain an estimate of the third factor, it is necessary to set up some natural source of point discharge, bush or tree, which it is possible to regard as typical of the district and to measure the current passing upwards from it. The choice of a typical tree in the Somerset East district is an easy one, for it is fairly thickly covered with *Acacia Karroo*, a small thorn-tree growing to an average height of about 12 feet and plentifully provided with long and sharp thorns. A suitable tree was therefore cut down at the base and mounted upon ebonite-sulphur insulators. Similar insulators were placed in the stay-wires, which kept it upright, and shields were provided to protect the insulators against dust and rain. The tree was 7 metres to the N.E. of the hut and was joined to the current-measuring instrument by means of a wire passing in in insulators up the centre of an iron pipe. This instrument was a unipivot galvanometer with one terminal joined to the tree and the other to earth, and could be read to tenths of a micro-ampere.

The top of the tree was 4 metres above the ground and the branches spread out in a rough circle of 1.5 metres radius. The leaves withered in a few days but the thorns remained. Fresh twigs and branches were wired to it occasion-

* Wilson, 'Phil. Trans.,' *loc. cit.*

† Schonland and Craib, *loc. cit.*

ally, but it is doubtful if this was really necessary. A photograph of the tree is shown in Plate 6.

§ 3 *Observations of the Tree Current during Storms*

The following table shows approximately the relation found to hold between the strength of the electric field below the cloud and the upward current due to point discharge from the tree.

Table I

Field	Current
v/m	microamperes
- 3,500	0.07
- 5,500	0.20
- 11,000	1.00
- 16,000	4.00

The rapid rise in the current with increasing field is very marked and in accordance with other observations upon point discharge. The maximum current observed was 4.5 microamperes. Data for positive fields are too few to draw any conclusion as to the effect of the sign of the field of force upon the current.

While a storm is overhead the electric field is constantly altering as a result of lightning discharges and the subsequent recovery of the cloud charges, and these changes in the field affect the current from the tree. The sudden field-changes give rise to ballistic deflections of the galvanometer needle, after which the current increases until the next flash occurs. To determine the mean value of the current while the storm was near to the station the galvanometer reading was taken at regular intervals and without reference to the actual field prevailing at the moment. The mean values obtained are shown in column 6 of the following table. Columns 3, 2, 4 and 5 give the distance of the active part of the cloud, the average value of the steady field, the time during which observations were made, and the number of observations used to find the average current. Column 7 shows the total quantity of positive electricity discharged upwards from the tree during the period of observation.

The table shows that during 230 minutes of strong negative fields the tree discharged 0.0129 coulomb of positive electricity upwards, while during 10 minutes of strong positive fields it discharged 0.0001 coulomb of negative electricity. The latter effect was due to a mammatiform cloud residue, the actual storm having receded far away.

Table II

1	2	3	4	5	6	7
Storm	Average steady field	Distance	Time	No. of observations	Average current	Quantity discharged
	v/m	kms	mins		microamperes	coulombs
30	- 10 000	4-6	30	10	1.0	0.0018
31	8 000	1-1	20	5	2.5	0.0030
36	10 000	1-10*	122	30	0.8	0.0059
38	- 11 000	5-7	35	10	+0.6	0.00126
38	6 000	D*	5	4	0.15	0.00005
43	11 000	4-5	18	10	0.75	0.00081
48	6 000	D*	10	5	0.20	0.00012

* Active centre at more than 10 kms

These observations may be supplemented by the statement that during the passage of seven storms over the station in 1927 the steady field exceeded - 5000 v/m for 300 minutes and + 5000 v/m for 5 minutes. The corresponding figures for cloud residues were 53 and 37 minutes respectively, but for the present we shall consider active storms only and it is evident that the positive fields and negative upward currents can in this case be neglected.

It is interesting to compare these observations with those made by Wormell* in England, who used a single point-discharger at a height of 8 metres, which is stated to be likely to produce similar effects to those from a small tree. The currents obtained in the two cases are of the same order of magnitude, though in Wormell's experiments values as high as 10 microamperes were frequently observed. A similar predominance of upward currents was found. It would, however, appear that the point-discharger used by him was more effective than my tree, for currents of the order of 3 microamperes were found to be produced by fields of strength 3000 v/m, which in my experiments would only give rise to about 0.1 microampere.

The downward current from the tree during fine weather was measured on several occasions and found to be about 9.1×10^{-11} amps in a field of strength 60 v/m.

§ 4. Estimate of the Total Upward Ionisation Current below an Active Storm

In order to form an estimate of the total upward current due to point-discharge below an active thundercloud, it is necessary to determine (a) the principal

* 'Roy Soc. Proc.,' A, vol. 115, p. 443 (1927).

sources of point discharge (b) the average upward current from each such source at various distances from the active centre of the thundercloud and (c) the number and distribution of these sources below the cloud. To obtain this information especially that under (b) at all accurately would require a more exhaustive study of the problem than has yet been made. Sufficient information is however available for an estimate of the order of magnitude of the upward current.

(a) and (c) As already mentioned the principal source of point discharge is the thorn tree described. Four fifths of the district over which the storms travel is thickly covered with this tree the remainder consisting of cleared ground with occasional taller trees of the blue gum variety. The thorn trees are on the average about 5 m tall and as they would shield small bushes between them from the full effects of the electric field they may be considered as the only important sources of point discharge. The grass in the open spaces is very poor and short and can hardly be an important factor.

(b) —To obtain an idea of the total effect of these trees it is necessary to decide at what distance from the active centre of the storm the field and so the tree current may be considered as negligible. The evidence so far obtained indicates that the field is usually very small at a distance of about 8 kms and grows rapidly as the storm approaches reaching — 5000 v/m at about 5 kms and — 16 000 v/m when the storm is practically overhead. At a distance of 6 kms the field is about — 3000 v/m and falls off rapidly with further increase in the distance.

The average effective fields are less than and often only half the above values owing to the sudden reductions in field strength caused by lightning discharges. Thus the tree current will be considerably less than 0.1 microampere in a field of maximum strength — 3000 v/m and we may proceed by neglecting the contributions from all trees more than 5 or 6 kms away from the active centre. This distance is measured from the lower pole of the cloud whose height may be taken as 3 kms so that all the trees within a circular area of radius 4 to 5 kms may be expected to make an effective contribution to the upward current.

Those trees near the centre of this area will be giving a mean upward current of about 2.5 microamperes and those at the circumference about 0.1 microampere. The data available are hardly sufficient for an accurate knowledge of the current from trees at various distances from the centre. Table II however indicates that an average value of 0.8 microampere over the whole area will probably not be very far from the truth.



Thorn tree as Source of Point discharge (v p 254)



Intertraction Streamers (t p 262)

(Facing p 268)

In order to form the estimate of the total upward point discharge current it will therefore be assumed that the trees are 5 metres apart that the effective area has a radius of 4.5 kms and that the average upward current from a tree within this area is 0.8 microampere. From these figures the total number of trees effective in point discharge below the thundercloud is 2.6×10^6 and the average total upward current from them is 2.1 amperes.

§ 5 *The Effect of Lightning Flashes between Cloud and Ground*

In order to estimate the effect of flashes of lightning upon the transfer of electricity between the cloud and the ground we require the sign and magnitude of the average quantity so transferred and also the average frequency of such flashes.

As concerns the sign it has been shown in a previous paper* that the great majority of flashes to ground (more than 90 per cent) produce a positive change of field and so convey a negative charge to the earth. Further the electric moments of 73 distant discharges were measured in 1926 and found to have a mean value of 93 coulomb kilometres†. This result has been confirmed by further unpublished measurements made in 1927 and if the average vertical length of the discharge path whether to ground or in the cloud be taken at 3 kms, it gives 15 coulombs for the average quantity of electricity involved in a discharge.

To determine the average frequency of flashes to ground use is made of the fact that practically every positive change of field observed from a distant storm is caused by a discharge to ground. The photographic records of 30 such storms show that 89 positive and 734 negative sudden changes of field occurred during 232 minutes so that a flash to ground took place on the average once in every 2.6 minutes. This result is in accord with outside observations of the storms.

The effect of the momentary currents carried by lightning discharges is thus equivalent to a steady current of 15/156, or about 0.1 ampere, in an upward direction.

§ 6 *The Convection Current carried by Charged Rain*

In order to form an estimate of the part played by charged rain, the average current entering the test plate during periods of rainfall has been determined from the photographic records obtained with the capillary electrometer. Such measurements include the effect of ionisation currents as well as rain currents,

* Schonland, *loc. cit.*

† Schonland and Orall, *loc. cit.*

but the former were found to be negligible in comparison with the latter, since the surface of the test-plate was not provided with any important source of point-discharge. The method has been shown by Wilson* to be free from the disturbing effects of splashing.

Observations were also made of the duration of the rainfall. The results for seven storms are shown in the following table, the last column of which gives the quantity of positive electricity carried to the earth in each shower of rain, measured in coulombs per square centimetre of the test-plate.

Table III

Storm No	Distance	Field	Current	Duration	Quantity
	kms	v/m	amps /sq cm	mins	coulombs/sq cm
25	6	- 5,000	+ 7.9×10^{-12}	10	} 21.3×10^{-11}
25	3	8,000	+ 23.0†	12	
30	5	- 10,000	+ 6.5	12	
34	3	- 8,000	+ 10.0	15	9.0
36	3-5	} - 16,000	+ 6.7	12	} 7.1
36	4-6		+ 6.5	6	
38	10*	- 8,000	3.0	10	- 1.8
38	10*	+ 6,000	- 1.0	10	- 0.6
41	4		No rain		
43	4		No rain		

* Active centre at more than 10 kms

† Heavy rain

It will be seen that in all cases of strong negative fields due to active storms the rain was positively charged. The only occasion on which negatively charged rain was associated with a negative field was when storm 36 was receding and at a distance of about 10 kms. The occurrence of negatively charged rain in association with the positive field due to a cloud residue of storm 38 is interesting. Although the current is small its sign and value were carefully determined.

The largest rain-current observed was $+ 2.3 \times 10^{-12}$ amps /sq cm. Higher values were found on two occasions in 1926 when currents of $+ 2.0 \times 10^{-11}$ (?) and $+ 6.0 \times 10^{-12}$ amps /sq cm were recorded, but the rainfall was then heavier than any which occurred in 1927. For the storms under discussion the average rain-current will be taken as 1.0×10^{-12} amps /sq cm.

We now require an estimate of the average area over which rain was falling. If the average velocity of the storm be taken as 25 kms per hour and the

* Wilson, 'Roy Soc Proc.,' A, vol. 92, p. 555 (1916).

average duration of the rainfall at any point as 12 minutes, this area is about 5 kms in diameter and amounts to about 20 sq kms. The total convection current over this area is therefore $20 \times 10^{10} \times 10^{-13}$ or 0.02 ampere. This current is quite negligible in comparison with the 2.1 amperes carried upward from point-discharge.

This result can be seen in another way, the tree may be taken to represent the main source of point-discharge within an average area of 20 sq metres, so that the loss of positive electricity by point-discharge from this area during the five storms of Table II was at least 0.013 coulomb. Table III shows that the gain of positive electricity by the agency of charged rain during the same five storms was 1.84×10^{-10} coul/sq cm or 0.000037 coulomb over the area of 20 sq metres. The ratio of the loss to the gain is 350 to 1.

§ 7 *The Total Current between Active Storms and the Earth*

The estimates of the preceding sections may now be combined to find the total current between an active thundercloud and the ground. This current is made up as follows:

Point-discharge	2.1 ampere
Lightning discharges	0.1 ampere (equivalent)
Charged rain	-0.02 ampere

The total current may therefore be estimated as 2.2 amperes in such a direction as to convey a negative charge to the earth.

These observations confirm Wilson's remark that "of the three kinds of electric current which may accompany precipitation—the convection current carried by rain, the momentary currents of lightning discharges, and continuous currents due to the intense electric fields—it is quite possibly the last which contributes most to the interchange of electricity between the earth and the atmosphere."

The comparatively small value of the effect of lightning discharges is interesting. It would seem probable that this effect is more important in Europe than in South Africa, but it is hardly likely to be an important factor when averaged over the surface of the earth. Observations from as far north as Nyassaland (lat 14° S) agree with those made in South Africa and in India as to the marked preponderance of discharges within the cloud.

It is, however, to be expected that a thunderstorm occurring over a region which is not well covered with trees and other natural sources of point discharge

* "Dict. App. Physics," loc. cit.

will be more active electrically and give rise to more discharges to ground than one over what is botanically termed "park" land, for the dissipation of the cloud charges by point-discharge currents will be much reduced. This is probably the reason why the treeless regions of South Africa, such as the Orange Free State and the high-veld of the Transvaal, are noted for the powerful electrical display produced by thunderstorms. It may be added, however, that a large proportion of Africa south of the Equator, perhaps more than 75 per cent, is "park" land.

The small value found for the current due to charged rain must be associated with the fact that the rainfall during these two months was considerably below the usual value* and the district suffered severely from drought. Two of the storms, as is shown in Table III, produced no rain at all and none gave as much as half an inch of rain. It is possible, therefore, that the rain effect is abnormally low, but unlikely that it could ever seriously challenge that due to point discharge.

That these clouds are usually quite capable of dealing with continuous dissipation currents of the order of several amperes can be shown from a study of the "recovery curves" of the electric field changes caused by distant lightning discharges. The recovery curves, as found by Wilson in England,† are approximately exponential and suggest a constant rate of regeneration of the cloud charges. This rate may be found from the initial linear portion of the curves, when the dissipation is absent. A number of measurements have been made from the photographic records of the electric fields and they indicate that, in the absence of dissipation, the cloud charges would recover their original strength in about 3.5 seconds. This is the mean of some 80 observations. If the average charge on a cloud pole be taken, as before, to be 15 coulombs, regeneration must take place at an average rate of about 4 coulombs per second so that when the dissipation and regeneration currents ultimately balance each other, a dissipation of 2 or 3 amperes below the cloud is not at all beyond the capabilities of the generating process, even allowing for dissipation within the cloud itself.

§ 8 *The Replenishment of the Earth's Negative Charge*

It has been shown in the preceding sections that the thunderstorms which passed over the station produced currents of the order of 2 amperes below them and in such a direction as to convey a negative charge to the earth. Since point discharge was the main factor in the causation of these currents, their direction

* 2.02 inches instead of 6 inches or more. This is the rainy season.

† Wilson, 'Phil. Trans.,' loc. cit.

was set by the direction of the electric fields of force below the clouds, and this was predominantly negative. Up to the present 13 active storms have been observed to pass over the station and occasions of strong positive fields beneath them have been extremely rare and fleeting.

Since the observations discussed in previous papers upon the electric fields of these storms and of others at greater distances can only be interpreted in terms of a thundercloud with a positive charge elevated above a negative one, there is good reason for believing that similar strong negative fields of force prevailed below those storms which did not pass over the station. The conclusions of other observers* are in agreement with this view, at any rate in respect of the majority of the thunderclouds examined by them. It is therefore not unlikely that the estimate given for the cloud-earth current may apply to most of the storms which occur over the surface of the earth.

It is unnecessary to stress the importance of this conclusion in connection with Wilson's views on the replenishment of the earth's negative charge, but it must be pointed out that further information is required before it is possible to determine the full effect of these factors upon the electrical condition of the earth. The currents so far considered have only been those between active thunderstorms and the ground, and these are practically always directed upwards. There are, however, occasions when fairly strong electric fields exist below clouds which are not active in producing lightning, and these fields are sometimes positive in sign, giving rise to downwardly directed point-discharge currents. Up to the present the observations do not suggest that there is any predominance of these downward currents under shower-clouds. In January and February, 1927, the field below inactive clouds exceeded $+5000$ v/m for 37 minutes and -5000 v/m for 53 minutes, so that the effects of the larger currents below them practically balanced. For an accurate estimate, however, it would be necessary to carry out experiments with integrating devices such as those recently described by Wormell (*loc cit*). In the Somerset East district, charged shower-clouds seem to occur only in the wake of thunderstorms.

My indebtedness to the writings of Prof Wilson is apparent throughout this paper, and I have to thank him for his interest in these experiments, Prof A. Ogg for providing facilities for the work, Mr J. Linton for much help, and the South African Research Board for a grant in aid.

* Appleton, Watt and Herd, 'Roy. Soc. Proc.' A, vol. 111, p. 615 (1926), Wormell, *loc. cit.*

§ 9 Summary

The paper describes observations made to examine the part played by (a) point-discharge currents, (b) lightning discharges between cloud and ground, and (c) charged rain, in the electrical interchange between an active thunder-cloud and the earth. From these observations, (a) and (b) are estimated to produce continuous currents of the order of 2.1 and 0.1 (equivalent) amperes respectively in an upward direction and (c) to produce a reverse downward current of the order of 0.02 ampere. The resultant current is thus estimated at 2.2 amperes in such a direction as to convey a negative charge to the earth.

Note on the Explanation of a so-called "Interaction" Phenomenon

By N K ADAM

(Communicated by G I Taylor, F R S —Received November 8, 1927)

[PLATE 6 (Lower figure)]

Sir Almroth Wright* observed that a disc of filter paper soaked in coloured albumen solution, fixed to the under side of a cover-glass which was floated upon a salt solution, showed coloured streamers radiating out along the surface. In seeking an explanation, I concluded† that the streamers were due to the upper layer of the salt becoming lighter, owing to loss of salt to the filter paper by diffusion, and that this alteration of specific gravity caused currents outwards towards the surface of the solution beyond the cover-glass which is slightly higher than the under side of the coverglass, and the only region to which upward streaming currents could go. In confirmation of this view, I showed that if the cover-glass was tilted the streamers (which I assumed to indicate the direction of the currents) only went to the upper side of the cover-glass, and if the positions of salt and albumen were reversed, so that the upper layers of solution would become more dense by diffusion, the streamers indicated downward currents. Sir A. Wright‡ has criticised my explanation, and the

* 'Roy. Soc. Proc.' A, vol. 112, p. 213 (1926)

† *Ibid.*, A, vol. 113, p. 478 (1926)‡ *Ibid.*, A, vol. 114, p. 579 (1927)

criticism which seems to have most weight is that the upward currents would be expected to produce a uniform spreading cloud of colour, not a system of radial streamers. I have therefore tested directly whether a slow upward current of water, impinging on a disc of filter paper soaked in dye solution, drives out the colour in a uniform cloud or in streamers. The photograph* shows that fine streamers are actually produced. The disc was supported in the surface of water, about 3 mm. above a tube 1 cm. in diameter delivering water at a rate of about 36 c.c. per minute. Variations of the rate of flow slightly altered the appearance of the streamers, but a uniform cloud was *never* produced.

A slow current of coloured liquid, impinging on a plate in the surface, does not produce streamers, the streamers are therefore to be ascribed to the manner in which the colour washes out from the filter paper. Very probably the colour leaves mainly at certain irregularities on the upper side, or the edge of the paper. Glazed and waxed paper also caused streamers, though these were less definite in the case of the waxed paper. Drops of coloured liquid emerging from a hole in a glass plate did not produce fine streamers, but a few rather coarse streamers appeared when coloured liquid was placed in a tin with a number of small holes in the bottom. The streamers in the case of the filter paper seem possibly due to the fibres of the paper.

* See Plate 6, facing p. 256

Examples of the Zeeman Effect at Intermediate Strengths of Magnetic Field

By K DARWIN

(Communicated by Prof C G DARWIN, FRS —Received December 8, 1927)

Introduction

In a recent paper* called "The Zeeman Effect and Spherical Harmonics," Prof Darwin gives a set of formulæ from which can be determined the frequencies and intensities of the lines in the standard Zeeman Effect. Except for $s - p$ doublets these quantities could previously only be calculated for strong or weak magnetic fields, and the interest of the new formulæ lies in the fact that from them we can also calculate the frequency and intensity at any intermediate field. Approximate algebraic solutions are available for strong or weak fields, but the new method makes numerical solutions for all strengths easily practicable. The present work gives the application of the new formulæ to three cases which involve simple but lengthy calculation. These are the $s - p$ and $p - d$ doublets and the $s - p$ triplets, but we describe first the case of the $s - p$ triplets as this illustrates most fully the method under consideration. As these cases involve respectively 10, 34 and 19 lines, it will be readily seen that the discussion of any more complicated systems would lead to a large amount of work. The simplest case of all, that of the $s - p$ doublets, is already known from the work of Voigt (by entirely different methods). As, however, so much of the material for working out the $s - p$ doublets by the new method is the same as we require for the $p - d$ doublets, we have included in a brief form the results for the simpler case. The theory and procedure is, of course, similar for all the three examples considered, so we now give an outline of the calculations and results before entering into the detail for the several cases separately.

Referring to § 5 of the previous paper, we find the following rules for forming the "chains of equations" on which the whole calculation is based.

Take

$$\begin{aligned} k &= 0, 1, 2, \dots && \text{for } s, p, d \quad \text{terms} \\ r &= 0, \frac{1}{2}, 1, && \text{for singlets, doublets, triplets} \end{aligned}$$

* 'Roy Soc Proc,' A, vol 115, page 1 (1927). Equivalent formulæ are given by Heisenberg and Jordan ('Z f Physik,' vol 37, p 263 (1926)).

Let u be any integer between k and $-k$ inclusive, and let s be any multiple of $\frac{1}{2}$ such that $(r+s)$ is an integer, and also $-r \leq s \leq r$. ω is the Larmor frequency and β is the constant of multiplet separation in energy units. The a 's are numerical coefficients in the characteristic functions of the atom, but for their precise interpretation reference must be made to the previous paper. With any of the permitted values of u and s write down the equation

$$\begin{aligned} -a_{u-1, s+1} \beta (k-u+1) (r+s+1) + a_{u, s} [W - \beta 2us - \omega (u+2s)] \\ - a_{u+1, s-1} \beta (k+u+1) (r-s+1) = 0, \quad (1) \end{aligned}$$

in which all the coefficients are integers whatever r may be. Set down the corresponding equations in $a_{u-1, s+1}$ and $a_{u+1, s-1}$, and carry on in both directions until stopped by the condition $|u| \leq k$ or $|s| \leq r$. The determinant of this system of equations will give a set of values for W (corresponding to $m = u+s$) where each value represents the separation of a level from the mean centre of the multiplet. We distinguish the different roots of the determinant by the value of j , the greatest having $j = k+r$ and the rest being numbered by units downwards in order of decreasing magnitude.

Having formed the chains of equations and chosen a value for ω , which measures the strength of the magnetic field, we have to solve for W the determinant arising from the chain of equations corresponding to each value of m . In the three cases we shall deal with, the determinant is never of higher order than the third. A chain of equations gives us only ratios between the a 's, so to obtain numerical values we have to introduce a normalising equation. In the previous paper the formulae for intensities (4.4, 4.5 and 4.6) have as denominators factors such as

$$\sum_m (a_u^k)^j (r+s)! (r-s)! (k+u)! (k-u)!, \quad (2)$$

where \sum_m means the summation over all values of u and s such that $u+s=m$.

This quantity we shall call N_m^{kj} . We might have taken $N_m^{kj} = 1$ as a normalising equation to simplify the calculation of intensities, but since a common numerical factor often runs right through N_m^{kj} , it was found more convenient to omit this factor in normalising. The numerical coefficients are consequently different for each case, and so a list of normalising equations will be given for each system of levels as we deal with it. For the purpose of numerical solution it was natural to fix the scale of the multiplets by choosing β as a simple number in each case. The values chosen (for reasons given below) were $\frac{1}{2}$ for the p -triplet, 1 for the p -doublet, and $\frac{1}{2}$ for the d -doublet levels,

in the s -levels β does not occur. The values adopted for ω were in all cases in the respective scales $\frac{1}{2}, \frac{1}{3}, 1, 2, 5$.

Having normalised according to the appropriate equation we have obtained numerical values for each W and its a 's, and the next step is to combine the levels by taking the differences between the values of W for values of k differing by unity, for all values of j , and all permissible values of m . We thus obtain the frequency of a line in energy units, or rather the difference between its frequency and that of the mean centre of the multiplet. The general expressions for intensities (4, 4, 5 and 4, 6 of the previous paper) consist of three formulæ

$$\left. \begin{aligned} & \left[\sum_m a_{n,s}^{k,j} a_{n,s}^{k-1,j} (r+s)! (r-s)! (k+u)! (k-u)! \right]^2 / N_m^{k,j} N_m^{k-1,j} \\ & \text{for the perpendicular components } m \rightarrow m-1 \\ & \left[\sum_m a_{n,s}^{k,j} a_{n,s}^{k-1,j} (r+s)! (r-s)! (k+u)! (k-u)! \right]^2 / N_m^{k,j} N_m^{k-1,j} \\ & \text{for the other perpendicular components } m \rightarrow m+1, \text{ and} \\ & 4 \left[\sum_m a_{n,s}^{k,j} a_{n,s}^{k-1,j} (r+s)! (r-s)! (k+u)! (k-u)! \right]^2 / N_m^{k,j} N_m^{k-1,j} \\ & \text{for the parallel components } m \rightarrow m \end{aligned} \right\} \quad (3)$$

These appear rather formidable but in practice they simplify somewhat because many of the factorials reduce to $0!$ or $1!$. Also our choice of normalising equations makes most of the denominator disappear, and the remainder is incorporated in a numerical factor in which a factor from the numerator is also included. Finally the whole system of intensities is multiplied by a numerical coefficient such that in weak fields all the intensities are integers. These numbers were $3/2$ for the $s-p$ doublets and triplets, and $15/2$ for the $p-d$ doublets. The intensity formulæ as given below have already been treated in this way.

We thus calculate the frequency ν (more strictly the difference of the frequency from that of the mean centre of the multiplet), and the intensity I , for all lines at any strength of field, and the complete results appear in Tables I to VI. In addition we give the results of approximate algebraic solutions for very large and very small values of ω . These "strong field" and "weak field" solutions were obtained on exactly the same principles as the numerical solutions for intermediate fields, so need no preliminary discussion. The numerical work was done with a 10-inch slide rule throughout, and the results are accurate to that degree.

For each of the three cases we have drawn a graph which shows clearly

the general features of the transition from the anomalous Zeeman Effect to the Paschen Back Effect. For this we should naturally plot ν against ω , but the divergence of the lines for large values of ω is so great that in order to show more detail we have distorted both co-ordinates in the ratio $1/(\omega + 1)$. This reduces the divergence of the lines and makes the chosen values of ω ($\omega = \frac{1}{5}, \frac{1}{2}, 1, 2, 5$) occur at even distances along the axis. The parallel components, $m = m$, are drawn as continuous lines, and both sets of perpendicular components $m = m \pm 1$ as broken lines, since there is no difficulty in distinguishing the two latter types. The intensities are roughly indicated by the thickness of the lines, the exact values being given in the tables. In the $p-d$ doublet graph however, we wished to include lines whose intensities are exceedingly small compared to the important lines, namely, the "forbidden lines" where $j = \frac{3}{2} \rightarrow j = \frac{1}{2}$ so that in this one graph the width of the lines cannot be made to correspond proportionally to the intensities.

Before proceeding further I wish to express my obligation to my husband, Prof Darwin. I owe to him the original suggestion and plan of the work and should have been quite unable to carry it out without his guidance and criticism at every stage.

s - p Triplets

We have to construct the 'chains of equations' for the particular case, first of the s -terms, then of the p terms. The notation which has been found convenient to distinguish the different values of W and the a 's is $W_{u,v}^{i,j}$ and $a_{u,v}^{i,j}$. Since however k has one value throughout for the s -terms, and another value throughout for the p -terms, the index k is omitted until we come to combine the two sets of terms. The index j is also omitted until it is necessary to distinguish between different roots in the equations for W arising from each chain.

For the s -terms we have, by the foregoing rules, $k = 0$ and $r = 1$, whence $u = 0$ since $|u| \leq k$, and $s = +1, 0$, or -1 since $|s| \leq r$, so that $m = +1, 0$, or -1 .

The chains of equations then degenerate to

$$\begin{aligned} a_{0,1}[W_1 - 2\omega] &= 0 \quad \text{which gives } W_1 = 2\omega \\ a_{0,0}[W_0] &= 0 & W_0 &= 0 \\ a_{0,-1}[W_{-1} + 2\omega] &= 0 & W_{-1} &= -2\omega \end{aligned}$$

Thus an exact solution for W is effected at once for any given value of ω . Here we normalise all three a 's as unity

For the p -terms we have $k = 1$ and $r = 1$ whence $u = 1, 0$, or -1 and $s = 1, 0$, or -1 so that $m = 2, 1, 0$, -1 or -2 . We take $\beta = \frac{1}{2}$ rather than 1, because this makes the lines for no field have frequencies of 1, -1 , -2 , instead of 2, -2 , -4 , and thus the chains of equations are

$$m = 2 \quad a_{1,1}(W - 1 - 3\omega) = 0$$

$$m = 1 \quad \begin{aligned} a_{0,1}(W - 2\omega) - a_{1,0} &= 0 \\ -a_{0,1} + a_{1,0}(W - \omega) &= 0 \end{aligned}$$

$$m = 0 \quad \begin{aligned} a_{-1,1}(W + 1 - \omega) - \frac{1}{2}a_{0,0} &= 0 \\ -2a_{-1,1} + a_{0,0}(W) - 2a_{1,-1} &= 0 \\ -\frac{1}{2}a_{0,0} + a_{1,-1}(W + 1 + \omega) &= 0 \end{aligned}$$

$$m = -1 \quad \begin{aligned} a_{-1,0}(W + \omega) - a_{0,-1} &= 0 \\ -a_{-1,0} + a_{0,-1}(W + 2\omega) &= 0 \end{aligned}$$

$$m = -2 \quad a_{-1,-1}(W - 1 + 3\omega) = 0$$

The normalising equations are as follows --

$$\begin{aligned} m = 2 \quad (a_{1,1}^1)^2 &= 1 \\ m = 1 \quad (a_{0,1}^1)^2 + (a_{1,0}^1)^2 &= 1 \\ m = 0 \quad 4(a_{-1,1}^1)^2 + (a_{0,0}^1)^2 + 4(a_{1,-1}^1)^2 &= 1 \\ m = -1 \quad (a_{-1,0}^1)^2 + (a_{0,-1}^1)^2 &= 1 \\ m = -2 \quad (a_{-1,-1}^1)^2 &= 1 \end{aligned}$$

To illustrate the procedure let us now take $\omega = 1$, the middle value of the five numerical values of ω for which the calculations have been made, and work with that throughout. As before we have to solve for W the determinants formed from each chain. The several values of W in the quadratic and cubic equations so formed are distinguished by the index j , the roots being numbered from the highest ($j = k + r = 2$) downwards. From the first and last chains (of one member) we have at once

$$\begin{aligned} W_2^{1,2} &= 4, & a_{1,1}^{1,2} &= 1, \\ W_{-2}^{1,2} &= -2, & a_{-1,-1}^{1,2} &= 1 \end{aligned}$$

We may observe that chains of one member, unlike longer ones, have a con-

stant value of unity for a for all values of ω . From the second chain ($m = 1$) we have

$$(W - 2\omega)(W - \omega) = 1$$

Solving the quadratic numerically by the usual method of completing the square we get

$$W_1^{1/2} = 2.617 \quad \text{and} \quad W_1^{1/1} = 0.383$$

From either of the equations we can now determine the ratio of the a 's corresponding to either value of W , for we have

$$a_{10}/a_{01} = W - 2\omega,$$

$$a_{01}/a_{10} = W - \omega,$$

and these form in practice a useful check on one another and on the solution for W^* . With this ratio and the appropriate normalising equation $(a_{01})^2 + (a_{10})^2 = 1$ we can now get numerical values for the a 's corresponding to the two roots, and these are

$$\begin{aligned} a_{01}^{1/2} &= 0.851, & a_{01}^{1/1} &= 0.526, \\ a_{10}^{1/2} &= 0.526, & a_{10}^{1/1} &= -0.851 \end{aligned}$$

An exactly similar treatment of the other quadratic (arising from the chain $m = -1$) gives the following results —

$$\begin{aligned} W_1^{1/1} &= -0.383, & W_1^{1/1} &= -2.617, \\ a_{10}^{1/2} &= 0.851, & a_{10}^{1/1} &= 0.526, \\ a_{0-1}^{1/2} &= 0.526, & a_{0-1}^{1/1} &= -0.851 \end{aligned}$$

It will be noticed that a numerical equality appears between the roots of the quadratics, and also among the values of a derived from the different roots of each. It can be seen from the form of the equations for any value of ω that this will be so, but it is just an accidental property and can be proved to be due to the fact that k and r are both equal to 1, and to occur in no other case. It will be readily seen, however, that this symmetry caused a welcome economy of labour in dealing with the pairs of quadratics!

The cubic (for $m = 0$) was solved by Newton's method, i.e., if x_1 is an

* In the case when ω is large, one of the two ratios gives a much more precise value than the other, and we must choose the ratio which gives the more accurate result with the particular value of W we are using. Similar discrimination is needed for the cubic equation when ω is large.

approximation to one of the roots of the equation $f(x) = 0$, then a better approximation is $x_1 - \frac{f(x_1)}{f'(x_1)}$. Our equation when $\omega = 1$ is

$$f(W) \equiv W^3 + 2W^2 - 2W - 2 = 0$$

and so

$$f'(W) \equiv 3W^2 + 4W - 2$$

Taking a few values of W , the following solutions were guessed

$$W^2 = +1.1, \quad W^1 = -0.7, \quad W^0 = -2.5$$

Two further approximations, and sometimes only one, then suffice to give three decimal places correctly. In the present case the solutions were

$$W^2 = 1.169$$

$$W^1 = -0.689$$

$$W^0 = -2.482$$

The third root can, of course, be obtained by considering the sum or products of the roots, or if they have been found independently (as here) we have a check on their accuracy, the sum being -2.002 . To determine the α 's we have the three relations

$$\frac{\alpha_{-1,1}}{\alpha_{0,0}} = \frac{1}{2(W+1-\omega)}$$

$$\frac{\alpha_{1,-1}}{\alpha_{0,0}} = \frac{1}{2(W+1+\omega)}$$

from the original equations, and the normalising equation

$$4(\alpha_{-1,1})^2 + (\alpha_{0,0})^2 + 4(\alpha_{1,-1})^2 = 1$$

From these we get

$\alpha_{1,1}^{1,2} = 0.319$	$\alpha_{-1,1}^{1,1} = -0.378$	$\alpha_{1,1}^{1,0} = -0.0864$
$\alpha_{0,0}^{1,2} = 0.746$	$\alpha_{0,0}^{1,1} = 0.521$	$\alpha_{0,0}^{1,0} = 0.428$
$\alpha_{1,-1}^{1,2} = 0.1176$	$\alpha_{1,-1}^{1,1} = 0.1986$	$\alpha_{1,-1}^{1,0} = -0.444$

and these values can be checked on the middle equation of the chain which contains all three α 's

The above example shows the process of the work for $\omega = 1$. The values of W for all ω 's are to be found in Table I. To save space the values of the α 's (133 in number) have not been tabulated as they are only subsidiary quantities necessary to calculate intensities. The first and last columns give the results of the approximate algebraic solutions for weak and strong fields to three

Table I—Triplet Levels

	<i>s</i> terms		<i>p</i> terms ($\beta = 1/2$)						
	W_1^{01}	W_0^{01}	W_1^{01}	W_0^{11}	W_1^{10}	W_0^{11}	W_1^{10}	W_0^{11}	W_1^{12}
Weak									
$\omega=1.0$	2.00	0	$1 + 3\omega$	$1 + \frac{1}{2}\omega$	$1 - \frac{1}{2}\omega$	$1 + \frac{1}{2}\omega$	$1 - \frac{1}{2}\omega$	$1 - \frac{1}{2}\omega$	$1 - 3\omega$
$\omega=1/2$	0.4	0	1.6	1.00	1.00	0.990	0.04	-1.304	-0.4
$\omega=1$	1.0	0	2.0	1.041	1.041	-0.893	-2.148	-1.779	-0.0
$\omega=2$	2.0	0	4.0	1.169	1.169	-0.689	-3.487	-2.617	-2.0
$\omega=5$	10.0	0	16.0	1.681	1.681	0.368	-3.323	-4.414	-5.0
Strong									
$\omega=1$	2.00	0	$3\omega + 1$	$\omega + \frac{1}{2}$	$\omega - \frac{1}{2}$	0	ω	$2\omega - \frac{1}{2}$	$-3\omega + 1$

powers of ω . The work was, of course, on exactly the same principles as that for the numerical solutions but the following slight variations in method were found convenient. Consider the quadratic ($m = 1$) for weak fields. We write the equation

$$(W - 2\omega)(W - \omega) = 1$$

as

$$W = 1 + \frac{3\omega W - 2\omega^2}{W + 1}$$

Substituting for W in the small term, this gives

$$W = 1 + 3\omega/2$$

as second approximation and substituting again we get

$$\begin{aligned} W &= \frac{3\omega(1 + 3\omega/2) - 2\omega^2}{2 + 3\omega/2} \\ &= 1 + 3\omega/2 + \omega^2/8 \end{aligned}$$

The second root is obtained at once from the fact that the sum of the roots is 3ω . The solution of the cubic by the same method is even simpler, because ω only occurs in the equation as a square. Thus from

$$(W - 1)(W + 1)(W + 2) = \omega^2 W$$

we get as first root $1 + \omega^2/6$. The determination of the a 's is by the same process as in the numerical solutions and so need not be given here. For strong fields the results are developed in powers of $1/\omega$ by a similar method. The approximations can be checked by substituting $\omega = 1/5$ and $\omega = 5$ respectively.

We have now to combine the s and p terms and obtain the frequencies of the lines by taking the differences between the W 's for all permissible transitions. To determine the combinations we have $k = 1 \rightarrow 0$ and the three types $m \rightarrow m - 1$, $m \rightarrow m + 1$, and $m \rightarrow m$. This gives seven lines with $m \rightarrow m$, and six each with $m \rightarrow m - 1$ and $m \rightarrow m + 1$. We will give as example the process for the algebraic solution in weak fields, for $m \rightarrow m - 1$ and $j(2 \rightarrow 1)$

$$\begin{array}{l} W_1^{1,2} - W_1^{0,1} \\ = (1 + 3\omega) - 2\omega \\ = 1 + \omega \end{array} \quad \begin{array}{l} W_1^{1,2} - W_0^{0,1} \\ = (1 + 3\omega/2 + \omega^2/8) - 0 \\ = 1 + 3\omega/2 + \omega^2/8 \end{array} \quad \begin{array}{l} W_0^{1,2} - W_{-1}^{0,1} \\ = (1 + \omega^2/6) - (-2\omega) \\ = 1 + 2\omega + \omega^2/6 \end{array}$$

The numerical solutions and the algebraic approximations are given in Table II, the frequencies occupying the first half of each column and the intensities the second. In writing the frequencies for strong fields terms in $1/\omega$ have been omitted to save space but these terms appear in Table I which shows the levels and so are available if required. In cases where the larger terms are absent the leading term is given. The development of a line arising from any particular values of j and m for increasing strength of field can be seen at once by reading downwards the appropriate column in Table II.

The general expressions for intensities (3) reduce in the present case to the following simple forms the denominators being always unity owing to the form chosen for the normalising equations combined with the adjustment of the numerical coefficients. The notation for the intensities is $\left[\begin{smallmatrix} k & j \\ m & m \end{smallmatrix} \rightarrow \begin{smallmatrix} k-1 & j \\ m & m \end{smallmatrix} \right]$

$$\begin{array}{ll}
 m \rightarrow m-1 & \left[\begin{smallmatrix} 1 & j \\ 2 & \end{smallmatrix} \rightarrow \begin{smallmatrix} 0 & 1 \\ 1 & \end{smallmatrix} \right] = 6 \\
 & \left[\begin{smallmatrix} 1 & j \\ 1 & \end{smallmatrix} \rightarrow \begin{smallmatrix} 0 & 1 \\ 0 & \end{smallmatrix} \right] = 6 (a'_{10})^2 \\
 & \left[\begin{smallmatrix} 1 & j \\ 0 & \end{smallmatrix} \rightarrow \begin{smallmatrix} 0 & 1 \\ -1 & \end{smallmatrix} \right] = 24 (a'_{1-1})^2 \\
 m \rightarrow m+1 & \left[\begin{smallmatrix} 1 & j \\ 0 & \end{smallmatrix} \rightarrow \begin{smallmatrix} 0 & 1 \\ 1 & \end{smallmatrix} \right] = 24 (a'_{11})^2 \\
 & \left[\begin{smallmatrix} 1 & j \\ -1 & \end{smallmatrix} \rightarrow \begin{smallmatrix} 0 & 1 \\ 0 & \end{smallmatrix} \right] = 6 (a'_{10})^2 \\
 & \left[\begin{smallmatrix} 1 & j \\ -2 & \end{smallmatrix} \rightarrow \begin{smallmatrix} 0 & 1 \\ -1 & \end{smallmatrix} \right] = 6 \\
 m \rightarrow m & \left[\begin{smallmatrix} 1 & j \\ 1 & \end{smallmatrix} \rightarrow \begin{smallmatrix} 0 & 1 \\ 1 & \end{smallmatrix} \right] = 12 (a'_{01})^2 \\
 & \left[\begin{smallmatrix} 1 & j \\ 0 & \end{smallmatrix} \rightarrow \begin{smallmatrix} 0 & 1 \\ 0 & \end{smallmatrix} \right] = 12 (a'_{00})^2 \\
 & \left[\begin{smallmatrix} 1 & j \\ -1 & \end{smallmatrix} \rightarrow \begin{smallmatrix} 0 & 1 \\ -1 & \end{smallmatrix} \right] = 12 (a'_{0-1})^2
 \end{array}$$

Wherever the a 's have a constant value of unity for all ω 's they are omitted and this is so for all the s terms and for the end chains of the p -terms

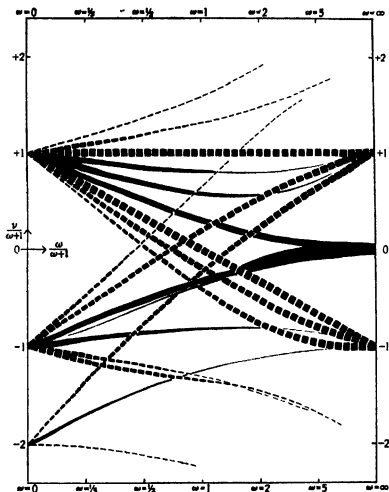


FIG. 1. *s-p* triplet. The co-ordinates are distorted so as to include the strong fields while showing detail for the weak. The abscissa runs from zero field to infinite field in the scale $\omega/(\omega+1)$. The ordinate measures $\nu/(\omega+1)$, where ν is the difference of the frequencies of the lines from that of the mean centre of the multiplet. The intensities are roughly shown by the breadth of the lines, the continuous lines being the parallel components and the broken lines the perpendicular components.

As an example we will determine the intensities at the field $\omega = 1$ of the three lines due to $m \rightarrow m-1$ and $j = 2 \rightarrow j = 1$

$$\begin{aligned} \begin{bmatrix} 1, 2 & \rightarrow & 0, 1 \\ 2 & & 1 \end{bmatrix} &= 6 \\ \begin{bmatrix} 1, 2 & \rightarrow & 0, 1 \\ 1 & & 0 \end{bmatrix} &= 6 (0.526)^2 = 1.661 \\ \begin{bmatrix} 1, 2 & \rightarrow & 0, 1 \\ 0 & & -1 \end{bmatrix} &= 24 (0.1176)^2 = 0.332 \end{aligned}$$

These and all similar results appear in the columns headed I in Table II. On the extreme right of Table II is a column giving the sum of the intensities of all the lines for each strength of field. This sum should have a constant value of 18 for each set of the perpendicular components, and of 36 for the parallel components, and the deviations from these figures (the greatest being of the order 1/300) measure the accuracy of the numerical work. Another check on the values of the intensities consists in applying the summation rules [see Kronig ('Z f Physik,' vol 31, p 885 (1925)) and Fowler ('Phil Mag,' vol 1, p 1079 (1925))] This we did satisfactorily for a few cases, but it seemed an unnecessary labour to do so throughout.

s - p and p - d Doublets

Before beginning the numerical work, we may note that in the case of the doublets, unlike that of the triplets, a complete algebraic solution would be possible as it involves quadratic equations only. For the examples we are discussing, the *s - p* and *p - d* doublets, we have to obtain the levels for the *s*-terms, the *p*-terms, and the *d*-terms, and then combine them appropriately. We begin therefore with a short account of the work leading to Table III, which gives the three sets of levels, before considering the resulting lines. We use throughout the previous notation $W_m^{k,j}$ and $a_u^{k,j}$, and the same values of ω as were used in the case of the triplets, namely, $\omega = \frac{1}{2}, \frac{1}{4}, 1, 2, 5$, "weak" and "strong". For the *p*-terms we take $\beta = 1$, but for reasons which will appear shortly we choose $\beta = 1/5$ for the *d*-terms. The approximate solution for weak and strong fields, is not carried to as high a degree of accuracy as was done for the triplets, and is therefore not in any way novel. The work required in this case to obtain the third term throughout is considerably longer, and the results seem scarcely of sufficient interest to justify it. As the approximate solutions for the triplets were given in some detail we shall not comment further on the corresponding work in this case, but shall merely include the results in the tables. As before, the values of a (224 in number) have not been tabulated.

For the *s*-terms, which are the simplest, we have $k = 0$, $r = \frac{1}{2}$ (for doublets), and the chains of equations give

$$W_{1/2}^{0,1/2} = \omega, \quad W_{-1/2}^{0,1/2} = -\omega$$

The *a*'s are taken as unity

For the p -terms we have $k = 1$, $r = \frac{1}{2}$, and we take $\beta = 1$. The chains of equations then are

$$\begin{aligned} a_{1, 1/2} (W_{3/2} - 2\omega - 1) &= 0 \\ a_{0, 1/2} (W_{1/2} - \omega) - a_{1, -1/2} (2) &= 0 \\ -a_{0, 1/2} (1) + a_{1, -1/2} (W_{1/2} + 1) &= 0 \\ a_{-1, 1/2} (W_{-1/2} + 1) - a_{0, -1/2} (1) &= 0 \\ -a_{-1, 1/2} (2) + a_{0, -1/2} (W_{-1/2} + \omega) &= 0 \\ a_{-1, -1/2} (W_{-3/2} + 2\omega - 1) &= 0 \end{aligned}$$

In this case we normalise according to the following equations —

$$\begin{aligned} m = 3/2 \quad (a_{1, 1/2}^1)^2 &= 1 \\ m = 1/2 \quad (a_{0, 1/2}^1)^2 + 2(a_{1, -1/2}^1)^2 &= 1 \\ m = -1/2 \quad 2(a_{-1, 1/2}^1)^2 + (a_{0, -1/2}^1)^2 &= 1 \\ m = -3/2 \quad (a_{-1, -1/2}^1)^2 &= 1 \end{aligned}$$

We will work out the results for $\omega = 1$ as an illustration, as we did for the triplets. From the first and last chains we have

$$\begin{aligned} W_{3/2}^1 &= 3 \quad \text{and} \quad W_{-3/2}^1 = -1, \\ a_{1, 1/2}^1 &= 1, \quad a_{-1, -1/2}^1 = 1 \end{aligned}$$

The first quadratic (which arises from the chain for $m = \frac{1}{2}$) is

$$(W - \omega)(W + 1) - 2 = 0,$$

which gives the solutions

$$W_{1/2}^1 = +1.732 \quad \text{and} \quad W_{1/2}^1 = -1.732$$

As before the roots are distinguished by the value of j decreasing by units, the highest root having $j = k + r = 3/2$

From the two equations we have the ratio given by

$$\frac{a_{1, -1/2}}{a_{0, 1/2}} = \frac{W - \omega}{2},$$

and

$$\frac{a_{0, 1/2}}{a_{1, -1/2}} = W + 1,$$

and combining this with the normalising equation we get

$$\begin{aligned} a_{0, 1/2}^1 &= 0.888, \quad a_{0, 1/2}^1 = 0.458, \\ a_{1, -1/2}^1 &= 0.325, \quad a_{1, -1/2}^1 = -0.626 \end{aligned}$$

The solution of the second quadratic ($m = -\frac{1}{2}$) is on exactly the same lines and need not be given.

Considering now the d -terms we have to form the chains of equations when $k = 2$ and $r = \frac{1}{2}$. In most spectra the d levels of the more important lines are much closer together than the p levels. In order to represent this fact, but to avoid the d levels exhibiting nothing but a Paschen Back Effect, we have arbitrarily chosen β as $1/5$, 1 being the value we used for the p levels. We thus get the following chains

$$\begin{aligned}
 a_{2, 1/2} (W^{5/2} - \frac{2}{5} - 3\omega) &= 0 \\
 a_{1, 1/2} (W_{3/2} - \frac{1}{5} - 2\omega) - a_{2, -1/2} \frac{4}{5} &= 0 \\
 -a_{1, 1/2} \frac{1}{5} + a_{2, -1/2} (W_{3/2} + \frac{2}{5} - \omega) &= 0 \\
 a_{0, 1/2} (W_{1/2} - \omega) - a_{1, 1/2} \frac{2}{5} &= 0 \\
 -a_{0, 1/2} \frac{2}{5} + a_{1, -1/2} (W_{1/2} + \frac{1}{5}) &= 0 \\
 a_{-1, 1/2} (W_{-1/2} + \frac{1}{5}) - a_{0, -1/2} \frac{2}{5} &= 0 \\
 -a_{-1, 1/2} \frac{2}{5} + a_{0, -1/2} (W_{-1/2} + \omega) &= 0 \\
 a_{-2, 1/2} (W_{-3/2} + \frac{2}{5} + \omega) - a_{-1, -1/2} \frac{1}{5} &= 0 \\
 -a_{-2, 1/2} \frac{1}{5} + a_{-1, -1/2} (W_{-3/2} - \frac{1}{5} + 2\omega) &= 0 \\
 a_{-2, -1/2} (W_{-5/2} - \frac{2}{5} + 3\omega) &= 0
 \end{aligned}$$

The quadratics were dealt with exactly as before, the normalizing equations being in this case as follows —

$$\begin{aligned}
 m = 5/2 & \quad a_{(2, 1/2)}^2 = 1, \\
 m = 3/2 & \quad (a_{1, 1/2})^2 + 4(a_{2, -1/2})^2 = 1, \\
 m = 1/2 & \quad 2(a_{0, 1/2})^2 + 3(a_{1, -1/2})^2 = 1, \\
 m = -1/2 & \quad 3(a_{-1, 1/2})^2 + 2(a_{0, -1/2})^2 = 1, \\
 m = -3/2 & \quad 4(a_{-2, 1/2})^2 + (a_{-1, -1/2})^2 = 1, \\
 m = -5/2 & \quad (a_{-2, -1/2})^2 = 1
 \end{aligned}$$

We now use these data to obtain the frequencies and intensities of the $s - p$ and $p - d$ doublet lines

s - p Doublets.

For the frequencies we have to take the differences of the *W*'s for the *s*-terms and the *p*-terms for all possible transitions of *j* and *m*, but as the process was given in detail for the triplets we do not describe it here. It is sufficient to say that the results are arranged in Table IV on exactly the same plan as the

Table IV *s - p* Doublets

	<i>j</i> (3/2 → 1/2)				<i>j</i> (1/2 → 1/2)			
	<i>ν</i>	<i>I</i>	<i>ν</i>	<i>I</i>	<i>ν</i>	<i>I</i>	<i>ν</i>	<i>I</i>
<i>m</i> → <i>m</i> - 1	3/2 → 1/2		1/2 → -1/2		1/2 → -1/2			
Weak	1 + $\frac{1}{2}m$	3	1 + $\frac{1}{2}m$	1	- 2 + $\frac{1}{2}m$	2		
<i>m</i> = 1/5	1 2	3 0	1 335	0 913	- 1 735	2 06		
<i>m</i> = 1/2	1 5	3 0	1 847	0 799	- 1 347	2 23		
<i>m</i> = 1	2 0	3 0	2 732	0 684	- 0 732	2 37		
<i>m</i> = 2	3 0	3 0	4 560	0 408	+ 0 440	2 59		
<i>m</i> = 5	6 0	3 0	10 312	0 144	3 686	2 86		
Strong	$m + 1$	3	$2m + \frac{3}{2}$	0	$m - 1 - \frac{2}{m}$	3		
<i>m</i> → <i>m</i> + 1	-1/2 → 1/2		-3/2 → -1/2		-1/2 → 1/2			
Weak	1 - $\frac{1}{2}m$	1	1 - m	3	- 2 - $\frac{1}{2}m$	2		
<i>m</i> = 1/5	0 967	1 096	0 8	3 0	- 2 267	1 922		
<i>m</i> = 1/2	+ 0 184	1 241	0 5	3 0	- 2 684	1 786		
<i>m</i> = 1	- 0 586	1 500	+ 0 0	3 0	- 3 414	1 500		
<i>m</i> = 2	- 2 000	2 005	- 1 0	3 0	- 5 000	1 002		
<i>m</i> = 5	- 5 552	2 720	- 4 0	3 0	- 10 446	0 275		
Strong	$-m - 1 + \frac{2}{m}$	3	$-m + 1$	3	$-2m - \frac{2}{m}$	0		
<i>m</i> → <i>m</i>	1/2 → 1/2		-1/2 → -1/2		1/2 → 1/2		-1/2 → -1/2	
Weak	1 - $\frac{1}{2}m$	4	1 + $\frac{1}{2}m$	4	- 2 - $\frac{1}{2}m$	2	- 2 + $\frac{1}{2}m$	2
<i>m</i> = 1/5	0 935	4 16	1 067	3 83	- 2 135	1 832	- 1 867	2 18
<i>m</i> = 1/2	0 847	4 43	1 184	3 52	- 2 347	1 592	- 1 684	2 48
<i>m</i> = 1	0 732	4 74	1 414	3 01	- 2 732	1 263	- 1 414	3 01
<i>m</i> = 2	0 560	5 18	2 000	2 005	- 3 560	0 814	- 1 000	4 00
<i>m</i> = 5	0 312	5 73	4 448	0 547	- 6 312	0 236	- 0 448	5 44
Strong	$0 + \frac{2}{m}$	6	$m - 1 + \frac{2}{m}$	0	$-m - 1 - \frac{2}{m}$	0	$0 - \frac{2}{m}$	6

corresponding ones in Table II, the frequencies appearing in the first half of each column and the intensities in the second half. The expressions for intensities take the following very simple form. As before, the denominators

can be omitted because the form of the normalising equation makes them all equal to unity, and where α is constant for all values of ω it has been included in the numerical factor

$$\begin{array}{ll}
 m \rightarrow m-1 & \begin{bmatrix} 1, 3/2 \rightarrow 0, 1/2 \\ 3/2 \rightarrow 1/2 \end{bmatrix} = 3 \\
 & \begin{bmatrix} 1, j \rightarrow 0, 1/2 \\ 1/2 \rightarrow -1/2 \end{bmatrix} = 6 (a_{1, 1/2}^1)^2 \\
 m \rightarrow m+1 & \begin{bmatrix} 1, j \rightarrow 0, 1/2 \\ -1/2 \rightarrow 1/2 \end{bmatrix} = 6 (a_{1, 1/2}^1)^2 \\
 & \begin{bmatrix} 1, 3/2 \rightarrow 0, 1/2 \\ -3/2 \rightarrow -1/2 \end{bmatrix} = 3 \\
 m \rightarrow m & \begin{bmatrix} 1, j \rightarrow 0, 1/2 \\ 1/2 \rightarrow 1/2 \end{bmatrix} = 6 (a_{0, 1/2}^1)^2 \\
 & \begin{bmatrix} 1, j \rightarrow 0, 1/2 \\ -1/2 \rightarrow -1/2 \end{bmatrix} = 6 (a_{0, 1/2}^1)^2
 \end{array}$$

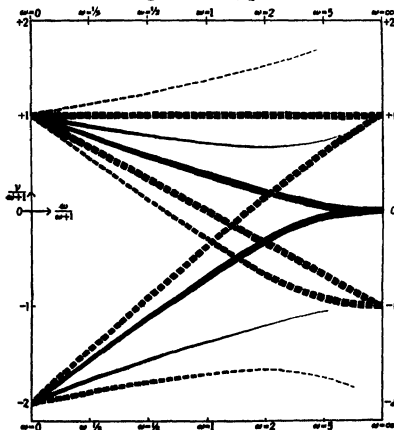


FIG. 2. $s-g$ doublets. The curves are plotted in the same way as in fig 1, and the intensities are again shown by the breadth of the lines.

The expressions hold for all values of j , and the straightforward calculation they involve needs no further comment

p - d Doublets

We have here to take the differences of the W 's for the p -terms and d -terms for all possible transitions. Again we will merely indicate the arrangement of the results. Table V gives all the lines arising from the transitions $j = 5/2 \rightarrow j = 3/2$ and $j = 5/2 \rightarrow j = 1/2$ the frequencies being placed in the first half of each column as before, and Table VI on an exactly similar plan gives the lines for $j = 3/2 \rightarrow j = 3/2$ and $j = 3/2 \rightarrow j = 1/2$. The calculation of intensities is considerably more laborious for the $p - d$ doublets than for the other two cases, as the general expressions do not reduce to such simple forms. We can give them, however, with their denominators omitted throughout, and with a omitted wherever it has the constant value unity for all strengths of field.

$$\begin{aligned}
 m \rightarrow m-1 \quad & \begin{bmatrix} 2, j \\ 5/2 \end{bmatrix} \rightarrow \begin{bmatrix} 1, j' \\ 3/2 \end{bmatrix} = 90 \\
 & \begin{bmatrix} 2, j \\ 3/2 \end{bmatrix} \rightarrow \begin{bmatrix} 1, j' \\ 1/2 \end{bmatrix} = 45 (a_{1,1/2}^2 a_{0,1/2}^{1,j'} + 4a_{2,-1/2}^2 a_{1,-1/2}^{1,j})^2 \\
 & \begin{bmatrix} 2, j \\ 1/2 \end{bmatrix} \rightarrow \begin{bmatrix} 1, j' \\ -1/2 \end{bmatrix} = 15 (2a_{0,1/2}^2 a_{-1,1/2}^{1,j} + 3a_{1,-1/2}^2 a_{0,-1/2}^{1,j})^2 \\
 & \begin{bmatrix} 2, j \\ -1/2 \end{bmatrix} \rightarrow \begin{bmatrix} 1, j' \\ -3/2 \end{bmatrix} = 30 (a_{0,-1/2}^2)^2 \\
 m \rightarrow m+1 \quad & \begin{bmatrix} 2, j \\ 1/2 \end{bmatrix} \rightarrow \begin{bmatrix} 1, j' \\ 3/2 \end{bmatrix} = 30 (a_{0,1/2}^2)^2 \\
 & \begin{bmatrix} 2, j \\ -1/2 \end{bmatrix} \rightarrow \begin{bmatrix} 1, j' \\ 1/2 \end{bmatrix} = 15 (3a_{-1,1/2}^2 a_{0,1/2}^{1,j} + 2a_{0,-1/2}^2 a_{1,-1/2}^{1,j})^2 \\
 & \begin{bmatrix} 2, j \\ -3/2 \end{bmatrix} \rightarrow \begin{bmatrix} 1, j' \\ -1/2 \end{bmatrix} = 45 (4a_{-2,1/2}^2 a_{-1,1/2}^{1,j} + a_{-1,-1/2}^2 a_{0,-1/2}^{1,j})^2 \\
 & \begin{bmatrix} 2, j \\ -5/2 \end{bmatrix} \rightarrow \begin{bmatrix} 1, j' \\ -3/2 \end{bmatrix} = 90 \\
 m \rightarrow m \quad & \begin{bmatrix} 2, j \\ 3/2 \end{bmatrix} \rightarrow \begin{bmatrix} 1, j' \\ 3/2 \end{bmatrix} = 90 (a_{1,1/2}^2)^2 \\
 & \begin{bmatrix} 2, j \\ 1/2 \end{bmatrix} \rightarrow \begin{bmatrix} 1, j' \\ 1/2 \end{bmatrix} = 60 (2a_{0,1/2}^2 a_{0,1/2}^{1,j'} + 3a_{1,-1/2}^2 a_{1,-1/2}^{1,j'})^2 \\
 & \begin{bmatrix} 2, j \\ -1/2 \end{bmatrix} \rightarrow \begin{bmatrix} 1, j' \\ -1/2 \end{bmatrix} = 60 (3a_{-1,1/2}^2 a_{-1,1/2}^{1,j'} + 2a_{0,-1/2}^2 a_{0,-1/2}^{1,j'})^2 \\
 & \begin{bmatrix} 2, j \\ -3/2 \end{bmatrix} \rightarrow \begin{bmatrix} 1, j' \\ -3/2 \end{bmatrix} = 90 (a_{-1,-1/2}^2)^2
 \end{aligned}$$

The results appear in Table V and VI, and it will be noticed that the intensities of the "forbidden lines" ($j = 5/2 \rightarrow j = 1/2$) are zero at strong and weak fields, and rise to a small value (in no case above 15) at intermediate fields.

It may be remembered that in Table II we checked the intensities of the triplets by taking their sum at each strength of field. We have not recorded this detail for the doublets, but when a similar summation is carried out in this case we find that the total intensity for either set of the perpendicular components comes to 300, and that for the parallel components to 600, with a maximum error of 1 in 300.

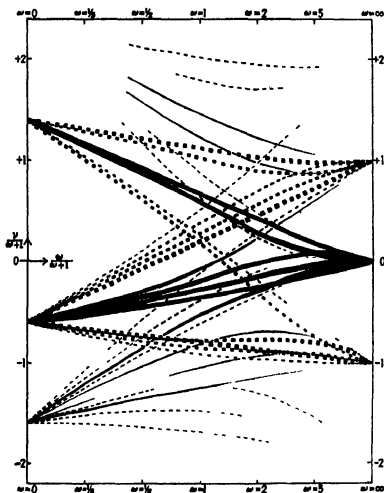


FIG. 3. $p-d$ doublets. The curves are plotted in the same way as in fig. 1, but in order to include the weaker lines the breadth of the curves could not be made strictly proportional to the intensities.

Table VI $p - d$ Doublets.

		$f(3/2 \rightarrow 3/2)$						$f(1/2 \rightarrow 1/2)$					
		p	I	p	I	p	I	p	I	p	I	p	I
$m \rightarrow m - 1$	Weak	$-\frac{1}{2} + \frac{1}{2}m$	6	$-\frac{1}{2} + \frac{1}{2}m$	6	$-\frac{1}{2} + \frac{1}{2}m$	6	$-\frac{1}{2} + \frac{1}{2}m$	6	$-\frac{1}{2} + \frac{1}{2}m$	6	$-\frac{1}{2} + \frac{1}{2}m$	6
	$m = 1/5$	-1 500	7 20	-1 305	9 04	-1 239	7 50	-1 370	75 8	-1 320	25 00	-1 370	75 8
	$m = 1/2$	-1 277	8 24	-1 125	11 00	-0 962	9 70	-1 817	77 3	-1 728	98 90	-1 817	77 3
	$m = 1$	-1 229	8 10	-0 788	12 55	-0 232	12 28	-2 235	79 4	-2 040	23 85	-2 235	79 4
	$m = 2$	-1 026	8 28	-0 804	9 80	+0 876	14 02	-3 084	81 9	-2 068	22 80	-3 084	81 9
	$m = 3$	-0 743	2 545	+0 307	2 780	-3 852	14 08	-5 081	88 5	-5 203	41 80	-5 081	88 5
Strong		$-\frac{2}{5} - \frac{5}{25}m$	6	$\frac{4}{5} - \frac{5}{25}m$	0	$-\frac{6}{5} - \frac{5}{25}m$	15	$-\frac{2}{5} + \frac{4}{5} - \frac{5}{25}m$	90	$-\frac{1}{5} + \frac{4}{5} - \frac{5}{25}m$	45	$-\frac{1}{5} + \frac{4}{5} - \frac{5}{25}m$	45
$m \rightarrow m + 1$	Weak	$-\frac{1}{2} - \frac{1}{2}m$	6	$-\frac{1}{2} - \frac{1}{2}m$	6	$-\frac{1}{2} - \frac{1}{2}m$	6	$-\frac{1}{2} - \frac{1}{2}m$	6	$-\frac{1}{2} - \frac{1}{2}m$	6	$-\frac{1}{2} - \frac{1}{2}m$	6
	$m = 1/5$	-1 928	4 080	-1 024	5 870	-1 714	4 240	-1 248	24 05	-1 220	72 2	-1 248	24 05
	$m = 1/2$	-2 451	3 130	-2 209	2 275	-1 940	1 232	0 985	22 30	0 928	68 6	0 985	22 30
	$m = 1$	-3 374	1 882	-2 944	0 879	-2 451	0 232	+0 500	19 54	+0 267	57 1	+0 500	19 54
	$m = 2$	-5 204	0 640	-4 804	0 023	-3 804	3 085	-0 564	16 61	-0 806	44 6	-0 564	16 61
	$m = 3$	-11 245	0 190	-10 38	0 033	-9 292	1 472	-3 788	14 90	-4 297	43 7	-3 788	14 90
Strong		$-\frac{2}{5} - \frac{6}{5} - \frac{5}{25}m$	0	$-\frac{2}{5} - \frac{6}{5} - \frac{5}{25}m$	0	$-\frac{2}{5} + \frac{6}{5} - \frac{5}{25}m$	0	$-\frac{2}{5} + \frac{4}{5} - \frac{5}{25}m$	15	$-\frac{1}{5} + \frac{4}{5} - \frac{5}{25}m$	45	$-\frac{1}{5} + \frac{4}{5} - \frac{5}{25}m$	45
$m \rightarrow m$	Weak	$-\frac{1}{2} - \frac{1}{2}m$	18	$-\frac{1}{2} - \frac{1}{2}m$	2	$-\frac{1}{2} + \frac{1}{2}m$	2	$-\frac{1}{2} + \frac{1}{2}m$	2	$-\frac{1}{2} + \frac{1}{2}m$	2	$-\frac{1}{2} + \frac{1}{2}m$	2
	$m = 1/5$	-1 765	13 15	-1 043	0 554	-1 556	4 510	-1 417	24 8	-1 407	98 2	-1 417	24 8
	$m = 1/2$	-3 020	8 06	-1 788	0 005	-1 546	9 76	-1 256	39 65	-1 206	98 5	-1 256	39 65
	$m = 1$	-2 497	8 02	-2 106	0 714	-1 848	17 09	-1 047	65 2	-1 358	92 2	-1 047	65 2
	$m = 2$	-3 498	1 806	-2 884	1 713	-2 124	17 54	-0 806	84 0	-1 256	98 4	-0 806	84 0
	$m = 3$	-6 431	0 452	-5 537	1 123	-4 495	5 46	-0 845	89 4	-1 067	88 9	-0 845	89 4
Strong		$-\frac{7}{5} - \frac{4}{5} - \frac{5}{25}m$	0	$-\frac{7}{5} - \frac{4}{5} - \frac{5}{25}m$	0	$-\frac{7}{5} + \frac{4}{5} - \frac{5}{25}m$	0	$-\frac{4}{5} + \frac{4}{5} - \frac{5}{25}m$	90	$-\frac{4}{5} + \frac{4}{5} - \frac{5}{25}m$	45	$-\frac{4}{5} + \frac{4}{5} - \frac{5}{25}m$	45

The Analysis of the Absorption Spectrum of Cobalt Chloride in Concentrated Hydrochloric Acid

By WALLACE R BRODE, Ph D, Fellow of the John Simon Guggenheim Memorial Foundation, Liverpool University

(Communicated by E O C Baly, F R S—Received 15th December, 1927)

[PLATE 7]

This paper presents the absorption spectrum of cobalt chloride in concentrated hydrochloric acid as a solvent, and a discussion of the data obtained with regard to certain theoretical possibilities of its complex structure. No attempt has been made to present or discuss theories concerning the nature of the cobalt ions or complexes in various solutions and compounds.

The absorption spectrum of cobalt chloride in hydrochloric acid has been observed and studied by a number of investigators*. In many of the earlier papers the work was qualitative in character and the complexity of the absorption band was undetected. In the first of these investigations the band was recorded as a smooth curve with but two or three apparent maxima. With an increase in the accuracy of the methods and apparatus for absorption spectra measurement, recent observers have resolved this complex band into four bands.

Because of the apparent complexity of the absorption band and the possibilities of the application of these component parts to absorption spectra theories as well as to the determination of the nature of the cobalt ion in the solution, it was felt desirable to make a detailed study of the absorption spectrum of this coloured solution. The observations were, for the most part, made on a new model of the Hilger-Nutting spectrophotometer. Seven bands of rather high intensity, as well as two weak bands, were observed in this investigation. It has been possible to analyse this complex band into components by a mathematical procedure, and it has been further shown that a definite mathematical relation exists between these analysed component bands.

* Russell, 'Roy Soc Proc,' vol 32, p 258 (1881), Hartley, 'Trans Roy Soc Dublin,' (2) vol. 7, p 263 (1900), 'J Chem. Soc.,' vol 83, p 401 (1903), Jones and co-workers, 'Am. Chem. J.,' vol 37, p. 126 (1907), Publications of the Carnegie Institution of Washington, Nos 60, 110, 130, and 160, Hill and Howell, 'Phil Mag.,' vol 48, p 833 (1924).

Apparatus and Solutions

The apparatus used in this investigation was a new model of the Hilger-Nutting* spectrophotometer. In this instrument the essential parts, i.e., light source, light deflectors, photometer, and spectrometer, are all mounted on a single rigid metal base, and other improvements have been made which have increased the accuracy and general scope of the apparatus. The cells used consisted of glass tubes and end plates which could fit in an adjustable holder for various lengths of tubing. In general 0.5 cm. cells were used, but for observations on extremely dilute and concentrated solutions, cells varying from 0.05 to 10.0 cm. were used. The solutions were prepared from a reagent quality of nickel free cobalt chloride ($\text{CoCl}_2 \cdot 6\text{H}_2\text{O}$) which had been recrystallized from distilled water. The hydrochloric acid used as the solvent was the synthetic material containing quality of approximately 37 per cent HCl. Measurements made on the same solution at various times over a period of several days gave no indication of any change in the intensity of the absorption bands.

Method of Observation

Each indicated observation point in the data herewith presented represents the average of not less than ten separate photometer readings at the selected wave-length. Observations were made at every 2 m μ from 715 to 575 m μ , and at every 5 m μ from 575 to 440 m μ . The data are presented graphically in fig. 1, and the average values, together with the average deviations, are recorded in Table I. Although in previous papers† the method of setting the transmission at definite extinction coefficient values and coming to a match by adjustment of the wave-length has been recommended, in the case of these cobalt chloride solutions this procedure would have failed to give the accuracy necessary for the resolution of the general absorption band into its components. This earlier suggested method of observation is intended for the study of bands which are quite sharp and pointed. The absorption spectrum of cobalt chloride in hydrochloric acid presents a rather flat band, so that the setting of the wave-length to definite values and the adjustment of the extinction coefficient by means of the photometer yield more accurate and consistent results.

A study of Table I will give a definite idea of the accuracy of the data presented. It will be noticed that in general the average deviation is less

* Adam Hilger, Ltd., London.

† Brode, 'J. Am. Chem. Soc.', vol 46, p 581 (1924)

than 0.025 units in the extinction coefficient and that the error of observation in most cases is less than the size of the circle used to indicate the observed points in fig. 1.

Table I—Absorption Spectrum Data for Cobalt Chloride in a concentrated Hydrochloric Acid Solution between Wave-length values of 720 and 595 $m\mu$. Concentration = 0.10 g $\text{CoCl}_2 \cdot 6\text{H}_2\text{O}$ per 100 cc of solution. Cell thickness = 0.5 cm

Wave Length ($m\mu$)	Frequency (f)	No of Observations	Extinction Coefficient	
			Average	Av Deviation from the mean
720	416.6	6	0.420	0.045
715	418.9	8	0.385	0.032
711	421.9	10	0.303	0.038
709	423.1	10	1.032	0.032
707	424.3	10	1.082	0.027
705	425.5	10	1.207	0.013
703	426.7	10	1.257	0.025
701	427.9	11	1.334	0.015
699	429.1	12	1.358	0.036
697	430.4	12	1.413	0.030
695	431.7	18	1.460	0.022
693	432.9	10	1.457	0.019
691	434.1	12	1.404	0.025
689	435.3	10	1.364	0.028
687	436.8	10	1.330	0.020
685	438.0	14	1.312	0.022
683	439.2	12	1.302	0.029
681	440.4	10	1.323	0.019
679	441.9	10	1.340	0.026
677	443.1	11	1.331	0.034
675	444.4	10	1.314	0.019
673	445.7	10	1.363	0.025
671	447.1	10	1.396	0.026
669	448.4	14	1.392	0.019
667	449.7	12	1.384	0.020
665	451.1	12	1.357	0.014
663	452.5	10	1.337	0.021
661	453.8	10	1.306	0.014
659	455.2	10	1.269	0.022
657	456.6	12	1.175	0.027
655	458.0	10	1.067	0.031
653	459.4	12	0.993	0.023
651	460.8	10	1.008	0.028
649	462.2	10	0.982	0.024
647	463.7	14	0.974	0.020
645	465.1	10	0.953	0.049
643	466.5	10	0.913	0.024
641	468.0	10	0.895	0.028

Table I—(continued)

Wave length (m μ .)	Frequency (f)	No of Observations.	Extinction Coefficient	
			Average	Av Deviation from the mean.
639	469.5	10	0.878	0.025
637	470.9	13	0.885	0.018
635	472.4	11	0.914	0.024
633	473.9	12	0.921	0.025
631	475.4	14	0.928	0.029
629	476.9	11	0.932	0.027
627	478.4	10	0.920	0.019
625	480.0	10	0.896	0.023
623	481.5	10	0.864	0.020
621	483.1	10	0.800	0.021
619	484.6	10	0.777	0.031
617	486.2	10	0.730	0.028
615	487.8	10	0.724	0.023
613	489.3	10	0.748	0.024
611	490.9	10	0.752	0.029
609	492.6	10	0.707	0.027
607	494.3	10	0.645	0.030
605	495.8	10	0.410	0.045
603	497.5	8	0.302	0.032
601	499.1	8	0.274	0.033
599	500.8	7	0.238	0.026
597	502.5	5	0.211	0.030
595	504.1	5	0.179	0.046

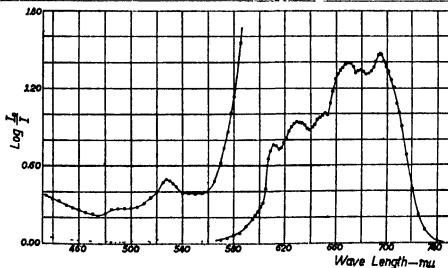
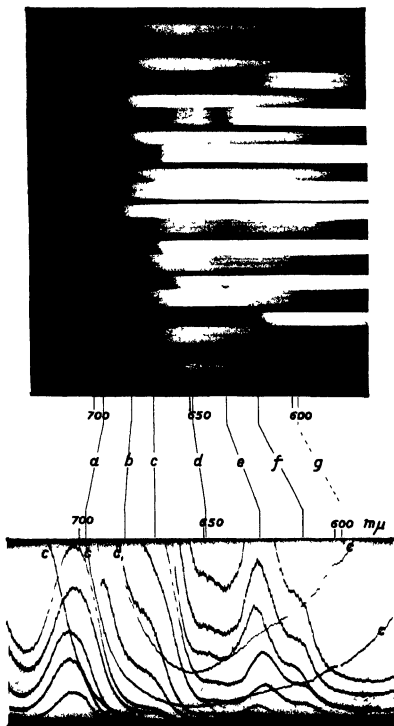


FIG. 1.—The Absorption Spectrum of Cobalt Chloride in concentrated Hydrochloric Acid, (a) 570 to 740 m μ ; concentration = 1.00 g. of $\text{CoCl}_2 \cdot 6\text{H}_2\text{O}$ per litre of solution, cell thickness = 0.5 cm. (b) 435 to 585 m μ ; concentration = 12.0 g. of $\text{CoCl}_2 \cdot 6\text{H}_2\text{O}$ per litre of solution, cell thickness = 0.5 cm.

To check the data obtained by the Hilger-Nutting spectrophotometer method and to remove the possibility of personal or instrumental error, photographs were made with Ilford panchromatic plates on a Judd-Lewis photometer and a Littrow spectrograph. These plates were read by means of a Moll recording microphotometer. The spectrum between 600 and 700 $m\mu$ (1.5 cm. on the plate) was magnified to 15 cm. by the recording microphotometer. Plate 7 shows a portion of one of these plates and an "exhibition" set of photometer readings. In this set of photographs, as was true with all other observations given in this paper, a comparison cell of the same length containing the solvent was used. These comparison photographs are the upper spectrum in the upper half of the plate and the lower spectrum in the lower half, the cells being reversed in the photometer to correct slight instrumental deviations. Because of the rather small slit used, 0.10 mm., a number of slit lines appear in the photograph, but these did not interfere with the photometer observations which measured the photographic density of the entire width of the spectrum photograph. The photometer record under the photograph in Plate 7 was prepared from the plate above it for illustrative purposes. In making the actual measurements on this and other plates only one absorption spectrum, together with its corresponding comparison spectrum and reference line for wave-length calibration were recorded on a photometer strip. Only three comparison spectra photographs (c) are recorded on the photometer strip in Plate 7. These show the steep falling off on the left or red side of the plate caused by the decrease in the sensitivity of the plate and a more gradual falling off of the plate density on the right, caused by an amber screen which was placed in front of the two photometer beams so as to cut off the unwanted blue portion of the spectrum and prevent to some extent fogging of the plate by stray light. From the data thus obtained (Table II) and as can also be seen in the photographs and photometer curves, the existence and position of the absorption bands observed by the Hilger-Nutting spectrophotometer method have been confirmed.

Discussion of Data

A study of fig. 1 will show the presence of seven bands in the intense portion of the spectrum and two or more in the weak portion (575 to 440 $m\mu$). Since the absorption band at 528 has a molecular extinction coefficient of less than 1/200 that of the first (a) intense band, it becomes negligible when recorded on the same scale of concentration and thickness as the intense bands. For the present this band will be left out of the discussion although it will be



referred to again in later papers. These seven bands appear on first observation to be at wave-length values of 695, 679, 666, 648, 626, 610, and 595 $m\mu$. In the study of the relations between bands in absorption spectra, as well as series phenomena in other branches of spectroscopy, it is more convenient to record or plot the data on a frequency scale instead of a wave-length scale. When plotted on a frequency scale, constant frequency differences and other similar effects can be readily observed. The apparent maxima positions of the seven bands, as shown in fig 2, occur at the following frequency values 432, 442, 450, 465, 478, 491 and 505 f (f = fresnel = vibrations + seconds $\times 10^{12}$). For convenience in the discussion of these bands they may be designated as $a, b, c, d, e, f,$ and g , commencing with the band of lowest frequency (429 f)

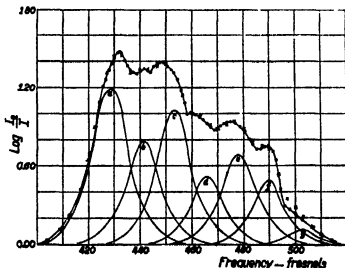


FIG. 2.—The Absorption Spectrum of Cobalt Chloride in concentrated Hydrochloric Acid and its Analysis into Component Bands

It will be noticed (Table II) that the differences between these frequency values are not constant, but a comparison of these values with the graph (fig 2) will to a considerable extent explain these differences. For example, when two nearly equal similar bands or curves add together to produce a compound curve, the resulting maxima of the compound curve will be nearer together than the maxima of the two components. (For a more extended discussion of this effect, with practical examples, reference may be made to a forthcoming article* by the author, on the effect of position isomerism on

* 'J. Am. Chem. Soc.'

the absorption spectra of simple azo dyes) This reasoning may also be applied to the two outer members of a three component compound curve, and in cases where the resulting maxima of the compound curve are approximately the same intensity, the frequency of the centre component may be assumed to be approximately at its true frequency A further study of the addition effects of three similar curves to produce a compound curve will show that where the bands are intense, the apparent maxima of the compound curve will be nearer together than the apparent maxima of a less intense similar compound curve

From the above generalizations we may take (b) and (c) as being at frequencies 442 and 478 f respectively The differences between (a) and (b), and between (b) and (c) should be less than the differences between (d) and (e) and between (e) and (f), and this is confirmed in Table II An examination of a very concentrated solution failed to reveal any band near 400 f, so it may be assumed that the low frequency side of component (a) is, for a considerable distance along the curve, the same as the observed compound curve

Further advance in the resolution or analysis of this complex band into its components may now be made in two different directions, both of which in the end give the same results and thereby lend additional weight to the veracity of the necessary assumptions The first method requires the assumption that these component bands be of the same general shape The term "same general shape" means that the extinction coefficient at any point on the curve is to the extinction coefficient of a point at equal frequency distance from the maximum of any other curve of the series as the respective extinction coefficients of their maxima are to each other A consideration of this assumption will show that, for a given compound curve, only one set of such bands of a definite number can be constructed, and also that all compound curves are not capable of being so resolved into such a series of bands The fact that this curve is capable of being so resolved is in itself an argument for the treatment of the observed curve or absorption band as a series of compounded curves Additional argument is found in the facts that these constructed curves of similar shape are equally spaced, and also that the frequencies of these constructed curves are integral multiples of this constant frequency difference

Table II—The Positions of the Maxima of the component Bands

Band	Observed Hilger-Nutting Method			Judd-Lewis-Lattrow Method ($m\mu$)
	Wave-Length ($m\mu$)	Frequency (f)	Diff	
a	695	432	10	(697)
b	679	442	8	(680)
c	666	450	15	672
d	648	465	13	649
e	626	478	13	620
f	610	491	14	613
g	(595)	(505)		(595)
		Av Diff	12 2	

Values in parentheses are not as accurate as the other observations

Calculated

Method 1		Method 2		Multiple relations	Band No
(f)	Diff	(f)	Diff		
429	13	429 80	12 28	$12\ 28 \times 35 = 429\ 80$	35
442	12	442 08	12 28	$12\ 28 \times 36 = 442\ 08$	36
454	12	454 36	12 28	$12\ 28 \times 37 = 454\ 36$	37
466	12	466 64	12 28	$12\ 28 \times 38 = 466\ 64$	38
478	12	478 92	12 28	$12\ 28 \times 39 = 478\ 92$	39
490	14	491 20	12 28	$12\ 28 \times 40 = 491\ 20$	40
504		503 48		$12\ 28 \times 41 = 503\ 48$	41
Av Diff	12 5	Av Diff	12 28		

The second method of attack is to assume that these bands are symmetrical, although not necessarily similar in shape, and that a constant frequency difference, which may be approximately determined from column four of Table II, exists between the bands. The assumption of a constant frequency

difference has some basis in the fact that with the exception of certain small variations which can be explained, the apparent maxima have approximately the same frequency differences. From these assumptions, the known positions of bands (b) and (c) and the shape of the low frequency side of band (a) it is possible to construct a series of curves which will add together to produce the observed compound curve. This second method of analysis is not as applicable as the first, except in the case of compound curves consisting of but two components, when certain restrictions with regard to the symmetry may be modified. In the analysed curves of cobalt chloride, the curves were approximately symmetrical and this method could be applied with success.

In fig 2 the \times values are those obtained by the addition of the constructed curves. The curves obtained by both methods of analysis were identical in shape and frequency position. From these curves the constant frequency difference was determined as 12.28 f and the multiple values of this fundamental value represented by the component bands are respectively (a) = 35, (b) = 36, (c) = 37, etc., to (g) = 41.

With regard to the intensities of the various components, it should be noted that the odd and even numbered bands, calling (a) 35, (b) 36, etc., form separate series, and that in this particular case the intensities of the odd numbered bands are greater than the next higher even numbered band. This effect will be discussed in greater detail in further papers on this subject.

A similar method of analysis has been applied to the bands observed in potassium permanganate* which have been shown to exist as similar components at constant frequency differences. These observations were again checked and this relation confirmed before starting on the study of the cobalt chloride absorption band in hydrochloric acid. Chromic anhydride† presents an absorption spectrum with marked inflections, which has recently been resolved into a series of integral bands with equal frequency differences. Other inorganic materials whose absorption bands have been shown to consist of integrally related bands with constant frequency differences include uranyl salts‡ and certain nitrates§.

* Hagenbach and Percy, 'Helv. Chem. Acta,' vol 5, p 454 (1922)

† Viterbi and Kraus, 'Gazz. Chim. Ital.,' vol. 57, p 690 (1927)

‡ Jones, 'Publication of the Carnegie Institution of Washington,' No 160 (1911)

§ Morton and Riding, 'Roy. Soc. Proc.,' A, vol 113, p 717 (1927).

Summary

1 The absorption spectrum of cobalt chloride in concentrated hydrochloric acid as a solvent has been determined between wave-length values of 750 and 440 m μ .

2 The principal absorption band has been shown to consist of at least seven component bands

3 The observed absorption curve can be resolved into seven similarly shaped bands of different intensities, which can be added together to produce the observed curve

4 A constant frequency difference exists between adjacent bands

5 The frequencies of these component bands are integral multiples of this constant frequency difference

6 There appears to be a relation between the odd and even numbered multiples and their relative intensities of absorption

Acknowledgment is made to Dr R A Morton who suggested this problem and has materially assisted in the carrying out of the work. The author also wishes to thank Prof E C C Baly, F R S, for his helpful suggestions and permission to use certain apparatus in the carrying out of this work, and the John Simon Guggenheim Memorial Foundation for financial assistance

DESCRIPTION OF PLATE 7

Photographic measurements on the absorption spectrum of Cobalt Chloride in concentrated Hydrochloric Acid made on a Littrow Spectrograph with Judd-Lewis Photometer, and measurements of the photographic density of the plate as recorded by a Moll recording Microphotometer

*The Distribution of Intensity in the Band Spectrum of Helium
the Band at λ 4650.*

By W H J CHILDS, B Sc, Demonstrator in Physics, King's College,
London

(Communicated by O W Richardson, F R S—Received December 15, 1927)

Introduction

A recent development* of the analysis of the band spectrum of helium, by which the absence of certain lines in the various branches is explained and the quarter quantum numbers are replaced by half integers, makes it appear probable that alternate lines are entirely missing, *i.e.*, a set of rotation states is completely suppressed. Valuable information regarding this phenomenon (of which few examples are as yet known) may be expected from a study of the intensity relations in this spectrum. Such intensity relations can be predicted by expressions which have been developed of late with the aid of the correspondence principle and summation rules, but which by reason of the lack of sufficiently accurate quantitative intensity measurements have so far been little tested. It is thought that the measurements described in this paper, whilst not yet entirely free from photographic peculiarities are a sufficient improvement on those previously available, which have been obtained by eye estimation† or by microphotometer,‡ to warrant their use in a comparison with the predicted values.

Experimental Details

(a) *Apparatus*—The tubes used were three in number. The first was of the ordinary Plücker form, with narrow capillary, the bands being well developed in the bulbs when excited by the condensed discharge with a small spark gap. The pressure of the contained helium was of the order of 1 cm. and a small amount of hydrogen was present. The second tube was T-shaped and was constructed of 15 mm. bore tubing, except for the upper half of the stem, which was made of 6 mm. bore tube. The electrodes were of copper strip sealed directly into the glass. The third tube was the usual straight pattern, but in this case the bulbs were made of 25 mm. bore tube with a connecting piece of

* R. S. Mulliken, 'Phys. Rev.', vol. 23, p. 1202 (1926)

† Curtis and Long, 'Roy. Soc. Proc.', A, vol. 108, p. 513 (1925)

‡ McLennan, Smith and Lea, 'Roy. Soc. Proc.', A, vol. 113, p. 183 (1926)

elliptical cross section. The electrodes were again of copper strip but in this case covered with a layer of electrolytically deposited silver.

The tubes were excited either by means of an induction coil and mercury break, or by a transformer. The details of the discharge circuit are given in the accompanying diagram No. 1. *K* is an adjustable parallel plate condenser of

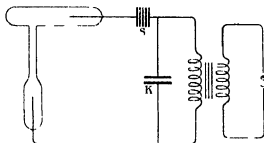


FIG. 1

a few millimicrofarads capacity and *S* represents a multiplate quenched spark gap. The two larger tubes when excited by means of the transformer furnished sources of band spectra of considerable intrinsic brilliancy.

Most of the plates were obtained with the Hilger constant deviation spectrometer with camera attachment but in one case a large quartz spectrograph (Hilger E I) was used.

Three types of photographic plate were employed, namely, Ilford special rapid panchromatic, Imperial Eclipse, and Ilford Empress.

(b) *Method* — The method finally adopted after a series of trials may be outlined as follows —

The spectrum is photographed in the ordinary way, but each plate is calibrated by exposing it (with the same exposure time as was necessary for the band spectrum) to a number of sources whose relative intensities are known. The plate is then developed and the densities of both the lines and calibration marks obtained by means of devices which will be described in another paper. From the measurements on the calibration marks a curve connecting light intensity with photographic density can be drawn, and this can then be used to translate the densities of the band line images into relative intensities.

The calibration marks were obtained by means of a stepped aperture, which was illuminated by a tungsten filament lamp, and a cylindrical lens. In this way there were projected on to the slit of the spectroscope five strips of increasing intensity. A plate exposed to these showed on development five images (of continuous spectra) of progressively increasing density.

The intensity scale was examined in the following manner. Two sets, say, A and B, of intensity marks were obtained on a plate, the intensities in set A being approximately $4/3$ those in set B. The densities of each set of images were then measured and plotted against intensity mark number, and in each case a smooth curve drawn through the points so obtained. It is now necessary to search for points in A and B which have the same density. Suppose mark No. 1 in set A has the same density as that of 1.5 (obtained by interpolation) in set B, and also that 1.5 in set A has the same density as that of 2 in set B. From this information it is deduced that intensity mark 1.5 has $4/3$ the intensity of mark 1, and that mark 2 has $4/3$ the intensity of mark 1.5. Proceeding in this manner the relative intensities over the whole scale can be determined.

Since the band under discussion is at $\lambda 4650 \text{ \AA}$, it is not to be expected that the result will be seriously affected by variations of plate sensitivity. The sensitivity curve of the plates was roughly estimated by making use of the assumption that the calibration lamp gave the black body distribution of intensity corresponding to its "colour temperature".* The temperature of the filament, under the conditions of use, was obtained from the resistances at room and working temperatures and was found to be 2300° A , in close agreement with a check value obtained with a pyrometer. The corresponding colour temperature is 2350° A . Making use of the relation

$$J_\lambda = \alpha \lambda^{-5} e^{-\frac{c}{\lambda T}} \text{ where } \alpha = 1.445 \text{ cm degree,}$$

the following values of spectral distribution are obtained ---

J_λ	λ
1.00	4625 \AA
1.10	4685 \AA
1.18	4730 \AA

The dispersion of the prism did not need to be taken into account since over this narrow range it was found to be linear.

Measurements of the calibration marks on the plates were made for four wavelengths $\lambda\lambda 4626, 4656, 4687, 4719$, and the results showed that over the region occupied by the $\lambda 4650 \text{ \AA}$ band the plate sensitivity was constant.

* Hyde, Cady and Forsythe, 'Phys. Rev.', vol 10, p 401 (1917), also "Report on Properties of Tungsten," Worthing and Forsythe, 'Intern. Comm. Illum.'

Methods used for Measuring Densities

Densities were obtained from the photographic plates by four methods, as shown in the table of results. These methods will be described more fully elsewhere, a summary only is given here.

*Selenium Cell used as a Photometer—Method of Fournier d'Albe **

An enlarged image of the photographic plate, formed by a suitable projection device, is thrown on to a linear selenium cell. By an occulting mechanism this cell is illuminated and darkened for equal periods of time, the amplitude of the resulting galvanometer deflection being taken as a measure of the intensity of the light falling on the cell. If it is required the cell can be calibrated so that true photographic densities may be obtained, but such a proceeding is unnecessary when calibration marks are present on a plate. Variations in the cell constants and the candle power of the projection lamp will affect the measurements, so that the next method is to be preferred.

Selenium Cell used as a Photometer—Method of Toy and Rawlins †

A modification of this method was used. An auxiliary lamp in the same circuit as the projection lamp is used, with a shutter device to vary the intensity, to illuminate the cell. A suitable switching arrangement enables either lamp to be used, the shutter is adjusted until on changing over from one lamp to the other there is no variation in the resistance of the selenium. The reading of the shutter is then taken as a measure of the light transmitted by the photographic plate. Again it is unnecessary to calibrate the shutter if calibration marks are on each plate.

Optical Photometer ‡

This was available through the courtesy of Dr I. C. Martin. The plate is examined by means of a microscope with a field of view consisting of two parts. One of these is illuminated by light transmitted by a small portion of the plate, the other by light which has traversed an absorbing wedge. The wedge is adjusted until the two parts of the field have equal intensities, when the position of the wedge is taken as a measure of the intensity of the light transmitted by the plate.

* 'Roy Soc Proc,' A, vol 89, p 75 (1913)

† 'Proc Phys Soc,' vol 36, p 432 (1924)

‡ 'Trans Opt. Soc,' vol 26, p 109 (1924)

Moll Recording Apparatus (and laboratory model)*

The principle of this type of densitometer is well known. Unfortunately only low resolving power apparatus was available. The record with the Moll apparatus was obtained by Messrs Adam Hilger.

Results of Measurements

Four plates were suitable for measurement. These will be referred to as A, B, C and D. Particulars of them are given in the accompanying table.

Plate	Type of Plate	Discharge	Tube No	Spectrograph	Remarks
A	I S R P	Coil	2	C D	Calibrated
B	I E	Transformer	3	C D	"
C	I S R P	Transformer	3	C D	"
D	I S R P	Coil	1	E 1	Uncalibrated

I S R P = Ilford special rapid panchromatic
I E = Ilford Empress

Most attention was given to A and B, C and D were regarded as supplying checking results. The details are given in the following tables Nos I, II and III, the weighted means of the measurements of plates A and B have also been plotted and are shown in figs 2, 3, 4. The intensities in these diagrams have been multiplied by a factor such that in each case the strongest line has intensity 100.

Results for Plate A

Table I

The intensities are given in the arbitrary units as obtained from the intensity scale supplied by the calibration marks.

Weight	P2	P3	P4	P5	P6	P7	P8	Method of density measurement used
3	19.5	32	33	30	25.5	19.5	11.5	Selenium cell used as a photometer by method of Fournier d'Albe
3	18	33	33.5	30	24	16.5	8	
2	18	35	36	32	28	20	13	
5	23	34	35	31	25	19	—	Selenium cell used as a photometer by method of Toy and Rawlings Optical microphotometer of Dr Martin Method of Toy and Rawlings
3	24	33	35	31	27	22	—	
5	20	33	36	31	24	17	—	

* 'Proc. Phys. Soc.', vol 33, p 207 (1921)

Table I —(continued)

Q1	Q2	Q3	Q4	Q5	Q6	Q7	Q8	R'1	R'2	R'3	R'4	R'5	R'6 + R'7
30	43	46 5	43	37	31	27 5	18 5	33	32	32	31	28 5	27
29 5	43	47 5	45	39 5	35	25	15 5	32	31	31 5	30 5	24	27
31	46	53	48	44	38	29	23	49	49	49	45	41	40
32	45	51	47 5	42	37	28	22	32	32	34	32	29	29
—	48	54	51	43	37	28	—	33	35	33	31	28	28
34	44	49	46	42	37	28	18	34	33	34	32	29	30

The weights assigned and methods used are the same as given in the table of P lines

Weighted Means —

P1	P2	P3	P4	P5	P6	P7	P8
—	20 5	33	35	31	25	19	11
Q1	Q2	Q3	Q4	Q5	Q6	Q7	Q8
32	44 5	50	47	41	36	27 5	19 5
R'1	R'2	R'3	R'4	R'5	R'6 + R'7		
34 5	34	34 5	33	29	29 5		

Results for Plate B

Table II

The intensities are given in the arbitrary units as obtained from the intensity scale supplied by the calibration marks

Owing to the poor results obtained from the recording densitometers these were not included when taking the weighted mean

Weight	P2	P3	P4	P5	P6	P7	P8	Method of density measurement used
3	35	46	46	41	27	19	—	Selenium cell used as a photometer by method of Fournier d'Albe
3	36	49	47	43	30	21	—	" " "
5	37	49	47	44	30	22	—	" " "
5	37	51	50	40	29	19	—	Selenium cell Method of Toy and Rawling
4	36	51	50	43	31	—	—	Optical microphotometer of Dr Martin
—	—	30	29	27	19	15	—	Moll self recording densitometer
—	30	38	38	35	24	—	—	Laboratory self recording densitometer

Table II- (continued)

Q1	Q2	Q3	Q4	Q5	Q6	Q7	Q8	R'1	R'2	R'3	R'4	R'5	R'6+R'7
47	66	70	63	54	44	27	7	54	49	47	40	29	27
51	67	72	64	53	45	29	18	54	51	49	44	33	33
53	66	69	62	55	47	30	15	57	54	52	45	34	33
53	67	71	65	58	48	29	15	59	57	54	47	35	36
52 5	66 5	71	65 5	56 5	43	31	—	56 5	55	49	45	31	36
	43	42	37	31	29	18		55	53	50	26	22	22
—	—	60	54	45	39	23	—	48	47	43	38	30	29

The weights assigned and methods used are the same as given in the table of P lines

Weighted Means —

P2	P3	P4	P5	P6	P7	P8	
36 5	49 5	48	42	39 5	20 5	—	
Q1	Q2	Q3	Q4	Q5	Q6	Q7	Q8
51 5	66 5	70 5	64	55 5	46	29 5	14
R'1	R'2	R'3	R'4	R'5	R'6+R'7		
56 5	54	51	44 5	32 5	33 5		

Results for Plate C

Table III

The intensities are given in arbitrary units as obtained from the intensity scale supplied by the calibration marks

P2	P3	P4	P5	P6	P7	P8	Method of density measurement used					
53	70	70	64	45	31	—	Selenium cell	Method of Fournier d'Albe				
54	70	69	65	44	30	—	Method of Toy and Rawling					

Q1 and Q2	Q3	Q4	Q5	Q6	Q7	R'1	R'2	R'3	R'4	R'5	R'6+R'7
94	100	89	76	70	45	77	74	68	61	47	45
94	100	88	77	69	44	85	78	73	65	51	51

The methods used are the same as given in the table of P lines

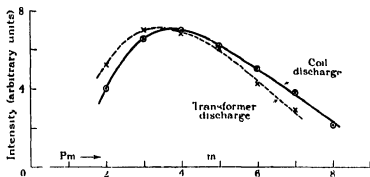


FIG 2 —The Distribution of Intensity in the P Branch

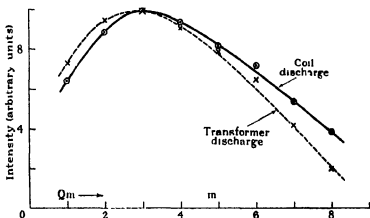


FIG 3 —The Distribution of Intensity in the Q Branch

It will be noticed that in each case the intensity of Q6 rises above the smooth curve. This is believed to be real since it is shown in so many of the records, but whether it is a genuine case of anomalous intensity of a band line, or merely the coincidence of some foreign line with Q6 remains uncertain.

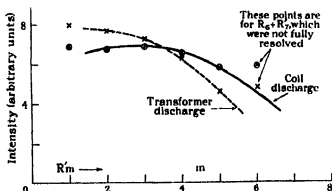


FIG 4 —The Distribution of Intensity in the R' Branch

Results for Plate D

m	1	2	3	4	5	6	7	8
P	—	46	69	69*	67	51	39*	—
Q		97†	100*	95	85	69	58	44
R'		85	81	78	75	67	67†	—

* These values were assumed See text below

† Q1 and Q2, R 6 and R7 were blends

Assume with Sampson* the expression connecting density with intensity

$$D - A/D = \gamma \{\log I - \log i\}$$

where D = density of photographic image, I = intensity of light which caused the image A, γ , i are constants

The densities on plate D were measured The values for Q3, P4, P7 were then assumed from the results of Plate A and the constants A, γ , i obtained The expression was then used to obtain the intensities of the remaining lines

Remarks on the Measurements

It will be noted that there are sometimes systematic differences between sets of measurements on the same branch This is due to the fact that a slight error of focussing in the projection device does not appreciably affect the calibration mark readings, whilst the narrow spectral lines are somewhat sensitive to such faults If, however, two sets of readings which do not agree are converted so that in each case the intensities are expressed relatively to that of the strongest line the agreement is much better Even the measurements obtained with the recording thermopile densitometers are in fair agreement when so treated It is clear from this that the final error will be small when the weighted means are taken.

It is believed that chance errors, such as those due to faulty setting of the cell on a spectral line, variations in intensity of the projection lamp or specks of dust on the plate have been to a large extent eliminated by the policy of obtaining several records by entirely different methods and taking weighted means The manner in which the points fall with relation to the smooth curves shown in the figures seems to suggest that no serious experimental errors are present

The conclusion that the plate sensitivity is constant over the region occupied by the band depends on the assumption that the intensity distribution in the

* R A Sampson, 'Monthly Notices, R.A.S.', vol 83, p 174 (1923)

spectrum of the calibration lamp is the same as that of a black body at 2350 Å. If this assumption is not approximately correct the intensities will only be correct for lines in the neighbourhood of Q1, i.e., λ 4650 Å. Elsewhere the values will be in error by an amount depending on the wave-length difference from λ 4650, this error will be quite regular, however, and easily corrected for if future measurements show that such is necessary. The effect of selective absorption in the prism may be combined with the change of sensitivity of the plate with wave-length to give what might be called the "apparent sensitivity", strictly speaking it is this sensitivity which was found to be constant over the range λ 4625-4730.

An error is likely to arise from the following circumstances. It is known that a plate does not integrate correctly a series of short exposures. Now the calibration marks are obtained from a steady source whilst the source of the band lines is only approximately steady, so that the band line intensities obtained by interpolation of the calibration curve may be a little distorted. It is to be expected that the weaker lines would be relatively strengthened.

Since the effect increases with the ratio $\left\{ \frac{\text{rest time}}{\text{exposure time}} \right\}$ it is also to be expected

that the results obtained from the coil discharge will be more affected than those from the transformer discharge. It was hoped that information on this point would be obtained from a comparison of plates A and B, but an unexpected excitation effect has prevented this. It will be seen, however, that the ratio of the maximum intensity in the P branch to the maximum intensity in the Q branch is very nearly the same in all plates, a result which would hardly be expected if a serious intermittency effect was present. That the plates of the transformer discharge were not seriously affected can be seen from the following considerations. Supposing the effect to exist, it is not to be expected that the results obtained from a plate in which only the initial half of the calibration curve is used would agree with those gained from a plate requiring the use of the whole calibration curve. Such a test is provided by plates B and C, which are in fair agreement with one another.

Discussion of the Results

The first step in the development of the theory of the distribution of energy among the lines of a band was the explanation of the distribution in oscillation-rotation bands. The expression for this, as derived by R. H. Fowler, Dieke and Kamble is of the form

$$\text{Intensity } J \propto \epsilon^{-\frac{E}{kT}}$$

Here ϵ is a term which involves both a probability of transition and the *a priori*

probability of an initial state, whilst $e^{-\frac{E}{kT}}$ is the Boltzmann factor, E representing the energy of the initial states as derived from frequency data. The inclusion of this factor implicitly assumes a thermal equilibrium. In the expression as originally derived, s appears to be equal to a/p , where a is approximately a constant* and p is the mean of the *a priori* probabilities of the initial and final states. In order to obtain agreement with observation it is necessary to place

$$p = 2j$$

where j = rotational quantum number

Information regarding electronic bands with a zero branch cannot be obtained unless some molecular model is assumed. It has lately been shown, by Birge and others, that the electronic levels of molecules are closely similar to those of "corresponding" atoms, i.e., atoms with the same number of outer electrons. Extending this hypothesis still further Mulliken, with the aid of the atomic analogy, has assigned inner quantum numbers j , to these levels. The assumed values of j , are identical with the Sommerfeld j values of corresponding atomic states. This inner quantum number j , is related to the fine structure of the bands in that the σ and ρ of the Kramers-Pauli expression

$$F(j) = B[\sqrt{j^2 - \sigma^2} - \rho]^2$$

are to be interpreted as its components, ρ is the component parallel to the vector of the nuclear angular momentum, whilst σ is the component parallel to the nuclear axis. This assumption of the inner quantum numbers analogous to those of corresponding atoms supplies the model necessary for the application of the correspondence principle or summation rule to the calculation of the distribution of energy in the branches of electronic bands. Using the close analogy of $\Delta j = 0, \pm 1$ in line spectra to $\Delta j = 0, \pm 1$ (Q, P, R branches) in band spectra, and of $\Delta k = 0, \pm 1$, in line spectra to $\Delta \sigma = 0, \pm 1$ in band spectra, Hönl and London† have applied summation rule methods to the problem. Assuming that $p = 2j$ (as in the oscillation-rotation bands) the expressions‡ applicable to the $\lambda 4650 \text{ Å}$ He₂ band are

* If vibrations are present the value of a is not quite the same in the P and R branches, and differs more and more as j increases.

† Hönl and London, 'Z f Physik,' vol. 33, p. 808 (1923)

‡ These expressions are given as modified by Mulliken in a recent paper, 'Phys. Rev.', vol. 29, p. 391 (1927), where many known cases of intensity distribution are reviewed and used, not only to provide evidence for the predicted intensity relations but also to justify the author's attempt (by means of the introduction of the presumed inner quantum number) to correlate all known band-spectra.

$$(7) \quad \nu_P = a(j - \sigma)(j - \sigma + 1)/j, \quad \nu_Q = 2aj(j - \frac{1}{2} + \sigma)(j + \frac{1}{2} - \sigma)/(j^2 - \frac{1}{4}), \\ \nu_R = a(j + \sigma)(j + \sigma - 1)/j$$

The appropriate value of σ in this case is unity. This value is not directly obtained, but only from a consideration of missing first lines.

A consequence of the adoption of the inner quantum number in the case of the helium bands is that the rotational energy terms assume the form $B(j^2 - \sigma^2)$ instead of the form $B(j - \epsilon)^2$ used in the analysis of Curtis and Long. It should be pointed out that two disturbing factors are present in the He_2 bands for which no explanation is provided by the theoretical considerations given above and for which, consequently, no allowance is made in the calculation of intensities. The first is that there are two rotation states, named A and B substates by Mulliken, to each value of j . Such doubling must not be confused with that which occurs in the violet C N bands. In the case of the doublet series of helium bands it is supposed that the P and R branches result from $B \rightarrow B$ transitions, whilst $A \rightarrow B$ are the transitions for the Q branch. In order to reconcile this arrangement with the observed spectrum the further assumption is required that alternate levels are suppressed. The resulting system of levels with the revised numeration is shown in fig. 5.

The following general conclusions with regard to the intensities in the λ 4650 band have been arrived at by Mulliken.

(1) The Q branch is the strongest, and its maximum intensity should be a little more than twice that of the P branch.

The fact that the Q branch is the strongest can be gathered at once from a glance at a reproduction of the spectrum. The prediction that at its greatest it should be twice as strong as the maximum intensity of the P branch is not fulfilled, figs. 2 and 3 showing that the ratio is more nearly 10 : 7. There is other evidence in support of a lower ratio than 2 : 1. In the first place neither eye estimation or microphotometer favour such a ratio. Secondly, Eriksson and Hulthen have published* a photogram of the Al H band at λ 4354 Å which is classified by Mulliken with He_2 λ 4650 Å and for which similar intensity relations should hold. This record shows that Q_{10} and P_{11} are the strongest lines of their respective branches, and that their intensities as measured from the ordinates of the recording densitometer curve are as 100 : 75. It is true that this is not the ratio of the intensities, but from the writer's experience he

* 'Z f Physik,' vol. 34, p. 775 (1925)

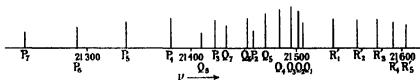
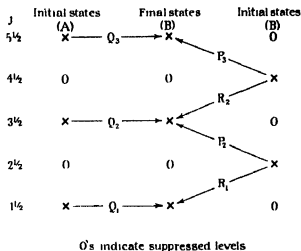


FIG 5—The System of Levels for the λ 4650 Band The lower part of the diagram shows the general appearance of this band, intensities being indicated by the lengths of the lines

would say that it is not likely to be in error by the amount necessary to make the ratio 100 : 50.

(2) Following from the scheme of rotation states adopted, the positions of maximum intensity should be such that if P_4 is the strongest line of the P branch, then R'_3 should be strongest in the R' branch. The maximum of the Q branch should occur between Q_3 and Q_4 .

This is borne out well by the results. The positions of the maxima are in the right order* ($P > Q > R'$) and differ by the correct amounts.

(3) The R' branch should initially be stronger than the P branch whilst for

* It should perhaps be mentioned that the intensity of R'_1 (and to a lesser extent that of R'_2) is likely to be given a little too great by reason of some faint adjacent lines which are shown in grating plates, but which the constant deviation spectrometer was unable fully to resolve.

larger j values the two should become asymptotically equal. This also is borne out by the observations.

Effective Temperatures of the Sources

Whilst the inclusion of the Boltzman factor may be justified in the case of absorption bands such as those of HCl, it is by no means certain that a distribution such as it connotes is to be expected when a gas is subjected to an electric discharge, in fact, it would be a surprising circumstance if such a distribution were found to exist. Adopting this distribution, the position of the line of maximum intensity enables an estimate of the temperature of the source to be made. In many cases the "effective" temperature thus obtained is much higher than the true temperature. A high value for this "effective" temperature in the case of the helium bands is perhaps to be expected when it is considered that the emitting molecule, presumably formed from excited atoms and containing the energy which these atoms have gained in the electric field of the tube, is an unstable one, and may not exist long enough to come into equilibrium with the surrounding gas.

A point of general interest shown by the results is the shift of the intensity maximum to lower rotation states in the case of the transformer discharge, in spite of the fact that the true temperature of the gas in such a discharge is greater than when a coil is used. Some information as to the "effective" temperatures in these cases may be obtained in the following manner.

If it be assumed that the distribution of intensity is of the type indicated by theory, a straight line of slope T should result if values of $\log J/\epsilon$ are plotted against $\log e^{-\frac{h}{kT}}$. Such curves, shown in fig. 7, have been drawn for the P, Q and R' branches of plates A and B, with values of ϵ_P , ϵ_Q and ϵ_R taken from Mulliken's paper. In each case the curves are distorted for low rotation states, either the ϵ values are too low or the J values are too high.

It is of importance to ascertain whether or no this distortion can be removed by adjusting the ϵ numbers without departing from an arithmetic progression. The success of such an attempt would show, of course, the possibility of attributing the intensity distribution to a linear ϵ factor, but, of equal importance, it would demonstrate that so far as the thermal distribution factor was concerned, nothing more complex than the Boltzman factor need be used. It may be stated at once that adjustment is possible, the necessary sequences and the results of the adjustment are shown in the accompanying table.

Plate	Branch	Sequence (Mulliken)	Sequence* (Adjusted)	Temperature
				° A
A	P	2, 4, 6 --	3, 5, 7, --	925
A	Q	3, 7, 11, --	11, 15, 19, --	1250
A	R'	3, 5, 7, --	4, 6, 8, --	1060
B	P	2, 4, 6, --	3, 5, 7, --	730
B	Q	3, 7, 11, --	11, 15, 19, --	1050
B	R'	3, 5, 7, --	4, 6, 8, --	760

* The unit of the sequence is not determined here, and is not necessarily the same for each branch. In order to obtain agreement with the observed intensities the units, for the P, Q and R branches respectively, must have magnitudes 1 0 41 0 91

It will be noticed at once that the temperatures obtained from the Q branches are much higher than those obtained from the P or R' branches, a result which is suggestive when it is remembered that the initial states of the Q branch have been assumed by Mulliken to be A sub-states, whilst those of the P and R' branches are B sub-states. It is hoped that further information regarding this effect will be gained from investigations now in progress on other bands of this spectrum.

Fortunately information regarding the temperature of the emitting molecules is available from another source. From the expression obtained by Lord Rayleigh for the half width of a spectral line of wave-length λ emitted by a particle of mass m (compared with the hydrogen atom) at a temperature T

$$\delta\lambda = 3.57 \times 10^{-7} \times \lambda \times \sqrt{T/m}$$

it is found that the width of a band line when the temperature is 1000° A should be approximately 0.038 Å. The width corresponding to a temperature of 400° A is approximately 0.024 Å. During a previous investigation the writer had obtained photographs of the band lines (coil excitation) as examined by a Fabry and Perot étalon of gap 1 cm. With this gap and in this region of the spectrum a change of unit order represents 0.108 Å.

The photographs showed the rings quite sharply defined. The fringe width natural to the étalon (supposing perfect adjustment and truly monochromatic light) may be obtained from a knowledge of the reflecting power of the films, for this instrument a value of 0.2 of an order was obtained. The fringe width calculated for a temperature of 400° A is thus approximately 0.35 order, whilst that corresponding to a temperature of 1000° A is approximately 0.55 order. The width obtained from the photograph was approximately 0.30 order,*

* This does not agree with the value 0.08 Å found by Leo, 'Ann. d. Physik,' vol. 81, p. 757 (1926), from Lummer plate photographs.

indicating that the distribution of translational velocities among the emitting molecules is that which corresponds to the true temperature of the gas in the tube

Rigorous Test of the λ Values

Reference to the diagram of rotation states shows that R1 and P2, R2 and P3 have the same initial states, so that in each case the ratio of the intensities should give the ratio λ_R/λ_P , quite independently of any assumptions as to the temperature or the type of distribution. In this way a strict test of the theory may be made. The observed and calculated values are shown in fig 6A. The observed values are of the correct magnitude, but except for the first (for which as already stated R1 is likely to be too strong) they are somewhat low. In

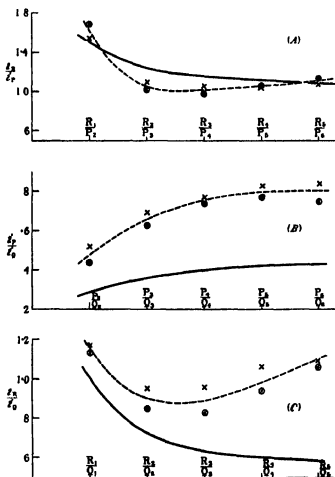


FIG 6 —○ Plate A, × Plate B, — Mulliken

view, however, of the assumptions made with regard to the distribution of intensity in the spectrum of the calibration lamp it would be unwise to attach much significance to this

Unfortunately it is not possible to test the Q branch in so rigorous a manner, for the initial states of this branch are not common to the P or R branches. It

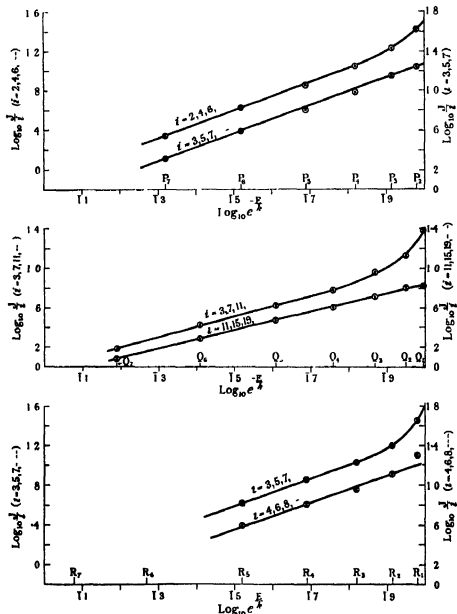


FIG 7

follows that the values of i_P/i_Q , for example, cannot be obtained without some knowledge of the temperature and without making some assumptions as to the type of distribution. If two lines having the same end-states are taken, however, these assumptions control the values through an expression of the form $\exp - (E'_Q - E'_P)/KT$ which, at least near the band origin, will not differ much from unity. The values of i_P/i_Q and i_R/i_Q , adopting the values of the temperatures given in the previous section, are shown in figs 6, B, C, in comparison with the theoretical values. It is to be emphasised that this is a test for the scheme of i numbers which is almost independent of assumptions, and as such the results from it must have some importance. They indicate that, in general, the theory is not far from accounting for the intensity distribution, but that, on the other hand, the actual numerical i values* will need revision, if they are to agree with observation.

It is evident from a consideration of fig 6 that it should be possible

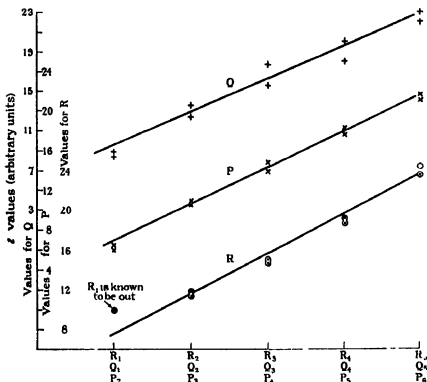


FIG 8—Showing the Linearity of the i Factors

* It must be remembered that the theory assumes a thermal equilibrium for its calculation of these numbers, if there is evidence to show the existence of a non thermal distribution then it must not be expected to obtain agreement

to obtain values of τ_P , τ_Q , τ_R , which are almost entirely independent of assumptions of temperature and distribution

For the ratios τ_R/τ_P , τ_R/τ_Q , τ_P/τ_Q , are known so that $\tau_P/\tau_Q \times \tau_Q/\tau_R$, τ_P/τ_R , may be found. Accordingly $\tau_P/\tau_R \times \tau_R/\tau_P$, τ_P/τ_P , τ_R/τ_R is known. By a similar process we can obtain values for τ_{R_1}/τ_{R_2} , τ_{R_2}/τ_{R_1} . If now we assume that $\tau_{R_1} = 1$ the remaining values τ_{R_1} , τ_{R_2} may be found.

Using the values we can then obtain τ_P , τ_Q . Unfortunately the errors, when determining the τ_R values, are cumulative. Nevertheless, the results are interesting as being possibly a more direct route to the τ values than that given in the preceding section. The results of this treatment are shown in fig. 8. If the smoothed values of fig. 6 are used the results are more regular, the τ_Q values in this case lying practically upon a straight line.

Comparison of Observed with Predicted Values

Adopting a temperature of 980° A. for the coil discharge and 750° A. for the transformer discharge, with the τ_P , τ_Q , τ_R values given by Mulliken, enables the predicted energy distribution to be calculated. The results of such calculation are given in figs. 9A and 9B. It will be seen that the observed intensity curves are of the predicted type but that quantitatively the agreement is not good. As suggested by fig. 7 the measurements are in better accord with the following expressions —

Plate A —

$$J_P = (\tau_P + 1) e^{-E/980\text{K}}, \quad J_Q = 0.41 (\tau_Q + 8) e^{-E/1250\text{K}}, \\ J_R = 0.91 (\tau_R + 1) e^{-E/980\text{K}}$$

Plate B—

$$J_P = (\tau_P + 1) e^{-E/750\text{K}}, \quad J_Q = 0.41 (\tau_Q + 8) e^{-E/1050\text{K}}, \\ J_R = 0.91 (\tau_R + 1) e^{-E/750\text{K}}$$

A comparison of these expressions with the experimental results is made in figs. 9A and 9B. It would be premature to say that the predictions are not confirmed, decision must be reserved until the other bands of this spectrum have been examined.

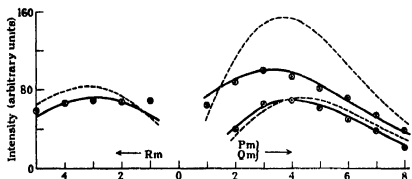


FIG 9A —Plate A --- Calculated (Mulliken) — Calculated (empirical) ○ Observed
 $T = 980^{\circ} \text{ A}$ $T = 980^{\circ} \text{ A}$ (P and R branches)
 $T = 1250^{\circ} \text{ A}$ (Q branch)

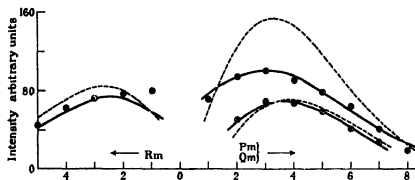


FIG 9B —Plate B --- Calculated (Mulliken) — Calculated (empirical) ○ Observed
 $T = 750^{\circ} \text{ A}$ $T = 750^{\circ} \text{ A}$ (P and R branches)
 $T = 1050^{\circ} \text{ A}$ (Q branch)

The Bearing of Intensity Measurements on the Question of Numeration

The results of intensity measurements in the case of helium have an immediate application to the question of numeration, about which some uncertainties have lately arisen. That adopted in this paper is the one recently put forward by Mulliken, for which there is much external evidence. Too much space would be required to give this in detail,* but the essential point lies in the existence of certain structural similarities between the helium bands and those of other symmetrical molecules (the negative bands of nitrogen are referred to in particular) which suggest that for the sake of consistency the same quantum numeration should be employed for all

* Reference should be made to Kratzer, 'Z f Physik,' vol 16, p 353 (1923), Curtis and Long, 'Roy Soc Proc,' vol. 108, p 583 (1925), and "Report on Band Spectra," pp. 204-209, R S Mulliken, 'Phys Rev,' vol. 28, p 1202 (1926)

For nitrogen, so far as structure is concerned, either the half- or quarter-integral numerations may be used, although each leads to difficulties when other properties of the bands are considered. If half-integral numbers are employed for the successive states it is difficult to explain the alternating intensities which exist in these bands, for there is no obvious reason why the levels should be split into two groups having different *a priori* probabilities. If, on the other hand, the quarter-integral numeration is adopted, $\pm e$, if the states are associated with rotational quantum numbers $m = j - \epsilon$ where ϵ has the values $+\frac{1}{4}$, $+\frac{3}{4}$ then with each value of ϵ is associated one of the groups of alternate lines. It is then natural to attribute different *a priori* probabilities to the two values of ϵ . The latter interpretation unfortunately leads to an improbable value of moment of inertia which is correctly given only if the former numeration is employed.

With the helium bands, if the assumption is made that the missing lines near the origin are due to the prohibition of the state for which $j' = 0$, the quarter-integral numeration seems inevitable. This numeration suffers from two defects. Firstly, the selection principles involved are purely arbitrary, and secondly, it offers no explanation for the absence of two lines which are observed to be missing in the band at $\lambda 5730$. Mulliken has recently considered this question of missing first lines in some detail, and, pointing out that the prohibition of the $j' = 0$ state may not always be correctly assumed, has in the case of helium obtained some very strong evidence pointing to the suppression of alternate rotation states. The scheme thus built up not only accounts for the observed branches in a natural manner but also gives an explanation of the missing lines of the band $\lambda 5730$. Accordingly the present tendency is to adopt a half-integral numeration for both the negative nitrogen and helium bands, thereby securing a gain in consistency without sacrificing accuracy of representation. The alternate lines in the case of helium are assumed to be so faint as to escape detection. The cause of the alternation of intensity is left unexplained. An examination of the $\lambda 4650$ band shows that, if present, these lines cannot have intensities greater than one-tenth of normal.

Since the discrepancies between the observed and calculated intensity values of this paper may be attributed to a number of causes it is somewhat difficult to decide the degree to which they confirm the adoption of the scheme of levels of diagram No. 5. For underlying the method by which the values of the calculated intensity were obtained is the assumption of thermal equilibrium, it is improbable that this assumption is strictly justified in the case of emission bands. The fact that the Q branch is less intense than the theory demands

may perhaps be connected in some way with the assumption that this branch originates from a set of states (A states) entirely different from those involved in the P and R branches. These two types of state are possibly affected differently by any cause, such as onsetting instability or a departure from thermal equilibrium, which tends to distort the Maxwellian distribution. The only strict test of the theory is a comparison (such as that made in diagram No. 6) of the intensities of lines which have their origin in the same state. It was from a consideration of these points that the conclusion was drawn that the measurements, in general, do not clash with theory, i.e., that the bands are of the predicted type. If this be admitted, it is direct evidence in favour of Mulliken's scheme of numeration, for, as he points out,* the agreement would not exist if the j values had not been assigned on the assumption of alternate missing lines.

Summary

Some measurements of the intensity distribution in the helium band λ 4650 Å (first of the main series) are given enabling the predictions of the summation rule to be tested. The predicted distribution is of the correct type, but agreement with observation is by no means complete. Notably the P and R' branches are much stronger, relative to the Q branch, than the theory indicates. It is found that an expression of the form $\epsilon^{-E/kT}$ where ϵ is a linear function of j' is adequate to describe the observed distribution.

As with many other bands the temperature obtained by assuming that the distribution of angular momentum is governed by the Boltzman factor is much higher than the true temperature of the gas. In this case effective temperatures of approximately 750° A and 1000° A are found, depending on the conditions of excitation. A higher temperature is obtained from the Q branch than from the P and R branches. Examination of the Doppler width of the band lines shows, however, that there is a distribution of translational velocities corresponding to the true temperature.

The work on these bands is being continued with improvements both to densitometry and general technique.

In conclusion the writer wishes to acknowledge his indebtedness to Prof W. E. Curtis for advice and criticism throughout the work.

* 'Phys. Rev.', vol. 29, p. 405 (1927)

The Heating Effects of Thorium and Radium Products.

By S W WATSON, M A (1851 Exhibition Scholar, University of South Africa),
and M C HENDERSON, Ph B

(Communicated by Prof Sir E Rutherford, P R S —Received December 21, 1927)

1 *Introduction*

The heating effect of radium and its decay products has been studied by many experimenters, and the observed heatings compared with those calculated from the energy of the alpha, beta and gamma radiations. The most important of these measurements, as far as the α -rays are concerned, are those of Meyer and Hess,* Rutherford and Robinson,† and Hess‡ (See Meyer and Schweidler, 'Radioaktivität,' 2nd edn, 1927, p 225, *et seq*, for a complete list of references)

From the measurements of these authors it appeared that practically the whole of the observed heating could be accounted for by the absorption of the α -, β - and γ -rays. Fresh determinations of the quantities involved in the theoretical heating have, however, thrown doubt upon this conclusion. The chief source of uncertainty to-day in this respect is the value of the number (Z) of alpha particles emitted per second by a gram of radium. The most recent determinations of this quantity are those of Hess and Lawson,§ and Geiger and Werner,|| who obtained the values 3.72×10^{10} and 3.40×10^{10} respectively¶. The former value leads to a calculated heating which agrees within 1 or 2 per cent with the observed emission, some uncertainty arising here through the difficulty of accurately estimating the fraction of the energy of the beta and gamma rays which is absorbed in any given experimental arrangement. If, on the other hand, Geiger and Werner's value be correct, it follows that about 10 per cent of the observed heating must arise through some activity other than that of the known α -, β -, and γ -rays.

It was felt that a measurement of the relative amounts of heat emitted by several radioactive substances might throw light on the above problem. If the

* 'Wien. Ber,' vol. 121, IIa, p 603 (1912)

† 'Wien. Ber,' vol. 121, IIa, p 1491 (1912), 'Phil Mag,' vol. 25, p 312 (1913)

‡ 'Wien. Ber,' vol. 121, IIa, p 1419 (1912)

§ 'Wien. Ber,' vol. 127, IIa, p 405 (1918), 'Phil Mag,' vol. 48, p 200 (1924)

|| 'Z f Physik,' vol. 21, p 187 (1924)

¶ A recent preliminary announcement by Jedrzejowski ('Compt. Rend.,' vol. 184, p. 1551 (1927)) gives 3.50×10^{10} .

amounts should prove to be in proportion to the calculated emissions, the result would strengthen the evidence in favour of the view that the heat development is due almost entirely to the absorption of the α -, β - and γ -rays, and would consequently give a fairly reliable estimate of the number of alpha particles emitted per second by a gram of radium. The substances the heat emissions of which have been measured by the authors are radon (radium emanation) in equilibrium with its products of short life, radium (B + C), radium C, thorium (B + C), and thorium C.

The comparison of the calculated heatings of thorium and radium products was made possible by the results described in a separate paper* by the writers, which gives the ratio between the numbers of alpha particles expelled per second by Ra C and by Th C of equivalent gamma-ray activities. The results agree well with the experiments of Shenstone and Schlundt,† who used a different method. These comparisons should be free from many of the sources of uncertainty which enter into an absolute determination of the rate of emission of α -particles by either body separately.

The comparison of the heating effects of several products has already been made in the case of radium and its products of rapid decay by Rutherford and Robinson (*loc cit*), who gave the following percentage distribution —

Product	Theoretical	Observed
Rn	27.7	29
Ra A	29.7	31
Ra (B + C)	42.6	40

(The theoretical percentages based on the data used in Section 5 of the present paper, including 90 per cent of the β -ray energy, would be 27.1, 29.7 and 43.2 respectively.) The results indicated an agreement to about 5 per cent between the observed and calculated distribution of heating among the various products. The method was, however, a differential one, and by measuring the heating of Ra (B + C) and Ra C separately a more definite result might be expected. This has now been done and the comparison extended to the thorium products. It will be seen that the results indicate in each case an agreement between the observed and calculated heatings to within 2 per cent and that the absolute values correspond very closely to the value of $Z = 3.72 \times 10^{10}$.

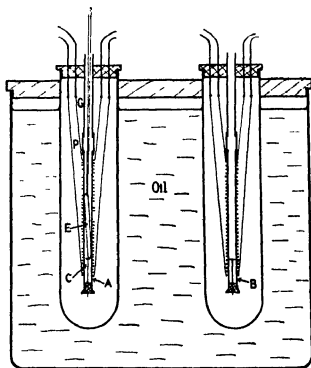
* 'Proc Camb Phil Soc,' vol 24, p 133 (1928)

† 'Phil Mag,' vol 43, p 1038 (1922)

2 The Apparatus

The method used was similar in principle to that employed by Rutherford and Robinson * It consisted in measuring the change of balance of a Wheatstone bridge when two opposite arms were heated by the radioactive substance The bridge was standardised by a heating coil, made as similar as possible to the radioactive source

The arms of the bridge were four coils of number 47 S W G silk-covered copper wire, each coil containing 6 metres of wire and having very nearly 42 ohms resistance Two coils, forming two opposite arms of the bridge, were wound upon an aluminium tube (A) in two layers, each layer forming one of the coils The other two coils were wound upon a similar tube (B) In this way a double sensitivity was obtained Each aluminium tube was 6.1 cm in length, 3.6 mm in external diameter, and 0.35 mm in wall thickness The windings



occupied a length of 4.9 cm on each tube A small platform (C) of copper wire formed a seating for the glass tube (E) containing the radioactive material or the heating coil, and was supported in a small cork which closed the lower

* *Loc cit*

end of the tube Each aluminum tube was supported inside a 1-inch test-tube by a piece of thin-walled glass tubing (G) and a piece of thin paper tubing (P), introduced to improve the thermal insulation During an experiment the second aluminum tube held an empty "dummy" source The two test-tubes were suspended in a large beaker filled with paraffin oil, and the latter was surrounded by about 10 inches of cotton wool and wood turnings Two paper tubes led vertically from the tops of the glass tubes (G) and formed the entrances through which the source of heat and the dummy were lowered

A thermo-junction immersed in the oil between the test-tubes indicated that the temperature of the oil did not change by more than a degree in the course of a day, and usually by only a few tenths of a degree

The bridge could be exactly balanced at any time by adjusting an external resistance of approximately 7000 ohms in parallel with one of the bridge coils The galvanometer used was a moving coil instrument of 24 ohms resistance and gave a deflection of 200 mm per microampere at 1 metre scale distance

The sources were sealed into glass tubes about 2 cm in length, 1.9 mm in diameter and 0.2 mm in wall thickness The dummy was an empty glass tube of the same dimensions The heating coil was made of 42 S.W.G. Eureka wire, resistance 34.80 ohms, and was sealed into another similar tube

In order to eliminate the heating effect of the current in the leads of the heating coil and errors due to conduction of heat along them, the dummy was provided with a pair of leads of the same copper wire (47 S.W.G.) as those of the heating coil and connected in series with them The tubes containing the sources were also provided with similar compensating leads, and during an experiment these leads (again in series with those of the dummy) carried a current which would have given approximately the observed heating if the coil had been in place instead of the radioactive source

The sensitivity of the bridge for a total current through it of 4 milliamperes was about 235 mm for a heat emission of 1 cal./hour, or about 24 mm per millicurie of radon. It was found that a change of 1 ohm out of about 7000 in the shunt box produced a change of balance of 0.2 mm From this it was calculated that a 2-cm deflection corresponded to a difference of temperature between the two arms of the bridge of about 0.01° C, so that by reading to 0.2 mm a difference of 10^{-4} degrees could be detected

The sources were measured against the laboratory radium standard (6.38 mg radium element) by a gamma-ray electroscope covered with lead and aluminium equivalent to 18 mm of lead The electroscope arrangement was identical

with that used in finding the number of alpha particles emitted by Th C* The radium standard has recently been checked at the National Physical Laboratory It is probably accurate to one-half per cent

3 Procedure

In each day's work the bridge current was allowed to run continuously The bridge was balanced and the small regular change of balance followed throughout the day and corrected for The change in balance was found to be roughly proportional to the difference in temperature between the oil bath and the room, and was caused by differences of conduction along the supports of the two tubes, together with the fact that a small general change of temperature of the copper coils would not be accompanied by a corresponding change of resistance of the large manganin shunt resistance After the source and dummy had been lowered into their respective tubes, the galvanometer deflection reached its equilibrium value in about 15 minutes Readings were taken alternately with the bridge current direct and reversed to eliminate any thermoelectric effects and a small zero creep At least six were taken at intervals of $1\frac{1}{2}$ minutes after the deflection had become steady In the case of a rapidly decaying source a much larger number was taken, the decay being followed for over half an hour after the maximum deflection had been reached The source and dummy were then removed and the balance change observed after conditions had again become steady Experiments were made alternately with the radioactive source and heating coil, as many times as the decaying strength of the source permitted

The observed deflection, in the case of a rapidly decaying source, has to be corrected for a lag of the apparatus The correction was obtained in two ways The simpler method depended on the determination of the cooling curve of the apparatus after a slightly warmed dummy source had been inserted When the initial disturbances had died away, the deflection diminished exponentially to zero with a definite half-value period (T_s) The mean of several determinations, lying between 1.1 and 1.3 minutes, was 1.2 minutes It can readily be shown that the observed deflection at any instant, when a decaying source of heat (half-value period T_s) is in place, must be multiplied by the factor $\frac{T_s - T}{T_s}$ to give the deflection corresponding to a steady rate of heat supply equal to the instantaneous value for the decaying source (This calculation is

exactly analogous to that used in correcting radioactive sources for transient equilibrium)

The second method was a direct one, in which the heating coil was inserted and the current through it reduced in such a way that the heat evolution decreased exponentially with a given period. The two methods gave results in excellent agreement except in the case corresponding to Ra C (see Section 4 (c))

The heating produced in the coil was calculated from its resistance and the current passing through it, the latter being found from the voltage of the cell and the total resistance of the circuit. The voltage was measured on an accurate Weston voltmeter, which was standardised from time to time against a cadmium cell

4 Experimental Results

In the following tables the strength of the source is given in "milligrams," by which is meant the number of milligrams of radium which would produce the same gamma-ray ionisation when measured through 18 mm of lead. The values have been corrected in every case for absorption of the γ -rays from the source in the walls of the containing tube and in the wire on which the source was deposited. This correction lay between 0.2 and 1.2 per cent.

(a) *Radon* ---Thirty experiments in all were made with this product, extending over a period of several months. The mean value of the heating was 101.7 cal./hour per gram, and in only one case did an individual result differ from this by more than 1.3 per cent. The probable error as given by the formula $2/3\sqrt{\Sigma d^2/n(n-1)}$ is less than 0.2 per cent.

Table I gives the result of the last eight experiments in which the largest sources were used, so that these results should be the most reliable.

Table I ---Radon

Strength of source	Heating	Cal./gram hour
mg	cal./hour	
33.86	3.437	101.5
33.30	3.394	101.9
28.16	2.873	102.0
23.60	2.403	101.8
23.14	2.330	100.7
24.53	2.509	103.3
20.73	2.099	101.2
17.72	1.794	101.3
Observed heating		101.6

Taking account of possible sources of systematic error, viz, the radium standard used, the standard cells, and possible inequality in the heat losses, it is felt that this result can be relied upon to within about 1 per cent. It will be seen in Section 5 (a) that the theoretical value is 102.4 cal/gram-hour.

(b) *Radium (B + C)*—The ordinary method of preparation of this kind of source on a wire, viz, by exposure to radon for two hours in an electric field, was found to give too irregular a decay for accurate work. Such irregularities frequently occur with sources prepared by this method. Therefore a quantity of radon was introduced into the tube itself and allowed to stand overnight with only a very small mercury surface exposed in a constriction in the tube. The radon was then pumped off and the tube cut off, washed out with alcohol, baked and sealed. The resulting source followed very closely the normal decay as given by Bracelin's* corrections to the tables published by Lawson and Hess.†

The results are shown in Table II, where the strength of the source given in column 2 represents the amount of Ra C present as given by the γ -ray measurements. A small correction is applied in section 5 (b) for the γ -ray effect due to Ra B. The lag correction is given by $\frac{1.2 \text{ min.}}{34 \text{ min.}} = -3.5 \text{ per cent}$, 34 minutes being the time in which the observed heating would have fallen to half value at its actual rate of decay.

Table II—Ra (B + C)

Time after removal	Mg	Cal./hour	Cal./gram-hour
min			
72.5	11.19	0.467	44.4
75.5	10.54	0.470	44.6
78.5	9.92	0.443	44.7
81.5	9.33	0.417	44.7
84.5	8.76	0.392	44.7
89.5	7.89	0.354	44.9
92.5	7.40	0.333	44.8
95.5	6.92	0.312	45.1
Mean			44.7
Correction for lag = -3.5 per cent =			1.6
Observed heating			43.1

(c) *Radium C*—This source was prepared by rotating a 1/5 mm. nickel wire in a solution of Ra (B + C) in hot hydrochloric acid. The active deposit was

* 'Proc. Camb. Phil. Soc.', vol. 23, p. 150 (1926)

† 'Wien. Ber.', vol. 127, IIa, pp. 626-7 (1918)

allowed to stand for 25 minutes before dissolving in order to allow the Ra A to decay to a negligible value. After 15 minutes' rotation the wire was washed, dried, and sealed into its glass tube. The source decayed normally with a period of 19.7 minutes, which is the period given by Bracelin.*

Table III—Ra C

Time after removal	Mg	Cal./hour	Cal./gram hour
min			
41	8.72	0.402	46.1
50	6.37	0.295 ₄	46.4
59	4.62	0.215	46.5
68	3.38	0.157	46.5
Mean			46.4
Correction for lag = - 7.4 per cent =			3.5
Observed heating			42.9

The calculated lag correction in this case was $1.2/19.7 = 6.1$ per cent, while an experimental determination with a heating coil gave 8.7 per cent. The mean of these two values was used in the above calculation. The discrepancy was perhaps due to difficulty in diminishing the heating current with sufficient regularity at so rapid a rate.

(d) *Thorium (B + C)*—The deposits of this product were obtained on platinum wires $\frac{1}{4}$ mm in diameter by electrolysis of a solution of radiothorium in weak hydrochloric acid. The first decayed at the normal rate for a source obtained by long exposure to the emanation. The results are shown in Table IV (a).

The second source consisted initially of Th B and Th C in transient equilibrium proportion together with a large excess of Th C. The results are shown in Table IV (b), a correction being applied to the first two readings for the heat which would have been emitted if this excess Th C had been accompanied by the corresponding quantity of Th B. The correction is based on the difference between the mean observed heatings of Th (B + C) and Th C, viz., 2.8 cal./hour per gram of Th B. (It will be seen in Section 5 (d) and (e) that this large difference is the result of two effects—the beta rays of Th B and the transient equilibrium between Th C and Th C'')

Table IV—Th (B + C).

Time after removal	Mg Th (B + C)	Mg excess Th C	Total mg	Cal /hour	Cal./gram hour	Correction for deficit of Th B	Corrected Cal./gram-hour
hrs m							
(a)							
1 41			3 65	0 1880	51 5		51 5
3 30			3 27	0 1670	51 1		51 1
5 28			2 88	0 1482	51 3		51 3
(b)							
0 53	5 14	1 99	7 13	0 3526	49 5	+0 8	50 3
2 54	4 47	0 48	4 95	0 2474	50 0	+0 2	50 2
5 13	3 85	0 07	3 92	0 1977	50 4		50 4
7 06	3 40	0 02	3 42	0 1747	51 1		51 1
22 11	1 26 ₁	—	1 26	0 0640	50 6		50 6
Mean							50 8
Correction for lag = - 0 2 per cent. =							0 1
Observed heating							50 7

(c) *Thorium C*—This product was obtained by rotating a nickel wire $\frac{1}{8}$ mm in diameter for 2 hours in a hot solution of radiothorium in weak hydrochloric acid. The wire was then washed and dried and sealed into its glass tube. The gamma-ray decay was slightly too slow, giving a half-value period of 62.4 minutes for the first 4 hours. Measurements on the next day by both β - and γ -rays showed it to be decaying with the period of Th B. It was estimated from the decay curve that the source contained initially about 0.7 per cent of Th B, and that during the heating measurements, an hour after separation, the amount present was 1.4 per cent of the equilibrium proportions. It will be seen from the results for Th (B + C) and for Th C that the heating due to this amount of Th B is quite negligible.

Table V Th C

Time after removal	Mg	Cal /hour	Cal /gram-hour
min			
48	4 47	0 2205	49 3
51	4 33	0 2111	48 9
54	4 19	0 2037	48 6
57	4 05	0 1968	49 1
60	3 91	0 1921	49 1
63	3 80	0 1842	48 5
66	3 66	0 1785	48 8
Mean			48 9
Correction for lag = $\frac{1.2}{62} = - 1.9$ per cent. =			1 0
Observed heating			47 9

5 Calculated Rate of Heat Production

(a) *Radon*—The energy of the alpha particles per gram per second is given by $\frac{1}{2}\Sigma nmv^2$, where n is the number expelled per gram per second, m the mass of a particle, and v its velocity, the summation including the alpha particles from the radon, Ra A, and Ra C. A small factor $(1 + \frac{1}{2}\beta^2 + \dots)$ amounting on the average to 1.002 may be applied for the relativity increase of energy. In the case of Ra C, n is equal to Z , the number of alpha particles ejected per second by a gram of radium, but for the radon and Ra A the number is 0.9 per cent lower on account of the transient equilibrium. For the present we shall assume Hess and Lawson's* value for Z , viz., 3.72×10^{10} . Using the velocity of the Ra C alpha particle as given by Rutherford and Robinson,† and those of the other products as deduced from Geiger's rule $v^2 = kR$ (confirmed by Briggs‡), we have

Rn	$v = 1.613 \times 10^9$ cm/sec	$v^2 = 2.602 \times 10^{18}$
Ra A	1.688	2.849
Ra C	1.922	3.694

Taking m_α as 6.595×10^{-24} gm.,

$$\frac{1.002}{2} \Sigma m_\alpha n v^2 = \frac{1.002}{2} \times 6.595 \times 10^{-24} \times 3.72 \times 10^{10} \times \left(\frac{2.602 + 2.849}{1.009} + 3.694 \right) \times 10^{18} = 1.118 \times 10^6 \text{ ergs/gm.-sec}$$

Multiplying by $3600/4.186 \times 10^7$ we obtain 96.1 cal./gram-hour.

The energy of the recoil atoms is on the average $\frac{4}{218}$ of this figure, or 1.8 cal./gram-hour.

The energy of the β -rays has been determined experimentally by Gurney,§ who gives the distribution in the β -ray spectra of Ra B, Ra C, Th B and Th C. The mass per unit area of absorbing material in our apparatus was 0.193 gm./cm². It appears from measurements by Madgwick|| that in our apparatus rays up to Hp 4000 would be almost entirely stopped, these alone possess about 40 per cent. of the total β -ray energy. For rays above Hp 4000 the energy absorbed was calculated, in groups covering small ranges of velocity, from data given by Rawlinson, Danyaz, Varder, Madgwick and others. It was

* *Loc. cit.*

† 'Phil. Mag.', vol. 28, p. 552 (1914).

‡ 'Roy. Soc. Proc.', A, vol. 114, p. 344 (1927).

§ 'Roy. Soc. Proc.', A, vol. 109, p. 540 (1925); vol. 112, p. 380 (1926).

|| 'Proc. Camb. Phil. Soc.', vol. 23, p. 970 (1927).

estimated that about 80 per cent of the β -ray energy would be absorbed in the case of both Ra (B + C) and Th (B + C), while the rays of Ra B and Th B would be entirely absorbed

The estimated contributions of the β -rays to the heating are given in Table VI In the worst case, that of Ra (B + C), an error of 10 per cent in the estimate would only affect the total theoretical heating by 1 per cent, while in the case of radon the percentage effect would be only half as great

Table VI

	Total energy of beta rays (Gurney)	Energy absorbed
	cal /gram hour	cal /gram hour
Ra C	4 3	3 2
Ra B	1 3	1 7
Ra (B + C)	5 6	4 5
Th C	4 1	3 1 _s
Th B	0 6 _s	0 6 _s
Th (B + C)	4 7 _s	3 8

The heating effect of the gamma rays under our conditions was estimated from the results of Ellis and Wooster* to be less than 0.1 per cent of the whole heating and can be neglected

The calculated heating of radon in our apparatus is therefore

Alpha rays	96.1
Recoil atoms	1.8
Beta rays	4.5
Total	102.4 cal /gram-hour

(b) Ra (B + C) —For the alpha rays we have —

$$1.002 \times \frac{1}{4} m_{\alpha} v^2 = 39.1 \text{ cal /gram-hour}$$

$$\text{For the recoil atoms } \frac{4}{214} \times 39.1 = 0.7$$

$$\text{For the beta rays (see following paragraph)} \quad 3.7$$

$$\text{Total} \quad 43.5 \text{ cal /gram-hour}$$

Gurney's data were obtained with sources of radon, in which equal numbers of Ra B and Ra C atoms break up per second. In an active deposit source

* 'Phil Mag,' vol 50, p 521 (1925)

this is very far from being the case, and a calculation shows that at the time the heating measurements were made (68 to 90 minutes after removal) approximately two-fifths as many atoms of Ra B break up as of Ra C in unit time. Therefore the contribution of the Ra B beta rays to the heating is only 0.5 calorie instead of 1.3. This gives a figure of 3.7 instead of 4.5 cal./gram-hour for the β -ray heating under the experimental conditions.

A further small correction has been applied to the theoretical heatings based on the result given by Slater,* that in an electroscope covered with 18 mm of lead 1 per cent of the ionisation is caused by Ra B, when equal numbers of Ra B and Ra C atoms are disintegrating per second. We are assuming that the ionisation in the electroscope is a measure of the activity of the Ra C. The effect to be corrected for is the difference between the ionisations caused by the Ra B in the radium standard† and that in the source of heat. In the case of radon the two effects are equal and opposite, so that no correction is required. In the experiment with Ra (B + C) the average value of the correction over the period of the electroscope readings is $1 - 0.4$, or 0.6 per cent. In the case of Ra C the full correction of 1 per cent applies.

The correction for the γ -rays of Th B has been estimated to be also about 1 per cent at 18 mm of lead. The corresponding correction for the radium standard in the Th (B + C) and Th C heatings has been taken into account in the determination of the relative number of α -particles, and need not be applied here.

The final theoretical figure for Ra (B + C) is then $43.5 + 0.6$ per cent = 43.8 cal./gram-hour.

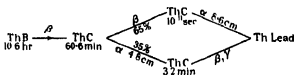
(c) Ra C

Alpha rays	39.1 (as for Ra (B + C))
Recoil atoms	0.7
Beta rays	3.2
Total	43.0
Correction for γ -rays of Ra B in radium standard = + 1 per cent	0.4
Theoretical heating	43.4 cal./gram-hour

* 'Phil Mag,' vol 44, p 302 (1922)

† The effects of the γ rays of the radium itself and of the Ra D in the standard probably do not exceed 0.2 per cent.

(d) *Thorium (B + C)*—In a previous paper* it was found that 4.03×10^{10} alpha particles are emitted per second by a source of Th C corresponding in gamma-ray activity to a gram of radium, when measured through 18 mm of lead. This result can be employed directly to calculate the theoretical development of heat by Th C (as is done in the following section), but in applying it to a source controlled by the decay of Th B, several transient equilibrium factors must be taken into account. The disintegration scheme is shown below, the γ -rays arise from Th C'',† while the α -rays come from Th C and C'



The period of Th C' is so short that Th C and Th C' are always present in a fixed ratio. In a source of Th C a disintegration of one atom of Th C' per second is accompanied by $\frac{\lambda_{C'} - \lambda_C}{\lambda_{C'}}$ or 0.947 atom per second of Th C and hence by 0.947 alpha particle of 4.8 cm range. In a source of Th (B + C), corresponding to one atom of Th C' per second we have $\frac{(\lambda_C - \lambda_B)(\lambda_{C'} - \lambda_B)}{\lambda_C \lambda_{C'}}$ or 0.900 atom of Th B per second, hence $0.900 \times \frac{\lambda_C}{\lambda_C - \lambda_B}$ or 0.995 atom per second of Th C, and thus 0.995 \pm 8 cm alpha particle. Therefore for the same γ -ray activity there are $\frac{0.995}{0.947}$ times as many α -particles of either range emitted per second from Th (B + C) as from Th C. For a γ -ray effect equal to that of a gram of radium through 18 mm of lead the number of particles expelled per second from Th (B + C) will be $4.03 \times 10^{10} \times \frac{0.995}{0.947}$, or 4.24×10^{10} (assuming the value 3.72×10^{10} for radium).

If we take the branching ratio as 35.65, the heat production of Th (B + C) can be calculated as follows —

Th C α	$v =$	1.696×10^9	cm/sec
Th C' α	$v =$	2.063×10^9	cm/sec

* Watson and Henderson, *loc. cit*

† Hahn and Meitner, 'Phys. Zeit.', vol 13, p 390 (1912)

The energy of the alpha rays and recoil atoms is

$$1.003 \Sigma \frac{1}{2} m_0 v^2 \left(1 + \frac{4}{212}\right) \text{ ergs/gm-sec} \quad 46.4 \text{ cal/gram-hour}$$

Beta rays	3.8
	50.2

(Section 5 (b)) Correction for γ -rays of Th B

= - 1 per cent =	0.5
------------------	-----

Theoretical heating	49.7 cal/gram-hour
	--

(c) *Thorium C*—As mentioned in the preceding paragraph, the number of alpha particles per second per equivalent gram of Th C is 4.03×10^{10} , so that the theoretical heating is—

Alpha rays and recoil atoms $\frac{4.03}{4.24} \times 46.4$	44.1 cal/gram-hour
---	--------------------

Beta rays	3.1 ₅
-----------	------------------

Theoretical heating	47.2 ₅ cal/gram-hour
	--

6 Comparison of Observed and Calculated Results, and Discussion

The results may be tabulated as follows —

Table VII

Product	Observed heating	Theoretical heating	100 × $\frac{\text{Observed}}{\text{Theoretical}}$	Relative to Rn
Rn	101.6	102.4	99.2	100.0
Ra (B + C)	43.1	43.8	98.4	99.2
Ra C	42.9	43.4	98.9	99.7
Th (B + C)	50.7	49.7	102.0	102.8
Th C	47.9	47.2 ₅	101.4	102.2

The relative results given in the last column are independent of the assumed rate of emission of alpha particles by radium, the value of the radium standard used, and any systematic errors in the heat measurements.

The agreement in the case of the thorium products is not as good as in that of the radium products, but the discrepancy lies within the probable errors in the determination of the relative numbers and velocities of the alpha particles,

the branching ratio, the estimated heating from the beta particles, and the heat measurements themselves. The good general agreement of the results is consistent with the supposition that no considerable amount of heat is radiated from the atom in forms which we have not taken into account, such as electromagnetic radiation soft enough to be absorbed in the type of calorimeter used.

It is interesting to note that the β -ray emitters Ra B and Th B show no abnormal effects. Herszfeld^{*} and Wertenstein^{*} found that the β -ray heating of Ra B did not exceed 2 per cent of the heating caused by the α - and β -rays of Ra C.

If Geiger and Werner's value of 3.4×10^{10} α -particles per second per gram of radium is correct, it follows that from 10 to 12 per cent of the heating must be caused by easily absorbed radiation not included in the above calculations. This would require about 40, 70 and 80 quanta per atom, for instance, for radium, Ra C and Th C respectively, if the radiation were of a wave-length of 1 Å U, and correspondingly more quanta for softer radiation. There is at present no evidence for the existence of soft radiation in such quantity. If such an additional emission of energy does occur, the proportion which it bears to the total energy must be very nearly the same for a large number of radioactive bodies, this is seen from Table VIII, where the results of various observers are compared with the corresponding theoretical heatings calculated on the basis of 3.72×10^{10} α -particles per second. The table includes the members of the radium family alone, since the comparison for Th B and Th C involved additional sources of uncertainty, as mentioned above. The theoretical values have been recalculated from the same data as have been used earlier in this paper, including the fractions indicated of the values given by Gurney and by Ellis and Wooster (*loc cit*) for the heating effects of the β - and γ -rays respectively. In the case of the γ -rays of radium, calculated by Lawson[†] to give 0.9 cal/gram-hour, it is assumed that 0.5 cal/gram-hour will represent the heating due to the amount absorbed in the calorimeter used by Meyer and Hess, and by Hess.

The high degree of uniformity of these results seems to be consistent with the view that the rate of emission of alpha particles can be calculated from the heating effects, which, as far as they go, support Hess and Lawson's result.

^{*} 'Jour de Phys.', vol 1, p 143 (1920)

[†] 'Nature,' vol 116, p 897 (1925)

Table VIII

Observers	Product	Observed cal /gm hr	Theoretical cal /gm hr	100 > $\frac{\text{Observed}}{\text{Theoretical}}$
Meyer and Hess*	Ra + Rn + A + B + C including all β rays and 18 per cent of the γ rays	132.3	130.8	101
Hess*	Ra alone	25.2	25.1	100
Rutherford and Robinson*	Rn + A + B + C including 90 per cent of the β ray energy	103.5	103.1	100
Present experimenters	Rn + A + B + C	101.6	102.4	99
Present experimenters	Ra C and Ra (B + C) (mean)			99

* *Loc cit*

Meitner,* estimating the energy of the β - and γ -rays on a somewhat hypothetical basis, found the total observed heating of radium to agree with a value 3.5×10^{10} α -particles per second per gram of radium, this, however, was before the experimental determinations were made by Gurney and by Ellis and Wooster. Thibaud† calculated the energy of the γ -rays from his estimates of the intensities of the lines in the γ -ray spectra. His value for the γ -rays of Ra (B + C) is 6.3 cal /gram-hour, which is considerably lower than Ellis and Wooster's result (8.6 cal /gram-hour), but his γ -ray intensities are probably inaccurate (*cf* intensities given by Ellis and Wooster, 'Proc Camb Phil Soc,' vol 23 (VI), p 717 (1927))

7 Summary

The rates of heat evolution by five combinations of radioactive bodies, viz , Rn + Ra (A + B + C), Ra (B + C), Ra C, Th (B + C), Th C, have been measured by a resistance thermometer method. The results obtained agree within 2 per cent with the theoretical values based on Hess and Lawson's data for the rate of emission of alpha particles by radium (3.72×10^{10} per gram per second). If there is any evolution of heat other than that produced by the known radiations (as is required by Geiger and Werner's value for the rate of emission of alpha particles) it must be in nearly the same proportion in a large number of radioactive products, and must occur in an easily absorbed form in a quantity corresponding, if electromagnetic, to a large number of quanta per atom disintegrating.

* 'Naturwiss.,' vol 12, p 1146 (1924)

† 'Compt. Rend.,' vol. 180 (I), p. 1166 (1925)

The authors wish to express their thanks to Sir Ernest Rutherford for his interest and advice, to Dr J Chadwick, who suggested the work and was a constant source of assistance and valuable criticism, and who also prepared several of the radioactive sources, and to Mr G R Crowe, who prepared the remaining sources

An Investigation into the Existence of Zero-Point Energy in the Rock-Salt Lattice by an X-Ray Diffraction Method

By R W JAMES, M A, I WALLER, Ph D, and D R HARTREE, Ph D

(Communicated by W L Bragg, F R S —Received December 22, 1927)

1 *Introduction*

In the present paper we shall attempt to collate the results of four separate lines of research which, taken together, appear to provide some interesting checks between theory and experiment. The investigations to be considered are (1) the discussion by Waller* and by Wentzel,† on the basis of the quantum (wave) mechanics, of the scattering of radiation by an atom, (2) the calculation by Hartree of the Schrödinger distribution of charge in the atoms of chlorine and sodium, (3) the measurements of James and Miss Firth‡ of the scattering power of the sodium and chlorine atoms in the rock-salt crystal for X-rays at a series of temperatures extending as low as the temperature of liquid air, and (4) the theoretical discussion of the temperature factor of X-ray reflexion by Debye§ and by Waller||. Application of the laws of scattering to the distribution of charge calculated for the sodium and chlorine atoms, enables us to calculate the coherent atomic scattering for X-radiation, as a function of the angle of scattering and of the wave-length, for these atoms in a state of rest, assuming that the frequency of the X-radiation is higher than, and not too near the frequency of the K-absorption edge for the atom¶. From the observed

* 'Phil. Mag.', vol 4, p 1228 (1927), 'Nature,' July 30, 1927

† 'Z f Physik,' vol 43, pp 1, 779 (1927)

‡ 'Roy. Soc. Proc., A, vol 117, p. 62 (1927)

§ 'Ann. d. Physik,' vol 43, p 49 (1914)

|| 'Z f Physik,' vol 17, p 398 (1923), 'Upsala Dissertation,' 1925

¶ This condition is fulfilled with sufficient accuracy in all the applications of the scattering laws made here. If the frequency of the X-radiation approaches the K absorption limit, anomalous scattering will occur

scattering power at the temperature of liquid air, and from the measured value of the temperature factor, we can, by applying the theory of the temperature effect, calculate the scattering power at the absolute zero, or rather for the atom reduced to a state of rest. The extrapolation to a state of rest will differ according to whether we assume the existence or absence of zero point energy in the crystal lattice. Hence we may hope, in the first place to test the agreement between the observed scattering power and that calculated from the atomic model, and in the second place to see whether the experimental results indicate the presence of zero-point energy or no.

2 *The Scattering of Radiation by Bound Electrons*

In the previous work in which attempts have been made to determine the distribution of charge within the atom from the observed scattering curves or *F*-curves, for the atoms,* or to test atomic models by comparing the *F*-curves calculated from them with the observed curves the classical law of scattering due to J. J. Thomson has always been employed, and it has been assumed that all the radiation scattered from the atoms in the crystal lattice is coherent.

Now since the discovery of the Compton effect it has been evident that these assumptions are not justifiable. A certain fraction of the incident radiation is scattered with a change of wave-length, and since no diffraction maxima corresponding to radiation with a modified wave-length can be detected, this radiation may be presumed to be incoherent, so that no definite phase relationship exists between the incident radiation and this part of the scattered radiation.

Owing to the existence of this incoherent radiation it appeared that serious errors might have been introduced into the older calculations of *F*-curves and attempts were made by Williams† and by Jauncey‡ to recalculate some of the *F*-curves which had been deduced from theoretical atomic models so as to make allowance for this.

The advent of the quantum mechanics, however, has made it necessary to reconsider the whole question of scattering, and we shall outline briefly some of the results so far obtained, which appear to be of considerable importance.

* In this paper *F* will always denote the ratio of the amplitude of the coherent radiation scattered from an atom in a state of rest to the amplitude scattered from a free electron according to the classical theory of J. J. Thomson. Corresponding to the applications made here, we shall assume *F* to depend only on $(\sin \theta)/\lambda$, λ being the wave-length of the radiation employed and 2θ the angle of scattering. The *F* curves give *F* as a function of $(\sin \theta)/\lambda$.

† 'Phil Mag.', vol 2, p 657 (1926)

‡ 'Phys Rev.', vol 29, p 605 (1927)

What follows refers in the first instance to scattering by an electron moving in a stationary atomic field. We shall neglect relativity corrections, which cannot introduce an error greater than a few per cent in the applications made here.

We may consider what happens as the radiation falling upon the electron gradually decreases in wave-length. As the wave-length diminishes, so that the frequency of the incident radiation becomes large compared with the characteristic absorption-frequencies associated with the electron, the dispersion formula which holds for optical frequencies gradually transforms into the classical scattering formula for a free electron, due to J J Thomson, and this remains true until the wave-length approaches the linear dimensions of the initial "orbits" of the electron. As the wave-length becomes shorter, the scattering of coherent radiation diminishes and becomes more concentrated in the forward direction of the incident light. We could picture the effect by supposing the electron to consist of a spatial distribution of charge each element of which scatters according to the classical law. For such a distribution the resultant scattering in directions other than the forward direction will be diminished by interference. The distribution of charge which would actually give the angular distribution of coherent scattered radiation calculated by the wave mechanics is precisely the Schrödinger distribution of charge for the scattering electron in the particular stationary state concerned (in practice the normal state). The electron will in fact have an F curve which can be calculated from its Schrödinger distribution of charge.

As the coherent scattering diminishes, incoherent scattering will occur which, as the wave-length decreases, approximates more and more closely in intensity and distribution to the Compton effect, and practically merges into it when the momentum of the incident quantum is large compared with that corresponding to electronic motions in the atom. The sum of the intensities of the coherent and incoherent radiation during this whole process is given by the Thomson formula*.

For an atom containing more than one electron, the total Schrödinger density of charge may be found by taking the sum of the densities corresponding to the separate electrons. If the frequency of the incident radiation is higher than, and not too near, the frequency of the K -absorption edge of the atom, we may therefore expect, and this is the point of importance for our present purpose, that the coherent part of the scattered radiation may be directly

* If the frequency of the incident radiation is so high that relativity corrections must be taken into account, this result is no longer true.

calculated by applying the classical Thomson formula for the amplitude of the scattered radiation to each element of that distribution of electricity which is defined by the Schrödinger density distribution for the initial state of the scattering atom (in practice the normal state)* In this case it is no longer true that the intensity of the radiation scattered in any direction is given by the Thomson formula, although we may expect to obtain some degree of approximation to the intensity by applying the results given for one electron to each electron of an atom containing several electrons †

The importance of these results in comparing theory and experiment is at once evident. Distributions of charge deduced from observed F curves will be the Schrödinger density distributions, and conversely, if the Schrödinger distribution for any atom can be calculated, the scattering curve to be expected with X-rays whose frequencies lie within the limits already defined can at once be calculated according to the classical laws given above.

3 Calculation of the Schrödinger Distribution of Charge for Sodium and Chlorine

In order to calculate accurately the Schrodinger density of charge for an atom containing N electrons, it is first necessary to find the characteristic values and functions for a Schrodinger wave equation in $3N$ variables. However, a simpler method which appears to give a good approximation to the distribution of charge of the core electrons of an atom on the wave-mechanics is available, it has already been given in some detail by one of us (D R H) in two papers‡ and will here be described only briefly.

An approximation to the interactions of the various electrons in an atom is made by supposing that a central field of force acts on each one. As the Schrödinger charge distribution for a complete n_k group is spherically symmetrical, this is probably a close approximation for expressing the interactions of any electron with a closed group, and for the interactions of the electrons within a single closed group it is the simplest approximation which can be

* Cf a note by one of us (I W) in 'Naturwissenschaften,' December 2, 1927. If the atom contains N electrons, the Schrödinger characteristic functions (Eigenfunktionen) ϕ_n are functions of the $3N$ co-ordinates of the electrons. The density distribution for one electron in the state n is found by integrating $-\epsilon|\phi_n|^2$ with respect to the co-ordinates of all the other electrons, where $-\epsilon$ is the charge on one electron. It should be pointed out that in this treatment the "retardation" of the forces between the electrons has not been strictly taken into account: this point will be discussed in another paper.

† Cf Williams, 'Mem. Proc. Manchester Lit. Phil. Soc.', vol. 71, p. 23 (1927).

‡ 'Camb. Phil. Soc. Proc.', vol. 24, pp. 80, 111 (1928).

made to avoid the detailed solution of the many-electron problem, and seems justified by results given in the papers already mentioned

For any atom or ion all of whose n_s groups are complete, a field which may be called the "self-consistent field" may be found as follows. Consider first a given field which can be thought of as the sum of contributions from the nucleus and from the various groups of core electrons, it may be called the "initial field". For each n_s corresponding to a group of core electrons the field is corrected approximately for the fact that the distributed charge of any one electron of this group does not contribute to the field acting on that electron, the solution of the wave equation for one of the core electrons in the field so modified can be evaluated, and from it the distribution of charge for the group can be found (it is centrally symmetrical as the group is assumed to be complete), finally the field of the nucleus and distribution of charge of all the core electrons can be calculated, and may be called the "final field". If this is the same as the initial field used to calculate it, it is called the "self-consistent field".

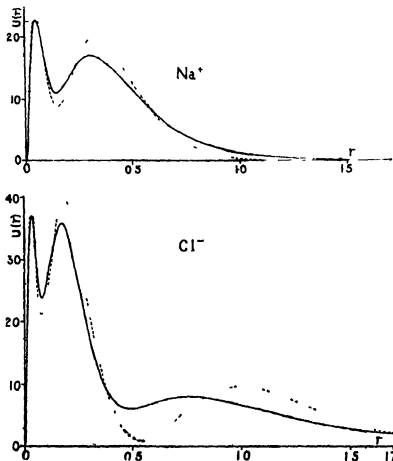
The process of determining the self-consistent field of a given atom is one of successive approximation, the numerical work involved in finding a close approximation to it is by no means prohibitive, and it seems probable that the distribution of charge in such a field is a good approximation to the actual distribution in the atom (so far as it can be thought of as in ordinary space at all), and very possibly the best that can be obtained without much more elaborate theoretical and numerical work.

Details of the methods used for solving the wave equation numerically, and for working out the successive approximations to the self-consistent field of an atom are given in the papers already referred to. Tables of the distribution of charge for the final stage of the successive approximation to the self-consistent fields of Na^+ and Cl^- are also given in the second paper, these tables give the radial charge density $U(r)^*$ in electrons per unit radius as a function of the radius, the unit of length being the "atomic unit" $a_H = \hbar^2/4\pi^2me^2 = 0.529 \text{ \AA}$, in the present paper the Ångström unit will be used as the unit of length. Curves of $U(r)$ as a function of r for Na^+ and Cl^- are given here in figs 1 and 2. For comparison, the distributions given earlier by Pauling† are also shown, these are calculated by a method which takes the radial distribu-

* I.e., $U(r)$ is the charge contained in a spherical shell between radii r and $r + dr$; in the papers referred to $U(r)$ is called $-dZ/dr$. For an ion consisting of closed groups, this charge is distributed uniformly over the sphere.

† Roy. Soc. Proc. 'A', vol. 114, p. 181 (1927).

tion for any electron as being that given by the wave mechanics for an electron in the Coulomb field of a point charge, the appropriate value of the charge



FIGS. 1 and 2.—Distribution of Charge in Na^+ and Cl^- Ions calculated by Wave Mechanics. Radial Density $U(r)$ in electrons per A.U. radius plotted as a function of radius r in \AA.U.

Full curve — calculated by method of self-consistent field

Broken curve - - - calculated by Pauling's method

being given by an empirical table. For the distribution in a Coulomb field, the peaks of the radial density curve are sharper and narrower than for the distribution in the non-Coulomb field of an actual atom, also Pauling's "size screening constants" give too large a scale for the distribution, especially for the outermost core electrons. The combined result of these two differences is that the maxima and minima of Pauling's radial density curve are too

pronounced, and this is particularly the case for the outermost minimum, and more so for the heavier than for the lighter elements

4 *The Observed F Curves and their Correction for Temperature*

The experimental values of F which will be compared with theory were obtained in the course of an investigation of the temperature factor of X-ray reflexion from rock salt*. Previous comparisons of F with atomic models have been based on the work of Bragg, James, and Bosanquet†. Later work by Havighurst,‡ Harris, Bates and MacInnes,§ and Bearden|| has confirmed the general accuracy of the earlier experiments. In all cases the observations were made at room temperature, and to correct them, so as to correspond to the atom in a state of rest, a temperature factor of X-ray reflexion now known to be considerably too small was used. The absolute values of the intensity of reflexion from rock salt have now been measured at the temperature of liquid air. Under these conditions the intensities of the spectra of high order are greatly increased, and it is possible to follow the scattering curve to angles of scattering considerably greater than a right angle. In fact, spectra have recently been measured at an angle of scattering as large as 130° . The results of these observations make it quite evident that the F -curves hitherto deduced from experiment fall away far too rapidly as the angle of scattering increases. This is of especial importance in connection with the Fourier analyses of electron distribution which have been based on these curves, and we shall return to this point later.

The values of F as deduced directly from the experimental results will be a function of the temperature, since the atoms in the crystals are in a state of thermal vibration which will affect the average distribution of charge density. To obtain the true F as defined in § 2, which refers to the atom in a state of rest, it is necessary to study the manner in which the intensity of X-ray reflexion by crystals depends on the temperature. The theory of the decrease of intensity of reflexion of X-rays with temperature was first discussed by Debye,¶ who concluded that for a simple cubic lattice, consisting of atoms of one kind only,

* James and Firth, *loc. cit.*

† 'Phil. Mag.', vol. 41, p. 309 (1921), vol. 42, p. 1 (1921), vol. 44, p. 433 (1922)

‡ 'Phys. Rev.', vol. 28, pp. 5, 860, 882 (1926)

§ 'Phys. Rev.', vol. 28, p. 235 (1926)

|| 'Phys. Rev.', vol. 29, p. 20 (1927)

¶ *Loc. cit.*

the intensity of an interference maximum formed at a glancing angle θ with wave-length λ should be multiplied by a factor e^{-M} , where

$$M = \frac{6\lambda^2}{\mu k \Theta} \frac{\phi(x)}{x} \frac{\sin^2 \theta}{\lambda^2} \quad (1)$$

Here h is Planck's constant, μ the mass of an atom of the crystal, k Boltzmann's gas constant, Θ the characteristic temperature of the crystal, $x = \Theta/T$, and $\phi(x)$ is a function of x , which approaches unity as x approaches zero, and zero for large values of x , and which is evaluated and tabulated by Debye in his paper. A later treatment by one of us (I W),* based on a different method of connecting the amplitudes of the atomic vibrations with the normal vibrations of the crystal, showed that the factor should really be e^{-2M} for the intensity, and consequently e^{-M} for the amplitude of the spectrum. It was also shown that for a crystal unit composed of more than one kind of atom, the structure-amplitude for spectra in which the contributions from all the atoms are in phase should be of the form $\sum F_\kappa e^{-M_\kappa}$ where F_κ is the F factor for an atom of type κ , supposed at rest, and M_κ is the value of M appropriate to that atom, and in general differs for different atoms, the summation being taken over all the atoms in the crystal unit. Formulae expressing M_κ as a function of the forces between the atoms were also given.

The experiments of James and Miss Firth showed that, for rock-salt, the observed temperature factor agreed quantitatively with the amended Debye theory from 86° absolute up to about 500° absolute, for spectra whose structure amplitudes were of the type $(Fe^{-M})_{Cl} + (Fe^{-M})_{Na}$. But it was also found that for spectra of the type $(Fe^{-M})_{Cl} - (Fe^{-M})_{Na}$ the decrease in intensity with temperature was considerably smaller than for those of the other type. This can only occur if M is different for chlorine and sodium. From these results Waller and James† deduced the ratios of the values of Fe^{-M} at room temperature, and at the temperature of liquid air, for the chlorine and for the sodium atoms separately. This does not suffice to determine the M 's, since all we are able to obtain from the ratio of Fe^{-M} at two temperatures is the value ΔM , or the difference between the values of M for those temperatures. By adding to M any constant quantity, independent of the temperature, we should not alter ΔM , and thus the existence of such a constant could not be inferred from the ratio of Fe^{-M} at two temperatures.

Now M is, for atoms of one kind, proportional to the energy of vibration of

* 'Upsala Dissertation,' 1925.

† 'Roy Soc. Proc., A, vol. 117, p. 214 (1927)

these atoms M may be regarded as composed of two parts M' and B . If no zero-point energy exists, B is zero and M is identical with M' , vanishing at absolute zero. The quantity B , which is independent of temperature, represents the constant contribution to the energy of vibration due to zero-point energy. We therefore have the equation

$$M = M' + B, \quad (2)$$

B being proportional to the zero-point energy.

What we can determine, by supposing our measurements carried out at temperatures as low as we please, is M' . We cannot determine M experimentally. If, however, we can obtain a theoretical estimate of B , we can calculate F , using measured values of M' , either on the assumption that there is zero-point energy or that there is not. Thus two separate F curves may be obtained for each atom, which may be compared with that calculated for the atomic model.

Assuming each atom to be bound in a cubically symmetrical way, the theory of the temperature factor shows that if $\overline{u_x^2}$ is the mean-square amplitude of vibration parallel to any direction x ,

$$M = \frac{8\pi^2 \sin^2 \theta}{\lambda^3} \overline{u_x^2} = \frac{8\pi^2 \sin^2 \theta}{\lambda^3} \{ \alpha + \beta T + \gamma/T + \delta/T^3 + \dots \} \quad (3)$$

the expansion being convergent for temperatures higher than about 50° abs for rock-salt. In this formula, γ can easily be calculated, while α and β , which depend on the interatomic forces, cannot be calculated directly. For δ , a rough estimate, which can readily be obtained, is enough. If we assume the zero-point energy to have the value proposed by Planck, half a quantum per degree of freedom, then α is equal to zero, and β can be determined from the experimental results in the manner described by Waller and James*. On this assumption therefore, we may obtain M , and hence F , for the atoms of chlorine and sodium. M was found to be greater for sodium than for chlorine, indicating that the average amplitude of vibration of the sodium atoms is greater than that of the chlorine atoms.

It is not easy to calculate accurately the theoretical values of α for absence of zero-point energy. The F -curves given by James and Miss Firth correspond approximately to this state of affairs, although the separate values of M for the two atoms were not taken into account, and the formula used to extrapolate to absolute zero is really valid only for a simple cubic lattice.

The curves calculated on the two assumptions are given in fig. 3, and it will

* *Loc. cit.*

be seen that the difference between them is very considerable, especially for large angles of scattering.

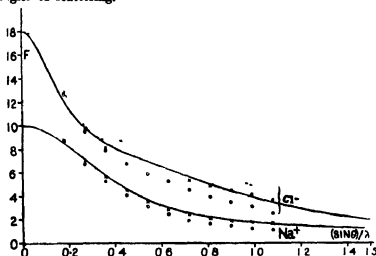


FIG 3—Comparison of F values deduced from observation with those calculated from theory F plotted as a function of $\sin \theta/\lambda$ for Na^+ and Cl^- ions, θ = glancing angle, λ = wave-length in A U. Full curves show values of F for distribution of charge calculated by wave mechanics, broken curve shows values of F for distribution of charge for orbital atomic model. Crosses show values of F deduced from observation, assuming zero point energy, circles show values of F deduced from observation, assuming no zero point energy.

The values of F for Cl^- and Na^+ calculated from the Schrodinger densities, and the observed values corrected to correspond to the ions in a state of rest on the assumption that zero-point energy exists are also given in Table I

Table I

$(\sin \theta)/\lambda$	$F(\text{Na}^+)$		$F(\text{Cl}^-)$		$(\sin \theta)/\lambda$	$F(\text{Na}^+)$		$F(\text{Cl}^-)$	
	Calc	Obs *	Calc	Obs *		Calc	Obs *	Calc	Obs *
0 00	10 00	—	18 00	—	0 60	3 22	3 00	6 49	6 03
0 05	9 87	—	17 11	—	0 70	2 63	2 40	5 77	5 45
0 10	9 50	—	15 23	—	0 80	2 23	2 12	5 06	4 89
0 15	8 92	—	13 19	—	0 90	1 96	1 93	4 41	4 45
0 20	8 21	8 30	11 50	11 70	1 00	1 75	1 79	3 84	3 96
0 25	7 45	7 30	10 23	10 15	1 10	1 59	1 65	3 33	3 50
0 30	6 68	6 44	9 30	9 02	1 20	1 48	—	2 89	—
0 35	5 93	5 79	8 60	8 32	1 30	1 40	—	2 51	—
0 40	5 23	5 07	8 06	7 70	1 40	1 34	—	2 21	—
0 45	4 61	4 45	7 62	7 30	1 50	1 29	—	1 99	—
0 50	4 07	3 94	7 23	6 78					

* The observed values in this table were read from curves plotted from the corrected values of F given by Waller and James (*loc cit*)

5 Comparison of the Corrected *F* curves with those calculated from the Atomic Models

From the Schrodinger distribution of density for the ions of sodium and chlorine, obtained in the manner described in section 3, we have calculated the *F*-curves, assuming that every element of charge scatters according to the classical laws, and that the contributions from the charges in different parts of the atom can be combined using the ordinary rules of interference. The radial distributions plotted in figs 1 and 2 give the radial density $U(r)$ in electrons per Å U radius as ordinates and r in Å U as abscissae, $U(r)$ being the amount of charge lying between distances r and $r + dr$ from the centre of the atom. The contribution dF to the *F*-curve from such a shell, for a spectrum formed at a glancing angle θ , and hence for an angle of scattering 2θ , is given by

$$dF = U(r) \frac{\sin \phi}{\phi} dr,$$

where $\phi = (4\pi r \sin \theta)/\lambda$, and hence, for the whole atom, *F* for this spectrum is given by

$$F = \int_0^{\infty} U(r) \frac{\sin \phi}{\phi} dr \quad (4)$$

An interpretation of this formula is that *F* is the number of electrons in the atom multiplied by the mean value of $(\sin \phi)/\phi$, weighted according to the radial density of charge. This integral is evaluated graphically or numerically for a series of values of $(\sin \theta)/\lambda$ close enough to allow interpolation to the accuracy required.

Some curves of $U(r) \sin \phi/\phi$ are given in fig 4, to illustrate the way in which, as $(\sin \theta)/\lambda$ increases, the outer parts of the atom rapidly become of small importance, and how at large angles of scattering the form of the *F* curve depends almost entirely on the two K electrons.

The values of *F* calculated in this way are tabulated in Table I and are plotted in fig 3 where they may be compared with the values obtained from the experimental results. It will be seen that for both chlorine and sodium there is a very close agreement between the calculated values of *F* and the observed values corrected, assuming the existence of zero-point energy. The calculated curve for each ion is shown as a full line, the crosses show the values obtained from experiment assuming Planck's value of the zero-point energy, and the circles the approximate values assuming absence of zero-point energy*.

* For clearness, the results of experiment are shown by points rather than by curves.

For both chlorine and sodium, the observed curve is higher than the calculated one for small values of θ . This is probably due to an incorrect allowance

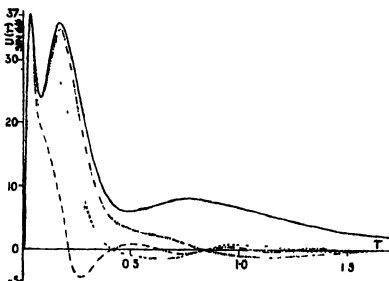


FIG. 4—Showing contributions from different parts of the atomic distribution of charge to F at various glancing angles $U(r) (\sin \phi)/\phi$ in electrons per \AA U radius [$\phi = 4\pi r (\sin \theta)/\lambda$] plotted against r in $\text{\AA} \cdot U$ for

$$(\sin \theta)/\lambda = 0, \text{ thus } \text{---} \text{---} \text{---}$$

$$(\sin \theta)/\lambda = 0.3 \text{ ---} \text{---} \text{---}$$

$$(\sin \theta)/\lambda = 0.6, \text{ thus } \text{---} \text{---} \text{---}$$

$$(\sin \theta)/\lambda = 1.2 \text{ ---} \text{---} \text{---}$$

for extinction, which is difficult to measure and which chiefly affects the intense spectra. For somewhat higher angles the observed curve falls below the calculated one, but crosses it again and lies slightly above it for values of $(\sin \theta)/\lambda$ greater than about 0.9.

It is a little difficult to be sure to what extent these deviations are real. The calculated distribution of charge for the outermost electrons of Cl^- is slightly uncertain, on account of difficulties in the calculation due to the negative charge on the ion, the consequent error in F might amount to 0.2 and would probably be greatest just about where the difference between the observed and calculated curves is greatest, but this is not enough to explain the whole difference, otherwise the precision of the numerical work should be adequate to give values of F to 0.03. Whether the simplifying assumptions made in calculating the distribution of charge would introduce appreciable error in F cannot at present be determined.

The observed curves are obtained by taking half the sum and half the difference of the smoothed curves for $(F_{\text{e}^-})_{\text{Cl}} + (F_{\text{e}^-})_{\text{Na}}$ and $(F_{\text{e}^-})_{\text{Cl}} - (F_{\text{e}^-})_{\text{Na}}$.

and it is possible that some of the deviations are introduced in this process. On the difference curve for example, no points between $(\sin \theta)/\lambda = 0.154$, corresponding to the (111) spectrum, and $(\sin \theta)/\lambda = 0.295$, corresponding to the (113) spectrum, can be obtained by observation. Between these two points the curve is falling rapidly and its subsequent course for higher values of $(\sin \theta)/\lambda$ makes interpolation between (111) and (113) very doubtful. To obtain a more direct comparison of theory and experiment, we have calculated from the theoretical density distributions the curves for $(Fe^{-M})_{Cl} \pm (Fe^{-M})_{Na}$ at 86° absolute, using the values of M deduced from the experimental results. These curves are given in fig. 5. The circles in the same figure give the observed values for a series of spectra at the temperature of liquid air. In obtaining the values of M it was, of course, necessary to use

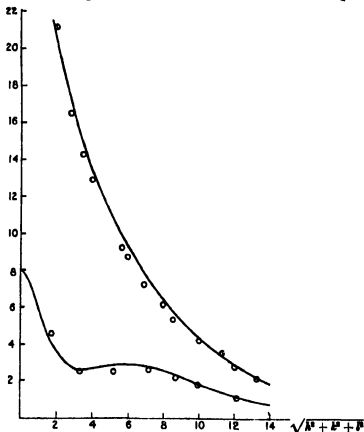


FIG. 5.—Value of the structure amplitude $(Fe^{-M})_{Cl} \pm (Fe^{-M})_{Na}$ calculated from the wave mechanics atomic model and corrected to 86° abs. by using the observed temperature factor, extrapolated assuming the existence of zero point energy, plotted against $\sqrt{h^2 + k^2 + l^2} = 11.26 (\sin \theta)/\lambda$, $[(hkl)$ the index of a spectrum]. The circles show the observed values at the temperature of liquid air (86° abs.)

the separate F-curves for the two atoms, so that the results are not entirely free from uncertainty due to lack of knowledge of the exact form of the curve for the different spectra. The uncertainty, however, is now only in a correction, and the comparison between theory and experiment is more direct. The agreement between calculation and observation is surprisingly good, but there seems still to be a systematic deviation of the experimental points from the theoretical curve. The values for high angles of scattering are, of course, difficult to measure accurately, since the intensities of the spectra concerned are very small. But there can be no reasonable doubt that the difference between the F curves with and without zero-point energy are well beyond the limits of experimental error. *If the theoretical model is accurate, the experimental results seem to indicate very definitely the existence of zero-point energy.*

Now for high angles of scattering the form of the F curve, as we have seen, depends almost entirely on the K electrons, and it is very unlikely that the atomic model can be much in error so far as these are concerned, since the proportional deviation from a Coulomb field is so small over the main part of the range for which the radial density is appreciable. The mean amplitude of vibration of the atoms corresponding to zero-point energy is of the same order as the radius of the K electron region. From the ratios of the values of F with and without zero-point energy, we have calculated approximately the root-mean square amplitudes of vibration at absolute zero. We find 0.12 Å for sodium and 0.11 Å for chlorine. Now the K maximum in the density distribution occurs at 0.035 Å from the nucleus for chlorine and 0.052 Å for sodium. The F curve due to the K electrons will thus depend greatly upon whether there is or is not zero-point energy, and since it is practically this curve that we measure at high angles of scattering, conditions are favourable for distinguishing between the two cases, and the discrimination depends much less on the exact theory used to obtain the atomic model than might have been expected.

It may be pointed out here that, since on the wave mechanics the charge-distribution of an atom or ion, all of whose electrons are in closed n_s groups, is centrally symmetrical, the value of F given by equation (4) holds for a single atom, whereas on the orbit model it only holds for reflection from a crystal in the direction of a spectrum so that we can average the radial distribution of scattering electrons over a large number of atoms.

For comparison, the F curve for Cl^- calculated for the orbital atomic model by an approximate method given by one of us in an earlier paper* is also shown

* D. B. Hartree, 'Phil. Mag.', vol. 50, p. 289 (1925). Integer values of the azimuthal quantum number k are assumed in the numerical data from which these curves were calculated, the use of half integer values of k would have only a small effect on the F curves.

in fig 3 Its most striking difference from the F curve deduced from the wave mechanics is a pronounced "bump" in the curve for the orbit model* The existence of this bump for the orbit model and its absence for the wave theory model can easily be explained On the orbit model, near the outer apex of an orbit, radius r_0 , the radial density (averaged over a large number of atoms at an instant of time, or over a long time for one atom) tends to infinity as $r \rightarrow r_0$ from below, and is zero for $r > r_0$. This strong concentration of charge just inside the outer apex weights very heavily the value of $(\sin \phi)/\phi$ there in the integration of (4) for F , as the glancing angle increases, the value of $\phi = (4\pi \sin \theta)/\lambda$ for a value of r just less than the outer apical distance of the outermost groups of orbits passes through successive maxima and minima of $(\sin \phi)/\phi$, and on account of the heavy local weighting of the value of $(\sin \phi)/\phi$ at this radius, these maxima and minima appear quite noticeably as the bumps on the F -curve The same applies to the contributions to F from the inner groups of orbits On the wave mechanics, the charge density remains always finite and continuous, and although it has maxima and minima, there is nothing like the heavy weighting of the values of $(\sin \phi)/\phi$ over a small range which occurs with the orbital model, so that the maxima and minima of this quantity do not now have such a noticeable effect on the F -curve Their effect does not, however, disappear entirely, for Cl^- the F -curve has a portion almost straight at about $(\sin \theta)/\lambda = 0.5$, between two portions concave upwards This straight piece corresponds to the bump on the curve calculated on the orbit model

6 On the Fourier Method of obtaining Charge Distributions

In this paper, we have preferred to calculate the F -curves from the theoretical atomic models, and to compare them with the curves obtained from the experimental results, rather than to employ the apparently much more direct method of deducing a distribution of charge from the F -curves and comparing this with the atomic models The method of Fourier analysis due to Duane,[†] which was used in this way by Havighurst[‡] and by Compton,[§] will, of course, give the Schrödinger charge densities By its means we may determine a "sheet-

* For Na, the F curve for the orbital model has a similar though less pronounced hump This curve also lies above the curve calculated from the distribution of charge according to the wave mechanics

† 'Proc. Nat. Acad. Sci.', vol. 11, p. 489 (1925)

‡ 'Proc. Nat. Acad. Sci.', vol. 11, p. 803 (1925)

§ "X-rays and Electrons," p. 151

density," in planes parallel to a set of reflecting planes of the crystal, in which case the coefficients of the terms of the Fourier series are proportional to the values of F for the successive spectra from these planes, or we may, when the F -curve for one kind of atom can be obtained, deduce the radial density $U(r)$, the coefficients then being proportional to nF_n , where F_n is the value of F for the n th order spectrum. In either case, the series must be continued until the coefficients become so small that the contributions of all further terms to the density distribution are negligible. Now at the highest angle of scattering at which F has been determined it is still far from negligible.

To employ a Fourier series with a limited number of terms is simply to introduce false detail into the atomic model deduced from it, on the other hand, to extrapolate the F -curves is to assume much of what we are attempting to determine. These objections apply particularly to the radial analysis, for here the terms of the series converge very slowly, since each F is multiplied by its order. They apply with somewhat less force to the sheet analysis, but this, on the other hand, is not sensitive to the details of the radial distribution for large values of r , while it is inconveniently sensitive for very small values.

If we apply Fourier analyses to results obtained with long wave-lengths we shall obtain detail far beyond the resolving power of our apparatus, but it will be false detail, and will correspond to nothing in the atomic structure. The method which we have employed, of comparing the F -curves deduced from the atomic models with the experimental F -curves, cannot, of course, give fine detail either. Various atomic models differing in their fine structure, would give practically indistinguishable F -curves. It has the merit, however, of involving no extrapolations and does compare theory directly with experiment. The difference between the F -curves deduced with and without zero point energy is quite definite and allows a decision between the two cases to be made by experiment. Using the Fourier method we should have had to distinguish between two different radial densities, and the occurrence of false detail in the calculated distributions, due to lack of knowledge of the higher coefficients, would have made the decision difficult. To employ the Fourier method with advantage, it would be necessary to obtain F -curves with much shorter wave-lengths than have hitherto been used, which would, of course, enable higher orders of spectra to be observed. This is strictly analogous to increasing the resolving power of an optical apparatus by using ultra-violet light as an illuminant.

Summary

It can be shown that within certain limits of frequency, the F-curve, or atomic scattering curve, of an atom for X-radiation can be calculated by applying the classical law of scattering to the Schrödinger distribution of charge

This result is used to compare the F-curves calculated from the Schrödinger distributions for the ions Na^+ and Cl^- , obtained theoretically by an approximate method, with those obtained experimentally from observations on the rock-salt crystal at different temperatures

It is found that the F-curves so calculated agree very closely with the experimental curves on the assumption that the crystal possesses zero-point energy of amount half a quantum per degree of freedom, as proposed by Planck The difference between the F-curves with and without this energy is considerable, since the amplitudes of vibration of the atoms at the absolute zero are somewhat greater than the radii of the regions within which the density distributions of the K electrons are concentrated, and it is upon these electrons that the F-curves at high angles of scattering mainly depend

In conclusion we wish to express our indebtedness to Prof W L Bragg, F R S, for his constant help and advice at every stage of this work

The Quantum Theory of the Electron Part II

By P A M DIRAC, St John's College, Cambridge

(Communicated by R H Fowler, F R S —Received February 2, 1928)

In a previous paper by the author* it is shown that the general theory of quantum mechanics together with relativity require the wave equation for an electron moving in an arbitrary electromagnetic field of potentials, A_0 , A_1 , A_2 , A_3 to be of the form

$$F\psi \equiv \left[p_0 + \frac{e}{c} A_0 + \alpha_1 \left(p_1 + \frac{e}{c} A_1 \right) + \alpha_2 \left(p_2 + \frac{e}{c} A_2 \right) + \alpha_3 \left(p_3 + \frac{e}{c} A_3 \right) + \alpha_4 mc \right] \psi = 0 \quad (1)$$

The α 's are new dynamical variables which it is necessary to introduce in order to satisfy the conditions of the problem. They may be regarded as describing some internal motion of the electron, which for most purposes may be taken to be the spin of the electron postulated in previous theories. We shall call them the spin variables.

The α 's must satisfy the conditions

$$\alpha_\mu^2 = 1, \quad \alpha_\mu \alpha_\nu + \alpha_\nu \alpha_\mu = 0 \quad (\mu \neq \nu)$$

They may conveniently be expressed in terms of six variables ρ_1 , ρ_2 , ρ_3 , σ_1 , σ_2 , σ_3 that satisfy

$$\left. \begin{aligned} &\rho_r^2 = 1, \quad \sigma_r^2 = 1, \quad \rho_r \sigma_s = \sigma_s \rho_r, \quad (r, s = 1, 2, 3) \\ \text{and} \quad &\rho_1 \rho_2 = \rho_3, \quad \rho_2 \rho_3 = \rho_1, \quad \sigma_1 \sigma_2 = \sigma_3, \quad \sigma_2 \sigma_3 = \sigma_1 \end{aligned} \right\}, \quad (2)$$

together with the relations obtained from these by cyclic permutation of the suffixes, by means of the equations

$$\alpha_1 = \rho_1 \sigma_1, \quad \alpha_2 = \rho_1 \sigma_2, \quad \alpha_3 = \rho_1 \sigma_3, \quad \alpha_4 = \rho_3.$$

The variables σ_1 , σ_2 , σ_3 now form the three components of a vector, which corresponds (apart from a constant factor) to the spin angular momentum vector that appears in Pauli's theory of the spinning electron. The ρ 's and σ 's vary with the time, like other dynamical variables. Their equations of motion, written in the Poisson Bracket notation [], are

$$\dot{\rho}_r = c [\rho_r, F], \quad \dot{\sigma}_r = c [\sigma_r, F].$$

* 'Roy Soc Proc,' A, vol 117, p. 610 (1928). This is referred to later by *loc. cit.*

It should be observed that these equations of motion are consistent with the conditions (2), so that if the conditions are satisfied initially they always remain satisfied. For example, we have

$$i\hbar/c \dot{\sigma}_1 = \sigma_1 H - F\sigma_1 = 2s\rho_1\sigma_3(p_3 + e/c A_3) - 2s\rho_1\sigma_3(p_3 + e/c A_3)$$

Thus σ_1 anticommutes with σ_1 , so that

$$d\sigma_1^2/dt = \sigma_1\sigma_1 + \sigma_1\sigma_1 = 0$$

The ρ 's and σ 's, and therefore also any function of them, can be represented by matrices with four rows and columns. A possible representation, in which ρ_3 and σ_3 are diagonal matrices, is given in (*loc cit*) § 2. Such a representation can apply only to a single instant of time, since the ρ 's and σ 's vary with the time. To get a scheme of representation which holds for all times, so that the equations of motion are valid in it, we should have to have only constants of the motion as diagonal matrices. It is, however, quite correct for the purpose of solving the wave equation (1) to take a matrix representation for the ρ 's and σ 's which holds only for a single instant of time (as was done in *loc cit*), since the wave function is then the transformation function connecting the ρ 's, σ 's and x 's at this particular time with a set of variables that are constants of the motion, as is required for the general interpretation of quantum mechanics.

Before we proceed with the theory of atoms with single electrons that was begun in *loc cit*, the proof will be given of the conservation theorem, which states that the change in the probability of the electron being in a given volume during a given time is equal to the probability of its having crossed the boundary. This proof is supplementary to the work of *loc cit* § 3, and is necessary before one can infer that the theory will give consistent results that are invariant under a Lorentz transformation.

§ 1 The Conservation Theorem

We shall first make a slight generalisation of the usual interpretation of wave mechanics to apply to cases when the Hamiltonian is not Hermitian. Let the wave equation, written in certain variables q , be

$$(H - W)\psi = 0 \quad (1)$$

Consider also the equation

$$(\hat{H} - \hat{W})\phi = 0$$

or

$$(\hat{H} + W)\phi = 0, \quad (2)$$

where the symbol \bar{a} denotes the matrix obtained from the matrix a by transposing rows and columns. If ψ_m, ϕ_n are suitably normalised solutions of (1) and (2) respectively, referring to the states m and n , we take $\phi_n \psi_m$ to be the corresponding matrix element of the probability of the q 's having specified values. If H is Hermitian, \bar{H} is the conjugate imaginary of H (obtained by writing $-i$ for i) and the solutions of (2) are just the conjugate imaginaries to the solutions of (1), so that in this case our probability $\phi_n \psi_m$ becomes the usual one $\bar{\psi}_n \psi_m$. In the general case it is necessary to use the transposed Hamiltonian instead of the conjugate imaginary Hamiltonian in (2) in order to secure that if ϕ_n, ψ_m are initially orthogonal or mutually normalised ($i.e., \int \phi_n \psi_m dq = 1$), they always remain orthogonal or mutually normalised respectively.

Our wave equation for an electron in an electromagnetic field is

$$[p_0 + e'A_0 + \rho_1(\boldsymbol{\sigma} \cdot \mathbf{p} + e'\mathbf{A}) + \rho_3 mc] \psi = 0 \quad (3)$$

where $e' = e/c$. The Hamiltonian here will be Hermitian if a matrix scheme for the spin variables is chosen in which they are Hermitian. However, if one now applies a Lorentz transformation to this wave equation and divides out by the coefficient of the new p_0 , the resulting new Hamiltonian will not, in general, be Hermitian, although, as shown in *loc cit*, § 3, it may be brought back to its original Hermitian form by a canonical transformation of the matrix scheme for the spin variables. In the following work we require to have the same matrix representation of the spin variables for all frames of reference, so we cannot assume our Hamiltonian is Hermitian, and must use the above generalised interpretation.

The equation obtained by transposing rows and columns in the operator of (3) is

$$[-p_0 + e'A_0 + \bar{\rho}_1(\bar{\boldsymbol{\sigma}} \cdot -\mathbf{p} + e'\mathbf{A}) + \bar{\rho}_3 mc] \phi = 0 \quad (4)$$

The probability per unit volume of the electron being in the neighbourhood of any point is given, according to the above assumption, by $\phi \psi$, where this product must now be understood to mean the sum of the products of each of the four components of ϕ (referring respectively to the four rows or columns of the matrices ρ, σ) into the corresponding component of ψ . We have to prove that this probability is the time component of a 4-vector, and that the divergence of this 4-vector vanishes.

From (3)

$$[\rho_3(p_0 + e'A_0) + \rho_1\rho_2(\sigma, p + e'A) + mc]\rho_3\psi = 0$$

or

$$[\gamma_0(p_0 + e'A_0) + \sum_{r=1,2,3} \gamma_r(p_r + e'A_r) + mc]\chi = 0, \quad (5)$$

where

$$\gamma_0 = \rho_3, \quad \gamma_r = \rho_1\rho_2\sigma_r, \quad \chi = \rho_3\psi$$

Equation (5) is symmetrical between the four dimensions of space and time, and shows that $\gamma_0, -\gamma_1, -\gamma_2, -\gamma_3$ are the contravariant components of a 4-vector. If we multiply (4) by ρ_3 on the left-hand side, we get

$$[\gamma_0(-p_0 + e'A_0) + \sum_r \tilde{\gamma}_r(-p_r + e'A_r) + mc]\phi = 0, \quad (6)$$

since

$$\tilde{\gamma}_0 = \rho_3, \quad \tilde{\gamma}_r = \tilde{\sigma}_r\tilde{\rho}_3\tilde{\rho}_1 = \tilde{\rho}_3\tilde{\sigma}_1\tilde{\rho}_r$$

The operator in this equation is just the transposed operator of (5). The probability per unit volume of the electron being in any place is now given by

$$\phi\psi = \phi\rho_3\chi = \phi\gamma_0\chi, \quad (7)$$

where $\phi\alpha\chi$ denotes the sum of the products of each component of ϕ into the corresponding component of $\alpha\chi$, α being any function of the spin variables, represented by a matrix with four rows and columns [Note that quite generally $\phi\alpha\chi = \chi\tilde{\alpha}\phi$]. Expression (7) is the time component of a 4-vector, whose spacial components, namely,

$$-\phi\gamma_1\chi, \quad -\phi\gamma_2\chi, \quad -\phi\gamma_3\chi,$$

must give $1/c$ times the probability per unit time of the electron crossing unit area perpendicular to each of the three axes respectively.

We must now show that the divergence of this 4-vector vanishes, i.e., that

$$\frac{1}{c} \frac{\partial}{\partial t} (\phi\gamma_0\chi) - \sum_r \frac{\partial}{\partial x_r} (\phi\gamma_r\chi) = 0 \quad (8)$$

Multiplying (5) by ϕ and (6) by χ and subtracting, we get

$$\phi[\gamma_0 p_0 + \sum_r \gamma_r p_r]\chi + \chi[\tilde{\gamma}_0 p_0 + \sum_r \tilde{\gamma}_r p_r]\phi = 0,$$

which gives

$$\phi \left[\gamma_0 \frac{\partial}{\partial t} - \sum_r \gamma_r \frac{\partial}{\partial x_r} \right] \chi + \chi \left[\tilde{\gamma}_0 \frac{\partial}{\partial t} - \sum_r \tilde{\gamma}_r \frac{\partial}{\partial x_r} \right] \phi = 0,$$

or

$$\phi \left[\gamma_0 \frac{\partial}{\partial t} - \sum_r \gamma_r \frac{\partial}{\partial x_r} \right] \chi + \frac{1}{c} \frac{\partial \phi}{\partial t} \gamma_0 \chi - \sum_r \frac{\partial \phi}{\partial x_r} \gamma_r \chi = 0$$

This gives immediately the conservation equation (8) as the γ 's are here constant matrices.

§ 2 The Selection Principle

In *loc. cit.* the quantum number j was introduced, which determines the magnitude of the resultant angular momentum for an electron moving in a central field of force. j can take both positive and negative integral values. Again, the magnetic quantum number $m = M_z/\hbar$, say, that determines the component of the total angular momentum in some specified direction, was shown to take half odd integral values from $|j| + \frac{1}{2}$ to $|j| - \frac{1}{2}$. The state $j = 0$ is thus excluded, and the weight of any state j is $2|j|$. The equation obtained to determine the energy levels, i.e., equation (25) or (26), involves j only through the combination $j(j+1)$ except in the last term, which represents the spin correction. Thus two values of j which give the same value for $j(j+1)$ form a spin doublet, so that $j = j'$ and $j = -(j' + 1)$ form a spin doublet when $j' > 0$. The connection between j -values and the usual notation for alkali spectra is therefore given by the following scheme —

$$\begin{array}{ccccccc}
 j = -1 & & 1 & -2 & & 2 & -3 & & 3 & -4 \\
 \text{S} & & \underbrace{\hspace{1.5cm}} & \text{P} & & \underbrace{\hspace{1.5cm}} & \text{D} & & \underbrace{\hspace{1.5cm}} & \text{F}
 \end{array}$$

There is no azimuthal quantum number k in the present theory, an orbit for an electron in an atom being defined by three quantum numbers n, j, m only. One might on this account expect the selection rules, the relative intensities of the lines of a multiplet, etc., in the usual derivation of which k plays an important part, to be different in the present theory, but it will be found that they do just happen to be the same.

We shall first determine the selection rule for j . We use the following two theorems —

(i) If a dynamical variable X anticommutes with j , its matrix elements all refer to transitions of the type $j \rightarrow -j$.

(ii) If a dynamical variable Y satisfies

$$[[Y, j\hbar], j\hbar] = -Y, \quad (9)$$

its matrix elements all refer to transitions of the type $j \rightarrow j \pm 1$.

To prove (i) we observe that the condition $jX + Xj = 0$ gives

$$j' X(j'j'') + X(j'j'') j'' = 0$$

or

$$(j' + j'') X(j'j'') = 0$$

Hence $X(j'j'') = 0$ unless $j'' = -j'$.

A proof of (11) involving angle variables has been given in a previous paper * A simple proof analogous to the foregoing proof of (1) is as follows Equation (9) gives

$$Yj^3 - 2jYj + j^3Y = Y$$

or

$$Y(j'j'')j'^3 - 2j'Y(j'j'')j'' + j'^3Y(j'j'') = Y(j'j'')$$

Hence $Y(j'j'') = 0$ except when

$$j''^3 - 2j'j'' + j'^3 = 1,$$

i.e., when

$$j'' = j' \pm 1$$

We shall now evaluate $[x_3, j\hbar], j\hbar]$ The definition of j is

$$j\hbar = \rho_3 \{(\sigma, m) + \hbar\}$$

Hence

$$\begin{aligned} [x_3, j\hbar] &= \rho_3 \{ \sigma_1 [x_3, m_1] + \sigma_2 [x_3, m_2] \} \\ &= \rho_3 (\sigma_1 x_2 - \sigma_2 x_1), \end{aligned} \quad (10)$$

so that

$$[[x_3, j\hbar], j\hbar] = [\sigma_1 x_2 - \sigma_2 x_1, (\sigma, m)]$$

Now

$$\hbar [\sigma_1, (\sigma, m)] = \sigma_1 (\sigma, m) - (\sigma, m) \sigma_1 = 2\hbar (\sigma_2 m_2 - \sigma_3 m_3)$$

or

$$\frac{1}{2}\hbar [\sigma_1, (\sigma, m)] = \sigma_2 m_2 - \sigma_3 m_3,$$

and similarly

$$\frac{1}{2}\hbar [\sigma_2, (\sigma, m)] = \sigma_1 m_2 - \sigma_3 m_1$$

Hence

$$\begin{aligned} \frac{1}{2}\hbar [[x_3, j\hbar], j\hbar] &= (\sigma_2 m_2 - \sigma_3 m_3) x_2 + \frac{1}{2}\hbar \sigma_1 (\sigma_2 x_1 - \sigma_1 x_3) \\ &\quad - (\sigma_1 m_2 - \sigma_3 m_1) x_1 - \frac{1}{2}\hbar \sigma_2 (\sigma_2 x_3 - \sigma_3 x_2) \\ &= \sigma_3 (m, x) - m_2 (\sigma, x) + \frac{1}{2}\hbar \{ -\sigma_2 (\sigma, x) - x_3 \} \\ &= -M_2 (\sigma, x) - \frac{1}{2}\hbar x_3, \end{aligned}$$

so that

$$[[x_3, j\hbar], j\hbar] = -2u(\sigma, x) - x_3$$

Thus x_3 does not quite satisfy the condition that Y satisfies in (9), owing to the extra term $-2u(\sigma, x)$ This extra term, however, anticommutes with j If we now form the expression $x_3 - cu(\sigma, x)$, where c is some quantity that commutes with j , we can choose c so as to make this expression satisfy completely the condition that Y satisfies in (9) We have, in fact,

$$\begin{aligned} [[x_3 - cu(\sigma, x), j\hbar], j\hbar] &= -2u(\sigma, x) - x_3 + cu \frac{1}{2}j^3 (\sigma, x) \\ &= -\{x_3 - cu(\sigma, x)\} \end{aligned}$$

* 'Roy Soc Proc,' A, vol 111, p 281 (1926), § 3.

if ϵ is chosen such that

$$\begin{aligned} -2 + 4j^2\epsilon &= c, \\ \epsilon, \text{ if} \\ c &= 1/2(j^2 - \frac{1}{2}) \end{aligned}$$

Hence x_3 can be expressed as the sum of two terms, namely,

$$\frac{u}{2(j^2 - \frac{1}{2})}(\sigma, x) \quad \text{and} \quad x_3 - \frac{u}{2(j^2 - \frac{1}{2})}(\sigma, x),$$

of which the first anticommutes with j , and therefore contains only matrix elements referring to transitions of the type $j \rightarrow -j$, while the second satisfies the condition that Y satisfies in (9), and therefore contains only matrix elements referring to transitions of the type $j \rightarrow j \pm 1$. A similar result holds for x_1 and x_2 . Hence the selection rule for j is

$$j \rightarrow -j \quad \text{or} \quad j \rightarrow j \pm 1$$

Thus from states with $j = 2$ transitions can take place to states with $j = 1, -2$ or 3 . Comparing this selection rule with the above scheme connecting j -values with the S, P, D notation, we see that it is exactly equivalent to the two selection rules for j and k of the usual theory, and is therefore in agreement with experiment.

§ 3 The Relative Intensities of the Lines of a Multiplet

The relative intensities of the various components into which a line is split up in a weak magnetic field must be the same on the present theory as on previous theories, as they depend only on the Vertauschungs relations connecting the co-ordinates x_i with the components of total angular momentum M_i , which are taken over unchanged into the present theory. It will therefore be sufficient, for determining the relative intensities of the lines of a multiplet, to consider only one Zeeman component of each line, say, the component for which $\Delta u = 0$, ϵ , the component that comes from x_3 .

We shall determine the matrix elements of x_3 , when expressed as a matrix in a scheme in which r, j, u and p_3 are diagonal. x_3 is diagonal in (ϵ , commutes with) all of these variables except j . The part of x_3 referring to transitions $j \rightarrow -j$ we found to be

$$\frac{u}{2(j^2 - \frac{1}{2})}(\sigma, x) = \frac{u}{2(j^2 - \frac{1}{2})} \epsilon p_1 r, \quad (11)$$

using the ϵ introduced in *loc cit* § 6. ϵp_1 anticommutes with j , so that it can

contain only matrix elements of the type $\epsilon\rho_1(j, -j)$, and from the condition $(\epsilon\rho_1)^2 = 1$ we must have

$$|\epsilon\rho_1(j, -j)| = 1$$

Hence

$$|x_3(j, -j)| = \frac{u}{2(j^2 - \frac{1}{4})} r |\epsilon\rho_1(j, -j)| = \frac{u}{2(j^2 - \frac{1}{4})} r \quad (12)$$

Again, we have from (10)

$$\begin{aligned} \{x_3 - i[x_3, jh]\} \{x_3 + i[x_3, jh]\} &= \{x_3 - i\rho_3(\sigma_1x_3 - \sigma_2x_1)\} \{x_3 + i\rho_3(\sigma_1x_3 - \sigma_2x_1)\} \\ &= x_3^2 + (\sigma_1x_3 - \sigma_2x_1)^2 = r^2, \end{aligned}$$

which gives

$$\{(j+1)x_3 - x_{3j}\} \{x_3(j+1) - jx_3\} = r^2$$

If we equate the (j, j) matrix elements of each side of this equation, we get on the left-hand side the sum of three terms, namely, the $(j, -j)$ matrix element of the first $\{ \}$ bracket times the $(-j, j)$ element of the second, the $(j, j+1)$ element of the first times the $(j+1, j)$ element of the second, and the $(j, j-1)$ element of the first times the $(j-1, j)$ element of the second. The second of these three terms vanishes, leaving

$$(2j+1)^2 |x_3(j, -j)|^2 + 4 |x_3(j, j-1)|^2 = r^2$$

Hence

$$|x_3(j, j-1)|^2 = \frac{1}{4} r^2 \left\{ 1 - \frac{u^2}{(j - \frac{1}{2})^2} \right\} = \frac{1}{4} r^2 \frac{(j+u-\frac{1}{2})(j-u-\frac{1}{2})}{(j-\frac{1}{2})^2}. \quad (13)$$

Writing $-j$ for j , we get

$$|x_3(-j, -j-1)|^2 = \frac{1}{4} r^2 \frac{(j+u+\frac{1}{2})(j-u+\frac{1}{2})}{(j+\frac{1}{2})^2} \quad (14)$$

The three matrix elements of x_3 given in (12), (13) and (14) are associated with the three components of the multiplet formed by the combination of two doublets. The ratios of these matrix elements will, to a first approximation, remain unchanged when one makes a transformation from the matrix scheme in which r, j, u, ρ_3 are diagonal to a scheme in which the Hamiltonian is diagonal, and will therefore give the relative intensities of the Zeeman components $\Delta u = 0$ of the lines in a combination doublet. These ratios are in agreement with those of previous theories based on the spinning electron model.

§ 4 The Zeeman Effect

If there is a uniform magnetic field of intensity H in the direction of the x_3 axis, we can take the magnetic potentials to be

$$A_1 = -\frac{1}{2} H x_2, \quad A_2 = \frac{1}{2} H x_1, \quad A_3 = 0$$

The additional terms appearing in the Hamiltonian F will now be

$$\Delta F = \rho_1 \sigma' (\sigma, \Lambda) = -\frac{1}{2} \hbar e' \rho_1 (\sigma_1 x_2 - \sigma_2 x_1)$$

From (10) it follows that $\rho_3 (\sigma_1 x_2 - \sigma_2 x_1)$ or $(\sigma_1 x_2 - \sigma_2 x_1)$, like x_3 , contains only matrix elements of the type $(j, -j)$ or $(j, j \pm 1)$. Now ρ_1 anticommutes with j , and therefore contains only matrix elements of the type $(j, -j)$. Hence ΔF contains only matrix elements of the type (j, j) or $(j, -j \pm 1)$.

In *loc cit*, § 6, it was found [see equation (24)] that the Hamiltonian could be expressed as

$$F \equiv p_0 + V + \epsilon p_r + i \epsilon \rho_3 j \hbar / r + \rho_3 m c \quad (15)$$

It follows from (10) that $(\sigma_1 x_2 - \sigma_2 x_1)$ anticommutes with (σ, x) , and therefore also with ϵ . Thus if we put

$$\Delta F = i \hbar \epsilon \rho_3 \eta r,$$

so that

$$\eta = \frac{1}{2} \hbar e / c \hbar \quad \epsilon \rho_3 (\sigma_1 x_2 - \sigma_2 x_1) / r,$$

η commutes with ϵ . Further, η commutes with ρ_3 , r and p_r , so that it commutes with all the variables occurring in (15) except j . If we now express η as a matrix in j , we shall have obtained an expression for ΔF in terms of the variables occurring in (15). We have from (10) and (13)

$$|\rho_3 (\sigma_1 x_2 - \sigma_2 x_1) (j, j-1)|^2 = |x_3 (j, j-1)|^2 = \frac{1}{4} r^2 \frac{(j+u-\frac{1}{2})(j-u-\frac{1}{2})}{(j-\frac{1}{2})^2},$$

and similarly

$$|\rho_3 (\sigma_1 x_2 - \sigma_2 x_1) (j, j+1)|^2 = |x_3 (j, j+1)|^2 = \frac{1}{4} r^2 \frac{(j+u+\frac{1}{2})(j-u+\frac{1}{2})}{(j+\frac{1}{2})^2}.$$

We have seen that the matrix elements of $\epsilon \rho_1$, all of which are of the type $(j, -j)$, must be of modulus unity. Hence

$$\begin{aligned} |\eta (j, -j-1)|^2 &= \left(\frac{\hbar e}{2 c \hbar r} \right)^2 |\epsilon \rho_1 (j, -j)|^2 |\rho_3 (\sigma_1 x_2 - \sigma_2 x_1) (-j, -j-1)|^2 \\ &= \left(\frac{\hbar e}{4 c \hbar} \right)^2 \frac{(j+u+\frac{1}{2})(j-u+\frac{1}{2})}{(j+\frac{1}{2})^2} \\ \text{and similarly} \quad & \\ |\eta (j, -j+1)|^2 &= \left(\frac{\hbar e}{4 c \hbar} \right)^2 \frac{(j+u-\frac{1}{2})(j-u-\frac{1}{2})}{(j-\frac{1}{2})^2} \end{aligned} \quad \left. \vphantom{\left(\frac{\hbar e}{4 c \hbar} \right)^2} \right\} \quad (16)$$

Again, from (10) and (11)

$$\rho_3 (\sigma_1 x_2 - \sigma_2 x_1) (-j, j) = -2ij \quad x_3 (-j, j) = -\frac{u}{(j^2 - \frac{1}{4})} i j \cdot (\epsilon \rho_1) (-j, j),$$

so that

$$\eta (j, j) = \frac{\hbar e}{2 c \hbar} \frac{uj}{j^2 - \frac{1}{4}} \quad (17)$$

If we now write down in full, as in *loc cit*, the wave equation corresponding to (15), and include the extra term ΔF , we shall have

$$[(F + \Delta F) \psi]_+ = (p_0 + V) \psi_+ - \hbar \frac{\partial}{\partial r} \psi_+ - \left(\frac{2}{r} + \eta r \right) \hbar \psi_+ + mc \psi_+ = 0,$$

$$[(F + \Delta F) \psi]_- = (p_0 + V) \psi_- + \hbar \frac{\partial}{\partial r} \psi_- - \left(\frac{2}{r} + \eta r \right) \hbar \psi_- - mc \psi_- = 0,$$

where η is now an operator, operating on ψ_+ and ψ_- , that commutes with everything except j . On eliminating ψ_+ this gives, corresponding to (25) of *loc cit*,

$$\frac{\partial^2}{\partial r^2} \psi_- + \left[\frac{(p_0 + V)^2 - m^2 c^2}{\hbar^2} - \frac{j(j+1)}{r^2} + \eta - \eta j - j\eta - \eta^2 r^2 \right] \psi_- - \frac{1}{p_0 + V + mc} \frac{\partial V}{\partial r} \left[\frac{\partial}{\partial r} + \frac{2}{r} + \eta r \right] \psi_- = 0$$

We can neglect the $\eta^2 r^2$ term, which is proportional to the square of the field strength, and also the ηr term in the last bracket, which is of the order of magnitude of field strength times spin correction. The only first order effect of the field is the insertion of the terms $\eta - \eta j - j\eta$ in the first bracket. This bracket may now be written as

$$\left[\frac{2mE}{\hbar^2} + \frac{E^2}{c^2 \hbar^2} + \frac{2(E + mc^2)}{c \hbar^2} V + \frac{V^2}{\hbar^2} - \frac{j(j+1)}{r^2} + \eta - \eta j - j\eta \right], \quad (18)$$

where E is the energy level, equal to $p_0 c - mc^2$.

If the field is weak compared with the doublet separation, we can obtain a first approximation to the change in the energy levels by neglecting the non-diagonal matrix elements of ΔF or of η . The extra terms $\eta - \eta j - j\eta$ in (18) are now a constant instead of an operator, namely, the constant

$$-(2j-1)\eta(j, j) = -\frac{\hbar e}{c \hbar} \frac{u j}{j + \frac{1}{2}}$$

from (17). The energy levels will be reduced by $\hbar^2/2m$ times this constant, if we neglect the fact that the characteristic E occurs in (18) in other places besides the term $2mE/\hbar^2$, which means neglecting the interaction of the magnetic field with the relativistic variation of mass with velocity. The increase in the energy levels caused by the magnetic field is thus

$$\frac{\hbar e}{2mc} \frac{j}{j + \frac{1}{2}} u \hbar = \omega g u \hbar$$

where ω is the Larmor frequency $He/2mc$, and g , the Lande splitting factor, has the value

$$g = j/(j + \frac{1}{2})$$

For the succession of j -values, $1, 1, -2, 2, -3, \dots$ g has the values, $2, \frac{2}{3}, \frac{1}{2}, \frac{1}{3}, \dots$, in agreement with Lande's formula for alkali spectra

We now take the case of a magnetic field that is strong compared with the doublet separation, but weak compared with the separations of terms of different series. This requires that the matrix elements of η of the type $\eta(j, -j-1)$ with $j > 0$ shall be taken into account, although those of the type $\eta(j, -j+1)$ can still be neglected. The reduction in the energy levels will now be approximately $h^2/2m$ times one or other of the characteristic values of the extra terms $\eta - \eta j - j\eta$ in (18). These characteristic values are the roots ξ of the equation

$$\begin{vmatrix} (\eta - \eta j - j\eta)(j, j) - \xi & (\eta - \eta j - j\eta)(j, -j-1) \\ (\eta - \eta j - j\eta)(-j-1, j) & (\eta - \eta j - j\eta)(-j-1, -j-1) - \xi \end{vmatrix} = 0$$

or

$$\begin{vmatrix} -(2j-1) & \eta(j, j) - \xi & 2\eta(j, -j-1) \\ 2\eta(-j-1, j) & (2j+3) & \eta(-j-1, -j-1) - \xi \end{vmatrix} = 0$$

This gives, with the help of (16) and (17)

$$\xi^2 + \frac{He}{ch} \left[\frac{u\eta}{j + \frac{1}{2}} + \frac{u(j+1)}{j + \frac{1}{2}} \right] \xi + \left(\frac{He}{ch} \right)^2 \left[\frac{u^2 j(j+1)}{(j + \frac{1}{2})^2} - \frac{(j + \frac{1}{2})^2 - u^2}{4(j + \frac{1}{2})^2} \right] = 0,$$

which reduces to

$$\xi^2 + \frac{He}{ch} 2u\xi + \left(\frac{He}{ch} \right)^2 (u^2 - \frac{1}{4}) = 0$$

Hence

$$\xi = -\frac{He}{ch} (u \pm \frac{1}{2})$$

The increase in the energy levels due to the magnetic field is therefore

$$-\frac{h^2}{2m} \xi = \frac{h^2}{2m} \frac{He}{ch} (u \pm \frac{1}{2}) = \omega (u \pm \frac{1}{2}) h,$$

in agreement with the previous spinning electron theory of the Paschen-Back effect

One might expect that with still stronger magnetic fields the matrix elements $(j, -j+1)$ of η would come into play, and would cause interference between the Zeeman patterns of terms whose quantum numbers k in the usual notation differ by 2. The matrix elements $(j, -j+1)$ of $\eta - \eta j - j\eta$, however, vanish for arbitrary η , so that no effect of this nature occurs

*The Emission of Light by Flames containing Sodium and the
Absorption of Light by Mercury Vapour*

By H A WILSON, F R S, Rice Institute, Houston, Texas

(Received November 24, 1927)

The light from Bunsen flames containing sodium and other metals was investigated by Gouy* in 1879. He found that the intensity of the light is a function of the amount of sodium per square centimetre in the flame and that this function is approximately proportional to the square root of the amount of sodium per square centimetre when this is not extremely small.

If d denotes the thickness of the flame, ρ the amount of sodium per unit volume in it and I the light intensity emitted in a direction perpendicular to the flame surface then Gouy's results show that $I = A\rho d/\sqrt{\rho d} + B$ where A and B are constants. When ρd is not very small the constant B can be neglected and $I = A\sqrt{\rho d}$. The following values of I and ρd for a sodium flame, both in arbitrary units, were given by Gouy

ρd	1	2	5	10	20	50	100	250	500	1,000	5,000	10,000
I	1	1.0	4.1	6.7	10.0	15.8	21.7	34.1	48.5	69.5	152	208
$\frac{2.1\rho d}{\sqrt{\rho d} + 2}$	1.2	2.1	4.0	6.1	9.0	14.5	20.8	33.1	47	66.4	149	210
$2.1\sqrt{\rho d}$	2.1	3.0	4.7	6.7	9.4	14.9	21.0	33.2	47	66.5	149	210

The third row contains values of $2.1\rho d/\sqrt{\rho d} + 2$ which I have calculated. These values agree fairly well with those of I . The last row contains values of $2.1\sqrt{\rho d}$ which agree with Gouy's values of I as well as those of the more complicated expression when ρd is greater than 10.

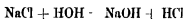
That the intensity of the light emitted is very nearly proportional to the square root of the amount of sodium is shown by the following experiments. Nine sensibly equal Bunsen flames all supplied with sodium by the same sprayer were arranged in a row. The light emitted in the direction of the row was measured with a Hilger spectrophotometer. By putting an opaque screen between two of the flames in the row the light intensities due to 1, 4 and 9 flames could be compared. It was found that these intensities were as 1 : 2 : 3 within the limit of error which was 1 to 2 per cent.

Solutions with concentrations of sodium proportional to 1, 4, 9, 16 were

* 'Ann. chim. phys.', vol. 18, p. 5 (1879)

used in the sprayer, and it was found that the light intensities were as 1 2 3 4 for any number of flames from 1 to 9. These results therefore confirm Gouy's conclusion that $I \propto \sqrt{pd}$ when pd is not extremely small.

So far as the writer is aware no satisfactory explanation of this square root law of Gouy's has been offered. It has been suggested that the substance in the flame which emits the light is produced by a chemical reaction such as



The amount of water vapour in the flame is large, so that according to this reaction if only a small fraction of the NaCl is converted into NaOH then the amount of NaOH produced will be proportional to the square root of the NaCl present. If then the light is proportional to the NaOH present it will vary as the square root of the NaCl supplied to a given flame.

Such an explanation is clearly quite inadequate for it makes the light emitted per unit volume of the flame vary as the square root of the concentration of the sodium in the flame, so that the light emitted should vary as $d\sqrt{p}$ whereas in fact it varies as \sqrt{pd} .

It is now known that the sodium light is emitted by sodium atoms and it is believed that sodium salts in flames are practically completely dissociated into metallic sodium. The light emitted in the flame should therefore be proportional to the amount of sodium in the flame, but all the light emitted does not escape from the flame because the sodium atoms absorb some of it. It ought to be possible to explain Gouy's square root law by taking into account the absorption of the sodium light by the sodium vapour.

The sodium atoms absorb the light at the centres of the D lines much more strongly than that at the edges, and it appears that by taking this into account a simple explanation of the square root law of emission can be obtained.

For this purpose we may regard the sodium atom as a simple oscillator, the equation of motion of which may be taken to be

$$mx + kx + \mu\dot{x} = Fe,$$

where m is the mass of the vibrating particle, which may be an electron, k the viscous resistance to the motion at unit velocity, μ a constant, F the electric intensity in the light at the atom, e the charge on the particle and x the displacement of the particle from its equilibrium position. If we take $F = F_0 \cos pt$ and calculate the average value of the power expended on the atom or \overline{eFx} we find

$$\overline{eFx} = e^2 F_0^2 k p^2 / 2 \{ (\mu - mp^2)^2 + p^2 k^2 \}$$

The flux of energy per square centimetre per second in the light is equal to $cE_0^2/8\pi$ where c is the velocity of light so that the atomic absorption coefficient γ or the fraction of the light energy flowing through 1 sq cm absorbed by the atom is given by

$$\gamma = 8\pi e^2 \overline{F^2} / c k_0^2 = 8\pi e^2 k p^2 / c \{(\mu - mp^2)^2 + p^2 k^2\}$$

If γ_0 is the value of γ when $\mu = mp^2$ then

$$\gamma = \gamma_0 k^2 p^2 / \{(\mu - mp^2)^2 + k^2 p^2\}$$

The absorption is inappreciable unless mp^2 is nearly equal to μ so that we may put $p = p_0 - \Delta$ where $p_0 = \sqrt{\mu/m}$ and Δ/p_0 is a small quantity, and so obtain

$$\gamma = \gamma_0 \left(1 + \frac{4m^2 \Delta^2}{k^2} \right)$$

The light emission from a layer of sodium vapour containing n atoms per square centimetre may now be calculated as follows. If we suppose a layer containing n atoms per square centimetre put in front of a black body at the same temperature the layer must make no difference to the total light emitted so that the layer containing n atoms must absorb as much light as it emits. If E denotes the intensity of the black body radiation per unit range of Δ near the D lines then the radiation emitted by the layer, in a direction perpendicular to its surface, is given by

$$I = E \int_{-\infty}^{+\infty} (1 - e^{-n\gamma_0/(1+4m^2\Delta^2/k^2)}) d\Delta$$

If $n\gamma_0$ is greater than about 2 or 3 this equation can be easily shown to reduce approximately to

$$I = E \frac{k}{m} \sqrt{\pi\gamma_0 n} \left(1 - \frac{1}{4n\gamma_0} - \frac{3}{32n^2\gamma_0^2} - \dots \right)$$

Thus it appears that the emission from a layer containing n atoms per square centimetre is proportional to \sqrt{n} when n is not too small in agreement with Gouy's results.

When n is very small the above integral for I shows that I is proportional to n which also agrees with Gouy's results.

In a recent paper, by A. L. Hughes and A. R. Thomas,* a valuable series of measurements of the absorption by mercury vapour of the mercury line 2546Å emitted by a resonance lamp, is described.

The first two columns of the following table contain their results. I_0 denotes

* 'Physical Review,' October, 1927

the intensity of the light before passing through a layer of mercury vapour containing n atoms per square centimetre and I that after passing through the layer

$\log(I_0/I)$	$n \cdot 10^{12}$	$\frac{1}{\sqrt{n}} \log(I_0/I) \cdot 10^7$	$\frac{\sqrt{n+4 \times 10^{12}}}{n} \log(I_0/I) \cdot 10^7$
0.1518	1.35	1.31	2.60
0.2255	2.41	1.44	2.60
0.3004	4.31	1.77	2.46
0.3700	7.49	2.12	2.02
0.8077	12.8	2.26	2.58
1.079	21.1	2.35	2.57
1.407	34.5	2.39	2.53
1.790	55.5	2.41	2.50
2.216	87.0	2.36	2.42

The third column contains values of $\frac{1}{\sqrt{n}} \log \frac{I_0}{I}$ which I have calculated, and it appears that this quantity is nearly constant for values of n greater than about 10^{12} .

The last column contains the values of $\frac{\sqrt{n+4 \times 10^{12}}}{n} \log \frac{I_0}{I}$ which are nearly constant for all values of n . When n is very small the equation $\frac{\sqrt{n+4 \times 10^{12}}}{n} \log \frac{I_0}{I} = 2.5 \cdot 10^{-7}$ gives $\bar{\gamma} = \frac{1}{n} \log \frac{I_0}{I} = 1.25 \times 10^{-12}$ for the average atomic absorption coefficient $\bar{\gamma}$. That is the average value for all the frequencies present in the line 2546 Å.

As Hughes and Thomas point out, the variation of the absorption with the number of atoms must be due to the mercury absorbing the centre of the line 2546 Å much more than the edges, so that we might expect the theory given above for sodium flames to apply also to this case.

We may suppose that the energy in the incident radiation for which Δ or $\nu_0 - \nu$ lies between Δ and $\Delta + d\Delta$, to be equal to $A e^{-\alpha^2 \Delta^2} d\Delta$ where A and α are constants. The ratio of the transmitted to the incident radiation energy should then be given by

$$\frac{I}{I_0} = \frac{\int_{-\infty}^{+\infty} A e^{-\alpha^2 \Delta^2} \gamma^n d\Delta}{\int_{-\infty}^{+\infty} A e^{-\alpha^2 \Delta^2} d\Delta}$$

where $\gamma = \gamma_0/(1 + 4m^2 \Delta^2/k^2)$ as before

Putting $x = \alpha \Delta$ this gives

$$\frac{I}{I_0} = \frac{1}{\sqrt{\pi}} \int_{-\infty}^{+\infty} e^{-x^2 - n\gamma_0(1 + 4m^2x^2/\alpha^2k^2)} dx$$

When $n\gamma_0$ is not too small the 1 in $1 + 4m^2x^2/\alpha^2k^2$ can be omitted without serious error and we get approximately

$$I/I_0 = e^{-\frac{n\gamma_0}{m} \sqrt{n\gamma_0}}$$

or $\log \frac{I_0}{I} = \frac{\alpha k}{m} \sqrt{n\gamma_0}$ which agrees with Hughes and Thomas' results for the larger values of n

When n is very small we have

$$\begin{aligned} \frac{I}{I_0} &= \frac{1}{\sqrt{\pi}} \int_{-\infty}^{+\infty} e^{-x^2} \left(1 - \frac{n\gamma_0}{1 + 4m^2x^2/\alpha^2k^2} \right) dx \\ &= 1 - \frac{n\gamma_0}{\sqrt{\pi}} \int_{-\infty}^{+\infty} \frac{e^{-x^2}}{1 + 4m^2x^2/\alpha^2k^2} dx \end{aligned}$$

The average atomic absorption coefficient $\bar{\gamma}$ calculated above from Hughes and Thomas' results by making n very small is therefore given by

$$\bar{\gamma} = \frac{\gamma_0}{\sqrt{\pi}} \int_{-\infty}^{+\infty} \frac{e^{-x^2}}{1 + 4m^2x^2/\alpha^2k^2} dx$$

If the distribution of energy in the mercury line 2516A were known γ could be estimated and so k/m could be calculated by means of this equation

In conclusion it may be said that the experimental results on the emission of light by sodium flames and on the absorption of resonance radiation by mercury vapour appear to be consistent with the view that the atoms absorb light like simple damped oscillators

The Hexahydrated Double Sulphates containing Thallium

By A E H TUTTON, D Sc, M A, F R S, Past-President of the Mineralogical Society

(Received February 2, 1928)

The author's prolonged study of the monoclinic isomorphous series of hexahydrated double sulphates and selenates, $R_2M\left(\begin{smallmatrix} S \\ Se \end{smallmatrix} O_4\right)_2 \cdot 6H_2O$, in which M may be magnesium, zinc, cadmium, copper, nickel, cobalt, iron (ferrous), or manganese, was completed as regards the salts in which R is the alkali metal potassium, rubidium, caesium, or the base ammonium, NH_4 , by the memoir* communicated in the year 1922. The metal thallium, in its thalious capacity, is also capable, like ammonium, of isomorphously replacing the alkali metals, but it has been found so difficult to grow crystals of these thallium double salts adequately perfect to yield results comparable in accuracy and completeness to those obtained for the salts of the alkalis, that hitherto only four of the fourteen possible thallium salts of the series have been described by the author, although all but one (thallium ferrous selenate) were prepared and examined by him as long ago as 1909,† when thallium zinc sulphate and selenate were described, the crystals of the remainder proving inadequately perfect (distorted or more or less opaque). It was much later, in 1925, that two other of the thallium double sulphates, those containing nickel and cobalt as the M-metal, were described,‡ having at length also been obtained in good crystals.

During the last two years the author has returned to the work, and with the large experience gained in the course of this long investigation, has at length succeeded in growing sufficiently perfect crystals of the whole 10 remaining salts, and has been able to effect not only a complete goniometrical measurement but a full optical and volume investigation. The results are communicated in the present memoir, as regards the double sulphates, and in the immediately succeeding paper as regards the double selenates, thus finally completing and rounding off the author's long task by bringing it to a satisfactory conclusion.

The double sulphates described in this paper are thallium-magnesium, thallium-ferrous, thallium-manganese, and thallium-copper sulphates. Only

* 'Roy. Soc. Proc.,' A, vol 101, p 245 (1922)

† 'Roy. Soc. Proc.,' A, vol 83, p 211 (1909)

‡ 'Roy. Soc. Proc.,' A, vol 108, p 240 (1925)

the two first mentioned have been studied before, by Werther* in the year 1864, who, however, only measured a few of the principal angles and attempted no optical or other physical investigation

Thallium Magnesium Sulphate $\text{Tl}_2\text{Mg}(\text{SO}_4)_2 \cdot 6\text{H}_2\text{O}$

Morphology

Ten crystals from four crops were used for the crystal angle measurements

Crystal System —Monoclinic (Class No 5, holohedral prismatic)

Ratio of Axes $a : b : c = 0.7442 : 1 : 0.5000$ Values of Werther 0.7422 : 1 : 0.5002

Axial Angle $\beta = 106^\circ 30'$ Value of Werther $106^\circ 24'$

Forms Observed $a\{100\}$, $b\{010\}$, $c\{001\}$, $p\{110\}$, $q\{011\}$, $r'\{201\}$, $o'\{111\}$, and $n'\{121\}$. The forms $a\{100\}$ and $n'\{121\}$ were not observed by Werther. There is a fairly good cleavage parallel to $r'\{201\}$.

Habit The most typical habit is illustrated in fig. 1

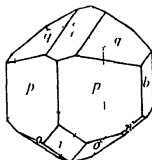


FIG. 1.— Tl Mg Sulphate

Morphological Angles These are given in the accompanying table

The Average Difference (ignoring sign) of interfacial angle between this salt and potassium magnesium selenate, that is, for the replacement of potassium by thallium, is $40'$. The maximum difference occurs for the important monoclinic axial angle $ac = (100) (001)$, and is $1^\circ 42'$.

The differences in the four main angles brought about by the replacement of sulphur by selenium, that is, between this salt and the corresponding thallium magnesium selenate, will be found on p. 395.

* Journ. Prakt. Chem., vol. 92, p. 128 (1864).

Interfacial Angles of Thallium Magnesium Sulphate

Angle	No. of measurements	Limits	Mean observed	Calculated	Diff.	Values of Wertheimer
$\left\{ \begin{array}{l} aa \\ aa' \\ w \\ c \\ ca \\ sr \\ sr' \\ cr \end{array} \right. \begin{array}{l} (100) (001) \\ (100) (101) \\ (101) (001) \\ (001) (201) \\ (001) (101) \\ (101) (201) \\ (201) (100) \\ (201) (001) \end{array}$	$\left\{ \begin{array}{l} 1 \\ 11 \\ 15 \end{array} \right.$	$\left\{ \begin{array}{l} - \\ 64.9-61.21 \\ 115.18-115.49 \end{array} \right.$	$\left\{ \begin{array}{l} 73.15 \\ - \\ 64.18 \\ - \\ 115.12 \end{array} \right.$	$\left\{ \begin{array}{l} 73.30 \\ 15.4 \\ 28.26 \\ 64.23 \\ 38.31 \\ 25.50 \\ 42.7 \\ 115.37 \end{array} \right.$	$\left\{ \begin{array}{l} 5 \\ - \\ 5 \\ - \\ - \\ - \\ - \\ - \end{array} \right.$	$\left\{ \begin{array}{l} 73.36 \\ - \\ 64.24 \\ - \\ - \\ - \\ - \\ - \end{array} \right.$
$\left\{ \begin{array}{l} ap \\ pp \\ ph \\ ph' \\ pp' \end{array} \right. \begin{array}{l} - (100) (110) \\ (110) (120) \\ (120) (010) \\ (110) (010) \\ (110) (110) \end{array}$	$\left\{ \begin{array}{l} - \\ 32 \\ 18 \end{array} \right.$	$\left\{ \begin{array}{l} - \\ - \\ 74.11-54.10 \\ 70.49-71.21 \end{array} \right.$	$\left\{ \begin{array}{l} - \\ - \\ 54.29 \\ 71.2 \end{array} \right.$	$\left\{ \begin{array}{l} 35.31 \\ 19.28 \\ 35.1 \\ * \\ 71.2 \end{array} \right.$	$\left\{ \begin{array}{l} - \\ - \\ - \\ - \\ 0 \end{array} \right.$	$\left\{ \begin{array}{l} - \\ - \\ - \\ - \\ 70.54 \end{array} \right.$
$\left\{ \begin{array}{l} eq \\ gh \end{array} \right. \begin{array}{l} - (001) (011) \\ (011) (010) \end{array}$	$\left\{ \begin{array}{l} 39 \\ 32 \end{array} \right.$	$\left\{ \begin{array}{l} 25.24-25.54 \\ 61.11-61.11 \end{array} \right.$	$\left\{ \begin{array}{l} 25.37 \\ 64.23 \end{array} \right.$	$\left\{ \begin{array}{l} * \\ 61.23 \end{array} \right.$	$\left\{ \begin{array}{l} - \\ 0 \end{array} \right.$	$\left\{ \begin{array}{l} 25.38 \\ - \end{array} \right.$
$\left\{ \begin{array}{l} aa' \\ eq \\ af \\ qs \\ aa' \end{array} \right. \begin{array}{l} - (100) (111) \\ (111) (011) \\ (100) (011) \\ (011) (111) \\ (111) (100) \end{array}$	$\left\{ \begin{array}{l} - \\ - \\ - \\ - \\ - \end{array} \right.$	$\left\{ \begin{array}{l} - \\ - \\ - \\ - \\ - \end{array} \right.$	$\left\{ \begin{array}{l} - \\ - \\ - \\ - \\ - \end{array} \right.$	$\left\{ \begin{array}{l} 48.15 \\ 26.55 \\ 75.10 \\ 34.43 \\ 70.7 \end{array} \right.$	$\left\{ \begin{array}{l} - \\ - \\ - \\ - \\ - \end{array} \right.$	$\left\{ \begin{array}{l} - \\ - \\ - \\ - \\ - \end{array} \right.$
$\left\{ \begin{array}{l} ca \\ ap \\ cp \\ po \\ os \end{array} \right. \begin{array}{l} - (001) (111) \\ (111) (110) \\ (001) (110) \\ (110) (111) \\ (111) (001) \end{array}$	$\left\{ \begin{array}{l} - \\ 40 \\ 14 \\ 11 \end{array} \right.$	$\left\{ \begin{array}{l} - \\ 70.24-76.54 \\ 58.28-58.59 \\ 44.22-44.53 \end{array} \right.$	$\left\{ \begin{array}{l} - \\ 76.38 \\ 58.30 \\ 44.42 \end{array} \right.$	$\left\{ \begin{array}{l} 34.0 \\ 42.38 \\ * \\ 58.35 \\ 44.47 \end{array} \right.$	$\left\{ \begin{array}{l} - \\ - \\ - \\ 4 \\ 5 \end{array} \right.$	$\left\{ \begin{array}{l} - \\ - \\ 76.42 \\ - \\ - \end{array} \right.$
$\left\{ \begin{array}{l} ba \\ oa \\ oa' \end{array} \right. \begin{array}{l} - (010) (111) \\ (111) (101) \\ (111) (111) \end{array}$	$\left\{ \begin{array}{l} - \\ - \\ - \end{array} \right.$	$\left\{ \begin{array}{l} - \\ - \\ - \end{array} \right.$	$\left\{ \begin{array}{l} - \\ - \\ - \end{array} \right.$	$\left\{ \begin{array}{l} 70.31 \\ 19.29 \\ 38.58 \end{array} \right.$	$\left\{ \begin{array}{l} - \\ - \\ - \end{array} \right.$	$\left\{ \begin{array}{l} - \\ - \\ - \end{array} \right.$
$\left\{ \begin{array}{l} ba \\ ba' \\ no \\ os \\ oa \end{array} \right. \begin{array}{l} (010) (111) \\ (010) (121) \\ (121) (111) \\ (111) (101) \\ - (111) (111) \end{array}$	$\left\{ \begin{array}{l} 32 \\ 3 \\ 3 \\ - \\ 16 \end{array} \right.$	$\left\{ \begin{array}{l} 65.0-61.17 \\ 47.0-47.30 \\ 17.40-18.20 \\ - \\ 49.35-49.48 \end{array} \right.$	$\left\{ \begin{array}{l} 65.9 \\ 47.14 \\ 17.56 \\ - \\ 49.30 \end{array} \right.$	$\left\{ \begin{array}{l} 65.8 \\ 47.10 \\ 17.58 \\ 24.52 \\ 49.44 \end{array} \right.$	$\left\{ \begin{array}{l} 1 \\ 1 \\ 2 \\ - \\ 5 \end{array} \right.$	$\left\{ \begin{array}{l} - \\ - \\ - \\ - \\ 49.42 \end{array} \right.$
$\left\{ \begin{array}{l} ng \\ qp \\ qn \\ np \\ ps \\ pq \end{array} \right. \begin{array}{l} (101) (011) \\ (011) (110) \\ (011) (121) \\ (121) (110) \\ - (110) (101) \\ - (110) (011) \end{array}$	$\left\{ \begin{array}{l} 38 \\ 3 \\ 3 \\ 3 \\ - \\ 38 \end{array} \right.$	$\left\{ \begin{array}{l} - \\ 87.22-87.50 \\ 35.38-36.52 \\ 51.31-51.56 \\ - \\ 92.11-92.41 \end{array} \right.$	$\left\{ \begin{array}{l} - \\ 87.32 \\ 35.45 \\ 51.41 \\ - \\ 92.28 \end{array} \right.$	$\left\{ \begin{array}{l} 37.32 \\ 87.33 \\ 35.48 \\ 51.45 \\ 54.55 \\ 92.27 \end{array} \right.$	$\left\{ \begin{array}{l} - \\ 1 \\ 3 \\ 4 \\ - \\ 1 \end{array} \right.$	$\left\{ \begin{array}{l} - \\ - \\ - \\ - \\ - \\ - \end{array} \right.$
$\left\{ \begin{array}{l} sq \\ qp' \\ ps' \\ pq' \end{array} \right. \begin{array}{l} - (101) (011) \\ (011) (110) \\ (110) (101) \\ (110) (011) \end{array}$	$\left\{ \begin{array}{l} 40 \\ - \\ 40 \\ 40 \end{array} \right.$	$\left\{ \begin{array}{l} - \\ 62.19-62.55 \\ - \\ 117.2-117.39 \end{array} \right.$	$\left\{ \begin{array}{l} 62.30 \\ - \\ 117.20 \end{array} \right.$	$\left\{ \begin{array}{l} 45.9 \\ 62.38 \\ 72.13 \\ 117.22 \end{array} \right.$	$\left\{ \begin{array}{l} 1 \\ - \\ 2 \end{array} \right.$	$\left\{ \begin{array}{l} - \\ - \\ - \end{array} \right.$
$\left\{ \begin{array}{l} ra \\ op \\ pr \end{array} \right. \begin{array}{l} (201) (111) \\ (111) (110) \\ - (110) (201) \end{array}$	$\left\{ \begin{array}{l} 23 \\ 18 \\ 25 \end{array} \right.$	$\left\{ \begin{array}{l} 35.3-35.20 \\ 91.45-92.2 \\ 52.45-53.5 \end{array} \right.$	$\left\{ \begin{array}{l} 35.11 \\ 91.52 \\ 52.54 \end{array} \right.$	$\left\{ \begin{array}{l} 35.16 \\ 91.53 \\ 52.51 \end{array} \right.$	$\left\{ \begin{array}{l} 5 \\ 1 \\ 3 \end{array} \right.$	$\left\{ \begin{array}{l} - \\ - \\ - \end{array} \right.$
Total number of measurements		538				

Volume

Relative Density—The mean of two very concordant results for the specific gravity at 20°/4° was 3.573. The method used was that of the author's "pycnometer with cap"†

$$\text{Molecular Volume} = \frac{M}{d} = \frac{727.30}{3.573} = 203.55$$

Molecular Distance Ratios (Tropo Axial Ratios)—

$$\lambda : \psi : \omega = 6.1723 : 8.2939 : 4.1470$$

Optics

Orientation of Optical Ellipsoid—The symmetry plane $b\{010\}$ is the plane of the optic axes, and the sign of the Double Refraction is negative. Extinction determinations with sections parallel to the symmetry plane showed that the γ -axis of the ellipsoid (indicatrix), which is the obtuse bisectrix (second median line) of the optic-axial angle and vibration direction for the γ index of refraction, lies 9° 4' behind the vertical crystal-axis c , and the α -axis, the acute bisectrix (first median line) and vibration direction for the α -index, lies 25° 34' above the inclined crystal-axis a , in the obtuse angle of the crystal-axes ac . Fig. 5 on p. 389 will assist in making this clear. The β -index corresponds to vibration along the symmetry axis b .

Refractive Indices—These are as follows, determined with excellent ground 60°-prisms, each so orientated as to yield two of the three indices directly.

Refractive Indices of TIMg Sulphate

Light *	α	β	γ
Li	1.5660	1.5836	1.5900
C	1.5665	1.5841	1.5905
Na	1.5705	1.5884	1.5949
Tl	1.5751	1.5935	1.6001
Cd	1.5776	1.5960	1.6027
F	1.5808	1.5993	1.6063
G	1.5878	1.6063	1.6174

$$\text{Mean index for Na light, } \frac{\alpha + \beta + \gamma}{3} = 1.5846$$

$$\text{Double refraction, } n_{\gamma-\alpha} = 0.0244$$

* Li means light of the wave length of the red lithium line, C that of the red hydrogen line, Na that of the yellow sodium line, Tl that of the green thallium line, Cd that of the green cadmium line, F that of the greenish blue hydrogen line, and G that of the violet hydrogen line near the G of the spectrum, all as supplied by the spectroscopic monochromatic illuminator.

† See the author's 'Crystallography and Practical Crystal Measurement,' 2nd Ed., vol. 1, p. 626. The immersion method of Retgers is not available for any of these heavy thallium salts, as their densities are greater than that of methylene iodide, 3.34. The author also made and experimented with Clerici's heavy liquid, a mixture of thallium formate and malonate, but found it quite unsuitable, and lighter than the selenates in any case.

General Formula for the intermediate index β , corrected to a vacuum (correction + 0.0004) —

$$\beta = 1.5698 + \frac{521.354}{\lambda^2} + \frac{4.800.600.000.000}{\lambda^4} +$$

The α -indices are closely reproduced if the constant 1.5698 be diminished by 0.0179, and the γ -indices if it be increased by 0.0065

Axial Ratios of the Optical Ellipsoid (Indicatrix)

$$\alpha : \beta : \gamma = 0.9887 : 1 : 1.0041$$

Molecular Optical Constants - These are set forth in the three following tables

Table of Specific Refraction and Dispersion (Lorenz)

Specific refraction, $\frac{n^2 - 1}{(n^2 + 2)d} = n$						Specific dispersion, $n_D - n_0$		
For ray C (Ha)			For ray H γ near G					
α	β	γ	α	β	γ	α	β	γ
0.0912	0.0937	0.0945	0.0942	0.0966	0.0975	0.0030	0.0029	0.0030

Table of Molecular Refraction and Dispersion (Lorenz)

Molecular refraction, $\frac{n^2 - 1}{n^2 + 2} \frac{M}{d} = m$						Molecular dispersion, $m_D - m_0$		
For ray C (Ha)			For ray H γ near G					
α	β	γ	α	β	γ	α	β	γ
68.31	68.13	68.74	68.40	70.23	70.80	2.18	2.10	2.15

Molecular Refraction (Gladstone and Dale)

$\frac{n - 1}{d} M$ for ray C			Mean molecular refraction for ray C, $\frac{1}{2}(\alpha + \beta + \gamma)$
α	β	γ	
118.31	118.90	120.20	118.14

Optical Axial Angle—The optic axial angle in air is too large to be clearly determinable, the axial brushes being on the extreme edges of the field and disappearing before they can be brought to the cross spider lines, although portions of the innermost rings are visible. Excellent determinations of the true angle within the crystal, $2V_a$, were obtained with two pairs of plates ground so as to be perpendicular to the acute and obtuse bisectrices, immersed in monobromonaphthalene. The following are the mean values obtained, the individual values differing only by less than $10'$ from these mean angles.

Light	$2V_a$ ° ,	Light	$2V_a$ ° ,
Li	74 41	Tl	75 14
C	74 42	Cd	75 23
Na	74 57	F	75 34

Dispersion of the Median Lines—Observations with the plates perpendicular to the acute bisectrix immersed in cinnamon oil, which is very close indeed in refractive index to the indices of the crystal, showed that the first median line lies $10'$ nearer to the crystal axis a for green thallium light than for red C-hydrogen light.

Thallium Ferrous Sulphate, $Tl_2Fe(SO_4)_2 \cdot 6H_2O$

Morphology

Twelve good little crystals from four different crops were used for the crystal-angle measurements. The crystals of this salt are coloured pale green.

Crystal System—Monoclinic. Class No 5 holohedral-prismatic.

Ratios of Axes— $a : b : c = 0.7427 : 1 : 0.4999$. Values of Werther 0.7366 : 1 : 0.4964.

Axial Angle— $\beta = 106^\circ 16'$. Value of Werther $105^\circ 52'$.

Forms Observed— $a\{100\}$, $b\{010\}$, $c\{001\}$, $p\{110\}$, $p'\{120\}$, $q\{011\}$, $r'\{201\}$, $o'\{111\}$. There is the usual cleavage parallel $r'\{201\}$, common to the series.

Habit. This salt is distinguished by the exceptionally prominent development of the form $r'\{201\}$, as will be apparent from the drawing of a typical crystal which is reproduced in fig. 2. Indeed, the crystals are frequently tabular parallel to and largely formed by the two faces of this form. The relative development of the other forms is as shown in the figure, except that the faces of $o'\{111\}$ are not often so relatively large, the faces of the primary prism $p\{110\}$ being as a rule much larger than these o' -faces. Only linear traces of $a\{100\}$ and $p'\{120\}$ were observed, inadequate for accurate measurement. The

large r' -faces were often badly formed but in the crystals chosen for measurement they were unusually good

Morphological Angles -- These are given in the accompanying table (p. 374)

The Average Difference of interfacial angle between this salt and its potassium analogue, that is, for the replacement of potassium by thallium, ferrous iron remaining the M-metal, is $41'$. The maximum difference of angle, which occurs for the systematic axial angle ac (100) (001), is $1^\circ 44'$

The differences in the four principal angles brought about by replacing sulphur by selenium will be found on p. 310



FIG. 2 — Tl Fe Sulphate

Volume

Relative Density The mean of two very concordant determinations of specific gravity at $20^\circ/4^\circ$ by the method of the 'pycnometer with cap' affords the value 3.650

$$\text{Molecular Volume} \quad \frac{M}{d} = \frac{758.62}{3.650} = 207.84$$

Topic Axial Ratios

$$a : b : c = 6.2050 : 8.3547 : 1.1765$$

Optics

Orientation of Optical Ellipsoid The plane of the optic axis is the symmetry plane $b(010)$, and the sign of the Double Refraction negative. Extinction determinations with sections parallel to the symmetry plane showed that the axis γ of the ellipsoid (indicatrix), the obtuse bisectrix of the optic axial angle and vibration direction for the refractive index ϵ , lies $32^\circ 31'$ from the normal to $c(001)$ and $16^\circ 15'$ behind the vertical crystal axis c , the α -axis which is the acute bisectrix of the optic axial angle and vibration direction for the α -index, lies $32^\circ 31'$ above the inclined axis a , in the obtuse axial angle ac . Fig. 5 on p. 389 will render this clearer. The vibration direction for the β index is the symmetry axis b .

Refractive Indices These were determined by means of several excellent

Interfacial Angles of Thallium Ferrous Sulphate

Angle	No of measurements	Limits	Mean observed	Calculated	Diff	Values of Werther
$\left\{ \begin{array}{l} ac = (100) (001) \\ aa = (100) (101) \\ ac = (101) (001) \\ cr' = (001) (201) \\ ca' = (001) (101) \\ ar = (101) (201) \\ ra = (201) (100) \\ rc = (201) (001) \end{array} \right.$	 — — 20 — — — 18	 — — 63 48-64 48 — — — 115 28-116 0	 — — 64 15 — — — 115 43	 73 44 45 14 28 30 64 13 18 29 25 44 42 3 115 47	 — — — 2 — — 4	 74 8 — — 64 15 — — — —
$\left\{ \begin{array}{l} ap = (100) (110) \\ pp = (110) (120) \\ pb = (120) (010) \\ pb = (110) (010) \\ pp = (110) (110) \\ pp = (110) (110) \end{array} \right.$	 — — — 20 19 18	 — — — 54 20-54 46 70 39-71 28 108 44-109 15	 — — — 54 30 71 2 108 50	 35 31 19 28 35 1 54 29 * 108 58	 — — — 1 — 1	 — — — — 70 38 109 22
$\left\{ \begin{array}{l} iq = (001) (011) \\ qb = (011) (010) \\ qq = (011) (011) \end{array} \right.$	 48 30 21	 25 11-25 54 64 5-64 45 128 30-128 54	 25 38 64 22 128 42	 * 64 22 128 44	 — 0 2	 25 32 — 128 57
$\left\{ \begin{array}{l} ao = (100) (111) \\ aq = (111) (011) \\ aq = (100) (011) \\ qo = (011) (111) \\ oa = (111) (100) \end{array} \right.$	 — — — — —	 — — — — —	 — — — — —	 48 26 26 56 75 22 34 42 69 56	 — — — — —	 — — — — —
$\left\{ \begin{array}{l} io = (001) (111) \\ ip = (111) (110) \\ cp = (001) (110) \\ pm' = (110) (111) \\ oi = (111) (001) \\ pi = (110) (001) \end{array} \right.$	 — — 36 14 12 33	 — — 76 33-77 4 58 10-58 36 44 35-45 7 102 49-103 32	 — — 76 49 58 26 14 47 103 11	 34 5 12 44 * 58 27 44 44 103 11	 — — — 1 3 0	 — — 77 7 — — —
$\left\{ \begin{array}{l} bo = (010) (111) \\ on = (111) (101) \end{array} \right.$	 — —	 — —	 — —	 70 27 19 33	 — —	 — —
$\left\{ \begin{array}{l} bo' = (010) (111) \\ oa' = (111) (101) \\ oa' = (111) (111) \end{array} \right.$	 2 — 1	 65 6-65 10 — —	 65 8 — 49 44	 65 10 24 50 49 40	 2 — 4	 — — 49 13
$\left\{ \begin{array}{l} sq = (101) (011) \\ qp = (011) (110) \\ pm = (110) (101) \\ pq = (110) (011) \end{array} \right.$	 — 29 — 30	 — 87 0-87 34 — 92 25-92 55	 — 87 21 — 92 39	 37 36 87 22 55 2 92 38	 — 1 — 1	 — — — —
$\left\{ \begin{array}{l} sq' = (101) (011) \\ qp = (011) (110) \\ ps' = (110) (101) \\ pq = (110) (011) \end{array} \right.$	 — 30 — 29	 — 62 40-63 2 — 116 51-117 31	 — 62 51 — 117 10	 45 7 62 49 72 4 117 11	 — 2 — 1	 — — — —
$\left\{ \begin{array}{l} r'o = (201) (111) \\ o'y = (111) (110) \\ pr' = (110) (201) \\ rp = (201) (110) \end{array} \right.$	 6 7 43 44	 34 57-35 29 91 56-92 15 52 28-53 8 126 41-127 31	 35 7 92 6 52 49 127 11	 35 9 92 2 52 49 127 11	 2 4 0 0	 — — — —
Total number of measurements	510					

60°-prisms, each ground to afford two indices, and the mean results are as under —

Refractive Indices of Tl Fe Sulphate

Light	α	β	γ
La	1 5880	1 6041	1 6110
C	1 5886	1 6048	1 6117
Na	1 5929	1 6093	1 6162
Tl	1 5980	1 6146	1 6223
Cd	1 6009	1 6175	1 6256
F	1 6040	1 6209	1 6292
G	1 6115	1 6285	1 6370

Mean index for Na light, $\frac{\alpha + \beta + \gamma}{3} = 1 6061$

Double refraction, $\text{Na}_{\gamma-\alpha} = 0 0233$

General Formula for the intermediate index β , corrected to a vacuum —

$$\beta = 1 5916 + \frac{420 091}{\lambda^2} + \frac{7 130 200 000 000}{\lambda^4} +$$

The α indices are also closely reproduced if the constant 1 5916 is diminished by 0 0164, and the γ -indices if it be increased by 0 0069

Axial Ratios of Optical Ellipsoid (Indicatrix) —

$$\alpha \ \beta \ \gamma = 0 9898 \ 1 \ 1 0043$$

Molecular Optical Constants —These are given in the next three tables

Table of Specific Refraction and Dispersion (Lorenz)

Specific refraction, $\frac{n^2 - 1}{(n^2 + 2)d} = n$						Specific dispersion $n_{\alpha} - n_{\gamma}$		
For ray C (Ha)			For ray H γ near G					
α	β	γ	α	β	γ	α	β	γ
0 0921	0 0943	0 0952	0 0952	0 0973	0 0983	0 0020	0 0030	0 0031

Table of Molecular Refraction and Dispersion (Lorenz)

Molecular refraction, $\frac{n^2 - 1}{n^2 + 2} \frac{M}{d} = m$						Molecular dispersion, $m_a - m_c$		
For ray C (H α)			For ray H γ near G					
α	β	γ	α	β	γ	α	β	γ
70.00	71.56	72.22	72.20	73.81	74.60	2.20	2.25	2.38

Molecular Refraction (Gladstone and Dale)

$\frac{n^2 - 1}{d} = M$ for ray C			Mean molecular refraction for ray C $\frac{1}{3}(\alpha + \beta + \gamma)$
α	β	γ	
122.23	125.70	127.14	125.03

Optic Axial Angle—Plates ground perpendicular to the acute and obtuse bisectrices afforded the following results, the interference figures having been very sharp and clear

Light	Apparent angle in air,	True angle within the
	$2E$ ° ' "	crystal, $2V_a$ ° ' "
Li	129 35	68 14
C	129 45	68 16
Na	131 35	69 0
Tl	133 47	69 26
Cd	135 26	69 13
F	137 20	69 59

Dispersion of the Median Lines—Observations in oil of cinnamon, the indices of which are very close to those of the crystals, indicated that the median lines are so dispersed in the symmetry plane that the first median line lies about 23' nearer to the crystal-axis a for green thallium light than for red C'-hydrogen light

Thallium Manganese Sulphate, $\text{Th}_2\text{Mn}(\text{SO}_4)_2 \cdot 6\text{H}_2\text{O}$

Morphology

Ten good little crystals were used for the goniometry, selected from four crops of outstanding excellence

Crystal System—Monoclinic Class No 5, holohedral-prismatic

Ratios of Axes—

$$a : b : c = 0.7454 : 1 : 0.4964$$

Axial Angle— $\beta = 106^\circ 22'$

Forms Observed— $a\{100\}$, $b\{010\}$, $c\{001\}$, $p\{110\}$, $p'\{120\}$, $p'''\{130\}$, $q\{011\}$, $r'\{201\}$, $o\{111\}$, $o'\{\bar{1}\bar{1}\bar{1}\}$, $n'\{\bar{1}21\}$

A typical habit is represented in fig 3. It is characterised by more extensive development of the form $r'\{201\}$ than is usual among the thallium salts of the series. The cleavage is parallel to the two faces of this form, and is particularly well developed in this salt.

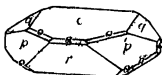


FIG 3—Th Mn Sulphate

Morphological Angles—The results of the angular measurements are given in the accompanying table (p. 378)

Volume

Relative Density Three concordant determinations of specific gravity gave as the mean accepted value 3.685, for the temperature $20^\circ/4^\circ$

$$\text{Molecular Volume} = \frac{M}{d} = \frac{757.72}{3.685} = 205.62$$

Topic Axial Ratios—

$$\lambda : \psi : \omega = 6.2194 : 8.3357 : 4.1378$$

Optics

Orientation of Optical Ellipsoid (Indicatrix)—The optic axes lie in the symmetry plane $b\{010\}$, and the double refraction is of negative sign. The axis γ (vibration direction for the γ -index of refraction) of the indicatrix lies $14^\circ 15'$ behind the vertical crystal-axis c , in the acute axial angle ac , and is the second median line (obtuse bisectrix) of the optic axial angle, the α -axis of the indicatrix (vibration direction of α -index), the acute bisectrix (first median line),

Interfacial Angles of Thalium Manganese Sulphate

Angle	No of measurements	Limits	Mean observed	Calculated	Diff
$\left\{ \begin{array}{l} ac \\ as \\ al \\ cr' \\ ca' \\ ar' \\ ra' \end{array} \right. \begin{array}{l} - (100) : (001) \\ - (100) (101) \\ = (101) (001) \\ (001) (201) \\ - (001) (101) \\ = (101) (201) \\ = (201) (100) \end{array}$	$\left\{ \begin{array}{l} 6 \\ --- \\ --- \\ 9 \\ --- \\ --- \\ 6 \end{array} \right.$	$\left\{ \begin{array}{l} 73\ 23-73\ 54 \\ --- \\ --- \\ 63\ 35-64\ 17 \\ --- \\ --- \\ 42\ 10-42\ 43 \end{array} \right.$	$\left\{ \begin{array}{l} 73\ 40 \\ --- \\ --- \\ 63\ 51 \\ --- \\ --- \\ 42\ 24 \end{array} \right.$	$\left\{ \begin{array}{l} 73\ 38 \\ 45\ 24 \\ 28\ 14 \\ 63\ 53 \\ 18\ 8 \\ 25\ 45 \\ 42\ 29 \end{array} \right.$	$\left\{ \begin{array}{l} 2 \\ --- \\ --- \\ 2 \\ --- \\ --- \\ 5 \end{array} \right.$
$\left\{ \begin{array}{l} ap \\ pp' \\ p'p \\ p''b \\ p''b \\ pb \\ pp \\ pp \end{array} \right. \begin{array}{l} - (100) (110) \\ (110) (120) \\ = (120) (130) \\ = (120) (010) \\ (130) : (010) \\ - (110) (010) \\ (110) (110) \\ (110) (110) \end{array}$	$\left\{ \begin{array}{l} 8 \\ 13 \\ 1 \\ 8 \\ 1 \\ 14 \\ 18 \\ 11 \end{array} \right.$	$\left\{ \begin{array}{l} 35\ 21-35\ 43 \\ 10\ 9-10\ 39 \\ --- \\ 11\ 40-15\ 1 \\ --- \\ 54\ 3-54\ 40 \\ 71\ 1-71\ 20 \\ 108\ 39-109\ 8 \end{array} \right.$	$\left\{ \begin{array}{l} 35\ 33 \\ 10\ 28 \\ 9\ 52 \\ 34\ 52 \\ 25\ 0 \\ 54\ 23 \\ 71\ 10 \\ 108\ 48 \end{array} \right.$	$\left\{ \begin{array}{l} 35\ 35 \\ 19\ 28 \\ 9\ 58 \\ 34\ 57 \\ 24\ 59 \\ 54\ 25 \\ * \\ 108\ 50 \end{array} \right.$	$\left\{ \begin{array}{l} 2 \\ 0 \\ 6 \\ 5 \\ 1 \\ 2 \\ --- \\ 2 \end{array} \right.$
$\left\{ \begin{array}{l} cq \\ qb \end{array} \right. \begin{array}{l} - (001) (011) \\ - (011) (010) \end{array}$	$\left\{ \begin{array}{l} 17 \\ 15 \end{array} \right.$	$\left\{ \begin{array}{l} 25\ 10-25\ 46 \\ 64\ 15-64\ 43 \end{array} \right.$	$\left\{ \begin{array}{l} 25\ 28 \\ 64\ 32 \end{array} \right.$	$\left\{ \begin{array}{l} * \\ 64\ 32 \end{array} \right.$	$\left\{ \begin{array}{l} --- \\ 0 \end{array} \right.$
$\left\{ \begin{array}{l} ao \\ oq \\ oq' \\ qo' \\ o'n \end{array} \right. \begin{array}{l} (100) (111) \\ = (111) (011) \\ = (100) (011) \\ = (011) : (111) \\ - (111) (100) \end{array}$	$\left\{ \begin{array}{l} --- \\ --- \\ --- \\ --- \\ --- \end{array} \right.$	$\left\{ \begin{array}{l} --- \\ --- \\ --- \\ --- \\ --- \end{array} \right.$	$\left\{ \begin{array}{l} --- \\ --- \\ --- \\ --- \\ --- \end{array} \right.$	$\left\{ \begin{array}{l} 48\ 32 \\ 26\ 44 \\ 75\ 16 \\ 34\ 27 \\ 70\ 17 \end{array} \right.$	$\left\{ \begin{array}{l} --- \\ --- \\ --- \\ --- \\ --- \end{array} \right.$
$\left\{ \begin{array}{l} co \\ op \\ cp \\ po' \\ o'r \\ pr \end{array} \right. \begin{array}{l} - (001) (111) \\ - (111) (110) \\ - (001) : (110) \\ - (110) : (111) \\ - (111) (001) \\ = (110) (001) \end{array}$	$\left\{ \begin{array}{l} 2 \\ 2 \\ 40 \\ 4 \\ 4 \\ 40 \end{array} \right.$	$\left\{ \begin{array}{l} 33\ 50-33\ 59 \\ 42\ 36-42\ 57 \\ 76\ 26-76\ 58 \\ 58\ 36-58\ 55 \\ 44\ 20-44\ 48 \\ 103\ 4-103\ 24 \end{array} \right.$	$\left\{ \begin{array}{l} 33\ 54 \\ 42\ 50 \\ 76\ 45 \\ 58\ 45 \\ 44\ 32 \\ 103\ 15 \end{array} \right.$	$\left\{ \begin{array}{l} 33\ 50 \\ 42\ 55 \\ * \\ 58\ 49 \\ 44\ 26 \\ 103\ 15 \end{array} \right.$	$\left\{ \begin{array}{l} 4 \\ 3 \\ --- \\ 4 \\ 6 \\ 0 \end{array} \right.$
$\left\{ \begin{array}{l} bo \\ oa \end{array} \right. \begin{array}{l} (010) (111) \\ = (111) (101) \end{array}$	$\left\{ \begin{array}{l} 2 \\ --- \end{array} \right.$	$\left\{ \begin{array}{l} 70\ 20-70\ 44 \\ --- \end{array} \right.$	$\left\{ \begin{array}{l} 70\ 29 \\ --- \end{array} \right.$	$\left\{ \begin{array}{l} 70\ 32 \\ 19\ 28 \end{array} \right.$	$\left\{ \begin{array}{l} 1 \\ --- \end{array} \right.$
$\left\{ \begin{array}{l} bu \\ bu' \\ n'o \\ o'n' \\ o'n' \end{array} \right. \begin{array}{l} - (010) (111) \\ - (010) (121) \\ = (121) (111) \\ - (111) (101) \\ - (111) (111) \end{array}$	$\left\{ \begin{array}{l} 4 \\ 1 \\ 1 \\ --- \\ 2 \end{array} \right.$	$\left\{ \begin{array}{l} 64\ 56-65\ 27 \\ --- \\ --- \\ --- \\ 49\ 27-49\ 10 \end{array} \right.$	$\left\{ \begin{array}{l} 65\ 11 \\ 47\ 21 \\ 17\ 54 \\ --- \\ 49\ 33 \end{array} \right.$	$\left\{ \begin{array}{l} 65\ 15 \\ 47\ 19 \\ 17\ 56 \\ 24\ 45 \\ 49\ 30 \end{array} \right.$	$\left\{ \begin{array}{l} 4 \\ 2 \\ 2 \\ --- \\ 1 \end{array} \right.$
$\left\{ \begin{array}{l} ag \\ gp \\ gn' \\ n'p \\ pa \\ pg \end{array} \right. \begin{array}{l} - (101) (011) \\ - (011) (110) \\ = (011) (121) \\ = (121) (110) \\ - (110) (101) \\ = (110) (011) \end{array}$	$\left\{ \begin{array}{l} --- \\ 28 \\ --- \\ --- \\ --- \\ 28 \end{array} \right.$	$\left\{ \begin{array}{l} --- \\ 87\ 10-87\ 48 \\ --- \\ --- \\ --- \\ 92\ 13-92\ 41 \end{array} \right.$	$\left\{ \begin{array}{l} --- \\ 87\ 36 \\ --- \\ --- \\ --- \\ 92\ 24 \end{array} \right.$	$\left\{ \begin{array}{l} 37\ 19 \\ 87\ 31 \\ 35\ 34 \\ 51\ 57 \\ 55\ 10 \\ 92\ 29 \end{array} \right.$	$\left\{ \begin{array}{l} --- \\ 5 \\ --- \\ --- \\ --- \\ 5 \end{array} \right.$
$\left\{ \begin{array}{l} a'g \\ gp \\ pa' \\ pg \end{array} \right. \begin{array}{l} = (101) (011) \\ = (011) : (110) \\ = (110) (101) \\ = (110) (011) \end{array}$	$\left\{ \begin{array}{l} --- \\ 37 \\ --- \\ 36 \end{array} \right.$	$\left\{ \begin{array}{l} --- \\ 62\ 34-63\ 48 \\ --- \\ 116\ 46-117\ 32 \end{array} \right.$	$\left\{ \begin{array}{l} --- \\ 63\ 47 \\ --- \\ 117\ 12 \end{array} \right.$	$\left\{ \begin{array}{l} 44\ 45 \\ 62\ 48 \\ 72\ 27 \\ 117\ 12 \end{array} \right.$	$\left\{ \begin{array}{l} --- \\ 1 \\ --- \\ 0 \end{array} \right.$
$\left\{ \begin{array}{l} r'o' \\ o'p \\ pr' \end{array} \right. \begin{array}{l} = (201) : (111) \\ = (111) : (110) \\ = (110) (201) \end{array}$	$\left\{ \begin{array}{l} 10 \\ 13 \\ 11 \end{array} \right.$	$\left\{ \begin{array}{l} 34\ 43-35\ 34 \\ 91\ 33-92\ 5 \\ 52\ 51-53\ 13 \end{array} \right.$	$\left\{ \begin{array}{l} 35\ 9 \\ 91\ 47 \\ 53\ 2 \end{array} \right.$	$\left\{ \begin{array}{l} 35\ 7 \\ 91\ 44 \\ 53\ 9 \end{array} \right.$	$\left\{ \begin{array}{l} 2 \\ 3 \\ 7 \end{array} \right.$
Total number of measurements	432				

lies $30^{\circ} 37'$ above the inclined crystal-axis a , in the obtuse axial angle ac . The symmetry axis b is the vibration direction for the β -index of refraction.

Refractive Indices—The mean values obtained were —

Light	α	β	γ
Li	1.5820	1.5854	1.6041
U	1.5826	1.5960	1.6047
Na	1.5861	1.5996	1.6084
Tl	1.5900	1.6035	1.6123
Cd	1.5927	1.6063	1.6152
F	1.5959	1.6096	1.6186

Mean index for Na light, $\frac{\alpha + \beta + \gamma}{3} = 1.5980$

Double refraction, $\text{Na}_{\gamma} = 0.0223$

General Formula for intermediate index β for any wave-length λ , corrected to a vacuum —

$$\beta = 1.5786 + \frac{832.324}{\lambda^2} - \frac{3.105400000000}{\lambda^4}$$

The α -indices are also closely reproduced by the formula if the constant 1.5786 be reduced by 0.0135 and the γ -indices if it be increased by 0.0088.

Axial Ratios of Optical Ellipsoid —

$$\alpha : \beta : \gamma = 0.9916 : 1 : 1.0055$$

Molecular Optical Constants These work out as follows, for the red ray C, H α .

	α	β	γ
Specific refraction $\frac{n^2 - 1}{(n^2 + 2)d}$	0.0906	0.0923	0.0934
Molecular refraction (Lorenz) $\frac{n^2 - 1}{n^2 + 2} \frac{M}{d}$	68.68	69.96	70.79
Molecular refraction (Gladstone) $\frac{n - 1}{d} M$	119.80	122.55	124.34

Mean molecular refraction (Gladstone), $\frac{\alpha + \beta + \gamma}{3} = 122.23$

Optic Axial Angle The angle in air, 2E, was not quite measurable, but

the true angle $2V_a$ within the crystal is given below, as the mean of several well agreeing determinations

Light	$2V_a,$		Light	$2V_a,$
Li	71 14		Tl	71 41
C	71 16		Cd	71 49
Na	71 26		F	71 59

Dispersion of the Median Lines—This is small, and is such that the first median line lies nearer to the inclined crystal-axis a for green thallium light than for red C-hydrogen light by $16'$, this being the mean of two determinations affording $15'$ and $17'$ respectively, made with the two crystals immersed in oil of cinnamon, the refractive index of which is almost identical with the mean crystal-index

Thallium Copper Sulphate, $Tl_2Cu(SO_4)_2 \cdot 6H_2O$

Morphology

Eleven little crystals from three different crops were used for the crystal-angle measurements. The crystals of this salt are coloured bright blue

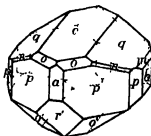


FIG. 4.— Tl_2Cu Sulphate

Crystal System—Monoclinic Class No 5, holohedral-prismatic

Ratios of Axes— $a : b : c = 0.7499 : 1 : 0.5033$

Axial Angle— $\beta = 105^\circ 33'$

Forms Observed— $a\{100\}$, $b\{010\}$, $c\{001\}$, $p\{110\}$, $p'\{120\}$, $p''\{130\}$, $q\{011\}$, $m\{021\}$, $r\{201\}$, $r'\{201\}$, $o\{111\}$, $o'\{111\}$, and $n\{121\}$. The form $r\{201\}$ is exceedingly rarely present on any of the salts of this whole isomorphous series. *Cleavage* occurs parallel to $r'\{201\}$

Habit—The most typical habit is illustrated in fig 4

Morphological Angles—The results of the goniometrical measurements are given in the accompanying table

Interfacial Angles of Thallium Copper Sulphate

Angle	No of measurements	Limits	Mean observed	Calculated	Diff
$\left\{ \begin{array}{l} ac = (100) (001) \\ as = (100) (101) \\ ac = (101) (001) \\ ar = (100) (201) \\ rr' = (201) (001) \\ cr' = (001) (201) \\ cr' = (001) (101) \\ r'p' = (101) (201) \\ ra = (201) (100) \\ r'c = (201) (001) \end{array} \right.$	$\left\{ \begin{array}{l} 2 \\ - \\ - \\ 1 \\ 1 \\ 16 \\ - \\ - \\ 2 \\ 15 \end{array} \right.$	$\left\{ \begin{array}{l} 74 \ 25-74 \ 27 \\ - \\ - \\ - \\ 63 \ 35-63 \ 47 \\ - \\ - \\ 41 \ 48-41 \ 53 \\ 116 \ 12-116 \ 28 \end{array} \right.$	$\left\{ \begin{array}{l} 74 \ 26 \\ - \\ - \\ 30 \ 51 \\ 43 \ 35 \\ 63 \ 41 \\ - \\ 41 \ 51 \\ 116 \ 19 \end{array} \right.$	$\left\{ \begin{array}{l} 71 \ 27 \\ 45 \ 43 \\ 28 \ 44 \\ 30 \ 52 \\ 43 \ 35 \\ 63 \ 42 \\ 78 \ 18 \\ 25 \ 21 \\ 41 \ 51 \\ 116 \ 18 \end{array} \right.$	$\left\{ \begin{array}{l} 1 \\ - \\ - \\ 1 \\ 0 \\ 1 \\ - \\ - \\ 0 \\ 1 \end{array} \right.$
$\left\{ \begin{array}{l} ap = (100) (110) \\ pp' = (110) (120) \\ p'p'' = (120) (130) \\ p'b = (120) (010) \\ p''b = (130) (010) \\ pb = (110) (010) \\ pp = (110) (110) \end{array} \right.$	$\left\{ \begin{array}{l} 4 \\ 2 \\ 1 \\ 2 \\ 1 \\ 27 \\ 16 \end{array} \right.$	$\left\{ \begin{array}{l} 35 \ 46-35 \ 52 \\ 19 \ 25-19 \ 33 \\ - \\ 34 \ 38-34 \ 42 \\ - \\ 53 \ 53-54 \ 27 \\ 71 \ 26-71 \ 55 \end{array} \right.$	$\left\{ \begin{array}{l} 35 \ 49 \\ 19 \ 29 \\ 9 \ 55 \\ 34 \ 40 \\ 24 \ 47 \\ 54 \ 10 \\ 71 \ 39 \end{array} \right.$	$\left\{ \begin{array}{l} 35 \ 50 \\ 19 \ 28 \\ 9 \ 55 \\ 31 \ 42 \\ 21 \ 47 \\ * \\ 71 \ 40 \end{array} \right.$	$\left\{ \begin{array}{l} 1 \\ 1 \\ 0 \\ 2 \\ 0 \\ - \\ 1 \end{array} \right.$
$\left\{ \begin{array}{l} cq = (001) (011) \\ qb = (011) (010) \\ bm = (010) (021) \\ mq = (021) (011) \end{array} \right.$	$\left\{ \begin{array}{l} 40 \\ 36 \\ 6 \\ 5 \end{array} \right.$	$\left\{ \begin{array}{l} 25 \ 26-26 \ 5 \\ 63 \ 55-64 \ 22 \\ 45 \ 41-45 \ 3 \\ 18 \ 4-18 \ 24 \end{array} \right.$	$\left\{ \begin{array}{l} 25 \ 52 \\ 64 \ 7 \\ 45 \ 50 \\ 18 \ 14 \end{array} \right.$	$\left\{ \begin{array}{l} * \\ 64 \ 8 \\ 45 \ 51 \\ 18 \ 15 \end{array} \right.$	$\left\{ \begin{array}{l} - \\ 1 \\ 3 \\ 1 \end{array} \right.$
$\left\{ \begin{array}{l} ao = (100) (111) \\ oq = (111) (011) \\ aq = (100) (011) \\ go' = (011) (111) \\ o'a = (111) (100) \end{array} \right.$	$\left\{ \begin{array}{l} - \\ - \\ - \\ - \\ - \end{array} \right.$	$\left\{ \begin{array}{l} - \\ - \\ - \\ - \\ - \end{array} \right.$	$\left\{ \begin{array}{l} - \\ - \\ - \\ - \\ - \end{array} \right.$	$\left\{ \begin{array}{l} 48 \ 56 \\ 27 \ 7 \\ 76 \ 3 \\ 34 \ 28 \\ 69 \ 29 \end{array} \right.$	$\left\{ \begin{array}{l} - \\ - \\ - \\ - \\ - \end{array} \right.$
$\left\{ \begin{array}{l} co = (001) (111) \\ op = (111) (110) \\ cp = (001) (110) \\ po' = (110) (111) \\ o'o = (111) (001) \end{array} \right.$	$\left\{ \begin{array}{l} 16 \\ 16 \\ 42 \\ 35 \\ 35 \end{array} \right.$	$\left\{ \begin{array}{l} 34 \ 0-34 \ 41 \\ 42 \ 50-43 \ 20 \\ 77 \ 11-77 \ 41 \\ 57 \ 45-58 \ 12 \\ 44 \ 23-44 \ 54 \end{array} \right.$	$\left\{ \begin{array}{l} 34 \ 21 \\ 43 \ 5 \\ 77 \ 27 \\ 57 \ 57 \\ 44 \ 36 \end{array} \right.$	$\left\{ \begin{array}{l} 34 \ 25 \\ 43 \ 2 \\ * \\ 57 \ 57 \\ 44 \ 36 \end{array} \right.$	$\left\{ \begin{array}{l} 4 \\ 3 \\ - \\ 0 \\ 0 \end{array} \right.$
$\left\{ \begin{array}{l} bn = (010) (121) \\ no = (121) (111) \\ bo = (010) (111) \\ os = (111) (101) \\ oo = (111) (111) \end{array} \right.$	$\left\{ \begin{array}{l} 1 \\ 1 \\ 7 \\ - \\ 3 \end{array} \right.$	$\left\{ \begin{array}{l} - \\ - \\ 70 \ 8-70 \ 24 \\ - \\ 39 \ 37-39 \ 39 \end{array} \right.$	$\left\{ \begin{array}{l} 54 \ 17 \\ 15 \ 54 \\ 70 \ 14 \\ - \\ 39 \ 38 \end{array} \right.$	$\left\{ \begin{array}{l} 54 \ 13 \\ 15 \ 58 \\ 70 \ 11 \\ 19 \ 49 \\ 39 \ 38 \end{array} \right.$	$\left\{ \begin{array}{l} 4 \\ 4 \\ 3 \\ - \\ 0 \end{array} \right.$
$\left\{ \begin{array}{l} bo' = (010) (111) \\ o'o' = (111) (101) \\ o'o' = (111) (111) \end{array} \right.$	$\left\{ \begin{array}{l} 25 \\ - \\ 12 \end{array} \right.$	$\left\{ \begin{array}{l} 64 \ 55-65 \ 19 \\ - \\ 49 \ 42-49 \ 58 \end{array} \right.$	$\left\{ \begin{array}{l} 65 \ 5 \\ - \\ 49 \ 50 \end{array} \right.$	$\left\{ \begin{array}{l} 65 \ 6 \\ 24 \ 54 \\ 49 \ 48 \end{array} \right.$	$\left\{ \begin{array}{l} 1 \\ - \\ 2 \end{array} \right.$
$\left\{ \begin{array}{l} qg = (101) (011) \\ gp = (011) (110) \\ pm = (110) (101) \\ pq = (110) (011) \end{array} \right.$	$\left\{ \begin{array}{l} - \\ 39 \\ - \\ 39 \end{array} \right.$	$\left\{ \begin{array}{l} - \\ 86 \ 15-86 \ 52 \\ - \\ 93 \ 12-93 \ 45 \end{array} \right.$	$\left\{ \begin{array}{l} - \\ 86 \ 33 \\ - \\ 93 \ 27 \end{array} \right.$	$\left\{ \begin{array}{l} 37 \ 55 \\ 86 \ 34 \\ 55 \ 31 \\ 93 \ 20 \end{array} \right.$	$\left\{ \begin{array}{l} - \\ 1 \\ - \\ 1 \end{array} \right.$
$\left\{ \begin{array}{l} a'q = (101) (011) \\ qa = (011) (121) \\ ap = (121) (110) \\ qp = (011) (110) \\ pa' = (110) (101) \\ pq = (110) (011) \end{array} \right.$	$\left\{ \begin{array}{l} - \\ 1 \\ 1 \\ 40 \\ - \\ 36 \end{array} \right.$	$\left\{ \begin{array}{l} - \\ - \\ - \\ 63 \ 0-63 \ 23 \\ - \\ 116 \ 38-117 \ 0 \end{array} \right.$	$\left\{ \begin{array}{l} - \\ 26 \ 32 \\ 36 \ 40 \\ 63 \ 10 \\ - \\ 116 \ 49 \end{array} \right.$	$\left\{ \begin{array}{l} 45 \ 5 \\ 26 \ 28 \\ 36 \ 44 \\ 63 \ 12 \\ 71 \ 43 \\ 116 \ 48 \end{array} \right.$	$\left\{ \begin{array}{l} - \\ 4 \\ 4 \\ 2 \\ - \\ 1 \end{array} \right.$

Interfacial Angles of Thallium Copper Sulphate—(continued)

Angle	No of measure- ments	Limits	Mean observed	Calcu- lated	Diff
$r'o = (201) (111)$	31	34 52–35 8	34 58	34 59	1
$o'p = (111) (110)$	31	91 53–92 21	92 9	92 10	1
$o'm = (111) (021)$	4	36 25–36 37	36 29	36 28	1
$m'p = (021) (110)$	4	55 38–55 44	55 42	55 42	0
$p'r' = (110) (201)$	36	52 38–53 0	52 52	52 51	1
Total number of measure- ments	612				

The Average Difference of angle between this thallium copper salt and the corresponding potassium copper sulphate, that is, brought about by the replacement of potassium by thallium, is 28', and the maximum angular change (largest of all the angular changes), which occurs in the principal angle, the monoclinic axial angle ac , is $1^\circ 5'$. The effect of replacing sulphur by selenium will be found dealt with on p. 416.

Volume

Relative Density The accepted value, the mean of three good determinations is 3.728

$$\text{Molecular Volume } \frac{M}{d} = \frac{766.22}{3.728} = 205.53$$

Topio Axial Ratios

$$a : b : c = 6.2003 : 8.2682 : 4.1614$$

Optics

Orientation of Optical Ellipsoid (Indicatrix)—The plane of the optic axes is the symmetry plane $b(010)$. The sign of the double refraction is negative. The axis γ (the vibration direction for the γ -index of refraction) of the indicatrix lies $17^\circ 20'$ behind the vertical crystal-axis c , in the acute crystal-axial angle ac , and is the obtuse bisectrix (second median line) of the optic axial angle, the α -axis of the indicatrix (corresponding to the α -index), the acute bisectrix (first median line), lies $32^\circ 53'$ above the crystal-axis a , in the obtuse crystal-axial angle ac . The vibration direction for the β -index of refraction is the symmetry axis b .

Refractive Indices —These are as under —

Light	α	β	γ
Li	1.5944	1.6044	1.6188
C	1.5950	1.6050	1.6144
Na	1.5996	1.6096	1.6190
Ti	1.6048	1.6149	1.6244
Cd	1.6081	1.6182	1.6277
F	1.6120	1.6222	1.6318

$$\text{Mean index for Na light, } \frac{\alpha + \beta + \gamma}{3} = 1.6094$$

$$\text{Double refraction } \text{Na}_{\gamma} = 0.0184$$

General Formula for the intermediate refractive index β , corrected to a vacuum

$$\beta = 1.5883 + \frac{665.095}{\lambda^2} + \frac{3.061.000.000.000}{\lambda^4} +$$

The α -indices are also closely reproduced by the formula if the constant 1.5883 is diminished by 0.0100, and the γ indices if it be increased by 0.0094

Axial Ratios of Optical Ellipsoid

$$\alpha : \beta : \gamma = 0.9938 : 1 : 1.0058$$

Molecular Optical Constants These are as follows, for the red hydrogen ray C —

	α	β	γ
Specific refraction $\frac{n^2 - 1}{(n^2 + 2)d}$	0.0911	0.0924	0.0935
Molecular refraction (Lorenz) $\frac{n^2 - 1}{n^2 + 2} \frac{M}{d}$	69.84	70.79	71.67
Molecular refraction (Gladstone) $\frac{n - 1}{d} M$	122.29	124.35	126.28

$$\text{Mean molecular refraction (Gladstone) } \frac{\alpha + \beta + \gamma}{3} = 124.31$$

Optic Axial Angle —The optic axes do not emerge in air, owing to the wide-

ness of the true optic axial angle, $2V_a$. Closely concordant (within $4'$ at most) measurements of the latter afforded the following mean values --

Light	$2V_a$ °	Light	$2V_a$ °
Li	85 22	Tl	85 10
C	85 21	Cl	85 7
Na	85 16	F	85 2

Dispersion of the Median Lines This is such that the first median line lies nearer to the crystal-axis a for green thallium light than for red C-hydrogen light by $16'$. Oil of cinnamon was used as the immersion liquid for this particular determination, its refractive index being practically identical with the mean index of the crystal.

Discussion of the Results

The main point of interest in discussing the results of this investigation is to make clear how these thallium salts of the great series $R_2M(SO_4)_2 \cdot 6H_2O$ differ from the other salts of the series already fully described, namely, those containing as the R-base one of the alkali metals of the same family group, potassium, rubidium, or caesium, or the radicle ammonium NH_4 . Differences there must be, as it is now certain that except in the cases of cubic crystals--where the symmetry itself fixes the angles unalterably--change of chemical composition, even the isomorphous replacement by family analogues, invariably causes morphological and physical change. The author's previous work has already shown what is the nature of the change when those four bases replace each other. It has been conclusively proved that there are small eutropic changes of interfacial angle and larger eutropic alterations of the optical and other physical properties in the cases of the alkali-metallic replacements. By "eutropic" is meant that the changes are proportional to or follow the order of the change of mass of the atoms interchanged, that is, that they are functions of the atomic number or atomic weight. The introduction of ammonium, while not acting eutropically, as we are here dealing with a radicle complex and not a simple analogous atom, effects changes which in regard to many of the properties--especially structural unit-cell size and edge-dimensions, and molecular refraction--resemble remarkably closely those accompanying the introduction of rubidium, the middle member of the alkali family-group, so that the rubidium and ammonium salts are strikingly isostructural and similar in all molecular properties. The work already achieved on four thallium salts of the series has shown that these thallium salts likewise, although not quite so closely, resemble the analogous ammonium and rubidium salts, to the

extent indeed of being very nearly isostructural with them. But they have been shown to exhibit one very remarkable outstanding difference, namely, very much higher refractive power, their refractive indices being so much higher that, as will be seen in the next memoir, the double selenates containing thallium are practically as highly refractive as the liquid so much used in optical work for its high refractivity, monobromonaphthalene. We may now proceed, therefore, to examine the further results here in this memoir presented for the remainder of the double sulphates containing thallium.

Dealing first with the *Interfacial Angles*, instead of giving a series of tables showing the whole of the angles of the thallium salts alongside those for the alkali-metallic and ammonium salts, which would occupy a large space,* a table is next shown in which are concisely and comparatively given the average and maximum changes of angle for each replacement. The average change is obtained by making a list of all the individual changes of angle (36 quite different angles being compared), and taking their mean, irrespectively of the change being an increase or decrease. In the case of passing from a potassium salt to a rubidium one, and thence to the analogous caesium one, the change is always of the same sign, as the rubidium value is always intermediate between the values for the potassium and caesium salts, by virtue of the progression according to atomic number. But with the introduction of ammonium or thallium the changes may be of either sign, there being no progress in order of mass, but only such a change of angle as is of a like order of magnitude, corresponding to true isomorphism (in the wider sense now understood, which recognises the minute but very real differences between the members of isomorphous series not cubic in symmetry). The maximum angular change is simply the biggest change that is observed on reviewing all the changes, and in the cases of the thallium salts and many of the other salts it is that which occurs in the principal angle, the supplement of the important monoclinic axial angle β , namely, $ac = (100) (001)$.

No thallium-cadmium salts are included in this investigation, for they appear to be incapable of existence. All attempts to prepare them have merely afforded white opaque granular deposits, which break up into a white microcrystalline powder on drying, the crystallites of which show no resemblance under the microscope to the salts of this series. Potassium-cadmium sulphate and selenate with $6H_2O$ have previously been shown to be also incapable of existence.

* Three such tables have already been given for the zinc, nickel, and cobalt double sulphates containing thallium, and may with advantage be consulted, on p. 220 of the 1900 memoir (*loc. cit.*) and pp. 243 and 253 of the 1925 memoir (also *loc. cit.*)

Table of Average and Maximum Changes of Angle in Double Sulphates

	Average change for replacement of K by				Maximum change for replacement of K by			
	Rb	Cs	NH ₄	Tl	Rb	Cs	NH ₄	Tl
Mg group	29	58	56	40	71	141	138	102
Zn "	26	56	50	35	65	139	124	88
Ni "	27	54	49	33	63	122	117	84
Co "	27	56	52	36	66	137	127	90
Fe "	32	65	62	41	72	145	138	104
Cu "	22	47	39	28	53	115	101	65
Mean	27	56	51	36	65	133	124	80

The manganese salts do not appear in this table as the potassium salt of this group also does not exist, and cannot therefore be compared. As regards these six groups compared, for which all the members have been obtained and investigated, the results are striking. In every case the change of angle, whether average or maximum, on the introduction of caesium for potassium is twice as much as when rubidium is interchanged for potassium, thus corresponding exactly to the change of atomic weight or number. The atomic numbers are 19 for K, 37 for Rb, and 55 for Cs, that is, 18 additional electrons are added in the first replacement and 36 in the second, in one or two additional shells around the nucleus. The introduction of ammonium or thallium provokes amounts of change which are lower than when caesium is introduced but higher than when rubidium is interchanged, the thallium value being the lower and nearer to the rubidium value, while the ammonium value is nearer to the caesium one.

It is really astonishing how exact this is, as regards the alkali-metallic changes, whether we consider each group alone, or the mean given at the foot of the table. For instance, in the latter case 56' and 27' or 133' and 65' stand wonderfully closely to 2 : 1. If an additional table be now given for the values of the axial angle β itself, the changes for the two replacements K by Cs or Rb will be seen always to stand, almost exactly to a minute of arc, as two to one.

Comparison of the Monoclinic Axial Angles β for Double Sulphates

Containing	Magnesium	Ferrous iron	Manganese	Copper
Potassium	104 48	104 32	—	104 28
Rubidium	105 59	105 44	105 57	105 18
Caesium	107 6	106 52	107 7	106 10
Ammonium	107 6	106 50	106 51	106 9
Thallium	106 30	106 16	106 22	106 33

It will be clear that the axial angle for the rubidium salt is in all four cases half-way between the axial angles of the corresponding potassium and caesium salts, that the axial angle of the ammonium salt is very close to that for the caesium salt, and that in the case of the thallium salt the value is intermediate between the values for the rubidium and caesium salts. Precisely similar results were obtained for the zinc, nickel, and cobalt groups already completely dealt with in previous papers.

Passing next to the changes in *Molecular Volume* and *Topic Axial Ratios*, which literally mean the volumes and edge-dimensions of the unit cells of the structural units, the following tables will be instructive.

Density and Molecular Volume of Double Sulphates

Containing	Potassium	Rubidium	Caesium	Ammonium	Thallium
Magnesium	2 034 100 58	2 380 206 18	2 076 218 00	1 723 207 78	1 573 203 55
Zinc	2 246 106 16	2 591 205 58	2 875 217 97	1 932 206 38	1 720 206 46
Nickel	2 237 191 99	2 380 203 43	2 872 215 90	1 923 203 91	1 770 201 97
Cobalt	2 219 195 68	2 567 205 03	2 844 218 11	1 901 206 40	1 782 201 40
Iron (ferrous)	2 177 188 05	2 518 207 81	2 796 220 77	1 864 208 86	1 650 207 84
Manganese		2 461 212 26	2 740 224 95	1 831 212 13	1 685 205 62
Copper	2 233 196 10	2 571 206 24	2 858 218 64	1 926 206 08	1 728 205 03

Specific gravity at 20°/4° is on the left-hand, and molecular-volume on the right, in the column.

As regards specific gravity, the usual progress with atomic weight or number is clear in the case of the alkali metals, but the ammonium salt is lighter than any, and the thallium salt nearly a whole unit heavier than the caesium salt.

With respect to the particularly interesting molecular volume, the unit cell content, there is an increase of an average of 9.6 units when rubidium replaces potassium, and an increase of a further 12.7 units in the mean when caesium replaces rubidium. But the cell volume of the ammonium salt is strikingly close to that of the rubidium salt, expressing the structure which the author has so fully proved in previous communications, and thallium also acts

similarly to ammonium, although the volumes of the thallium salts are not quite as close to those of the rubidium salt

Table of Topic Axial Ratios of Double Sulphates

Containing	Magnesium			Ferrous iron			Manganese			Copper		
	χ	ψ	ω	χ	ψ	ω	χ	ψ	ω	χ	ψ	ω
Potassium	6 0711	8 1899	4 0692	6 0533	8 2056	4 1192	—	—	—	6 0709	8 1053	4 1240
Rubidium	6 1803	8 3518	4 1550	6 1692	8 3628	4 1848	6 2404	8 4536	4 1846	6 2017	8 2800	4 1640
Cæsium	6 2008	8 6012	4 2541	6 2021	8 6242	4 2716	6 3286	8 7004	4 2746	6 3332	8 5249	4 2164
Ammonium	6 2320	8 4217	4 1418	6 2096	8 4172	4 1749	6 2670	8 4690	4 1761	6 1786	8 2790	4 1942
Thallium	6 1723	8 2639	4 1470	6 2050	8 3547	4 1765	6 2134	8 3357	4 1378	6 2003	8 2682	4 1614

This table only gives the values for the four groups of which the thallium salts are now described. But similar tables were given for the zinc group in the 1909 paper, and for the nickel and cobalt groups in the 1925 paper (both *loc cit*). And all these tables indicate the same facts, namely, a regular progression in the relative dimensions of the structural-unit cells, when potassium is replaced in turn by rubidium and then by cæsium, and closeness of the dimensions of the cells of the rubidium, ammonium and thallium salts containing the same M-metal.

It must be remembered that these measures of cell volume and cell edges are relative. To get the absolute dimensions the X-ray analysis is required, a task which is not yet feasible on account of the complexity of the molecule, the low (monoclinic) symmetry, and the presence of the six molecules of water. The author has hopes, however, that further progress will enable the problem to be tackled, and these relative measures converted into absolute ones, as was done for the simple sulphates of potassium, rubidium, cæsium and ammonium by Prof Ogg and Mr Hopwood* in the laboratory of Sir William Bragg. The wonderfully close confirmation of the author's relative dimensions for these salts renders one confident that in this case also of the more complicated double sulphates a like confirmation is bound to occur †.

* 'Phil Mag,' vol 32, p 518 (1926)

† A further memoir has just (February, 1928) been published by Prof Ogg [Phil Mag, vol 5, p 354 (1928)] giving the results of a much more detailed study of the four simple sulphates of K, Rb, Cs and NH_4 with crystals supplied by the author. The full structure has been worked out, the space group being $V_h 16$, with four molecules of R_2SO_4 to the structural unit cell. The results as regards the relations of the four salts and the absolute dimensions of the structural units are fully confirmed.

Passing now to the optical properties, the *Orientation of the Optical Indicatrix* is the first fundamental property for which a comparison should be instituted. The whole of these double sulphates and, as will be shown in the next memoir, also the double selenates, exhibit in strikingly similar fashion the fact which is graphically illustrated in fig 5. The ellipsoid of three different rectangular

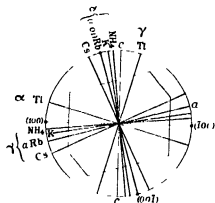


FIG 5

axes, of different lengths, represented relatively by the three refractive indices α , β , γ if we consider the Fletcher indicatrix as the representative ellipsoid, is only so far fixed that one of its axes, the intermediate one β in the case of this series of salts, is identical in direction with the single symmetry axis b of the monoclinic crystal. It is free to rotate about this axis whenever a change of one interchangeable metal for another is effected, and it does actually so rotate. It has been shown in previous communications that for any potassium salt its position is such that one of its two other axes, which lie in the symmetry plane, is as shown in fig 5, near to and somewhat to the left of the vertical crystal-axis c . For the corresponding rubidium salt it lies a little more to the left, and for the caesium salt still more so. The ammonium salt has this same axis very close to the c -axis, between it and the potassium position. It is now shown for the four thallium salts here described, and a similar fact was shown for the previously described thallium salts containing zinc, nickel, and cobalt, that this axis lies to the right of the crystal-axis c . The amounts are shown in the little table which follows —

Inclination of γ -axis of Ellipsoid to Right of Crystal-axis c

	$^{\circ}$	$'$
In Tl-Mg-sulphate	9	4
„ Tl-Fe-sulphate	16	15
„ Tl-Mn-sulphate	14	15
„ Tl Cu-sulphate	17	20

The values for the zinc, nickel, and cobalt salts were found in the former work to be respectively $13^{\circ} 29'$, $14^{\circ} 40'$ and $15^{\circ} 40'$ behind the axis c .

The sign of the double refraction is negative in all these thallium salts. Also in all of them this direction just located is the vibration direction of the light affording the γ -index of refraction, and is the second median line (obtuse bisectrix) of the optic axial angle.

Taking next the *Refraction Constants*, the next table compares the three most characteristic of these, namely, in the upper part the mean refractive index $1/3(\alpha + \beta + \gamma)$ for sodium light, in the middle part the double refraction, that is, the difference between the two extreme indices α and γ for sodium light, and in the lower part the mean molecular refraction according to the Gladstone formula (that of Lorenz showing precisely the same facts). Full comparative tables of the refractive indices themselves for six wave-lengths have already been given in the 1909 paper (p. 222) for the zinc group, and in the 1925 paper (pp. 247 and 257) for the nickel and cobalt groups, which exhibit quite similar relationships to the four groups of which the thallium salts are now described, it is therefore unnecessary to occupy space here in giving four other similar tables, and a table of the form now given (*see* p. 391) is really more instructive.

The outstanding feature displayed by the thallium salts at once strikes the eye, namely, their relatively very high refractive index, double refraction, and molecular refraction.

The properties already sufficiently proved in former memoirs, the eutropic progression shown by the potassium, rubidium, and caesium salts, especially clear as regards double refraction (a diminution with atomic weight and number) and molecular refraction (a steady and accelerating increase), and the similarity of molecular refraction shown by the rubidium and ammonium salts, are concisely exhibited by this table.

The *Optic Axial Angle* phenomena do not call for any special comparison, as they are only another natural expression of the refraction relationships along the three axes of the optical ellipsoid, which determine where the two circular

Refraction Constants of the Double Sulphates

Containing	Magnesium	Ferrous iron	Manganese	Copper	Mean refractive indices	Double refraction	Molecular
Potassium	1.4694	1.4850	—	1.4907	}		
Rubidium	1.4711	1.4889	1.4827	1.4943			
Cæsium	1.4877	1.5044	1.4979	1.5087			
Ammonium	1.4744	1.4925	1.4851	1.4990			
Thallium	1.5846	1.6061	1.5980	1.6094			
Potassium	0.0148	0.0210	—	0.0184	}		
Rubidium	0.0107	0.0162	0.0140	0.0150			
Cæsium	0.0059	0.0091	0.0079	0.0105			
Ammonium	0.0070	0.0119	0.0112	0.0144			
Thallium	0.0244	0.0277	0.0227	0.0194			
Potassium	91.23	95.59	—	95.91	}		
Rubidium	96.74	101.11	101.98	101.44			
Cæsium	106.25	110.82	111.43	110.65			
Ammonium	98.03	102.71	102.37	102.25			
Thallium	118.14	125.05	122.23	124.71			

sections of the ellipsoid shall be situated, perpendicular to which are the optic axes. But it should be emphasised that throughout the whole seven thallium double sulphates the acute bisectrix of the optic axial angle is the minimum axis α of the indicatrix ellipsoid, for which the axes are proportional to the refractive indices, and the maximum axis γ is the obtuse bisectrix. The intermediate axis β is always the symmetry crystal-axis b , perpendicular to the unique systematic symmetry plane, which contains the α and γ axes. The maximum index γ being the nearer to the intermediate index β , and the minimum axis α further therefrom, the double refraction is of negative sign, and this prevails throughout the whole set of thallium double sulphates. The study of the interference figures during the measurements of optic axial angle have consistently also indicated a slight dispersion (for different wave-lengths of light) of the bisectrices, the first and second median lines which are themselves the α and γ axes of the ellipsoid— in the symmetry plane, in amount varying from a quarter to three-quarters of a degree, and in the same sense, which is always such as brings the first median line nearer to the inclined crystal-axis a for green thallium than for red hydrogen light.

Conclusion

The results for these four remaining double sulphates containing thallium are precisely in line with those previously derived from the study of the thallium salts of the zinc, nickel, and cobalt groups. Thallium does not eutropically replace the alkali metals, but although the changes in exterior angles and

internal physical properties are not proportional to the heavy mass, as represented by the high atomic number of thallium (81), this heavier and more complicated atomic nature and structure do register themselves in the transcendent optical refraction and spectral dispersion exhibited by the thallium double salts. The exact position of the thallium salt of any group, as regards all the properties other than this refraction of light, is, indeed, very close to that occupied by the similarly non-eutropic ammonium salt, which has been throughout shown in previous memoirs to be so close to that of the analogous rubidium salt that almost perfect isostructure—identity of unit-cell shape and size—has been proved. The true isomorphism of these thallium salts with those containing the three most closely allied alkali metals (family-group and even series analogues) and ammonium is perhaps best of all proved by this fact, that for all morphological and optical (other than refraction) properties and constants its position is not an extreme one, but one not far removed from that of the middle member of the group of three eutropic salts, the values never being below those of the potassium salt nor above those of the caesium salt.

One further fact is shown by these thallium salts, in common with the salts of any other individual R-base when studied by themselves, namely, the astonishingly small effect on the crystal characters and constants of change of the M-metal. Attention has been called to this in many previous memoirs during this long investigation, and it is a fact which never fails to be impressive in view of the relatively great changes invoked by interchange of the alkali metals. It is to be expected that further work on the structure of the atoms of the metals, and the possible X-ray analysis of the crystals themselves, will tend to elucidate the mystery and furnish a reason for this striking fact.

The Hexahydrated Double Selenates containing Thallium Completion of the Thallium Salts and of the whole Monoclinic Series

By A E H TUTTON, D Sc, M A, F R S, Past-President of the Mineralogical Society

(Received February 2, 1928)

The introduction to the preceding memoir (p 367) applies equally to this paper, in which are described the six double selenates containing thallium as the R-metal and magnesium, ferrous iron, nickel, cobalt, manganese, and copper as the M-metal respectively. The optical and volume properties and constants of the zinc-thallium selenate are also included, as these were not determinable with the crystals described in 1909,* while lately the author has obtained quite excellent crystals of this salt suitable for all purposes.

While this work has been in progress a paper by L C LINDSLEY and L M DENNIS has appeared,† concerning five of these thallium double selenates, those in which the M-metal is copper, cobalt, nickel, magnesium, and manganese, which they consider to have made for the first time. This is, of course, an error, as all of them were made by the author previous to 1909, as will be clear from p 367 of the preceding paper, but, as there stated, the crystals obtained were not of adequate perfection for complete goniometrical, optical and density measurements and determinations. Lindsley and Dennis, however, only give measurements of two angles, and these are supplementary to each other, being the acute and obtuse angles of the primary prism $p\{110\}$. They give no optical or other physical data. They found in the case of each salt an increase of about $40'$ in the acute angle of the prism, and a like amount of diminution of the supplementary obtuse angle, compared with the corresponding angle on the crystals of the analogous double sulphate.

The iron salt, $\text{Tl}_2\text{Fe}(\text{SeO}_4)_2 \cdot 6\text{H}_2\text{O}$, does not appear to have been previously obtained by anyone, doubtless for the same reason as was pointed out by the author in a special communication‡ on the interaction of iron and selenic acid. For iron does not react with selenic acid as it does with sulphuric acid, but reduces it (doubtless through the nascent hydrogen first formed) immediately to elementary selenium, which is deposited as a red precipitate. But a satis-

* 'Roy Soc Proc,' A, vol 83, pp 216-218 (1909)

† 'Journ Amer Chem Soc,' vol. 47, p 377 (1925)

‡ 'Roy Soc Proc,' A, vol 94, p 352 (1918)

factory method of obtaining pure ferrous selenate was eventually discovered by the author, consisting in the use of pure ferrous sulphide instead of metallic iron, dilute selenic acid decomposes it like dilute sulphuric acid, with liberation of hydrogen sulphide, which is not sufficiently powerful a reducing agent to decompose selenic acid, yet is efficient enough to prevent any oxidation of the ferrous selenate to ferric during the warming caused by the heat of reaction. The ferrous selenate may be obtained in good crystals by evaporating the filtered liquid under reduced pressure, over oil of vitriol under the receiver of an air pump. Thallium ferrous selenate has been obtained in excellent crystals by mixing cold solutions of these crystals and of thallium selenate crystals, and evaporating likewise to the crystallisation point under much reduced pressure and at a fairly low temperature, using excess of ferrous selenate over and above that required for equivalent molecular proportions.

One outstanding fact is, indeed, noticeable with regard to the formation of all these thallium double salts, both sulphates and selenates, namely, that the deposition of the double salt crystals only occurs when there is considerable excess of the M-salt present. From solutions containing equal molecular proportions of the thallium R-salt and of the M-salt, thallium sulphate or selenate usually first crystallises out, even two or three nights (crops in succession being obtained of them), and it is only when the M-salt has been thereby rendered in considerable excess that one at length obtains a crop of the double salt crystals. This fact is probably connected with the low solubility of thallium sulphate and selenate, and as the selenate is the less soluble of the two the phenomenon is accentuated in the preparation of the thallium double selenates. Another difficulty caused by this slight solubility of the thallium simple salts is that one can only start with such very dilute solutions as are alone possible with those salts, rendering the process of further evaporation to the crystallising point of the double salt a lengthy business, often of many days or even weeks. Especially is this so in the case of the preparation of thallium ferrous sulphate or selenate, as no warming to accelerate evaporation is possible, for even gentle warming causes rapid oxidation to the ferric salt, and instead of the desired hexahydric monoclinic salt octahedral crystals of thallium ferric alum $\text{TlFe}(\text{SO}_4)_2 \cdot 12\text{H}_2\text{O}$ or the corresponding selenic alum are deposited, from a brown turbid liquid.

Thallium Magnesium Selenate, $\text{Tl}_2\text{Mg}(\text{SeO}_4)_2 \cdot 6\text{H}_2\text{O}$

Morphology

Eleven good little crystals were used for the goniometry, selected from five crops of outstanding excellence.

Crystal System Monoclinic (Class No 5 holohedral-prismatic)

Ratios of Axes $a : b : c = 0.7185 : 1 : 0.4993$

Axial Angle $\beta = 105^\circ 36'$

Forms observed $b\{010\}$, $c\{001\}$, $p\{110\}$, $q\{011\}$, $r'\{201\}$, $n'\{111\}$, and $n''\{121\}$

The last-mentioned form was represented sometimes by quite large faces

Cleavage — Parallel $r'\{201\}$, the cleavage direction common to the whole series

Habit — Short prismatic to more or less tabular parallel to the basal plane $c\{001\}$. A typical crystal is portrayed in fig. 1

Morphological Angles The accompanying table represents the results of the goniometry (p. 396)

The Average Angular Difference between this salt and the corresponding potassium magnesium selenate, that is the mean of all the differences in interfacial angles brought about by replacing potassium by thallium is $31'$

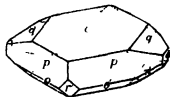


FIG. 1 — Tl Mg Selenate

The Maximum Angular Difference, which happens to occur for the principal angle, the monoclinic axial angle β , namely, $ac = (100) : (001)$, is $1^\circ 18'$

The difference in the four main angles, occasioned by replacing sulphur by selenium, that is, between thallium magnesium sulphate and selenate, is as follows. For $ac = (100) : (001)$, $54'$ for $pp = (110) : (1\bar{1}0)$, $32'$ for $eq = (001) : (011)$, $1'$ and for $cp = (001) : (110)$, $46'$. All these changes are in the direction of increase of the angle, on changing sulphur for selenium.

Volume

Relative Density The mean of two excellent determinations gave as the accepted value of the specific gravity 3.721 for the author's standard temperature of $20^\circ/4^\circ$

$$\text{Molecular Volume} = \frac{M}{d} = \frac{820.90}{3.721} = 220.61$$

$$\text{Topic Axial Ratios} \quad \rho : \psi : \omega = 6.3580 : 8.4943 : 4.2412$$

Interfacial Angles of Thallium Magnesium Selenate

Angle	No of measure- ments	Limits	Mean observed	Calcu- lated	Diff
$ac = (100) (001)$	--	--	--	74 24	--
$as = (100) (101)$	--	--	--	45 49	--
$ar = (101) (001)$	--	--	--	28 35	--
$cr = (001) (201)$	7	63 22-63 39	63 27	63 30	J
$ca' = (001) (101)$	--	--	--	38 5	--
$sr' = (101) (201)$	--	--	--	25 25	--
$ra = (201) (100)$	--	--	--	42 6	--
$rc = (201) (001)$	6	116 21-116 55	116 34	116 30	4
$ap = (100) (110)$	--	--	--	35 47	--
$pp' = (110) (120)$	--	--	--	19 28	--
$ph = (120) (010)$	--	--	--	34 45	--
$pb = (110) (010)$	24	53 58-54 37	54 14	54 13	1
$pp = (110) (110)$	26	71 16-71 52	71 34	*	--
$pp = (110) (110)$	24	108 6-108 41	108 25	108 26	1
$cq = (001) (011)$	38	25 16-25 58	25 41	*	--
$qb = (011) (010)$	20	64 9-64 50	64 22	64 19	3
$qq = (011) (011)$	12	128 15-128 56	128 39	128 38	1
$ao = (100) (111)$	--	--	--	48 59	--
$oq = (111) (011)$	--	--	--	27 0	--
$aq = (100) (011)$	--	--	--	75 59	--
$qa' = (011) (111)$	--	--	--	34 19	--
$oa = (111) (100)$	--	--	--	69 42	--
$co = (001) (111)$	--	--	--	34 15	--
$op = (111) (110)$	--	--	--	43 9	--
$cp = (001) (110)$	42	77 7-77 47	77 24	*	--
$po' = (110) (111)$	4	58 7-58 32	58 15	58 14	1
$o'c = (111) (001)$	4	43 58-44 37	44 19	44 22	1
$pc = (110) (001)$	42	102 11-102 58	102 35	102 36	1
$bo = (010) (111)$	--	--	--	70 18	--
$os = (111) (101)$	--	--	--	19 42	--
$bo = (010) (111)$	1	--	65 13	65 14	1
$bn' = (010) (121)$	--	--	--	47 18	--
$n'o' = (121) (111)$	--	--	--	17 56	--
$o's' = (111) (101)$	--	--	--	24 46	--
$o'o' = (111) (111)$	1	--	49 37	49 32	5
$sq = (101) (011)$	--	--	--	37 42	--
$qp = (011) (110)$	20	86 10-87 7	86 45	86 44	1
$qn' = (011) (121)$	6	35 3-35 41	35 21	35 23	2
$n'p = (121) (110)$	6	51 15-51 48	51 26	51 21	5
$ps = (110) (101)$	--	--	--	55 34	--
$pq = (110) (011)$	24	92 55-93 37	93 13	93 16	3
$sq = (101) (011)$	--	--	--	44 49	--
$qp = (011) (110)$	17	63 4-63 38	63 19	63 15	4
$ps' = (110) (101)$	--	--	--	71 56	--
$pq = (110) (011)$	17	116 24-116 55	116 41	116 45	4
$r'o' = (201) (111)$	1	--	34 49	34 54	5
$o'p = (111) (110)$	1	--	92 12	92 7	5
$pr' = (110) (201)$	6	52 53-53 9	53 3	52 59	4
$r'p = (201) (110)$	3	126 40-127 7	126 56	127 1	5
Total number of measure- ments	352				

Optics

Orientation of Optical Ellipsoid—The optic axes lie in the symmetry plane $b\{010\}$. The double refraction is negative. The first median line, the α -axis of the indicatrix ellipsoid, corresponding to the α -index of refraction, lies $20^\circ 3'$ above the crystal-axis a , in the obtuse crystal-axial angle ac , the second median line, the γ -index and axis, is for sodium light $4^\circ 27'$ behind the vertical crystal-axis c , in the acute crystal-axial angle ac . The β -axis is the symmetry axis b .

Refractive Indices—The 60° -prism observations afforded the following results

Light	α	β	γ
Li	1.6205	1.6292	1.6359
C	1.6210	1.6297	1.6364
Na	1.6250	1.6377	1.6404
Tl	1.6297	1.6384	1.6451
Cd	1.6326	1.6414	1.6482
P	1.6363	1.6452	1.6521

$$\text{Mean index for Na light, } \frac{\alpha + \beta + \gamma}{3} = 1.6330$$

$$\text{Double refraction Na}_{\gamma-\alpha} = 0.0154$$

General formula for the intermediate index β , corrected to a vacuum —

$$\beta = 1.6162 + \frac{504.123}{\lambda^2} + \frac{4.071.000.000.000}{\lambda^4} +$$

The α -indices are closely reproduced if the constant 1.6162 be diminished by 0.0087, and the γ -indices if the constant be increased by 0.0067.

Axial Ratios of the Optical Ellipsoid (Indicatrix) —

$$\alpha : \beta : \gamma = 0.9947 : 1 : 1.0041$$

Molecular Optical Constants—The values of these constants for the red hydrogen ray C are given in the next table

	α	β	γ
Specific refraction $\left. \begin{array}{l} \frac{n^2 - 1}{(n^2 + 2)d} \end{array} \right\}$	0.0945	0.0956	0.0964
Molecular refraction (Lorenz) $\left. \begin{array}{l} \frac{n^2 - 1}{n^2 + 2} \frac{M}{d} \end{array} \right\}$	77.59	78.47	79.13
Molecular refraction (Gladstone) $\left. \begin{array}{l} \frac{n - 1}{d} M \end{array} \right\}$	137.00	138.92	140.40

$$\text{Mean molecular refraction (Gladstone), } \frac{\alpha + \beta + \gamma}{3} = 138.77$$

Optical Axial Angle The following are the values of the true optic axial angle within the crystal, $2V_a$, obtained as the mean of several closely agreeing results. The apparent angle in air, $2E$, was so large that it was not quite completely visible through the section-plates perpendicular to the acute bisectrix.

Light	$2V_a$	Light	$2V_a$
Li	77 17	Th	77 50
C	77 20	Cl	77 58
Na	77 33	F	78 10

Dispersion of the Median Lines The dispersion of the two median lines in the symmetry plane is such that the first median line lies nearer to the crystal-axis a by $18'$ for green thallium light than for red C-hydrogen light. The plate in each case was immersed first in carbon bisulphide and afterwards in monobromonaphthalene, two liquids which possess refractive indices respectively slightly lower and higher than the crystals. The indications in the two liquids were identical to within $2'$.

Thallium Zinc Selenate, $\text{Th}_2\text{Zn}(\text{SeO}_4)_2 \cdot 6\text{H}_2\text{O}$

Morphology

This was dealt with in the 1909 memoir (*loc. cit.*)

Volume

Relative Density—The accepted mean value of three good determinations of the specific gravity at $20^\circ/4^\circ$ is 3.958.

$$\text{Molecular Volume} = \frac{M}{d} = \frac{861.62}{3.958} = 217.69$$

$$\text{Topic Axial Ratios } \chi : \psi : \omega = 6.3173 : 8.4468 : 4.2420$$

Optics

Orientation of Optical Ellipsoid (Indicatrix)—The plane of the optic axes is the symmetry plane $b\{010\}$. The sign of the double refraction is negative. The maximum axis γ of the indicatrix, corresponding to (direction of vibration for) the γ -index of refraction, lies $6^\circ 46'$ behind the vertical crystal-axis c , in the acute axial angle ac (which is $74^\circ 6'$), it is the second median line (obtuse bisectrix) of the optic axial angle. The minimum axis α of the indicatrix, the direction of vibration for the α -index of refraction and the acute bisectrix (first median line) of the optic axial angle, lies $22^\circ 40'$ above the crystal-axis a in the obtuse axial angle ac .

The β -index of refraction has the symmetry axis b for its vibration direction
Refractive Indices—These are set out in the accompanying table

Light	α	β	γ
Li	1.6352	1.6475	1.6549
C	1.6358	1.6481	1.6555
Na	1.6414	1.6549	1.6615
Fl	1.6479	1.6606	1.6687
Cl	1.6520	1.6648	1.6731
F	1.6576	1.6700	1.6793

$$\text{Mean index for Na light } \frac{\alpha + \beta + \gamma}{3} = 1.6523$$

$$\text{Double refraction } \Delta n_{\gamma\alpha} = 0.0201$$

General formula for the intermediate index β for any wave-length λ corrected to a vacuum —

$$\beta = 1.6271 + \frac{825.988}{\lambda^2} + \frac{4.108.100.000.000}{\lambda^4} +$$

The α -indices are also approximately reproduced if the constant 1.6271 be diminished by 0.0125, and the γ -indices if it be increased by 0.0076

Axial Ratios of Optical Ellipsoid (Indices) α —

$$\alpha : \beta : \gamma = 0.9924 : 1 : 1.0046$$

Molecular Optical Constants—These are given below for the red hydrogen ray C —

	α	β	γ
Specific refraction $\frac{n^2 - 1}{(n^2 + 2)d}$	0.0905	0.0919	0.0928
Molecular refraction (Lorenz) $\frac{n^2 - 1}{n^2 + 2} \frac{M}{d}$	78.02	79.22	79.93
Molecular refraction (Gladstone) $\frac{n - 1}{d} M$	138.41	141.08	142.70

$$\text{Mean molecular refraction (Gladstone), } \frac{\alpha + \beta + \gamma}{3} = 140.73$$

Optic Axial Angle—The following values, the mean of several closely agreeing

values from different crystals, were obtained for the optic axial angle in air, $2E$, and for the true angle within the crystal, $2V_a$.

Light	$2E$		$2V_a$	
	°	'	°	'
Li	120	15	68	12
C	120	19	68	15
Na	120	47	68	34
Tl	121	18	69	1
Cd	121	28	69	14
F	121	50	69	30

Dispersion of the Median Lines—The median lines are so dispersed in the symmetry plane, that the first median line lies nearer to the axis a by $30'$ (mean of two determinations with different crystals, affording respectively $33'$ and $27'$) for green thallium light, than it does for red C-hydrogen light. The observations were made with the crystal in each case successively immersed in carbon bisulphide and monobromonaphthalene, the refractive indices of which liquids are very slightly lower than, and higher than, those of the crystals, the indications in the two liquids were identical within 2 minutes.

Thallium Nickel Selenate, $\text{Ti}_2\text{Ni}(\text{SeO}_4)_2 \cdot 6\text{H}_2\text{O}$

Morphology

Twelve crystals from four crops were used for the crystal-angle measurements. The crystals of this salt are coloured bright green.

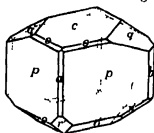


FIG. 2.— Ti Ni Selenate

Crystal System—Monoclinic. Class No 5, holohedral-prismatic.

Ratios of Axes— $a : b : c = 0.7456 : 1 : 0.5019$

Axial Angle— $\beta = 105^\circ 36'$

Forms Observed— $a\{100\}$, $b\{010\}$, $c\{001\}$, $p\{110\}$, $p'\{120\}$, $q\{011\}$, $r'\{201\}$, $o\{111\}$, $o'\{1\bar{1}1\}$, $n'\{121\}$

Cleavage—The cleavage direction is parallel $r'\{201\}$, as usual in this series.

Habit—The most typical habit is illustrated in fig. 2.

Interfacial Angles of Thalium Nickel Selenate

Angle	No of measurements	Limits	Mean observed	Calculated	Diff
$\left\{ \begin{array}{l} ac = (100) (001) \\ as = (100) (101) \\ ac = (101) (001) \\ cr' = (001) (201) \\ cs' = (001) (101) \\ sr' = (101) (201) \\ r'a = (201) (100) \\ r'c = (201) (001) \end{array} \right.$	$\left\{ \begin{array}{l} 3 \\ - \\ - \\ 13 \\ - \\ - \\ 1 \\ 12 \end{array} \right.$	$\left\{ \begin{array}{l} 74 \ 23-74 \ 32 \\ - \\ - \\ 63 \ 49-64 \ 10 \\ - \\ - \\ 41 \ 37-41 \ 44 \\ 115 \ 49-116 \ 26 \end{array} \right.$	$\left\{ \begin{array}{l} 74 \ 27 \\ - \\ - \\ 63 \ 54 \\ - \\ - \\ 41 \ 41 \\ 116 \ 7 \end{array} \right.$	$\left\{ \begin{array}{l} 74 \ 24 \\ 45 \ 38 \\ 28 \ 46 \\ 63 \ 49 \\ 38 \ 22 \\ 25 \ 27 \\ 11 \ 47 \\ 116 \ 11 \end{array} \right.$	$\left\{ \begin{array}{l} 3 \\ - \\ - \\ 5 \\ - \\ - \\ 6 \\ 4 \end{array} \right.$
$\left\{ \begin{array}{l} ap = (100) (110) \\ pp' = (110) (120) \\ p'b = (120) (010) \\ pb = (110) (010) \\ pp = (110) (110) \\ pp = (110) (110) \end{array} \right.$	$\left\{ \begin{array}{l} 3 \\ 2 \\ 1 \\ 10 \\ 26 \\ 21 \end{array} \right.$	$\left\{ \begin{array}{l} 35 \ 32-35 \ 56 \\ 19 \ 20-19 \ 28 \\ - \\ 54 \ 6-54 \ 32 \\ 71 \ 3-71 \ 48 \\ 108 \ 19-108 \ 50 \end{array} \right.$	$\left\{ \begin{array}{l} 35 \ 43 \\ 19 \ 24 \\ 34 \ 51 \\ 54 \ 17 \\ 71 \ 26 \\ 108 \ 34 \end{array} \right.$	$\left\{ \begin{array}{l} 35 \ 43 \\ 19 \ 24 \\ 34 \ 49 \\ 54 \ 17 \\ * \\ 108 \ 34 \end{array} \right.$	$\left\{ \begin{array}{l} 0 \\ 1 \\ 2 \\ 0 \\ - \\ 0 \end{array} \right.$
$\left\{ \begin{array}{l} cq = (001) (011) \\ qb = (011) (010) \\ qq = (011) (011) \end{array} \right.$	$\left\{ \begin{array}{l} 48 \\ 12 \\ 22 \end{array} \right.$	$\left\{ \begin{array}{l} 25 \ 11-26 \ 10 \\ 63 \ 50-64 \ 20 \\ 128 \ 3-128 \ 46 \end{array} \right.$	$\left\{ \begin{array}{l} 25 \ 48 \\ 64 \ 9 \\ 128 \ 24 \end{array} \right.$	$\left\{ \begin{array}{l} * \\ 64 \ 12 \\ 128 \ 24 \end{array} \right.$	$\left\{ \begin{array}{l} - \\ 1 \\ 0 \end{array} \right.$
$\left\{ \begin{array}{l} ao = (100) (111) \\ oq = (111) (011) \\ aq = (100) (011) \\ go' = (011) (111) \\ o'a = (111) (100) \end{array} \right.$	$\left\{ \begin{array}{l} - \\ - \\ - \\ - \\ - \end{array} \right.$	$\left\{ \begin{array}{l} - \\ - \\ - \\ - \\ - \end{array} \right.$	$\left\{ \begin{array}{l} - \\ - \\ - \\ - \\ - \end{array} \right.$	$\left\{ \begin{array}{l} 48 \ 50 \\ 27 \ 9 \\ 75 \ 59 \\ 34 \ 32 \\ 69 \ 29 \end{array} \right.$	$\left\{ \begin{array}{l} - \\ - \\ - \\ - \\ - \end{array} \right.$
$\left\{ \begin{array}{l} co = (001) (111) \\ op = (111) (110) \\ cp = (001) (110) \\ po' = (110) (111) \\ o'c = (111) (001) \\ pc = (110) (001) \end{array} \right.$	$\left\{ \begin{array}{l} 2 \\ 2 \\ 45 \\ 7 \\ 5 \\ 44 \end{array} \right.$	$\left\{ \begin{array}{l} 34 \ 0-34 \ 33 \\ 42 \ 41-43 \ 21 \\ 77 \ 5-77 \ 44 \\ 57 \ 41-58 \ 21 \\ 44 \ 25-44 \ 55 \\ 102 \ 14-103 \ 5 \end{array} \right.$	$\left\{ \begin{array}{l} 34 \ 21 \\ 43 \ 1 \\ 77 \ 23 \\ 58 \ 2 \\ 44 \ 35 \\ 102 \ 37 \end{array} \right.$	$\left\{ \begin{array}{l} 34 \ 24 \\ 42 \ 59 \\ * \\ 58 \ 1 \\ 44 \ 36 \\ 102 \ 37 \end{array} \right.$	$\left\{ \begin{array}{l} 1 \\ 2 \\ - \\ 1 \\ 1 \\ 0 \end{array} \right.$
$\left\{ \begin{array}{l} bo = (010) (111) \\ os = (111) (101) \\ oo = (111) (111) \end{array} \right.$	$\left\{ \begin{array}{l} 4 \\ - \\ 1 \end{array} \right.$	$\left\{ \begin{array}{l} 70 \ 0-70 \ 27 \\ - \\ - \end{array} \right.$	$\left\{ \begin{array}{l} 70 \ 14 \\ - \\ 39 \ 33 \end{array} \right.$	$\left\{ \begin{array}{l} 70 \ 16 \\ 19 \ 44 \\ 39 \ 28 \end{array} \right.$	$\left\{ \begin{array}{l} 2 \\ - \\ 5 \end{array} \right.$
$\left\{ \begin{array}{l} bo' = (010) (111) \\ bn' = (010) (121) \\ n'o' = (121) (111) \\ o's' = (111) (101) \\ o'o' = (111) (111) \end{array} \right.$	$\left\{ \begin{array}{l} 2 \\ 1 \\ 1 \\ - \\ 1 \end{array} \right.$	$\left\{ \begin{array}{l} 65 \ 6-65 \ 10 \\ - \\ - \\ - \\ - \end{array} \right.$	$\left\{ \begin{array}{l} 65 \ 8 \\ 47 \ 16 \\ 17 \ 54 \\ - \\ 49 \ 36 \end{array} \right.$	$\left\{ \begin{array}{l} 65 \ 10 \\ 47 \ 13 \\ 17 \ 57 \\ 24 \ 50 \\ 49 \ 40 \end{array} \right.$	$\left\{ \begin{array}{l} 2 \\ 1 \\ 3 \\ - \\ 1 \end{array} \right.$
$\left\{ \begin{array}{l} ag = (101) (011) \\ gp = (011) (110) \\ gn' = (011) (121) \\ n'p = (121) (110) \\ ps = (110) (101) \\ pq = (110) (011) \end{array} \right.$	$\left\{ \begin{array}{l} - \\ 28 \\ 6 \\ 4 \\ - \\ 20 \end{array} \right.$	$\left\{ \begin{array}{l} - \\ 86 \ 32-86 \ 59 \\ 35 \ 19-35 \ 55 \\ 51 \ 0-51 \ 24 \\ - \\ 93 \ 1-93 \ 27 \end{array} \right.$	$\left\{ \begin{array}{l} - \\ 86 \ 47 \\ 35 \ 30 \\ 51 \ 15 \\ - \\ 93 \ 14 \end{array} \right.$	$\left\{ \begin{array}{l} 37 \ 54 \\ 86 \ 42 \\ 35 \ 32 \\ 51 \ 10 \\ 55 \ 24 \\ 93 \ 18 \end{array} \right.$	$\left\{ \begin{array}{l} - \\ 5 \\ 2 \\ 5 \\ - \\ 4 \end{array} \right.$
$\left\{ \begin{array}{l} s'q = (101) (011) \\ qp = (011) (110) \\ ps = (110) (101) \\ pq = (110) (011) \end{array} \right.$	$\left\{ \begin{array}{l} - \\ 29 \\ - \\ 30 \end{array} \right.$	$\left\{ \begin{array}{l} - \\ 63 \ 7-63 \ 24 \\ - \\ 116 \ 27-116 \ 56 \end{array} \right.$	$\left\{ \begin{array}{l} - \\ 63 \ 14 \\ - \\ 116 \ 45 \end{array} \right.$	$\left\{ \begin{array}{l} 45 \ 6 \\ 63 \ 12 \\ 71 \ 42 \\ 116 \ 48 \end{array} \right.$	$\left\{ \begin{array}{l} - \\ 2 \\ - \\ 3 \end{array} \right.$
$\left\{ \begin{array}{l} r'o' = (201) (111) \\ o'p = (111) (110) \\ pr' = (110) (201) \end{array} \right.$	$\left\{ \begin{array}{l} 3 \\ 5 \\ 16 \end{array} \right.$	$\left\{ \begin{array}{l} 34 \ 52-35 \ 8 \\ 91 \ 45-92 \ 34 \\ 52 \ 29-52 \ 57 \end{array} \right.$	$\left\{ \begin{array}{l} 35 \ 0 \\ 92 \ 14 \\ 52 \ 41 \end{array} \right.$	$\left\{ \begin{array}{l} 34 \ 58 \\ 92 \ 17 \\ 52 \ 45 \end{array} \right.$	$\left\{ \begin{array}{l} 2 \\ 3 \\ 4 \end{array} \right.$
Total number of measurements		441			

Morphological Angles The results of the interfacial angular measurements are given in the accompanying table (*see p 401*)

The Average Angular Difference between this salt and its potassium analogue K-Ni-selenate, is 28', and the Maximum Angular Difference, which occurs for the angle $ac = (100) (001)$, the monoclinic axial angle, is $1^{\circ} 9'$. These represent the characteristic differences in the crystal angles brought about by the replacement of potassium by thallium. The replacement of sulphur by selenium causes the following changes in the main interfacial angles (the differences between Tl-Ni-sulphate and selenate for $ac = (100) (001)$, 48' for $pp = (110) (1\bar{1}0)$, 38' for $cq = (001) (011)$ 11' and for $cp = (001) (110)$ 41' all are increases of angle on passing from the sulphate to the selenate

Volume

Relative Density - The mean of four trustworthy determinations gave for the accepted value of the specific gravity at $20^{\circ}/4^{\circ}$, 3.993

$$\text{Molecular Volume} = \frac{M}{d} = \frac{855.02}{3.993} = 214.13$$

$$\text{Topic Axial Ratios} - \gamma : \psi : c = 0.2680 : 8.4066 : 4.2193$$

Optics

Orientation of Optical Ellipsoid - The optic axes lie in the symmetry plane $b(010)$, and the sign of the double refraction is negative. The γ -axis of the ellipsoid (vibration direction of γ -index of refraction), the obtuse bisectrix (second median line) of the optic axial angle, lies $10^{\circ} 19'$ behind the vertical crystal-axis c , the α -axis of the ellipsoid the acute bisectrix (first median line) lies $25^{\circ} 55'$ above the crystal-axis a , in the obtuse angle ac of the crystal axes

Refractive Indices - The results of 60°-prism observations are as under

Light	α	β	γ
Li	1.6334	1.6464	1.6512
C	1.6339	1.6459	1.6517
Na	1.6378	1.6498	1.6560
Tl	1.6443	1.6563	1.6626
Cd	1.6490	1.6600	1.6666
P	1.6523	1.6643	1.6709

$$\text{Mean index} = \frac{\alpha + \beta + \gamma}{3} \text{ for Na light} = 1.6479$$

$$\text{Double refraction, Na-}\gamma - \alpha = 0.0182$$

The vibration-directions of α and γ are as given in the previous section. The vibration direction of β is the symmetry axis b .

General formula for the intermediate index β , corrected to a vacuum

$$\beta = 1.6504 - \frac{882.386}{\lambda^2} + \frac{30.390800(000.000)}{\lambda^4}$$

The α -indices are closely reproduced if the constant 1.6504 is diminished by 0.0120, and the γ -indices if it be increased by 0.0062.

Axial Ratios of Optical Ellipsoid (Indices α, β, γ)

$$\alpha : \beta : \gamma = 0.9927 : 1 : 1.0037$$

Molecular Optical Constants The following are the values of these constants for the red C-ray of hydrogen

	α	β	γ
Specific refraction $\frac{n^2 - 1}{(n^2 + 2)d}$	0.0895	0.0909	0.0915
Molecular refraction (Lorenz) $\frac{n^2 - 1}{n^2 + 2} \frac{M}{d}$	76.56	77.71	78.26
Molecular refraction (Gladstone) $\frac{n - 1}{d} M$	135.74	138.31	139.55

Mean molecular refraction (Gladstone), $\frac{\alpha + \beta + \gamma}{3} = 137.87$

Optic Axial Angle The following are the results of the measurements of $2E$, the angle in air, and of $2V_a$, the true optic axial angle within the crystal. The observations with the usual ground plates, immersed in monobromonaphthalene were confirmed as regards $2V_a$ by measurements also in carbon bisulphide. For the very high refractive index of the crystals happens to be intermediate between, and very close to, the indices of these two highly refractive liquids. The values as determined in the two liquids were almost identical, being only a few minutes apart.

Light	$2E$ °	$2V_a$ °
Li	107.24	58.5
C	107.31	58.10
Na	109.20	58.59
Tl	112.3	59.51
Cl	114.10	60.17
F	115.38	60.53

Dispersion of the Median Lines—This is such that the first median line lies about 35' nearer to the crystal-axis a for thallium green light than for red C-hydrogen light. This was rendered quite clear as the result of the measurements in carbon bisulphide and monobromonaphthalene.

Thallium Cobalt Selenate, $\text{Ti}_2\text{Co}(\text{SeO}_4)_2 \cdot 6\text{H}_2\text{O}$

Morphology

Eleven good little crystals were used for the goniometry, selected from five crops of outstanding excellence. The crystals of this salt are ruby red in colour.

Crystal System—Monoclinic. Class No 5, holohedral-prismatic.

Ratios of Axes— $a : b : c = 0.7463 : 1 : 0.5021$

Axial Angle— $\beta = 105^\circ 40'$

Forms Observed— $a\{100\}$, $b\{010\}$, $c\{001\}$, $p\{110\}$, $p'\{120\}$, $q\{011\}$, $r\{201\}$, $o\{111\}$, $o'\{1\bar{1}1\}$, and $n'\{121\}$. There is a good cleavage parallel $r\{201\}$.

Habit—The most typical habit is illustrated in fig. 3.

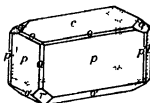


FIG. 3— Ti Co Selenate

Morphological Angles—These are given in the accompanying table (p. 405).

The Average Angular Change occurring on the replacement of potassium by thallium, that is on passing from potassium cobalt selenate to thallium cobalt selenate, is $34'$. The maximum change is $1^\circ 23'$, and it occurs for the principal angle, the monoclinic axial angle β [$ac = (100) (001)$].

The angular change on replacing sulphur by selenium, in the case of the four main angles, is as follows. For $ac = (100) (001)$, $45'$, for $pp = (110) (1\bar{1}0)$, $31'$, for $oq = (001) (011)$, $12'$, and for $cp = (001) (110)$, $39'$.

Volume

Relative Density—The mean of two excellent determinations gave as the accepted density at $20^\circ/4^\circ$ the value 3.998.

$$\text{Molecular Volume} = \frac{M}{d} = \frac{855.27}{3.998} = 213.92$$

Topic Axial Ratios— $\chi : \psi : \omega = 6.2696 : 8.4010 : 4.2181$

Interfacial Angles of Thallium Cobalt Selenate

Angle	No of measure ments	Limits	Mean observed	Calcu lated	Diff
$ac = (100) (001)$	—	—	—	74 20	—
$as = (100) (101)$	—	—	—	45 36	—
$ac = (101) (001)$	—	—	—	28 44	—
$cr' = (001) (201)$	2	63 42- 63 57	63 50	63 50	0
$ca' = (001) (101)$	—	—	—	38 22	—
$a'r' = (101) (201)$	—	—	—	25 28	—
$ra = (201) (100)$	1	—	41 53	41 50	3
$r'c = (201) (001)$	3	116 3-116 18	116 12	116 10	2
$ap = (100) (110)$	2	35 40- 35 42	35 41	35 41	0
$pp' = (110) (120)$	2	19 26- 19 30	19 28	19 28	0
$p'b = (120) (010)$	2	34 48- 34 52	34 50	34 51	1
$pb = (110) (010)$	6	54 9- 54 30	54 18	54 19	1
$pp = (110) (110)$	25	71 1- 71 38	71 21	*	—
$pp = (110) (110)$	24	108 19-108 58	108 39	108 30	0
$cq = (001) (011)$	36	25 20- 25 59	25 48	*	—
$qb = (011) (010)$	2	64 6- 64 20	64 13	64 12	1
$qq = (011) (011)$	12	128 4-128 38	128 23	128 24	1
$ao = (100) (111)$	—	—	—	48 49	—
$oq = (111) (011)$	—	—	—	27 7	—
$aq = (100) (011)$	—	—	—	75 56	—
$go' = (011) (111)$	—	—	—	34 35	—
$o'a = (111) (100)$	—	—	—	69 20	—
$co = (001) (111)$	1	—	34 22	34 22	0
$op = (111) (110)$	1	—	42 54	42 58	4
$cp = (001) (110)$	44	77 4- 77 48	77 20	*	—
$po = (110) (111)$	8	57 55- 58 16	58 4	58 1	3
$o'r = (111) (001)$	8	44 28- 44 40	44 35	44 39	4
$pr = (110) (001)$	42	102 26-102 56	102 40	102 40	0
$bo = (010) (111)$	—	—	—	70 16	—
$os = (111) (101)$	—	—	—	19 44	—
$oo = (111) (111)$	—	—	—	39 28	—
$bo = (010) (111)$	—	—	—	65 9	—
$bn' = (010) (121)$	—	—	—	47 12	—
$n'o' = (121) (111)$	—	—	—	17 57	—
$o'n' = (111) (101)$	—	—	—	24 51	—
$o'o' = (111) (111)$	—	—	—	49 42	—
$sq = (101) (011)$	—	—	—	37 52	—
$qp = (011) (110)$	22	86 29- 86 58	86 48	86 46	2
$qn' = (011) (121)$	7	35 19- 35 40	35 32	35 33	1
$n'p = (121) (110)$	7	51 7- 51 26	51 17	51 13	4
$ps = (110) (101)$	—	—	—	55 22	—
$pq = (110) (011)$	21	93 0- 93 27	93 10	93 14	4
$s'q = (101) (011)$	—	—	—	45 6	—
$qp = (011) (110)$	22	63 1- 63 24	63 11	63 10	1
$ps' = (110) (101)$	—	—	—	71 44	—
$pq = (110) (011)$	22	116 40-117 4	116 40	116 50	1
$r'o' = (201) (111)$	2	35 0- 35 4	35 2	35 0	2
$o'p = (111) (110)$	2	92 5- 92 20	92 13	92 15	2
$po' = (110) (201)$	2	52 32- 52 50	52 41	52 45	4
Total number of measure ments	328				

Optics

Orientation of Optical Ellipsoid—The plane of the optic axes is the symmetry plane $b\{010\}$, and the double refraction is of negative sign. The first median line, the vibration-direction of the α -index of refraction, lies $24^\circ 2'$ above the inclined crystal axis a , in the obtuse angle of the crystal axes ac , and the second median line, corresponding to the γ -index, is $8^\circ 22'$ behind the vertical axis c , in the acute angle ac . The intermediate axis of the optical ellipsoid (indicatrix), corresponding to the index β , is the symmetry axis b .

Refractive Indices—The results obtained from 60° -prisms are the following

Light	α	β	γ
Ia	1.6397	1.6490	1.6545
C	1.6402	1.6495	1.6550
Na	1.6442	1.6535	1.6590
Tl	1.6485	1.6578	1.6635
Cd	1.6515	1.6608	1.6666
F	1.6552	1.6646	1.6706

$$\text{Mean index for Na light, } \frac{\alpha + \beta + \gamma}{3} = 1.6522$$

$$\text{Double refraction, } Na_{\gamma-\alpha} = 0.0150$$

General formula for the intermediate index β , corrected to a vacuum, is

$$\beta = 1.6322 + \frac{798.284}{\lambda^2} - \frac{1.561300000}{\lambda^4}$$

The α -indices are equally well reproduced if the constant 1.6322 be diminished by 0.0093, and the γ -indices if it be increased by 0.0056.

Axial Ratios of the Optical Ellipsoid (Indicatrix)

$$\alpha : \beta : \gamma = 0.9944 : 1 : 1.0033$$

Molecular Optical Constants—These are as follows for the ray C (the red line of hydrogen, H α)—

	α	β	γ
Specific refraction	0.0901	0.0911	0.0918
$\frac{n^2 - 1}{(n^2 + 2)d}$			
Molecular refraction (Lorenz)			
$\frac{n^2 - 1}{n^2 + 2} \frac{M}{d}$	77.09	77.96	78.50
Molecular refraction (Gladstone)			
$\frac{n - 1}{d} M$			
	136.96	138.94	140.12

$$\text{Mean molecular refraction (Gladstone), } \frac{\alpha + \beta + \gamma}{3} = 138.67$$

Optic Axial Angle—The following are the values of the optic axial angle in air, $2E$, and of the true angle within the crystal, $2V_o$, obtained as the mean of several closely concordant determinations—

Light	$2E$		$2V_o$	
Li	111	4	66	11
C	111	10	66	15
Na	112	30	66	42
Tl	113	40	67	1
Cd	114	25	67	18
F	115	10	67	36

Dispersion of the Median Lines—The dispersion of the two median lines in the symmetry plane, is such that the first median line lies $20'$ nearer to the crystal-axis a for thallium green light than for red C-hydrogen light. Monobromonaphthalene and carbon bisulphide were used in succession as immersion liquids in the determination, their refractive indices being just slightly higher and lower respectively than those of the crystals.

Thallium Ferrous Selenate, $Tl_2Fe(SeO_4)_2 \cdot 6H_2O$

This salt has not hitherto been described, doubtless owing to the difficulty of preparing ferrous selenate. For as described in a previous communication,* when one attempts to prepare it by the action of selenic acid on iron the former is immediately reduced by the nascent hydrogen first formed, a red precipitate of selenium being thrown down. The author found, however as stated in the memoir just referred to, that if one uses ferrous sulphide instead of iron, ferrous selenate is produced, the escaping hydrogen sulphide not being able to reduce selenic acid, while it prevents any oxidation of the ferrous salt to ferric. The ferrous selenate may either be crystallised out or the filtered solution used directly for the preparation of the double salt by adding solution of thallium selenate. The best crystals of the double salt are obtained however by the former method by mixing the aqueous solution of thallium selenate with a solution of the pale green crystals of ferrous selenate. As cold solutions only must be used, owing to the ready oxidation of ferrous salts by warming and thallium selenate is but slightly soluble in water the mixed solution is both

* 'Roy. Soc. Proc., A, vol. 94, p. 352 (1918)

very dilute and may contain considerable excess of ferrous selenate over and above the amount calculated for equivalent molecular proportions. This is no detriment, however, but rather an advantage, for if equivalent amounts are used thallium selenate invariably crystallises out first, and several nightly crops may be deposited before the double salt begins to crystallise. The dilution being considerable and evaporation at the ordinary temperature being essential, it must be accomplished under reduced pressure, under the receiver of an air pump, over a dish of vitriol.

Four good crops of the double selenate were eventually obtained, the first two of which were troubled with partial turbidity, although quite clear in parts, but the third and fourth crops were composed of perfectly transparent, limpid, brilliantly refractive crystals of a pure and very pale green (at first almost colourless) tint, eminently suitable for goniometrical and optical investigation, of a size up to 5 mm. in their longest dimension.

Morphology

Twelve very perfect crystals from the two best developed crops were used for the crystal-angle measurements, the results of which are set out as follows. The crystals were coloured a very pale bluish green when fresh from the mother liquor, but become more yellowish green after a few days.

Crystal System — Monoclinic. Class No 5, holohedral-prismatic.

Ratios of Axes — $a : b : c = 0.7445 : 1 : 0.5011$

Axial Angle — $\beta = 105^\circ 27'$

Forms Observed — $a\{100\}$, $b\{010\}$, $c\{001\}$, $p\{110\}$, $p'\{120\}$ (only traces), $q\{011\}$, $r'\{201\}$, $o'\{111\}$. There is a good cleavage parallel to $r'\{201\}$.

Habit — The third crop referred to was a very beautiful one, largely of crystals 2–3 mm. in diameter, and more or less spherical, although on the whole slightly tabular parallel to the basal pinakoid $c\{001\}$. The fourth crop was composed of a few of the larger crystals already referred to, very suitable for optical work. The faces of both crops were remarkably perfect, affording single brilliant signal-images, even from the forms $c\{001\}$ and $p\{110\}$ which are so usually striated in the salts of this series. The faces of $r'\{201\}$ and $o'\{111\}$ were particularly good, which is again exceptional. The $q\{011\}$ faces were developed to about an equal extent to the $c\{001\}$ faces, as in the rubidium salts of the series. Good and fairly large faces of $a\{100\}$ were common, with smaller but equally good b -faces. No measurable faces of $p'\{120\}$ or $o\{111\}$ were observed on any of the crops.

Interfacial Angles of Thallium Ferrous Selenate

Angle	No of measurements	Limits	Mean observed	Calculated	Diff
$\left\{ \begin{array}{l} ac = (100) (001) \\ ac = (100) (101) \\ ac = (101) (001) \\ cr' = (001) (201) \\ cr' = (001) (101) \\ s'r' = (101) (201) \\ r'a = (201) (100) \\ r'e = (201) (001) \end{array} \right.$	$\left\{ \begin{array}{l} 10 \\ - \\ - \\ 17 \\ - \\ - \\ 12 \\ 12 \end{array} \right.$	$\left\{ \begin{array}{l} 74\ 25-74\ 37 \\ - \\ - \\ 63\ 32-63\ 44 \\ - \\ - \\ 11\ 11\ 41\ 54 \\ 116\ 10-116\ 30 \end{array} \right.$	$\left\{ \begin{array}{l} 74\ 32 \\ - \\ - \\ 63\ 38 \\ - \\ - \\ 41\ 40 \\ 116\ 22 \end{array} \right.$	$\left\{ \begin{array}{l} 74\ 33 \\ 45\ 44 \\ 28\ 49 \\ 63\ 42 \\ 38\ 20 \\ 25\ 22 \\ 41\ 15 \\ 116\ 18 \end{array} \right.$	$\left\{ \begin{array}{l} 1 \\ - \\ - \\ 4 \\ - \\ - \\ 4 \\ 4 \end{array} \right.$
$\left\{ \begin{array}{l} ap = (100) (110) \\ pp = (110) (120) \\ p'b = (120) (010) \\ pb = (110) (010) \\ pp = (110) (110) \\ pp = (110) (110) \end{array} \right.$	$\left\{ \begin{array}{l} 21 \\ - \\ - \\ 22 \\ 16 \\ 16 \end{array} \right.$	$\left\{ \begin{array}{l} 35\ 37-35\ 50 \\ - \\ - \\ 54\ 12\ 54\ 26 \\ 71\ 11-71\ 35 \\ 108\ 25-108\ 50 \end{array} \right.$	$\left\{ \begin{array}{l} 35\ 41 \\ - \\ - \\ 54\ 19 \\ 71\ 24 \\ 108\ 36 \end{array} \right.$	$\left\{ \begin{array}{l} 35\ 41 \\ 19\ 28 \\ 31\ 51 \\ * \\ 71\ 22 \\ 108\ 38 \end{array} \right.$	$\left\{ \begin{array}{l} 0 \\ - \\ - \\ - \\ 2 \\ 2 \end{array} \right.$
$\left\{ \begin{array}{l} qg = (001) (011) \\ qb = (011) (010) \\ qq = (011) (011) \end{array} \right.$	$\left\{ \begin{array}{l} 33 \\ 22 \\ 16 \end{array} \right.$	$\left\{ \begin{array}{l} 25\ 26-25\ 53 \\ 64\ 0-64\ 21 \\ 128\ 15-128\ 47 \end{array} \right.$	$\left\{ \begin{array}{l} 25\ 47 \\ 64\ 13 \\ 128\ 26 \end{array} \right.$	$\left\{ \begin{array}{l} * \\ 64\ 13 \\ 128\ 26 \end{array} \right.$	$\left\{ \begin{array}{l} - \\ 0 \\ 0 \end{array} \right.$
$\left\{ \begin{array}{l} ao = (100) (111) \\ oq = (111) (011) \\ aq = (100) (011) \\ qo' = (011) (111) \\ o'a = (111) (100) \end{array} \right.$	$\left\{ \begin{array}{l} - \\ - \\ 4 \\ 3 \\ 3 \end{array} \right.$	$\left\{ \begin{array}{l} - \\ - \\ 76\ 4-76\ 9 \\ 34\ 31-34\ 36 \\ 69\ 16-69\ 20 \end{array} \right.$	$\left\{ \begin{array}{l} - \\ - \\ 76\ 7 \\ 34\ 34 \\ 69\ 18 \end{array} \right.$	$\left\{ \begin{array}{l} 48\ 56 \\ 27\ 11 \\ 76\ 7 \\ 34\ 32 \\ 69\ 21 \end{array} \right.$	$\left\{ \begin{array}{l} - \\ - \\ 0 \\ 2 \\ 3 \end{array} \right.$
$\left\{ \begin{array}{l} co = (001) (111) \\ op = (111) (110) \\ cp = (001) (110) \\ po' = (110) (111) \\ o'c = (111) (001) \\ pc = (110) (001) \end{array} \right.$	$\left\{ \begin{array}{l} - \\ - \\ 35 \\ 17 \\ 19 \\ 40 \end{array} \right.$	$\left\{ \begin{array}{l} - \\ - \\ 77\ 20-77\ 40 \\ 57\ 50-58\ 7 \\ 44\ 22\ 44\ 42 \\ 102\ 20-103\ 46 \end{array} \right.$	$\left\{ \begin{array}{l} - \\ - \\ 77\ 30 \\ 57\ 54 \\ 44\ 33 \\ 102\ 31 \end{array} \right.$	$\left\{ \begin{array}{l} 34\ 27 \\ 17\ 3 \\ * \\ 57\ 57 \\ 44\ 33 \\ 102\ 30 \end{array} \right.$	$\left\{ \begin{array}{l} - \\ - \\ - \\ 1 \\ 0 \\ 1 \end{array} \right.$
$\left\{ \begin{array}{l} bo = (010) (111) \\ os = (111) (101) \end{array} \right.$	$\left\{ \begin{array}{l} - \\ - \end{array} \right.$	$\left\{ \begin{array}{l} - \\ - \end{array} \right.$	$\left\{ \begin{array}{l} - \\ - \end{array} \right.$	$\left\{ \begin{array}{l} 70\ 15 \\ 19\ 45 \end{array} \right.$	$\left\{ \begin{array}{l} - \\ - \end{array} \right.$
$\left\{ \begin{array}{l} bo' = (010) (111) \\ bn' = (010) (121) \\ n'o' = (121) (111) \\ o's' = (111) (101) \\ o'o' = (111) (111) \end{array} \right.$	$\left\{ \begin{array}{l} 12 \\ 2 \\ 1 \\ - \\ 5 \end{array} \right.$	$\left\{ \begin{array}{l} 65\ 8-65\ 22 \\ 47\ 20-47\ 20 \\ - \\ - \\ 49\ 26-49\ 35 \end{array} \right.$	$\left\{ \begin{array}{l} 65\ 14 \\ 47\ 20 \\ 17\ 53 \\ - \\ 49\ 32 \end{array} \right.$	$\left\{ \begin{array}{l} 65\ 13 \\ 47\ 17 \\ 17\ 56 \\ 24\ 47 \\ 49\ 34 \end{array} \right.$	$\left\{ \begin{array}{l} 1 \\ 3 \\ 3 \\ - \\ 2 \end{array} \right.$
$\left\{ \begin{array}{l} sq = (101) (011) \\ qp = (011) (110) \\ qn' = (011) (121) \\ n'p = (121) (110) \\ ps = (110) (101) \\ pq = (110) (011) \end{array} \right.$	$\left\{ \begin{array}{l} - \\ 18 \\ 10 \\ 10 \\ - \\ 78 \end{array} \right.$	$\left\{ \begin{array}{l} - \\ 86\ 32-87\ 45 \\ 75\ 25-75\ 29 \\ 51\ 4-51\ 11 \\ - \\ 93\ 12-92\ 29 \end{array} \right.$	$\left\{ \begin{array}{l} - \\ 86\ 39 \\ 75\ 27 \\ 51\ 8 \\ - \\ 93\ 21 \end{array} \right.$	$\left\{ \begin{array}{l} 37\ 55 \\ 86\ 37 \\ 35\ 30 \\ 51\ 7 \\ 55\ 28 \\ 93\ 23 \end{array} \right.$	$\left\{ \begin{array}{l} - \\ 2 \\ 3 \\ 1 \\ - \\ 2 \end{array} \right.$
$\left\{ \begin{array}{l} s'q = (101) (011) \\ qp = (011) (110) \\ ps' = (110) (101) \\ pq = (110) (011) \end{array} \right.$	$\left\{ \begin{array}{l} 34 \\ - \\ - \\ 34 \end{array} \right.$	$\left\{ \begin{array}{l} - \\ 63\ 16-63\ 30 \\ - \\ 116\ 26-116\ 51 \end{array} \right.$	$\left\{ \begin{array}{l} - \\ 63\ 22 \\ - \\ 116\ 38 \end{array} \right.$	$\left\{ \begin{array}{l} 45\ 4 \\ 63\ 21 \\ 71\ 35 \\ 116\ 39 \end{array} \right.$	$\left\{ \begin{array}{l} - \\ 1 \\ - \\ 1 \end{array} \right.$
$\left\{ \begin{array}{l} r'o' = (201) (111) \\ o'p = (111) (110) \\ p'o' = (110) (201) \\ r'p = (201) (110) \end{array} \right.$	$\left\{ \begin{array}{l} 20 \\ 20 \\ 35 \\ 34 \end{array} \right.$	$\left\{ \begin{array}{l} 34\ 47-34\ 56 \\ 92\ 16-92\ 27 \\ 52\ 30-52\ 55 \\ 127\ 10-127\ 23 \end{array} \right.$	$\left\{ \begin{array}{l} 34\ 51 \\ 92\ 23 \\ 52\ 45 \\ 127\ 15 \end{array} \right.$	$\left\{ \begin{array}{l} 34\ 53 \\ 92\ 25 \\ 52\ 42 \\ 127\ 18 \end{array} \right.$	$\left\{ \begin{array}{l} 2 \\ 2 \\ 3 \\ 3 \end{array} \right.$
Total number of measurements		613			

A typical crystal of these particularly satisfactory crops is illustrated in fig 4

The crystals of the other two earlier crops, which showed slight turbidity at the periphery, were more tabular, often plates, parallel $c\{001\}$, and they showed relatively very large development of the pyramidal form $n'\{\bar{1}21\}$, the faces of which were often larger than those of the primary prism $p\{110\}$

The average difference (ignoring sign) of interfacial angle between this salt and potassium ferrous selenate (that is, for the replacement of potassium by thallium), the first member of the iron group of the series, is $39'$, and the maximum difference [which occurs for the axial angle ac , $(100) (001)$] is $1^\circ 37'$

The differences in the four main angles between this salt and the corresponding sulphate, thallium ferrous sulphate (that is, for the replacement of sulphur by selenium) are as follows, all being increases of angle For $ac = (100) (001)$,

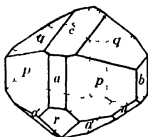


Fig 4 $-Tl Fe Selenate$

$49'$, for $pp = (110) (\bar{1}\bar{1}0)$, $20'$, for $aq = (001) (011)$, $9'$, and for $cp = (001) (110)$, $41'$

Volume

Relative Density—Three concordant determinations afforded the mean value 3.940, for the specific gravity at $20^\circ/4^\circ$

$$\text{Molecular Volume} = \frac{M}{d} = \frac{852.22}{3.940} = 216.30$$

Topic Axial Ratios— $\chi \ \psi \ \omega = 6.2846 \ 8.4415 \ 4.2300$

Optics

Orientation of Optical Ellipsoid—The optic axes lie in the symmetry plane $b\{010\}$. The double refraction is negative. The maximum axis γ of the optical ellipsoid (indicatrix), the vibration-direction for the γ -index of refraction, lies $9^\circ 9'$ behind the vertical crystal-axis c , in the acute axial angle ac (which is $74^\circ 33'$), it is the obtuse bisectrix (second median line) of the optic axial angle

The minimum axis α of the indicatrix, the vibration direction of the α -index and the first median line (acute bisectrix) of the optic axial angle, lies $24^{\circ} 36'$ from the inclined crystal-axis a in the obtuse axial angle ac . The β -indicatrix axis, the vibration direction for the β -index, is the symmetry axis b .

Refractive Indices—Excellent concordant determinations were obtained with several prisms and gave the following mean values—

Light	α	β	γ
Li	1.6291	1.6453	1.6527
C	1.6297	1.6460	1.6533
Na	1.6352	1.6511	1.6589
Tl	1.6415	1.6578	1.6655
Cd	1.6452	1.6617	1.6695
F	1.6496	1.6662	1.6741

Mean index for Na light, $\frac{\alpha + \beta + \gamma}{3} = 1.6485$

Double refraction, $\text{Na}_{\gamma-\alpha} = 0.0237$

General formula for the intermediate index β , for any wave-length λ , corrected to a vacuum (correction $+0.0004$)—

$$\beta = 1.6265 + \frac{745.318}{\lambda^2} - \frac{4.616.300.000.000}{\lambda^4} +$$

The α -indices are also approximately reproduced if the constant 1.6265 is diminished by 0.0162, and the γ -indices if it be increased by 0.0075.

Axial Ratios of Optical Ellipsoid (Indicatrix)—

$$\alpha : \beta : \gamma = 0.9902 : 1 : 1.0045$$

Molecular Optical Constants—These are as follows for the red hydrogen ray C—

	α	β	γ
Specific refraction $\left. \begin{array}{l} \frac{n^2 - 1}{(n^2 + 2)d} \end{array} \right\}$	0.903	0.0921	0.0929
Molecular refraction (Lorenz) $\left. \begin{array}{l} \frac{n^2 - 1}{n^2 + 2} \frac{M}{d} \end{array} \right\}$	76.93	78.50	79.21
Molecular refraction (Gladstone) $\left. \begin{array}{l} \frac{n - 1}{d} M \end{array} \right\}$	136.20	139.71	141.31

Mean molecular refraction (Gladstone), $\frac{\alpha + \beta + \gamma}{3} = 139.07$

Optic Axial Angle—The following values were obtained for the optic axial angle in air, $2E$, and for the true angle within the crystal, $2V_a$. Very concordant, almost identical, values were yielded by the half-dozen different determinations with separate clear crystals

Light	$2E$		$2V_a$	
	°	'	°	'
Li	125	25	69	1
C	125	48	69	5
Na	130	6	69	36
Tl	134	18	70	3
Cl	135	18	70	20
F	140	30	70	45

Dispersion of the Median Lines—The dispersion of the median lines is such that the first median line lies nearer to the axis a by half a degree (individual determinations gave 25–28') for green thallium light than for red C-hydrogen light. Carbon bisulphide and monobromonaphthalene were successively used as immersion liquids, the refractive indices of which are just lower and higher respectively than those of the crystals, the results afforded being identical to within 3'

Thallium Manganese Selenate, $Tl_2Mn(SeO_4)_2 \cdot 6H_2O$

Morphology

Ten good crystals were used for the goniometry, selected from the four best crops



FIG. 5— $Tl Mn Se$ selenate

Crystal System—Monoclinic Class No. 5, holohedral-prismatic

Ratios of Axes— $a : b : c = 0.7463 : 1 : 0.4993$

Axial Angle— $\beta = 105^\circ 29'$

Forms Observed— $a\{100\}$, $b\{010\}$, $c\{001\}$, $p\{110\}$, $p'\{120\}$, $q\{011\}$, $r\{\bar{2}01\}$, $o\{111\}$, $o'\{\bar{1}11\}$, and $n'\{\bar{1}21\}$. There is a good cleavage parallel $r'\{\bar{2}01\}$

Habit—A typical crystal is shown in fig. 5 as regards general habit, but a large proportion of the crops obtained were composed of crystals showing only the faces of $c\{001\}$ and $p\{110\}$ or only mere linear traces of the other forms

Interfacial Angles of Thallium Manganese Selenate

Angle	No of measurements	Limits	Mean observed	Calculated	Diff
$\left\{ \begin{array}{l} ac = (100) (001) \\ as = (100) (101) \\ ac = (101) (001) \\ cr' = (001) (201) \\ cs' = (001) (101) \\ sr' = (101) (201) \\ ra = (201) (100) \end{array} \right.$	$\left\{ \begin{array}{l} 6 \\ - \\ - \\ 14 \\ - \\ - \\ 9 \end{array} \right.$	$\left\{ \begin{array}{l} 74.32-71.36 \\ - \\ - \\ 63.11-63.19 \\ - \\ - \\ 41.40-42.11 \end{array} \right.$	$\left\{ \begin{array}{l} 74.43 \\ - \\ - \\ 63.11 \\ - \\ - \\ 41.56 \end{array} \right.$	$\left\{ \begin{array}{l} 74.31 \\ 43.48 \\ 28.43 \\ 63.33 \\ 38.11 \\ 25.22 \\ 41.56 \end{array} \right.$	$\left\{ \begin{array}{l} 2 \\ - \\ - \\ 2 \\ - \\ - \\ 0 \end{array} \right.$
$\left\{ \begin{array}{l} ap = (100) (110) \\ pp' = (110) (120) \\ p p' = (120) (130) \\ p b = (120) (010) \\ p''b = (130) (010) \\ pb = (110) (010) \\ pp = (110) (110) \\ pp = (110) (110) \end{array} \right.$	$\left\{ \begin{array}{l} 15 \\ 1 \\ - \\ 1 \\ - \\ 1 \\ 20 \\ 20 \end{array} \right.$	$\left\{ \begin{array}{l} 35.12-35.53 \\ - \\ - \\ - \\ - \\ 54.13-54.40 \\ 71.11-71.49 \\ 108.14-108.54 \end{array} \right.$	$\left\{ \begin{array}{l} 35.39 \\ 19.29 \\ - \\ 34.44 \\ - \\ 54.21 \\ 71.25 \\ 108.35 \end{array} \right.$	$\left\{ \begin{array}{l} 35.43 \\ 19.28 \\ 9.57 \\ 34.19 \\ 24.52 \\ 54.17 \\ * \\ 108.3 \end{array} \right.$	$\left\{ \begin{array}{l} 4 \\ 1 \\ - \\ 5 \\ - \\ 4 \\ - \\ 0 \end{array} \right.$
$\left\{ \begin{array}{l} rg = (001) (011) \\ qb = (011) (010) \\ qq = (011) (011) \end{array} \right.$	$\left\{ \begin{array}{l} 30 \\ 7 \\ 10 \end{array} \right.$	$\left\{ \begin{array}{l} 25.20-25.57 \\ 64.12-64.36 \\ 128.20-128.51 \end{array} \right.$	$\left\{ \begin{array}{l} 25.42 \\ 64.22 \\ 128.31 \end{array} \right.$	$\left\{ \begin{array}{l} * \\ 64.18 \\ 128.36 \end{array} \right.$	$\left\{ \begin{array}{l} - \\ 4 \\ 3 \end{array} \right.$
$\left\{ \begin{array}{l} ao = (100) (111) \\ og = (111) (011) \\ ag = (100) (011) \\ go = (011) (111) \\ oa = (111) (100) \end{array} \right.$	$\left\{ \begin{array}{l} - \\ - \\ - \\ - \\ - \end{array} \right.$	$\left\{ \begin{array}{l} - \\ - \\ - \\ - \\ - \end{array} \right.$	$\left\{ \begin{array}{l} - \\ - \\ - \\ - \\ - \end{array} \right.$	$\left\{ \begin{array}{l} 48.50 \\ 27.6 \\ 76.5 \\ 34.21 \\ 69.32 \end{array} \right.$	$\left\{ \begin{array}{l} - \\ - \\ - \\ - \\ - \end{array} \right.$
$\left\{ \begin{array}{l} co = (001) (111) \\ op = (111) (110) \\ cp = (001) (110) \\ po' = (110) (111) \\ oc = (111) (001) \\ pc = (110) (001) \end{array} \right.$	$\left\{ \begin{array}{l} 1 \\ 1 \\ 40 \\ 2 \\ 2 \\ 10 \end{array} \right.$	$\left\{ \begin{array}{l} - \\ - \\ 77.12-77.52 \\ 57.58-58.1 \\ 44.9-44.31 \\ 102.12-102.52 \end{array} \right.$	$\left\{ \begin{array}{l} 34.24 \\ 43.2 \\ 77.29 \\ 58.2 \\ 44.21 \\ 102.32 \end{array} \right.$	$\left\{ \begin{array}{l} 34.21 \\ 43.8 \\ * \\ 58.6 \\ 44.20 \\ 102.31 \end{array} \right.$	$\left\{ \begin{array}{l} 3 \\ 6 \\ - \\ 4 \\ 4 \\ 1 \end{array} \right.$
$\left\{ \begin{array}{l} bo = (010) (111) \\ os = (111) (101) \end{array} \right.$	$\left\{ \begin{array}{l} - \\ - \end{array} \right.$	$\left\{ \begin{array}{l} - \\ - \end{array} \right.$	$\left\{ \begin{array}{l} - \\ - \end{array} \right.$	$\left\{ \begin{array}{l} 70.18 \\ 10.42 \end{array} \right.$	$\left\{ \begin{array}{l} - \\ - \end{array} \right.$
$\left\{ \begin{array}{l} bo' = (010) (111) \\ bn' = (010) (121) \\ n'o' = (121) (111) \\ o'n' = (111) (101) \end{array} \right.$	$\left\{ \begin{array}{l} - \\ - \\ - \\ - \end{array} \right.$	$\left\{ \begin{array}{l} - \\ - \\ - \\ - \end{array} \right.$	$\left\{ \begin{array}{l} - \\ - \\ - \\ - \end{array} \right.$	$\left\{ \begin{array}{l} 65.16 \\ 47.21 \\ 17.65 \\ 24.44 \end{array} \right.$	$\left\{ \begin{array}{l} - \\ - \\ - \\ - \end{array} \right.$
$\left\{ \begin{array}{l} sq = (101) (011) \\ qp = (011) (110) \\ qn' = (011) (121) \\ n'p = (121) (110) \\ ps = (110) (101) \\ pq = (110) (011) \end{array} \right.$	$\left\{ \begin{array}{l} 19 \\ 2 \\ 2 \\ 2 \\ - \\ 20 \end{array} \right.$	$\left\{ \begin{array}{l} - \\ 86.12-86.59 \\ 35.10-35.30 \\ 51.4-51.20 \\ - \\ 93.3-93.38 \end{array} \right.$	$\left\{ \begin{array}{l} - \\ 86.38 \\ 35.20 \\ 51.12 \\ - \\ 93.20 \end{array} \right.$	$\left\{ \begin{array}{l} 17.48 \\ 86.40 \\ 35.25 \\ 51.15 \\ 55.32 \\ 93.20 \end{array} \right.$	$\left\{ \begin{array}{l} - \\ 2 \\ 5 \\ 3 \\ - \\ 0 \end{array} \right.$
$\left\{ \begin{array}{l} s'q = (101) (011) \\ qp = (011) (110) \\ ps' = (110) (101) \\ pq = (110) (011) \end{array} \right.$	$\left\{ \begin{array}{l} - \\ 15 \\ - \\ 14 \end{array} \right.$	$\left\{ \begin{array}{l} - \\ 63.2-63.44 \\ - \\ 116.14-116.55 \end{array} \right.$	$\left\{ \begin{array}{l} - \\ 63.23 \\ - \\ 116.38 \end{array} \right.$	$\left\{ \begin{array}{l} 44.54 \\ 63.21 \\ 71.45 \\ 116.39 \end{array} \right.$	$\left\{ \begin{array}{l} - \\ 2 \\ - \\ 1 \end{array} \right.$
$\left\{ \begin{array}{l} r'o' = (201) (111) \\ o'p = (111) (110) \\ pr' = (110) (201) \end{array} \right.$	$\left\{ \begin{array}{l} 2 \\ 3 \\ 12 \end{array} \right.$	$\left\{ \begin{array}{l} 34.44-34.59 \\ 92.8-92.20 \\ 52.38-52.57 \end{array} \right.$	$\left\{ \begin{array}{l} 34.54 \\ 92.16 \\ 52.49 \end{array} \right.$	$\left\{ \begin{array}{l} 34.51 \\ 92.19 \\ 52.50 \end{array} \right.$	$\left\{ \begin{array}{l} 3 \\ 3 \\ 1 \end{array} \right.$
Total number of measurements		312			

Morphological Angles—The results of the goniometrical measurements are given in the accompanying table (*see* p 413)

It was shown in the memoir on the manganese group of double selenates,* that a potassium salt of the group has never been obtained, and appears to be incapable of existence, being outside the limits of stability. No comparison of the thallium salt with an analogous potassium salt can, therefore, be made.

The effect of the replacement of sulphur by selenium, afforded by a comparison of thallium manganese sulphate with the present salt, is to produce the following angular changes, all increases: $ac = (100) (001)$, $53'$, $pp = (110) (1\bar{1}0)$, $15'$, $cq = (001) (011)$, $14'$, and $cp = (001) (110)$, $44'$.

Volume

Relative Density—The mean accepted value, from two excellent determinations, is 3.833, for the temperature $20^\circ/4^\circ$.

$$\text{Molecular Volume} = \frac{M}{d} = \frac{851.32}{3.833} = 222.10$$

Topic Axial Ratios— $f \quad \psi \quad \omega = 6.3584 \quad 8.5200 \quad 4.2540$

Optics

Orientation of Optical Ellipsoid (Indicatrix)—The plane of the optic axes is the symmetry plane $b\{010\}$. The sign of the double refraction is negative. The maximum axis γ of the indicatrix, vibrations along which correspond to the γ refractive index, lies $8^\circ 21'$ behind the vertical crystal-axis c , in the acute axial angle ac , and is the obtuse bisectrix (second median line) of the optic axial angle. The minimum axis α of the indicatrix, the acute bisectrix (first median line), corresponding (as regards direction of vibration) to the α -index of refraction, lies $23^\circ 50'$ above the inclined crystal-axis a , in the obtuse axial angle ac . The symmetry axis b is the vibration-direction of the light affording the β -index of refraction.

Refractive Indices—The determinations afforded the following results—

Light	α	β	γ
Li	1.6213	1.6364	1.6464
C	1.6219	1.6370	1.6470
Na	1.6276	1.6429	1.6531
Tl	1.6343	1.6496	1.6598
Cd	1.6379	1.6534	1.6640
F	1.6422	1.6579	1.6685

Mean index for Na-light, $\frac{\alpha + \beta + \gamma}{3} = 1.6412$

Double refraction, $N_{\gamma-\alpha} = 0.0255$

* 'Roy Soc Proc.,' A, vol 101, p 225 (1922)

General formula for the intermediate index β for any wave-length γ , corrected to a vacuum —

$$\beta = 1.6147 + \frac{914.363}{\lambda^2} + \frac{2.723.900.000.000}{\lambda^4} +$$

The α -indices are also closely reproduced by the formula if the constant 1.6147 is diminished by 0.0153, and the γ -indices if it be increased by 0.0102

Axial Ratios of Optical Ellipsoid (Indicatrix) —

$$\alpha : \beta : \gamma = 0.9907 : 1 : 1.0062$$

Molecular Optical Constants — These are as under, for the red hydrogen ray C —

	α	β	γ
Specific refraction $\frac{n^2 - 1}{(n^2 + 2)d}$	0.0919	0.0936	0.0948
Molecular refraction (Lorenz) $\frac{n^2 - 1}{n^2 + 2} \frac{M}{d}$	78.21	79.72	80.71
Molecular refraction (Gladstone) $\frac{n - 1}{d} M$	138.12	141.48	143.70

Mean molecular refraction (Gladstone), $\frac{\alpha + \beta + \gamma}{3} = 141.10$

Optic Axial Angle — The angle in air, $2E$, was not observable, but the true optic axial angle, $2V_a$, within the crystal was found, as the mean of several closely agreeing determinations, to be as under —

Light	$2V_a$	Light	$2V_a$
	° ,		° ,
Li	72 1	Tl	72 53
C	72 4	Cd	73 10
Na	72 27	F	73 32

Dispersion of the Median Lines — The two median lines are dispersed in the symmetry plane in such a manner that the first median line lies 27' nearer to the crystal-axis a for thallium green light than for red C-hydrogen light

Thallium Copper Selenate, $\text{Ti}_2\text{Cu}(\text{SeO}_4)_2 \cdot 6\text{H}_2\text{O}$ *Morphology*

Eleven good little crystals were used for the goniometry, selected from four crops of outstanding excellence. The crystals of this salt are bright blue in colour.

Crystal System - Monoclinic Class No 5, holohedral-prismatic.

Ratios of Axes - $a : b : c = 0.7531 : 1 : 0.5048$

Axial Angle $\beta = 104^\circ 59'$

Forms Observed - $a\{100\}$, $b\{010\}$, $c\{001\}$, $p\{110\}$, $p'\{120\}$, $p'''\{130\}$, $q\{011\}$, $m\{021\}$, $l\{031\}$, $r'\{101\}$, $r'\{201\}$, $o\{111\}$, $o'\{111\}$, and $n'\{121\}$. The form $l\{031\}$ is exceedingly rare in the series.

Cleavage - There is an excellent cleavage parallel $r'\{201\}$.

Habit - Short prismatic to more or less tabular parallel to the basal plane $o\{001\}$. A typical crystal is portrayed in fig. 6.

Morphological Angles - The results of the measurements of the interfacial angles are given in the accompanying table (see pp. 417-18).

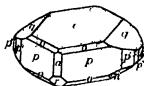


FIG. 6 - Ti_2Cu Selenate

The Average Angular Difference between this salt and the corresponding potassium salt K-Cu-selenate , that is, the effect on the interfacial angles of replacing potassium by thallium, is $43'$. The difference which occurs for the important axial angle β , $ac = (100) (001)$, is $1^\circ 34'$. This is exceeded, however, by one other angle, for which the maximum angular difference of $1^\circ 39'$ occurs.

The effect of replacing sulphur by selenium, as seen on comparing Ti-Cu-sulphate and Ti-Cu-selenate , on the four main angles, is as follows. For $ac = (100) (001)$, $34'$, for $pp = (110) (1\bar{1}0)$, $22'$, for $cq = (001) (011)$, $8'$, and for $cp = (001) (110)$, $29'$.

Volume

Relative Density - The mean of two closely agreeing determinations of the specific gravity at $20^\circ/4^\circ$ gave as the accepted value 3.944.

Molecular Volume - $\frac{M}{d} = \frac{859.82}{3.944} = 218.01$

Topic Axial Ratios - $\chi : \psi : \omega = 6.3294 : 8.4045 : 4.2426$

Interfacial Angles of Thallium Copper Selenate

Angle	No of measurements	Limits	Mean observed	Calculated	Diff
$\left\{ \begin{array}{l} ac = (100) (001) \\ as = (100) (101) \\ ac = (101) (001) \\ cr' = (001) (201) \\ cs' = (001) (101) \\ s's' = (101) (201) \\ r'a = (201) (100) \\ r'e = (201) (001) \end{array} \right.$	$\left\{ \begin{array}{l} 6 \\ --- \\ --- \\ 15 \\ - \\ - \\ 1 \\ 13 \end{array} \right.$	$\left\{ \begin{array}{l} 75 \ 0-75 \ 1 \\ --- \\ --- \\ 61 \ 4 \ 63 \ 30 \\ --- \\ --- \\ 41 \ 38-41 \ 43 \\ 115 \ 16 \ 116 \ 30 \end{array} \right.$	$\left\{ \begin{array}{l} 75 \ 2 \\ --- \\ --- \\ 63 \ 17 \\ --- \\ --- \\ 41 \ 41 \\ 116 \ 46 \end{array} \right.$	$\left\{ \begin{array}{l} 75 \ 1 \\ 46 \ 6 \\ 28 \ 55 \\ 63 \ 17 \\ 38 \ 7 \\ 25 \ 10 \\ 41 \ 42 \\ 116 \ 43 \end{array} \right.$	$\left\{ \begin{array}{l} 1 \\ - \\ - \\ 0 \\ - \\ - \\ 1 \\ 2 \end{array} \right.$
$\left\{ \begin{array}{l} ap = (100) (110) \\ pp' = (110) (120) \\ p'b = (120) (010) \\ p'p'' = (120) (130) \\ p''b = (130) (010) \\ pb = (110) (010) \\ pp = (110) (110) \end{array} \right.$	$\left\{ \begin{array}{l} 3 \\ 2 \\ 2 \\ 1 \\ 1 \\ 35 \\ 18 \end{array} \right.$	$\left\{ \begin{array}{l} 35 \ 38 \ 36 \ 19 \\ 19 \ 22 \ 19 \ 31 \\ 34 \ 27-34 \ 39 \\ --- \\ --- \\ 51 \ 39 \ 51 \ 12 \\ 71 \ 44-72 \ 32 \end{array} \right.$	$\left\{ \begin{array}{l} 35 \ 37 \\ 19 \ 26 \\ 34 \ 33 \\ 9 \ 53 \\ 24 \ 40 \\ 53 \ 59 \\ 72 \ 1 \end{array} \right.$	$\left\{ \begin{array}{l} 36 \ 1 \\ 19 \ 28 \\ 34 \ 31 \\ 9 \ 53 \\ 24 \ 38 \\ * \\ 72 \ 2 \end{array} \right.$	$\left\{ \begin{array}{l} 4 \\ 2 \\ 2 \\ 0 \\ 2 \\ - \\ 1 \end{array} \right.$
$\left\{ \begin{array}{l} cq = (001) (011) \\ qb = (011) (010) \\ bl = (010) (031) \\ lm = (031) (021) \\ bm = (010) (021) \\ nq = (021) (011) \end{array} \right.$	$\left\{ \begin{array}{l} 37 \\ 38 \\ 1 \\ 2 \\ 14 \\ 1 \end{array} \right.$	$\left\{ \begin{array}{l} 25 \ 48 \ 26 \ 9 \\ 63 \ 51-64 \ 12 \\ --- \\ 34 \ 15-34 \ 30 \\ 28 \ 37 \ 128 \ 55 \\ --- \end{array} \right.$	$\left\{ \begin{array}{l} 26 \ 0 \\ 64 \ 0 \\ 44 \ 22 \\ 11 \ 24 \\ 45 \ 46 \\ 18 \ 11 \end{array} \right.$	$\left\{ \begin{array}{l} * \\ 64 \ 0 \\ 34 \ 21 \\ 11 \ 22 \\ 45 \ 43 \\ 18 \ 17 \end{array} \right.$	$\left\{ \begin{array}{l} - \\ 0 \\ 1 \\ 1 \\ 3 \\ 6 \end{array} \right.$
$\left\{ \begin{array}{l} ao = (100) (111) \\ oq = (111) (011) \\ aq = (100) (011) \\ qo' = (011) (111) \\ o'a = (111) (100) \end{array} \right.$	$\left\{ \begin{array}{l} --- \\ --- \\ - \\ - \\ - \end{array} \right.$	$\left\{ \begin{array}{l} --- \\ --- \\ - \\ - \\ - \end{array} \right.$	$\left\{ \begin{array}{l} --- \\ - \\ - \\ - \\ - \end{array} \right.$	$\left\{ \begin{array}{l} 49 \ 20 \\ 27 \ 14 \\ 76 \ 34 \\ 34 \ 18 \\ 69 \ 8 \end{array} \right.$	$\left\{ \begin{array}{l} - \\ - \\ - \\ - \\ - \end{array} \right.$
$\left\{ \begin{array}{l} co = (001) (111) \\ op = (111) (110) \\ cp = (001) (110) \\ po' = (110) (111) \\ or = (111) (001) \\ pe = (110) (001) \end{array} \right.$	$\left\{ \begin{array}{l} 2 \\ 2 \\ 42 \\ 12 \\ 18 \\ 28 \end{array} \right.$	$\left\{ \begin{array}{l} 34 \ 15-34 \ 53 \\ 43 \ 5-43 \ 31 \\ 77 \ 42-78 \ 8 \\ 57 \ 24 \ 57 \ 58 \\ 44 \ 3-44 \ 14 \\ 101 \ 55-102 \ 20 \end{array} \right.$	$\left\{ \begin{array}{l} 34 \ 14 \\ 43 \ 18 \\ 77 \ 56 \\ 57 \ 39 \\ 44 \ 21 \\ 102 \ 4 \end{array} \right.$	$\left\{ \begin{array}{l} 34 \ 39 \\ 43 \ 17 \\ * \\ 57 \ 36 \\ 44 \ 28 \\ 102 \ 4 \end{array} \right.$	$\left\{ \begin{array}{l} 7 \\ 1 \\ - \\ 3 \\ 4 \\ 0 \end{array} \right.$
$\left\{ \begin{array}{l} bo = (010) (111) \\ os = (111) (101) \\ oo = (111) (111) \end{array} \right.$	$\left\{ \begin{array}{l} 3 \\ --- \\ 1 \end{array} \right.$	$\left\{ \begin{array}{l} 69 \ 58-70 \ 7 \\ --- \\ --- \end{array} \right.$	$\left\{ \begin{array}{l} 70 \ 3 \\ --- \\ 69 \ 53 \end{array} \right.$	$\left\{ \begin{array}{l} 70 \ 1 \\ 19 \ 59 \\ 39 \ 58 \end{array} \right.$	$\left\{ \begin{array}{l} 2 \\ - \\ 5 \end{array} \right.$
$\left\{ \begin{array}{l} bo' = (010) (111) \\ bn' = (010) (121) \\ n'o' = (121) (111) \\ o's' = (111) (101) \\ o'o' = (111) (111) \end{array} \right.$	$\left\{ \begin{array}{l} 6 \\ --- \\ - \\ 1 \\ 3 \end{array} \right.$	$\left\{ \begin{array}{l} 64 \ 55-65 \ 13 \\ --- \\ --- \\ - \\ 49 \ 39-49 \ 55 \end{array} \right.$	$\left\{ \begin{array}{l} 65 \ 5 \\ --- \\ --- \\ 24 \ 51 \\ 49 \ 47 \end{array} \right.$	$\left\{ \begin{array}{l} 65 \ 6 \\ 47 \ 8 \\ 17 \ 58 \\ 24 \ 54 \\ 49 \ 48 \end{array} \right.$	$\left\{ \begin{array}{l} 1 \\ - \\ - \\ 1 \\ 1 \end{array} \right.$
$\left\{ \begin{array}{l} sq = (101) (011) \\ qp = (011) (110) \\ qn' = (011) (121) \\ n'p = (121) (110) \\ pn = (110) (101) \\ pq = (110) (011) \end{array} \right.$	$\left\{ \begin{array}{l} --- \\ 33 \\ 1 \\ 1 \\ - \\ 33 \end{array} \right.$	$\left\{ \begin{array}{l} --- \\ 85 \ 55-86 \ 12 \\ --- \\ --- \\ --- \\ 93 \ 44-94 \ 3 \end{array} \right.$	$\left\{ \begin{array}{l} --- \\ 86 \ 2 \\ 35 \ 18 \\ 50 \ 40 \\ - \\ 93 \ 58 \end{array} \right.$	$\left\{ \begin{array}{l} 38 \ 7 \\ 86 \ 0 \\ 35 \ 16 \\ 50 \ 44 \\ 55 \ 53 \\ 94 \ 0 \end{array} \right.$	$\left\{ \begin{array}{l} --- \\ 2 \\ 2 \\ 4 \\ - \\ - \\ 2 \end{array} \right.$
$\left\{ \begin{array}{l} s'q = (101) (011) \\ qp = (011) (110) \\ po' = (110) (101) \\ pq = (110) (011) \end{array} \right.$	$\left\{ \begin{array}{l} --- \\ 31 \\ - \\ 32 \end{array} \right.$	$\left\{ \begin{array}{l} --- \\ 63 \ 26-63 \ 41 \\ --- \\ 116 \ 13 \ 117 \ 44 \end{array} \right.$	$\left\{ \begin{array}{l} --- \\ 63 \ 33 \\ - \\ 116 \ 27 \end{array} \right.$	$\left\{ \begin{array}{l} 45 \ 0 \\ 63 \ 32 \\ 71 \ 28 \\ 116 \ 28 \end{array} \right.$	$\left\{ \begin{array}{l} - \\ 1 \\ - \\ 1 \end{array} \right.$

Interfacial Angles of Thallium Copper Selenate—(continued)

Angle	No of measurements	Units	Mean observed	Calculated	Diff
$\left\{ \begin{array}{l} r'o' = (201) \text{ (111)} \\ o'p = (111) \text{ (110)} \\ o'm = (111) \text{ (021)} \\ mp = (021) \text{ (110)} \\ pr' = (110) \text{ (201)} \end{array} \right.$	13 14 3 5 30	$\begin{array}{cc} \circ & ' \\ 34 & 42-35 & 7 \\ 92 & 13-92 & 37 \\ 36 & 16-36 & 32 \\ 55 & 43-56 & 5 \\ 52 & 36-52 & 58 \end{array}$	$\begin{array}{cc} \circ & ' \\ 34 & 49 \\ 92 & 24 \\ 36 & 22 \\ 55 & 59 \\ 52 & 47 \end{array}$	$\begin{array}{cc} \circ & ' \\ 34 & 49 \\ 92 & 20 \\ 36 & 25 \\ 55 & 55 \\ 52 & 51 \end{array}$	0 4 3 4 4
Total number of measurements	507				

Optics

Orientation of Optical Ellipsoid (Indicatrix)—The optic axes lie in the symmetry plane $b\{010\}$. The sign of the double refraction is negative. The maximum axis γ of the indicatrix, light vibrations along which correspond to the γ -index of refraction, lies $14^\circ 25'$ behind the vertical crystal-axis c , in the acute axial angle ac , it is the obtuse bisectrix (second median line) of the optic axial angle. The minimum axis α of the indicatrix, the acute bisectrix (first median line) of the optic axial angle and direction of vibration for the α -index, lies $29^\circ 24'$ above the crystal-axis a , in the obtuse axial angle ac . The vibration-direction for the β -index of refraction is the symmetry axis b .

Refractive Indices—These are found to be as follows —

Light	α	β	γ
Li	1.6330	1.6504	1.6655
C	1.6345	1.6511	1.6662
Na	1.6366	1.6565	1.6720
Tl	1.6461	1.6631	1.6787
Cd	1.6495	1.6666	1.6823
F	1.6537	1.6709	1.6867

$$\text{Mean index for Na-light, } \frac{\alpha + \beta + \gamma}{3} = 1.6560$$

$$\text{Double refraction, } N_{\alpha-\gamma} = 0.0324$$

General formula for the intermediate index β , for any wave-length λ , corrected to a vacuum —

$$\beta = 1.6353 + \frac{485.126}{\lambda^2} + \frac{9.191.500.000.000}{\lambda^4} +$$

The α -indices are also fairly reproduced if the constant 1.6353 be diminished by 0.0168, and the γ -indices if it be increased by 0.0154.

Axial Ratios of the Optical Ellipsoid (Indicatrix) —

$$\alpha \quad \beta \quad \gamma = 0.9898 \quad 1 \quad 1.0094$$

Molecular Optical Constants — These are given below for the red hydrogen ray C —

Specific refraction	}	α	β	γ
$\frac{n^2 - 1}{(n^2 + 2)d}$		0.0907	0.0926	0.0943
Molecular refraction (Lorenz)	}			
$\frac{n^2 - 1}{n^2 + 2} \frac{M}{d}$		78.00	79.62	81.08
Molecular refraction (Gladstone)	}			
$\frac{n - 1}{d} M$		138.32	141.94	145.23

Mean molecular refraction (Gladstone), $\frac{\alpha + \beta + \gamma}{3} = 141.82$

Optic Axial Angle — This very large angle is invisible in air, although one optic axis is visible through a pair of *c*-faces, much to one side of the centre. The measurements for the true angle within the crystal, which were carried out with the plates immersed in monobromonaphthalene, afforded the following mean result, the individual values being almost identical

Light	$2V_a$	Light	$2V_a$
	° ' ,		° ' ,
L ₁	85 14	Tl	85 4
C	85 13	Cd	85 1
Na	85 9	F	84 56

Dispersion of the Median Lines — The first and second median lines are dispersed in the symmetry plane to the slight extent that the first median line lies nearer to the inclined crystal-axis *a* for green thallium light than for red C-hydrogen light by 17'. This was the mean of two determinations (yielding 15' and 19' respectively) in monobromonaphthalene, the refractive index of which is practically identical with that of these highly refractive crystals.

Discussion of Results

The considerations on p. 384 of the preceding memoir on the double sulphates containing thallium apply equally to the double selenates, so that it is only necessary to proceed at once with the discussion of the various properties

As regards the *Interfacial Angles* the next table gives a comparison of the average and maximum changes brought about by the replacement of potassium by thallium and by the other interchangeable R-bases

Table of Average and Maximum Changes of Angle in Double Selenates

	Average change for replacement of K by				Maximum change for replacement of K by			
	Rb	Cs	NH ₄	Tl	Rb	Cs	NH ₄	Tl
Mg group	24	52	51	31	56	128	129	78
Zn "	27	52	49	41	64	131	122	102
Ni "	23	47	45	28	57	119	110	60
Co "	25	51	49	31	61	136	126	83
Fe "	27	55	54	39	69	139	130	97
Cu "	33	61	47	43	79	148	125	99
Mean	26	53	50	36	65	134	125	88
Mean of both sulphates and selenates	27	55	51	36	65	133	125	89

It will be evident how analogous the selenate results are to those yielded by the sulphates, from the fact that the mean values for the whole of the two series are practically identical with those for the selenate series. The change, whether average or maximum, is directly proportional to the change in atomic number when rubidium or caesium is introduced instead of potassium, the figures in the second column in each case being double those in the first, correct in the mean to 3'. The introduction of ammonium or thallium for potassium provokes intermediate changes, the former change being nearer the amount for the caesium replacement, and the latter nearer to what occurs when rubidium is the replacing element.

The monoclinic *Axial Angle* β is reviewed comparatively for all the double selenates now described in the next table, from which it will be seen that the increase of this angle occurs eutropically (that is, proportionately to the change in atomic weight or number, rubidium being exactly midway in regard to these constants) only for the alkali-metallic salts.

The half-way position of the rubidium salt, between the potassium and caesium salts, will be very clear from this table. The ammonium salt possesses an axial angle very nearly identical with that of the caesium salt, while the thallium salt comes between the rubidium and caesium salt, the value being

Comparison of Monoclinic Axial Angles β for Double Selenates

Containing	Magnesium	Nickel	Cobalt	Ferrous iron	Manganese	Copper
	\circ $'$	\circ $'$	\circ $'$	\circ $'$	\circ $'$	\circ $'$
Potassium	104 18	104 27	104 17	103 50		103 25
Rubidium	105 14	105 20	105 14	104 57	105 9	104 44
Cæsium	106 17	106 11	106 18	106 2	106 22	105 12
Ammonium	106 27	106 17	106 23	106 9	106 16	105 30
Thallium	105 36	105 36	105 40	105 27	105 29	104 59

nearer to that of the former. Similar relationships were shown in the 1909 memoir (*loc cit*) to hold in the zinc group of double selenates, and all these conclusions are exactly similar to those drawn in the preceding memoir for the double sulphates.

The changes in interfacial angles brought about by replacing sulphur by selenium may next be discussed. The next table shows the changes, all being increases, in the four main angles.

Angular Differences between Analogous Sulphates and Selenates

Angle	Tl Mg salts	Tl Ni salts	Tl Co salts	Tl Fe salts	Tl Mn salts	Tl Cu salts
$ac = (100) (001)$	74	48	15	49	53	34
$pp = (110) (1\bar{1}0)$	32	18	11	20	15	22
$q = (001) (011)$	4	11	12	9	14	8
$cp = (001) (110)$	46	41	39	41	44	29

For the Tl-Zn salt previously (1909) described (*loc cit*) the numbers were 22', 38', 6' and 21'. It will be observed that the changes never reach a whole degree, and are characteristically such as have been shown by the author invariably to accompany isomorphous replacement in crystal systems of lower than cubic symmetry.

With regard next to the *Volume Constants*, the next two tables compare the densities, molecular volumes, and topic axial ratios.

From them, just as from the similar tables given in the preceding memoir for the double sulphates, the relative volumes and edge-dimensions of the structural-unit cells of the space-lattice are seen to progress eutropically for the three alkali-metallic salts, while the ammonium salt is almost precisely iso-structural with the ammonium salt, their volumes and dimensions being nearly identical, and the thallium salts also resemble, although not so closely, the corresponding rubidium salts in these respects.

Density and Molecular Volume of Double Selenates

Containing	Potassium	Rubidium	Cæsium	Ammonium	Thallium
Magnesium	2 365 208 63	2 684 218 15	2 939 231 20	2 058 219 42	1 721 220 61
Zinc	2 558 208 80	2 868 218 35	3 121 230 77	2 261 217 73	1 958 217 69
Nickel	2 559 206 14	2 856 216 00	3 114 229 17	2 243 216 53	1 993 214 13
Cobalt	2 530 208 60	2 837 218 49	3 091 230 73	2 228 218 10	1 998 213 92
Iron (ferrous)	2 494 210 39	2 800 220 29	3 048 233 21	2 191 220 39	1 940 216 30
Manganese	—	2 763 222 92	3 008 236 01	2 158 223 35	1 833 222 10
Copper	2 539 209 60	2 839 219 94	3 073 233 79	2 223 220 64	1 944 218 01

The replacement of sulphur by selenium in the thallium double salts causes an expansion of the unit-cell volume by an average of 12.91 units, corresponding to an increase per atom of selenium of 6.5 units. This is in accord with previous observations, for the increase has varied in different groups of the salts from 6.0 to 6.8 units.

Proceeding now to the *Optics*, the *Orientation of the Optical Ellipsoid* shows a similar rotation about the symmetry axis *b* as in the double sulphates, so that fig. 5 on p. 389 of the preceding memoir is valid equally for the double selenates. The positions in the thallium salts of that axis of the indicatrix ellipsoid which is the vibration direction of the γ -index of refraction and is the obtuse bisectrix of the optic axial angle, that is, the second median line, is given in the next little table. It is not so far removed behind the vertical crystal axis *c* as it is in the double sulphates.

Inclination of γ -Axis of Ellipsoid to Right of Crystal-Axis *c*

	°	'		°	'
In Tl Mg selenate	4	27	In Tl Fe selenate	9	9
„ Tl Zn „	6	46	„ Tl Mn „	8	21
„ Tl Ni „	10	19	„ Tl Cu	14	25
Tl Co „	8	22			

Topic Axial Ratios of Double Selenates

	Magnesium			Zinc			Nickel			Cobalt			Ferrous iron			Manganese			Copper		
	X	ψ	ω	X	ψ	ω	X	ψ	ω	X	ψ	ω	X	ψ	ω	X	ψ	ω	X	ψ	ω
K	6 0462 8	1562 4	1141 6	1812 8	2880 4	2045 6	1677 8	2596 4	1786 6	2197 8	2688 4	1856 6	2230 8	3085 4	1908	—	—	—	1819 8	2338 4	2347
Rb	6 1436 8	3326 4	1754 6	2613 8	4662 4	2492 6	2533 8	4561 4	2542 6	2901 8	4693 4	2508 6	3109 8	5006 4	2505 6	3333 8	3332 4	2734 6	3179 8	4295 4	2704
Cs	6 2415 8	5808 4	2561 6	3710 8	7106 4	3300 6	3317 8	6878 4	3378 6	3618 8	7028 4	3418 6	3847 8	7366 4	3196 6	4297 8	7850 4	3547 6	4378 8	7022 4	3346
NH ₄	6 1648 8	3670 4	1810 6	2742 8	4684 4	2681 6	2520 8	4543 4	2678 6	3057 8	4651 4	2587 6	3212 8	5043 4	2684 6	3577 8	5603 4	2750 6	2868 8	4063 4	3308
Tl	6 3580 8	4943 4	2412 6	3173 8	4468 4	2420 6	2680 8	4066 4	2163 6	2696 8	4010 4	2181 6	2846 8	4415 4	2700 6	3584 8	5200 4	2540 6	3204 8	4047 4	2426

The sign of the *Double Refraction* is negative in all these double selenates, as in the double sulphates

The *Refraction Constants* are compared in the next table, in an analogous manner to the double sulphates, as described on p 390 of preceding memoir

Refraction Constants of the Double Selenates

Containing	Mg	Zn	Ni	Co	Fe	Mn	Cu	
Potassium	1 5033	1 5212	1 5293	1 5252	1 5207		1 5226	Mean Refrac- tive Index
Rubidium	1 5059	1 5238	1 5293	1 5275	1 5220	1 5164	1 5218	
Cæsium	1 5108	1 5367	1 5445	1 5402	1 5357	1 5289	1 5325	
Ammonium	1 5111	1 5408	1 5372	1 5335	1 5292	1 5217	1 5311	
Thallium	1 6330	1 6523	1 6479	1 6522	1 6485	1 6412	1 6560	
Potassium	0 0170	0 0214	0 0246	0 0222	0 0250	—	0 0248	Double Refraction
Rubidium	0 0124	0 0189	0 0192	0 0170	0 0195	0 0164	0 0165	
Cæsium	0 0058	0 0080	0 0094	0 0099	0 0108	0 0088	0 0112	
Ammonium	0 0099	0 0145	0 0175	0 0156	0 0165	0 0128	0 0186	
Thallium	0 0154	0 0201	0 0182	0 0150	0 0237	0 0255	0 0324	
Potassium	104 40	108 19	108 39	108 89	108 87	—	108 89	Molecular Refraction
Rubidium	109 73	113 71	114 12	114 54	114 33	114 43	114 08	
Cæsium	119 48	123 12	124 02	123 86	124 22	124 10	123 69	
Ammonium	111 42	114 81	115 57	115 61	115 90	115 79	116 10	
Thallium	138 77	140 73	137 87	138 67	139 07	141 10	141 82	

The thallium double selenates are seen to distinguish themselves by exceptionally high refractive indices and molecular refraction, as they have been shown to do in the cases of the double sulphates. Indeed the maximum index of refraction in some cases exceeds that of the very highly refractive liquid monobromonaphthalene (1 6657 for Na-light), so much used on that account as the immersion liquid in determinations of optic axial angle with complementary plates perpendicular to the acute and obtuse bisectrices. For instance, the γ -index of thallium copper selenate for Na-light is 1 6720.

The double refraction middle part of the table shows best the regular diminution in this property with atomic number which occurs in the cases of the three alkali metals.

As regards molecular refraction, here again the eutropic progression is clearly displayed in the relations of the three alkali-metallic salts, and also the near identity of the molecular refractions of the rubidium and ammonium salts is plainly revealed, while the transcendent position of the thallium salts is strikingly evident. As regards the effect on the molecular refraction of replacing sulphur by selenium, there is an increase of about 14 units, the exact mean of all the 34 cases being 13 8. If we exclude the thallium salts for which the

mean rise is more than the average for all, namely, 16.4, the average for the alkali-metallic and ammonium salts is only 13.2. As there are two sulphur atoms replaced by selenium, the effect per atom is thus 6.6 or 6.9 units, according as the salts containing thallium are included or excluded from the comparison.

With respect to the *Optic Axial* angle phenomena it is only necessary to emphasise that for this double selenate series, as for the double sulphates, the double refraction is throughout of negative sign, the minimum α -axis of the ellipsoid being the first median line (acute bisectrix), and the γ -axis the second, and that these two axes of the optical ellipsoid (indicatrix) are dispersed in the symmetry plane to a similar small extent, varying in the seven different salts from 17' to 35', in the same sense, which brings the first median line nearer to the inclined crystal-axis a for green thallium light than for red hydrogen light.

Conclusion

The results for the double selenates are thus analogous in every respect to those for the double sulphates containing thallium. The replacement of sulphur by selenium causes all the constants to be pushed on somewhat, just as it does in the alkali-metallic and ammonium salts, the unit cells of the structural space-lattice for instance being enlarged, and the interfacial angles and physical properties correspondingly altered. The amounts of change are never larger, however, than such as have now been shown generally to accompany isomorphous replacement.

The net effect of replacing sulphur in all the double sulphates by selenium is to leave the relations of the thallium double selenates to the double selenates containing potassium, rubidium, caesium, and ammonium almost precisely the same as has been stated in the preceding communication for the double sulphates. The two series confirm each other absolutely as regards those relationships. While the potassium, rubidium, and caesium salts containing the same M-metal show the regular eutropic change following change of atomic number and weight, the ammonium and thallium salts do not show any relationship to atomic or molecular weights, but only such changes as are similar in amount, lying between the limits of the potassium and caesium salts, and being thus of the small order just referred to, characteristic of isomorphous replacement. Yet the ammonium salts do show one constant and significant property, that of being nearly perfectly isostructural with the analogous rubidium salts and of exhibiting constants very close to those of the rubidium salts. And the thallium salts, likewise, show tendency in the same direction, but the similarity never

proceeds as completely towards identity as in the case of the ammonium salts. This fact, however, in regard to all morphological properties, such as crystal angles, and the directional size and volume of the unit space-lattice cell, obviously brings the thallium salts well inside the isomorphous series, and not as extreme members, these latter being the potassium and caesium salts. One outstanding and very striking exceptional property the thallium salt possesses, however, which at once distinguishes it from all the other R-base salts of the series, namely, its very high optical refractivity.

Compared with the remarkable determinative effect on the crystal form and properties which interchange of the five R-bases has been shown to exert, the very slight effect of interchanging the M-metals is again shown in the cases of the seven thallium salts. A glance at the tables on pp 421 and 424, showing the changes in the important axial angle β of the crystals and in the molecular refraction, two typical morphological and optical properties, will at once render this fact quite plain. That the structure of the atoms themselves, and their positions in the periodic table, determining their structure, are prime causes must be evident, and this is a line of study which it is hoped in future work to take up and elucidate.

It is, however, already certain that the eutropic progress of the potassium, rubidium and caesium salts is due to the progressive enlargement of the atoms of these alkali metals, by a complete shell of 18 electrons each time we pass from one to another, corresponding to the increase of 18 in atomic number, from 19 to 37 and 55. It corresponds, indeed, to the passage from argon to krypton and xenon, the complete-shell (and therefore inert) elements next below them in atomic number, 18, 36 and 54. And the very mobile extra electron left outside the outermost complete shell amounts for the great (maximum) electro-positive chemical activity which these alkali metals display, enabling them to form this magnificently crystallising series of isomorphous salts.

This communication now closes the author's long descriptive and comparative study of this great isomorphous series of 77 salts, rounding off the work on the alkali-metallic and ammonium salts which was brought to a conclusion in the 1922 memoir* (which gave as an appendix, p 262, a complete list of the memoirs published since the inception of the research in the year 1890) by a description of the whole of the analogous thallium salts of the series, a task which has proved much more difficult, but is now satisfactorily completed.

* 'Roy Soc Proc,' A, vol. 101, p 245 (1922)

*The Bending of a Centrally-Loaded Isotropic Rectangular Plate
Supported at Two Opposite Edges*

By A E H LOVE, FRS

(Received February 6, 1928)

1 The plate will be taken to be of uniform isotropic material, the elastic quality of which is specified by its Young's modulus E and Poisson's ratio σ , and it will be taken to be of small uniform thickness $2h$. The flexural rigidity D of the plate is then given by the formula

$$D = \frac{1}{3} E h^3 / (1 - \sigma^2) \quad (1)$$

The initially plane middle surface of the plate will be taken as the plane of rectangular cartesian co-ordinates x, y , and the edges of the plate will be taken to cut this plane in segments of the lines $x = \pm a, y = \pm b$, so that the length of the plate is $2a$, and the breadth $2b$.

The plate will be taken to be bent by concentrated pressure P , applied to one of its faces in a line normal to the faces and passing through the origin, the centre of the rectangle. The deflexion w , or the displacement of a point of the middle surface in the direction of the pressure P , is the quantity to be determined.

The problem has a certain interest in connection with the experimental determination of the constants E and σ . See § 12 *infra*.

It is known* that w is given by a formula of the form

$$w = \frac{P}{8\pi D} \{ (x^2 + y^2) \log r + \chi \}, \quad (2)$$

where r denotes the distance of the point (x, y) from the origin, and χ is a certain bi-harmonic function determined by the boundary conditions, that is to say χ is free from singularity within the rectangle, satisfies the equation

$$\nabla^4 \chi \equiv \frac{\partial^4 \chi}{\partial x^4} + \frac{\partial^4 \chi}{\partial y^4} + 2 \frac{\partial^4 \chi}{\partial x^2 \partial y^2} = 0 \quad (3)$$

at all points within the rectangle, and further satisfies certain conditions at the boundary.

The edges $x = \pm a$ will be taken to be supported, and the edges $y = \pm$

* See my "Elasticity," Chapter XXII

to be free. The conditions to be satisfied at the supported edges $x = \pm a$ are

$$w = 0, \quad \nabla^2 w = 0, \quad (4)$$

where ∇^2 stands for $\partial^2/\partial x^2 + \partial^2/\partial y^2$. The conditions to be satisfied at the free edges $y = \pm b$ are*

$$\nabla^2 w - (1 - \sigma) \frac{\partial^2 w}{\partial x^2} = 0, \quad \frac{\partial}{\partial y} \left\{ \nabla^2 w + (1 - \sigma) \frac{\partial^2 w}{\partial x^2} \right\} = 0 \quad (5)$$

They express respectively the vanishing of flexural couple and transverse force.

The problem is reduced to the determination of the function w .

2. To determine this function we begin by transforming to a circular boundary. The region within the rectangle in the plane of the complex variable $z (\equiv x + iy)$, can be represented conformally on the half-plane $Y > 0$ in the plane of a complex variable $Z (\equiv X + iY)$ by the equation†

$$Z = \sqrt{k} \operatorname{sn} \left\{ \frac{K}{a} (z + ib) \right\}, \quad (6)$$

where the modulus k of the elliptic function is determined by the equation

$$K'/K = 2b/a, \quad (7)$$

so that k depends in a known way upon the ratio of the breadth of the rectangle to its length.

The region within the circle $|\zeta| = 1$ in the plane of an auxiliary complex variable $\zeta (\equiv \xi + i\eta)$ can be represented conformally on the same half-plane $Y > 0$ by the equation

$$\zeta = \frac{z - Z}{z + Z} \quad (8)$$

and from the elimination of Z between the equations (6) and (8) there results an equation by which the region within the rectangle in the z plane is transformed into the region within the circle in the ζ plane.

The differential forms of the two equations of transformation are

$$\frac{K}{a} dz = \frac{1}{\sqrt{k}} \left\{ \left(1 - \frac{Z^2}{k} \right) (1 - kZ^2) \right\}^{-1} dZ,$$

and

$$dZ = -2i (1 + \zeta)^{-2} d\zeta,$$

* These can be obtained from results given in my "Elasticity," Chapters XXII and XXIV, or from those given in Rayleigh, "Sound," vol. 1, § 215.

† See A. R. Forsyth, "Theory of Functions of a Complex Variable," 2nd edn., Cambridge, 1900, p. 639.

and, if a real positive acute angle α is determined by the equation

$$\tan \frac{1}{2}\alpha = \sqrt{k}, \quad (9)$$

these differential formulæ combined with (8) give

$$dz = -\frac{2ia}{K(1+k)} \frac{d\zeta}{\sqrt{(1-2\zeta^2 \cos 2\alpha + \zeta^4)}}, \quad (10)$$

from which, with the condition that $z = 0$ at $\zeta = 0$, it appears that

$$z = -\frac{2ia}{K(1+k)} \sum_{n=0}^{\infty} \frac{1}{2n+1} P_n(\cos 2\alpha) \zeta^{2n+1}, \quad (11)$$

where P_n is the symbol of Legendre's n th coefficient. This formula holds at all points on or within the circle $|\zeta| = 1$, and shows that the function z/ζ is a holomorphic function of ζ , or of z , in the region bounded by the circle, or the rectangle. It follows that the function $\log(r/\rho)$, where ρ stands for $|\zeta|$, is harmonic within the rectangle, that is to say is free from singularity and satisfies the equation $\nabla^2 \{\log(r/\rho)\} = 0$.

Since the product of $x^2 + y^2$ and a harmonic function is bi-harmonic, it follows that, instead of the formula (2), we may take

$$w = \frac{P}{8\pi D} \{(x^2 + y^2) \log \rho + f\} \quad (12)$$

Then f is a bi-harmonic function to be determined by means of the boundary conditions (4) and (5).

3. Let us suppose temporarily that all four edges of the plate are supported. Then we shall have the displacement w expressed by the equation (12), in which f is bi-harmonic and, at the edges, we shall have

$$f = 0, \quad \nabla^2 f = -\nabla^2 \{(x^2 + y^2) \log \rho\} \quad (13)$$

Now we have, everywhere in the rectangle except at the origin,

$$\nabla^2 \{(x^2 + y^2) \log \rho\} = 4 \log \rho + 4 \left(x \frac{\partial}{\partial x} + y \frac{\partial}{\partial y} \right) \log \rho$$

At all the edges $\rho = 1$ so that this becomes, at the edge $y = b$,

$$\nabla^2 \{(x^2 + y^2) \log \rho\} = 4b \frac{\partial \rho}{\partial y}$$

Also, at the same edge ($y = b$),

$$\frac{\partial \rho}{\partial y} = \left| \frac{d\zeta}{dz} \right|,$$

for it is the ratio of corresponding short lengths in the two planes. The other edges can be treated in the same way, and we see that, at the edges $y = \pm b$ we must have

$$\chi = 0, \quad \nabla^2 \chi = -4b \left| \frac{d\zeta}{dz} \right|, \quad (14)$$

and at the edges $x = \pm a$ we must have

$$\chi = 0, \quad \nabla^2 \chi = -4a \left| \frac{d\zeta}{dz} \right| \quad (15)$$

From the symmetry of the conditions it is seen that χ must be an even function of x and an even function of y . Certain even bi-harmonic functions of x and y vanishing at all the edges, are known in the forms

$$X_n = \left(\frac{y \sinh vy}{b \sinh vb} - \frac{\cosh vy}{\cosh vb} \right) \cos vx, \quad (16)$$

where $v = (2n + 1)\pi/2a$, n may be any positive integer, and the letters x, y may be interchanged, a, b being interchanged at the same time. We see that we could determine χ by the formula

$$\chi = \sum A_n X_n + \sum B_n Y_n,$$

where Y_n is the function obtained from X_n by these interchanges, if we could determine the constants A_n and B_n . For this purpose we should require an expansion of $|d\zeta/dz|$ at $y = b$ in a series of the form $\sum x_n \cos vx$, and similarly for $x = a$.

4 We proceed to form an expression for $|d\zeta/dz|$ at $y = b$, and to expand it in a Fourier series valid in the interval $a \geq x \geq -a$. We have

$$\frac{d\zeta}{dz} = \frac{-2i}{(1+Z)^2},$$

and

$$\frac{dZ}{dz} = \frac{K}{a} \sqrt{k} \operatorname{cn} \left\{ \frac{K}{a}(z+ib) \right\} \operatorname{dn} \left\{ \frac{K}{a}(z+ib) \right\}$$

Also, at $y = b$,

$$\frac{K}{a}(z+ib) = \frac{K'}{a} + iK'',$$

so that

$$Z = \frac{1}{\sqrt{k} \operatorname{sn}(Kx/a)}, \quad \frac{dZ}{dz} = -\frac{K}{a\sqrt{k}} \frac{\operatorname{dn}(Kx/a) \operatorname{cn}(Kx/a)}{\operatorname{sn}^2(Kx/a)}$$

In these we put

$$x = -a + at/K \quad (17)$$

Then, at $y = b$ in the interval $2K \geq t \geq 0$, we have

$$\frac{d\zeta}{dz} = \frac{2kK^2\sqrt{k}}{a} \frac{\operatorname{sn} t}{(1\sqrt{k} \operatorname{cn} t - \operatorname{dn} t)^2},$$

and

$$\left| \frac{d\zeta}{dz} \right| = \frac{2K(1-k)\sqrt{k}}{a} \frac{\operatorname{sn} t}{1-k\operatorname{sn}^2 t} \quad (18)$$

We expand the function $\operatorname{sn} t/(1-k\operatorname{sn}^2 t)$ in a Fourier series of the form $\sum a_n \cos(n\pi t/2K) + b_n \sin(n\pi t/2K)$. The function being uneven, we know beforehand that the coefficients a_n must vanish. Disregarding this for the moment, we have

$$2Ka_n = \int_{-2K}^{2K} \frac{\operatorname{sn} t}{1-k\operatorname{sn}^2 t} \cos \frac{n\pi t}{2K} dt,$$

$$2Kb_n = \int_{-2K}^{2K} \frac{\operatorname{sn} t}{1-k\operatorname{sn}^2 t} \sin \frac{n\pi t}{2K} dt$$

and

$$(a_n + ib_n) 2K = \int_{-2K}^{2K} \frac{\operatorname{sn} t}{1-k\operatorname{sn}^2 t} e^{i(n\pi t/2K)} dt = I, \quad (19)$$

To evaluate I we treat t as complex, and take the contour integral

$$\int \frac{\operatorname{sn} t}{1-k\operatorname{sn}^2 t} e^{i(n\pi t/2K)} dt$$

round the rectangle in the t plane with vertices at $-2K$, $2K$, $2K + 2iK'$, $-2K + 2iK'$. Since the elliptic function has the periods $4K$, $2iK'$, and the exponential function has the period $4K$, the contour integral is $(1-q^n)I$, where $q = e^{-\pi K'/K}$. The contour integral is equal to the product of $2\pi i$ and the sum of the residues of the function at those of its poles that are within the contour. These poles are at $\pm K + \frac{1}{2}iK'$ and $\pm K + \frac{3}{2}iK'$. The residue at any pole is the value of

$$-\frac{e^{i(n\pi t/2K)}}{2k \operatorname{cn} t \operatorname{dn} t}$$

at that pole. It follows that the contour integral is equal to

$$2\pi i \left\{ \frac{e^{in\pi/2} q^{n/4}}{2i(1-k)\sqrt{k}} - \frac{e^{-in\pi/2} q^{n/4}}{2i(1-k)\sqrt{k}} - \frac{e^{in\pi/2} q^{3n/4}}{2i(1-k)\sqrt{k}} + \frac{e^{-in\pi/2} q^{3n/4}}{2i(1-k)\sqrt{k}} \right\},$$

or we have

$$I = \frac{\pi}{(1-k)\sqrt{k}} 2i \sin \frac{n\pi}{2} \frac{q^{n/4}}{1+q^{n/2}} \quad (20)$$

We have the result that, at $y = b$ in the interval $a \geq x \geq -a$,

$$\left| \frac{d\zeta}{dz} \right| = \frac{\pi}{a} \sum_{n=0}^{\infty} \operatorname{sech} \frac{(2n+1)\pi b}{2a} \cos \frac{(2n+1)\pi x}{2a} \quad (21)$$

In the same way it can be proved that, at $x = a$, in the interval $b \geq y \geq -b$,

$$\left| \frac{d\zeta}{dz} \right| = \frac{\pi}{b} \sum_{n=0}^{\infty} \operatorname{sech} \frac{(2n+1)\pi a}{2b} \cos \frac{(2n+1)\pi y}{2b} \quad (22)$$

5 Reverting to the problem of § 3, we determine χ as the sum of two bi-harmonic functions χ_1 and χ_2 , where χ_1 is of the form

$$\chi_1 = \sum_{m=0}^{\infty} A_m \left(\frac{x \sinh \mu x}{a \sinh \mu a} - \frac{\cosh \mu x}{\cosh \mu a} \right) \cos \mu y, \quad (23)$$

μ being $(2m+1)\pi/2b$, and χ_2 is of the form

$$\chi_2 = \sum_{n=0}^{\infty} B_n \left(\frac{y \sinh \nu y}{b \sinh \nu b} - \frac{\cosh \nu y}{\cosh \nu b} \right) \cos \nu x, \quad (24)$$

ν being $(2n+1)\pi/2a$. At the edges $y = \pm b$, χ_1 satisfies the conditions

$$\chi_1 = 0, \quad \nabla^2 \chi_1 = 0,$$

at the edges $x = \pm a$, it satisfies the condition $\chi_1 = 0$, and, at these edges, it will satisfy the condition

$$\nabla^2 \chi_1 = -4a \left| \frac{d\zeta}{dz} \right|,$$

if

$$2A_m \frac{\mu \cosh \mu a}{a \sinh \mu a} = -4a \frac{\pi}{b} \operatorname{sech} \mu a \quad (25)$$

The coefficients B_n can be determined in the same way, and we have the solution of the problem in the form

$$\begin{aligned} w = \frac{P}{8\pi D} & \left[(x^2 + y^2) \log \rho \right. \\ & + 4a^2 \sum_{m=0}^{\infty} \frac{\sinh \mu a}{(2m+1) \cosh^2 \mu a} \left(\frac{\cosh \mu x}{\cosh \mu a} - \frac{x \sinh \mu x}{a \sinh \mu a} \right) \cos \mu y \\ & \left. + 4b^2 \sum_{n=0}^{\infty} \frac{\sinh \nu b}{(2n+1) \cosh^2 \nu b} \left(\frac{\cosh \nu y}{\cosh \nu b} - \frac{y \sinh \nu y}{b \sinh \nu b} \right) \cos \nu x \right], \quad (26) \end{aligned}$$

μ and ν being $(2m+1)\pi/2b$ and $(2n+1)\pi/2a$

This problem of the centrally loaded isotropic rectangular plate, supported at all four edges, was solved by Hencky,* by starting with the form (2), and he

* H. Hencky, "Der Spannungszustand in rechteckigen Platten" (Diss.), München, 1913

completed the solution for a square ($a = b$). The problem is simplified very much by starting, as above, with the form (12). I have verified that, when $a = b$, the above formula (26) and Hencky's formulae lead to the same numerical value for the central deflexion, viz., $(0.1457) (Pa^2/\pi D)$.

6 The bi-harmonic function f_1 will be useful in the problem of the plate supported at the edges $x = \pm a$, and free at the edges $y = \pm b$. The conditions to be satisfied in this problem were laid down in § 1. For brevity we write

$$\lambda_0 = (x^2 + y^2) \log p$$

Then we seek a solution in the form

$$w = (P/8\pi D) (f_0 + f_1 + f_2 + f_3 + f_4), \quad (27)$$

where f_1 is the function so denoted in § 5, and all the functions f_1, f_2, f_3, f_4 are bi-harmonic, and are even functions of both x and y .

The function χ_0 expresses a displacement, vanishing at all the edges, and maintained by central load and by certain flexural couples and transverse forces at the edges, and the function f_1 has been adjusted to give no flexural couple at the edges $y = \pm b$, and to give no displacement at any edge, and so that the flexural couples answering to it at the edges $x = \pm a$ balance those answering to f_0 .

All the functions f_2, f_3, f_4 will be adjusted to give no displacement and no flexural couple at the edges $x = \pm a$.

The function f_2 will be adjusted to give no transverse force at the edges $y = \pm b$, and so that the flexural couples answering to it at these edges balance those answering to f_0 .

The functions f_3 and f_4 will be adjusted to give no flexural couple at the edges $y = \pm b$. The transverse forces answering to f_3 at these edges will balance those answering to χ_0 , and the transverse forces answering to f_4 at these edges will balance those answering to f_1 .

The combined solution gives no displacement or flexural couple at the edges $x = \pm a$, and no flexural couple or transverse force at the edges $y = \pm b$.

7 The boundary conditions satisfied by f_2 are, at the edges $x = \pm a$,

$$f_2 = 0, \quad \nabla^2 f_2 = 0, \quad (28)$$

and at the edges $y = \pm b$,

$$\frac{\partial}{\partial y} \left\{ \nabla^2 f_2 + (1 - \sigma) \frac{\partial^2 \chi_2}{\partial x^2} \right\} = 0, \quad \left\{ \nabla^2 - (1 - \sigma) \frac{\partial^2}{\partial x^2} \right\} (f_0 + f_2) = 0 \quad (29)$$

We seek a solution in the form

$$f_2 = \sum_{n=0}^{\infty} (B_n \cosh ny + B_n' \sinh ny) \cos nx,$$

v being $(2n+1)\pi/2a$. This satisfies conditions (28), and it will satisfy the first of conditions (29) if, at $y = \pm b$,

$$\frac{\partial}{\partial y} \{2v^2 B_n \cosh vy - (1-\sigma)v^2 (B_n vy \sinh vy + B_n' \cosh vy)\} = 0,$$

that is, if

$$B_n \{(1+\sigma) \sinh vb - (1-\sigma) vb \cosh vb\} - B_n' (1-\sigma) \sinh vb = 0$$

so that χ_2 can be expressed in the form

$$\chi_2 = \sum_{n=0}^{\infty} B_n [vy \sinh vy - \{vb \coth vb - (1+\sigma)/(1-\sigma)\} \cosh vy] \cos vx \quad (30)$$

At the edge $y = b$, $\log \rho$ and its x -derivatives vanish, and $\nabla^2 \chi_0 = 4b |d\zeta/dz|$, and therefore the contribution of χ_0 to the left-hand member of the second of conditions (29) is

$$4\pi(b/a) \sum_{n=0}^{\infty} \operatorname{sech} vb \cos vx$$

The contribution of f_2 to the same is

$$\sum_{n=0}^{\infty} B_n \{2v^2 \cosh vb + (1+\sigma)v^2 (vb \sinh vb - vb \coth vb \cosh vb) + (1+\sigma)v^2 \cosh vb\} \cos vx$$

Hence this condition is satisfied if

$$B_n = -\frac{4\pi b}{v^2 a} \frac{\tanh vb}{(3+\sigma) \cosh vb \sinh vb - (1-\sigma) vb} \quad (31)$$

The function χ_2 is determined by the formulæ (30) and (31)

8 The boundary conditions satisfied by χ_3 are, at the edges $x = \pm a$

$$\chi_3 = 0, \quad \nabla^2 \chi_3 = 0, \quad (32)$$

and, at the edges $y = \pm b$,

$$\nabla^2 \chi_3 - (1-\sigma) \frac{\partial^2 \chi_3}{\partial x^2} = 0, \quad \frac{\partial}{\partial y} \left[\left\{ \nabla^2 + (1-\sigma) \frac{\partial^2}{\partial x^2} \right\} (\chi_0 + \chi_2) \right] = 0 \quad (33)$$

We seek a solution in the form

$$\chi_3 = \sum_{n=0}^{\infty} (C_n' vy \sinh vy + C_n'' \cosh vy) \cos vx,$$

v being $(2n+1)\pi/2a$. This satisfies conditions (32), and it will satisfy the first of conditions (33) if

$$2C_n' \cosh vb + (1-\sigma)(C_n' vb \sinh vb + C_n'' \cosh vb) = 0$$

We therefore take γ_3 to have the form

$$\chi_3 = \sum_{n=0}^{\infty} C_n \left\{ \frac{vy \sinh vy}{vb \sinh vb + \{2/(1-\sigma)\} \cosh vb} - \frac{\cosh vy}{\cosh vb} \right\} \cos vx \quad (34)$$

To determine the constants C_n we have to express the contribution of f_0 to the left-hand member of the second of conditions (33). We have

$$\frac{\partial \chi_0}{\partial y} = 2y \log \rho + (x^2 + y^2) \frac{\partial \log \rho}{\partial y},$$

and

$$\begin{aligned} \nabla^2 \frac{\partial \chi_0}{\partial y} &= 4 \frac{\partial \log \rho}{\partial y} + \left\{ 4 \frac{\partial \log \rho}{\partial y} + 4 \left(x \frac{\partial}{\partial x} + y \frac{\partial}{\partial y} \right) \frac{\partial \log \rho}{\partial y} \right\} \\ &= 8 \frac{\partial \rho}{\partial y} + 4x \frac{\partial}{\partial x} \left(\frac{1}{\rho} \frac{\partial \rho}{\partial y} \right) - 4y \frac{\partial^2 \log \rho}{\partial x^2} \end{aligned}$$

Along the edge $y = b$, where ρ is constantly 1 for all values of x , and $\partial \rho / \partial y$ is $|d\zeta/dx|$, this gives

$$\frac{\partial}{\partial y} \nabla^2 f_0 = 4 \left(x \frac{\partial}{\partial x} + 2 \right) \left| \frac{d\zeta}{dx} \right|$$

Again

$$\frac{\partial^2}{\partial x^2} \frac{\partial \chi_0}{\partial y} = 2y \frac{\partial^2 \log \rho}{\partial x^2} + 2 \frac{\partial \log \rho}{\partial y} + 4x \frac{\partial}{\partial x} \frac{\partial \log \rho}{\partial y} + (x^2 + y^2) \frac{\partial^3}{\partial x^2} \frac{\partial \log \rho}{\partial y}$$

and, therefore, along the edge $y = b$,

$$\frac{\partial}{\partial y} \frac{\partial^2 \chi_0}{\partial x^2} = \left\{ 2 + 4x \frac{\partial}{\partial x} + (x^2 + b^2) \frac{\partial^2}{\partial x^2} \right\} \left| \frac{d\zeta}{dx} \right|$$

It follows that the contribution of χ_0 to the left-hand member of the second of conditions (33) is

$$\left\{ (10 - 2\sigma) + 4(2 - \sigma)x \frac{\partial}{\partial x} + (1 - \sigma)(x^2 + b^2) \frac{\partial^2}{\partial x^2} \right\} \left| \frac{d\zeta}{dx} \right| \quad (35)$$

In this we may take, according to (21),

$$\left| \frac{d\zeta}{dx} \right| = \frac{\pi}{a} \sum_{l=0}^{\infty} \operatorname{sech} \lambda b \cosh \lambda x, \quad (21, b_{1s})$$

λ being written for $(2l+1)\pi/2a$, and we have to express (35) as a series of the type $\Sigma \gamma_n \cos nx$ in the interval $a > x > -a$.

9 To this end we begin by observing that the series in the right-hand member of (21, b_{1s}) can be differentiated term by term as often as may be wished, for the coefficients $\operatorname{sech} \lambda b$ secure uniformity of convergence of the derived series. Thus we have, in the interval $a > x > -a$,

$$\left. \begin{aligned} x \frac{d}{dx} \left| \frac{d\zeta}{dx} \right| &= \frac{\pi}{a} \sum_{l=0}^{\infty} (-\lambda x \operatorname{sech} \lambda b \sinh \lambda x), \\ (x^2 + b^2) \frac{d^2}{dx^2} \left| \frac{d\zeta}{dx} \right| &= \frac{\pi}{a} \sum_{l=0}^{\infty} \{ -\lambda^2 (x^2 + b^2) \operatorname{sech} \lambda b \cosh \lambda x \} \end{aligned} \right\} \quad (36)$$

The functions represented in the above interval by the series in the right-hand members of (36) are even in x , and they are capable of expansion by Fourier

series, for they are continuous and have continuous derivatives of all orders at every point within the interval. We wish to expand them in Fourier series of cosines of multiples of $\pi x/2a$. Before it can be expanded in such a series, a function, even in x , must be defined in a wider interval $2a > x > -2a$. Let $f(x)$ denote the function to be expanded, and let a new function $F(x)$ be defined by the conditions

$$\left. \begin{aligned} \text{in } a > x > -a, \quad F(x) &= f(x), \\ \text{in } 2a > x > a, \quad F(x) &= -f(2a - x), \\ \text{in } -2a < x < -a, \quad F(x) &= -f(2a + x) \end{aligned} \right\} \quad (37)$$

Then $F(x)$ is defined at all points of the interval $2a > x > -2a$ except the end points and the points $x = \pm a$, at which it is, and legitimately may be, left undefined. The function $F(x)$ can be expanded in a Fourier series of cosines of multiples of $\pi x/2a$, and this series is convergent, and its sum is $f(x)$, at every point in the sub-interval $a > x > -a$. Further it can be proved without difficulty that all the coefficients of cosines of even multiples of $\pi x/2a$ are zero, and that, if the series is

$$F(x) = \sum_{n=0}^{\infty} \alpha_n \cos vx,$$

then

$$\alpha_n a = 2 \int_0^a f(x) \cos vx dx, \quad (38)$$

v being $(2n+1)\pi/2a$.

10 To apply this process to the functions represented by the right-hand members of (36) we have to evaluate the integrals

$$\int_0^a \sum_{l=0}^{\infty} (-\operatorname{sech} \lambda b - \lambda x \sin \lambda x) \cos vx dx = U_n \text{ say,}$$

and

$$\int_0^a \sum_{l=0}^{\infty} (-\operatorname{sech} \lambda b - \lambda^2 x^2 \cos \lambda x) \cos vx dx = V_n \text{ say,}$$

λ being $(2l+1)\pi/2a$, and v being $(2n+1)\pi/2a$. The factor $\operatorname{sech} \lambda b$ secures uniformity of convergence, and therefore the order of the operations summation and integration may be interchanged. We thus find

$$\left. \begin{aligned} U_n &= -\frac{a}{4} \left\{ -\operatorname{sech} \lambda b + (2n+1) \sum_{l=0}^{\infty} \frac{2l+1}{(l-n)(l+n+1)} (-1)^{l+n} \operatorname{sech} \lambda b \right\} \\ V_n &= -\frac{a}{4} \left\{ \left(\frac{2}{3} v^2 a^2 - 1 \right) \operatorname{sech} \lambda b \right. \\ &\quad \left. + (2n+1) \sum_{l=0}^{\infty} \frac{(2l+1)^2}{(l-n)^2 (l+n+1)^2} (-1)^{l+n} \operatorname{sech} \lambda b \right\} \end{aligned} \right\}, \quad (39)$$

where the accents attached to the signs of summation indicate that the terms in which $l = n$ are to be omitted from the sums

If we write

$$\left. \begin{aligned} L_n &= \sum_{l=0}^{\infty} (-1)^l \frac{2l+1}{(l-n)(l+n+1)} \operatorname{sech} \lambda b \\ M_n &= \sum_{l=0}^{\infty} (-1)^l \frac{(2l+1)^3}{(l-n)^2(l+n+1)^2} \operatorname{sech} \lambda b \end{aligned} \right\}, \quad (40)$$

the expression (35), which is the contribution of f_0 to the left-hand member of (33), will become

$$\begin{aligned} (\pi/a) \sum_{n=0}^{\infty} \{ [6 + \frac{1}{2}(1-\sigma) - (1-\sigma)v^2(b^2 + \frac{1}{3}a^2)] \operatorname{sech} \lambda b \\ + (-1)^n (2n+1) \{ 2(2-\sigma)L_n - \frac{1}{2}(1-\sigma)M_n \} \} \cos vx \end{aligned} \quad (41)$$

The contribution of f_3 to the left-hand member of (33) is found, after a little reduction, to be

$$\frac{1}{b} \sum_{n=0}^{\infty} C_n v^2 \frac{(3+\sigma) \tanh \lambda b - (1-\sigma) \lambda b \operatorname{sech}^2 \lambda b}{\tanh \lambda b + 2/(1-\sigma) \lambda b} \cos vx, \quad (42)$$

and thus the coefficients C_n are determined by the equation

$$\begin{aligned} C_n &= \frac{\pi b}{a} \frac{\tanh \lambda b + 2/(1-\sigma) \lambda b}{(3+\sigma) \tanh \lambda b - (1-\sigma) \lambda b \operatorname{sech}^2 \lambda b} \\ &\times \left[\left\{ (1-\sigma)(b^2 + \frac{1}{3}a^2) - \frac{13-\sigma}{2v^2} \right\} \operatorname{sech} \lambda b \right. \\ &\left. + (-1)^{n+1} \frac{4a^2}{(2n+1)\pi^2} \{ 2(2-\sigma)L_n - \frac{1}{2}(1-\sigma)M_n \} \right], \end{aligned} \quad (43)$$

where L_n and M_n are given by (40). These coefficients being known, the function χ_3 is given by (34)

11 The boundary conditions satisfied by χ_4 are, at $x = \pm a$,

$$\chi_4 = 0, \quad \nabla^2 \chi_4 = 0, \quad (44)$$

and, at $y = \pm b$,

$$\nabla^2 \chi_4 - (1-\sigma) \frac{\partial^2 \chi_4}{\partial x^2} = 0, \quad \frac{\partial}{\partial y} \left\{ \nabla^2 + (1-\sigma) \frac{\partial^2}{\partial x^2} \right\} (\chi_1 + \chi_4) = 0 \quad (45)$$

Just as in § 8 we find that the first three conditions are satisfied by taking χ_4 to have the form

$$\chi_4 = \sum_{n=0}^{\infty} D_n \left\{ \frac{vy \sinh vy}{b \sinh \lambda b + \{2/(1-\sigma)\} \cosh \lambda b} - \frac{\cosh vy}{\cosh \lambda b} \right\} \cos vx \quad (46)$$

To determine the coefficients D_n we have to express the contribution of χ_2 to the left-hand member of the second of conditions (45) at the edge $y = b$. We may write χ_1 in the form

$$\chi_1 = 4a^2 \sum_{k=0}^{\infty} \frac{\sinh \kappa a}{(2k+1) \cosh^2 \kappa a} \left(\frac{\cosh \kappa x}{\cosh \kappa a} - \frac{x \sinh \kappa x}{a \sinh \kappa a} \right) \cos \kappa y, \quad (47)$$

κ being $(2k+1)\pi/2b$. Then this contribution will be found, after a little reduction, to be

$$4a \sum_{k=0}^{\infty} (-1)^k \frac{\kappa^2 \sinh \kappa a}{(2k+1) \cosh^2 \kappa a} \left[\left(\frac{2(2-\sigma)}{\sinh \kappa a} - (1-\sigma) \frac{\kappa a}{\cosh \kappa a} \right) \cosh \kappa x + (1-\sigma) \frac{\kappa x \sinh \kappa x}{\sinh \kappa a} \right] \quad (48)$$

Just as in § 9 we expand this expression in a series of the form $\Sigma \gamma_n \cos vx$, valid in the interval $a > x > -a$. We put

$$\left. \begin{aligned} \cosh \kappa x &= \sum_{n=0}^{\infty} \alpha_n' \cos vx \\ x \sinh \kappa x &= \sum_{n=0}^{\infty} \beta_n' \cos vx \end{aligned} \right\} \quad (49)$$

Then

$$\begin{aligned} \alpha_n' a &= \int_{-a}^a \cosh \kappa x \cos vx \, dx, \\ \beta_n' a &= \int_{-a}^a x \sinh \kappa x \cos vx \, dx \end{aligned}$$

On performing the integrations it is found that

$$\left. \begin{aligned} \alpha_n' &= (-1)^n \frac{2v}{\kappa^2 + v^2} \frac{\cosh \kappa a}{a}, \\ \beta_n' &= (-1)^n \left\{ \frac{2v}{\kappa^2 + v^2} \sinh \kappa a - \frac{4\kappa v}{(\kappa^2 + v^2)^2} \frac{\cosh \kappa a}{a} \right\} \end{aligned} \right\} \quad (50)$$

Hence the contribution of χ_1 to the left-hand member of the second of conditions (45) at $y = b$ is

$$16 \sum_{n=0}^{\infty} (-1)^n v \left[\sum_{k=0}^{\infty} (-1)^k \frac{\operatorname{sech} \kappa a}{2k+1} \left\{ (2-\sigma) \frac{\kappa^2}{\kappa^2 + v^2} - (1-\sigma) \frac{\kappa^4}{(\kappa^2 + v^2)^2} \right\} \right] \cos vx \quad (51)$$

The contribution of χ_4 to the same is found, as in § 10, to be

$$\frac{1}{b} \sum_{n=0}^{\infty} D_n v^2 \frac{(3+\sigma) \tanh vb - (1-\sigma) vb \operatorname{sech}^2 vb}{\tanh vb + 2/[(1-\sigma) vb]} \cos vx, \quad (52)$$

and thus the coefficients D_n are determined by the equation

$$D_n = -16b \frac{(-1)^n}{v} \frac{\tanh vb + 2\{(1-\sigma)vb\}}{(3+\sigma)\tanh vb - (1-\sigma)vb \operatorname{sech}^2 vb} \\ \times \sum_{k=0}^{\infty} (-1)^k \frac{\operatorname{sech} \kappa a}{2k+1} \left\{ (2-\sigma) \frac{\kappa^2}{\kappa^2 + v^2} - (1-\sigma) \frac{\kappa^4}{(\kappa^2 + v^2)^2} \right\}, \quad (53)$$

v being $(2n+1)\pi/2a$, and κ being $(2k+1)\pi/2b$. These coefficients being known, χ_4 is given by (46)

All the terms of the solution expressed by (27) have now been found, and the problem is solved

12 From time to time it has been proposed to determine elastic constants, especially of crystals, by measuring, by an interferential method, the central deflexion of a centrally loaded rectangular plate, supported at two opposite edges. Reference may be made to a paper by A. E. H. Tutton,* where will be found an account of previous work on similar lines, and to a recent paper by W. Mandell†. Such measurements can be made with great accuracy, but, in order to infer the values of the elastic constants, it is necessary to apply a formula for the central deflexion of a plate so loaded and supported. The theory of crystalline plates has not been made out, and, unless the plates are thick enough (in proportion to their breadths) and narrow enough (in proportion to their lengths) to be treated as bars, no formula is available. For a long thin narrow bar, loaded centrally, and supported at its ends, there would be a formula for the central deflexion w_0 , which, in the notation of this paper, would be

$$w_0 = Pa^3/8Eh^3b, \quad (54)$$

and this would hold for a bar of crystalline material, provided that E is the Young's modulus of the material, answering to tension in the direction of the length of the bar‡.

The method could, of course, be used for isotropic materials, and then there would be available the formulæ of this paper. From these it would appear that the central deflexion w_0 of the plate, besides being inversely proportional to the Young's modulus E of the material, would depend also, in a way that is by no means simple, on the Poisson's ratio σ . In order to test, or exemplify, the approximation to the bar formula (54) as the ratio a/b increases, and to illustrate the dependence of the central deflexion on the value of σ , I calculated the values

* 'Phil. Trans.,' A, vol. 202, p. 143 (1904).

† 'Roy. Soc. Proc.,' A, vol. 116, p. 623 (1927).

‡ This is the formula used by Mandell.

of the quantity $w_0 E h^3 / P a^2$ for various values of the ratio a/b , and for two values of σ , viz., $\frac{1}{3}$ and $\frac{1}{2}$, between which the Poisson's ratios of many isotropic materials are known to lie. The results are recorded in the following table, where, in the line following the letter "B," is given the result of applying the bar formula (54) —

Table of $w_0 E h^3 / P a^2$

$\sigma \backslash a/b$	1,	2	3	4
$\frac{1}{3}$	0.1240	0.2230	0.3580	0.4878
$\frac{1}{2}$	0.1305	0.2344	0.3693	0.4918
B	0.1250	0.2300	0.3750	0.5000

It will be seen that the values of the Young's modulus, for isotropic material, that might be inferred by applying the formula (54) to a plate, of which the length is four times the breadth, would be likely to be affected by an error of about 2 per cent, the inferred values being too great, and the exact amount of the error depending upon the Poisson's ratio of the material.

It may be observed that, if there were any effective instrumental method of measuring the central deflexion of a centrally-loaded rectangular plate of isotropic material, supported at all four edges, the theory of § 5 of this paper would lead to a very exact determination of the constant $E/(1 - \sigma^2)$ for the material.

Relativity and Wave Mechanics *

By W. WILSON, F.R.S., Hildred Carlile Professor of Physics in the University of London

(Received, February 9, 1928)

The equations of motion of a charged particle can be expressed in the following general form†

$$\left(\frac{\partial \Pi_\lambda}{\partial q^\lambda} - \frac{\partial \Pi_\lambda}{\partial \tau} \right) \frac{dq^\lambda}{d\tau} = 0, \quad (1)$$

where

$$\Pi_\lambda = p_\lambda + eA_\lambda,$$

$$p_\lambda = m_0 g_{\lambda\lambda} \frac{dq^\lambda}{d\tau},$$

and A is the potential of the electromagnetic field in which the particle is moving, e is the charge on the particle, m_0 is its proper mass and τ is the proper time. Where summation is implied it is extended over values of the indices from $\lambda = 1$ to $\lambda = 4$. Equations (1) do not represent geodesics in the space-time continuum except in the special case where Π_λ reduces to the "mechanical momentum" p_λ . A very slight formal modification suffices, however, to convert them into equations representing a geodesic in a 5-dimensional continuum. To accomplish this we extend the metrical tensor $g_{\lambda\lambda}$ by introducing new components defined by

$$g_{5\lambda} = g_{\lambda 5} = -A_\lambda,$$

as well as a component g_{55} , the significance of which will be left for subsequent investigation. The momentum Π can now be put in the form

$$\Pi_\lambda = m_0 g_{\lambda\lambda} \frac{dq^\lambda}{d\tau}, \quad (\lambda = 1, 2, 3, 4, 5)$$

* Dr H. I. Flint has drawn my attention to a recent paper by O. Klein ('Z. f. Physik,' vol. 46, p. 188 (1928)) in which an extension to five dimensions, exactly similar to that given in the present paper, is described. The corresponding part of this paper was written some time ago and without any knowledge of Klein's work, and it is a fairly obvious corollary to ideas contained in the paper by the writer to which reference is made ('Roy. Soc. Proc., A,' vol. 102, p. 478 (1922)).

† 'Roy. Soc. Proc., A,' vol. 102, p. 478 (1922).

Since

$$g_{\alpha\beta} = \Lambda_{\alpha},$$

we must have

$$m_0 \frac{dq^\lambda}{d\tau} = e. \quad (2)$$

If we now extend the summation in equations (1) from $\lambda = 1$ to $\lambda = 5$ and add a fifth equation

$$\left(\frac{\partial H_5}{\partial q^\lambda} - \frac{\partial H_\lambda}{\partial q^5} \right) \frac{dq^\lambda}{d\tau} = 0, \quad (3)$$

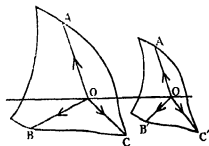
we shall have the equations of a geodesic in a 5-dimensional continuum, and we shall refer to them as the extended equations (1). It is suggested that the extended equations may have more than a formal significance, i.e., the component g_{55} and the co-ordinate q^5 may have some, at present unknown, physical significance.

Equations (1), as extended, can be expressed in the following equivalent form

$$\oint \Pi_\alpha dq^\alpha = 0, \quad (\alpha = 1, 2, 3, 4, 5), \quad (4)$$

where the limits of the integral are the continuous points of the actual path of the particle (a part of its "world line") and a neighbouring path. In fact the extended equations (1) can be derived from (4) by applying the theorem of Stokes. Equation (4) is an extended Hamilton's Principle.*

Let O and O' be neighbouring points on the world line of an electron (or any particle) and let ABC $A'B'C'$ be surfaces enclosing small volumes in



the 5-dimensional continuum and containing O and O' respectively. We shall regard $A'B'C'$ as the "parallel displacement" of ABC corresponding to the interval OO' . By this is meant that if ABC is the locus of the end points of displacement vectors OA, OB, OC, \dots , then $A'B'C'$ is the locus of the end points of the vectors OA', OB', OC', \dots which are the parallel displacements of OA, OB, OC respectively. For the sake of generality we will leave the metric of the continuum undefined. It is obviously permissible to contemplate other metrics than that associated with the fundamental tensor whose components $g_{\alpha\beta}$

* Roy Soc Proc., A, vol 102, p 481 (1922)

describe the gravitational and, in the theory now put forward, also the electromagnetic field in which the particle is moving. The metrical tensor implied in the volumes ABC $A'B'C'$ will be represented by $\mu_{\alpha\lambda}$ and we shall use μ to represent the determinant of the $\mu_{\alpha\lambda}$ and the symbol $\gamma_{\alpha\beta}^*$ to represent the Christoffel bracket expression

$$\frac{1}{2}\mu^{\alpha\lambda}\left(\frac{\partial\mu_{\alpha\lambda}}{\partial q^\beta}+\frac{\partial\mu_{\beta\lambda}}{\partial q^\alpha}-\frac{\partial\mu_{\alpha\beta}}{\partial q^\lambda}\right)$$

The contracted Christoffel expression $\gamma_{\alpha\beta}^*$ will be denoted by $\gamma_{\alpha\beta}$.

The volume ABC is represented by the integral

$$V = \int \int \mu^{\frac{1}{2}} dq^1 dq^2 \dots dq^5$$

To get an expression for the increment of this due to the displacement from O to O' it will suffice to consider the increment

$$\delta(\mu^{\frac{1}{2}} dq^1 \dots dq^5)$$

or

$$\delta(\mu^{\frac{1}{2}} \xi^1 \dots \xi^5),$$

if we write

$$dq^1 = \xi^1,$$

$$dq^2 = \xi^2,$$

and so on. The general expression for a parallel displacement is

$$\delta \xi^\alpha = -\Gamma_{\alpha\beta}^\alpha \xi^\beta \delta q^\beta,$$

and since the vectors

$$dq^\alpha = \xi^\alpha$$

in the integral have each only one component we have

$$\delta \xi^1 = -\Gamma_{1\alpha}^1 \xi^\alpha \delta q^\alpha,$$

$$\delta \xi^2 = -\Gamma_{2\alpha}^2 \xi^\alpha \delta q^\alpha$$

$$\delta \xi^5 = -\Gamma_{5\alpha}^5 \xi^\alpha \delta q^\alpha,$$

and therefore

$$\frac{\delta(\xi^1 \xi^2 \dots \xi^5)}{\xi^1 \xi^2 \dots \xi^5} = -\Gamma_\alpha \delta q^\alpha, \quad (5)$$

where

$$\Gamma_\alpha = \Gamma_{\beta\alpha}^\beta$$

It is known that

$$\frac{\delta \mu^{\frac{1}{2}}}{\mu^{\frac{1}{2}}} = \gamma_\alpha \delta q^\alpha \quad (6)$$

Combining (5) and (6) we get

$$\frac{\delta(\mu^1 dq^1}{\mu^1 dq^1} \frac{dq^1}{dq^a}) = (\gamma_a - \Gamma_a) \delta q^a$$

It follows therefore that the increment of the small volume ABC is expressed by

$$\frac{\delta \left| \int \mu^1 dq^1 \right|}{\int \mu^1 dq^1} = (\gamma_a - \Gamma_a) \delta q^a$$

or

$$\delta V/V = K_a \delta q^a, \quad (7)$$

where the vector $\gamma_a - \Gamma_a$ is denoted by K_a .

We will now adopt such a metric (assuming this to be possible) that

$$K_a = a \Pi_a \quad (8)$$

where a is a suitable universal constant

In the neighbourhood of a geodesic

$$\frac{\partial \Pi_a}{\partial q^b} = \frac{\partial \Pi_b}{\partial q^a},$$

and therefore

$$\Pi_a = \frac{\partial \chi}{\partial q^a},$$

where χ is some function of (q^1, q^2, \dots, q^n) and consequently

$$\frac{1}{V} \frac{\partial V}{\partial q^a} = K_a = a \Pi_a \quad (9)$$

The extended equations (1) are obviously unaffected by substituting for Π_a the vector

$$\Pi_a + \frac{\partial \eta}{\partial q^a},$$

where η is any function of (q^1, \dots, q^n)

The circumstances are exactly similar to those associated with the vector potential in electromagnetic problems, where it is usual to impose the condition that the divergence of the vector potential shall be zero. We shall therefore subject the arbitrary function η contained in Π to the condition expressed by

$$\text{div } \Pi = 0, \quad (10)$$

or, what is the same thing,

$$\frac{1}{\mu^4} \frac{\partial}{\partial q^x} \left\{ \mu^4 \mu^{x\lambda} \frac{1}{V} \frac{\partial V}{\partial q^\lambda} \right\} = 0$$

or, if we carry out the differentiation $\frac{\partial}{\partial q^x}$ and substitute $a\Pi_x$ for $\frac{1}{V} \frac{\partial V}{\partial q^x}$ (equation (9))

$$\frac{1}{\mu^4} \frac{\partial}{\partial q^x} \left\{ \mu^4 \mu^{x\lambda} \frac{\partial V}{\partial q^\lambda} \right\} = a^2 \mu^{x\lambda} \Pi_x \Pi_\lambda \quad (11)$$

If now a^2 be given the value $-4\pi^2/\hbar^2$ and if $\mu_{x\lambda} = m_0 g_{x\lambda}$ we see that (11) is Schrodinger's equation for a charged particle. The "volume" V is Schrodinger's function ψ . Equation (11) is really more general than Schrodinger's, since the summations with respect to κ and λ extend from 1 to 5. It becomes exactly Schrodinger's equation in certain limiting cases, for instance if V is independent of q^5 and if Π_5 is zero.

In a recent communication to the Society, H. T. Flint and J. W. Fisher have identified the Schrodinger function ψ with the gauge or metrical factor of space-time defined by

$$ds^2 = \lambda g_{x\lambda} dx^x dx^\lambda *$$

This view of the meaning of ψ has a close similarity to that adopted in the present paper.

Let us consider the case where the determinant, μ , is constituted as follows

$$\mu = \begin{vmatrix} \mu_{11} & 0 & 0 & 0 & 0 \\ 0 & \mu_{22} & 0 & 0 & 0 \\ 0 & 0 & \mu_{33} & 0 & 0 \\ 0 & 0 & 0 & \mu_{44} & \mu_{45} \\ 0 & 0 & 0 & \mu_{54} & \mu_{55} \end{vmatrix} \quad (12)$$

where the indices 1, 2, 3 refer to rectangular axes of co-ordinates, x, y, z respectively, and 4 refers to the time axis. This form of μ is suitable for dealing with an electron in what is approximately an electrostatic field. We easily find for the components of the contravariant metrical tensor μ^{xx}

$$\mu^{11} = 1/\mu_{11}, \quad \mu^{22} = 1/\mu_{22}, \quad \mu^{33} = 1/\mu_{33}, \quad \mu^{44} = \mu_{55}/(\mu_{44}\mu_{55} - \mu_{54}\mu_{45}) \quad (13)$$

and so on.

We shall now deal with a nuclear atom consisting of a nucleus with a charge Ne and a single electron with a charge $e' = -e$. The only way to advance is by

* 'Roy Soc. Proc.,' A, vol. 117, p. 625 (1928)

keeping reasonably close to the older theory, which must be somewhere near the truth. This forces us to regard μ as sensibly constant (for such a system as we are considering). We shall therefore write

$$\mu = -m_0 c^2 G, \quad (14)$$

where m_0 is the proper mass of the electron and G is a constant. We have

$$\mu_{11} = \mu_{22} = \mu_{33} = m_0, \quad (15)$$

$$\mu_{44} = -m_0 c^2, \quad \mu_{45} = \mu_{54} = -m_0 \phi,$$

where ϕ is the scalar (electro-static) potential. From (14) and (15) we have

$$\mu_{55} = m_0 (G - \phi^2/c^2) \quad (16)$$

Suppose further that

$$\Pi_5 = 0$$

This assumption is not so arbitrary as may appear at first sight. It may be regarded as part of the description of the model of the atom which has already the features represented by

$$\Pi_3 = \text{angular momentum} = \text{constant},$$

$$\Pi_4 = \text{constant},$$

and since we have introduced a fifth axis we shall suppose the corresponding momentum Π_5 to be constant and assign it the value zero.

Now

$$\Pi_5 = \mu_{54} \frac{dt}{d\tau} + \mu_{55} \frac{dq'}{d\tau},$$

therefore

$$-m_0 \phi \beta + \mu_{55} c' / m_0 = 0,$$

or

$$\mu_{55} = m_0^2 \phi \beta / c', \quad (17)$$

where β represents the ratio $\frac{dt}{d\tau}$.

Equations (16) and (17) impose a condition on β , which is *not now* identical with the $\frac{dt}{d\tau}$ in the ordinary restricted relativity. If the old relativistic expression for $\frac{dt}{d\tau}$ be represented by β_0 , we have of course

$$\beta_0 = (1 - v^2/c^2)^{-\frac{1}{2}}$$

From (16) and (17) we have

$$m_0 (G - \phi^2/c^2) = m_0^2 \phi \beta / c'$$

or

$$\beta = (G - \phi^2/c^2) c' / m_0 \phi \quad (18)$$

Putting $\phi = Ne/r$ and substituting in (18) we find, when r is very small

$$\beta = -Nec'/m_0c^2r \quad (19)$$

It is interesting to evaluate β_0 and compare it with β . We have (if we consider a circular orbit)

$$m_0\beta_0v^2/r = -Nec'/r^2,$$

and since $v^2 = c^2(1 - 1/\beta_0^2)$ we get

$$(\beta_0^2 - 1)/\beta_0 = -Nec'/m_0c^2r$$

or for small values of r

$$\beta_0 = -Nec'/m_0c^2r \quad (20)$$

If we make the final assumption that in the case we are considering the "wave" function V does not contain q^5 , so that terms like

$$\frac{\partial V}{\partial q^5} \quad \text{and} \quad \frac{\partial^2 V}{\partial q^5 \partial q^i}$$

vanish, then equation (11) becomes

$$\frac{\partial}{\partial q^i} \left(\mu^{\kappa i} \frac{\partial V}{\partial q^i} \right) = -\frac{4\pi^2}{h^2} \left(\Pi_{\kappa} \frac{dq^{\kappa}}{d\tau} \right) V, \quad (\kappa = 1, 2, 3, 4),$$

since μ is constant. From (13), (15) and (17), and from

$$\Pi_{\kappa} = p_{\kappa} \quad (\kappa = 1, 2, 3),$$

we get

$$\frac{1}{m_0} \nabla^2 V - \frac{\partial}{\partial t} \left(\beta \frac{\partial V}{\partial t} \right) = -\frac{4\pi^2}{h^2} \left(p_{\lambda} \frac{dq^{\lambda}}{d\tau} + E\beta \right) V, \quad (\lambda = 1, 2, 3), \quad (21)$$

where $E = m_0c^2\beta + e'\phi$ is the energy of the electron. This equation becomes identical with Schrodinger's equation for the hydrogen atom, as originally given,* if β is sensibly constant.

Equation (10) referred in the first instance to the immediate neighbourhood of the path of an electron or particle, while, in the guise of the wave equation, it is extended to hold everywhere. This assumes that Π has a meaning at places where there is no electron at all. In the wave equation $\Pi_{\kappa} dq^{\kappa}/d\tau$, but not Π_{κ} , is supposed to be given as a function of position, as are the $\mu^{\kappa i}$, etc., and the equation is therefore linear. A solution of it gives V , and consequently $\frac{1}{V} \frac{\partial V}{\partial q^i}$, at every point. If therefore any point and any direction, κ , whatever are selected, the solution of the wave equation gives the appropriate value of

* E. Schrodinger, 'Ann d. Phys.', vol. 79, p. 361 (1926).

Π_x , even if the electron is not present. Consequently the meaning to be attached to Π is the momentum the electron or particle would have if present at the point in question. We can now find a meaning for the wave function V (Schroedinger's ψ). If a particle at some instant is actually within a "volume" V_0 it will be within a volume V , which is the parallel displacement of V_0 , at some later (or earlier) instant. If its position at any time is unknown, the probability that it is in a specified volume will depend in some way on V . This is, in fact, the usual view of the meaning of V or ψ .

It is easy to see that in the case of neutral particles not under the influence of a gravitational or electromagnetic field, the wave equation (21) reduces to

$$\frac{1}{m_0} \nabla^2 V = \frac{1}{m_0 c^2} \frac{\partial^2 V}{\partial t^2} = - \frac{4\pi^2}{h^2} (-m_0 c^2) V,$$

or

$$\nabla^2 V = \frac{1}{c^2} \frac{\partial^2 V}{\partial t^2} = \frac{4\pi^2 m_0^2 c^2}{h^2} V \quad (22)$$

and therefore if there are neutral particles whose masses are sufficiently small, their wave equation (in the absence of a field) will be the familiar one for the propagation of light in empty space. This is in conformity with the original suggestions of L. de Broglie and it would appear that light (radiation) is a corpuscular phenomenon after all as Newton supposed it to be.

An X-Ray Study of some Simple Derivatives of Ethane —Part I

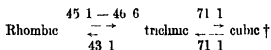
By KATHLEEN YARDLEY, M Sc (Mrs LONSDALE), Amy Lady Tate Scholar

(Communicated by Sir William Bragg, F R S - Received December 15 1927)

HEXACHLORETHANE — C_2Cl_6 Molecular weight, 236.76

This substance is typical of the halogen derivatives of ethane and will therefore be considered in some detail

Trimorphism — C_2Cl_6 is orthorhombic at ordinary temperatures, but at about 46°C it changes over to a trichinic form and at 71° the trichinic form becomes cubic*. The process is reversible —



Goszner points out that this trimorphism is also common to C_2Br_4 and to the so-called symmetrical and asymmetrical forms of $\text{C}_2\text{Cl}_4\text{Br}_2$, the four substances forming a completely isomorphous series. The transition temperatures in the case of symm $\text{C}_2\text{Cl}_4\text{Br}_2$ are 80° and 108° – 109°C . Those of the other two substances are not given in the literature. In the following paper only the orthorhombic forms have been studied.

Crystal Form — This has been described by Brooke,‡ Goszner§ and Federow||. Goszner gives

Orthorhombic bipyramidal

$$a \quad b \quad c = 0.5677 \quad 1 \quad 0.3160$$

$$\text{Density } \rho = 2.091 \text{ grs/cc}$$

The X-ray investigation described later shows that the a and c axes must be doubled. The forms observed on crystals grown from an alcohol + ether solution named in accordance with the true unit cell, are {100} {210} {101} and occasionally {010} {111}. The crystals, when viewed along the [010] direction, present a pseudo-hexagonal appearance (fig 1a) and this fact is

* Lehmann, 'Z f Kryst,' vol 1, p 106 (1877), *ibid*, vol 6, p 584 (1882)

† Schwarz, 'Z f Kryst,' vol 25, p 614 (1896), Goszner, *ibid*, vol 38, p 151 (1904)

‡ 'Ann Philos,' vol 23, p 364 (1824)

§ *Loc cit*, see also Groth, 'Chem Krystallographie,' vol 3, p 38

|| Federow, 'Das Krystallreich,' p 254

emphasised in Federow's setting. He defines the crystals of C_2Cl_6 and of its isomorphous relations as having the "complex symbol" $\begin{pmatrix} 6 \\ 61 \\ +1 \end{pmatrix}$ and renames the forms mentioned above as follows $\{010\bar{1}\}$ $\{110\bar{1}\}$ $\{0110\}$ and $\{1000\}$ $\{1110\}$

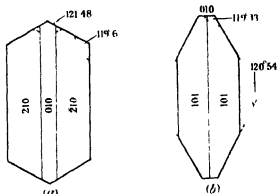


FIG 1

It should be noted, however, that in the $[001]$ direction the crystal also presents the appearance of a hexagon with two truncated corners (fig 1b). It will be seen later that the arrangement of the molecules in the unit cell accounts very simply for the pseudo-hexagonal appearance in the $[001]$ direction, but not so readily for that in the $[010]$.

No twinning or cleavage planes could be observed, nor were etch figures obtained for C_2Cl_6 . Gozner, however, records the following results of etching with ether on C_2Br_6 and $C_2Cl_4Br_2$ (symm), which may conveniently be inserted here, since they indicate the holohedry of the series.

On $\{100\}$ Eight-sided figures, having two edges parallel $[010]$, two parallel $[001]$ and two similar pairs parallel to the (100) (111) edges.

On $\{010\}$ Similar eight-sided figures, but with the last four edges having a different inclination.

On $\{210\}$ The figures were symmetrically disposed about all three symmetry planes.

X-Ray Goniometric Measurements—It was thought advisable to repeat the goniometric measurements for C_2Cl_6 as well as for the other members of the series, using the Bragg spectrometer simply as a goniometer. The method adopted was as follows. The position of the X-ray reflection on one side of a particular plane, say (210) , was carefully found, the slit of the ionisation chamber being wide open. Leaving the chamber in position the crystal was rotated

about the axis of the instrument until the reflection on the *same* side of the (210) or ($\bar{2}$ 10) entered the chamber. The angular distance between the two positions of the crystal gives the angle between the two planes. Other angles (110) (1 $\bar{1}$ 0), (230) ($\bar{2}$ 30), etc., can very quickly be measured, whether these planes occur as faces or not. In fact, the number of angles that can be measured in any zone is limited only by the intensity of the reflections from planes in that zone and by the patience of the observer. In the case of the optical goniometer the number and perfection of the occurring faces is the principal factor to be considered. This X-ray method is only applicable, of course, to orthogonal crystals, for which, however, it can give very accurate results. The X-ray method usually adopted, that of determining the exact angular positions of the reflecting planes, by observing the reflections from each side of them is much less accurate, since it involves a shift of the ionisation chamber. It is however, the only available one if the crystal is not orthogonal or if the angle between planes of different spacings is required. Photographic methods are far less reliable for goniometric measurements. A comparison of results for C_4Cl_6 follows —

	Brooke		Goszner		Yardley			
					(obs.)		(calc.)	
	°	'	°	'	°	'	°	'
(210) ($\bar{2}$ 10)	59	20	59	10	59	9	—	—
(230) ($\bar{2}$ 30)	—	—	—	—	119	6	119	8
(101) (10 $\bar{1}$)	58	0	58	12	58	5	—	—
(102) (10 $\bar{2}$)	—	—	—	—	31	2	31	2

Since the (230) and (102) planes do not occur as crystal faces, they were not available for optical measurement. The axial ratios calculated from the X-ray measurements are

$$a : b : c = 1 : 1.350 : 1.06302$$

Volatilisation of Crystals—On exposure to the air the edges of the crystals soon became rounded, and within a few hours the crystals had often disappeared. A series of time-intensity observations were therefore carried out, using a fresh crystal to begin with. A comparison was first made of the reflections from the (100) plane (fourth order), which is a well-developed face, and from the (001) plane (second order), which does not occur as a face at all. The complete reflection was plotted (ionisation current *v.* angle of deviation) for each plane at intervals of 30 minutes to 1 hour, the ionisation chamber slit being kept wide open throughout the observations. The "integrated reflection" obtained

by turning the crystal slowly and uniformly through the reflecting position was also measured at intervals, and a comparison was made with the NaCl (400) reflection

Curves *a*, *b* and *c* (fig 2) were obtained using a fairly small crystal. After about two hours the crystal unfortunately began to slip in its mount in such a

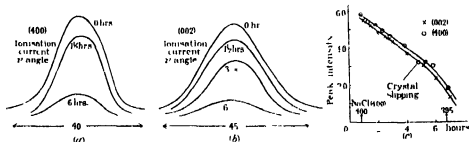


FIG. 2

way as to tilt the (100) plane while leaving the (001) plane vertical. The faces on the crystal, however, were still sufficiently recognisable for it to be replaced in position and the readings continued. The results showed that

- (1) The effects of volatilisation upon intensity are similar whether the plane examined is an occurring face or not
- (2) It is not dependent to any discernible extent on the spacing (2.88 Å for (400), 3.20 Å for (002))
- (3) The decrease in "peak intensity" is very nearly proportional to the time of exposure for the first few hours
- (4) The same is true of the "integrated intensity"

Other curves were obtained for the (400) and (002) reflections from a larger crystal, measuring about $5 \times 3 \times 2$ mm, which lasted for about 24 hours. At the end of the period of observation (23 hours) there were still quite moderate-sized {100} faces, though all other faces had completely disappeared and the crystal had become very thin in the [100] direction, with the result that after prolonged exposure the (400) reflection had diminished relatively less than the (002). In actual practice the crystals were never used when they had reached this stage. It is evident that the process of volatilisation is a simple surface effect and that the diminution of intensity with time is largely due to the decrease in area of the reflecting planes. In order to allow for this the crystals were chosen so that the planes in the zone to be examined were as far as possible of equal area, and one set of readings usually lasted about three hours. The reflection from one principal plane was measured at intervals and the reflections

from the remaining planes in the zone were increased proportionally to the times at which they were measured. Most of the intensities given in the tables are in terms of "peak ionisation current". The "integrated reflection" was only measured for the various orders of the main planes (100) (010) (001) (210) because, owing to the presence of a considerable amount of general radiation from the Rh target used, the peak current was much easier to measure during the limited time available for observations on each zone. Moreover, the two are found to be roughly proportional, and the integrated reflection is only really necessary where accurate calculation is to be based on the intensity observations. In order to make quite sure that the process of volatilisation would not affect the relative intensities of the reflections of different orders from any one plane, a separate investigation was carried out, the intensities of the two orders of (100) and of the four orders of (010) being measured at the beginning and end of an interval of some hours, during which time each intensity dropped to about one quarter of its former value. It was found that the intensity decreased proportionally for all the orders of either plane. The impossibility of grinding different faces on these soft, volatile crystals made accurate measurement of the "absolute intensity" quite out of the question. The intensity figures recorded for C_2Cl_6 and for the other substances may therefore only be regarded as relative. Also, it is not safe to compare the intensities of different planes except in a very general way. Those of the different orders of one plane may be compared with accuracy.

Size of Unit Cell It was mentioned above that the relative lengths of the original a and c axes had to be doubled to obtain the true unit cell. This was found necessary because, although the spacings of a large number of axial planes could be accounted for by assuming a unit cell of the original dimensions which would contain *one* molecule, the spacings of all planes ($h \neq 0$) having no zero index were double the calculated values if h were even and only normal if h were odd. The true unit cell contains *four* molecules of C_2Cl_6 and is of dimensions

$$a = 11.51, \quad b = 10.14, \quad c = 6.39 \text{ \AA}$$

Bravais Lattice Adopting this new cell as a basis for calculation it is found

- (a) That no measured spacing is a multiple of the corresponding calculated spacing,
- (b) That those planes whose measured spacings are sub-multiples of the calculated spacings belong exclusively to axial zones.

The latter fact proves that the Bravais lattice is Γ_0 , while both show that, as

far as can be judged from the massed experimental data, the cell now chosen is the correct one. The volatilisation of the crystals made rotation photographs difficult and complete sets of oscillations even more so, but such as were obtained agreed with the ionisation results and showed no spots which were not in agreement with the above cell. Laue photographs were easier to obtain, since larger crystals could be used, and photographs taken with the beam perpendicular to (100) showed a large number of spots, all of which could be assigned indices without further enlargement of the axes.

Results of Observation—Table I gives the spacings and intensities observed on the ionisation spectrometer. All axial planes (and all general planes in the

Table I

Plane	Spacing		Intensities observed								Remarks
	(calc)	Obs	1	2	3	4	5	6	7	8	
100	11 31 _s	2 87 _s				115	—			12	Quartered
010	10 14 _s	5 07		74	—	18	—	72	—	28	Halved
001	6 39 _s	3 20		46	—	4				—	"
011	5 40 _s	5 44	50	4	16	1	—			—	Normal
021	3 97 _s	2 01		0 5	—					—	Halved
012	3 04 _s	1 52	—	1	—					—	"
031	2 98 _s	3 02	13	2						—	Normal
041	2 35 _s	1 18	—	2						—	Halved
032	2 32 _s	1 19	—	0 5						—	"
013	2 08 _s	2 09	28	—						—	Normal
023	1 96 _s	0 98 _s	—	3						—	Halved
057	1 46 _s	1 40	1 5							—	Normal
101	5 58 _s	5 60	32	62	2 5	2	—	—		—	"
201	4 27 _s	4 28	19	24	8	1	—	—		—	"
401	3 29 _s	3 29	12	5	—	—				—	"
102	2 08 _s	3 07 _s	63	11	—	—				—	"
401	2 62 _s	2 60	24	—						—	"
302	2 45 _s	2 44 _s	33	2	—	—				—	"
501	2 17 _s	2 16	10							—	"
103	2 09 _s	2 05	5	—						—	"
203	1 99 _s	1 97	12							—	"
601	1 83 _s	1 86	2							—	"
403	1 71 _s	1 70	4							—	"
104	1 58 _s	1 57	4 5							—	"
205	1 25 _s	1 24 _s	7							—	"
405	1 16 _s	1 17	1 5							—	"
605	1 06 _s	1 06	3							—	"
110	7 61 _s	1 89 _s	—	—	—	15	—	—		2	Quartered
210	5 00 _s	5 01	100	22	41	1	—	—		—	Normal
120	4 64 _s	1 15	—	—	—	11				—	Quartered
230	2 91 _s	2 92	11	18						—	Normal
410	2 77 _s	1 38	—	9						—	Halved
250	1 91 _s	1 91	7							—	Normal
610	1 88 _s	1 87	25	—						—	"
111	4 89 _s	4 90	35	3	9	4				—	"
211	3 94 _s	3 96	6	3						—	"
122	2 63 _s	2 63	10	3						—	"

zones which were examined) with indices simpler than those actually recorded were looked for, but without success. Thus it may be inferred that the reflections from the different orders of the planes (043) (014) (105) (304) (130) (310) (140) (311) (233), etc., were too weak, in general, to be observed. Altogether, the number of different orders of different planes looked for amounted to several hundreds in the case of C_2Cl_6 , although only about 87 actual reflections were observed on the spectrometer.

The following planes gave first order reflections —

	Calc	Obs	Intensity		Calc	Obs	Intensity
121	3 75 ₄	3 72	MS	332	1 98 ₄	1 98	M
221	3 27 ₁	3 26	MW	213	1 96 ₁	1 90	W
112	2 04 ₇	2 04 ₁	MS	313	1 82 ₄	1 82	MW
131	2 89 ₂	2 85	VS	441	1 82 ₄	1 83	MS
321	2 76 ₁	2 76	W	531	1 82 ₄	1 82 ₄	W
212	2 69 ₄	2 69	W	611	1 40 ₄	1 79	W
331	2 35 ₄	2 35	S	432	1 80 ₄	1 81	W
421	2 33 ₁	2 32	M	173	1 78 ₁	1 74	VW
141	2 31 ₀	2 20	M	522	1 75 ₃	1 75	VW
322	2 21 ₁	2 21	W	423	1 74 ₄	1 73	MW
232	2 15 ₄	2 23 ₇	W	431	1 61 ₅	1 61 ₅	MS
511	2 11 ₀	2 11	VW	433	1 52 ₄	1 53	MW
113	2 05 ₂	2 05	MS	144	1 34 ₂	1 35	VW
				344	1 27 ₂	1 27 ₂	VW

VS	Very strong	M	Moderate
S	Strong	MW	Moderately weak
MS	Moderately strong	W	Weak
		VW	Very weak

Space-Group and Molecular Symmetry Certain planes on the [001] zone gave no reflections from any orders except the fourth, eighth, etc., their spacings thus being apparently quartered. The only space group in the orthorhombic bipyramidal class for which quarterings would be expected is Q_h^{24} . In that case, however, all the axial zones should show quarterings in certain planes*. Since that is not so, it is evident that the explanation of these quarterings must be looked for not from space-group but from intensity considerations.

Reflections were absent in odd orders from all planes in the [001] zone for which h was odd, also from all planes in the [100] zone for which $h + l$ was odd. All other planes were, in general, normal. Assuming that all these halvings are real, the only possible space-group is Q_h^{16} . If the crystals should prove to be pyramidal only (i.e., if there is no real plane of symmetry parallel to (010)), then the space-group would be C_{2v}^6 . No suggestion has ever been

* Niggli, 'Geom. Kryst. des Diskontinuums,' Leipzig (1919). Astbury and Yardley, 'Phil. Trans.,' A, vol 224, p 221 (1924).

made that the crystals are not holohedral, but this possibility is not dismissed by the X-ray evidence. It will be assumed throughout this paper, however, that the crystal class is correct. In that case each of the four molecules in the unit cell must possess either a plane or a centre of symmetry*. Intensity considerations very definitely eliminate the latter possibility. The halving found show that

(010) is a pure plane of symmetry,

(100) is a glide plane, translation $\frac{b}{2} \mid \frac{c}{2}$,

(001) is a glide plane, translation $\frac{a}{2}$

The co-ordinates of equivalent points referred to a 'centre of symmetry as origin (cf Wyckoff,† who adopts a different origin of co-ordinates) are --

$$\begin{array}{ccccccc} x & y & z, & x \frac{1}{2} - y & z, & \frac{1}{2} + x & y \frac{1}{2} - z, & \frac{1}{2} + x \frac{1}{2} - y \frac{1}{2} - z \\ -x & -y & -z, & -x \frac{1}{2} + y & -z, & \frac{1}{2} - x & -y \frac{1}{2} + z, & \frac{1}{2} - x \frac{1}{2} - y \frac{1}{2} + z \end{array}$$

If the molecules possess

- (a) A centre of symmetry (fig 3a), the points at which the centres of the molecules must lie are

$$000, \quad 0 \frac{1}{2} 0, \quad \frac{1}{2} 0 \frac{1}{2}, \quad \frac{1}{2} \frac{1}{2} \frac{1}{2}.$$

- (b) A plane of symmetry (fig 3b), the co-ordinates of corresponding points in the planes of the molecules are

$$x \frac{1}{4} z, \quad -x - \frac{1}{4} - z \quad \frac{1}{2} + x \frac{1}{4} \frac{1}{2} - z \quad \frac{1}{2} - x - \frac{1}{4} \frac{1}{2} + z,$$

and there are two parameters x and z to be determined

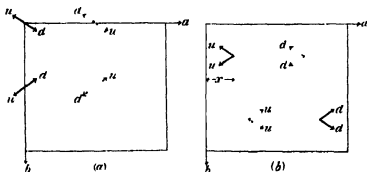


FIG 3

* Niggli, &c., *loc cit*

† Wyckoff, 'The Analytical Expression of the Results of the Theory of Space Groups,' Carnegie Institute, Washington (1922)

The planes in the [001] zone may be divided into three classes according to their behaviour to X-rays (see Table 1) —

- (1) Planes ($h\ k\ 0$) for which h is even but not a multiple of 4 give normal reflections, e.g., (210) (610) (230) (250)
- (2) Planes ($h\ k\ 0$) for which h is a multiple of 4 are halved (010) (410)
- (3) Planes ($h\ k\ 0$) for which h is odd are quartered (100) (110) (120)

The disappearance of all but fourth, eighth orders for (3) and of odd orders for (2) was remarkably complete in the case of C_2Cl_6 and was confirmed by the absence of *any* observable reflection for planes such as (140) (320), whose second orders should, if present, have been easily measurable, and for (430) (810), whose first orders might have been expected from space-group considerations alone. Now these results can only be obtained by an arrangement of units as shown in fig 4a, the projection of all four units, A, B, C, D on the (001) plane being *identical*

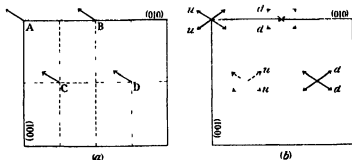


FIG 4

Since the centro-symmetrical molecules would have no degrees of freedom (i.e., no variable parameters), they would not be free to take up these positions, nor could any arrangement of their atoms cause such a complete disappearance of expected planes

The parameter x (b) alternative) can, however, be adjusted so that four plano-symmetrical molecules would lie in the A, B, C, D positions. For such an arrangement $x = \frac{1}{8}$ ($\frac{3}{8}$, $\frac{5}{8}$ or $\frac{7}{8}$). According to the space-group 4 and C (and similarly B and D) must be mirror-images of each other in the (100) plane. In order that their projections on (001) should be identical, the molecule itself must possess, in addition to its real plane of symmetry parallel to (010), a pseudo-plane parallel to (100) or a pseudo-centre (fig 4b). It is now easy to see a possible reason why the crystals present the appearance of a truncated hexagon when viewed along the [001] direction (fig 5)

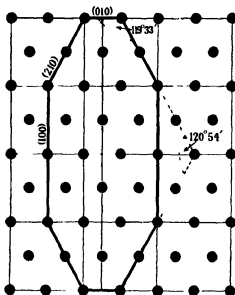


FIG 5

If the molecule possesses a pseudo plane parallel to (100), the projections of the four molecules on (010) would be as shown in fig 6a, the projections of A and

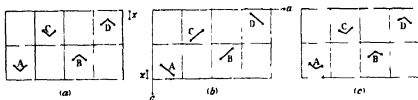


FIG 6

C being identical, as are also those of B and D. This would cause a complete disappearance of the second orders of (101) (102), etc (and in general those of $(h\ 0\ l)$ where h is odd) and of the first orders of (401) (403), etc (i.e., of $(h\ 0\ l)$ where h is a multiple of 4). Now many of these reflections not only occur but are very strong. The molecule, therefore, does not possess a pseudo-plane at right angles to its real plane of symmetry.

In the case of a pseudo-centre the projection on (010) would be as shown in fig 6b. Here the apparently identical molecules are an undefined distance $2z$ apart in the [001] direction, and it is theoretically possible to adjust the value of $2z$ so that none of the reflections actually found would be expected to vanish.

A third alternative, fig 6c, is possible, though highly improbable. This is the case in which the projections on (001) of the two "arms" of the molecule

are similar, though they are otherwise quite unlike each other. This possibility will not be considered in any detail.

We are therefore left with a molecule having a real plane and a pseudo-centre of symmetry, which, as a whole, possesses one unknown degree of freedom, the parameter z . Simple mathematical considerations can be used to limit the possible values of z .

The pseudo-centres of the molecules lie in the positions $(\frac{1}{8}, \frac{1}{4}, z)$, $(-\frac{1}{8}, -\frac{1}{4}, -z)$, $(-\frac{3}{8}, \frac{1}{4}, -z)$, $(\frac{3}{8}, -\frac{1}{4}, z)$, and thus for each atom lying at $(\frac{1}{8} + p, \frac{1}{4} + q, z + r)$ there will be other atoms at $(\frac{1}{8} - p, \frac{1}{4} - q, z - r)$, $(\frac{1}{8} + p, \frac{1}{4} - q, z + r)$, $(\frac{1}{8} - p, \frac{1}{4} + q, z - r)$ and 12 other positions. The resultant effect of all these atoms will be proportional to

$$\begin{aligned} & \sum_{p,q,r} A_{pqr} \left\{ \cos 2\pi n \left[\frac{h}{8} + \frac{k}{4} + lz + (hp + kq + lr) \right] \right. \\ & \quad + \cos 2\pi n \left[\frac{h}{8} + \frac{k}{4} + lz - (hp + kq + lr) \right] \\ & \quad + \cos 2\pi n \left[\frac{h}{8} + \frac{k}{4} + lz + (hp - kq + lr) \right] \\ & \quad \left. + \cos 2\pi n \left[\frac{h}{8} + \frac{k}{4} + lz - (hp - kq + lr) \right] + 12 \text{ other terms} \right\} \\ &= \sum_{p,q,r} 4A_{pqr} \left\{ \cos 2\pi n \left(\frac{h}{8} + \frac{k}{4} + lz \right) [\cos 2\pi n (hp + kq + lr) \right. \\ & \quad \left. + \cos 2\pi n (hp - kq + lr)] \right. \\ & \quad \left. + \cos 2\pi n \left(\frac{5h}{8} + \frac{k}{4} + \frac{l}{2} - lz \right) [\cos 2\pi n (hp + kq - lr) \right. \\ & \quad \left. + \cos 2\pi n (hp - kq - lr)] \right\} \\ &= 8 \sum_{p,q,r} A_{pqr} \left\{ \cos 2\pi n \left(\frac{h}{8} + \frac{k}{4} + lz \right) \cos 2\pi n (hp + lr) \cos 2\pi n kq \right. \\ & \quad \left. + \cos 2\pi n \left(\frac{h+l}{2} + \frac{h}{8} + \frac{k}{4} - lz \right) \cos 2\pi n (hp - lr) \cos 2\pi n kq \right\} \end{aligned}$$

Let

$$\cos 2\pi n (hp + lr) = X, \quad \cos 2\pi n (hp - lr) = Y,$$

$$\begin{aligned} \text{Exp} = 8 \sum_{p,q,r} A_{pqr} \cos 2\pi n kq \left\{ X \cos 2\pi n \left(\frac{h}{8} + \frac{k}{4} + lz \right) \right. \\ \left. + Y \cos 2\pi n \left(\frac{h+l}{2} + \frac{h}{8} + \frac{k}{4} - lz \right) \right\}, \end{aligned}$$

$$X = Y \text{ if } h = 0 \text{ or } l = 0$$

Then expression vanishes when

$$\cos 2\pi n \left(\frac{h}{8} + \frac{k}{4} + lz \right) + \cos 2\pi n \left(\frac{h+l}{2} + \frac{h}{8} + \frac{k}{4} - lz \right) = 0,$$

i.e., when

$$\cos 2\pi n \left(\frac{3h}{8} + \frac{k}{4} + \frac{l}{4} \right) \cos 2\pi n \left(\frac{h}{4} + \frac{l}{4} - lz \right) = 0,$$

i.e., when

$$n \left(\frac{3h}{2} + k + l \right) = \text{odd integer}, \quad (1)$$

or when

$$n (h + l - 4lz) = \text{odd integer}, \quad (2)$$

$l = 0$ for zone [001]

Then from (2) odd orders must vanish if h is odd, and from (1) odd orders vanish if h is odd and h a multiple of 4

$n = 2, 6, 10 \quad 4N - 2$ orders vanish if h is odd

Table I shows that these conditions are fulfilled $h = 0$ can be considered in the general case where

$$X \neq Y$$

Then the expression vanishes when the terms vanish separately That is, when

$$n \left(\frac{h}{2} + k + 4lz \right) = \text{odd integer}$$

and

$$n \left(2h + 2l + \frac{h}{2} + k - 4lz \right) = \text{odd integer}$$

These conditions are both fulfilled if

$$\frac{nh}{2} + nk + 4nlz = \text{odd integer}$$

There are eight different cases to be considered —

$$\left. \begin{array}{l} nh = 4N \\ nk = 2M + 1 \end{array} \right\} \left. \begin{array}{l} 4N \\ 2M \end{array} \right\} \left. \begin{array}{l} 4N + 1 \\ 2M + 1 \end{array} \right\} \left. \begin{array}{l} 4N + 1 \\ 2M \end{array} \right\} \left. \begin{array}{l} 4N - 1 \\ 2M + 1 \end{array} \right\} \left. \begin{array}{l} 4N - 1 \\ 2M \end{array} \right\} \left. \begin{array}{l} 4N + 2 \\ 2M + 1 \end{array} \right\} \left. \begin{array}{l} 4N + 2 \\ 2M \end{array} \right\}.$$

For example,

$$\begin{array}{ll} \text{If} & nh = 0, 4, 8 \quad 4N \\ \text{and} & nk = 0, 2, 4 \quad 2M \end{array}$$

then reflections will vanish for which $nlz = \frac{1}{4}, \frac{3}{4}, \frac{5}{4} \quad \frac{2P+1}{4}$

There have been observed —

$$(401) (421) (441) \quad \text{therefore } z \neq \frac{1}{4}, \frac{3}{4},$$

$$(002) (022) (042) (062) (082) (402) (422) \quad \text{therefore } z \neq \frac{1}{8}, \frac{3}{8}, \frac{5}{8}$$

$$(043) \quad \text{therefore } z \neq \frac{1}{12}, \frac{1}{4}, \frac{5}{12}$$

$$(004) (024) (044) (064) (404) (804) (114) \quad \text{therefore } z \neq \frac{1}{16}, \frac{3}{16}, \frac{5}{16}$$

$$(405) \quad \text{therefore } z \neq \frac{1}{20}, \frac{3}{20}, \frac{1}{4}$$

$$(046) \quad \text{therefore } z \neq \frac{1}{24}, \frac{1}{8}, \frac{5}{24}$$

By similar reasoning we find that the *observed* planes exclude all the following values of z —

$$0 \quad \frac{1}{32} \quad \frac{1}{24} \quad \frac{1}{20} \quad \frac{1}{16} \quad \frac{1}{12} \quad \frac{3}{32} \quad \frac{1}{10} \quad \frac{1}{8} \quad \frac{3}{20} \quad \frac{5}{32} \quad \frac{1}{6} \quad \frac{3}{16} \quad \frac{1}{5} \quad \frac{5}{24} \quad \frac{7}{32} \quad \frac{1}{4}$$

$$\frac{9}{32} \quad \frac{7}{24} \quad \frac{3}{10} \quad \frac{5}{16} \quad \frac{1}{3} \quad \frac{11}{32} \quad \frac{7}{20} \quad \frac{3}{8} \quad \frac{2}{5} \quad \frac{13}{32} \quad \frac{5}{12} \quad \frac{7}{16} \quad \frac{9}{20} \quad \frac{11}{24} \quad \frac{15}{32} \quad \frac{1}{2}$$

showing that z is not equal to any very simple fraction. It was hoped that by estimating the average corrected intensity ($I_{\text{obs}} - \frac{1 + \cos^2 2\theta}{\sin 2\theta}$) of the reflections which eliminate any particular value of z and plotting a curve for intensity vs z , a distinct minimum would be obtained which would point to the most probable value of the parameter. The curve obtained, however, showed a number of minima corresponding to the higher values of l (i.e., to the reflections of large θ), no doubt because the correction made for θ was insufficient, since it did not allow also for the falling off of scattering power of the constituent atoms with angle. It was not, therefore, possible to obtain a definite value for the parameter z .

In spite of this failure, a considerable amount of information about the position of the atoms can be deduced from the [001] zone alone. The details are best left, however, until results for some of the other isomorphous members of the series have been given.

HEXABROMETHANE— C_2Br_6 $M = 503.52$

Crystal Data—The habit is similar to that of C_2Cl_6 . Goszner* and Schimper† have measured the angles between faces and their results are compared with those found as before on the Bragg spectrometer—

		Goszner	Schimper	Yardley
		°	°	°
(210) (210)	=	58 50	58 50	58 50
(101) (101)	—	58 15	57 50	58 6
(102) (102)	—	—	—	31 7

Readings on the spectrometer were difficult to obtain because of the high absorption of the Rh $K\alpha$ radiation by the Br atoms. Using the values of $\frac{\mu}{\rho}$ for Mo $K\alpha$ given in Wingardh's tables‡ and extrapolating for Rh $K\alpha$ by means of the relation $\frac{\mu}{\rho} \propto \lambda^{2.8}$, we find that for C_2Cl_6 $\frac{\mu}{\rho} = 47.7$, whereas for C_2Br_6 $\frac{\mu}{\rho} = 269.7$, a value nearly six times as large. For this reason the intensity of nearly all the reflections was small and often the peaks were ill-defined and difficult to measure. The spectrometer readings give an axial ratio of

$$a : b : c = 1.1278 : 1 : 0.6270$$

as compared with Goszner's value

$$a : b : c = (2 \times) 0.5639 : 1 : (2 \times) 0.3142$$

The latter is possibly the more correct in this particular case, but the difference is small.

The density $\rho = 3.823$ grs./c.c.*

Results of Observations—This substance was much more stable than C_2Cl_6 and would stand a longer exposure

* *Loc. cit.*

† Groth, 'Chem. Krystallographie,' vol. 3, p. 39.

‡ 'Z. f. Physik,' vol. 8, p. 363 (1922).

Table II

Plane	Spacing		Intensity observed							
	Calc	Obs	1	2	3	4	5	6	7	8
100	12 07 ₂	3 00 ₂	—	—	—	12	—	—	—	8
010	10 70 ₂	5 35 ₂	—	9	—	4	—	19	—	3 5
001	6 72 ₂	3 36	—	4	—	0 5	—	—	—	—
011	5 69 ₂	5 68	10	—	4	—	—	—	—	—
031	3 15 ₂	3 19	2	(very broad)						
013	2 19 ₂	Obs only	—	—	—	—	—	—	—	—
101	5 87 ₂	5 82	8 5	8	—	—	—	—	—	—
201	4 49 ₂	4 45	2	2	—	—	—	—	—	—
102	3 23 ₂	3 22	10	2	—	—	—	—	—	—
401	2 75 ₂	2 70	2	—	—	—	—	—	—	—
302	2 58 ₂	2 52	2	—	—	—	—	—	—	—
210	5 25 ₂	5 29	2	1 5	2 5	—	—	—	—	—
230	3 07 ₂	Obs only	—	—	—	—	—	—	—	—
610	1 97 ₂	1 96 ₂	1	—	—	—	—	—	—	—

Laue photographs were taken with the X-rays perpendicular to the planes (100) and (010). These showed reflections from about 60 planes, the minimum value of $n\lambda$ found being 0.39, Å (using a Cu anticathode).

TETRACHLORDIBROMETHANE— $C_2Cl_4Br_2$ $M = 325.68$

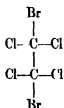
Two crystalline forms have been described. The first is said to be the symmetrical compound, $CCl_2Br-CCl_2Br$, and its preparation is given by Bourgoin*. This substance volatilises slowly in the air at ordinary temperatures without decomposition, but on heating in a closed capillary tube it melts with decomposition at 197.5° C. The second, the so-called asymmetrical compound, $CCl_3-CClBr_2$, has been prepared by Bourgoin† and Paterno‡. The crystals do not volatilise at ordinary temperatures, but on exposure to the air they go cloudy, eventually becoming quite opaque and falling to a white powder. This applied to crystals prepared in the laboratory by both the methods referred to. Probably the change is due to a slow alteration of crystalline form. On heating in a closed capillary tube the substance melts with partial decomposition (and sublimation) at 211° C. A mixture of the two compounds melts with partial decomposition at 198° C. Bourgoin† found that on heat treatment with aniline the symmetrical compound decomposed into Br_2 and C_2Cl_4 , whereas the asymmetrical compound

* 'Bull Soc Chim,' vol 24, p 114 (1875)

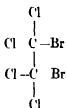
† 'Bull Soc Chim,' vol 23, p 4 (1874)

‡ 'Jahrb Fort Chemie,' p 250 (1871)

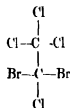
gave Cl_2 and $\text{C}_2\text{Cl}_4\text{Br}_2$. Bourgoin himself suggested (a) and (b) as the probable structural formulae of the two molecules, but in all subsequent literature the



symm (a)



asymm (b)



asymm (c)

formula (c) has been adopted for the asymmetric molecule, as for a tetrahedral carbon atom (a) and (b) would be identical

Crystal Data—Goszner* gives

Symm compound $\rho = 2.713$

$$a \ b \ c = (2 \ 0 \ 0) \ 5616 \ 1 \ (2 \ 0 \ 0) \ 3129$$

Asymm compound $\rho = 2.794$

$$a \ b \ c = (2 \ 0 \ 0) \ 5612 \ 1 \ (2 \ 0 \ 0) \ 3149 \dagger$$

The majority of crystals of both compounds showed well-developed {101} and {210} forms, with smaller {100} and {010}, the latter occasionally being absent altogether. In general, however, the crystals of the symm substance were found to be elongated in the [001] direction, and those of the asymm substance in the [010] direction. This fact made the comparison of Laue photographs of the two substances more difficult than if their habits had been precisely similar. The two sets of crystal angles, according to Goszner, differ only by a few minutes, and they were therefore repeated on the Bragg spectrometer.

		Symm $\text{C}_2\text{Cl}_4\text{Br}_2$		Asymm $\text{C}_2\text{Cl}_4\text{Br}_2$	
		Goszner	Yardley	Goszner	Yardley
		$\begin{smallmatrix} \circ & ' \\ \hline \end{smallmatrix}$	$\begin{smallmatrix} \circ & ' \\ \hline \end{smallmatrix}$	$\begin{smallmatrix} \circ & ' \\ \hline \end{smallmatrix}$	$\begin{smallmatrix} \circ & ' \\ \hline \end{smallmatrix}$
{210} : {210}	=	58 54	58 58	58 30	58 35
{101} : {101}	=	57 59	58 0	58 30	58 32
{102} : {102}	=	—	31 0	—	31 18

* *Loc cit*

† Wrongly given as 0.3171 throughout the text of Goszner's paper, his actual measurements lead to the value 0.3149.

The spectrometer readings give as axial ratios

Symm	a	b	$c = 1$	1308	1	0	6270
Asymm	a	b	$c = 1$	1220	1	0	6288

The small differences between the two crystalline forms are therefore fully confirmed. Apart from these geometrical differences, however, the X-ray evidence shows that the two isomers are remarkably alike.

Results of Observations—The three axial lengths were found to be

Symm	$a = 11.73 \text{ \AA}$	$b = 10.37 \text{ \AA}$	$c = 6.50 \text{ \AA}$
Asymm	$a = 11.61 \text{ \AA}$	$b = 10.35 \text{ \AA}$	$c = 6.51 \text{ \AA}$

The results for the asymm form led to a density of 2.745 instead of 2.791, and attempts by means of the flotation method to repeat Goszner's high value were quite unsuccessful. The intensity measurements for the two substances showed none of the distinct differences that might be expected if the two molecules were really $\text{CCl}_2\text{Br}-\text{CCl}_2\text{Br}$ and $\text{CCl}_3-\text{CClBr}_2$ respectively. Even the intensities of the different orders of (100) were very much alike, although this plane shows the biggest difference in spacing. In both cases the quartering discussed in connection with C_2Cl_6 was not so complete as for that substance or for C_2Br_6 . A small, but quite distinct, second order was observed for both forms. This might be explained either by a slight variation in α ($\frac{1}{8}$ for C_2Cl_6) or to a slight departure from the *pseudo*-symmetry postulated for C_2Cl_6 . The terms "symmetrical" and "asymmetrical" are misleading from a crystallographic point of view. Whatever their molecular structures may be, both forms possess the same amount of real symmetry, *i.e.*, one plane. There is no way of giving the "asymm" molecule, $\text{CCl}_3-\text{CClBr}_2$, a pseudo-centre of symmetry, but it is still possible to think of ways of arranging the atoms so that their projection on one particular plane would apparently have two planes of symmetry, without requiring the disappearance of observed planes. One such way,

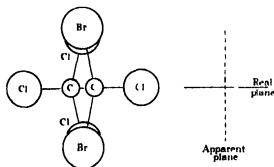


FIG 7

which would permit a tetrahedral arrangement of the carbon valency bonds is shown in fig 7 (p 465)

Table III

Symmetrical $C_2Cl_4Br_2$									
Plane	Spacing		Intensities observed						
	Calc	Obs	1	2	3	4	5	6	7 8
100	11 73 ₂	5 86	—	0 5	—	25	—	—	2
010	10 37 ₂	5 19	—	7 5	—	3 5	—	10	2 5
001	6 50 ₂	3 25 ₂	—	10	—	1	—	—	—
011	5 50 ₂	5 47	3	1	2	—	—	—	—
013	2 12 ₂	2 15	1	—	—	—	—	—	—
101	5 68 ₂	5 66	9	14	—	—	—	—	—
201	4 35 ₂	4 33	4	2	2	—	—	—	—
102	3 13 ₂	3 14	13	4	—	—	—	—	—
401	2 67 ₂	2 68	3	—	—	—	—	—	—
302	2 50 ₂	2 52	3	—	—	—	—	—	—
110	7 77 ₂	1 95	—	—	—	2 5	—	—	—
210	5 10 ₂	5 10	12	2 5	5	—	—	—	—
120	4 73 ₂	1 19	—	—	—	0 5	—	—	—
610	1 92 ₂	1 91 ₂	4 5	—	—	—	—	—	—
111	4 98 ₂	4 92	8	—	—	—	—	—	—
121	3 83 ₂	3 89	3 5	—	—	—	—	—	—
131	2 95 ₂	2 91	8	—	—	—	—	—	—

Asymmetrical $C_2Cl_4Br_2$									
Plane	Calc	Obs	1	2	3	4	5	6	7 8
100	11 61 ₂	5 80	—	0 5	—	20	—	—	2
010	10 35 ₂	5 19	—	12 5	—	3	—	10	2
001	6 50 ₂	3 25	—	12	—	1	—	—	—
101	5 67 ₂	5 66	4	12	—	—	—	—	—
201	4 31 ₂	4 31	2	4	1	—	—	—	—
102	3 13 ₂	3 11	20	3	—	—	—	—	—
110	7 72 ₂	1 95	—	—	—	3 5	—	—	—
210	5 06 ₂	5 10	39	4	12 5	0 5	—	—	—
120	4 72 ₂	1 19	—	—	—	2 5	—	—	—
230	2 90 ₂	2 98 ₂	3 5	6 5	—	—	—	—	—
610	1 90 ₂	1 91 ₂	4	—	—	—	—	—	—

Laue photographs of the two substances taken with the X-rays perpendicular to (100) (010) and (001) showed a large number of spots, but revealed no obvious differences. The presence or absence of some of the weaker planes may quite well have been due to slight missetting of the crystals or to their slightly different habits.

PENTABROMFLUORETHANE $\text{-C}_2\text{Br}_5\text{F}$ $M = 442.61$

A pure specimen of this compound was very kindly lent to me by Prof Swarts* and beautiful crystals could be grown from ethyl alcohol

Crystal Data—The crystals obtained were in the form of thin and rather brittle plates, which were found to be completely isomorphous with C_2Cl_5 , etc. The tabular faces were {100}, the {010} and {101} were well-developed boundary faces, while the {210} were either absent or very small. The pseudo hexagonal appearance in the [001] direction was therefore no longer obvious, though two or three small specimens were found which, instead of being tabular on {100}, were pseudo-hexagonal prisms on {010} as basal plane, bounded by almost equally developed {100} {101} faces. The following angles were accurately measured as before,

$$\begin{array}{ll} (210) \quad (2\bar{1}0) = 57^\circ 39' & (101) \quad (10\bar{1}) = 57^\circ 54' \\ (230) \quad (2\bar{3}0) = 62^\circ 21' & (102) \quad (10\bar{2}) = 30^\circ 59' \end{array}$$

giving an axial ratio

$$a \quad b \quad c = 1 \quad 1.012 \quad 1 \quad 0.6098$$

Experimental Technique—This compound absorbs the Rh K α radiation almost as much as C_2Br_6 , and in order to obtain good reflections a very thin flake was used (these were not available for C_2Br_6) mounted on a crystal holder, which was a modification of that described by W. L. Bragg and G. B. Brown†. Instead of a rotating circle, a fixed vertical circle A was used, of external diameter 10 cm. A scale was marked on the front of the circle and an arm carrying a vernier and a third small rotating circle B could be moved through about 190° on the circle A and clamped in any desired position. By means of simple X-ray measurements the {100} planes were adjusted to be parallel to the plane of A and then any plane in the [100] zone could be brought into a vertical position by a suitable motion of the arm, and the reflection from it measured. The advantage of this method of adjustment was that the X-rays could always travel through the least possible thickness of the crystal. Other zones were arranged so that the same condition was fulfilled, the inevitable absorption was greatest in the case of planes making a small angle with (100). At the same time the ionisation chamber slit could be shortened vertically so that no extraneous reflection could enter from any other plane that might be nearly vertical also. [This precaution was taken throughout the measurements on the series, and in

* 'Bull. Acad. R. Belg.', vol. 33, p. 473 (1897), abstract in 'Rec. Trav. Chim. Pays Bas,' vol. 17, p. 236 (1898).

† 'Roy. Soc. Proc. A,' vol. 110, p. 50 (1926).

the case of the more important intensity measurements the comparison of the orders was made with three different directions in the plane set vertical in turn. No variation of the relative intensities was found, showing that in none of these positions did any extraneous reflections enter the chamber.]

Results of Observations—The crystals of C_2Br_3F volatilised very slowly, a large plate lasting for about a week even when left exposed. The density measured by flotation in Rohrbach's solution was 3.46 grs/cc, but this value was probably about 1 per cent too low, (calculated from the X-ray measurements the density would be 3.49).

Table IV

Plane	Spacing		Intensities observed							
	Calc	Obs	1	2	3	4	5	6	7	8
100	11.84 ₂	5.92 ₂	—	—	—	10	—	1	—	2
010	10.75 ₂	5.37	—	4	—	10	—	28	—	10
001	6.55 ₂	3.28	—	12	—	—	—	—	—	—
011	5.60 ₂	5.59	1	1	—	—	—	—	—	—
021	4.15 ₂	2.03 ²	—	2	5	—	—	—	—	—
031	3.14 ₂	3.09 ₂	3	—	—	—	—	—	—	—
013	2.11 ₂	2.14	2	—	—	—	—	—	—	—
101	5.73 ₂	5.74 ₂	4	13	—	—	—	—	—	—
201	4.39 ₂	4.37	1	5	1	—	—	—	—	—
301	3.38 ₂	3.38	2	5	—	—	—	—	—	—
102	3.16 ₂	3.16	16	1	—	—	—	—	—	—
401	2.89 ₂	2.70	5	—	—	—	—	—	—	—
302	2.52 ₂	2.57	1	5	—	—	—	—	—	—
501	2.22 ₂	2.22 ₂	1	5	—	—	—	—	—	—
103	2.15 ₂	2.11	5	—	—	—	—	—	—	—
203	2.05 ₂	2.06	2	—	—	—	—	—	—	—
110	7.96 ₂	1.99	—	—	—	6	—	—	—	—
210	5.18 ₂	5.23	26	1	5	8	—	—	—	—
120	4.89 ₂	1.31	—	—	—	3	5	—	—	—
230	3.06 ₂	3.06 ₂	14	9	—	—	—	—	—	—
610	1.94 ₂	1.94 ₂	1	5	—	—	—	—	—	—
111	5.06 ₂	5.12	5	—	—	—	—	—	—	—
121	3.92 ₂	3.91	2	—	—	—	—	—	—	—
131	3.04 ₂	3.02 ₂	3	—	—	—	—	—	—	—

A Laue photograph taken with the X-rays perpendicular to (100) showed a minimum value of $n\lambda$ of 0.35₂ Å.

TRICHLORTRIBROMETHANE— $C_2Cl_3Br_3$ $M = 370.14$

This compound, whose structural constitution is uncertain, was prepared by Mouneyrat's method*. It is isomorphous with the rest of the series.

Crystal Data—Good crystals were grown from the mother liquors and these

* 'Bull Soc Chim,' vol 19, p 501 (1898)

were considerably elongated in the [001] direction. They showed well-developed {100} and {101} forms with smaller terminal faces {210} and occasionally {010}. On recrystallisation from benzene, however, the relative importance of the faces was completely changed. The {210} and {101} were now the main forms, {010} being fairly well developed and {100} quite small. The following angles were measured on the Bragg spectrometer,

$$\begin{array}{ll} (210) \quad (\bar{2}10) = 58^\circ 49' & (101) \quad (10\bar{1}) = 58^\circ 7' \\ (230) \quad (2\bar{3}0) = 61^\circ 13' & (102) \quad (10\bar{2}) = 31^\circ 3' \\ (120) \quad (1\bar{2}0) = 47^\circ 53' \end{array}$$

giving an axial ratio

$$a \quad b \quad c = 1 \quad 1.270 \quad 1 \quad 0.6262$$

Structural Formula—This substance may be either $\text{CCl}_3 \cdot \text{CBr}_3$ or $\text{CCl}_2\text{Br} \cdot \text{CClBr}_2$. A compound which according to its synthesis is most probably $\text{CCl}_2\text{Br} \cdot \text{CClBr}_2$ has been prepared by Besson* by the action of Br on $\text{CCl}_2 \cdot \text{CClBr}$ in sunlight at 100°C . This substance melts under pressure at 178° – 180° and its density is given as 2.11. The compound prepared by Mouneyrat and described here does not melt under pressure but begins to give off Br at 200° in a closed tube and at 235° has completely disappeared. The density calculated from the X-ray data is 3.03. It appears, therefore, to be quite a distinct isomeric form, and the belief expressed by Mouneyrat that the formula is $\text{CCl}_3 \cdot \text{CBr}_3$ is possibly justified.

Results of Observation—The crystals do not volatilise, but on exposure they rapidly grow cloudy. Laue photographs were taken with the X-rays perpendicular to (100) (010) and (001), and the minimum value found for n_λ was 0.48 Å. From the spectrometer results (Table V) it will be seen that the (100) plane now shows weak sixth and tenth orders as well as a doubtful second order (The latter was difficult to measure accurately because it was superimposed on the "wash" of general radiation from the large fourth order.)

Table V

Plane	Spacing		Intensities observed									
	Calc	Obs	1	2	3	4	5	6	7	8	9	10
100	11 77 ₂	5 89 ₂	—	7	—	67	—	2	—	6 5	—	1 5
010	10 44 ₂	5 22 ₂	—	28	—	9 5	—	31	—	6	—	—
001	6 54 ₁	3 26	—	40	—	—	—	—	—	—	—	—
011	5 54 ₂	5 57	7	8	5 30	—	—	—	—	—	—	—
031	3 07 ₂	3 06	11	—	—	—	—	—	—	—	—	—
013	2 13 ₂	2 18	12	—	—	—	—	—	—	—	—	—
101	5 71 ₂	5 71	15	57	1	2	—	—	—	—	—	—
201	4 37 ₂	4 35	1	9	4 5	—	—	—	—	—	—	—
102	3 16 ₂	3 14 ₂	66	10	—	—	—	—	—	—	—	—
401	2 72 ₂	2 66	10	—	—	—	—	—	—	—	—	—
302	2 51 ₂	2 51	17	—	—	—	—	—	—	—	—	—
210	5 12 ₂	5 12	7	2	1	—	—	—	—	—	—	—
120	4 77 ₂	1 20	—	—	—	2	—	—	—	—	—	—
230	2 99 ₇	3 00 ₂	6	5	—	—	—	—	—	—	—	—
111	5 01 ₂	5 03	7	—	1	—	—	—	—	—	—	—
121	3 85 ₇	3 92	20	3	—	—	—	—	—	—	—	—
131	2 97 ₂	2 97 ₂	2 5	—	—	—	—	—	—	—	—	—
331	2 42 ₂	2 42	9	—	—	—	—	—	—	—	—	—
441	1 88 ₂	1 87	2 5	—	—	—	—	—	—	—	—	—

TETRABROMDIMETHYLETHANF $\text{CH}_3 \text{ CBr}_2 \text{ CBr}_2 \text{ CH}_3$ $M = 373.75$

This compound was prepared by the v Pechmann-Bauer method * Federow† describes two crystalline modifications. The first, a stable tetragonal form, is described in Part II of this paper. The second is an unstable orthorhombic form.

(a) *Low Temperature Orthorhombic Modification*—Federow grew this form from ligroin at -10°C , he gives very approximate angular measurements

$$(110) (1\bar{1}0) = 56^\circ - 56\frac{1}{2}^\circ \quad (011) (0\bar{1}1) = 59^\circ - 60\frac{1}{4}^\circ$$

and also mentions the presence of $\{010\}$ planes. From these he deduces the ratio

$$a : b : c = 0.535 : 1 : 1.746$$

If we change his a, b, c axes into c', a', b' axes, the occurring forms become $\{101\}$, $\{110\}$ and $\{100\}$ and the new axial ratio

$$a' : b' : c' = 0.573 : 1 : 0.306$$

This bears a close resemblance to the original form of the axial ratios of C_2Cl_6 , etc., and the crystal habit is the same as for those substances.

* 'Ber d Deut Chem Ges,' vol 42, p 668 (1909)

† 'J Prakt Chem,' vol 42, p 145 (1900), also 'Z f Kryst,' vol 21, p 399 (1903)

Some of the $C_2Br_4(CH_3)_2$ prepared in the laboratory was allowed to crystallise from ether + ligroin surrounded by a freezing mixture in a vacuum flask, and a few orthorhombic crystals were obtained. These showed well-developed {101} and {210} forms, with smaller {100} and {010} faces. A Laue photograph of a small crystal taken with the X-rays perpendicular to the (100) plane was entirely similar to those of the other members of the series. The crystal, however, was not quite single. The spectrometer readings were made using a fairly large crystal and in some haste because of its probable instability. The crystal did, in fact, go cloudy and fall to pieces after a few days.

The following angles are probably correct to within 5'–10' —

$$\begin{array}{ll} (210) (100) = 28^\circ 17' & (102) (100) = 71^\circ 25' \\ (101) (100) = 60^\circ 10' & (210) (230) = 29^\circ 47' \end{array}$$

These give an axial ratio

$$\begin{array}{l} a \quad b \quad c = 1.073 \quad 1 \quad 0.601 \\ = 2 \times 0.536 \quad 1 \quad 2 \times 0.300 \end{array}$$

It will be seen that the a/b ratio is about 7 per cent smaller than Federow's admittedly inaccurate value. The X-ray data lead to a density of 2.945.

Table VI

Plane	Spacing		Intensities observed									
	Calc.	Obs.	1	2	3	4	5	6	7	8	9	10
100	11.70 ₆	2.94 ₃	—	—	—	5	—	—	—	—	—	—
010	10.90 ₉	5.42 ₂	—	3	—	11	—	6	—	—	2	—
001	6.55 ₈	3.27 ₄	—	1	—	—	—	—	—	—	—	—
101	5.72 ₉	5.84 ₁	—	2	5	—	—	—	—	—	—	—
102	3.15 ₇	3.20 ₁	3	5	—	—	—	—	—	—	—	—
210	5.15 ₇	5.20 ₁	2	5	—	11	—	—	—	—	—	—
230	3.08 ₄	3.10 ₁	3	5	—	—	—	—	—	—	—	—
111	5.06 ₈	5.15 ₇	Very broad									
311	3.20 ₆	3.12 ₁	3	—	—	—	—	—	—	—	—	—

(b) *Second Orthorhombic Modification*—It was found during the attempts to obtain fresh batches of tetragonal crystals that an orthorhombic modification, isomorphous with the series but quite distinct from the low-temperature form, could be obtained by recrystallisation from benzene at ordinary temperatures. It yielded very good crystals, many of which were plates on {010} (not

on {100} as in the case of other members of the series) elongated in the [001] direction, and bounded by small {101} and smaller {210} and {101} faces. These showed the full symmetry of the bipyramidal class. Others, however, were so unequally developed that their symmetry was not obvious. The latter were tabular on a pair of {101} faces, the remaining pair being very small. These plates were bounded by {210} faces, the {010} and {100} being entirely absent. The following angles are correct to within 1' 2'

$$\begin{array}{lll} (210) \quad (\bar{2}10) = 58^\circ 32' & (033) \quad (0\bar{3}\bar{3}) = 64^\circ 25' & (101) \quad (10\bar{1}) = 58^\circ 42' \\ (610) \quad (\bar{6}10) = 21^\circ 10' & (013) \quad (01\bar{3}) = 23^\circ 42' & (102) \quad (10\bar{2}) = 31^\circ 25' \end{array}$$

Hence

$$a \quad b \quad c = 1 \quad 1206 \quad 1 \quad 0 \quad 6296$$

Table VII

Plane	Spacing		Intensities observed							
	Calc	Obs	1	2	3	4	5	6	7	8
100	11 70 ₀	2 92 ₃	—	—	—	45	—	—	—	1 5
010	10 44 ₁	5 22 ₂	—	17	—	3 5	—	15	—	1 5
001	6 57 ₂	3 27 ₄	—	21	—	1 5	—	—	—	—
011	5 56 ₂	5 57	5	4	12	—	—	—	—	—
013	2 14 ₂	2 15	8	—	—	—	—	—	—	—
101	5 73 ₁	5 71	10	35	—	—	—	—	—	—
201	4 37 ₀	4 34 ₂	2	4 5	5	—	—	—	—	—
102	3 16 ₂	3 14	42	4	—	—	—	—	—	—
401	2 67 ₂	2 65 ₂	16	—	—	—	—	—	—	—
302	2 51 ₂	2 49	17	—	—	—	—	—	—	—
210	5 10 ₂	5 09 ₂	21	4	13 5	—	—	—	—	—
230	2 99 ₁	Obs only	—	—	—	—	—	—	—	—
610	1 91 ₁	1 92	7	—	—	—	—	—	—	—
111	5 02 ₂	4 99	9	—	—	—	—	—	—	—
112	3 02 ₂	3 02	10	—	—	—	—	—	—	—
131	2 97 ₂	2 96	0	—	—	—	—	—	—	—

It will be seen that there are marked differences between Tables VI and VII. The (010) plane shows the biggest change both in spacing and in the relative intensity of its various orders.

General Survey of the Isomorphous Series—There are certain conclusions common to all members of this isomorphous series.

The space-group is Q_h^{16} .

There are four molecules in the unit cell, each possessing a plane of symmetry parallel to (010).

In the case of C_2Cl_6 , C_2Br_6 and probably $C_2Br_4(CH_3)_2$, the molecules also possess a pseudo-centre, the four pseudo-centres lying in the positions

$$(\frac{1}{2} \frac{1}{2} z) (-\frac{1}{2} -\frac{1}{2} -z) (-\frac{3}{2} \frac{1}{2} \frac{1}{2} -z) (\frac{3}{2} -\frac{1}{2} \frac{1}{2} +z)$$

The parameter z does not appear to equal any very simple fraction

Considering the [001] zone alone, the number of possible atomic arrangements is, to a certain extent, limited

(1) The two C atoms may lie in the (010) plane or at equal distances on either side of that plane—one parameter x

(2) The six halogen atoms (or methyl groups) must be arranged in one of four possible ways —

- (a) All six may lie in the (010) plane
- (b) Two may lie in the (010) plane and four outside it
- (c) Four may lie in the (010) plane and two outside it
- (d) All six may lie outside the (010) plane

Possibility (d) may be eliminated at once because $C_2Br_4F_2$ and $C_2Cl_3Br_3$ are among the molecules possessing a plane of symmetry, so that at least two halogens must lie in that plane

(a) may also be eliminated because if the halogen atoms all lay in successive (020) planes, the intensities of the second, fourth, sixth, etc., orders of (010) should fall off very nearly "normally," the scattering power of the C atoms being comparatively small. In general, however, the sixth, eighth order reflections are relatively far more intense than the second and fourth, showing that heavy

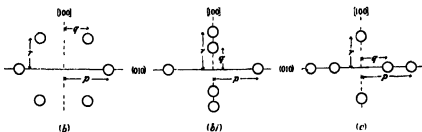


FIG 8

atoms must lie between the (020) planes. Since the projection of the molecule C_2Cl_6 on (001) must also possess an apparent plane parallel to (100), the possible arrangements left are (fig 8)

(b 1) is highly improbable. It would mean either that the four atoms lay in

a row along the b axis, or that the projection of the atoms on (100) must be of the form shown in fig 9, which seems almost impossible for a molecule such as C_2Cl_6 . If $q = 0$ or $r = 0$, this would reduce to a special case of (c), or if $r = q \neq 0$ to a special case of (b).

The two most probable arrangements, therefore, are (b) and (c). In each of these the halogen atoms have only one variable parameter r in the [010]

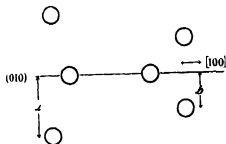


FIG 9—Three variable parameters in [001] direction

direction, and it is possible to calculate all probable values of the structure factor S . Assuming the crystal to be ideally imperfect (an assumption which must be nearly true for soft organic crystals), the following relation holds —

$$I_{\text{obs.}} = K R^2 \frac{1 + \cos^2 2\theta}{\sin 2\theta} e^{-B \sin^2 \theta}$$

Here θ is the angle of reflection and K is a constant independent of θ . If the crystal were not assumed to be ideally imperfect, K would contain a factor dependent on the intensity. The temperature factor $e^{-B \sin^2 \theta}$ cannot yet be evaluated for these crystals and is therefore neglected. Then

$$R \propto \sqrt{I_{\text{obs.}} + \frac{1 + \cos^2 2\theta}{\sin 2\theta}}$$

Now R is the product of the structure factor S and the composite Hartree factor ΣF , which allows for the falling off of scattering power of the constituent atoms with angle. Hence the ratio R/S should be a function of θ which decreases as θ increases*. Table VIII gives observed values R for the different orders of (010).

* Bragg, 'Roy Soc Proc,' A, vol 105, p 16 (1924)

Table VIII

	C ₂ Cl ₄	C ₂ Br ₄	C ₂ Cl ₂ Br ₂ (s)	C ₂ Cl ₂ Br ₂ (a)	C ₂ Br ₂ F ₂	C ₂ Cl ₂ Br ₂	C ₂ Br ₂ (CH ₃) ₂ (a)	C ₂ Br ₂ (CH ₃) ₂ (b)
b =	10 14 _s	10 70 _s	10 37 _s	10 35 _s	10 75 _s	10 44 _s	10 90 _s	10 44 _s
(020)	58 5	39	45	50 5	21 5	51 5	40	67
(040)	40	37	46 5	41 5	48 5	42 5	109	38
(060)	100	100	100	100	100	100	100	100
(080)	73 5	50	48	43	70 5	49 5	68	37
(0100)	<15 5	—	<22 5	<31 5	—	<23	—	—
(0120)	<17	—	<25	<39	—	<23	—	—

In each case R for (060) has been taken as 100, to emphasise the fact that the values are only relative. Where maximum values of R are quoted for (0100) and (0120), it means that those orders were carefully looked for and that they could have been observed if R had been greater than the given value.

The structure factor S for any plane (0 n 0) where n is even is given by (fig 10)

$$(b) S \propto A + 2B \cos 2\pi n \frac{\tau}{b} + 4C \cos 2\pi n \frac{x}{b},$$

$$(c) S \propto D + 2E \cos 2\pi n \frac{\tau}{b} + 4C \cos 2\pi n \frac{x}{b},$$

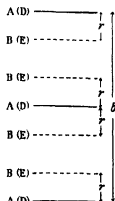


Fig 10

where C is the scattering power of carbon and A, B, D, E are the initial scattering powers of the atoms given below

Table IX

	C ₂ Cl ₄	C ₂ Br ₄	C ₂ Cl ₂ Br ₂ (s) and (a)	C ₂ Br ₂ F ₂	C ₂ Cl ₂ Br ₂	C ₂ Br ₂ (CH ₃) ₂ (a) and (b)
A	4Cl	4Br	4Br or 4Cl	2Br + 2F	2Cl + 2Br	4(CH ₃) or 4Br
B	4Cl	4Br	4Cl or 2Cl + 2Br	4Br	2Cl + 2Br	4Br or 2Br + 2(CH ₃)
D	8Cl	8Br	4Cl + 4Br or 8Cl	6Br + 2F	6Cl + 2Br or 6Br + 2Cl	4Br + 4(CH ₃) or 8Br
E	2Cl	2Br	2Cl or 2Br	2Br	2Br or 2Cl	2Br or 2(CH ₃)

Only two values of x have been considered —

$$x = 0 \text{ (C — C in (010) plane)}$$

$$x = \frac{1.54}{2} = 0.77 \text{ \AA} \text{ (C — C perpendicular to (010) plane)}$$

For the purposes of calculation we must know whether the atoms are ionised or not. The following are the initial scattering powers ($\theta = 0$) in each case —

	C	F	CH ₃	Cl	Br
Not ionised	6	9	9	17	34
Ionised	3	10	10	18	35

↗
(partly sharing)

The values of S for the following different arrangements have been worked out for all possible values of $\phi = 2\pi \frac{r}{b}$

- (1) Arrangement (b), atoms not ionised, $x = 0$
- (2) Arrangement (b), atoms ionised, $x = 0$
- (3) Arrangement (b), atoms not ionised, $x = 0.77 \text{ \AA}$
- (4) Arrangement (b), atoms ionised, $x = 0.77 \text{ \AA}$
- (5) (6) (7) (8) Corresponding conditions for arrangement (c)

It was found from these calculations that only for one substance, $C_2Br_4(CH_3)_2$, (b), could decreasing values of $\frac{R}{S} = f(\theta)$ be found for arrangement (c), whereas arrangement (b) gave some sort of agreement for every substance examined. It may definitely be stated, therefore, that of the six halogen atoms (or methyl groups) in each molecule, two lie in the plane of symmetry (010) and the other four are arranged in pairs on either side.

It was also found that for three of the series a decreasing $f(\theta)$ could not be obtained with the C atoms at distance 0.77 \AA from the (010) planes. This leaves arrangements (1) and (2), results for which are tabulated below.

A value of ϕ for which R/S is a decreasing $f(\theta)$ cannot be found for either symm or asymm $C_2Cl_4Br_2$, assuming that the two Br atoms lie in the (010) plane. This would indicate that the formula of both isomers is CCl_2CClBr_2 . It is true that the agreement even for the latter formula is not good, $f(\theta)$ for the first order being distinctly large, but this may easily be due to the fact that we have assumed only one variable parameter in the [010] direction, whereas for the molecule CCl_2CClBr_2 there would probably be two, one for the pair

Table X.

$C_2Cl_4 = Cl-C-C-Cl$ Cl Cl Cl Cl			$C_2Br_4 = Br-C-C-Br$ Br Br Br Br			$C_2Cl_3Br = Cl-C-C-Br$ Cl Br Cl Br		
Sin θ	Not ionised. (1)	Ionised. (2)	Sin θ	Not ionised. (1)	Ionised. (2)	Sin θ	Not ionised. (1)	Ionised. (2)
0.0605	2.425	3.215	0.0574	2.37	2.925	0.0598	2.875	3.46
0.1211	3.38	2.60	0.1148	2.63	2.40	0.1176	3.415	2.75
0.1816	1.96	1.65	0.1722	1.56	1.55	0.1764	1.51	1.69
0.2422	1.09	1.23	0.2390	0.925	1.03	0.2353	0.815	0.83
0.3027	<1.67	<0.96				0.2940	<1.23	<1.055
0.3633	<0.97	<0.92				0.3638	<0.84	<0.93
$\frac{2\pi r}{b} = \phi =$	51°(129°)	51.5°(128.5°)					52.5°(127.5°)	52.5°(127.5°)
$C_2Cl_3Br = Br-C-C-Cl$ Cl Cl Cl Cl			$C_2Cl_4Br_2 = Br-C-C-Br$ Cl Br Cl Br			$C_2Cl_3Br = Cl-C-C-Cl$ Cl Br Cl Br		
Sin θ	Not ionised. (1)	Ionised. (2)	Sin θ	Not ionised. (1)	Ionised. (2)	Sin θ	Not ionised. (1)	Ionised. (2)
0.0592	1.065	1.41	0.0592	4.90	6.85	0.0593	7.54	12.35
0.1184	1.99	3.60	0.1184	2.185	1.95	0.1187	2.275	1.99
0.1776	0.965	1.06	0.1776	1.745	1.63	0.1780	1.60	1.67
0.2368	0.73	0.87	0.2368	1.015	1.075	0.2373	1.145	1.23
0.2960	<1.87	<13.15	0.2960	<0.485	<0.46	0.2966	<1.245	<1.14
0.3552	<0.28	<0.315	0.3552	<1.135	<1.285	0.3560	<1.035	<1.11
$\phi =$	55.5°(124.5°)	55.5°(124.5°)					54°(126°)	54°(126°)
$C_2Br_4(CH_3)_2 = (CH_3-C-C-CH_3)$ Br Br Br Br			$C_2Br_4(CH_3)_2 = Br-C-C-CH_3$ Br Br Br CH ₃			$C_2Br_4(CH_3)_2 = Br-C-C-Br$ Br CH ₃ Br CH ₃		
Sin θ	Not ionised. (1)	Ionised. (2)	Sin θ	Not ionised. (1)	Ionised. (2)	Sin θ	Not ionised. (1)	Ionised. (2)
0.0663	18.05	10.20	0.0663	3.45	5.68	0.0598	2.80	3.40
0.1196	3.33	3.165	0.1196	2.335	2.565	0.1176	2.22	2.94
0.1689	2.18	2.25	0.1689	1.925	1.28	0.1765	1.045	1.09
0.2253	1.90	1.965	0.2253	1.97	8.93	0.2353	1.19	1.375
$\phi =$	52.5°(127.5°)	52.5°(127.5°)					58.5°(121.5°)	58.5°(121.5°)

of Cl atoms outside the (010) plane, and one for the Br atoms similarly placed. This would apply in a greater or less degree to the other "uneven" molecules, CBr_3 , CBr_2F and CCl_3 , CBr_3 (or CCl_2Br , CClBr_2).

For $\text{C}_2\text{Br}_4(\text{CH}_3)_2$ (both modifications) a decreasing $f(\theta)$ was only obtained by assuming the CH_3 groups to lie in the (010) plane, so that the formula $\text{CBr}_2(\text{CH}_3) \cdot \text{CBr}_2(\text{CH}_3)$ is verified by this analysis.

For each of the eight isomorphous crystals examined, a decreasing $f(\theta)$ could be found for arrangement (2), which assumes ionised atoms. In most cases agreement was possible and sometimes even better for arrangement (1), which assumes not ionised atoms, and it seems likely that the real truth of the matter is somewhere between the two extremes. The deciding factor is, of course, the ratio of the scattering powers of halogen and carbon atoms. The values $\text{C} = 3$, $\text{Cl} = 18$ ($\frac{\text{C}}{\text{Cl}} = 0.17$) imply that the C—C bond consists of two equally shared electrons, but that each C atom gives up its three remaining valency electrons to the three Cl atoms surrounding it. The values $\text{C} = 6$, $\text{Cl} = 17$ ($\frac{\text{C}}{\text{Cl}} = 0.35$) imply that all the valency bonds are two-electron linkages. The C/Cl ratios used above are only really correct for $\theta = 0$, and since we do not know exactly how each ratio varies with increasing values of θ , the calculations cannot be applied rigidly. An intermediate value of the C/Cl ratio could be attained by supposing that the C—C bond consists of *two* shared electrons, while the C—Cl bonds consists of *one* shared electron (originally a C valency electron). This arrangement would be in agreement with Main Smith's statements* that chemical bonds in general consist of only one shared electron, but that the single bonds between C atoms in organic chemistry frequently consist of di-electronic junctions.

The values of r corresponding to the selected values of ϕ for arrangement (2) are —

C_2Cl_6	$r = 1.45 (3.62) \pm 0.04 \text{ \AA}$
C_2Br_6	$r = 1.58 (3.77) \pm 0.04 \text{ \AA}$
(s) $\text{C}_2\text{Cl}_4\text{Br}_2$	$r = 1.55 (3.64) \pm 0.04 \text{ \AA}$
(a) $\text{C}_2\text{Cl}_4\text{Br}_2$	$r = 1.55 (3.63) \pm 0.04 \text{ \AA}$
$\text{C}_2\text{Br}_5\text{F}$	$r = 1.58 (3.80) \pm 0.03 \text{ \AA}$
$\text{C}_4\text{Cl}_2\text{Br}_2$	$r = 1.52 (3.70) \pm 0.09 \text{ \AA}$
(a) $\text{C}_4\text{Br}_4(\text{CH}_3)_2$	$r = 1.59 (3.86) \pm 0.05 \text{ \AA}$
(b) $\text{C}_4\text{Br}_4(\text{CH}_3)_2$	$r = 1.78 (3.44) \pm 0.01 \text{ \AA}$

* 'J Soc Chem Ind,' vol 43, p 323 (1924) (Chem and Ind Rev)

Fig 11 shows the final arrangement of atoms in the [001] zone, the values of the parameters x , p , q have not yet been determined. That there are interest-

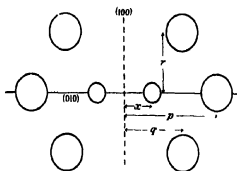


Fig 11

ing differences in respect of these values between the different compounds is shown in the following table, giving observed values of R for the (100) planes [$R_{100} = 100$ throughout]

Table XI

	C_2Cl_6	C_2Br_6	$C_2Cl_4Br_2$ symm	$C_2Cl_4Br_2$ asymm	$C_2Br_4F_2$	$C_2Cl_2Br_4$	$C_2Br_2(CH_3)_4$ (a)	$C_2Br_2(CH_3)_4$ (b)
$\alpha =$	11 51 ₅	12 07 ₅	11 73 ₅	11 61 ₄	11 84 ₁	11 77 ₁	11 70 ₁	11 70 ₅
200	< 9	< 12 5	10	11	< 9	< 8 5	< 22	< 7 5
400	100	100	100	100	100	100	100	100
600	< 12	< 22	< 18	< 20	22 5	21	< 40	< 13
800	47	72 5	41	45 5	37 5	44	< 46	26 5
1000	< 15 5	< 29	—	—	< 30	24	—	< 17 5
1200	< 17 5	< 32 5	—	—	< 33 5	< 28	—	< 20

There are also interesting resemblances between the reflections from various orders of the (210) planes and those of (010). It is hoped that further investigation will help to fix all the remaining parameters (three in the [100] direction and four in the [001] direction) with some certainty.

It is interesting to compare the form of the curves given by plotting R/S against $\sin \theta$ with Hartree's F curves*. Hartree's curves for Cl^- (18) and

* 'Phil Mag,' vol 50, p 289 (1925)

C^{4+} (2) are given in fig 12 together with the "observed" curves for ionised C_2Cl_4 and C_2Br_4 . Since only relative intensities were measured, the R/S scale

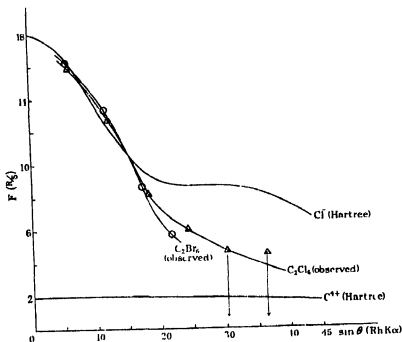


FIG 12—Arbitrary Scale for C_2Cl_4 and C_2Br_4

has been arbitrarily adjusted so as to bring the curves into a position suitable for comparison. The falling off of R/S for higher orders is more rapid than would be expected from Hartree's curves

Symmetry of the Carbon Valencies—The projection of the molecule shown in fig 11 is obviously consistent with a pseudo-trigonal molecule of the type usually assumed by chemists and indicated by other experiments. Mark and Pohland* have investigated the structures of ethane and of diborane by the powder method and have found that in these the molecule, C_2H_6 or B_2H_6 , apparently exists as a distinct entity and that the symmetry of the C (B) atom is at least C_3 , the axis of the C—C dumb-bell lying along the principal axis of the cell. They give the distance between the C centres as 1.55 Å and the distance between centres of nearest C atoms of neighbouring molecules as 3.5 Å. The exact positions of the H nuclei could not be fixed. More recently, Mark and Noethling† have shown that the methane C atom in tetramethylmethane lies

* 'Z f Kryst.', vol. 62, p. 103 (1925)

† 'Z f Kryst.', vol. 65, p. 435 (1927)

on a trigonal axis, the probable symmetry of the molecule being T_d , and C_{3v} , that of the substituted CH_3 .

It is also true that any other orientation of a pseudo-trigonal molecule in the unit cell of C_2Cl_6 , etc., would give results inconsistent with experimental observation. Now in these crystals the molecule, which apparently might have had a trigonal axis in addition to other symmetry, actually possesses only one plane. The C atoms lie in this plane and so do two of the Cl (or other halogen) atoms. Therefore two of the valency directions of each C lie in the plane, the other four being disposed in pairs about it. In other words, of the four valencies belonging to each C atom, two lie in the plane and two outside it. Thus each C atom may be regarded as having two "A" and two "B" valencies. The difference between the C atoms which leads to the absence of any other real symmetry must be that in the one case the A valencies lie in the plane and the B outside it, whereas for the other carbon atom in the molecule the B valencies lie in the plane and the A outside it (fig 13)

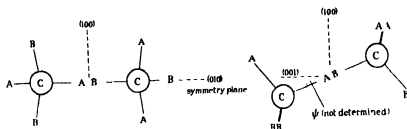


FIG. 13

This is the simplest arrangement of two similar four-valency atoms which combine to possess a plane but no other real element of symmetry. Combined with six like atoms the whole system could obviously, however, very closely simulate centro-symmetry (fig 14). It seems reasonable to trace a close

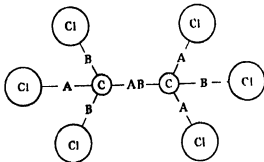


FIG. 14

connection between these two pairs of A and B valencies for the carbon atom and the nature of the four so-called "valency" electrons. According to Bohr's original scheme free C has four (2, 1) electrons whose orbits are tetrahedrally arranged. Later Fowler* showed that the doublet spectrum of ionised C (C II) is immediately explained if C^+ has two (2, 1) and one (2, 2) electrons, but is not consistent with the idea of four (2, 1) electrons in neutral carbon. The work of Main Smith† and of Stoner,‡ now generally accepted, indicates that the four outer electrons are arranged, two in (2, 1) orbits and two in (2, 2) orbits. The tetrahedral symmetry so generally attributed to the carbon atom is *not*, therefore, a necessary property of the outer electrons, and in the case of C_2Cl_4 it is shown to be non-existent. The most reasonable explanation of the existence of A and B valencies is to suppose that in the case of the A valency it is a (2, 1) electron that is shared with, or transferred to, another atom, and that the B valency similarly corresponds to a (2, 2) electron. In that case, the evidence shows that the junction between the two carbons in C_2Cl_4 is effected by the mutual sharing of a (2, 1) and a (2, 2) electron. If this is always the case, then it is not difficult to see why the C atom in diamond, for example, appears to possess complete T_d (hexakis-tetrahedral) symmetry. Fig 15 shows that each C atom, originally possessing two A and two B valencies (or electrons) in the crystal shares four pairs of (AB) electrons with its four neighbours. The atoms, therefore, attain a much higher degree of symmetry in the crystal by means of electron-sharing, if it is understood that the sharing is completely mutual, that is, that an (AB) electron-pair is equivalent to a (BA) electron-pair. This involves either the sharing of a single new orbit by the two electrons or the mutual influencing of each orbit by the other so that they become equivalent, or, finally, the absolutely equal sharing of the two distinct orbits by the two C residues. As it stands, fig 14 possesses at most tetrahedral symmetry, but by replacing both (AB) and (BA) by "P" junctions, the symmetry becomes cubic (hexakis-octahedral). It is nevertheless true that though the internal arrangement is strictly cubic, the external surface might, if the orbits can be regarded as capable of location in space, have a predominance of (2, 1) electrons on one side and of (2, 2) on the other. The question is, could this difference be detected by any physical or chemical means? It is difficult to see how such a difference is to be avoided by any arrangement of the Main Smith-Stoner type.

* 'Roy Soc Proc,' A, vol 165, p 299 (1924).

† *Loc cit*

‡ 'Phil Mag,' vol 48, p 719 (1924)

of C atoms, unless the true cell of diamond is considerably larger than has hitherto been determined

The problem suggests itself as to whether there is any chemical difference

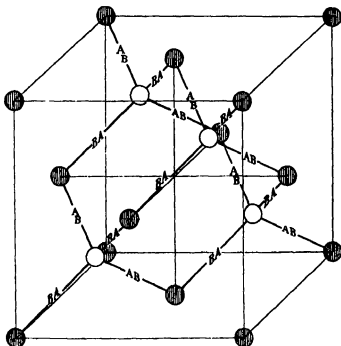


FIG 15

between an A and a B valency, whether, for example, an atom attached by means of an A valency might be more easily replaced than one attached by a B valency, or vice versa. If so, this might possibly account for the two forms of $C_2Cl_4Br_2$, both of which appear to have the formula $CCl_3 \cdot CClBr_2$, and which resemble each other so closely in other ways. In the one case the Br atoms might be attached by means of A valencies, and in the other case by B valencies. It would similarly be possible to have two forms of $CCl_2Br \cdot CClBr_2$. There are serious difficulties in the way of this idea, but since the two ends of the molecule are definitely unlike, the possibility of isomers is worth consideration.

Summary of Part I

The following substances have been examined in detail and are found to belong to an isomorphous series: C_2Cl_4 , C_2Br_4 , $C_2Cl_4Br_2$ (two forms), $C_2Br_4F_2$, $C_2Cl_2Br_2$, $C_2Br_4(CH_3)_2$ (two forms, one obtained at temperature below $0^\circ C$)

They crystallise in the space-group Q_h^{18} and the maximum and minimum values of the axial lengths are

$$a = 11\ 51_3 - 12\ 07_0\ \text{\AA}.$$

$$b = 10\ 14_5 - 10\ 90_0\ \text{\AA}$$

$$c = 6\ 39_4 - 6\ 57_3\ \text{\AA}$$

There are four molecules in the unit cell, each possessing a plane of symmetry parallel in the crystal to the (010) plane. This plane passes through the two carbon atoms and two of the halogen atoms (or through the two methyl groups in the case of $C_2Br_4(CH_3)_2$). The three molecules C_2Cl_6 , C_2Br_6 and $C_2Br_4(CH_3)_2$ also possess a pseudo-centre of symmetry which produces additional halvings not expected from space-group considerations. The formula of both forms of $C_2Cl_4Br_2$ appears to be $CCl_3\ CClBr_2$. From the molecular symmetry the symmetry of the carbon valencies is deduced, and it is shown that the carbon atom must possess two A and two B valencies. It is suggested that these are closely allied to the two (2, 1) and two (2, 2) electrons in the outer group of neutral carbon. Composite *F* curves are obtained for C_2Cl_6 and C_2Br_6 , which are compared with Hartree's curves for ionised Cl^- and $C^{+1\ + +}$.

An X-ray Study of some Simple Derivatives of Ethane —Part II

By KATHLEEN YARDLEY (Mrs LONSDALE), Amy Lady Tate Scholar[†]

(Communicated by Sir William Bragg, F R S —Received December 15, 1927)

TETRABROMDIMETHYLETHANE $\text{CH}_3\text{CBr}_2\text{CBr}_2\text{CH}_3$ $M = 373.75$

Two orthorhombic forms of this substance have been described in Part I of this paper. There is also, however, a stable tetragonal modification. Grown from ether or ligroin at ordinary temperatures, this modification shows only two forms, which Federow* calls {111} and {110}. The latter are small and often absent. At the first attempt a number of large (about $3 \times 3 \times 4$ mm) bipyramids of this type were obtained overnight. Measurements on the Bragg spectrometer gave —

$$(111) (110) = 28^\circ 55' \text{ (Federow, } 28^\circ 50') \text{}$$

$$(111) (11\bar{1}) = 76^\circ 29'$$

leading to the axial ratio

$$a : c = 1 : 1.280$$

The density found by the flotation method was 2.818 gr/cc. Unfortunately the absorption of such large crystals for Rh rays was too high for measurements to be made with any accuracy except for planes occurring as faces on the crystal. Moreover, the crystals were too soft to permit of any grinding of other planes. Only a very few measurements could be made, therefore, and these were insufficient for a reliable determination of the unit cell. All attempts to obtain Laue photographs of these large crystals were unsuccessful and when subsequent attempts were made to grow fresh smaller crystals, only the orthorhombic (*b*) modification could be obtained. In fact, no subsequent recrystallisations gave the tetragonal form.

On the ionisation spectrometer reflections were measured from the following planes —

Plane	Intensity	Plane	Intensity
220	12	111	14
002	? very broad	222	2
004	8	333	18
202	7	444	—
331	2	555	0.5

* *Loc. cit*

The lengths of the axes are

$$a = 8.80 \text{ \AA} \quad c = 11.27 \text{ \AA},$$

and this possible unit cell contains four molecules, which may lie in the "face-centred" positions. Doubling of the spacings of any of the above planes was carefully looked for but not found. Since, however, it is almost inconceivable that the molecule should itself possess four-fold symmetry, the four molecules in the above cell cannot be exactly alike, and some axial planes must be present in odd orders, though these may be very weak. The molecule might simulate four-fold symmetry quite easily if the four Br atoms (which are the principal diffracting centres) happened to lie in one plane and at the corners of a square.

DIBROMOTETRAMETHYLETHANE $\text{C}_2(\text{CH}_3)_4\text{Br}_2$ $M = 243.97$

Preparation and Crystal Data—The symmetrical compound $(\text{CH}_3)_2\text{CBr}\text{CBr}(\text{CH}_3)_2$ was prepared by Couetier's method,* and recrystallisation from alcohol gave crystals in the form of long tetragonal needles, which were very volatile. These were bounded by prism faces {100} and terminated by pyramid faces {111}. They were flexible, being easily bent about the [100] directions and there was a good cleavage parallel to {100}. No orthorhombic modification could be found. An attempt was also made to obtain the asymmetrical compound $(\text{CH}_3)_3\text{C}\text{CBr}_2(\text{CH}_3)_2$ using the methods described by Couetier† and Delacré‡. This compound, however, proved to be absolutely identical with that first prepared. The X-rays results were the same, the melting-points (under pressure) were the same, 182°C , and a mixed melting-point showed no depression. The crystals looked the same and behaved in the same way, and in fact it would appear that both methods of synthesis merely give the symmetrical compound.

No previous crystallographic measurements were available. The following angles were measured on the spectrometer—

$$(201) (20\bar{1}) = 114^\circ 30'$$

$$(101) (10\bar{1}) = 75^\circ 51'$$

$$(111) (11\bar{1}) = 95^\circ 32'$$

Hence

$$a : c = 1 : 0.7798$$

* 'Ann Chim Phys,' vol 26, p 433 (1892)

† *Loc cit*

‡ 'Chem Zentralbl,' vol 2, p 497 (1906)

Results of Observation—The density was found by the flotation method to be 1.811 gr/c.c. at 21° C. The spectrometer results are as follows —

Table I

Plane	Spacing		Intensities observed							
	Calc	Obs	1	2	3	4	5	6	7	8
100	10.44 _s	5.22	—	100	—	17	—	6	—	4.5
001	8.13 _s	4.09	—	21	—	15	—	—	—	—
110	7.38 _s	3.68 _s	—	61	—	10	—	—	—	—
120	4.87 _s	2.33	—	26	—	0.5	—	—	—	—
130	3.30 _s	1.64 _s	—	5.5	—	—	—	—	—	—
101	6.42 _s	3.21 _s	—	36	—	1.5	—	0.5	—	—
201	4.39 _s	2.19 _s	—	30	—	—	—	—	—	—
102	4.79 _s	1.87 _s	—	0.5	—	—	—	—	—	—
301	3.20 _s	1.59	—	6.5	—	—	—	—	—	—
111	5.47 _s	5.46	—	36	0	—	1	0.5	—	—
112	3.56 _s	1.79	—	3	—	—	—	—	—	—
221	3.36 _s	1.67	—	3.5	—	—	—	—	—	—
113	2.54 _s	2.53	17	—	—	—	—	—	—	—
115	1.59 _s	1.58 _s	2	—	—	—	—	—	—	—
211	4.05 _s	2.01	—	15.5	—	—	—	—	—	—
311	3.06 _s	3.05	15.5	4.5	—	—	—	—	—	—

The needle-like shape of the crystals made it possible for them to be enclosed in a fine glass capillary which could be sealed at both ends. So enclosed, they did not volatilise and small crystals could be examined fairly easily by photographic methods. Rotation and a complete series of oscillation photographs were taken with the principal axis vertical and a few oscillations were obtained with the [100] and [110] directions vertical. These confirmed the spectrometer results, the following reflections being recorded —

200	220	400	420	440	600	620
111	311	331				
002	202	222	402	422		
113	313	333				
004	204	224				
115						

No doublings of any of the spacings could be observed by either method. There are four molecules in this unit cell.

Laue photographs were taken perpendicular to (001), (110) and (100), with the object of confirming the size of the unit cell and also of determining the crystal class. These photographs, and the intensity measurements on the ionisation

spectrometer, showed the existence of apparent planes of symmetry parallel to {110} and {100}, thus indicating that the class is D_{2d} , C_{4v} , D_4 or D_{4h} . The crystal habit shows no polarity, but since only two forms were observed, the evidence either way is not conclusive

Table II

Plane	Intensity	Spacing	$\pi\lambda$	Plane	Intensity	Spacing	$\pi\lambda$
X rays \perp (100)				X rays nearly \perp (100) Extra planes			
120	W	4.67 ₂	4.20	100	VS	10.44 ₂	1.73
150	M	2.04 ₂	0.84	320	M	2.88 ₂	2.70
211	VS	4.05 ₂	3.12	310	W	3.30 ₂	2.65-1.55
311	M	3.06 ₂	1.79	111	M	5.47 ₂	4.93
321	W	2.73 ₂	2.82	531	VW	1.75 ₂	1.20
315	W	1.46 ₂	1.22	421	MW	2.24 ₂	2.11-1.39
935	W	1.35 ₂	1.05	101	VS	6.42 ₂	4.82-2.74
102	S	3.79 ₂	2.76	314	W	1.73 ₂	0.89-0.49
113	S	2.64 ₂	1.22	X rays \perp 001			
115	W	1.59 ₂	0.48 ₂	221	MS	3.36 ₂	2.78
112	M	3.56 ₂	2.42	211	M	4.05 ₂	4.00
Additional planes found with X rays nearly \perp (110)				322	MW	2.73	0.90 ₂
513	VW	1.63 ₂	1.53-1.39	311	M	3.06 ₂	2.25
313	VW	2.09 ₂	1.16-1.14	511	MW	1.98 ₂	0.94 ₂
				301	MW	3.20 ₂	2.48

As far as the spectrometer and oscillation photographic results² were concerned, no odd order reflections were found except for planes with "all odd" indices. This points to a face-centred arrangement of the molecules, each of which must possess nearly, if not quite, all of the symmetry of the class to which the crystals belong. If, however, the molecule $(CH_3)_2CBr-CBr(CH_3)_2$ does possess a tetrad axis, either of pure or of alternating symmetry, the $Br-C-C-Br$ atoms would have to be collinear, lying along the principal axis, an arrangement which is at least unlikely. Any evidence that would reveal differences between the four molecules in the cell was therefore looked for most carefully. From the table of Laue results it will be seen that on a photograph taken with the X-ray beam not quite perpendicular to the (100) plane four distinct spots appeared, due to reflections from (314) planes. The values of $\pi\lambda$ corresponding to these spots were 0.89, 0.83₂, 0.55₂ and 0.49 Å. Now the minimum wave-length of X-rays issuing from the Shearer tube (Cu anticathode) used in the investigation was not less than 0.34-0.35 Å, and

therefore $n\lambda$ for the second order of (314) should be at least 0.68 Å. Since the values 0.55, and 0.49 were found, these reflections must have been of the first order. No other first order reflections from planes with "mixed indices" were found, showing that the four molecules, though not quite alike, must be very nearly so.

Space-group and Molecular Symmetry—The unit cell containing the four molecules has, therefore, dimensions $10.45 \times 10.45 \times 8.14 \text{ Å}^3$, and the molecule must have at least two-fold symmetry. By analogy with the substances examined in Part I of this paper, one would expect a plane of symmetry in the molecule. The intense reflections from (200) and (220), as well as the more or less normal falling off of the intensities of the higher orders of these planes, indicate that the Br atoms lie in pairs along the directions

$$[001]_{00} \quad [001]_{01} \quad [001]_{10} \quad [001]_{11}$$

The methyl groups belonging to any one molecule can be so arranged as to give the molecule an apparent tetragonal axis. The deviation from tetragonal symmetry would then be due only to the deviation of the line joining the centres of the two carbon atoms from the tetrad axis (fig. 1)

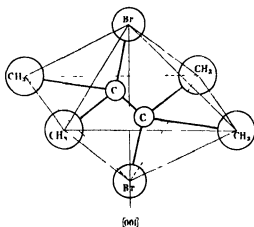


Fig. 1

Such a molecule could have —

- (1) A plane of symmetry perpendicular to the (001) plane
- (2) A centre of symmetry
- (3) An axis of symmetry perpendicular to the [001] direction.
- (4) A combination of all these elements, giving four-fold symmetry

An examination of the theory* shows that there are a large number of space-groups to which this substance might belong. Those in the classes given above which agree with the results found are —

- (a) D_{2d}^1 D_{2d}^2 D_{2d}^3 D_{2d}^4
- (b) C_{4v}^1 C_{4v}^2 C_{4v}^3 C_{4v}^4 C_{4v}^5 C_{4v}^6
- (c) D_4^1 D_4^2 D_4^3 D_4^4
- (d) D_{2h}^1 D_{2h}^2 D_{2h}^3 D_{2h}^4 D_{2h}^5 D_{2h}^6 D_{2h}^7 D_{2h}^8 D_{2h}^9 D_{2h}^{10} D_{2h}^{11} D_{2h}^{12} D_{2h}^{13} D_{2h}^{14} D_{2h}^{15}

In the majority of these, most of the halvings found would have to be regarded as accidental (as, in fact, many probably are). A number of these can be eliminated because the symmetry required by each of four units in the cell is highly improbable in the case of this molecule (*e.g.*, a plane parallel (001) and so on). Others could not lead to an even approximately face-centred arrangement of molecules, and we are finally left with —

- (a) D_{2d}^1 D_{2d}^2 Molecular symmetry plane $\parallel^1 \{110\}$
- (b) C_{4v}^2 C_{4v}^6 Molecular symmetry plane $\parallel^1 \{110\}$
- (c) D_4^3 D_4^4 Molecular symmetry dyad axis $\perp^1 \{110\}$
- (d) D_{2h}^{12} D_{2h}^{15} Molecular symmetry dyad axis \perp^1 plane $\parallel^1 \{110\}$

[Supposing that the planes of symmetry shown in the Laue photographs do not really exist, the space-group C_{4h}^1 , in which the molecule would have centrosymmetry, would also be a possibility]

It is not possible to decide between these eight space-groups at present, but if the molecule illustrated above (fig. 1), with its pseudo-tetragonal symmetry, be adopted, the structure must be one of two, and only two, types, whatever the actual space-group may be. These types are illustrated in fig. 2. Type (a) corresponds to the space-groups D_{2d}^1 C_{4v}^2 D_4^3 and D_{2h}^{12} , and type (b) to the space-groups D_{2d}^2 C_{4v}^6 D_4^4 and D_{2h}^{15} .

As actually drawn, the molecule has a dyad axis perpendicular to a plane which is parallel to $\{110\}$, and the class would then be D_{2h}^1 , but if, as is more likely, the molecule has a real plane and a pseudo-centre (by analogy with C_4Cl_4 , etc.) then the class would be D_{2d} or C_{4v} .

Attempts to place the atoms more accurately by means of intensity considerations have not been successful up to the present, but in every possible arrangement the diameter of the methyl group, considered as a whole, is at least 2.5–3.0 Å and possibly more, the distance between adjacent C and Br centres

* Niggli, *loc. cit.*, Astbury and Yardley, *loc. cit.*

is at least $4.07/2$, and, therefore, if the diameter of the C atom is taken as 1.54 and Br atoms of neighbouring molecules are assumed to be in contact along the

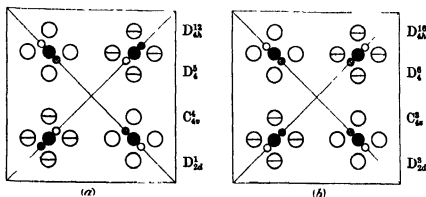


FIG. 2

- | | |
|----------------------------------|--|
| ● Br atom | ● C atom above level of CH ₃ groups |
| ○ CH ₃ group in (001) | ○ C atom below level of CH ₃ groups |
| ⊖ CH ₃ group in (002) | |

principal axis, the diameter of the Br atom must be at least 2.53 \AA . The cleavage parallel to the $\{100\}$ planes must take place at methyl-bromine contacts.

It is very interesting to notice that for

$$\begin{aligned} \text{C}_2(\text{CH}_3)_4\text{Br}_2 \quad a/c &= 1.07798 \\ &= 1.284/1 \end{aligned}$$

while for the tetragonal modification of

$$\text{C}_2\text{Br}_4(\text{CH}_3)_2 \quad a/c = 1.1280$$

The cell in each case contains four molecules approximately in the face-centred positions.

It seems likely that, whereas in the case of $\text{C}_2(\text{CH}_3)_4\text{Br}_2$ the Br atoms lie along the $[001]$ directions and the CH₃ groups along the $[100]$ directions, for $\text{C}_2\text{Br}_4(\text{CH}_3)_2$ the reverse may possibly be the case, but scarcity of data for the latter substance makes any such speculation rather dangerous.

HEXAMETHYLETHANE $\text{C}_2(\text{CH}_3)_6$

The preparation of this compound is described by Henri*. The evaporation of an ethereal solution in an almost closed flask gave small flaky crystals, obviously not single, but these volatilised so quickly that nothing could be

* 'Bull. Acad. R. Belg.', vol. 8, p. 352 (1906), also 'C. R.', vol. 142, p. 1075 (1906)

done with them. In any solvent other than ether the volatilisation of the substance was quicker than that of the solvent.

The same applied to the compound

PENTAMETHYLBROMETHANE $C_5(CH_3)_5Br$

PENTAMETHYLETHANOL $(CH_3)_5C \cdot (CH_3)_4OH$ $M = 116.1$

This was an intermediate product in the preparation of $C_6(CH_3)_6$ and though extremely volatile, it could be exposed to the air for a few seconds without completely disappearing.

It formed needle-like crystals remarkably like those of $C_2(CH_3)_4Br_2$, showing what appeared to be the same forms and capable of being bent in the same directions. Crystals were grown from ether in a *corke*d flask (the slight leakage round the cork enabled evaporation to take place very slowly). These were then quickly removed and placed in fine glass capillaries which were immediately sealed. The whole operation had to be performed in a few seconds in order to avoid volatilisation. The sealed-up crystals remained apparently unchanged for a few days. But gradually they disappeared and it was found that this was due to slight temperature variations along the length (generally about 1 cm.) of the tube, the substance having sublimed to form smaller crystals in the cooler parts of the tube.

Results of Observation—A few spectrometer observations were made, especially for the purpose of determining the system and class, and the axial lengths and angles. Also a complete series of 10° oscillation photographs were made about the axis of the needle as axis of rotation. The crystals were so fine and, by the time they had been transferred to the capillary tubes, their faces were so indistinct that it was most difficult to obtain good photographs with other main directions vertical. The results are therefore incomplete, but even at their present preliminary stage they are most interesting. Laue photographs were attempted, but these were not very successful, since it was extremely difficult to get a good setting of the crystal in the limited time available before sublimation had spoilt the specimen. The angle (100) (010) was fairly easily measureable on the spectrometer and proved to be $90^\circ \pm 5'$. The remaining axial angles could not be measured accurately but were also nearly, if not exactly, right angles. The cell is therefore probably orthorhombic (or pseudo-orthorhombic). The angle (210) ($2\bar{1}0$) was found to be $90^\circ 29'$, giving an axial ratio

$$a : b = 1.9830 : 1$$

The mean of a large number of observations of the spacings of (400) and (020) gave

$$a = 21.35 \text{ \AA}$$

$$b = 10.77 \text{ \AA}$$

and a less accurate measurement of the spacing of (002), whose area was extremely small, gave

$$c = 7.84 \text{ \AA}$$

These lead to the axial ratios

$$a : b : c = 1.9824 : 1 : 0.728$$

The axial lengths may be compared with those of $C_2(CH_3)_4Br_2$. For the latter substance the strongest reflections observed were due to planes of spacing —

$$d_{200} = d_{020} = 5.22_4 \text{ \AA}$$

$$d_{220} = 3.69_4$$

The strongest reflections for $C_2(CH_3)_4OH$ were due to —

$$d_{400} = 5.33_8 \text{ \AA}$$

$$d_{020} = 5.38_1$$

$$d_{420} = 3.79_1$$

The following reflections were found on the Bragg spectrometer —

Table III

Plane	Spacing		Intensities observed				Remarks
	Calc	Obs	1	2	3	4	
100	—	10.67 ₈	—	3	—	31	Spacings of axial planes are twice the measured values. Area small therefore inaccurate. Very carefully measured. Not so carefully measured.
010	—	5.38 ₃	—	30	—	—	
001	—	3.92	—	7	—	1	
210	7.58 ₈	3.79 ₃	—	18	—	—	
410	4.78 ₃	2.37 ₈	—	1	—	—	
211	5.45 ₈	5.48	25	—	—	—	" "

Table IV gives the planes observed on 10° oscillation photographs taken with the [001] direction vertical

Table IV

	Plane	Intensity	Plane	Intensity	Plane	Intensity
Central hyperbola	200	M S	130	V W	440	M W
	110	M S	330	M	730	W
	310	M W	620	M W	910	V W
	400	S	710	V W	640	V W
	020	S	530	W	930	V W
	220	M W	800	W	550	V W
	510	V W	040	V W	840	M S
	420	S	240	V W	1220	V W
	600	V W	820	M W	460	W
1st hyperbola	211	V S	611	M W	631	M
	411	V W	231	M	051	W
	321	W	521	V W	1031	W
2nd hyperbola	112	M	422	M S	712	M W
	202	M	602	M W	802	M S
	312	M W	132	M	042	M S
	222	M	332	M W	242	M W
	512	M	622	W		
3rd hyperbola	213	V S	323	V W	523	W
	413	W	613	V W	633	V W
4th hyperbola	424	M W				

The strongest reflections in the above tables are (400) (020) (420) (211) (213), the first four of which were also observed on the ionisation spectrometer. If the a axis were halved, so as to divide the cell into two pseudo-tetragonal parts, each containing four molecules, these planes would become

$$(200) \quad (020) \quad (220) \quad (111) \quad (113)$$

That these reflections are particularly strong shows that the molecules in each of the two halves are nearly in the face-centred positions, and are similar in scattering power. This is verified by most of the "moderately strong" reflections, such as

$$(840) \quad (422) \quad (802) \quad (042),$$

and by the fact that the rotation photographs of this substance and of $C_2(CH_3)_4Br_2$ show strong resemblances.

That the molecules do differ in orientation is shown, however, by the comparatively strong reflections from (200) (110) and by a number of weaker reflections. No reflections were observed from "all odd" planes, so that the Bravais lattice is Γ_c , the cell being centred (fig 3).

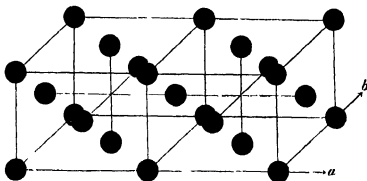


FIG 3

A glance at the tables shows that —

- (1) All planes (hkl) are halved if $h + k + l$ is odd.
- (2) ($h0l$) planes are only observed if h and l are both even—(200) (400) (600) (800) (002) (004) (202) (602) (802).
- (3) ($0kl$) planes are only observed if k and l are both even—(020) (040) (002) (004) (042) [Data insufficient]

The following space-groups are possible —

C_{2v}^{20} —dyad axis of cell parallel to [100] [010] or [001]

C_{2v}^{21} —dyad axis of cell parallel to [001]

C_{2v}^{22} —dyad axis of cell parallel to [100] [010] or [001]

Q^a, Q^o

Q_A^{25} —molecular symmetry a plane or centre

Q_A^{26} —molecular symmetry an axis, plane or centre

Q_A^{28} —molecular symmetry an axis or plane

Only two of these space-groups, C_{2v}^{21} and Q_A^{26} , permit any approximation to a double face-centred cell of the type illustrated in fig 3. In the case of Q_A^{26} the molecule would have to possess a plane of symmetry parallel to (001). Now if, as seems almost certain, the molecules of this substance are arranged very much like those of $C_2(CH_3)_4Br_2$, which it resembles so closely, then a plane parallel to (001) would be out of the question, since a hydroxyl group must lie on one side and a methyl group on the other side of that plane.

This leaves the space-group C_{2v}^{21} , the [001] direction being unique. There are glide-planes parallel to (100) and (010) which intersect in a screw dyad axis. The projections of the molecules on the three axial planes are shown in fig 4.

Fig 5 shows the probable arrangement of the molecule which may, however, be tilted to some extent, though not much, because $a/2$ and b are so very nearly

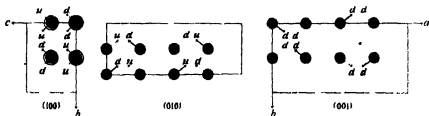


FIG 4

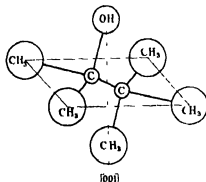


FIG. 5

equal The fact that the scattering power of the methyl group is not much different from that of the hydroxyl group makes it difficult to distinguish between a molecule and its reflection in the (001) plane

The density calculated from the X-ray data, assuming 8 molecules in the unit cell, is 0.85 grs /c.c It was found that the crystals floated in water, so that this assumption as to the number per cell is almost certainly correct It was also noticed that when placed in the water the crystals danced about on the surface in a way entirely similar to the behaviour of camphor in similar circumstances

Summary of Part II

The tetragonal form of $C_2Br_4(CH_3)_4$ has an axial ratio $a : c = 1 : 1.280$, and density 2.818 grs /c.c There are probably four molecules in approximately face-centred positions in a cell of size $8.81^3 \times 11.27 \text{ \AA}^3$ The data obtained are inadequate for a determination of the space-group $C_2(CH_3)_4Br_2$ forms

needle-like tetragonal crystals of axial ratio $a : c = 1 : 0.7798$ and density 1.811. There are four molecules in a unit cell of dimensions $10.45^3 \times 8.14 \text{ \AA}^3$. These molecules are in approximately face-centred positions and possess either a plane or dyad axis of symmetry or both. They also simulate tetragonal symmetry, showing that the line joining the Br atoms must be nearly perpendicular to the plane containing the four CH_3 groups. There are only two possible types of structure, which are illustrated. Attempts to obtain X-ray data for $\text{C}_2(\text{CH}_3)_4$ and $\text{C}_2(\text{CH}_3)_3\text{Br}$ failed because of the extreme speed with which these substances volatilised. $\text{C}(\text{CH}_3)_3$, $\text{C}(\text{CH}_3)_2\text{OH}$ is closely allied to $\text{C}(\text{CH}_3)_2\text{Br}$. $\text{C}(\text{CH}_3)_2\text{Br}$, the orthorhombic cell has dimensions $21.35 \times 10.77 \times 7.84 \text{ \AA}^3$, and the density is < 1 . The unit cell may be divided into two pseudo-tetragonal parts, each containing four molecules in approximately face-centred positions, the space-group is C_{2h}^{21} .

In conclusion, I wish to express my deep appreciation of the constant interest that Sir William Bragg, F.R.S., has shown in the progress of the work. The investigation was carried out at the Davy Faraday Laboratory of the Royal Institution, to the Managers of which I am indebted for all the usual facilities. My thanks are also due to Sir William Pope, F.R.S., for specimens of C_2Cl_6 and $\text{C}_2\text{Cl}_4\text{Br}_2$ (symm.) and to Prof. Swarts for a fine sample of $\text{C}_2\text{Br}_2\text{F}_2$. The remaining substances were all prepared at the Davy Faraday Laboratory by Mr W. B. Saville and Dr. Helen Gilchrist, and I am deeply grateful to these fellow-workers for the time and trouble so generously expended.

*The Behaviour of a Single Crystal of α -Iron subjected to
Alternating Torsional Stresses*

By H. GOUGH, M B E, D Sc, Ph D

(Communicated by Sir Thomas Stanton, F R S —Received December 22, 1927)

[PLATES 8-13]

The object of the investigation described in the present paper was to obtain some information relating to the mechanism of deformation and failure of a single crystal of α -iron subjected to alternating torsional stresses. With this particular type of applied straining action it has been shown previously that complete fracture of a metallic specimen may be produced while the total distortion of the specimen as a whole is extremely small and, in some cases, inappreciable. This has been shown to apply to ductile metals in the form of a finely divided aggregate* and also to the case of large single crystals of aluminium†. Fracture of this kind is of considerable scientific interest, its practical interest is due to the fact that a very large proportion of the failures of components of modern machines and prime movers are of precisely this type. The absence of change of shape of the specimen under these conditions of test does not permit of the employment of the method of distortion measurements devised by Taylor and Elam,‡ but experience§ has shown that careful observation of the characteristics of the slip bands formed affords a valuable and unique method of relating the mechanism of deformation with the crystal structure and the applied stressing system, and this method has been employed in the present experiment.

Apparatus Employed

1 *Alternating Torsion Machine*—The machine used for the application of cycles of reversed torsional straining was originally designed by Mr C E Stromeyer. It has been fully described elsewhere, both in its original form and in the somewhat improved form|| in which it is now employed.

2 *Measuring and Photographic Apparatus*—It was necessary to devise some

* Gough and Hanson, 'Roy Soc Proc,' A, vol. 104, p. 538 (1923).

† Gough, Hanson and Wright, 'Phil. Trans,' A, vol. 226, p. 1 (1925), Gough, Wright and Hanson, 'J Inst Metals,' vol. 36, p. 173 (1926).

‡ 'Roy. Soc. Proc,' A, vol. 102, p. 643 (1923).

§ 'Roy Soc. Proc,' vol. 90, p. 411 (1914).

|| 'Fatigue of Metals,' H. Gough, Scott, Greenwood & Son, London, 1924.

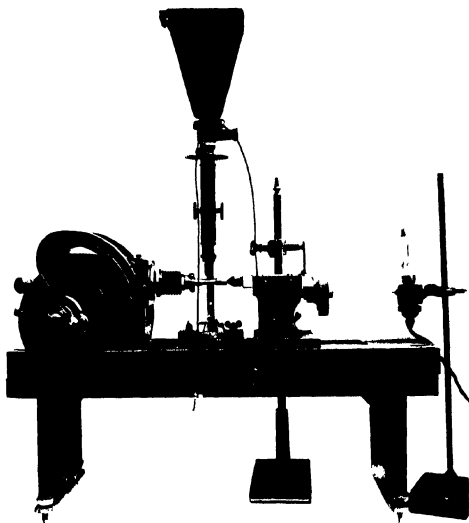


FIG 1—Apparatus used for Measurement and photomicrography



FIG 11 $\lambda = 190$ (10) $\downarrow L$

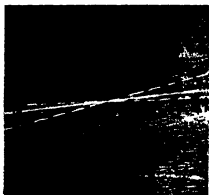


FIG 12 $\lambda = 200$ (20) $\downarrow L$

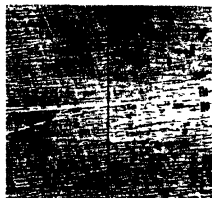


FIG 13 $\lambda = 210$ (30)



FIG 14 $\lambda = 35$

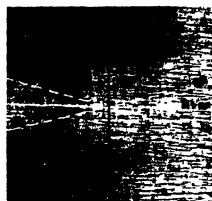


FIG 15 $\lambda = 40^\circ$

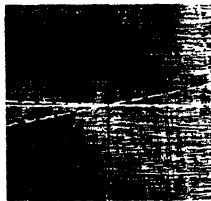


FIG 16 $\lambda = 50^\circ$

FIGS 11-15—Photo micrographs ($\times 80$ diams.)

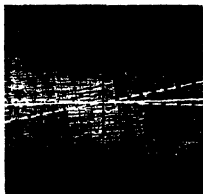


FIG 17 $\lambda = 60$



FIG 18 $\lambda = 65^\circ$

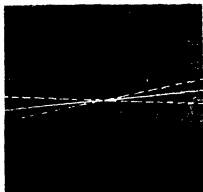


FIG 19 $\lambda = 75$



FIG 20 $\lambda = 255^\circ (75) \frac{1}{2} L$

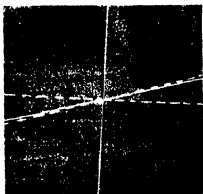


FIG 21 $\lambda = 94^\circ$

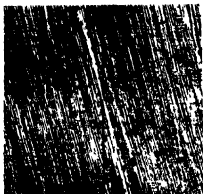


FIG 22 $\lambda = 120 \frac{1}{2} L$

FIGS 17-22—Photo micrographs (80 diam)

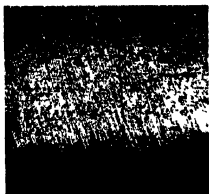


FIG 23 $\lambda = 136$ $\frac{1}{2} L$



FIG 24 $\lambda = 170$

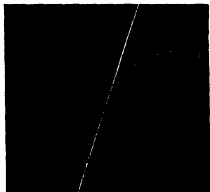


FIG 25 $\lambda = 926$ (146°) $\frac{1}{2} L$

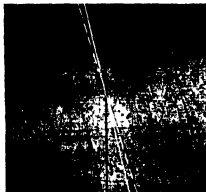


FIG 26 $\lambda = 160^\circ$

FIGS 21-26 Photo micrographs ($\times 80$ diams)

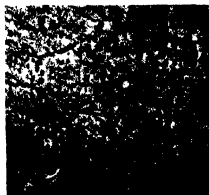


FIG 27 ($\times 120$ diams)

accurate form of apparatus whereby measurements could be made of the slope and position of slip band markings with reference to some datum line on the specimen. The apparatus shown in fig 1 has been fitted up for this purpose. It consists of a dividing head (fitted with the usual index) and a loose tail-stock (with screw adjustment) all mounted on an accurately machined bed plate. The specimen is carried on the centres of the head and tail stocks, and is clamped to the former, while being free to rotate on the latter. A metallurgical microscope, appropriately mounted, can be moved—in a machined slot in the base-plate—in a direction parallel to the axis of the specimen. The microscope can also be traversed in a horizontal direction perpendicular to the axis of the specimen. Attached to the eye-piece of the microscope and free to rotate with the eye-piece, is a circular disc accurately divided into degrees (permitting estimations of angles to one-tenth of a degree of arc). For photographic purposes the same apparatus is used merely replacing the eye piece of the microscope with a Leitz micro-camera attachment (Plate 8 shows this attachment in position). A thread is stretched directly under the plate holder of the camera, and means have been devised whereby this thread coincides with the image of the datum line with reference to which the slopes of the slip bands are measured. The shadow of this thread is photographed and reproduces accurately, on the plate, the position of the datum line. The apparatus thus enables the following operations to be performed with great accuracy, (a) the mounting of the specimen so that the position of the plane of reference is vertical, (b) the determination of the exact angle through which the specimen has been rotated in order to examine any required point on the surface, (c) the measurement of the slope of any surface mark with reference to the intersection on the surface of a plane perpendicular to the axis of the specimen and passing through the point under examination, and, finally (d) photographic record of the microstructure at any required point, the trace of the above reference plane being clearly indicated. It may be added that the above order of accuracy was found to be essential in the present experiment and that the apparatus proved very successful in operation.

Form of Specimen—The specimen is visible in fig 2. It is cylindrical in shape. The central portion is 0.35 inch in diameter and 0.6 inch in length. The enlarged ends are 0.45 inch in diameter and 0.75 inch long. Transition curves of large radius join the several portions. The specimen was machined from a crystal 0.46 inch in diameter and 9.2 inch long, kindly supplied by Prof. Edwards and Mr. Pfaff. On one enlarged end of the specimen eight lines are marked, each line being parallel to the axis of the specimen and spaced at

equal intervals apart. These lines are marked 0, 1, 2, ..., 7, and that numbered 0 will be referred to as "the zero reference mark of the specimen."

Conventions Employed—The specimen axis is the axis of reference. The reference plane is a plane passing through the axis of reference and containing the zero reference mark. The position of the normal of any plane is then denoted by θ and ψ , where θ is the angle between the normal of the plane and the axis of reference, while ψ is the angle between the projection of the normal on a plane perpendicular to the axis and a radial line (lying in this plane) drawn from the centre of the specimen and passing through the zero reference mark or the mark produced. The position of any point on the surface of the specimen is denoted by the symbol λ which represents the angle between two planes both containing the axis of reference, but while one plane contains the zero reference mark, the other contains the point under consideration (λ and ψ thus involve similar measurements, but it is convenient to restrict the use of these terms to points on the surface, and to the normals of planes respectively). The inclination of any mark (slip band, etc.) on the surface of the specimen is measured with respect to the trace of the surface at the point of a plane which is perpendicular to the axis of reference, this inclination is denoted by the symbol θ , prefixed by a \pm sign according to the usual convention.

Description of Experimental Work—After careful machining to the required form, the central portion of the specimen was deeply etched to remove the effect of the machining on the crystalline structure.

An X ray analysis was then made and the results obtained are as stated in Table I.

Table I—Spherical Co-ordinates (uncorrected) of Dodecahedral Planes as determined by X-ray Analyses

Stage of experiment	Plane	110	$\bar{1}\bar{1}0$	011	0 $\bar{1}\bar{1}$	101	1 $\bar{0}$ 1
Before test	θ	87.8	74.5	32.8	57.5	55.0	37.5
	ψ	318.7	50.2	353.7	192.2	265.2	110.2
After test	θ	87.5	74.3	33.7	57.8	55.7	37.4
	ψ	318.9	50.5	349.2	192.0	264.7	110.7

The surface of the parallel portion was then carefully polished. Using a gauge projection apparatus the envelope of the cross-section of the specimen was determined, the cross-section was found to be truly circular and concentric, the actual diameter being 0.3398 inch.

The specimen was then placed in the alternating torsion machine and subjected to 1,110,000 reversals of a range of torque of ± 17.3 inch-lbs ($f_s = \pm 1.0$ tons/inch²), at a frequency of 1000 cycles per minute. It was then removed and examined in a metallurgical microscope, using a 4 mm Apochromat objective (Zeiss). A searching examination of the complete circumference in the middle of the parallel portion of the specimen failed to reveal any slip band markings.

The specimen was replaced in the alternating torsion machine and the range of torque adjusted to ± 34.5 inch-lbs ($f_s = \pm 2.0$ tons/inch²). After a further 1,720,000 reversals (frequency 1000 cycles per minute) the specimen was removed and carefully examined. Again no slip bands could be detected. A large amount of time was spent in this examination, in which both direct and oblique illumination were employed as it is contrary to previous experience to expect that a "single crystal" would exhibit such perfect elasticity under the range of shear stress (± 2 tons per inch²) employed. When it was certain that there was no apparent change in the surface of the specimen, the crystal was replaced in the testing machine and a range of torque of ± 69.0 inch-lbs ($f_s = \pm 4$ tons/inch²) applied at a frequency of 1020 cycles per minute. After 4,280,000 reversals the specimen was again removed and examined. As before, a most careful examination failed to disclose any surface markings apart from mechanical scratches. The specimen was then subjected to 1,410,000 reversals at a range of torque $= \pm 104$ inch-lbs ($f_s = \pm 6$ tons/inch²). On examination, certain portions of the surface showed distinct slip-band markings, the majority of the surface, however, being entirely free from all signs of slip. The slip-bands were widely spaced and comparatively few in number. In appearance they varied from a very close approximation to straightness to a wavy appearance which could, in some cases, be resolved into a combination of shorter straighter bands of two different slopes. A careful survey was made of the entire circumference of the specimen and the inclinations of the slip-bands recorded. The general appearance of the microstructure was not such as to suggest that the limiting range of stress had yet been applied to the specimen. The specimen was, therefore, replaced in the testing machine and the range of applied torque adjusted to ± 140 inch-lbs ($f_s = \pm 8.1$ tons/inch²) at a frequency of 900 cycles per minute. The automatic cut-out of the machine was finely adjusted, so that if the specimen failed, the test would be stopped before the fatigue cracks had time to develop to a great extent. The machine was found stopped after 118,000 reversals. The specimen was removed from the machine and cleaned and a survey was made of the microstructure. The general appearance of the specimen can be described briefly as follows —

Cracks—The specimen had cracked in 14 different places, the general direction of these cracks being longitudinal (parallel to the axis of the specimen) although two of the cracks developed along two distinct branches. All of these cracks were confined to the left-hand half of the specimen, the central and right-hand portions being free from cracks. (An exact survey of these cracks on the developed surface of the specimen was made and is reproduced in fig 2.)

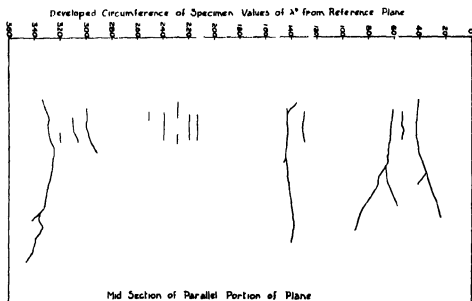


FIG 2—Developed Surface of a Specimen showing Positions and Shapes of Cracks

Gaps in Slip Bands—Four well-defined zones existed in the central and right-hand portions of the specimen in which no slip bands could be detected. The centres of these gaps occurred at, approximately,

$$\lambda = 5^\circ, 95^\circ, 185^\circ \text{ and } 275^\circ,$$

the width of each gap subtending an angle of, approximately, 10° , at the centre of the specimen.

Slip Bands—With the exception of the gaps noted above, the remainder of the surface exhibited clearly defined slip bands. These slip bands differed entirely in appearance at different portions of the specimen but may be described as belonging at any point to one of three main types—

- (i) One set of straight parallel slip bands
- (ii) Two sets of slip bands of differing slopes, those of each set appearing to be straight (or nearly so). In some cases, portions of one set joined portions of the second set, giving at a first glance a "wavy" appearance

- (iii) Distinctly "wavy" slip bands, having a well-defined average slope, and limits of slope, but impossible to resolve into combinations of straight slip bands

Different Appearance of Structure at Centre and in the Neighbourhood of the Cracks — In the left-hand half of the surface of the specimen, the *local* deformation—as judged by the microstructure—had been more severe (in the cracking stage) than in the centre or in the right-hand third. Thus at various positions along the same generator of the surface, it was possible to see the same slip bands in various conditions of development. For example, at values of $\lambda = 5^\circ, 95^\circ, 185^\circ$ and 275° no slip bands (or very faint traces only) were visible at the centre (see, for example, Plate 10, fig. 21), but at the centre of the left-hand third of the specimen, at these same points, junctions of two entirely different sets of well-developed slip bands were observed (see Plate 9, fig. 11). Again, at the points $\lambda = 138^\circ$ and 318° , very straight slip bands were visible (see Plate 11, fig. 24), but very careful manipulation of the lighting system was necessary to reveal these clearly at the centre, at the left-hand side, however, the same slope of slip bands was observed, but the bands themselves were of much closer pitch and easily visible over a wide range of lighting angles (see Plate 11, figs. 23, 25). Again, in many places at the centre where the structure showed clearly two sets of straight bands of different slopes (see Plate 10, fig. 19), the corresponding position towards the left revealed a closely-pitched system of wavy bands possessing the same limits of slope as at the centre but not resolvable into combinations of straight bands (see Plate 10, fig. 20).

Some emphasis has been laid on the differing appearance of the structure at these positions as it will be seen later that valuable information regarding the probable cause of the "waviness" of slip bands in iron has been obtained by a careful comparison of such differences.

Survey of Slip Bands — A complete survey was made of the slopes and appearances of the slip bands ($\lambda = 0^\circ$ to 360°) both at the centre of the specimen and also at a position towards the left-hand end of the parallel portion. The following were recorded —

- (i) general average slope of bands and their characteristics (whether straight or "wavy"),
 - (ii) limits of slopes of "wavy" bands,
 - (iii) individual slopes where two sets of bands were observed,
- together with general notes on appearance, change-over points, etc. Considerations of space forbid the presentation of these data in a complete form. It will

be sufficient to record the mean slope, also the limits of slope, of the slip bands at a number of points spaced round one-half of the circumference of the specimen (at points 180° apart, the slopes were of the same value but of opposite sign) These readings are as stated in Table II. A series of representative photomicrographs accompany the paper and illustrate various typical features exhibited by the micro-structure. In order to determine to what degree of accuracy the readings of the inclinations of the slip bands could be repeated, three complete series of measurements were made at different times. The results were found to be in very good agreement.

Table II—Some Data relating to Observed Slip Bands

Position of surface examined (val of λ)	Slope of slip bands		Position of surface examined (val of λ)	Slope of slip bands	
	Mean slope	Limits of slope		Mean slope	Limits of slope
0*	0	0 and - 0½	90*	- 82	80½ and - 80
5*	(a) 7	(a) 8 and - 8	95*	(a) - 80½	80½ and - 78
	(b) 77	(b) 73 and 86		(b) 0	—
10*	80	74 and 87	100*	0	—
15	83	74½ and 87	105	6½	—
20	84	75 and 87	110	12	12
25	84	76 and 87	115	14	17½ and 14
30	85	76 and 89	120	16½	18 and 15
35	87	75½ and 88	125	18	19 and 17
40	88	77 and - 81	130	18½	19 and 17
45	89	88 and - 81	135	19	straight parallel slip bands difficult to focus in microscope
50	89½	87 and - 82	140	19	
55	89½	88 and - 81	145	19	
60	- 89	87 and - 80½	150	18½	
65	- 88	87½ and 81	155	19½	19½ and 16
70	- 85	87 and - 81	160	15	20 and 16
75	- 86	87½ and - 80	165	12½	19½ and 14½
80	- 85	87½ and - 80	170	9	14½ and 5
85	- 84½	87 and - 80½	175	7½	12½ and 1½
					11 and - 2

* Central portion of specimen free from slip bands at these points

The specimen was again submitted to X-ray analysis, the results of which are as stated in Table I. Using a projection apparatus (magnification 50:1) it was found that no change in the form or dimensions of the cross-section of the specimen had occurred during the test. No permanent relative twist of the ends of the specimen could be detected. Thus the distortion of the specimen, as a whole, was inappreciable.

Interpretation of Slip Band Phenomena—It is now necessary to deduce a mechanism of slip, with relation to the crystalline structure of the material,

which is consistent with the changes in micro-structure resulting from the applied straining action. The complete surface of the specimen was, as mentioned previously, divided into four zones, namely, $5^\circ/95^\circ$, $95^\circ/185^\circ$, $185^\circ/275^\circ$, $275^\circ/5^\circ$, the junctions of these zones being marked by an absence of slip bands in the central portion of the specimen.

Previous experience with other single metallic crystals has shown that such gaps can be due to one of two changes, either (a) the applied stress system is insufficient to produce plastic strain, or (b) the direction of slip is tangential to the surface of the specimen at the point. An examination of the surface at corresponding points ($\lambda = 5^\circ$, 95° , 185° and 275°) in the neighbourhood of the cracks, showed, however, that an abrupt change occurred in the general direction of the slip bands at these points. Hence, the possibility (b) can be ignored and it is apparent that the stress governing the distortion reaches *minimum* values at these four positions. In previous work dealing with aluminium single crystals subjected to torsional straining, similar abrupt changes in the slope of slip band markings have been observed, and have proved to be associated with those positions on the surface where the direction of slip is replaced by another slip direction of the same crystallographic type. It appeared to be very probable that a similar mechanism of distortion had occurred in the present case, slip in the zone represented by $\lambda = 5^\circ$ to $\lambda = 95^\circ$ being confined to one slip direction which was replaced by a second slip direction (crystallographically similar) in the second zone represented by $\lambda = 95^\circ$ to $\lambda = 185^\circ$. Slip band measurements showed that the remaining two zones were merely a repetition of the first two zones.

Regarding the identification of the direction of slip the appearance of the micro-structure at $\lambda = 139^\circ$ was very suggestive. At this position and at the position diametrically opposite ($\lambda = 319^\circ$) the slip bands observed were straight, and entirely free from any suggestion of "waviness" or of duplex structure, which characterised the slip bands observed at all other parts of the surface. Further, it was extremely difficult to focus accurately these slip bands under direct illumination. By changing the lighting system in a number of ways it became apparent that a fairly close-spaced system of slip bands was present, but the differences of surface level due to these bands were very small. Now this appearance is typical of a position where the direction of slip is tangential to the surface of the specimen. If θ_s , ψ_s denote the spherical co-ordinates of the direction of slip, then whatever the type of slip may be, whether on a single plane or on duplex planes, or even of an irregular nature not confined to planes, straight slip bands will be formed at a value of λ equal to $(\psi_s \pm 90^\circ)$, and the

slope of these slip bands will be given by $\theta_s = \pm (90^\circ - \theta_d)$. In the present experiment the slopes of the straight slip bands at the points $\lambda = 139^\circ$ and $\lambda = 319^\circ$ were $\pm 19\frac{1}{2}^\circ$. Now all previous experiments on single crystals have shown that the slip direction corresponds to a line of high atomic density (e.g., 110 for aluminium,* 111 for iron,† 111 for tungsten,‡ 1120 for zinc§). The principal lines of atoms in the body-centred structure of iron correspond with the diagonals of the elementary cube. Calculation showed that the cube diagonals, of the present specimen, were situated as follows —

Table III — Spherical Co-ordinates of Cube Diagonals (Normals to Octahedral Planes)

Normal	θ	ϕ
	$^\circ$ $'$	$^\circ$ $'$
111	54 10	308 0
$\bar{1}\bar{1}\bar{1}$	39 6	51 44
11 $\bar{1}$	70 26	328 21
$\bar{1}\bar{1}1$	58 18	149 42

It is apparent that slip in the $\bar{1}\bar{1}1$ direction would be tangential to the surface of the specimen at the value of $\lambda = 228^\circ 21' \pm 90^\circ$, i.e., $138^\circ 21'$ or $318^\circ 21'$ and that the slope of the slip bands at these points would be represented by $\pm 19^\circ 34'$, i.e., $\pm (90^\circ - \theta_d)$, and this is identical with the nature of the slip bands observed at these points. Hence, strong evidence had been obtained that one of the slip directions concerned was a principal line of atoms of the lattice. (These principal lines, corresponding to the diagonals of the elementary cube and to the normals to the octahedral planes, will be referred to as the octahedral directions.)

Previous work on the deformation of single crystals of α -iron has been carried out by Pfeil,|| also Taylor and Elam || From his experiments Pfeil concluded that "slip in an iron crystal does not occur on cubic or dodecahedral planes, but on icositetrahedral planes. Movement on an icositetrahedral plane takes place in the direction of the trigonal axis to that plane." The observed deformations were not considered with regard to stress considerations. In the following

* See notes, *, †, ‡, p. 498

† Pfeil, 'J. Iron & Steel Inst.', vol. 15 (1926), Taylor and Elam, 'Roy. Soc. Proc.,' A, vol. 112, p. 337 (1926)

‡ Goucher, 'Phil. Mag.', vol. 6, p. 48 (1924).

§ Mark, Polanyi and Schmid.

|| Loc. cit.

year, Taylor and Elam published the results of distortion measurements on single crystals of iron subjected to static tensile and compressive straining. The strain analysis indicated that distortion proceeded by a uniform shear, the direction of slip coinciding with that of the most highly stressed octahedral direction. The slip plane, as determined by distortion measurements, did not, however, coincide—in the general case—with a crystallographic plane of low indices, but was apparently determined purely from shear stress considerations. Distortion measurements were not sufficient to determine whether the resulting distortion was produced by duplex slip on two planes. Information on this point was sought by a study of the slip band markings appearing on the polished surface of the specimens. Arising from this study, Taylor and Elam suggested a "rod" theory of deformation according to which "the particles of the metal stick together along a certain crystallographic direction, and the resulting distortion may be likened to that of a large number of rods which slide on one another. The rods stick together in groups or smaller bundles of irregular cross-section, and the slip lines which appear on a polished surface are the traces of these bundles on that surface. When the distortion of the crystal in bulk is a uniform shear these bundles stack together to form plates of irregular thickness, but lying in general with their planes parallel to the plane of slip determined by external measurements of the surface. The plane of these plates is determined by the direction of the principal stress. It has no direct relationship with the crystal axes. The slip lines appear to have no direct relation with any of the principal crystal planes."

Thus, the experiments of Pfeil and of Taylor and Elam indicated a common direction of slip. The suggested mechanisms of distortion, however, were fundamentally different, for whereas Pfeil considers that slip is confined to planes of one definite type (112) Taylor and Elam suggest that planes of low crystallographic indices do not necessarily enter into the distortion, the outlines of the "bundles of rods" concerned being irregular and not being controlled by stress considerations at all. At the same time, their observations do not exclude altogether the possibility that the outlines of the "rods" may coincide with portions of crystallographic planes, although a perusal of their work leads to an impression that Taylor and Elam do not favour this as a probability. Tungsten crystallises in the same type of lattice—body-centred cubic—as that of α -iron, and Goucher* has studied the deformation of single crystals of tungsten. He concluded that deformation may be accounted for in all cases by slip on {100}tetrahedral (112) planes and in the octahedral direction, with the single

* *Loc. cit.*

exception of a crystal subjected to special constraints which slipped on cube faces (100) and in the 100 direction. With regard to the present experiment, some evidence has been obtained that the 111 direction is a slip direction, thus agreeing with all the previous investigators. The general appearance of the micro-structure did not appear to be consistent with the hypothesis that distortion occurs by slip on planes of one type (Pfeil and Goucher), and while being generally similar to the structures recorded by Taylor and Elam, there were definite indications that the limits of slope of the slip bands followed some regular law and were not entirely irregular as the rod theory would indicate.

It was decided, as a first step, to examine the micro-structure of the specimen with regard to the general hypothesis that slip occurs on a plane (not necessarily of low indices, crystallographically) containing an octahedral direction and on which the resolved shear stress is a maximum. When torsional straining is applied the general case of four octahedral directions (as possible directions of slip) has to be considered. For the sake of simplicity, it is convenient to consider, mathematically, each octahedral direction individually, after which the *significant* direction at any point of the specimen can be exhibited graphically.

Considering any given octahedral direction (denoted by θ_a, ψ_a) a single infinity of planes contains this direction (applied to the stereographic projection, the normals of all such planes lie on the great circle corresponding to the intersection of the octahedral plane, θ_a, ψ_a , with the sphere). We require to find which of these planes gives the maximum value of resolved shear stress (in the octahedral direction), at any given point (denoted by λ) on the surface of the specimen. The spherical co-ordinates of this plane, also the slope of the trace of the plane on the surface of the specimen at the given point, are also required.

These expressions have been deduced in the following manner —

The Shear Stress Analysis of a Single Crystal of Iron subjected to a Pure Couple

At any point on the surface of a cylindrical torsion specimen, it is required to find —

- 1 The maximum value of the shear stress on all planes containing the normal to an octahedral plane and resolved in the direction of this normal
- 2 The spherical co-ordinates of the plane subjected to this maximum resolved shear stress.
- 3 The slope of the trace of this plane on the surface of the specimen at the point under consideration.

Notation — Let the pole of the spherical co-ordinates used be the axis of the specimen, and let the reference plane be a plane containing the pole and passing

through the reference mark \bigcirc on the specimen. Any point on the circumference of the specimen is then denoted by the angle λ , when λ is the dihedral angle between the reference plane and a second plane which contains the pole of the specimen and the point in question. Also let λ be considered of positive sign when it is measured in a counter-clockwise direction from the reference plane.

A plane is denoted by the spherical co-ordinates θ, ψ , of its normal, where θ is the angle the normal makes with the axis of the specimen, while ψ is the angle made with the reference plane of the projection of the normal on to a plane perpendicular to the axis. The same convention of signs is employed for ψ as for λ .

Let θ_s, ψ_s refer to the normal to an octahedral plane, and θ_0, ψ_0 to the normal to any other plane containing this normal. Let S_r denote the value of the shear stress on plane, θ_0, ψ_0 , resolved in the direction θ_s, ψ_s . Let $S =$ maximum shear stress at the surface of the specimen. Then

$$S = 2T/\pi r^2$$

where $T =$ applied couple and $r =$ radius of specimen

Then it has been shown previously* that

$$S_r = S [\sin \theta_0 \cos \theta_s \sin (\psi_0 - \lambda) + \cos \theta_0 \sin \theta_s \sin (\psi_s - \lambda)] \quad (1)$$

The condition that the plane θ_0, ψ_0 , shall contain the direction, θ_s, ψ_s , is given by

$$\tan \theta_0 = -\cot \theta_s \sec (\psi_s - \psi_0) \quad (2)$$

Substituting for $\sin \theta_0$ and $\cos \theta_0$ in (1) we obtain, after simplification

$$S_r = S [\sin^2 \theta_s \sin (\psi_s - \lambda) \cos (\psi_s - \psi_0) - \cos^2 \theta_s \sin (\psi_0 - \lambda)] / \cos \theta_s \sqrt{\tan^2 \theta_s \cos^2 (\psi_s - \psi_0) + 1} \quad (3)$$

It is now required to find the maximum value for S_r . Differentiating with respect to ψ_0 , and equating to zero, we obtain

$$\begin{aligned} \frac{dS_r}{d\psi_0} = 0 = S [& \{-\sin^2 \theta_s \sin (\psi_s - \lambda) \sin (\psi_0 - \psi_s) \\ & - \cos^2 \theta_s \cos (\psi_0 - \lambda)\} \{\sin^2 \theta_s \cos^2 (\psi_0 - \psi_s) + \cos^2 \theta_s\} \\ & + \{\sin^2 \theta_s \sin (\psi_s - \lambda) \cos (\psi_0 - \psi_s) - \cos^2 \theta_s \sin (\psi_0 - \lambda)\} \\ & \times \sin^2 \theta_s \cos (\psi_0 - \psi_s) \sin (\psi_0 - \psi_s)], \end{aligned}$$

which reduces to

$$\sin^2 \theta_s \cos (2\psi_s - \psi_0 - \lambda) + \cos^2 \theta_s \cos (\psi_0 - \lambda) = 0$$

* Gough, Wright and Hanson, 'J. Inst. Metals,' vol 36, p 173 (1926)

Writing

$$(\psi_0 - \lambda) = K + \beta \quad \text{and} \quad (\psi_d - \lambda) = K$$

we obtain

$$\sin^2 \theta_d \cos (K - \beta) + \cos^2 \theta_d \cos (K + \beta) = 0,$$

whence

$$\tan \beta = \cot K / \cos 2\theta_d, \quad (4)$$

and substituting in (3) we obtain

$$S_{r_{\max}} = S[\sin^2 \theta_d \sin K \cos \beta - \cos^2 \theta_d \sin (K + \beta)] / \sqrt{\sin^2 \theta_d \cos^2 \beta + \cos^2 \theta_d},$$

which reduces finally to

$$\begin{aligned} S_{r_{\max}} &= S \sqrt{\cos^2 K \cos^2 \theta_d + \sin^2 K \cos^2 2\theta_d} \\ &= S \sqrt{\cos^2 (\psi_d - \lambda) \cos^2 \theta_d + \sin^2 (\psi_d - \lambda) \cos^2 2\theta_d}, \end{aligned} \quad (5)$$

giving the value of the maximum resolved shear stress at any point on the circumference of the circle, denoted by λ , in terms of S , θ_d and ψ_d , which was required (The sign must be otherwise determined)

Determination of Co-ordinates of Plane of Maximum Resolved Shear Stress

The co-ordinates, θ_0 , ψ_0 , are determined from the relations

$$\tan (\psi_0 - \psi_d) = \cot (\psi_d - \lambda) \sec 2\theta_d \quad (4)$$

and

$$\tan \theta_0 = -\cot \theta_d \sec (\psi_d - \psi_0) \quad (2)$$

To determine Slope of Trace of Plane of Maximum Resolved Shear Stress on Surface of Specimen

The tangent plane at the point considered ($\psi = \lambda$) is expressed by

$$x \cos \lambda + y \sin \lambda = 0 \quad (\text{direction only considered})$$

The equation to the plane of maximum resolved shear stress (θ_0 , ψ_0) is

$$x \sin \theta_0 \cos \psi_0 + y \sin \theta_0 \sin \psi_0 + z \cos \theta_0 = 0$$

The general plane through the intersection of these planes is

$$x (\sin \theta_0 \cos \psi_0 + K \cos \lambda) + y (\sin \theta_0 \sin \psi_0 + K \sin \lambda) + z \cos \theta_0 = 0, \quad (6)$$

and is perpendicular to the tangent plane if

$$\sin \theta_0 \cos \psi_0 \cos \lambda + \sin \theta_0 \sin \psi_0 \sin \lambda + K = 0,$$

i.e., if

$$K = -\sin \theta_0 \cos (\psi_0 - \lambda)$$

Substituting, we obtain

$$-x \sin \theta_0 \sin (\psi_0 - \lambda) \sin \lambda + y \sin \theta_0 \sin (\psi_0 - \lambda) \cos \lambda + z \cos \theta_0 = 0$$

The " θ " co-ordinate of this plane (perpendicular to the tangent plane and containing the intersection of the plane of maximum resolved shear stress with the tangent plane) is equal to the slope of the trace of the plane of maximum resolved shear stress measured with relation to the perpendicular to the axis of the specimen. Denoting this slope by θ_s , it can be shown that

$$\tan \theta_s = \pm \tan \theta_0 \sin (\psi_0 - \lambda) \quad (7)$$

Using the relations (2) and (4), by suitable expansion and substitution, the following expression is finally obtained

$$\tan \theta_s = \frac{1 - 2 \sin^2 (\psi_s - \lambda) \sin^2 \theta_s}{\sin (\psi_s - \lambda) \tan \theta_s \cos 2\theta_s} \quad (8)$$

Thus giving the slope of the trace in terms of θ_s , ψ_s and λ only, as was required

Correction of X-Ray Crystal Analysis and Deduced Spherical Co-ordinates of the Octahedral and other Crystallographic Planes

The spherical co-ordinates of the dodecahedral planes of the specimen (before and after test) given in Table I require correction. In previous work on aluminium crystals it was found that sufficiently accurate and consistent corrections could be obtained using the stereographic net. This is much more difficult in the case of the iron crystal where readings of reflections from six dodecahedral planes were usually obtained from the X-ray analysis. In addition to giving due consideration to each of the six readings, the limits of accuracy placed on the experimental readings for each plane are $\pm 1^\circ$ for θ readings and $\pm 2^\circ$ for the ψ readings. As will be seen, it became necessary, at a later stage, to obtain, accurately, the spherical co-ordinates of a much larger number of crystallographic planes. At first, these were all deduced using the net, but undesirable errors crept in. Accordingly the correction of the X-ray readings and the position of the required planes have been calculated throughout. The X-ray readings were first corrected by the method of least squares,* and θ and ψ readings being weighted according to the ascribed accuracy of determination. The cube faces were then found by bisecting the angles between appropriate dodecahedral faces. The spherical co-ordinates of any required crystallographic plane were then calculated, using these co-ordinates and the Millerian indices of the required plane.

Thus if $l_1, m_1, n_1 (\theta_1, \psi_1)$, $l_2, m_2, n_2 (\theta_2, \psi_2)$, $l_3, m_3, n_3 (\theta_3, \psi_3)$ refer to the cube axes of the crystal (as found after correcting the X-ray analysis) while θ and ψ refer to any crystallographic plane whose Millerian indices are denoted

* See "The Combination of Observations," Brunt, 'Cambridge Univ. Press' (1923)

by a , b and c . Then, using the usual method of transformation of axes it can be shown that

$$\cos \theta = (a \cos \theta_1 + b \cos \theta_2 + c \cos \theta_3) (a^2 + b^2 + c^2)^{-1/2}, \quad (9)$$

$$\tan \psi = \frac{a \sin \theta_1 \sin \psi_1 + b \sin \theta_2 \sin \psi_2 + c \sin \theta_3 \sin \psi_3}{a \sin \theta_1 \cos \psi_1 + b \sin \theta_2 \cos \psi_2 + c \sin \theta_3 \cos \psi_3} \quad (10)$$

The calculated co-ordinates for various planes are given in Table IV

At present we are concerned only with the co-ordinates of the octahedral directions, θ & ψ ,

$$\begin{cases} \theta_{111} = 54^\circ 10' \\ \psi_{111} = 308^\circ 0' \end{cases} \begin{cases} \theta_{1\bar{1}\bar{1}} = 39^\circ 6' \\ \psi_{1\bar{1}\bar{1}} = 51^\circ 44' \end{cases} \begin{cases} \theta_{11\bar{1}} = 70^\circ 26' \\ \psi_{11\bar{1}} = 228^\circ 21' \end{cases} \begin{cases} \theta_{\bar{1}11} = 58^\circ 18' \\ \psi_{\bar{1}11} = 149^\circ 42' \end{cases}$$

Curves of Maximum Resolved Shear Stress and their Significance when studied in Relation to the general features of the Cracks and Slip Bands present on the Specimen

Using equation (5) and inserting the values of the co-ordinates of the four octahedral directions, the maximum resolved shear stress curves were plotted (see fig 3) (Note that for complete reversal of stress, the stress curves should be reflected about the zero stress line) The curves show that if the maximum

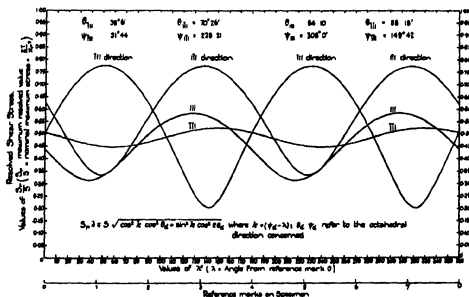


FIG. 3.—Diagram showing, at each point of the developed circumference of the specimen, the values of the maxima of the shear stresses on all planes resolved in the direction of the normals to the octahedral planes.

Table IV—Spherical Co-ordinates of Various Crystallographic Planes, also Stress Equation Constants

Column I Plane *	Column II		Column III	
	Spherical co ordinates		Stress constants	
	θ	ψ	A	a.
001	15 51	221 54	—	—
010	77 28	3 21	—	—
100	80 31	95 27	—	—
011 $\left(\begin{smallmatrix} 111 \\ 111 \end{smallmatrix}\right)$	33 31	350 50	$\left\{ \begin{array}{l} +0.704 \left(\begin{smallmatrix} 111 \\ 111 \end{smallmatrix}\right) \\ +0.451 \left(\begin{smallmatrix} 111 \\ 111 \end{smallmatrix}\right) \\ -0.327 \left(\begin{smallmatrix} 111 \\ 111 \end{smallmatrix}\right) \\ +0.690 \left(\begin{smallmatrix} 111 \\ 111 \end{smallmatrix}\right) \\ +0.490 \left(\begin{smallmatrix} 111 \\ 111 \end{smallmatrix}\right) \\ +0.459 \left(\begin{smallmatrix} 111 \\ 111 \end{smallmatrix}\right) \end{array} \right\}$	$\left\{ \begin{array}{l} 151 \ 10 \\ 46 \ 17 \\ 57 \ 6 \\ 123 \ 9 \\ 152 \ 42 \\ 73 \ 30 \end{array} \right\}$
101 $\left(\begin{smallmatrix} 111 \\ 111 \end{smallmatrix}\right)$	37 9	110 25	$\left\{ \begin{array}{l} -0.393 \\ +0.493 \end{array} \right\}$	$\left\{ \begin{array}{l} 23 \ 54 \\ 112 \ 25 \end{array} \right\}$
101 $\left(\begin{smallmatrix} 111 \\ 111 \end{smallmatrix}\right)$	58 12	191 26	$\left\{ \begin{array}{l} -0.775 \left(\begin{smallmatrix} 111 \\ 111 \end{smallmatrix}\right) \\ +0.336 \left(\begin{smallmatrix} 111 \\ 111 \end{smallmatrix}\right) \\ -0.562 \left(\begin{smallmatrix} 111 \\ 111 \end{smallmatrix}\right) \\ -0.518 \left(\begin{smallmatrix} 111 \\ 111 \end{smallmatrix}\right) \end{array} \right\}$	$\left\{ \begin{array}{l} 50 \ 48 \\ 43 \ 22 \\ 117 \ 18 \\ 165 \ 32 \end{array} \right\}$
101 $\left(\begin{smallmatrix} 111 \\ 111 \end{smallmatrix}\right)$	55 42	264 34	—	—
110 $\left(\begin{smallmatrix} 111 \\ 111 \end{smallmatrix}\right)$	87 54	319 7	—	—
110 $\left(\begin{smallmatrix} 111 \\ 111 \end{smallmatrix}\right)$	74 20	49 42	—	—
111	54 10	308 0	—	—
111	39 6	51 44	—	—
111	59 18	149 42	—	—
111	70 26	228 31	—	—
231	69 57	325 49	-0.421	6 17
121	58 50	330 18	+0.501	172 50
121	49 54	335 47	+0.584	163 7
121	21 0	23 58	+0.770	141 58
112 $\left\{ \begin{array}{l} 111 \\ 111 \end{array} \right\}$	19 42	55 4	+0.775	137 22
112 $\left\{ \begin{array}{l} 111 \\ 111 \end{array} \right\}$	23 26	83 16	+0.759	132 35
112 $\left\{ \begin{array}{l} 111 \\ 111 \end{array} \right\}$	53 57	123 23	+0.551	110 2
112 $\left\{ \begin{array}{l} 111 \\ 111 \end{array} \right\}$	63 58	128 22	+0.467	99 2
112 $\left\{ \begin{array}{l} 111 \\ 111 \end{array} \right\}$	74 8	132 34	+0.392	83 31
112 $\left\{ \begin{array}{l} 111 \\ 111 \end{array} \right\}$	76 4	303 55	-0.722	45 24
112 $\left\{ \begin{array}{l} 111 \\ 111 \end{array} \right\}$	69 43	294 39	-0.658	41 48
112 $\left\{ \begin{array}{l} 111 \\ 111 \end{array} \right\}$	63 54	284 35	-0.574	37 12
112 $\left\{ \begin{array}{l} 111 \\ 111 \end{array} \right\}$	51 19	241 22	+0.228	168 12
112 $\left\{ \begin{array}{l} 111 \\ 111 \end{array} \right\}$	50 59	237 23	+0.209	129 6
112 $\left\{ \begin{array}{l} 111 \\ 111 \end{array} \right\}$	52 19	213 36	+0.275	97 42
112 $\left\{ \begin{array}{l} 111 \\ 111 \end{array} \right\}$	67 24	172 33	+0.628	63 12
112 $\left\{ \begin{array}{l} 111 \\ 111 \end{array} \right\}$	73 34	163 1.	+0.700	59 18
112 $\left\{ \begin{array}{l} 111 \\ 111 \end{array} \right\}$	80 8	154 5	+0.749	55 59
112 $\left\{ \begin{array}{l} 111 \\ 111 \end{array} \right\}$	81 29	211 48	+0.578	133 42
112 $\left\{ \begin{array}{l} 111 \\ 111 \end{array} \right\}$	72 46	205 5	+0.557	140 0
112 $\left\{ \begin{array}{l} 111 \\ 111 \end{array} \right\}$	45 37	173 3	+0.402	170 30
112 $\left\{ \begin{array}{l} 111 \\ 111 \end{array} \right\}$	40 10	159 9	-0.355	4 36
112 $\left\{ \begin{array}{l} 111 \\ 111 \end{array} \right\}$	36 43	142 29	-0.323	23 18
112 $\left\{ \begin{array}{l} 111 \\ 111 \end{array} \right\}$	45 13	83 51	-0.398	84 42
112 $\left\{ \begin{array}{l} 111 \\ 111 \end{array} \right\}$	51 58	72 25	-0.449	95 54
112 $\left\{ \begin{array}{l} 111 \\ 111 \end{array} \right\}$	59 38	63 3	-0.498	104 51
112 $\left\{ \begin{array}{l} 111 \\ 111 \end{array} \right\}$	89 43	38 14	-0.585	127 54
112 $\left\{ \begin{array}{l} 111 \\ 111 \end{array} \right\}$	58 43	37 39	+0.498	2 58
112 $\left\{ \begin{array}{l} 111 \\ 111 \end{array} \right\}$	50 25	28 59	+0.483	13 36
112 $\left\{ \begin{array}{l} 111 \\ 111 \end{array} \right\}$	42 55	18 5	+0.469	24 57
112 $\left\{ \begin{array}{l} 111 \\ 111 \end{array} \right\}$	32 31	315 22	+0.449	68 47
112 $\left\{ \begin{array}{l} 111 \\ 111 \end{array} \right\}$	36 14	297 8	+0.456	81 11
112 $\left\{ \begin{array}{l} 111 \\ 111 \end{array} \right\}$	42 11	283 37	+0.468	93 14
112 $\left\{ \begin{array}{l} 111 \\ 111 \end{array} \right\}$	71 6	251 52	+0.515	130 14
112 $\left\{ \begin{array}{l} 111 \\ 111 \end{array} \right\}$	80 15	245 45	+0.523	139 44
112 $\left\{ \begin{array}{l} 111 \\ 111 \end{array} \right\}$	89 30	239 59	+0.535	149 6

* Note.—The indices in brackets (column I) refer to the octahedral direction which is contained by the plane. The six dodecahedral planes contain two such octahedral directions.

resolved shear stress hypothesis (octahedral direction) is correct, only the $\bar{1}\bar{1}1$ and the $1\bar{1}1$ directions are of importance with the present specimen. The following features of the curves are important —

Direction	"Peak" position of curve	"Effective" portions of curves.
$\bar{1}\bar{1}1$ $1\bar{1}1$	$\lambda = 138^\circ 4$ and $318^\circ 4$ $\lambda = 51^\circ 7$ and $231^\circ 7$	$\lambda = 93^\circ$ to 187° also $\lambda = 273^\circ$ to $\lambda = 7^\circ$ $\lambda = 7^\circ$ to 93° also $\lambda = 187^\circ$ to $\lambda = 273^\circ$

The "change-over" points being at $\lambda = 7^\circ, 93^\circ, 187^\circ$ and 273°

The positions of the cracks found on the specimen (see fig. 2) were situated at the following approximate positions —

Group 1	$\lambda = 36^\circ (+ 7^\circ, - 11^\circ),$	$53^\circ (\pm 1^\circ),$	$67^\circ (+ 23^\circ, - 10^\circ)$
Group 2	$\lambda = 130^\circ (\pm 1^\circ),$	$140^\circ (\pm 5^\circ)$	
Group 3	$\lambda = 213^\circ, 219^\circ,$	$228^\circ, 239^\circ,$	252°
Group 4	$\lambda = 295^\circ (\pm 5^\circ),$	$310^\circ (\pm 3^\circ),$	$320^\circ, 328^\circ (\pm 3^\circ)$

Thus the cracks are situated about four general positions which coincide, approximately, with the crests of the stress curves of fig. 3. The "significant" slip direction in fig. 3 changes at values of λ equal to $7^\circ, 93^\circ, 187^\circ$ and 273° , and the effective resolved shear stress is a minimum at these points. Reference to Table II will show that, at these positions on the specimen, no slip bands were visible in the central portion of the specimen, while sudden changes in the direction of the slip bands were observed at corresponding positions in the left-hand third of the specimen. Thus the positions of the cracks, zones free from slip bands, change-over points of the direction of slip and the special nature of the slip bands at the positions $\lambda = 139^\circ$ and 319° , are in such exact agreement with the stress distribution illustrated in fig. 3 as to leave no room for doubt that the general hypothesis on which the curves are calculated—maximum resolved shear stress in an octahedral direction—is the most important factor governing the process of distortion of the specimen. The slip band markings at any point on the specimen will now be considered in relation to the trace of the plane subjected to this maximum resolved shear stress at the point in question. It has been shown that the slope of the trace of this plane is given (see equation (8)) by the expression

$$\tan \theta_s = (1 - 2 \sin^2 (\psi_s - \lambda)) \sin^2 \theta_s / \sin (\psi_s - \lambda) \tan \theta_s \cos 2\theta_s.$$

Inserting the values of the spherical co-ordinates, θ_s, ψ_s , for one of the given octahedral directions, the expression can be evaluated for all values of λ (0° to

360°) This has been done for all the four octahedral directions and the results represented graphically. Figs 5 and 7* refer to the significant directions $\bar{1}\bar{1}1$ and $1\bar{1}1$. Each diagram represents a development of the complete circumference of the circle, values of λ are shown horizontally while positive and negative slopes are shown vertically above, and below, respectively, this datum line. Each curve refers entirely to one only of the octahedral directions. The values of θ , (calculated using equation (8)) give the dotted curves, the full curves will be considered later. If the data given in Table II in the column headed "Mean Slope" are plotted on figs 5 and 7, the points agree extremely well with the dotted curves of these figures in the following areas

$$\begin{aligned} \text{Fig 5 } (\bar{1}\bar{1}1 \text{ direction}) \text{ agrees at } & \begin{cases} \lambda = 7^\circ \text{ to } 93^\circ, \\ \lambda = 187^\circ \text{ to } 273^\circ, \end{cases} \\ \text{Fig 7 } (1\bar{1}1 \text{ direction}) \text{ agrees at } & \begin{cases} \lambda = 93^\circ \text{ to } 187^\circ, \\ \lambda = 273^\circ \text{ to } 7^\circ, \end{cases} \end{aligned}$$

and, as fig 3 shows, these are the particular octahedral directions which are significant according to the deduced stress analysis. The accompanying series of photo-micrographs illustrate the correspondence existing between the average slope of the slip bands at various points and the slope of the trace of the plane of maximum resolved shear stress on the surface of the specimen. In general, the photographs were taken at the centre of the specimen except in some cases where it is desired to bring out special features not easily seen at the centre. Such special positions are indicated by notes $\frac{1}{4}L$, $\frac{1}{2}L$, etc., meaning that the spot is to the left of the centre and $\frac{1}{4}$ or $\frac{1}{2}$ way from the centre towards the end of the parallel portion of the specimen. The vertical black line is the datum line, of zero slope, photographed in the manner previously described. Passing through the centre of each photographic negative, a line has been ruled at an angle corresponding to the calculated slope of the trace of the plane of maximum resolved stress as given by equation (8) and shown by the dotted curves in figs 5 and/or 7. This line appears as a full white line in the print. In fig 11 two white lines are seen ($\bar{1}\bar{1}1$ and $1\bar{1}1$). At this point ($\lambda = 190^\circ$ or 10°) the change over in direction of the slip bands has just been completed, and several widely-spaced bands of the $\bar{1}\bar{1}1$ series come to an end in the upper portion of the field. Figs 14, 23 and 25 (Plates 9-11) show the appearance of typical cracks. Fig. 21 shows some of the slip bands in an early stage of development as seen occasionally in those areas otherwise free from all slip band markings.

A careful examination of the photographs will show that the white line is in good general agreement with the average slope of the slip band markings

* See pp. 523, 524.

Previous reference has been made to the nature of the slip bands in the region $\lambda = 139^\circ$ and $\lambda = 319^\circ$. Plate 11, fig 24, shows the structure at $\lambda = 139^\circ$, the lighting had to be very carefully adjusted to obtain this photograph. Fig 23 taken slightly to the left of this spot, shows that a very closely spaced system of slip bands is present. As mentioned above, the nature and slope (19.6°) of the slip bands at the point $\lambda = 139^\circ$ are sufficient to identify the normal to the 111 direction ($\theta = 70^\circ 26'$, $\psi = 228^\circ 21'$) as the slip direction.

The evidence so far obtained is considered to have demonstrated in a satisfactory manner, the following details concerning the mechanism of distortion —

- 1 The direction of slip coincides with that of the most highly-stressed principal line of atoms
- 2 The average slope of the slip bands, at any point is a very close approximation to the slope of the trace of the plane of maximum resolved shear stress

In these important respects, therefore, an iron crystal subjected to reversed torsional stresses deforms in a similar manner to that previously shown by Taylor and Elam to govern distortion under static tensile and compressive stresses

More Detailed Consideration of the Appearance of the Slip Band Markings and its Bearing on the Mechanism of Deformation

The remaining step is to deduce the exact type of distortion that, governed by the chief condition of resolved shear stress (octahedral direction), would produce the observed forms of slip band markings. Several possible types of distortion will be discussed

1 *General Case* —The most general case assumes that slip will take place, at any point in the specimen, on that plane subjected to the shear stress denoted by the maximum ordinates of the stress curves of fig 3 at the particular value of λ concerned. (This plane will not, of course, in general, be a crystallographic plane of low indices, see fig 4 (b)). Should this type of slip occur, then the slope of the slip bands should, at any point on the surface of the specimen, agree with that denoted by the dotted lines at the significant portions of figs 5 and 7. Also these slip bands should have one definite slope at this point. These features are not, however, exhibited by the micro-structure and the above hypothesis of deformation can be definitely rejected (as it was previously rejected by Taylor and Elam in connection with their static tests)

2 *The "Rod" Theory of Taylor and Elam* —It follows from this theory that

the form of the slip bands will, at any point on the surface of the specimen, correspond to the trace of the "rods" or "bundles of rods" on the tangent plane to the surface at this point. Now, if the θ_s , ψ_s refer to the direction of slip, parallel straight slip bands should be found at values of λ equal to $\psi_s \pm \pi/2$. We have seen that the appearance of the structure at the point $\lambda = 139^\circ$ and $\lambda = 319^\circ$ agrees with this supposition. But the "bundles of rods" are assumed to be of irregular cross section bearing no relation to the crystal structure. Hence as λ increases from a value of $\psi_s \pm \pi/2$ towards ψ_s (or $\psi_s + \pi$) the character of the slip bands should change from a system of parallel straight lines to a wavy irregular shape, attaining maximum "waviness" at the latter points. These general characteristics are not consistent with the appearance of the micro-structure in the present case. At any point, the limits of slope of the slip band markings possessed very definite limits. Now in the region $\lambda = 7^\circ$ (187°) to $\lambda = 93^\circ$ (273°) where the $\bar{1}11$ direction is significant from stress considerations, calculation showed that the limits of slope of the slip bands were consistent with the traces of one definite pair of planes in the zone from $\lambda = 7^\circ$ to $\lambda = 40^\circ$, also that these planes agreed with the crystallographic planes 321 and 110. But in the area $\lambda = 40^\circ$ to $\lambda = 93^\circ$, although the observed limits of slope were again consistent with the traces of two planes on the surface, these planes proved to coincide with the 110 and $\bar{2}\bar{3}1$ planes. The spherical coordinates for the plane of *actual maximum shear stress* were calculated, from equations (2) and (4), and the positions of these planes have been plotted, for various values of λ (intervals of 10°) on the stereographic projection shown in fig. 4(b). The positions of these planes in the portion of the specimen represented by $\lambda = 7^\circ$ to 93° are very significant when considered in relation to the crystal planes 321, 110 and $\bar{2}\bar{3}1$, and the limits of slope of the slip bands in the same area (as explained above). They suggest that the mechanism of deformation is probably associated with slip on certain crystal planes—these planes being determined from shear stress considerations—rather than that of an irregular substructure of the material bearing no apparent relation to the crystal structure.

3 Examination of the Micro-structure with Relation to the Assumption that Deformation proceeds by Slip on a Crystal Plane (or pairs of Planes) of Low Indices—It becomes necessary to obtain data regarding the stress-distribution on certain types of planes likely to be involved and also, the slopes of the traces of these planes on the surface of the specimen. The direction of slip being identified as the octahedral direction, the locus of the normals to all possible slip planes are represented—on the stereographic projection—by the great

circle representing the intersection of the plane (whose normal is the direction of slip) on the surface of the sphere (see fig 4 (A)) All such planes are represented by the 110, 112, 123, 134, etc, series of Millerian indices (\pm e, one of the indices represents the sum of the other two), and it is necessary to limit in some way the number of types of planes to be examined. Now, as previously mentioned, evidence had been obtained that 110 and 123 planes were concerned. Experience of the mechanism of strain in other types of crystal structure (face-centred cubic and close-packed hexagonal) indicates that planes of slip are determined—to some extent yet unknown—by the atomic density of these planes (as well as by the condition that the direction of slip in the slip plane shall be a line of great linear atomic density). Now the planes containing the octahedral direction arranged in order of atomic density, are as follows —

Plane (General Type)	Atomic Density ($\times a^2$) *
110	0.708 (maximum for
112	0.408 lattice)
123	0.267
134	0.196
etc	

Thus, if 110 and 123 planes are possible slip planes, 112 planes would also be expected to warrant consideration. Planes such as 235, 145, and higher indices would not be expected to enter into the distortion as if slip could occur on these planes then, owing to their great number, the limits of slope of the resulting slip bands *would not be as widely divergent* as found in the present case. Hence it was decided to consider 110, 112 and 123 planes only. Fig 4 (A) is a stereographic projection of the cubic lattice showing these planes (the pole of the diagram being a normal to a cube face, 001). Fig 4 (B) shows the same system, the pole now corresponding to the axis of the present specimen. The relative orientation of the crystal and specimen axes is as determined from the (corrected) X-ray analysis made *after* test.

Resolved shear stress equations for each of the 12 planes containing each octahedral direction were calculated as follows —

Let

θ_p, ψ_p , refer to the plane

θ_d, ψ_d refer to the contained octahedral direction

* Where a is the lattice parameter

Then if

S_r = value of the shear stress on the plane resolved in the given direction at any point on the surface of the specimen (denoted by λ)

$S = 2T/\pi r^3$ where T is the applied torque and r is the radius of cross-section of the specimen

we have

$$S_r/S = A \cos (\lambda - \alpha) \quad (11)$$

where

$$A = \sqrt{-\frac{1}{2} (\cos 2\theta_p + \cos 2\theta_s + 2 \cos \theta_p \cos 2\theta_s)}$$

and

$$\alpha = \tan^{-1} [(\tan^2 \theta_p - 1) \cot (\psi_s - \psi_p)] + \psi_p$$

The sign of A is determined from the alternative form of equation (11), previously given as equation (1)

The values of A and α for each of the 42 planes (110, 112 and 123 types, each dodecahedral plane being common to two octahedral directions) were calculated, giving 49 equations, and the constants are as stated in column III of Table IV. The stress curves calculated from some of these equations are plotted in figs 6 and 8, relating to the $\bar{1}11$ and $1\bar{1}1$, directions, respectively*. These curves give the stress intensity for a uni-directional torque, for reversed stresses they should be reflected about the zero stress line. Note that the envelope to each family of curves is given by equation (5) and has been previously plotted in fig 3.

The slope of the traces of each of these planes on the surface of the specimen was also calculated in the usual manner

$$\theta_s = \tan^{-1} \{ \tan \theta_p \sin (\lambda - \psi_p) \}$$

These slopes are represented graphically in figs 5 and 7*. Note that all these planes have a common slope at the points $\lambda = \psi_s \pm 90^\circ$, where ψ_s refers to the direction of slip, and at these points straight parallel slip bands should be observed if the direction of slip contains the plane of maximum resolved shear stress at the point.

Fig 3 shows that the significant portions of these curves are as follows —

* Similar curves have been plotted relating to the $11\bar{1}$ and $\bar{1}\bar{1}1$ directions. These slip directions, however, were found to have no influence on the distortion.

Table V

Figure No	Direction of slip	Significant portions of curves
5 6	111	$\lambda = 7^\circ$ to 93° , also $\lambda = 187^\circ$ to 273°
7 8	111	$\lambda = 93^\circ$ to 187° , also $\lambda = 273^\circ$ to 7°

Consider one of the shear stress curves, for example, fig 6. At any value of λ , the maximum value of the resolved shear stress is represented by the ordinate of the *envelope* of the stress curve. The diagram shows also the two planes (of 110, 112 and 123 type) which most nearly approach this value. Thus, at $\lambda = 30^\circ$, the planes of nearest approach are the 110 and 321 planes (situated on opposite sides of the plane of actual maximum stress). But fig 5 also gives this general information, for we see that the dotted line representing the trace of the plane of maximum stress, at this point, is situated between the curves representing the slopes of the traces of the 110 and 321 planes. Hence, only the *slope diagrams*, figs 5 and 7, need be considered if the *actual value* of the resolved stress on the planes is not required, and this may be found a convenient method of studying the problem.

With this data available, several possible types of distortion were studied with relation to the observed slip bands.

(a) *Slip confined to one type of plane* (110, 112 or 123) — This is the mechanism of distortion previously encountered with aluminium crystals. It should result in definite series of parallel straight slip bands with clearly marked "change-over" points*. This mechanism is inconsistent with the observed micro-structure and needs no further consideration.

(b) *Duplex slip on two planes of similar crystallographic type* — Distortion might occur by slip on the most highly stressed pair of 110, 112 or 123 planes. This possibility was examined at length but was rejected as it failed entirely to produce those limits of slope exhibited by the micro-structure.

(c) *Duplex slip on two planes, not of the same crystallographic type, being situated on opposite sides of the plane of actual maximum resolved shear stress, each plane being either a 110, 112 or 123 plane and subjected to greater resolved shear stress than any other plane of these three types situated on the same side of the plane of actual maximum resolved shear stress*

* See notes *, †, p 498

Consider fig 4 (b) The position of the plane of actual maximum resolved shear stress, for various values of λ , have been calculated (using equations (2) and (4)), and their positions are denoted by these values of λ . The possibility now under consideration is duplex slip on one plane on each side of the plane of maximum resolved shear stress, each slip plane to be that one of the three general types 110, 112 or 123 subjected to greater resolved shear stress than any other plane of these types situated on that side. For example, the plane of maximum resolved shear stress, at the point $\lambda = 30^\circ$, is situated between the planes 321 and 110. On the left of this plane we have in order the planes 321, 211, 312, etc., on the right, we find 110, 231, 121, etc. From fig 6, the values of the resolved shear stresses at this point ($\lambda = 30^\circ$) are as follows -

Table VI

Plane	312	211	321	Plane of maximum resolved shear stress	110	231	121
Value of resolved shear stress in 111 direction (divided by $\sqrt{3}$)	0.505	0.635	0.69	0.72	0.715	0.675	0.605

Then the possibility under examination is that slip may occur on both the 321 and 110 planes, the relative amounts on each being adjusted so as to produce an approximate distortion equivalent to slip on the plane of maximum resolved shear stress. If slip of this type occurs then we see from fig 5, that the limits of slope of the slip bands observed at the point ($\lambda = 30^\circ$) should make angles of $+76^\circ$ (321) and $+88^\circ$ (110) with the datum line, while the *mean* slope should be $+86^\circ$, corresponding with the trace of the plane of actual maximum resolved shear stress.

Analysing the complete surface of the specimen in this manner, the relations between the limits of slope of the slip markings and the slip bands become as given in Table VII

Table VII

Value of λ (also $\lambda + \pi$)	Slip direction (see fig. 4)	Planes with whose traces the limits of slope of the slip bands should be in agreement
7° to 40 40 40 to 93	$\bar{1}11$	321 and 110 110 (also possibly 321 or 231 110 and 231)
93 to 111° 111 111 to 138° 21' 138 21'	$\bar{1}11$	213 and 101 213 also possibly 101 or 112 213 and 112 All planes (Slope = $90 - \theta_{111} = 10-34$) 112 and 123 123 also possibly 112 or 011 123 and 011
138 21' to 160 160 160 to 187		

(It is of interest to note, that with the type of distortion now under discussion the geometry of the body centred lattice restricts the pairs of possible slip planes into two general types only, i.e., 110/123 and 112/123. The form 112/110 cannot occur. Reference to fig. 4 (b) will make this apparent.)

A very careful comparison was then made of the micro structure of the specimen and the limits of slope deduced from figs. 5 and 6, also 7 and 8 according to the hypothesis stated above. The agreement found was remarkably close. Fig. 9 illustrates this agreement. The diagram represents a development of one-half of the circumference of the specimen. The slopes of

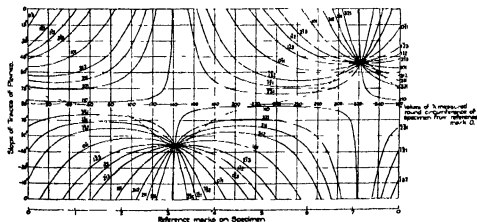


FIG 5—Diagram showing the slope of traces of the { Rhombic Dodecahedral (110) Icositetrahedral (112) Hexakis-Octahedra (123) } Planes, also of the planes of Maximum Resolved Shear Stress containing the $\bar{1}11$ direction.

the traces of the 110, 112 and 123 planes, containing the slip directions $\bar{1}11$ and $1\bar{1}1$, are plotted in those areas where these slip directions are significant (see fig. 3) and are represented by the full-line curves. The traces of the planes of

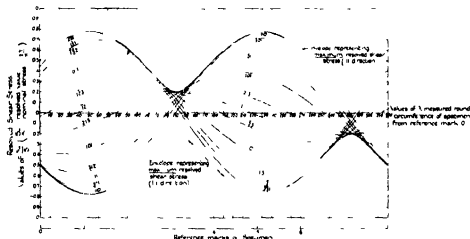


Fig. 6—Diagram of Resolved Shear Stress on { Rhombic Dodecahedral (110) } Planes containing the $\bar{1}11$ direction
Icositetrahedral (112)
Hexakis-Octahedral (123)

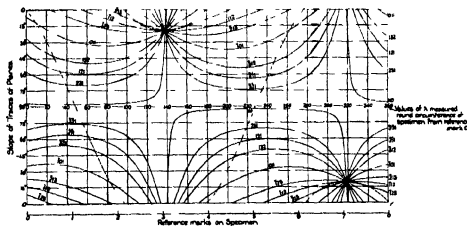


Fig. 7—Diagram showing the slope of traces of the { Rhombic Dodecahedral (110) } Planes,
Icositetrahedral (112)
Hexakis-Octahedral (123)
also of the Planes of Maximum Resolved Shear Stress containing the $\bar{1}11$ direction.

maximum resolved shear stress (for the $\bar{1}11$ and $1\bar{1}1$ directions) are indicated by the dotted lines. The experimental data relating to the observed slip bands—as given in Table II—are plotted on the same diagram, circles and dots denoting, respectively, the mean slope and limits of slope, as recorded in Table

II It is evident that the mean slopes of the slip bands correspond very closely with the traces of the planes of maximum resolved shear stress. But of much greater significance is the agreement between the limits of slope of the slip

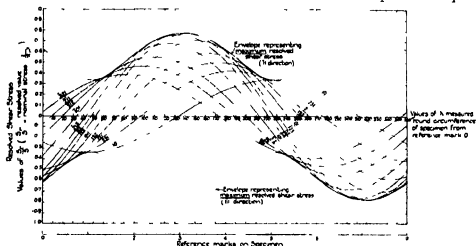


FIG 8—Diagram of Resolved Shear Stress on { Rhombic Dodecahedral (110) } Planes containing the 111 direction
{ Icositetrahedral (112) }
{ Hexakis Octahedral (123) }

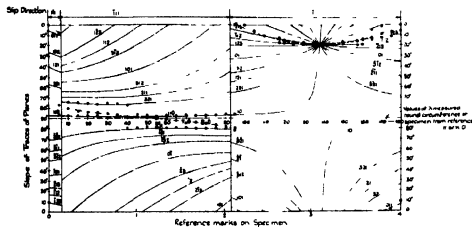


FIG 9—Diagram showing the slope of traces of the { Rhombic Dodecahedral (110) } Planes,
{ Icositetrahedral (112) }
{ Hexakis-Octahedral (123) }
also of the Planes of Maximum Resolved Shear Stress containing the 111 and 111 directions.

bands and the traces of certain crystal planes. Seven distinct changes of slope are seen to occur over the half-circumference of the specimen, and these changes agree exactly with those given in Table VII and predicted by the suggested mechanism of distortion now under discussion. In fact the agreement is so

close, holding over a wide range of slopes including many abrupt changes of slope, as to afford the very strongest evidence that this special type of duplex slip on certain crystallographic planes is the actual mechanism of distortion in the present case

On the photo-micrographs (Plates 9 to 11, figs 11 to 26) certain white dotted lines appear. These lines correspond to the slopes of the traces of the slip planes, at the particular value of λ concerned, according to the suggested duplex mechanism of distortion. They should represent the *limits of slope* of the slip band markings at the point, and the reader is thus enabled to form a personal opinion as to the degree of correspondence existing. It should be remembered that the given slopes apply exactly only to the centre of the field, at some values of λ these slopes are changing at a rapid rate.

Some of the micro-structures are of particular interest. At the point $\lambda = 40^\circ$ (fig 15) the plane of maximum resolved shear stress coincides with the 110 plane, and provided perfect conditions of surface and crystalline structure obtained, a single system of slip bands would be expected. In the centre of the field, this condition is closely approached. Yet the total limits of slope over the whole field are the greatest encountered (about 25°) over the whole specimen. This also would be expected, as from the stress considerations of the present theory, the point ($\lambda = 40^\circ$) marks a change-over point of the pairs of planes concerned. A clearly marked change-over would not be expected as similar tests on aluminium showed that, at such change-over points, the slip bands due to the two slip planes interpenetrate to some extent, producing a certain zone where traces of both planes are visible. The structure at $\lambda = 75^\circ$ (fig 19) is also extremely interesting. Here the plane of maximum shear stress is equidistant from the 110 and $\bar{2}\bar{3}1$ planes, which are equally stressed. The most obvious feature is the system of long slip bands, apparently straight and agreeing with the trace of the plane of maximum shear stress. Closer examination, however, shows the "rippled" shape of these bands, and the slopes of the ripples agree with those of the 110 and $\bar{2}\bar{3}1$ planes. As the shear stress on both these planes is equal at this point, and should produce approximately the same amount of slip on these planes, it is understandable that if the portions of the planes entering into the duplex slip are sufficiently small, straight slip bands would result. Thus the theory is consistent with straight slip bands in an entirely unexpected position. (According to the "rod" theory of Taylor and Elam straight slip bands (due to the $\bar{1}11$ direction) should only occur at the point $\lambda = 141^\circ 44'$ and should exhibit marked irregularity of outline at the spot considered, $\lambda = 75^\circ$). Also clearly discernible is a number of short

duplex bands, whose slopes agree with those of the traces of these two planes. Lastly there are many very short slip bands whose traces have one slope only, some that of the 110, others that of the $\bar{2}\bar{3}1$ planes. These three slopes can be clearly seen if the photograph is held horizontally a little below the level of the eye. Fig. 20 shows the appearance of an equivalent spot in the region of greater deformation. (This has been purposely photographed without a datum line.) The appearance is given of a very "ragged" system of slip bands, bearing little or no apparent relation to the structure of fig. 19. As a matter of fact, the limits of slope of the bands in the two photographs show marked agreement. Similar pairs of spots were examined at many points on the surface of the specimen, and these suggested strongly that, in order to obtain a true picture of the mechanism of distortion by slip band markings (that is to say, in order to produce a structure as shown in fig. 19) exceedingly small *total* deformations are necessary. For this purpose, alternating stresses are particularly suitable. Turning to the structure in the vicinity of a point at which the direction of slip is approximately tangential to the surface of the specimen, figs. 22 to 26 will repay study. At $\lambda = 120^\circ$, for example, the structure suggests a mixture of two sets of straight bands of slightly differing slope rather than that of one system of wavy bands. The significance of the structure at $\lambda = 139^\circ$ has been sufficiently discussed.

The theory of the mechanism of deformation of α -iron now presented for consideration may, therefore, be summarised as follows —

- 1 The direction of slip is the octahedral direction.
- 2 At any point on the surface of the specimen, there will exist a plane on which the value of the shear stress resolved in the contained octahedral direction is a maximum for all similar resolved shear stresses.
- 3 Slip will not, in general, occur on this plane, unless the plane coincides exactly with a dodecahedral (110), icositetrahedral (112) or hexakis octahedral (123) plane of the crystalline structure (and then only when conditions of perfect symmetry obtain). In other cases, the distortion is produced by slipping on two planes, each of which corresponds to one of the above crystal planes. These slip planes are situated on opposite sides of the plane of maximum resolved shear stress, although not, in general, equidistant from that plane.
- 4 Each slip plane is determined by the consideration that it is subjected to a greater value of resolved shear stress than any other possible slip plane on the same side of the plane of maximum resolved shear stress.
- 5 The slip bands will, in general, be of a duplex type, the *average* slope being

that of the trace of the plane of maximum shear stress on the surface of the specimen

6. The limits of slope of the slip bands will agree with the traces of the planes of slip

7 Under very small deformations, the slip bands appear either as short separate traces of the slip planes, or of a combination of these traces, and can be identified as such Under great deformations, however, the component slopes of the slip bands can be resolved only with great difficulty, sometimes they cannot be resolved at all In the latter case they present a very wavy, branched appearance bearing no apparent relation to the crystalline structure

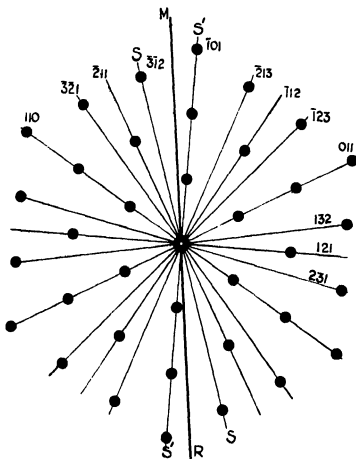


FIG 10

The significance of the above paragraphs numbered 2, 3 and 4 can be exhibited graphically as in fig 10 This diagram represents a view of the body-centred

lattice of α -iron situated such that the slip direction is normal to the plane of the diagram. The traces of all the planes of the 110, 112 and 123 types which contain the slip direction are indicated. Then, according to the conclusions derived from the present experiment, if MR represents the trace of the plane of maximum resolved shear stress (in the slip direction) distortion will occur by slip on the crystal planes SS and S'S', i.e., on the nearest planes of the given types situated immediately adjacent to the plane MR. An important point at once arises. Why, if slip occurs on two planes, does not the micro-structure reveal a system of two interlacing straight sets of slip bands? On this point, the present experiment throws no light whatever. It may be that owing to the presence of impurities, or to some other cause or causes, perfect lattice symmetry does not obtain, hence the line of atoms representing the common direction of slip (and the intersection of the slip planes) will be irregular. In such circumstances, it can be imagined that distortion would occur by movements of irregular obtuse angled wedges. But this is pure supposition, unwise at this stage of experiment. It does appear certain, however, that duplex slip of the type suggested (probably producing "crystal break-up") must result in considerable lattice distortion, at a much earlier stage than in a crystal where slip is confined to one plane. In fact if reference is made to the earlier work on single crystals of aluminium (see fig 7, 'Phil Trans Roy Soc,' Series A, vol 226) an example will be found of the micro-structure of a specimen slipping on *two* planes, which very strongly resembles the wavy irregular type of slip bands found in iron. This photograph has been reproduced on Plate 11 as fig 27. It is considered to be very suggestive in connection with the present work.

Shape of the Cracks causing Failure

The position and paths of the 14 cracks present on the specimen after test are shown in fig 2. The *positions* of the cracks have already been accounted for from stress consideration. It will be seen that the paths followed by the cracks bear no obvious relation to the traces of the planes of maximum resolved shear stress (cf figs 2, 5 and 7). The cracks are mostly parallel to the axes of the specimen or develop into a fork in the manner characteristic of iron. The predominating axial direction suggests that the effect of slipping on two planes so breaks up the structure that the crack develops along planes of actual maximum, *not* maximum resolved, shear stress. The bifurcation that occurs in some of the cracks probably develops at a later stage due to some local flaw in the material, and the effect of the presence of such a flaw in

producing a helicoidal or double helicoidal fracture has been previously demonstrated *

It may be of interest to recall some other experiments which seem to be consistent with the harmful effects of duplex slipping on the crystal structure of the type now suggested. In the pioneer work of Stanton and Bairstow† on the resistance to *impact* of iron and steel, they drew particular attention to the changes in micro-structure of iron subjected to repeated shock. They showed clearly that when a specimen is fractured under a small number of heavy blows, Neumann lamellæ were produced in great profusion. On the other hand, when failure occurred under fatigue, cracks resulted from the development of slip lines, and the process was the same under impact as under gradually applied alternating stress. Recently Pfeil‡ in his work on single crystals of iron, showed that Neumann lamellæ are formed on icositetrahedral planes by shocks of all magnitudes. He found, however, that a preliminary very small plastic deformation (0.28 per cent. or more) was sufficient to prevent the subsequent production of Neumann lamellæ by shocks. Rosenhain and McMinns§ also found the same phenomena quite independently, in specimens consisting of a crystalline aggregate. These experiments indicate that the mechanism of distortion of α -iron under static or fatigue stresses is accompanied by severe lattice distortion, and are especially interesting in connection with some of the features of the present research.

Total Deformation of the Test Piece

The total distortion of the test piece, as a whole, is most conveniently studied with regard to the relative movement during test between the specimen and crystal axes. The spherical co-ordinates of the cube axes as calculated from the corrected X-ray analyses, are as follows:

* "On the Concentration of Stress in the Neighbourhood of a small Spherical Flaw, and on the Propagation of Fatigue in 'Statically Isotropic' Materials," Southwell and Gough, 'Phil Mag.', vol. 1 (January, 1926)

† 'Proc Inst Mech Engrs' (November, 1908)

‡ *Lor. cit.*

§ 'Roy Soc Proc.', A, 108, p. 231 (1925)

Table VIII—Spherical Co-ordinates of Cube Axes of Specimen as calculated from Corrected X-ray Readings

Plane	Spherical co ordinates			
	Before test		After test	
	θ	ψ	θ	ψ
I00	81 7	96 5	80 31	95 27
010	77 36	4 6	77 28	3 21
001	15 19	220 46	15 51	221 34

The nature of the movement will, perhaps, be more apparent if expressed in terms of the movement of the specimen axis relative to the fixed crystal axes. Referring to fig 4 (a), the normals to the 010, I00 and 001 planes may be considered as x , y and z axes respectively, and the position of the specimen axis before and after test can then be calculated relative to these axes. The following results are obtained

$$\begin{aligned}\theta &= 15^{\circ} 19' & \theta_1 &= 15^{\circ} 51' \\ \psi &= 35^{\circ} 41' & \psi_1 &= 37^{\circ} 9'\end{aligned}$$

where θ , ψ and θ_1 , ψ_1 , refer to the axis before and after test, respectively. The dihedral angle represents the movement and its value is found to be $0^{\circ} 39'$ only. In view of this value, and of the possible errors in the X ray data from which it is deduced, it is obvious that the total distortion occurring during the test is of an extremely small amount and is, in fact, negligible.

Examination of the Cross Section of the Specimen

In view of experience with single crystals of aluminium, it was considered that an examination of the polished and/or etched cross-section of the specimen might reveal interesting features. Prof. Hanson very kindly rendered valuable assistance in this respect, and the polishing, etching and photography of the cross-section of the present specimen was carried out under his direction in the Metallurgical Department at Birmingham University.

The specimen was carefully cut across in a plane perpendicular to the axis (the θ of the plane thus having the approximate value of zero). Continuous polishing failed to reveal any structure (due to differential hardening) as had previously been encountered in aluminium crystals. Etching with a dilute

HNO_3 solution in alcohol revealed the presence of a number (about 36) of very small crystals present (It is possible that the very high initial range of elasticity exhibited by this specimen may be due, to some extent, to the presence of these crystals) The structure was, otherwise, featureless. The section was then deeply etched with a 5 per cent solution of HNO_3 in alcohol, and the appearance of the structure is exhibited in fig 28. In addition to the small crystals the structure exhibits four distinct zones. Reference to the scale surrounding this photograph and to fig 3 shows that the limits of these zones correspond to the change-over points of *significant* directions of slip. This fact affords additional evidence that the direction of slip is the octahedral direction. While opposite zones are of approximately uniform shapes and equal depths, adjacent zones differ widely in these respects. Now if the depth of the zone at any point was proportional to the value of the resolved shear stress at that point, we should expect to find maximum depths (see fig 3) at points $\lambda = 51^\circ$, 138° , 231° and 318° . This prediction is fulfilled. But the shear stress values at these points are nearly equal, yet the ratio of the depths of adjacent zones is approximately 2 3 1 (as measured from the photograph). This result, showing that the depth is not proportional to the shear stress, is not really surprising when we consider that the direction of slip differs in such adjacent zones. The effect of the etching might, however, be expected to be related to the amount of distortion in a direction perpendicular to the plane of the section. This possibility was examined. A polar diagram was constructed in which the ordinate at any point was equal to the maximum resolved shear stress value at the point (from fig 3) multiplied by the cosine of the θ co-ordinate of the direction of slip at that point. It was found that, constructing this diagram to a suitable scale, the shape of the diagram was in good agreement with the contours of the zones revealed by etching. Thus, at any point on the surface, if the depth of etched zone measured *radially from the surface* be denoted by x , then, apparently

$$x \propto f_s \times \cos \theta_s,$$

where f_s is the value of the maximum resolved shear stress at the point on the surface and θ_s refers to the slip direction.

The specimen was carefully repolished and etched with 4 per cent. iron alum, the specimen being moved, during the process, as specified by Dr Griffiths and Mr Lookspieser, the originators of the etching re-agent. The appearance of the specimen is exhibited in Plate 13, fig 30. Again, the zones are apparent. But whereas using the HNO_3 etching re-agent, the portions within the zones presented no distinctive features, the white dots in fig 30 are all of the same

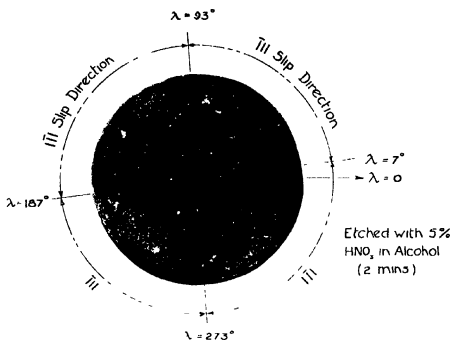


FIG 28 (7 diams)

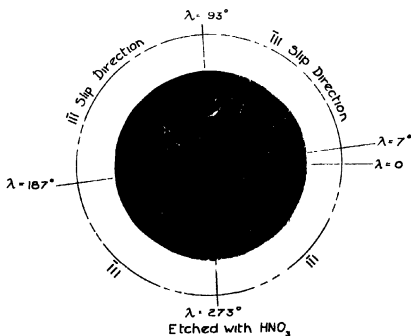


FIG 29 (~ 7 diams)

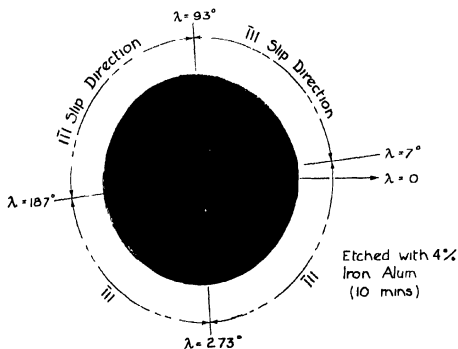


FIG 10 (7 diams)



Cross Section etched in 4% Iron Alum for 10 mins

FIG 11 (800 diams)

regular type Plate 13, fig 31, shows this structure at a much higher magnification The white dots are now seen to be regular etching pits, whose trace on the surface is, roughly, a parallelogram The orientation of these pits throughout the surface does not differ appreciably neither do the parallelograms differ appreciably in size Although a few isolated pits are visible in the area situated between the zones and the centre of the specimen, there is a very marked drop in the density of population of these pits once the zone is passed This is seen in a most striking manner when the microscope is traversed along a diameter of the specimen It was found that the shape of these pits agrees extraordinarily well with the trace of a cube on the surface of the section, assuming that the faces of the cube are the cube faces of the crystal For, from Table VIII we see that the spherical co-ordinates of the cube faces are as follows —

$$\theta_{001} = 15^\circ 51', \quad \psi_{010} = 3^\circ 21' \quad \psi_{100} = 95^\circ 27',$$

and the trace of a *unit* cube on the surface will be a parallelogram of the following dimensions and shape (relative to the trace of the reference plane $\gamma = 0$, on the surface) —

Trace of 100	inclination $5^\circ 27'$	}	included angle
Trace of 010	inclination $-86^\circ 39'$		
			$= 92^\circ 6'$

$$\frac{\text{Length of } 100 \text{ trace}}{\text{Length of } 010 \text{ trace}} = 1.01.$$

The inclination of the sides of the etching pits agree very well with the deduced values, but the actual dimensions of the sides are too irregular to compare with the required ratio, although the order of the results is the same Further, the shadow effects of the pits agree with the calculated "tip" of the 001 axes

Further examination of fig 31 shows the existence of a sub-structure consisting of triangular markings and a series of lines, approximately parallel It is hoped to make a detailed study of this sub-structure in the near future Plate 12, fig 29, shows the appearance of an etched cross-section in the neighbourhood of some of the cracks

It may perhaps be pointed out in view of the apparent regularity of shape of the cubic etch pits that the plane of the surface examined makes an angle of nearly 16° with the nearest cube face Obviously, extreme care must be used in determining crystal orientation by such means as observations of the shape of etch pits, needle impression, etc., such methods appear to involve the adoption of large errors and cannot be substituted for X-ray methods if accurate results are required.

Acknowledgments

The author desires to record his thanks to the following to Prof Edwards and Mr Pfeil who kindly supplied the iron crystal, to Prof Hanson who undertook the polishing and etching of the specimen and supplied figs 28 to 31, to Mr Cox, B A, who, by rendering generous assistance with the lengthy calculations involved, has materially assisted the progress of the work, and to Mr Binks, M Sc, who carried out the X-ray analyses of the crystal

Some Physical Properties of Gas-freed Sulphur

By C COLERIDGE FARR, D Sc, and D B MACLEOD, D Sc

(Communicated by C Chree, F R S—Received January 11, 1928)

In a paper by the authors* on the viscosity of liquid sulphur, it was shown how difficult it is to prepare a sample of sulphur whose viscosity is independent of previous heat treatment. This uncertainty extends to all the physical properties of sulphur and is noted in papers by Kell[†] and by Smith and his co-workers[‡]. Smith regards liquid sulphur as consisting of two modifications S_A and S_B , the proportion of S_B to S_A increasing as the temperature is raised, with a marked increase in the neighbourhood of 160° C. The presence, however, of such products as SO_2 , traces of H_2SO_4 , and H_2S exerts a considerable retarding influence on the attainment of inner equilibrium between these two varieties, thus causing a great variation in the physical properties at any given temperature.

Between the temperatures 160° C and 180° C the viscosity increases several thousand times. With sulphur purified in the ordinary way, by simple distillations or precipitations, remarkable variations in the viscosity are possible over this range of temperature. This property, therefore, provides an exceptionally sensitive test of the dependence of the sulphur on previous treatment, and a sample, whose viscosity was definite and constant at any temperature, would almost certainly be definite in its other physical properties.

* 'Roy Soc Proc,' A, vol 97, p. 80 (1920)

† 'J Chem. Soc,' vol 113, p 903 (1918)

‡ Smith and Holmes, 'Z Phys Chem,' vol 42, p 469 (1903), and vol 54, p 257 (1906), Carson, 'J Amer Chem Soc,' vol 29, p 499 (1907), Smith and Carson, 'Z Phys Chem,' vol 77, p 661 (1911)

At the time of the authors' earlier work on this subject (*loc cit*) means were not available for obtaining the highest vacua, and the sulphur suffered from contamination with mercury vapour. On the installation of an efficient liquid air plant in the laboratory it was decided to prepare a sample of sulphur as free as possible from all impurities, in a sealed vessel which could itself be used as a viscometer.

Method of Preparation of the Sulphur—Samples of purified sulphur were prepared, finally from sulphur crystallised from CS_2 and from commercial flowers of sulphur. Crystallised sulphur imported as "pure" showed on being distilled a considerable residue of carbonaceous matter, as, also, do any of the commercial samples.

The process of purification adopted consisted of two parts (1) a series of five distillations under CO_2 and (2) a series of three distillations under a vacuum the whole so arranged that no exposure to air was made during the process. The distillation apparatus is shown diagrammatically in fig. 1. A series of

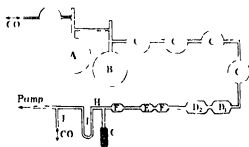


FIG. 1

flasks and receiving bulbs, thoroughly cleansed with boiling nitric acid and chromic acid, and washed with distilled water, were sealed together as follows. A and B were distilling flasks of 300 c.c. capacity, the bulbs C were of 200 c.c. capacity, and D_1 and D_2 were 100 c.c. pipettes. The bulbs E, which constituted the viscometer, were 25 c.c. pipettes sealed, usually, close together, but under some circumstances—for determining the viscosity at temperatures under 160°C —with a piece of fine bore tube between them about 15 cm. long and 1 mm. in bore. F was a spare pipette to condense the vapour escaping from E. G contained activated coconut charcoal. The U tube I, immersed in liquid air, prevented the diffusion of mercury vapour from the pump. The whole of the distilling apparatus was glass sealed and free from glass taps and rubber junctions.

By a suitable arrangement a current of purified and dried CO_2 could be passed

through the distillation apparatus either in the direction from A to J or from J to A

Crystallised sulphur, or ordinary distilled sulphur, was introduced into the flask A, which was then sealed off at the top, and only remained open to such currents of CO_2 as were desired through the side tube. The charcoal in G was first thoroughly heated and evacuated several times to remove moisture, etc., and then distillation commenced under a stream of dried CO_2 . During the first part of each distillation, the current of CO_2 was passed from J to A. It was then reversed and the middle portion of the sulphur carried forward. This was repeated, distilling from bulb to bulb until a suitable quantity had been distilled into D_1 . The end portion of the apparatus was then sealed off at a point between D_1 and the last bulb C and also at J. This cut off the CO_2 supply. The charcoal in G was then heated strongly in an electric oven and the U-tube I was immersed in liquid air, and the whole remaining portion from D was evacuated by means of an efficient Gaede pump. Meanwhile the sulphur in D was remelted to remove as much dissolved gas as possible. When a good vacuum had been secured a seal was made at H, leaving only the bulbs D and E and the hot charcoal bulb G.

After cooling, the charcoal bulb was immersed in liquid air, and remained so during the rest of the process. The viscometer bulbs E were then heated strongly in order to drive off gases condensed on or occluded in its glass, and the sulphur was distilled into it from D. It was found possible, by allowing the sulphur to condense and block the tube leading from D to E, to raise the tubes D to a temperature above 300°C , thus tending the more effectually to remove dissolved gases, and this blocking was allowed to take place several times during the distillation from D into E. When a suitable quantity of sulphur had been collected in E the bulbs D were drawn off. The same process of raising the temperature to about 350°C by blocking and then blowing off into F was adopted several times in the case of the bulb E. Finally the liquid air-cooled charcoal tube and F were separated from the viscometer E by sealing between E and F, the final seal being made whilst hot sulphur vapour was streaming through.

As a matter of fact, the viscometer itself proved a very satisfactory index of the quality of the vacuum, and of the effectiveness or otherwise of the attempts to drive off the final traces of gas. Where the heating had been insufficient, further heating would eliminate another slight trace of gas from the body of the sulphur, which would interfere with the even flow of the liquid through the constriction sufficiently to be noticeable towards the end of the flow. Such

tubes became useless, and only those, in which the vacuum was, and remained, very efficient, could be used for very prolonged observation, and were the only ones considered

Testing the Viscosity The viscometer, which consisted of two 25 c c pipettes (fig 2 (a)) contained about 12 c c of sulphur. It was mounted on a frame which could be rotated, the time taken for the sulphur to run from one end to the other being a measure of the viscosity of that tube. An iron vessel, with mica windows, well lagged and filled with paraffin was used as a bath. It was electrically heated and governed by an air thermostat, and with thorough mechanical stirring the temperature in it could be kept constant to a tenth of a degree for a considerable time. Measurements of the time of flow were always made within the range of temperature from 163°C to 169°C , that being the interval over which sulphur shows the most remarkable variations of viscosity. The test experiments consisted of measuring the viscosity under the following different conditions of heat treatment—(a) that of a tube of freshly prepared sulphur, (b) that of the same tube after it had been kept for several days—on one occasion it was five months—at a temperature somewhere between 130°C and 150°C in an electric oven, (c) the same tube heated to 330°C for 15 minutes in an electric oven and transferred rapidly to the paraffin bath (in this case the temperature never fell below that of the bath), (d) heated to 330°C for 15 minutes and cooled rapidly to 140°C and then transferred to the bath, (e) heated to 330°C and allowed to cool very slowly, remaining in and cooling with the oven until nearly the proper temperature for testing was reached, when it was rapidly transferred to the bath. A plotted example—one only of a number of similar experiments—of a series of readings with a satisfactory tube is shown in fig 3. The testing-bath having been adjusted to some temperature between the above-mentioned testing limits, 163°C and 169°C , the sulphur was removed from the heat-treatment oven into the bath and kept constantly moving for about 15 minutes so that it might acquire the temperature of the testing-bath. It is essential to take readings as promptly as possible, as with sulphur as usually purified there is a slow creep of viscosity values.



FIG 2

An inspection of fig 3 shows that whatever the previous heat-treatment has been all the values of the viscosity, with the exception of one observation made at a bath temperature of 166°C , lie upon the same curve. An error of observa-

tion of either seven or eight seconds in the time of flow, or of two-tenths of a degree in the temperature of the sulphur, would put this result upon the same

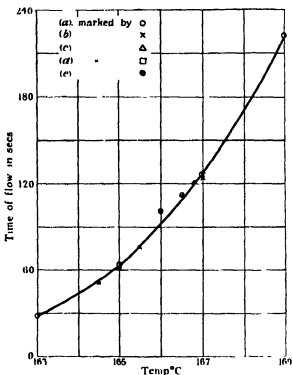


FIG 3

curve. Whilst the former error is unlikely, the latter is very probable as it was the first observation made with the sulphur after removal from the heat treatment oven, and although precautions were taken the sulphur may not have acquired the testing-bath temperature to that degree of accuracy. Another observation after the same heat treatment at a slightly higher testing-bath temperature does lie practically upon the curve.

In very striking contrast with these single valued results are those on p. 85, fig. 2, curves I and IV, of the authors' previous paper, which show that sulphur purified as is usually done and subjected to similar treatment gives values ranging in the proportion of one to eight when measured at the same fixed temperatures. It was found that a number of tubes prepared with considerable care, failed to give consistent values. These, on examination, were found to contain traces of residual gas, given off from the sulphur, probably, in the subsequent heat treatment. This indicates the importance of a small amount of gaseous impurity and the difficulty of removing it.

The authors thus consider it established that provided sulphur is prepared with sufficient care, and protected from exposure to air, it gives reproducible values of the viscosity

Melting-Point—It is interesting to note that from sulphur purified in this way, the less common crystalline form known as "Mother of Pearl" sulphur separates out with great ease, and exhibits a considerable degree of stability. For a description of the usual method of preparation of Mother of Pearl sulphur, or S_{III} , see paper by Smith and Carson (*loc cit*). With sulphur purified as above it was found unnecessary to induce the formation of S_{III} crystals by scratching or by other artificial means. The liquid sulphur was allowed to cool slowly to below 103°C when crystals of S_{III} would separate themselves. Further it was noticed that in tubes less satisfactorily prepared the S_{III} crystals settled out with greater difficulty and uncertainty. In order to study the melting point of S_{III} a tube as shown in fig 2 (b) was made. An inner tube A into which a thermometer could be placed, dipping in mercury, was fused into an outer bulb B which contained the sulphur. The bulb B was filled in a manner similar to the viscometer, the sulphur being sealed off under a vacuum.

The natural freezing point of S_{III} was determined as follows. After initial cooling of the tube of sulphur in air until crystals began to appear, the tube was quickly restored to the bath, and provided the bath did not remain below 103°C or above 106°C for long, the crystals could be kept in contact with the liquid indefinitely. The temperature of the liquid sulphur was raised above the approximate melting-point, but not sufficiently to remelt all the crystals present. It was then placed in the paraffin bath, whose temperature was below the approximate melting-point. The sulphur tube was vigorously shaken until a crop of crystals appeared and the temperature remained constant. The process was repeated, each time the paraffin bath being raised to a temperature a little nearer to the melting-point of sulphur. In this way, with the temperature of the paraffin bath at 103.2°C the inner thermometer gave readings from 103.8°C to 103.9°C as the temperature of the liquid sulphur during crystallisation. The thermometers were standardised against two sets of thermometers having N.P.L. certificates. Smith and Carson (*loc cit*) by a different method and using sulphur treated with ammonia obtained a value of 103.4°C as the natural freezing point of S_{III} .

The ideal melting-point of S_{III} , that is the melting-point in contact with pure S_A , cannot be determined with the same degree of accuracy. It was found possible with some of the tubes to crystallise the whole of the sulphur to S_{III}

and then remelt it, but more often the change to S_I or S_{II} would suddenly set in. The heat generated by this change, causing expansion, would frequently break the tube. The laboriousness of the work was greatly increased by tubes, prepared with much care, breaking after the sulphur had crystallised or on remelting. For this reason it was found desirable to prevent the sulphur crystallising as a whole, except in certain critical experiments. The ideal melting-point should be the temperature at which the sulphur just begins to melt after being totally crystallised. Observation showed this temperature to be in the near neighbourhood of 107°C , which is practically the same value as given by Smith and Carson 106.8° .

When the sulphur did not separate out as S_{III} it invariably crystallised as monoclinic, as indicated by a melting point between 119°C and 120°C . By partly remelting, crystals of monoclinic sulphur were secured in contact with the liquid. The natural freezing point of monoclinic sulphur was then determined in a manner similar to that adopted for S_{III} . The mean of a number of readings gave 114.6°C as its natural freezing point (compare Smith and Carson, 114.5°C).

With sulphur purified in the above way, the authors were unsuccessful, after repeated and careful efforts, in their attempts to obtain melting-points corresponding to the presence of rhombic sulphur. When the sulphur had crystallised as S_{III} , recrystallisation set in after a few hours, and the final product invariably melted in the region of 119 – 120°C . Tubes set aside for months remelted at the same temperature, which would indicate either that the tendency to form the stable rhombic sulphur had been retarded, or that re-heating rapidly restored the monoclinic variety after the transition temperature had been passed. It is hoped to throw more light on this aspect of the question by an X-ray study of the solid sulphur.

Supercooling—By slowly lowering the temperature of the bath, the sulphur could be kept liquid down to a temperature of 80°C , representing over 30° of supercooling. It actually remained liquid at 105° for several weeks without crystallising. It became of interest to obtain relative values of the viscosity over this range of temperature. A viscometer was prepared and filled on the same principle as the others, but the pipettes were separate by a length of semi-capillary tubing, the sulphur, of course, being much more limpid below 160°C . With this, comparative values of the viscosity were obtained from 81°C to 159°C . It was not found possible to calibrate the tube so as to give the viscosity in CGS units, and so the table only gives the time of flow corresponding to various temperatures. The minimum value was in the neighbourhood of

155° C At 80° C the sulphur is nearly four times as viscous as it is at 155° C These results are shown graphically in fig 4

Temperature (°C)	Time of flow in seconds	Temperature (°C)	Time of flow in seconds
80.8	111.4	144.0	34.5
84.7	100.6	148.2	32.8
88.7	91.0	154.3	31.6
93.8	78.8	155.3	31.5
97.9	73.1	157.0	31.9
104.5	63.1	158.6	60.0
110.3	57.0	159.2	165.0
120.4	47.6	159.3	232.0
134.0	39.0		

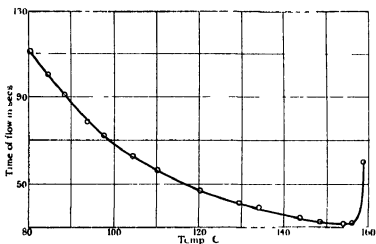


FIG 4

Conclusions

- (1) Purified sulphur, freed from gaseous impurities, acts as a simple substance, whose viscosity is definite at any given temperature, and independent of the previous heat treatment
- (2) From sulphur purified and prepared so as to be gas free, crystals of mother of pearl sulphur separate readily
- (3) Efforts to obtain rhombic sulphur, from sulphur similarly prepared, were unsuccessful
- (4) No sulphur, from which dissolved gases have not been very carefully removed, can be considered pure

*The Solution of the Wave Equation for the Scattering of Particles
by a Coulombian Centre of Force*

By N F MOTT, B A, St John's College, Cambridge

(Communicated by R H Fowler, F R S—Received February 2, 1928)

The problem of the scattering of a stream of charged particles by a Coulombian centre of force has been treated by Wentzel* and by Oppenheimer,† who use Born's method of successive approximations. They have shown that, if $ZZ'e^2/\hbar v$ is small, the quantum theory gives the well-known Rutherford formula. Furthermore, if $ZZ'e^2/\hbar v$ is large, we know that the quantum theory result must tend towards the classical, and it seemed probable that the two theories would agree for intermediate values of this constant. In this paper we shall show that this is actually the case.

We shall first consider the more general problem of scattering by a field $V(r)$. The wave equation is

$$\nabla^2 \phi + \frac{2m}{\hbar^2} (E - V) \phi = 0 \quad (1)$$

We want to find a solution of (1) which, when r is large, represents a plane wave $e^{ipz/\hbar}$ together with a wave travelling outward $f(\omega) e^{ipr/\hbar}/r$. Then $|f(\omega)|^2 d\omega$ will be the probability that the particle will be scattered in the solid angle $d\omega$.

We can solve (1) by separating the variables. If $L_n(r)$ is the characteristic solution of

$$\frac{1}{r^2} \frac{d}{dr} \left(r^2 \frac{dL}{dr} \right) + \left[\frac{2m}{\hbar^2} (E - V) - \frac{n(n+1)}{r^2} \right] L = 0, \quad (2)$$

then the most general solution of (1) that has axial symmetry is

$$\sum_n A_n P_n(\cos \theta) L_n(r) \quad (3)$$

We have to choose our A_n so that (3) shall be the required solution.

The following not very rigorous investigation suggests what these coefficients should be. The unit of length has been chosen so that $p/\hbar = 1$.

Suppose that, for large r

$$L_n(r) \sim \frac{2}{r} \sin(r + \phi_n)$$

where ϕ_n depends on n only

* 'Z f Physik,' vol 40, p 590 (1927)

† 'Z f Physik,' vol 43, p 413 (1927)

Now, a plane wave can be represented by the series

$$e^{iz} = (2\pi/r)^{\frac{1}{2}} \sum_{n=0}^{\infty} (n + \frac{1}{2}) i^n P_n(\cos \theta) J_{n+\frac{1}{2}}(r),$$

and hence we have to choose our coefficients A_n in such a way that, when r is large,

$$\sum_{n=0}^{\infty} P_n(\cos \theta) [A_n I_n(r) - (2\pi/r)^{\frac{1}{2}} i^n (n + \frac{1}{2}) J_{n+\frac{1}{2}}(r)] \quad (4)$$

represents an outgoing wave only

Suppose we replace both $I_n(r)$ and $J_{n+\frac{1}{2}}(r)$ by the first terms of their respective asymptotic expansions—this, of course, we are by no means entitled to do

The term within the square bracket in (4) becomes

$$\frac{1}{ir} \{ [A_n e^{i\phi_n} + (n + \frac{1}{2}) (-1)^n] e^{ir} - [A_n e^{-i\phi_n} + (n + \frac{1}{2}) e^{-ir}] \}$$

We are thus led to consider the possibility that we should set

$$A_n = - (n + \frac{1}{2}) e^{i\phi_n}$$

so that the solution that we require is

$$\sum_{n=0}^{\infty} (n + \frac{1}{2}) e^{i\phi_n} P_n(\cos \theta) I_n(r) \quad (5)$$

The outgoing wave would be

$$\frac{e^{ir}}{ir} \sum_{n=0}^{\infty} (n + \frac{1}{2}) P_n(\cos \theta) \{ e^{2i\phi_n} + (-1)^n \}, \quad (6)$$

but the series does not converge. It can be summed as the limit of a power series on its radius of convergence, and this does in fact give the right answer, in the case which we are about to investigate.

We shall now consider more rigorously the asymptotic behaviour of the function (5) for the case of the inverse square law, when $V = ZZ' e^2/r$. Z' may be either positive or negative, so that the results which we shall obtain are applicable both to α and to β particles.

We know both the solution of the equation (2) and the asymptotic expansion of that solution*. Using these results, the function (5) is easily seen to be

$$\sum_{n=0}^{\infty} (n + \frac{1}{2}) P_n(\cos \theta) \frac{1}{\Gamma(n + 1 + i\sigma)} \left(\frac{ir}{2}\right)^n \int_C (1 - t^2)^n \left(\frac{1+t}{1-t}\right)^{i\sigma} e^{irt} dt \quad (7)$$

where

$$\rho = ZZ' e^2/hv,$$

and the closed path of integration C encircles the points ± 1 in an anticlockwise direction.

* Cf. Schrödinger, 'Ann. d. Physik,' vol. 79, p. 365 (1926).

The sum (7) converges absolutely, but since the terms do not begin to diminish until n is of the order of r , we cannot investigate the behaviour of (7) when r is large by using an asymptotic expansion for the integral

We note that if $\rho = 0$, and if we replace C by a single line joining the points $-1, +1$, then the integral becomes a multiple of the Bessel function of order $n + \frac{1}{2}$, and the function (7) reduces to $e^{ir \cos \theta}$

In what follows we shall use the following symbols

$$F(x) = \frac{1}{2} (1 - x^2)/(x^2 - 2x \cos \theta + 1)^{3/2} \quad (8)$$

$$= \sum_{n=0}^{\infty} (n + \frac{1}{2}) x^n P_n(\cos \theta) \quad |x| < 1$$

and

$$\phi_p(x) = \sum_{n=0}^{\infty} (n + \frac{1}{2}) P_n(\cos \theta) x^n / \Gamma(n + 1 + \frac{1}{2}\rho) \quad (9)$$

It is not difficult to prove that, if the real part of x is positive,

$$\phi_p(x) = \frac{i}{2\pi} \int_{\gamma} (zx)^{-1/2} e^{iz} F(z) dz$$

where the path of integration γ starts from $-\infty$ encircles the points $z = 0, z = e^{i\theta}$, and returns to $-\infty$ (See fig 1)

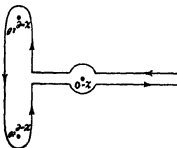


FIG. 1

If the real part of x is negative we must reflect the whole figure in the imaginary axis

We shall require the asymptotic behaviour of $\phi_p(x)$ when $|x|$ is large and $\arg x$ lies between 0 and π . Most of the integral then comes from the neighbourhood of $z = e^{-i\theta}$, and we find that

$$\phi_p(x) \sim x^{-1/2} (e^{-i\theta})^{-1/2} \phi_0(x) \quad (10)$$

where $\phi_0(x)$ is the value of $\phi_p(x)$ when $\rho = 0$, namely,*

$$\phi_0(x) = x^{-1/2} \frac{\partial}{\partial x} \{x^{1/2} e^{ix \cos \theta} J_0(x \sin \theta)\}$$

Assuming still that $|x|$ is large and that $\arg x$ lies in the same quadrant as before, we see that

$$\phi_0(x) \sim S \exp(ix e^{-i\theta}) \quad (11)$$

where S is a function containing no exponential term

* Watson, 'Bessel Functions,' p 149

The function (7) that we want is clearly

$$\int_c \phi_p \left(\frac{1}{2} \sqrt{1-t^2} \right) \left(\frac{1-t}{1+t} \right)^{-1/2} e^{i\pi t} dt \quad (12)$$

We take the path c as shown in fig. 2, a curve on the positive side of the real axis, with loops round the points $t = \pm 1$. We will suppose that the integration starts at the point P .



FIG. 2

We want to be able to use our approximation (7) for ϕ_p at all points of c , excepting the neighbourhoods of ± 1 . We can do this so long as $\arg \frac{1}{2} i\pi (1-t^2)$ lies between 0 and π , that is, so long as

$$|R^2 \cos 2\alpha| < 1 \quad (13)$$

where

$$t = R e^{i\alpha}$$

We evaluate the integral by the method of steepest descents. The exponential part of the integrand in (12) is

$$\exp [i\pi \{ t + \frac{1}{2} e^{-i\theta} (1-t^2) \}], \quad (14)$$

which gives us a saddle point at $t = e^{i\theta}$, and with this value of t , (14) becomes $e^{i\pi \cos \theta}$ as it should. We can choose, further, a steepest descents path through this saddle point, without violating the condition (13). Let us do this, then since all the integral (12) comes from the neighbourhood of the saddle point, we can set $t = e^{i\theta}$ in all the non-exponential part of the integrand. (12) then becomes

$$(e^{-2i\pi\theta} - 1) (2i\pi \sin^2 \frac{1}{2}\theta)^{-1/2} \int_1^{+1} \phi_0 \left(\frac{1}{2} i\pi \sqrt{1-t^2} \right) e^{i\pi t} dt$$

The integral is equal to $e^{i\pi \cos \theta}$, as we have pointed out, we have finally for (12), writing x for $r \cos \theta$,

$$- 2i e^{-i\pi\theta} \sin \pi\theta \exp (i\pi - i\pi \log r - x) \quad (15)$$

still neglecting the contributions made by the neighbourhoods of the poles

The function (15) does not represent a plane wave. Its wave fronts are the surfaces

$$x - \frac{ZZ'e}{mv^2} \log(r - x) = \text{const} \quad (16)$$

(Here we are using the ordinary unit of length again.) It is nevertheless the wave that we should expect to represent the incident stream of particles, as a moment's appeal to the Correspondence Principle will show.

Let us consider the problem in terms of the classical dynamics. A stream of particles starts with velocity v parallel to the axis of x . The trajectories of the particles form in space a family of hyperbolæ. A family of surfaces is orthogonal to these hyperbolæ, and the wave fronts of the wave which represents the oncoming particles should be just these surfaces. Now, although one asymptote of each of the hyperbolæ is parallel to the axis of x , yet, as we go a long way from the nucleus, the orthogonal surfaces do not become plane, the form to which they tend is, as a matter of fact, just (16). The wave is, as it were, distorted, even at infinity, by the nucleus which it is going to encounter.

We have now to see what is contributed to the integral (12) by the neighbourhoods of the poles $t = \pm 1$. In the neighbourhood of $t = -1$, put $t + 1 = z/ir$, the integral becomes

$$\frac{1}{2} (2ir)^{-i\rho-1} e^{-ir} \int \phi_p \{z(1 - z/2ir)\} z^{i\rho} (1 - z/2ir)^{-i\rho} e^z dz,$$

and since $r \gg 1$, and we are only interested in the region where $|z| \approx r$, we may replace this integral by

$$\frac{1}{2} (2ir)^{-i\rho-1} e^{-ir} \int_{\sigma} \phi_p(z) z^{i\rho} e^z dz \quad (17)$$

The path of integration σ comes from $-\infty$, encircles the point $z = 0$ in an anticlockwise direction, and goes back again to $-\infty$.

From the other pole we get a contribution

$$\frac{1}{2i} e^{-\frac{3\pi\rho}{2}} (2r)^{i\rho-1} e^{ir} \int_{\sigma} \phi_p(-z) z^{-i\rho} e^z dz \quad (18)$$

We have to evaluate the integrals in (17) and (18). We shall find that the integral in (17) vanishes, so that we are left with an outgoing wave only.

Let us consider the function

$$f(X) = \int_{\sigma} \phi_p(zX) z^{i\rho} e^z dz \quad (19)$$

The integral (19) exists for all values of X lying in some neighbourhood of $X = 1$, and $f(X)$ is a continuous function in this neighbourhood, so that

$$\lim_{X \rightarrow 1} f(X) = f(1)$$

Furthermore, if

$$|X| < 1 - \delta,$$

we have

$$f(X) = -2i \sin \nu \rho \sum_{n=0}^{\infty} (n + \frac{1}{2}) (-X)^n P_n(\cos \theta)$$

It follows that, for the integral in (17), we have

$$\int_{\sigma} \phi_{\rho}(z) z^{\nu} e^z dz = \lim_{X \rightarrow 1} f(X) \\ = 0, \text{ as we require}$$

We are therefore left with the outgoing wave (18) only

For the integral in (18) we obtain in the same way

$$\int_{\sigma} \phi_{\rho}(-z) z^{-\nu} e^z dz = 2i \sin \nu \rho \lim_{X \rightarrow 1} \sum_{n=0}^{\infty} (n + \frac{1}{2}) \frac{\Gamma(n+1-\nu \rho)}{\Gamma(n+1+\nu \rho)} X^n P_n(\cos \theta) \quad (20)$$

It is interesting to see that (20) is of the form (b)

The limit (20) can be evaluated as follows —

We have*

$$\Gamma(-\nu \rho + n + 1) / \Gamma(\nu \rho + n + 1) = A \int_P t^{-\nu \rho + n} (1-t)^{2\nu \rho - 1} dt$$

where $A = e^{\nu \rho} / 4 \Gamma(2\nu \rho) \sin \pi \nu \rho \sin 2\pi \nu \rho$ and P , the path of integration, starts from a point on the real axis, encircles the points 0, 1 according to the scheme (1+, 0+, 1-, 0-), and finally returns to the starting point. Hence we find that,† if $|X| < 1$,

$$\sum_{n=0}^{\infty} (n + \frac{1}{2}) \frac{\Gamma(n+1-\nu \rho)}{\Gamma(n+1+\nu \rho)} X^n P_n(\cos \theta) = A \int_P F(tX) t^{-\nu \rho} (1-t)^{2\nu \rho - 1} dt,$$

where the path of integration does not encircle the poles of $F(tX)$

Thus, $\cos \theta$ not being equal to unity, we have

$$\lim_{X \rightarrow 1} \sum_{n=1}^{\infty} (n + \frac{1}{2}) \frac{\Gamma(n+1-\nu \rho)}{\Gamma(n+1+\nu \rho)} X^n P_n(\cos \theta) \\ = A \int_P F(t) t^{-\nu \rho} (1-t)^{2\nu \rho - 1} dt \quad (21)$$

* Cf Whittaker and Watson, "Modern Analysis," 3rd Ed., p. 257

† Cf equation (8)

To evaluate this integral, it is convenient to assume for the moment that ρ is an imaginary number between 0 and $-\frac{1}{2}$, so that we can replace (21) by

$$\frac{1}{\Gamma(2i\rho)} \int_0^1 F(t) t^{-\rho} (1-t)^{2\rho-1} dt$$

The result that we shall obtain will clearly be valid for ρ real

We evaluate the definite integral by the following set of substitutions —

$$\begin{aligned} t &= e^{i\phi} \\ y &= \operatorname{cosec} \frac{\theta}{2} \sin \frac{\phi}{2} \\ \frac{1}{z} &= 1 - y^2 \end{aligned}$$

We obtain finally for (21)

$$\frac{\pi^{3/2} e^{\pi\rho} 2^{2\rho}}{\sin 2\pi\rho \Gamma(2i\rho) \Gamma(i\rho) \Gamma(\frac{1}{2} - i\rho)} (1 - \cos \theta)^{\rho-1}$$

We are now in a position to write down the asymptotic form of (7) Referring back to (16), (18) and (21) we see that it is

$$\begin{aligned} &- 2i e^{-\frac{\pi}{2}\rho} \sin \pi\rho e^{i\pi - i\rho \log(r-x)} \\ &+ \frac{\frac{1}{2}\pi^{3/2} 4^{i\rho} e^{-\frac{\pi}{2}\rho} \sin \pi\rho}{\sin 2\pi\rho \Gamma(2i\rho) \Gamma(i\rho) \Gamma(\frac{1}{2} - i\rho)} r^{-i\rho-1} e^{i\pi} (1 - \cos \theta)^{\rho-1} \end{aligned}$$

Let us divide through by the factor $- 2i e^{\frac{\pi}{2}\rho} \sin \pi\rho$, we obtain

$$e^{i\pi - i\rho \log(r-x)} + R r^{-1} e^{i\pi + i\rho \log(r-x) + i\alpha} \quad (22)$$

where

$$R = \frac{ZZ' e^2}{2m v^2} \operatorname{cosec}^2 \frac{\theta}{2}, \text{ using ordinary units of length,}$$

and

$$\alpha = \arg \left\{ \frac{18^{i\rho}}{\Gamma(2i\rho) \Gamma(i\rho) \Gamma(\frac{1}{2} - i\rho)} \right\}$$

The function (22), then, is the function that we want It represents an incident wave of unit amplitude, together with an outgoing wave, and it is the asymptotic form of a certain solution of the wave equation (1) The probability that a particle will be scattered in the solid angle $d\omega$ is $R^2 d\omega$, and this gives the Rutherford scattering formula exactly for all velocities of the incident particles

In conclusion, the author wishes to express his thanks to Mr R H Fowler, F R S, and to Dr P A M Dirac, for much invaluable help and encouragement

Summary

The scattering of particles by a Coulombian centre of force is investigated. A solution of the wave equation is obtained, which splits up into an incident wave, representing the oncoming electrons, and a scattered wave. It is found that the quantum theory result agrees exactly with that of the classical theory. The analysis is applicable both to α and to β particles.

A Redetermination of the Velocities of α Particles from Radium C Thorium C and C'

By G. H. BRIGGS, B.Sc., Ph.D., Lecturer in Physics in the University of Sydney

(Communicated by Sir Ernest Rutherford, P.R.S. — Received February 2, 1928.)

§ 1 The first accurate determinations of the velocity with which an α particle is expelled from a radio-active substance and of the value of E/M , the ratio of the charge to the mass, were made by Rutherford and Robinson by measuring the deflections in magnetic and electric fields. An α particle moving with velocity V perpendicular to the direction of a magnetic field H describes a circle of radius ρ where

$$H\rho = MV/E$$

Rutherford and Robinson* found for α particles expelled from radium C $H\rho = 3.983 \times 10^5$ E.M.U. and $V = 1.922 \times 10^9$ cm. per second. The mean value of E/M for α particles from radium emanation, radium A and radium C was 4820 E.M.U., which agreed to within the limits of experimental error with the value 4826 deduced from electrochemical data taking the atomic weight of helium as 3.998 and the value of the faraday as 9647. This value of the velocity of α particles from radium C has served as a standard from which the velocities of α particles from other radio-active substances have been calculated from the Geiger relation $V^3 = kR$.

The present paper gives an account of a redetermination of the quantity $H\rho$ for α particles from radium C by a method which is essentially similar to those used in previous determinations of this kind. From the value of $H\rho$

* 'Phil. Mag.', vol. 28, p. 552 (1914).

the velocity has been calculated using the theoretical value of E/M which can be found to a high degree of accuracy from more recent determinations of the atomic weight of helium and the value of the faraday, taking into account the relativity correction for the increase in mass of the α particle. For the atomic weight of helium we may take 4.000, the value deduced by Van Laar* from a consideration of the density determinations† of Watson, Heuse, Taylor, and in particular of Guye's discussion of Taylor's results. Taking the value of the faraday given by recent determinations 9649.4 E.M.U. the value of E/M for a slow moving α particle is 4824.7 and on applying the correction for the relativity change of mass this becomes 4814.8 for the α particle from radium C, neglecting the mass of the lost electrons‡. It may be noted that Rutherford and Robinson's experimental result, 4820 agrees as well with this latter value as with the value 4826 which they calculated.

§ 2 *Apparatus and Experiments with α Particles from Radium C*—The same apparatus was used for producing the magnetic deflection, as has already been described§ in accounts of experiments on the straggling and the decrease of velocity of α particles from radium C, so that only a brief description of it as modified for the present purpose will be given here.

The poles of the electromagnet were 24 by 8.6 cm and 2.7 cm apart. The source was a platinum wire 0.125 mm diameter and effective length 8 mm, activated with radium B and C by exposure to radium emanation. The source, slit and photographic plate were carried on three rigid supports permanently screwed to a brass base which could be slid into a brass box fixed between the poles of the electromagnet. In addition to the usual single slit there was a second slit 2.2 mm below the first serving merely to give additional data. These slits were 0.051 mm and 0.080 mm wide, and a shutter worked by a windlass was arranged over them to prevent α rays reaching the plate before the pressure had been sufficiently reduced.

The uniformity of the magnetic field was investigated by exploration with a small search coil having a large number of turns and the variations were found

* 'J. Chim. Phys.', vol. 17, p. 266 (1919).

† Watson, 'J. Chim. Soc.', vol. 97, p. 810 (1910), Heuse, 'Ber. Deutsch. Phys. Ges.', vol. 15, p. 518 (1913), Taylor, 'Phys. Rev.', vol. 10, p. 653 (1917), Guye, 'J. Chim. Phys.', vol. 16, p. 46 (1918).

‡ F. W. Aston ('Roy. Soc. Proc.', A, vol. 115, p. 487, 1927) using the mass spectrograph finds the mass of helium 4.00216. I understand this agrees with the corrected density determinations made by Baxter and Starkweather ('Proc. Nat. Acad. Sci.', vol. 12, p. 20, 1926). This makes E/M for helium 4812. [E.R.]

§ Briggs, 'Roy. Soc. Proc.', A, vol. 114, pp. 313, 341 (1927).

to be very small. With a field of 8800 gauss the field at the source was 2.2 gauss less than that at the slits, and for positions on the plate corresponding to the upper and lower deflected lines the differences were 4.4 and 0.5 gauss respectively. The total correction which has to be applied to the value of H at the slits to give the effective field when determined by the method given by Rutherford and Robinson amounts to only 0.5 gauss. This is the mean correction for the two deflections.

The magnetic fields were measured by a null method which was in principle similar to that described by Ellis and Skinner*. A circuit is arranged consisting of a search coil, the secondary of a mutual inductance and a fluxmeter or galvanometer connected in series. The search coil is reversed or pulled out of the field and simultaneously the current in the primary of the mutual inductance is broken. This current is adjusted until under suitable timing conditions there is no deflection of the detecting instrument. In the present experiments the search coil consisted of 16 turns of No. 37 bare copper wire wound on a polished cylinder of clear fused quartz whose maximum and minimum diameters determined at the National Physical Laboratory were 3.30925 and 3.30905 cm. This coil was held in an ebonite holder which ran in grooves on a slide, one end of which could be inserted into the box between the poles. By means of a cord and falling weight the coil could be pulled out rapidly from a definite position between the poles. In its motion it tripped a small key which reversed the current in the primary of the mutual inductance. It was found that a high sensitivity low resistance galvanometer highly damped was somewhat more suitable than a reflecting fluxmeter as detector. The sensitivity of the arrangement was such that the current for balance could be adjusted to 1 in 5000, though under the best conditions of timing there was always a rapid motion of the spot about 1 cm. from and back to zero. The current was measured by means of a potentiometer using a cadmium cell and standard resistance, both of which as well as the mutual inductance, had recently been tested at the National Physical Laboratory. During the course of the work the cell was compared with two other recently standardised cells. When pulled from between the poles the coil came to rest about 80 cm. from the electromagnet. The strength of the field at the resting point was determined to within 0.2 gauss as a function of the current through the electromagnet. For the currents employed it was about 17 gauss. The possibility of the ebonite holder which carried the coil disturbing the magnetic field was tested experimentally and any such effect was found to be less than 1 in 10,000.

* 'Roy Soc Proc., A, vol. 105, p. 60 (1924)

A difficulty arose with this method of measuring the field, for it was found that the current for balance had to be altered by about 1 in 2500 if the connections to the galvanometer were interchanged. This difference was found with several galvanometers and also with a fluxmeter, and it was not clear whether it indicated a possible source of error which would not be eliminated by taking the mean of the two currents for balance. It was, however, found possible to reproduce this effect under conditions in which the total quantity of electricity discharged through the galvanometer is necessarily zero. The effect showed itself as a slight lack of balance, but the direction of the final deflection of the galvanometer was unaltered on interchanging the galvanometer connections. This is the necessary condition that in the field measurements the effect should be eliminated by taking the mean of the two currents.

During an experiment the current in the electromagnet was kept constant to within 1 in 10,000. The magnetic field for the first half of the exposure was measured before placing the holder carrying the source, slit and plate in the box, and the field for the second half of the exposure, $\pm e$, with the field reversed, was measured at the end of this exposure after the holder had been removed. The time of exposure in each half was about 15 minutes. The field in the second half was generally less than in the first by about 1 in 250—a hysteresis effect since the current was allowed to fall considerably during the initial warming up of the coils of the electromagnet before beginning an experiment. The two magnetic fields were measured in each experiment. They ranged from 8200 to 8900 gauss and produced a double deflection of about 32 mm.

The widths of the pairs of lines for the two slits were 0.24 and 0.30 mm. The separations were measured from the density curves found with a microphotometer, and could be deduced either from the midpoint of the bases of the density curves found by producing the straight portions of the sides of the curves to cut the base line, or by measuring the distance between the peaks of the density curves. The two methods gave results agreeing to within 0.005 mm. The screw of the microphotometer was calibrated by photometering a glass scale divided into tenths of a millimetre made by the Cambridge Instrument Company and tested at the National Physical Laboratory. This tested glass scale was also used in the measurements of the distances from the source to the slits and slits to the plate. It may be noted that the increase in the deflection due to the finite length of the course is quite negligible—about 1 in 10^4 .

For the narrower slit, which was on the normal from the source to the plate, the semi-deflection d is given by

$$d^2 = \frac{1}{4p^2} (l_2^2 + d^2) [(l_1 + l_2)^2 + d^2],$$

ρ being the radius of curvature and l_1 and l_2 , the distances from source to slit and slit to plate respectively. In the calculation of $H\rho$, H may be taken as the mean of the two fields in an experiment and d as half the double deflection. The error introduced by doing this was shown by actual calculation to be quite negligible. For the wider slit the above formula is not sufficiently accurate. The exact formula for this case has been given in a previous paper* and shows that under the conditions of the experiment the double deflection for this slit should be greater than that for the other by 1 in 940, the difference found in the experiments was of this order. The double deflection for the wider slit was therefore decreased by this amount and the value of ρ deduced from the equation given above.

§ 3 *Results* — The values of $H\rho$ for four experiments are given in the following table. In the fourth experiment the source consisted of thorium B and C as well as radium B and C and only one slit was used. The results obtained for the α particles from thorium C and C' will be discussed later. In the other experiments the result for the slit in the normal position is given first.

Table I

Experiment	1	2	3	4	Mean
$H\rho$	$\begin{Bmatrix} 3.9953 \\ 3.9942 \end{Bmatrix}$	$\begin{Bmatrix} 3.9911 \\ 3.9910 \end{Bmatrix}$	$\begin{Bmatrix} 3.9928 \\ 3.9932 \end{Bmatrix}$	$\begin{Bmatrix} 3.9931 \\ - \end{Bmatrix}$	$3.993 \times 10^5 \text{ E.M.U. units}$

From the value for E/M , 4814.8, the velocity is found to be 1.923×10^9 cm per second. The probable error of the results for $H\rho$ and V is estimated to be less than 1 in 1000.

The value $H\rho = 3.993 \times 10^5$ is slightly higher than that found by Rutherford and Robinson, 3.983×10^5 , the difference being of the same order as the accuracy, 1 in 400, aimed at in their work. $H\rho$ was also measured by Marsden and Taylor† during their experiments on the decrease of velocity of α particles from radium C and found to be 4.00×10^5 with a probable error of 1 in 200, a value in good agreement with the present determination. The value found for the velocity in the present work is almost identical with Rutherford and Robinson's determination $V = 1.922 \times 10^9$ cm per second which was deduced from their result for $H\rho$ and the value of E/M found experimentally from the magnetic and electric deflections.

§ 4 *Experiments with Thorium C and C'* — One photograph was obtained using as a source a wire activated with the active deposits of both radium and thorium. This was prepared by depositing thorium B and C electrolytically

* *Loc. cit.*

† 'Roy. Soc. Proc.' A, vol. 88, p. 443 (1913)

on the platinum wire and then exposing the wire for about 15 minutes to radium emanation. A complete experiment involving double deflections and measurement of the magnetic fields was carried out as before. The three pairs of lines for the particles from radium C, thorium C and C' were not as well defined as those obtained previously for radium C alone and at the end of the experiment the source was found to be somewhat tarnished. When photometered it was evident that some of the particles had had their velocities reduced in varying amounts in escaping from the source, but the least deflected edges of the lines were found to be quite sharp. The deflections have therefore been taken as the separation of the inner edges found from the photometer curves plus the mean width of the lines found in experiments with radium C alone. This procedure seems to be justified since the value of $H\rho$ found in this way for the radium C line, which showed just as much broadening and asymmetry as those for thorium C and C', is in excellent agreement with the results found when using radium C alone.

In Table II are the results obtained for the velocities by comparing the values of ρ and taking $V = 1.923 \times 10^9$ for radium C and including the correction for the relativity change of mass with velocity. This correction reduces the ratio thorium C' to thorium C by less than 1 in 1000. The table also shows the velocity ratios and the values deduced from the relation $V^3 = kR$ using Henderson's* results 6.953, 4.778 and 8.616 cm for the ranges of the α particles from radium C, thorium C and thorium C'. The greatest difference between observed and calculated values is 0.6 per cent.

Table II

	Velocity	
	Observed	Calculated from the relation $V^3 = kR$
Thorium C	1.705×10^9 cm per second	1.697×10^9 cm per second
Thorium C'	2.053	2.065
	Velocity Ratios	
	Observed	Calculated
Thorium C'/Thorium C	1.204×10^9 cm per second	1.217×10^9 cm per second
Thorium C'/Radium C	1.068	1.074
Thorium C/Radium C	0.886	0.882

The value 0.886 found for the ratio of the velocities of the particles from thorium C and radium C may be compared with that deduced from the velocity curve for α particles from radium C previously found by the writer †. From this curve the velocity, in terms of that of radium C, corresponding to an α particle

* 'Phil Mag.', vol 42, p 549 (1921)

† *Loc cit*

of range 4.778 cm is 0.885 ± 0.001 . A Wood* found by a method essentially similar to that described here velocities of 2.060×10^8 and 1.714×10^8 cm per second for thorium C' and thorium C. The latter value is certainly too high since, as was shown by Wood, by applying Geiger's relation it indicates a range of 4.95 cm, whereas Henderson and Geiger have since found values less than 4.8 cm, such a difference cannot be accounted for by departures from the Geiger relation. For the ratio of the velocities of particles from thorium C and C', Rosenblum has recently found 1.209 †

§ 5 *The Velocities of α Particles from other Radio-active Substances*—Except in the few cases where direct measurements have been made the velocities of α particles from the various radio-active substances have been deduced from the Geiger relation. The writer has recently investigated the relation between velocity and distance traversed for α particles from radium C. In addition to the marked deviation from the Geiger relation at low velocities, which has been noted by other observers, there were departures from the law at higher velocities which, for example, amounted to 1 in 150 for an α particle of range 3 cm. The problem of deducing the velocity of an α particle of known range from this experimental curve is complicated by the phenomenon of straggling since the velocity and the distance traversed defining any point on this curve are mean values whereas the ranges as usually measured are somewhat greater than the mean range because of straggling. It is therefore necessary to estimate this difference.

In the writer's experiments with radium C the difference was found to be 0.6 mm. Theory and experiment indicate that this difference expressed as a fraction of the range will be approximately constant for α particles of all ranges. Taking Geiger's ‡ determination of the ranges, the mean ranges have thus been deduced and the velocities of the various α particles have been found from the velocity curve for radium C. These velocities are given in Table III together with the corresponding energies expressed in electron volts. These values for the energies have been calculated from the relativity formula taking as before 9649.4 E.M.U. for the value of the faraday. For comparison with the velocities deduced from the velocity curve the values found by the Geiger relation $V^2 = kR$, R being the measured range, are included in table. For uranium I and II the recent measurements by Laurence§ using the Wilson cloud method

* 'Phil. Mag.', vol 30 p 702 (1915)

† Rosenblum, 'C. R.', vol 180, p 1333 (1925)

‡ 'Z. f. Physik', vol 8, p 45 (1921)

§ 'Trans. Nova Scotia Ins. Sci.', vol 17, pt 1 p 103 (1927)

have been included. The value given for thorium C' is that found in the present experiments.

For α -rays from polonium I Curie* found by the magnetic deflection method a velocity of 1.593×10^9 cm per second, neglecting the relativity correction for the increase of mass of the α particle. If this correction is applied this result becomes 1.591×10^9 cm per second which is identical with the value found by the method described here.

Table III

Substance	Range in centimetres at 15° C	Velocity in centimetres per seconds		Energy in electron volts
		$10^3 \lambda/R$	From velocity curve for radium C	
Uranium I	2.67*	1.397×10^8	1.387×10^8	3.904×10^6
Uranium II	2.70†	1.402	1.392	4.023
	3.07*	1.463	1.459	4.420
	3.28†	1.496	1.493	4.629
Ionium	3.194	1.483	1.480	4.548
Radium	3.389	1.512	1.512	4.747
Radium Fm	4.122	1.614	1.619	5.445
Radium A	4.722	1.680	1.696	5.976
Radium C	6.971	1.923	1.923	7.088
Radium F	3.925	1.588	1.591	5.258
Protactinium	3.673	1.553	1.554	5.016
Radioactinium	4.676	1.684	1.689	5.927
Actinium X	4.369	1.646	1.651	5.663
Actinium Em	5.789	1.808	1.812	6.824
Actinium A	6.584	1.887	1.888	7.410
Actinium C	5.511	1.778	1.784	6.614
Thorium	2.90	1.436	1.438	4.234
Radiothorium	4.019	1.601	1.605	5.351
Thorium X	4.354	1.644	1.649	5.649
Thorium Em	5.063	1.729	1.734	6.248
Thorium	5.683	1.797	1.801	6.741
Thorium C	4.787	1.697	1.702	6.019
Thorium C'	8.617	2.064	2.053†	8.767†

* Geiger

† Observed

‡ Laurence

§ 6. Summary

The value of $H\rho = MV/E$ for an α particle from radium C has been redetermined and found to be 3.993×10^8 E.M.U. From the value of E/M for an α particle deduced from electro-chemical data and the above result the initial velocity of α particles from radium C is found to be 1.923×10^9 cm per second.

The probable error is estimated to be less than 1 in 1000. The values found by Rutherford and Robinson were $H\beta = 3.983 \times 10^5$ and $V = 1.922 \times 10^9$.

The initial velocities of α particles from thorium C and C' have been found to be 1.705×10^9 and 2.053×10^9 cm. per second. These results have been compared with those deduced from the relation $V^2 = kR$.

A table is also included giving the velocities for all the known substances emitting α particles. These results have been deduced from the writer's velocity curve for α particles from radium C and Geiger's measurements of the ranges.

The above experiments were carried out at the Cavendish Laboratory, Cambridge, and I should like to thank Prof. Sir Ernest Rutherford for his continued interest in the work. I wish also to thank Mr. H. J. J. Braddick, B.A., for his help, particularly in the exploration of the magnetic field, my wife for assistance during the course of the experiments and Mr. G. R. Crowe for the preparation of the radio active sources.

Commutative Ordinary Differential Operators

By J. L. BURCHNALL and T. W. CHAUNDY

(Communicated by A. L. DIXON, F.R.S.—Received December 22, 1926—Revised February 1, 1928.)

The paper is conveniently divided into two sections. The first contains the general argument and the main propositions unencumbered by proof; in the first paragraph of this section is collected material already published, the succeeding paragraphs of the section are devoted to new results. The second section of the paper includes proofs of these results together with certain corollaries not essential to the main argument.

PART I

I.—Preamble

We make certain notational conventions. There is a single independent variable x , the arbitrary dependent variable of a differential equation or operation is written y . With these exceptions Greek letters denote functions of x and English "lower-case" letters denote constants.

The distinctions extend to symbols of functional form, which will represent polynomials, unless the contrary is stated. Thus

$$f(t) \equiv a_0 t^n + a_1 t^{n-1} + \dots + a_n$$

in which the coefficients α_r are all constants, but

$$\phi(t) \equiv \alpha_0 t^n + \alpha_1 t^{n-1} + \dots + \alpha_n,$$

in which any coefficient α_r may involve x

Differentiations in x and in any other argument will be distinguished respectively by a prime and a suffix. Thus

$$\phi'(t) \equiv \alpha_0' t^n + \alpha_1' t^{n-1} + \dots + \alpha_n',$$

but

$$\phi_1(t) \equiv n\alpha_0 t^{n-1} + (n-1)\alpha_1 t^{n-2} + \dots + \alpha_{n-1}$$

English capitals will denote differential operators, and, in particular, D is the fundamental differential operator d/dx . The adjoint of an operator R is denoted by R' . We consider only *direct, finite* operators, i.e., operators expressible as $\phi(D)$, where the conventions regarding functional symbols are still to apply when their arguments are differential operators.

Now a pair of operators $\phi(D), \psi(D)$ is not in general commutative, but a pair $f(D), g(D)$, with constant coefficients, is commutative and more generally a pair $f(R), g(R)$, where R is itself any operator $\phi(D)$. But the class of commutative pairs, is not restricted to the class of pairs $f(R), g(R)$. This is shown by such an example as

$$\left. \begin{aligned} P &\equiv x^{-n} \delta(\delta - n)(\delta - 2n) & (\delta - mn + n) \\ Q &\equiv x^{-n} \delta(\delta - m)(\delta - 2m) & (\delta - mn + m) \end{aligned} \right\}, \quad (1)$$

where $\delta \equiv xD$. The pair PQ is commutative but not reducible to the form $f(R), g(R)$, if m, n are interprime.

We here consider the problem of determining the general pair of operators P, Q such that

$$PQ \equiv QP$$

We made an earlier attempt at this problem in a paper* presented to the London Mathematical Society in 1922. Our methods were then inadequate to resolve the general problem, but we were able to establish certain fundamental properties of commutative operators. These we reproduce in outline, as follows —

Two commutative differential operators P, Q of respective orders m, n satisfy an algebraic identity, with constant coefficients,

$$f(P, Q) = 0$$

of partial orders n, m in P, Q respectively (2)

* 'Proc. London Math. Soc.', vol. 21, p. 420 (1923)

We consider only the case in which m, n are interprime. Our theory is not yet complete for the case in which m, n have a common factor, if one of m, n is a factor of the other, the commutative pair is "reducible," i.e., expressible in terms of a commutative pair of diminished order.

By change of independent variable x and, if necessary, division by a constant, the operators can be reduced to the forms

$$\begin{aligned} P &\equiv D^m + \mu_1 D^{m-1} + \mu_2 D^{m-2} + \dots + \mu_m \\ Q &\equiv D^n + \nu_1 D^{n-1} + \nu_2 D^{n-2} + \dots + \nu_n \end{aligned}$$

The terms of highest order in $f(P, Q)$ are now $P^m - Q^n$ (3)

The identity $f(P, Q) = 0$ is a sufficient condition for the commutative identity $PQ - QP = 0$ (4)

If p, q are constants such that $f(p, q) = 0$, the equations $(P - p)y = 0$, $(Q - q)y = 0$ have a common solution $y = \eta(p, q, x)$, in general transcendental in its arguments (5)

It is convenient to speak of $\eta(p, q, x)$ as the "common root" of the operators $P - p, Q - q$

If in $f(p, q) = 0$ we fix p , we obtain m corresponding values q_r ($r = 1, 2, \dots, m$) of q . If η_r is the common root of $P - p, Q - q_r$, we call the set η_r ($r = 1, 2, \dots, m$) a "normal" set of roots of $P - p$. We similarly define a normal set of roots of $Q - q$.

A normal set of roots is a linearly independent set (6)

Since η is a common root of $P - p, Q - q$, we can write

$$P - p \equiv S R, \quad Q - q \equiv T R,$$

where R is the operator $D - \eta'/\eta$. The identities

$$P_1 - p \equiv R S, \quad Q_1 - q \equiv R T$$

define a new pair P_1, Q_1 , which are said to be obtained from P, Q by "transference."

The operators P_1, Q_1 obtained by transference are commutative and satisfy the same identity as P, Q (7)

Repeated transference applied to a commutative pair thus generates a (continuous) group of commutative pairs all satisfying the same identity

Finally we proved that if P, Q are commutative, then their adjoints P', Q' are likewise commutative and satisfy the same identity as P, Q (8)

So much of the theory we were able to establish in the first three sections of our earlier paper (*loc cit*) We now take up the discussion from that point

II—Integral Curves

In virtue of (2), (3) we evidently render our problem more precise in seeking, not the general commutative pair but the general pair satisfying a prescribed identity

$$f(P, Q) \equiv P^n - Q^m \mid \quad = 0 \quad (9)$$

The problem has evident analogies with that of uniformising the curve $f(p, q) = 0$ in the plane of co-ordinates (p, q) and we are not surprised to find that, in general, Abelian transcendents are involved in the solution

We are, in fact, uniformising by a somewhat unusual parameter D which is such that, even when the curve is not unicursal, the forms p, q are polynomial in D , although transcendental in the coefficients. There thus persists for the general curve a certain mimicry of the formulæ for a purely rational curve.

We have imposed a restriction on the form of $f(P, Q)$ and we must impose a similar restriction on the form of $f(p, q)$. For this purpose it is convenient to give a special meaning to "weight," by defining p, q as of weights m, n and so $p^a q^b$ as of weight $am + bn$. The terms of greatest weight in a polynomial we call the "leading terms" and their coefficients the "leading coefficients." We define the weight of a polynomial $\phi(p, q)$ as the weight of its leading term.

The class of curves $f(p, q) = 0$ which we shall consider will be those in which the leading terms in $f(p, q)$ are required to be exactly $p^n - q^m$ of weight mn . The unicursal curves of the class are the rational, *integral* curves

$$p = g(t) \quad q = h(t),$$

where $g(\), h(\)$ are polynomial forms, the corresponding operators being, of course, the reducible pair $g(D), h(D)$. In the general case with the same parametric equations, the functions $g(\), h(\)$ though no longer rational, are still integral. We therefore call such curves "integral" curves.

An integral curve of interprime orders m, n

$$0 = p^n - q^m +$$

has, for sufficiently large values of m, n , a complex singular point at infinity on one or other axis of co-ordinates (according as $m \gtrless n$). Taking this singular

point as of the essence of the definition, we define the g -number* of the curve as the maximum number of other double points. We find that

The g -number of an integral curve of interpriming orders m, n , is

$$g = \frac{1}{2}(m-1)(n-1) \quad (10)$$

Since the weight of a term $p^a q^b$ is $am + bn$, we are led to consider the elementary theory of "lattice-numbers" $am + bn$, where a, b are positive integers or zero. We prove that

Every number in the closed interval $\{(m-1)(n-1), mn-1\}$ can be expressed as a lattice number in one and only one way. Just half the numbers in the closed interval $\{1, (m-1)(n-1)\}$ are lattice numbers.

The number $2g-1 \equiv mn-m-n$ is non-lattice, the number $2g-2 \equiv mn-m-n-1$ is lattice. (11)

The g -number $\frac{1}{2}(m-1)(n-1)$ thus appears as the number of non-lattice numbers to bases (m, n) .

We next consider the intersections of a curve $\phi(p, q) = 0$ of weight w with the fundamental curve $f(p, q) = 0$ and we show that

A curve $\phi(p, q) = 0$ of weight w cuts the fundamental curve in exactly w finite points, provided that $\phi(p, q)$ has only one leading term †. (12)

It is understood, of course, that, in accordance with the convention already made, the coefficients of ϕ may involve the parameter x , but not the parameters p, q .

If the fundamental curve is unicursal, weight represents degree in the unicursal parameter and the truth of (12) is obvious.

By combining the results of (11) and (12) we see that

If $2g \leq w < mn$, then $\phi(p, q) = 0$ of weight w cuts the fundamental curve in just w finite points. (13)

If $2g \leq w < mn$ reference to (11) shows that there are $(w+1-g)$ numbers in the closed interval $(0, w)$ which are lattice and uniquely so. Since the weight

* If there are no other double points, the g number and the genus of the curve are the same. But in the presence of finite double points, the g number remains, while the genus is diminished. It therefore seems desirable to retain distinct titles for these two characteristic numbers.

† That this condition is necessary is seen by considering an example

$$\phi(p, q) \equiv \psi(p, q)f(p, q) + \chi(p, q),$$

where $\chi(p, q)$ is of weight less than w . The intersections of $\phi = 0$ with $f = 0$ are now the intersections of $\chi = 0$ with $f = 0$ which do not amount to w . Here $\phi(p, q)$ has at least two leading terms arising from the terms $p^m - q^n$ in $f(p, q)$.

of every term in $\phi(p, q)$ is a lattice number, the possible number of terms therein is $w + 1 - g$ and thus

If $2g \leq w < mn$, a single curve of weight w can be drawn to pass through $w - g$ arbitrary finite points of $f(p, q) = 0$ and it will cut the fundamental curve again in g other finite points (14)

After these arithmetical prolegomena we proceed to consider what conditions the vanishing of the identity $f(P, Q) = 0$ imposes on P, Q , showing subsequently that the P, Q so determined do actually satisfy the identity

III Necessary Conditions for a Commutative Pair

Suppose P, Q to be a pair of operators satisfying the identity $f(P, Q) = 0$ and take an arbitrary point (p, q) on the curve $f(p, q) = 0$

Then $f(P, q) = f(P, q) - f(P, Q)$, and so is algebraically divisible by $Q - q$. The quotient itself may be expanded in powers of D and divided by $P - p$. We may express the result of these operations analytically as

$$f(P, q) = T(P - p)(Q - q) + (\psi D^{m-1} + \psi_1 D^{m-2} + \dots + \psi_{m-1})(Q - q) \quad (15)$$

Dealing similarly with the adjoint operators P', Q' , which we have said satisfy the same identity, we have in conformity with (15)

$$f(P', q) = U(P' - p)(Q' - q) + (\phi D^{m-1} + \phi_1 D^{m-2} + \dots + \phi_{m-1})(Q' - q) \quad (16)$$

We prove that

If $\eta(p, q)$ is the common root of $P - p, Q - q$ and $\xi(p, q)$ the common root of $P' - p, Q' - q$, then $\xi\eta = \phi(p, q) = \psi(p, q)$, if the arbitrary constant multipliers of ξ, η be suitably chosen, (17)

and that

$\psi(p, q) = 0$ cuts the fundamental curve in $2g$ points of which, in general, one-half lie on $\psi_1(p, q) = 0$ and the other half on $\phi_1(p, q) = 0$ (18)

We call the g points common to ψ and ψ_1

$$(\alpha_s, \beta_s), \quad (s = 1, 2, \dots, g),$$

and the g points common to ψ and ϕ_1

$$(\gamma_s, \delta_s), \quad (s = 1, 2, \dots, g),$$

and we define g functions of x

$$\omega(\alpha_s, \beta_s), \quad (s = 1, 2, \dots, g),$$

by the linear equations

$$\left. \begin{aligned} \sum_{s=1}^g \alpha_s^a \beta_s^b \omega(\alpha_s, \beta_s) &= 0, \quad \text{if } am + bn < 2g - 2 \\ \sum_{s=1}^g \alpha_s^a \beta_s^b \omega(\alpha_s, \beta_s) &= -1, \quad \text{if } am + bn = 2g - 2 \end{aligned} \right\}, \quad (19)$$

where a, b are positive integers or zero

The number of these equations is the number of lattice numbers in the closed interval $(0, 2g - 2)$, which is also the number in the closed interval $(1, 2g)$, since $2g, 0$ are lattice, while $2g - 1$ is non-lattice. By (11) the equations are thus g in number and define the g functions $\omega(\alpha_s, \beta_s)$ precisely

We then show that with $\omega(\alpha_s, \beta_s)$ so defined,

The common root $\eta(p, q)$ is given by the formula

$$\frac{\eta'}{\eta} = -\rho - \sum_{s=1}^g \frac{f(p, \beta_s) \omega(\alpha_s, \beta_s)}{(p - \alpha_s)(q - \beta_s)}, \quad (20)$$

where ρ is independent of p, q but may involve x

From (20) we deduce precise expressions for $\omega(\alpha_s, \beta_s)$ in the form

$$\omega(\alpha_s, \beta_s) = \frac{-\alpha_s'}{f_s(\alpha_s, \beta_s)} = \frac{\beta_s'}{f_s(\alpha_s, \beta_s)} = \frac{-\psi'(\alpha_s, \beta_s)}{\frac{\partial(f, \psi)}{\partial(\alpha_s, \beta_s)}} \quad (21)$$

These expressions for $\omega(\alpha_s, \beta_s)$ show that the equations (19) define α_s, β_s as Abelian functions associated with the fundamental curve $f(p, q) = 0$

We write equations (19) more concisely as

$$\sum \alpha^a \beta^b \omega(\alpha, \beta) = 0, \quad -1 \quad (22)$$

The characteristic Abelian equations for the adjoint operators are

$$\sum \gamma^a \delta^b \omega(\gamma, \delta) = 0, \quad +1 \quad (23)$$

where

$$\omega(\gamma_s, \delta_s) = \frac{-\gamma_s'}{f_s(\gamma_s, \delta_s)} = \frac{\delta_s'}{f_s(\gamma_s, \delta_s)} = \frac{-\psi'(\gamma_s, \delta_s)}{\frac{\partial(f, \psi)}{\partial(\gamma_s, \delta_s)}} \quad (24)$$

Equations (23) are immediately deducible from (19) for the fundamental Abelian Theorem applied to the $2g$ intersections of $f = 0, \psi = 0$ gives

$$\sum \alpha^a \beta^b \omega(\alpha, \beta) + \sum \gamma^a \delta^b \omega(\gamma, \delta) = 0$$

The common root for the adjoint operator is given by the formula

$$\frac{\xi'}{\xi} = \sigma - \sum_{s=1}^g \frac{f(p, \delta_s) \omega(\gamma_s, \delta_s)}{(p - \gamma_s)(q - \delta_s)}, \quad (25)$$

where σ is independent of p, q but may involve x

Equations (20), (25) define ξ , η , save for factors $\exp\left(\int \rho \, dx\right)$, $\exp\left(\int \sigma \, dx\right)$,

as Abelian functions of the second kind associated with the fundamental curve $f(p, q) = 0$

Equations (19), (20), (21) do no more than exhibit, somewhat indirectly, conditions which operators P , Q must obey, if they are to be connected by the identity $f(P, Q) = 0$. We have still to show that there are such operators, and, if there are such, how they are to be determined from equations (19) (20) (21)

IV—Sufficiency of the Conditions

Suppose now that we are given an integral curve $f(p, q) = 0$, and that on it we can find a variable set of g points (α_s, β_s) whose co-ordinates depend on a parameter x and satisfy the g Abelian equations, written with the notation of (22) in the form

$$\sum \alpha_s^a \beta_s^b \omega(x, \beta) = 0, \quad -1 \quad (26)$$

where

$$\omega(\alpha_s, \beta_s) = \frac{-\alpha_s'}{f_q(\alpha_s, \beta_s)} = \frac{\beta_s'}{f_p(\alpha_s, \beta_s)} \quad (27)$$

By (14), through the g arbitrary points (α_s, β_s) on $f(p, q) = 0$ we can draw a curve $\psi(p, q) = 0$ of weight $2g$ which will cut the fundamental curve in g other points. This defines the function $\psi(p, q)$ save as to a possible factor involving x but not p, q . We make $\psi(p, q)$ precise by imposing a leading coefficient $+1$

We then show that

If $\theta_r(p, q)$ is a polynomial of weight $2g + r$ and leading coefficient $(-1)^r$ and if the curve $\theta_r(p, q) = 0$ passes through the g points (α_s, β_s) , then the relation

$$\theta_{r+1}(p, q) = \theta_r(p, q) \sum_{s=1}^g \frac{f(p, \beta_s) \omega(\alpha_s, \beta_s)}{(p - \alpha_s)(q - \beta_s)} + \theta_r'(p, q)$$

defines a polynomial $\theta_{r+1}(p, q)$ of weight $2g + r + 1$ and leading coefficient $(-1)^{r+1}$ such that the curve $\theta_{r+1}(p, q) = 0$ passes through the g points (α_s, β_s)

(28)

We write $\theta_0(p, q) \equiv \psi(p, q)$ and use the recurrence-formula to define the functions

$$\theta_1(p, q), \quad \theta_2(p, q), \quad \dots, \quad \theta_n(p, q)$$

We then show that

We can find $m + n$ functions of x only, viz., $\mu_1, \mu_2, \dots, \mu_m, \nu_1, \nu_2, \dots, \nu_n$ such that

$$\left. \begin{aligned} (-)^m \theta_m(p, q) + \sum_{r=1}^m (-)^{m-r} \mu_r \theta_{m-r}(p, q) &= p\psi(p, q), \\ (-)^n \theta_n(p, q) + \sum_{r=1}^n (-)^{n-r} \nu_r \theta_{n-r}(p, q) &= q\psi(p, q) \end{aligned} \right\} \quad (29)$$

Now define $\eta(p, q)$ by the relation

$$\frac{\eta'}{\eta} = - \sum_{s=1}^g \frac{f(p, \beta_s) \omega(\alpha_s, \beta_s)}{(p - \alpha_s)(q - \beta_s)} \quad (30)$$

The recurrence formula of (28) becomes

$$\theta_{r+1} = (D - \eta'/\eta) \theta_r,$$

and so

$$\theta_r = (D - \eta'/\eta)^r \psi = \epsilon_r D^r \eta^{-1} \psi \quad (31)$$

It follows at once from (29) that, if

$$\left. \begin{aligned} P' &\equiv (-D)^m + \mu_1 (-D)^{m-1} + \dots + \mu_m \\ Q' &\equiv (-D)^n + \nu_1 (-D)^{n-1} + \dots + \nu_n \end{aligned} \right\}, \quad (32)$$

then

$$(P' - p) \eta^{-1} \psi = (Q' - q) \eta^{-1} \psi = 0$$

Hence

$$(P'Q' - Q'P') \eta^{-1} \psi = (pq - qp) \eta^{-1} \psi = 0,$$

and

$$f(P', Q') \eta^{-1} \psi = f(p, q) \eta^{-1} \psi = 0$$

Since P', Q' are independent of p, q , variation of p, q gives arbitrarily many roots $\eta^{-1} \psi$ both of the alternant

$$P'Q' - Q'P'$$

and of the operator

$$f(P', Q')$$

Such roots being linearly distinct,* the alternant and the operator $f(P', Q')$ both vanish identically. The operators P', Q' are thus commutative and satisfy the prescribed identity. The same is therefore true of their adjoints P, Q .

Evidently P, Q might have been constructed independently on the basis of

$$\sum \gamma_s \delta_s^b \omega(\gamma_s, \delta_s) = 0, \quad +1,$$

the relations satisfied by the other intersections (γ_s, δ_s) of $\psi(p, q)$ with the fundamental curve

* Cf *loc cit*, p. 422

By either course we have proved that

The Abelian equations (26), (27) are sufficient for the definition of a pair of operators P , Q , commutative and satisfying the prescribed identity $f(P, Q) = 0$ (33)

V—Degrees of Freedom in Determination of P , Q

There are two standard transformations of a linear differential equation, namely, change of independent variable and multiplication of the dependent variable by a function of the independent variable. The commutative property and the form of the identity survive the latter transformation, since, if P , Q are commutative, so are $\tau^{-1}P\tau$, $\tau^{-1}Q\tau$, where τ is any function of x , and they satisfy the same identity. The presence of the arbitrary factor $\exp\left(\int \rho dx\right)$ in the formula (20) for $\eta(p, q)$ is thus explained.

If a change of independent variable $\zeta = \zeta(x)$ be effected, the transformed operators are still commutative, but their leading coefficients are no longer unity, being in fact

$$\{\sigma(\zeta)\}^{-n}, \quad \{\sigma(\zeta)\}^{-n},$$

where

$$\sigma(\zeta) \equiv \{\zeta'(x)\}^{-1}$$

At the same time the fundamental Abelian equations become

$$\sum \alpha^a \beta^b d\alpha/f_q(\alpha, \beta) = 0, \quad (am - bn < 2q - 2)$$

$$\sum \alpha^a \beta^b d\alpha/f_q(\alpha, \beta) = -\sigma(\zeta) d\zeta, \quad (am + bn + 2q = 2)$$

If then the leading coefficients are not prescribed, the commutative pair are sufficiently defined by the first $q - 1$ Abelian equations only. The last Abelian equation merely defines the particular independent variable, transformation to which ensures a leading coefficient unity.

Thus in constructing operators P , Q to satisfy the identity $f(P, Q) = 0$ we have two arbitrary functions of x at our disposal. They add little, however, to the interest of the problem and we can absorb them by prescribing that P , say, be brought to a standard form

$$D^n + \mu_2 D^{n-2} + \dots + \mu_n$$

with leading coefficient unity and second term missing

There still remain, however, g disposable constants introduced by the integration of the g linear differential equations (26) * Thus

The commutative pairs of prescribed form satisfying a prescribed identity $f(P, Q) = 0$ constitute a group $[P, Q]$ involving g arbitrary constants (34)

We anticipate the subject-matter of the next paragraph to say that transference by factors with *constant* leading coefficients does not alter the prescribed form, nor, of course, the identity The group is therefore closed for such transference and we prove that

Conversely all pairs of the group $[P, Q]$ may be obtained by transference from any one of them (35)

If P is of the prescribed form, its adjoint P' is of the form

$$(-D)^m + \mu_1(-D)^{m-1} + \dots + \mu_m,$$

which is restored to the prescribed form by changing the sign of x Thus the group $[P', Q']$ is obtained from the group $[P, Q]$ by change of sign of the independent variable We go further and show that

The constants of integration can be chosen to define a pair P, Q transforming exactly into their adjoints by change of sign of x (36)

VI --Transference

We conclude with an account of the general theory of transference

If (p_1, q_1) is a point of the fundamental curve, then $P - p_1, Q - q_1$ have a common root $\eta_1 \equiv \eta(p_1, q_1)$ and so a common end-factor,

$$T_1 \equiv D - \eta_1'/\eta_1$$

We can therefore write, as in (7),

$$P - p_1 \equiv RT_1, \quad Q - q_1 \equiv ST_1,$$

and obtain, by transference of T_1 , a new commutative pair P_1, Q_1 defined by

$$P_1 - p_1 \equiv T_1R, \quad Q_1 - q_1 \equiv T_1S,$$

and satisfying the prescribed identity We shall say that the transference has been effected "with respect to the point (p_1, q_1) " of the fundamental curve

The equations of this transference can be written more concisely as

$$T_1P = P_1T_1, \quad T_1Q = Q_1T_1 \quad (37)$$

* The last equation of the set still contributes its own arbitrary constant, since the standard form prescribed above defines not the new ζ but its derivative ζ'

We effect a transference on P_1, Q_1 themselves with respect to a second point (p_2, q_2) of the fundamental curve by the equations

$$T_2 P_1 = P_{12} T_2, \quad T_2 Q_1 = Q_{12} T_2 \quad (38)$$

Combining these with (37) we pass directly from P, Q to P_{12}, Q_{12} by the equations

$$T_2 T_1 P = P_{12} T_2 T_1, \quad T_2 T_1 Q = Q_{12} T_2 T_1 \quad (39)$$

Proceeding in this way we can contemplate the possibility of a transference "of order r " by aid of T , an operator of the r th order, in the equations*

$$TP = P, T, \quad TQ = Q, T \quad (40)$$

The properties of such a transference are given in the following theorems

A transference of order r can be split up into r successive linear transfereces with regard to points $(p_1, q_1), (p_2, q_2), \dots, (p_r, q_r)$ of the fundamental curve

(41)

The resultant of successive linear transfereces with respect to points $(p_1, q_1), \dots, (p_r, q_r)$ of the fundamental curve is independent of the order in which the points are taken and may be obtained by a single transference of order r in which the transference-operator is just that operator of order r which annihilates

$$\eta(p_1, q_1), \dots, \eta(p_r, q_r) \quad (42)$$

Transference with respect to the complete set of intersections of the fundamental curve with any curve $h(p, q) = 0$ restores the original operators and the transference operator is $h(P, Q)$

(43)

VII—Transference and the Abelian Theory

The relation of transference to the Abelian theory is intimate. The operators P_1, Q_1 obtained by transference with respect to the point (p_1, q_1) belong to the group $[P, Q]$, their g base-points satisfying the same Abelian equations as the base-points (α_i, β_i) of P, Q .

From the Abelian standpoint we view transference as a shift of base-points. The manner of this shift we prove to be as follows —

If a transference be effected with respect to r points $(p_1, q_1), \dots, (p_r, q_r)$, the transformed base-points (γ_m, δ_m) are co-residual with $(p_1, q_1), \dots, (p_r, q_r)$ and the original base-points (γ_s, δ_s)

(44)

* The leading coefficient of T should be unity in order that P_r may retain the prescribed form. The more general case of any leading coefficient merely involves the use of an additional transference of "zero order"

$$P_1 = r P r^{-1}, \quad Q_1 = r Q r^{-1}$$

Thus, viewed analytically, transference corresponds to addition of Abelian arguments. Hence also, if transference be effected with respect to a complete set of intersections of the fundamental curve with some curve $h(p, q) = 0$, the transformed base-points are co-residual with the original base-points, i.e., are coincident with them and so the original operators are restored. Thus the first part of (43) appears as a corollary of (44).

If transference be effected with respect to a double point (p_0, q_0) of the fundamental curve, this point, counting as two intersections of the fundamental curve with any curve through the point, appears as one of the transformed base-points $(\alpha_{0e}, \beta_{0e})$. At this point

$$\alpha_{0e}' = 0 = \beta_{0e}', \quad f_p(\alpha_{0e}, \beta_{0e}) = 0 = f_q(\alpha_{0e}, \beta_{0e}),$$

and $\omega(\alpha_{0e}, \beta_{0e})$ is indeterminate. Thus for operators obtained by transference with respect to a double point the Abelian theory no longer holds without modifications, other new features also appear. We hope in a subsequent paper to discuss the special case in which the fundamental curve $f(p, q) = 0$ defining the commutative operators has double points. Within the limits of the present paper we shall suppose that transference is always effected with respect to ordinary points of the curve.

PART 2

Proofs of the Theorems in Part I, §§ II-VII

We add proofs of the various theorems which we have asserted.

(10) The g -number of an integral curve of interprime orders m, n , is

$$g = \frac{1}{2}(m-1)(n-1)$$

The g -number is the number of double points of the rational integral curve of orders m, n ,

$$\begin{aligned} p(t) &\equiv t^m + a_1 t^{m-1} + \dots + a_m = 0 \\ q(t) &\equiv t^n + b_1 t^{n-1} + \dots + b_n = 0 \end{aligned}$$

The parameters s, t of a double point are given by

$$p(s) = p(t), \quad q(s) = q(t).$$

Removal of the irrelevant factor $s - t$ gives the equations

$$\begin{aligned} t^{m-1} + (s + a_1)t^{m-2} + \dots + (s^{m-1} + a_{m-1}) &= 0 \\ t^{n-1} + (s + b_1)t^{n-2} + \dots + (s^{n-1} + b_{n-1}) &= 0 \end{aligned}$$

The order in s of the t -eliminant is its weight in the coefficients, i.e., $(m-1)(n-1)$. Each double point accounts for two values of s . Hence the g -number is

$$g = \frac{1}{2}(m-1)(n-1)$$

- (11) Every number in the closed interval $\{(m-1)(n-1), mn-1\}$ can be expressed as a lattice number in one and only one way, just half the numbers in the closed interval $\{1, (m-1)(n-1)\}$ are lattice numbers. The number $2g-1 \equiv mn-m-n$ is non-lattice, the number $2g-2 \equiv mn-m-n-1$ is lattice.

Let a, b denote positive integers and x, y any integers. Then the equation

$$mx + ny = ma - nb$$

has the general solution

$$x = a \pm t, \quad y = -b \mp t,$$

where t is a positive integer or zero. The equation has therefore a solution in positive integers (x, y) , if, and only if, the closed interval $(a/n, b/m)$ contains an integer or zero. It is sufficient to suppose $a < n$. Then $ma - nb$ is non-lattice if, and only if, $0 < b < m$.

Every integer is expressible in one of the forms $\pm ma \pm nb$. Hence the only non-lattice numbers are $|ma - nb|$ where $0 < a < n$, $0 < b < m$. The number $|ma - nb|$ occurs again as $|m(n-a) - n(m-b)|$. There are thus just $\frac{1}{2}(m-1)(n-1)$ non-lattice numbers. The greatest of them is $|m(n-1) - n|$, i.e., $mn - m - n = 2g - 1$. They therefore all lie in the closed interval $\{1, (m-1)(n-1)\}$ and exactly half fill it.

If j is a non-lattice number $ma - nb$, then $mn - m - n - j$ is the lattice number $m(n-1-a) + n(b-1)$. Hence of every two numbers whose sum is $mn - m - n$, one is lattice, the other non-lattice. In particular, since 1 is non-lattice, the number

$$mn - m - n - 1 = 2g - 2$$

is lattice.

The equation

$$mx + ny = ma + nb$$

has the general solution

$$x = a \pm t, \quad y = b \mp t,$$

and hence the unique solution (a, b) in positive integers, if $a < n$, $b < m$. These two inequalities are certainly secured by the inequality $ma + nb < mn$.

- (12) A curve $\phi(p, q) = 0$ of weight w cuts the fundamental curve in exactly w finite points, provided that $\phi(p, q)$ has only one leading term.

The p -eliminant of $f(p, q) = 0$, $\phi(p, q) = 0$ is

$$\prod_{r=1}^n \phi(p_r, q)$$

where p_1, \dots, p_n are the roots in p of $p^n - q^n + \dots = 0$, and therefore

$$\prod_{r=1}^n p_r = (-1)^{n-1} q^n + \text{lower powers of } q$$

If $p^a q^b$ is the single leading term of ϕ , it contributes to the eliminant the term

$$\begin{aligned} \prod_{r=1}^n p_r^a q^b &= \pm q^{am+bn} + \text{lower powers of } q \\ &= \pm q^w + \text{lower powers} \end{aligned}$$

The first term on the right is the leading term of the eliminant which is therefore of degree w in q , and thus there are just w finite intersections

(17) If $\eta(p, q)$ is the common root of $P - p$, $Q - q$ and $\xi(p, q)$ the common root of $P' - p$, $Q' - q$, then

$$\xi\eta = \phi(p, q) = \psi(p, q),$$

if the arbitrary constant multipliers of ξ, η be suitably chosen.

It is sufficient to prove that $\eta^{-1}\psi$ is the common root of $P' - p$, $Q' - q$, for we may then take $\xi = \eta^{-1}\psi$

Now, if $\eta, \eta_1, \dots, \eta_m$ be a normal set of roots of $P - p$, then $Q - q$ annihilates η but none of the others, but $f(P, q)$ annihilates them all. Thus

$$f(P, q)/(Q - q)$$

annihilates all but η and

$$(D - \eta'/\eta) f(P, q)/(Q - q)$$

annihilates all of the normal set, and so contains $P - p$ as an end-factor. Hence from (15)

$$(D - \eta'/\eta) \{\psi D^{m-1} + \psi_1 D^{m-2} + \dots + \psi_{m-1}\} = \psi(P - p) \quad (45)$$

by consideration of dimensions. Taking adjoints we have

$$\{(-D)^{m-1}\psi + (-D)^{m-2}\psi_1 + \dots + \psi_{m-1}\}(-D - \eta'/\eta) = (P' - p)\psi.$$

The operator on the left annihilates η^{-1} and so $\eta^{-1}\psi$ is a root of $P' - p$.

To prove it also a root of $Q' - q$ we form in analogy with (15) the identity

$$f(p, Q) = V(P - p)(Q - q) + (\chi D^{n-1} + \chi_1 D^{n-2} + \dots + \chi_{n-1})(P - p)$$

interchanging the rôles of P, Q . By the foregoing argument $\eta^{-1}\chi$ is a root of $Q' - q$. Now

$$f(p, Q) + f(P, q) = f(p, Q) + f(P, q) - f(p, q) - f(P, Q),$$

and so it contains $(P - p)(Q - q)$ as an algebraic factor. Hence also

$$(\psi D^{m-1} + \psi_1 D^{m-2} + \dots + \psi_{m-1})(P - p) + (\chi D^{n-1} + \chi_1 D^{n-2} + \dots + \chi_{n-1})(Q - q)$$

contains $(P - p)(Q - q)$ as a factor. The dimensions do not permit this and so the expression vanishes identically. By comparing the coefficients of D^{m+n-1} we see that $\chi = -\psi$ and the theorem follows.

(18) $\psi(p, q) = 0$ cuts the fundamental curve in $2g$ points of which, in general, one-half lie on $\psi_1(p, q) = 0$ and the other half on $\phi_1(p, q) = 0$.

To determine the weight of $\psi(p, q)$ we suppose in (15) that weight in p, q and order in D are additive. Then the equation (15) is of greatest dimensions mn , and therefore ψ , having a co-factor of dimensions $m + n - 1$ is of weight $(m - 1)(n - 1) = 2g$ and hence by (12) cuts the fundamental curve in $2g$ points.

With the usual notation for P we write (45) as

$$(D - \eta'/\eta) \{ \psi D^{m-1} + \psi_1 D^{m-2} + \dots + \psi_{m-1} \} = \psi \{ D^m + \mu_1 D^{m-1} + \dots + \mu_m - p \}$$

By comparing coefficients of D^{m-1}, D^{m-2} we have

$$\left. \begin{aligned} \psi' + \psi_1 - (\eta'/\eta)\psi &= \mu_1\psi \\ \psi_1' + \psi_2 - (\eta'/\eta)\psi_1 &= \mu_2\psi \end{aligned} \right\} \quad (46)$$

Similarly by considering the adjoint we have

$$\psi' + \phi_1 - (\xi'/\xi)\psi = -\mu_1\psi$$

By use of (17) we deduce from these equations

$$\psi' + \psi_1 + \phi_1 = 0 \quad (47)$$

$$\psi(\mu_2\psi - \psi_2 - \psi_1' - \mu_1\psi_1) = \phi_1\psi_1. \quad (48)$$

The discussion presupposes that (p, q) is a point of the fundamental curve, otherwise $\eta(p, q)$ has no meaning. Hence by (48) the intersections of $\psi = 0$ with the fundamental curve lie on $\psi_1 = 0$ or on $\phi_1 = 0$.

By the symmetry existing between any adjoint pair it is clear that as many intersections will be on ϕ_1 as on ψ_1 . There is, however, the possibility that a point (α, β) might lie on both these curves. By (47) such a point lies also on $\psi' = 0$. Unless, then, this occurs only for isolated values of the variable, we have $f(\alpha, \beta) = 0 = \psi(\alpha, \beta)$ and so by differentiation

$$\begin{aligned} \alpha' f_\alpha(\alpha, \beta) + \beta' f_\beta(\alpha, \beta) &= 0 \\ \psi'(\alpha, \beta) + \alpha' \psi_\alpha(\alpha, \beta) + \beta' \psi_\beta(\alpha, \beta) &= 0. \end{aligned}$$

Hence, since also $\psi'(\alpha, \beta) = 0$, we must have $\alpha' = 0 = \beta'$, i.e., the point is fixed or else the Jacobian of f, ψ vanishes at every such (α, β) . The case is thus clearly exceptional, and, although we cannot yet discuss it completely to our satisfaction, we shall exclude it and so accept theorem (18)

$$(20) \quad \frac{\eta'}{\eta} = -\rho - \sum_{s=1}^g \frac{f(p, \beta_s) \omega(\alpha_s, \beta_s)}{(p - \alpha_s)(q - \beta_s)}$$

where ρ is independent of p, q but may involve x .

From (15), (45) we have

$$(D - \eta'/\eta) f(p, q) = \{(D - \eta'/\eta) T + \psi\} (P - p)(Q - q) \quad (49)$$

Choose (p_0, q_0) a new fixed point on the fundamental curve, giving the corresponding solution $\eta_0 \equiv \eta(p_0, q_0)$. Operating with (49) on η_0 we get

$$\frac{f(p_0, q)}{(p - p_0)(q - q_0)} (D - \frac{\eta'}{\eta}) \eta_0 = \left\{ (D - \frac{\eta'}{\eta}) T(p, q, D) + \psi \right\} \eta_0 \quad (50)$$

Now from (46), (47)

$$\psi \eta'/\eta = -\phi_1 - \mu_1 \psi$$

Hence $\psi \eta'/\eta$ is a polynomial in p, q which becomes $-\phi_1(\alpha_s, \beta_s)$ for the substitution $p, q = \alpha_s, \beta_s$. Now multiply (50) by $\psi(p, q)$ and make this substitution. This is legitimate, since in (50) no differential operator acts on any function of p, q except the operator $\psi(p, q)D$ which vanishes for the substitution. We therefore obtain

$$\frac{f(p_0, \beta_s)}{(\alpha_s - p_0)(\beta_s - q_0)} \phi_1(\alpha_s, \beta_s) \eta_0 = \phi_1(\alpha_s, \beta_s) T(\alpha_s, \beta_s, D) \eta_0$$

If we cancel the non-vanishing factor $\phi_1(\alpha_s, \beta_s)$, multiply by $\omega(\alpha_s, \beta_s)$, drop the suffix 0 and sum for s , we have

$$\eta \sum_{s=1}^g \frac{f(p, \beta_s) \omega(\alpha_s, \beta_s)}{(p - \alpha_s)(q - \beta_s)} = \sum_{s=1}^g \omega(\alpha_s, \beta_s) T(\alpha_s, \beta_s, D) \eta \quad (51)$$

The right-hand side can be expanded as the sum of terms of the form

$$\left\{ \sum_{s=1}^g \omega(\alpha_s, \beta_s) \alpha_s^m \beta_s^n \right\} D^r \eta$$

By (19) every such term vanishes unless $ma + nb \geq 2g - 2$. Now from (15) if weight in p, q and order in D are additive, then $T(p, q, D)$ is of greatest dimensions $m - m - n (= 2g - 1)$ and so on the right-hand side of (51) every term vanishes except D and the absolute term. In the co-factor of D the only surviving term is that of greatest weight $2g - 2$ in α_s, β_s .

To obtain the terms of greatest dimensions in (15) we replace $f(P, q)$ by $P^m - q^m$ and P, Q by D^m, D^n respectively. Then the leading terms of $T(p, q, D)$ form the quotient of $D^{mn} - q^m$ by $(D^m - p)(D^n - q)$, i.e., of

$$D^{(m-1)n} + qD^{(m-2)n} + \dots + q^{m-1} \text{ by } D^m - p.$$

Since m, n are interprime, no terms will cancel in the long division and so the quotient is of the form

$$\sum p^a q^b D^c$$

where every numerical coefficient is unity.

Hence (51) reduces to the form

$$\eta \sum_{s=1}^q \frac{f(p, \beta_s) \omega(\alpha_s, \beta_s)}{(p - \alpha_s)(q - \beta_s)} = -\eta' - \rho\eta,$$

where ρ is some function of x only. Thus (20) is established.

$$(21) \quad \omega(\alpha_s, \beta_s) = \frac{-\alpha_s'}{f_s(\alpha_s, \beta_s)} = \frac{\beta_s'}{f_p(\alpha_s, \beta_s)} = \frac{-\psi'(\alpha_s, \beta_s)}{\frac{\partial(f, \psi)}{\partial(\alpha_s, \beta_s)}}$$

If in (20) we multiply up by $\psi(p, q)$ and take the limit $p, q \rightarrow \alpha_s, \beta_s$, we get on the left, as we have already seen, $-\phi_1(\alpha_s, \beta_s)$ which, by (47), equals $\psi'(\alpha_s, \beta_s)$.

On the right we get

$$-\omega(\alpha_s, \beta_s) \lim_{p, q} \frac{f(p, \beta_s) \psi(p, q)}{(p - \alpha_s)(q - \beta_s)}$$

Since $f(p, q), f(\alpha_s, \beta_s), \psi(\alpha_s, \beta_s)$ are all zero we may write the limit as

$$\begin{aligned} \lim_{p, q} \frac{f(p, \beta_s) - f(\alpha_s, \beta_s)}{p - \alpha_s} \cdot \frac{\psi(p, q) - \psi(\alpha_s, \beta_s)}{q - \beta_s} \\ = \lim_{p, q} \frac{\psi(p, \beta_s) - \psi(\alpha_s, \beta_s)}{p - \alpha_s} \cdot \frac{f(p, q) - f(p, \beta_s)}{q - \beta_s} \end{aligned}$$

The subject of the limiting process is now a polynomial in p, q and we pass at once to the limit,

$$f_p(\alpha_s, \beta_s) \psi_s(\alpha_s, \beta_s) - \psi_s(\alpha_s, \beta_s) f_s(\alpha_s, \beta_s).$$

We thus have

$$\omega(\alpha_s, \beta_s) = -\psi'(\alpha_s, \beta_s) / \frac{\partial(f, \psi)}{\partial(\alpha_s, \beta_s)}$$

The other equations of (21) follow at once from

$$\alpha' f_s(\alpha, \beta) + \beta' f_s(\alpha, \beta) = 0$$

$$\psi'(\alpha, \beta) + \alpha' \psi_s(\alpha, \beta) + \beta' \psi_s(\alpha, \beta) = 0$$

which we obtain by differentiating $f(\alpha, \beta) = 0, \psi(\alpha, \beta) = 0$.

As a corollary to (20) we can prove that

If η_1, \dots, η_m is the set of normal roots of $P - p$, then

$$\prod_{r=1}^m \eta_r = \tau \prod_{s=1}^g (p - \alpha_s)$$

where τ involves x but not p

(52)

In (20) we fix p and sum for the m values of q given by the equation $f(p, q) = 0$. Then, since

$$\sum_q \frac{1}{\beta_s - q} = \frac{f_s(p, \beta_s)}{f'(p, \beta_s)},$$

we have

$$\sum_{r=1}^m \left(\frac{\eta'_r}{\eta_r} + \rho \right) = \sum_{s=1}^g \frac{f_s(p, \beta_s) \omega(\alpha_s, \beta_s)}{p - \alpha_s}$$

Now

$$\frac{f_s(p, \beta_s) - f_s(\alpha_s, \beta_s)}{p - \alpha_s}$$

is a polynomial in p, α_s, β_s of greatest weight $2g - 1$. Hence in

$$\sum_{s=1}^g \left\{ \frac{f_s(p, \beta_s) - f_s(\alpha_s, \beta_s)}{p - \alpha_s} \right\} \omega(\alpha_s, \beta_s)$$

no term involving p survives. It is thus a function of x only. So therefore is

$$\sum_{r=1}^m \frac{\eta'_r}{\eta_r} = \sum_{s=1}^g \frac{f_s(\alpha_s, \beta_s) \omega(\alpha_s, \beta_s)}{p - \alpha_s}$$

By (21) we can therefore write

$$\sum_{r=1}^m \frac{\eta'_r}{\eta_r} = \frac{\tau'}{\tau} = \sum_{s=1}^g \frac{\alpha'_s}{p - \alpha_s},$$

where τ involves x only. Our theorem follows by integration with respect to x .

More generally it is possible to prove that

If η_r is the common root of $P - p, Q - q$, corresponding to (p_r, q_r) , an intersection of a curve $h(p, q) = 0$ with the fundamental curve, then

$$\prod_r \eta_r = \tau \prod_{s=1}^g h(\alpha_s, \beta_s) \quad (53)$$

(28) If $\theta_r(p, q)$ is a polynomial of weight $2g + r$ and leading coefficient $(-1)^r$ and if the curve $\theta_r(p, q) = 0$ passes through the g points (α_s, β_s) , then the relation

$$\theta_{r+1}(p, q) = \theta_r(p, q) \sum_{s=1}^g \frac{f(p, \beta_s) \omega(\alpha_s, \beta_s)}{(p - \alpha_s)(q - \beta_s)} + \theta'_r(p, q)$$

defines a polynomial $\theta_{r+1}(p, q)$ of weight $2g + r + 1$ and leading coefficient $(-1)^{r+1}$ and the curve $\theta_{r+1}(p, q) = 0$ passes through the g points (α_s, β_s) .

Since $\theta_r(\alpha_n, \beta_n) = 0$, we may write, as in the proof of (21),

$$\frac{\theta_r(p, q) f(p, \beta_n)}{(p - \alpha_n)(q - \beta_n)} = \frac{\theta_r(p, q) - \theta_r(p, \beta_n)}{q - \beta_n} \frac{f(p, \beta_n) - f(\alpha_n, \beta_n)}{p - \alpha_n} \\ + \frac{\theta_r(p, \beta_n) - \theta_r(\alpha_n, \beta_n)}{p - \alpha_n} \frac{f(p, \beta_n) - f(p, q)}{q - \beta_n} \quad (54)$$

This is a polynomial of aggregate weight $4g + r - 1$ in p, q, α_n, β_n . If we multiply by $\omega(\alpha_n, \beta_n)$ and sum, then, in virtue of equations (26), the terms of weight in α_n, β_n less than $2g - 2$ disappear. Thus only terms of weight in p, q not exceeding $2g + r + 1$ survive. Since the weight of $\theta_r'(p, q)$ does not exceed $2g + r$, it follows that θ_{r+1} is of weight $2g + r + 1$.

If $(-)^r p^i q^j$ is the leading term in $\theta_r(p, q)$, the leading term in (54) is found in the expansion of

$$(-)^r \frac{p^i (q^j - \beta_n^j) (p^n - \alpha_n^n)}{(q - \beta_n)(p - \alpha_n)} + (-)^r \frac{(p^i - \alpha_n^i) \beta_n^j (q^n - \beta_n^n)}{(p - \alpha_n)(q - \beta_n)}$$

Every numerical coefficient is $(-1)^r$ and since $2g + r + 1$ has a single lattice representation $i'm + j'n$, the term of weight $2g + r + 1$ occurs but once, appearing in the first or second group according as $i' \geq$ or $<$.

This term appears in $\theta_{r+1}(p, q)$ multiplied by $\sum_i \alpha_n^i \beta_n^i \omega(\alpha_n, \beta_n)$, where $am + bn = 2g - 2$, and hence, in virtue of (26), the leading coefficient of $\theta_{r+1}(p, q)$ is $(-1)^{r+1}$.

Lastly

$$\theta_{r+1}(\alpha_n, \beta_n) = \theta_r'(\alpha_n, \beta_n) + \omega(\alpha_n, \beta_n) \lim_{p, q \rightarrow \alpha_n, \beta_n} \frac{f(p, \beta_n) \theta_r(p, q)}{(p - \alpha_n)(q - \beta_n)},$$

the limit being taken as $p, q \rightarrow \alpha_n, \beta_n$. But from (54) this limit is

$$\frac{\partial(f, \theta_r)}{\partial(\alpha_n, \beta_n)},$$

and as in the proof of (21)

$$\omega(\alpha_n, \beta_n) \frac{\partial(f, \theta_r)}{\partial(\alpha_n, \beta_n)} = -\theta_r'(\alpha_n, \beta_n)$$

Accordingly $\theta_{r+1}(p, q) = 0$ passes through the g points (α_n, β_n) .

(29) We can find $m + n$ functions of x only $\mu_1, \mu_2, \dots, \mu_m, \nu_1, \nu_2, \dots, \nu_n$ such that

$$(-)^m \theta_m(p, q) + \sum_{r=1}^m (-)^{m-r} \mu_r \theta_{m-r}(p, q) = p\psi(p, q),$$

$$(-)^n \theta_n(p, q) + \sum_{r=1}^n (-)^{n-r} \nu_r \theta_{n-r}(p, q) = q\psi(p, q)$$

It is sufficient to prove the theorem for the functions μ only. Now, since $p\psi(p, q)$ is of weight $2g + m$ and leading coefficient is $+1$,

$$p\psi(p, q) - (-)^m \theta_m(p, q)$$

is at most of weight $2g + m - 1$. Suppose that the coefficient of the term of this weight is μ_1 then

$$p\psi(p, q) - (-)^m \theta_m(p, q) - (-)^{m-1} \mu_1 \theta_{m-1}(p, q)$$

is at most of weight $2g + m - 2$

Proceeding in this way we can in succession define the functions of x

$$\mu_1, \mu_2, \dots, \mu_{m-1},$$

such that

$$p\psi(p, q) - (-)^m \theta_m(p, q) - \mu_1 (-)^{m-1} \theta_{m-1}(p, q) - \dots + \mu_{m-1} \theta_1(p, q)$$

is at most of weight $2g$

Equated to zero it represents a curve through the g points (α_s, β_s) , since ψ and every θ passes through them.

But by (14) a single curve of weight $2g$ can be drawn through g arbitrary points on the fundamental curve, and hence the curve is essentially $\psi = 0$.

Thus for some μ_m we have

$$(-)^m \theta_m(p, q) + \sum_{r=1}^{m-1} (-)^{m-r} \mu_r \theta_{m-r}(p, q) + \mu_m \psi(p, q) = p\psi(p, q)$$

The proof of (35) depends on the theory of transference and is given later at p. 581

(36) The constants of integration [in the Abelian equations] can be chosen to define a pair P, Q transforming exactly into their adjoints by change of sign of x .

Give x some numerical value and let the co-ordinates of the $2g$ points $(\alpha_s, \beta_s), (\gamma_s, \delta_s)$ thereupon assume the values $(a_s, b_s), (c_s, d_s)$. Then by Abel's theorem

$$\begin{aligned} \sum \int_{a_s, b_s}^{\infty} \alpha_s' \beta_s' d\alpha_s / f_s(\alpha_s, \beta_s) + \sum \int_{c_s, d_s}^{\infty} \gamma_s' \delta_s' d\gamma_s / f_s(\gamma_s, \delta_s) \\ = M_w + \sum \int_{a_s, b_s}^{\infty} \alpha_s' \beta_s' d\alpha_s / f_s(\alpha_s, \beta_s) + \sum \int_{c_s, d_s}^{\infty} \gamma_s' \delta_s' d\gamma_s / f_s(\gamma_s, \delta_s) \\ = M_w + k_w + k_w', \text{ say,} \end{aligned}$$

where $w = m + n \leq 2g - 2$ and M_w is a sum of periods

The Abelian equations (26) may be written in integrated form as

$$\begin{aligned}\sum_s \int_{\alpha_s}^{\beta_s} \alpha_s' \beta_s' d\alpha_s / f_g(\alpha_s, \beta_s) &= \frac{1}{2}M_w + k_w + h_w, \quad \text{if } w < 2g - 2, \\ &= \frac{1}{2}M_w + k_w + h_w + x, \quad \text{if } w = 2g - 2,\end{aligned}$$

and

$$\begin{aligned}\sum_s \int_{\gamma_s}^{\delta_s} \gamma_s' \delta_s' d\gamma_s / f_g(\gamma_s, \delta_s) &= \frac{1}{2}M_w + k_w' - h_w, \quad \text{if } w < 2g - 2, \\ &= \frac{1}{2}M_w + k_w' - h_w - x, \quad \text{if } w = 2g - 2,\end{aligned}$$

where the g constants h_w are the constants of integration and are still at our disposal.

If we write

$$h_w = \frac{1}{2}(k_w' - k_w),$$

the equations in γ, δ differ from those in α, β only in the sign of x . They therefore define a commutative pair with the property asserted, the pair is unique save for a sum of periods of the Abelian functions

- (41) Any transference of order r can be split up into r successive linear transfereces with regard to points $(p_1, q_1), (p_2, q_2), \dots, (p_r, q_r)$ of the fundamental curve

Let the equations of transference be

$$TP = P, T, \quad TQ = Q, T \quad (55)$$

Then, if ζ is any root of T , so also is $P\zeta$, and hence, if $\zeta_1, \zeta_2, \dots, \zeta_r$ is a linearly distinct set of roots of T , we get the r equations

$$P\zeta_s = a_{1s}\zeta_1 + a_{2s}\zeta_2 + \dots + a_{rs}\zeta_r, \quad (s = 1, 2, \dots, r),$$

where a_{ij} are some constants.

By the theory of "normal forms" we can find some

$$\zeta = c_1\zeta_1 + c_2\zeta_2 + \dots + c_r\zeta_r$$

which is a root not only of T but of $P - p$ for some p

More generally suppose that T and $P - p$ have just s linearly distinct common roots $\eta_1, \eta_2, \dots, \eta_s$. By (55), if η is any of them, then $Q\eta$ is also a root of T , by the commutative property of P, Q it is also a root of $P - p$. Thus $Q\eta$ is a common root of $P - p, T$, and so we have the system of s equations

$$Q\eta_s = b_{1s}\eta_1 + b_{2s}\eta_2 + \dots + b_{ss}\eta_s, \quad (s = 1, 2, \dots, s),$$

where b_{ij} are some constants

By a second appeal to the theory of normal forms we find some

$$\eta = d_1\eta_1 + d_2\eta_2 + \dots + d_r\eta_r,$$

which is a root of both T , $P - p$ and also, for some q , of $Q - q$. Hence T annihilates some $\eta(p, q)$ where (p, q) is a point of the fundamental curve.

Write $T_1 \equiv D - \eta'/\eta$, so that we have

$$P - p \equiv RT_1, \quad Q - q \equiv ST_1, \quad T = UT_1$$

If we write also

$$P_1 - p \equiv T_1R, \quad Q_1 - q \equiv T_1S,$$

we have from (55)

$$UP_1 = P_1U, \quad UQ_1 = Q_1U,$$

where now U is an operator of order $r - 1$, and T_1 is the operator of a linear transference in the point (p, q) . Dealing with U as we dealt with T , and so on, we at length break down T into the resultant of r successive linear transfereces of the type of T_1 .

(42) The resultant of successive linear transfereces with respect to points $(p_1, q_1), \dots, (p_r, q_r)$ of the fundamental curve is independent of the order in which the points are taken and may be obtained by a single transference of order r in which the transference-operator is just that operator of order r which annihilates

$$\eta(p_1, q_1), \dots, \eta(p_r, q_r)$$

Consider two points $(p_1, q_1), (p_2, q_2)$ and suppose that transference is first effected with respect to the point (p_1, q_1) . We may then write

$$\left. \begin{aligned} \eta_1 &= \eta(p_1, q_1), & T_1 &= D - \eta'_1/\eta_1 \\ T_1P &= P_1T_1, & T_1Q &= Q_1T_1 \end{aligned} \right\} \quad (56)$$

For the second transference we need η_{12} the common root of $P_1 - p_2$, $Q_1 - q_2$.

If $\eta_2 = \eta(p_2, q_2)$, we have by (56)

$$(P_1 - p_2)T_1\eta_2 = T_1(P - p_2)\eta_2 = 0,$$

and similarly

$$(Q_1 - q_2)T_1\eta_2 = 0$$

Hence

$$\eta_{12} = T_1\eta_2$$

The second transference is effected by means of the linear operator

$$T_2 \equiv D - \eta'_{12}/\eta_{12}$$

Then

$$T_2\eta_{12} = 0, \quad \text{e. g.,} \quad T_2T_1\eta_2 = 0$$

But

$$T_2T_1\eta_1 = 0, \quad \text{since} \quad T_1\eta_1 = 0$$

Thus η_1, η_2 are the roots of the operator $T_1 T_1$ which is thus symmetrical in $(p_1, q_1), (p_2, q_2)$

Now $T_2 T_1$ is the quadratic operator which effects the complete transference in respect of the pair of points $(p_1, q_1), (p_2, q_2)$. The order of the two points may therefore be interchanged in the composite transference, and so generally in a transference of any dimensions the points may be rearranged, by successive interchanges of neighbouring points, into any desired order.

It follows that any specified point (p_s, q_s) may be brought to the beginning of the series, and consequently T , the operator of the complete transference, exhibited with an end-factor $D - \eta_s'/\eta_s$. Hence T annihilates every

$$\eta(p_s, q_s), \quad (s = 1, 2, \dots, r)$$

- (43) Transference with respect to the complete set of intersections of the fundamental curve with any curve $h(p, q) = 0$ restores the original operators and the transference-operator is $h(P, Q)$

For $h(P, Q)$ is certainly a possible transference-operator, since

$$h(P, Q)P = Ph(P, Q), \quad h(P, Q)Q = Qh(P, Q)$$

It has therefore a complete set of roots of the form $\eta \equiv \eta(p_r, q_r)$, where (p_r, q_r) is a point of the fundamental curve.

Since $h(P, Q)\eta_r = h(p_r, q_r)\eta_r$, it follows that η_r is a root of $h(P, Q)$, if, and only if, (p_r, q_r) is an intersection of $h(p, q) = 0$ with the fundamental curve. Hence the roots of $h(P, Q)$ must correspond exactly to the complete intersection of $h(p, q) = 0$ and $f(p, q) = 0$. Since such a set of η 's is linearly distinct,* $h(P, Q)$ is the operator effecting transference in this complete set of intersections. As we have seen, such a transference restores the original operators.

We have incidentally proved that the order of the operator $h(P, Q)$ is the number of intersections of $h(p, q) = 0$ and the fundamental curve.

- (44) If a transference be effected with respect to r points $(p_1, q_1), \dots, (p_r, q_r)$, the transformed base-points (γ_r, δ_r) are co-residual with $(p_1, q_1), \dots, (p_r, q_r)$ and the original base-points (γ_s, δ_s) .

Consider first a transference with respect to the single point (p_1, q_1) . If $\eta_1 \equiv \eta(p_1, q_1)$, the equations of transference may be written

$$(D - \eta_1'/\eta_1)(P, Q) = (P_1, Q_1)(D - \eta_1'/\eta_1) \quad (57)$$

and the adjoint equations as

$$(P', Q')(D + \eta_1'/\eta_1) = (D + \eta_1'/\eta_1)(P', Q'). \quad (58)$$

* *Loc. cit.*, p. 423.

Write $\eta_{(1)}$ for the common root of $P_1 - p$, $Q_1 - q$ and $\xi_{(1)}$ for the common root of $P'_1 - p$, $Q'_1 - q$. Then from (57)

$$(D - \eta'_1/\eta_1)\eta = \eta_{(1)},$$

and from (58)

$$(D + \eta'_1/\eta_1)\xi_{(1)} = \xi,$$

where η is the common root of $P - p$, $Q - q$ and ξ that of $P' - p$, $Q' - q$.

Hence

$$\xi_1\eta_1\xi\eta_{(1)} = \xi_1\eta_1\xi\eta' - \xi_1\eta'_1\xi\eta, \quad (59)$$

$$\xi_1\eta_1\xi\eta_{(1)} = \xi_1\eta_1\xi_{(1)}'\eta_{(1)} + \xi_1\eta'_1\xi_{(1)}\eta_{(1)} \quad (60)$$

Now by (31) $\xi'\eta$ is a polynomial $\theta_1(p, q)$ of weight $2g + 1$ and passing through the g base-points (α_s, β_s) . Similarly $\xi\eta'$ is a polynomial of like weight passing through the adjoint base-points (γ_s, δ_s) . Moreover $\xi\eta$ is ψ which is of weight $2g$ and passes through (α_s, β_s) , (γ_s, δ_s) .

Thus from (59) we see that $\xi_1\eta_1\xi\eta_{(1)}$ is a polynomial of weight $2g + 1$ passing through the g points (γ_s, δ_s) . Similarly (60) shows that $\xi_1\eta_1\xi\eta_{(1)}$ passes through the g transformed base-points $(\alpha_{1s}, \beta_{1s})$.

We have now accounted for all but one of the intersections of $\xi_1\eta_1\xi\eta_{(1)}$ with the fundamental curve. But evidently from (59) the remaining intersection is (p_1, q_1) itself. Hence

$$(p_1, q_1), (\alpha_{1s}, \beta_{1s}), (\gamma_s, \delta_s), \quad (s = 1, \dots, g)$$

are residual. But

$$(\alpha_{1s}, \beta_{1s}), (\gamma_{1s}, \delta_{1s}), \quad (s = 1, \dots, g)$$

are also residual.

Thus $(\gamma_{1s}, \delta_{1s})$ are co-residual with (p_1, q_1) , (γ_s, δ_s) .

If a new transference is effected with regard to another (p_1, q_1) , then the new base-points $(\gamma_{12s}, \delta_{12s})$ are co-residual with $(\gamma_{1s}, \delta_{1s})$, (p_1, q_1) and so with (γ_s, δ_s) , (p_1, q_1) , (p_2, q_2) and so for further transfereces. The theorem is thus proved.

We conclude with the postponed proof of (35).

(35) All pairs of the group $[P, Q]$ may be obtained by transference from any one of them.

Let (P, Q) , (P_0, Q_0) be two commutative pairs of the group and let (γ_s, δ_s) , $(\gamma_{0s}, \delta_{0s})$ for $s = 1, \dots, g$, be their respective base-points. By (28) the $g + 1$ curves $\psi(p, q) = 0$, $\theta_1(p, q) = 0$, $\theta_s(p, q) = 0$ all pass through the g points (α_s, β_s) . We can therefore assign $g + 1$ functions of x

$$\rho, \rho_1, \dots, \rho_g$$

such that the curve

$$\rho\psi(p, q) + \sum_1^g \rho_s \theta_s(p, q) = 0 \quad (61)$$

passes also through the g points $(\gamma_{0s}, \delta_{0s})$. Its weight is that of the polynomial $\theta_g(p, q)$ which is $3g$. It therefore cuts the fundamental curve in g other points in addition to $(\alpha_s, \beta_s), (\gamma_{0s}, \delta_{0s})$. Call these g points (σ_s, τ_s) , for $s = 1, \dots, g$.

By Abel's theorem applied to the intersections of (61) with the fundamental curve we then have

$$0 = \sum \gamma_{0s}^a \delta_{0s}^b \omega(\gamma_{0s}, \delta_{0s}) + \sum \alpha_s^a \beta_s^b \omega(\alpha_s, \beta_s) + \sum \sigma_s^a \tau_s^b \omega(\sigma_s, \tau_s)$$

But by the fundamental theory

$$\sum \gamma_{0s}^a \delta_{0s}^b \omega(\gamma_{0s}, \delta_{0s}) = 0, +1,$$

$$\sum \alpha_s^a \beta_s^b \omega(\alpha_s, \beta_s) = 0, -1$$

Hence

$$\sum \sigma_s^a \tau_s^b \omega(\sigma_s, \tau_s) = 0$$

These equations are g in number and linear in the g expressions $\omega(\sigma_s, \tau_s)$. Hence, unless the determinant of the equations vanishes, every $\omega(\sigma_s, \tau_s)$ must vanish, that is to say every $d\sigma_s, d\tau_s = 0$.

These g intersections of (61) with the fundamental curve are thus fixed points, they are evidently the points (p_s, q_s) with regard to which the transformation we seek is effected.

We can exhibit the transference-operator itself without difficulty. For substituting in (61) from (31) we have

$$\left\{ \rho + \sum_1^g \rho_s D^s \right\} \xi = 0,$$

where

$$\xi = \xi(p_s, q_s).$$

Hence the operator

$$T' \equiv \rho + \sum_1^g \rho_s D^s$$

has the g roots $\xi(p_s, q_s)$. It therefore transforms the adjoints by the formulae

$$T'(P', Q') = (P'_0, Q'_0) T',$$

and hence its adjoint transforms P, Q, P_0, Q_0 by the formulae

$$(P, Q) T = T(P_0, Q_0)$$

We can similarly define the operator U which reverses this transference by the formulae

$$U(P, Q) = (P_0, Q_0) U.$$

[*Postscript added February 8, 1928*—By the kindness of Prof. Baker we have been enabled to see his note following before finally sending our paper to press.

We desire to say, firstly, that we very much appreciate the interest he has taken in our communication, and, secondly, that we do not wish it to appear that we regard our results as in any way at variance with Prof Baker's argument

We have considered the problem primarily as an enquiry in the theory of differential equations and in the algebra of plane curves, and we have passed on to the Abelian functions only so far as they have been inevitable

In the crucial matter of multiple points we are anxious to make our position clear. Much of the theory (and in particular the earlier theory) remains valid whether or not the fundamental curve has multiple points. For this reason we were reluctant to exclude them in express terms.

On the other hand we recognise that certain of the later results—as for instance, the Abelian equations and theorems on transference—no longer hold without qualification if multiple points are present. In actual fact we have accumulated certain material illustrative of this, which we hope will shortly be available for publication. This material, which has come from consideration of the simplest uncursal identity $P^n = Q^m$ will, we hope, throw light on the modification of the theory due to multiple points.

In the meantime we prefer to remain non-committal, neither necessarily excluding all multiple points nor definitely asserting what results are unaffected by their presence.]

Note on the foregoing paper, "Commutative Ordinary Differential Operators," by J. L. BURCHNALL and J. W. CHAUNDY

By Prof H F BAKER, F R S

(Received January 17, 1928)

The argument of this paper may be regarded as centred round the ascertainment of two linear differential equations, those denoted by

$$(P' - p) \eta^{-1} \psi = 0, \quad (Q' - q) \eta^{-1} \psi = 0,$$

these are, in fact, differential equations satisfied by a quotient of theta functions of several arguments when all of these arguments except one are taken constant, and the theory of the paper is in close connection with the classical method for approaching the definition of the theta function from the algebraical side. It would seem to be important to justify this assertion in precise terms, so as to make clear the general bearings of the results arrived at by the authors. The elementary algebraic method which they follow has in my opinion great interest, especially as it enables them to deal in part with the theory even when the curve has unknown multiple points, but one is not satisfied until the functions involved are defined by their behaviour and not by their algebraical form. I hope, therefore, that the writers will allow me to make the following remarks, and that I may be pardoned for explicit references to my own volume, 'Abel's Theorem,' 1897. This was written before the appearance of Weierstrass' lectures ('Werke,' vol. 4, 1902, 600 quarto pages), and is very imperfect, but it is briefer in one respect than Weierstrass' theory, by the use of the fundamental integral functions (Kronecker, Dedekind and Weber, Hensel). What there is of novelty in the following remarks relates mainly to these. The general ideas are expounded also in Clebsch and Gordan's 'Abelsche Functionen' (1866)—to which, as to Weierstrass' volumes, explicit references are given below. I consider in the first place a curve of which the multiple points are known and allowed for, but exemplify in examples how the theory can be applied when this is not so, the existence of a new multiple point being regarded as a particular case.

§ 1 We consider a general plane algebraic curve, whose equation is expressed (in Weierstrass' manner, 'Werke,' vol. 2, 1895, p. 235 ff) in terms of two functions which have poles only at one place. These two functions we shall denote by x, y (not by p, q , as in the paper before us), of respective orders α

and r , prime to one another, the equation may thus be supposed to contain two terms y^a and $-x^r$, but no terms of higher order (as rational functions) than ar , the order of y^a or x^r (cf 'Abel's Theorem,' pp 34, 93, 99) Thus a, r replace m and n respectively of the author's paper The genus of the curve can be shown to be

$$p = \frac{1}{2}(a-1)(r-1) - \delta,$$

or $g - \delta$, in the notation of the paper, δ being the equivalent number, in double points and cusps, of the multiple points of the curve which exist for finite values of x and y There exist rational functions infinite only at ∞ , that is at the single place for which $x = \infty, y = \infty$, of every order, *except p orders*, the greatest possible of these failing orders is $2p - 1$ Further, there exist $(a-1)$ integral rational functions, that is rational functions infinite only at ∞ , say, g_1, \dots, g_{a-1} , such that every integral function is expressible in the form

$$(x, 1)^k + (x, 1)^{k_1} g_1 + \dots + (x, 1)^{k_{a-1}} g_{a-1},$$

where $(x, 1)^i$ denotes a polynomial in x of degree i (see 'Abel's Theorem,' chap IV) If $\sigma_i + 1$ be the lowest power of x such that

$$g_i/x^{\sigma_i+1}$$

is not infinite for $x = \infty$, then $\sigma_i + 1$ is called the dimension of g_i , in other words, if r be the order of the function g_i , as a rational function, each of the integers

$$r_i - a, \quad r_i - 2a, \quad \dots, \quad r_i - \sigma_i a$$

is positive, but $r_i - (\sigma_i + 1)a$ is negative In fact, these positive numbers, taken for $i = 1, 2, \dots, (a-1)$, are the orders of non-existing integral rational functions, and we have

$$\sigma_1 + \sigma_2 + \dots + \sigma_{a-1} = p$$

The functions g_1, \dots, g_{a-1} are to be chosen so that, in the expression of an integral rational function in terms of these, there arises no term $x^k g_i$, whose order, $ka + r_i$, is greater than the order of the function

From the functions g_1, \dots, g_{a-1} can be computed other rational (not integral) functions, of which the number is a , say,

$$\gamma_0, \gamma_1, \dots, \gamma_{a-1}$$

having, for our present purpose two main properties In the first place the p everywhere finite integrals associated with the curve are given by

$$\int [(x, 1)^{\sigma_1-1} \gamma_1 + \dots + (x, 1)^{\sigma_{a-1}-1} \gamma_{a-1}] dx,$$

wherein the p coefficients in the polynomials $(x, 1)^p$ are arbitrary. In the second place, if $\gamma_i(x)$ denote the value of γ_i at a place (x) of the curve, and $g_i(\xi)$ denote the value of g_i at a place (ξ) of the curve, and if we put

$$(x, \xi) = \frac{\gamma_0(x) + \gamma_1(x)g_1(\xi) + \dots + \gamma_{n-1}(x)g_{n-1}(\xi)}{x - \xi}$$

then the integral, in (x) ,

$$\int_{(k)}^{(x)} (x, \xi) dx$$

has only two infinities, both logarithmic, at (ξ) , and at $x = \infty, y = \infty$. This integral will be denoted by

$$P_{\xi, \infty}^{x, k}$$

(k) being an arbitrary place on the curve, for which the integral vanishes.

It is important also to consider the rational function of (x) given by

$$(\alpha, x),$$

where (α, β) , or (α) denotes any definite finite place of the curve. This function has a pole of the first order when (x) is at (α) , being infinite there if (α) be not a branch place, like $-(x - \alpha)^{-1}$, and is otherwise infinite only when (x) is at the infinite place. If, for the neighbourhood of this latter place, we use a parameter t such that

$$x = t^{-a}, \quad y = t^{-r}p,$$

where p is a non-vanishing power series in t , the function (α, x) is expressible in this neighbourhood in the form

$$t^{-k_1} \mu_1 \omega_1(\alpha) + \dots + t^{-k_p} \mu_p \omega_p(\alpha),$$

where k_1, \dots, k_p are the orders of non-existing integral rational functions, μ_1, \dots, μ_p are non-vanishing power series in t not depending on (α) , and $\omega_1(\alpha), \dots, \omega_p(\alpha)$ are differential coefficients of linearly independent everywhere finite integrals, for the place (α) . For the sake of definiteness in a subsequent statement, we suppose $\omega_1(\alpha), \dots, \omega_p(\alpha)$ multiplied by such absolute constants that the constant terms in the power series μ_1, \dots, μ_p are all $+1$.

Among the non-existent orders k_1, \dots, k_p unity is certainly found, unless the curve be rational. Suppose for definiteness that $k_1 = 1$. By the known theory of inversion it is possible to determine p places of the curve, say $(\alpha_1, \beta_1), \dots, (\alpha_p, \beta_p)$, which will be briefly denoted by $(\alpha_1), \dots, (\alpha_p)$, such that the p equations

$$\omega_1(\alpha_1) d\alpha_1 + \dots + \omega_i(\alpha_p) d\alpha_p = du_i \quad (i = 1, \dots, p)$$

are satisfied, for arbitrary values, of general character, of the arguments u_1, \dots, u_p . Then, if

$$T = P_{x, \infty}^{\alpha_1, k_1} + \dots + P_{x, \infty}^{\alpha_p, k_p},$$

$(k_1), \dots, (k_p)$ denoting arbitrary fixed places, the function e^T depends on the place (x) of the curve, and on the values u_1, \dots, u_p through $(\alpha_1), \dots, (\alpha_p)$. As a function of (x) , the function e^T vanishes to the first order at each of the places $(\alpha_1), \dots, (\alpha_p)$, and becomes infinite to the first order at each of $(k_1), \dots, (k_p)$, it has essential singularity when (x) is at (∞) , but it is a single valued function of (x) . For such a function as e^T reference may be made to Clebsch and Gordan, 'Abelsche Functionen' (1866), p. 139, to Weierstrass, 'Werke,' vol. 4, p. 469 (and, for the hyperelliptic case, 'Werke,' vol. 1, p. 299, of date 1856), for the explicit representation as a quotient of theta functions of u_1, \dots, u_p , cf. 'Abel's Theorem,' pp. 275, 289.

§ 2 In the application of the foregoing to be made here, it is supposed that each of the arguments u_1, \dots, u_p is taken constant, or zero, then the function e^T depends on the place (x) , and on the argument u_1 .

There exists an integral rational function of (x) of order $2p$, with p zeros at the places $(\alpha_1), \dots, (\alpha_p)$, which is definite save for a multiplier independent of (x) . We suppose it chosen so that the term of highest order of infinity at (∞) is exactly t^{-2p} . This function of (x) , by the condition of vanishing at $(\alpha_1), \dots, (\alpha_p)$, will have coefficients which are functions of u_1 . We denote this function by ψ .

Now consider the function Y , given by

$$Y = \psi e^{-1},$$

from this define functions $\mathfrak{z}_1, \mathfrak{z}_2, \dots$, in turn, by means of the equations

$$\mathfrak{z}_1 e^{-T} = \frac{\partial}{\partial u_1} (\psi e^{-T}), \quad \mathfrak{z}_2 e^{-T} = \frac{\partial}{\partial u_1} (\mathfrak{z}_1 e^{-T}), \quad \dots,$$

so that in general

$$\mathfrak{z}_m e^{-1} = \left(\frac{\partial}{\partial u_1} \right)^m (\psi e^{-1}),$$

we can prove that \mathfrak{z}_m is an integral rational function of (x) , of order $2p + m$, vanishing at $(\alpha_1), \dots, (\alpha_p)$, with the term of highest infinity at ∞ equal to $(-1)^m t^{-2p-m}$, the coefficients in this function are functions of u_1 .

Consider \mathfrak{z}_1 , it is given by

$$\mathfrak{z}_1 = -\psi \left[(\alpha_1, x) \frac{\partial \alpha_1}{\partial u_1} + \dots + (\alpha_p, x) \frac{\partial \alpha_p}{\partial u_1} \right] + \frac{\partial \psi}{\partial u_1},$$

in the neighbourhood of the place (∞) the integral rational function of (x) which multiplies ψ , on the right here, is equal to

$$t^{-k_1} \mu_1 \sum_{i=1}^p \omega_1(\alpha_i) \frac{\partial \alpha_i}{\partial u_1} + \dots + t^{-k_p} \mu_p \sum_{i=1}^p \omega_p(\alpha_i) \frac{\partial \alpha_i}{\partial u_1},$$

which reduces, however, by the definition of $(\alpha_1), \dots, (\alpha_p)$ to

$$t^{-k_1} \mu_1,$$

with $k_1 = 1$, the integral function $\partial\psi/\partial u_1$, by definition of ψ , is of order less than $2p$. Thus \mathfrak{S} is an integral function of order $2p + 1$, the term of highest infinity at (∞) being, by the definition of μ_1 , exactly $-t^{-(2p+1)}$. Further, since ψe^{-T} does not (vanish or) become infinite at $(\alpha_1), \dots, (\alpha_p)$, the product $\mathfrak{S}_1 e^{-T}$ does not become infinite at any of these, thus \mathfrak{S}_1 vanishes at these places. A precisely similar argument is applicable to the equation

$$\mathfrak{S}_2 e^{-T} = \frac{\partial}{\partial u_1} (\mathfrak{S}_1 e^{-T}),$$

and so on, indefinitely, and the statement above made for \mathfrak{S}_m is thus justified.

Next consider the integral rational function $x\psi$, of order $a + 2p$. By what has been said, the difference

$$x\psi - (-1)^a \mathfrak{S}_a$$

is an integral rational function of (x) , of order $2p + a - 1$. Hence by proper choice of a factor σ_{a-1} , independent of (x) , but dependent on u_1 , the function

$$x\psi - (-1)^a \mathfrak{S}_a - \sigma_{a-1} \mathfrak{S}_{a-1}$$

is an integral rational function of (x) of order $2p + a - 2$, and so on. Finally there is an integral rational function of (x) ,

$$x\psi - (-1)^a \mathfrak{S}_a - \sigma_{a-1} \mathfrak{S}_{a-1} - \dots - \sigma_1 \mathfrak{S}_1$$

of order $2p$, where $\sigma_{a-1}, \dots, \sigma_1$ depend on u_1 only. As all the functions $\psi, \mathfrak{S}_a, \dots, \mathfrak{S}_1$ vanish in $(\alpha_1), \dots, (\alpha_p)$ this must be the same as $\sigma\psi$, where σ depends on u_1 only. We have thus shown that

$$\left[(-1)^a \left(\frac{\partial}{\partial u_1} \right)^a + \sigma_{a-1} \left(\frac{\partial}{\partial u_1} \right)^{a-1} + \dots + \sigma_1 \frac{\partial}{\partial u_1} + \sigma - x \right] (\psi e^{-T}) = 0$$

Similarly the function ψe^{-T} satisfies a linear differential equation

$$[Q' - y] (\psi e^{-T}) = 0,$$

of order r . The exact correspondence of the general point of view here followed with that in the paper referred to is thus sufficiently established.

If $(\gamma_1), \dots, (\gamma_p)$ be the zeros of the rational function of (x) , ψ , other than $(\alpha_1), \dots, (\alpha_p)$, and, for definiteness, we denote the positions of $(\alpha_1), \dots, (\alpha_p), (\gamma_1), \dots, (\gamma_p)$ when $u_1 = 0$ by $(a_1), \dots, (a_p), (c_1), \dots, (c_p)$, we have, by Abel's Theorem

$$P_{x,\infty}^{a_1} + \dots + P_{x,\infty}^{a_p} + P_{x,\infty}^{c_1} + \dots + P_{x,\infty}^{c_p} = \log \frac{\psi(x, u_1)}{\psi(x, 0)} \bigg/ \frac{\psi(\infty, u_1)}{\psi(\infty, 0)}$$

where, the term of highest infinity in ψ at (∞) being t^{-2p} , independent of u_1 , we have $\psi(\infty, u_1)/\psi(\infty, 0) = 1$. Thus, adopting in the definition of T , for $(k_1), \dots, (k_p)$, the places $(a_1), \dots, (a_p)$, we have

$$\psi e^{-T} = \psi(x, 0) e^U,$$

where

$$U = P_{\infty, \infty}^{y_1} + \dots + P_x^{y_r}.$$

Thus the result arrived at is that the function e^U satisfies the linear differential equation above found for ψe^{-T} . By Abel's Theorem this function U is the same function of $-u_1$ as is T of u_1 . But we do not pursue this.

§ 3 Particularly to illustrate § 1 in detail, it may be worth while to add one example. Take an ordinary general plane quartic curve. First take homogeneous co-ordinates (x, Y, z) , so that the point (x) , or $(1, 0, 0)$, is an inflexion of the curve, with $z = 0$ as inflexional tangent, so that the point (Y) , or $(0, 1, 0)$ is the point where this inflexional tangent meets the curve again, with $x = 0$ as the tangent to the curve at this point, and a proper line through (x) for $Y = 0$. The equation of the curve then becomes

$$xY^3 + cY^2z^2 + Yz(x, z)_2 - z(x, z)_3 = 0,$$

where c is a constant, $(x, z)_i$ means a homogeneous polynomial of degree i , and we can suppose the coefficient of x^3 in $(x, z)_3$ to be 1. Now put $y = xY$, and $z = 1$. Then we obtain the Weierstrass form

$$f(x, y) \equiv y^3 + cy^2 + yxu_2 - x^2u_1 = 0,$$

where $u_2 = (x, 1)_2$, $u_3 = (x, 1)_3$. For this the numbers a, r are respectively 3 and 5. To describe the character of this curve, we may supply a power of z to render the equation homogeneous of order 5 in x, y, z . Then the curve has a double point at $(0, 0, 1)$, with general tangents, has a higher cuspidal point at $(0, 1, 0)$, such that $x = 0$ meets the curve in two points there, while $z = 0$ meets the curve in five points there. The curve thus meets $x = 0$ also where $y + \alpha z = 0$, and meets $y = 0$, beside at the double point, at the three points given by $u_3 = 0$. If, more explicitly, the equation be

$$y^3 + cy^2 + yx(mx^2 + hx + n) - x^3(x^3 + \lambda x^2 + \mu x + \nu) = 0,$$

we have, for the expression in the neighbourhood of (∞) ,

$$x = t^{-3}, \quad y = t^{-5} (1 - \frac{1}{3}mt + \dots)$$

The two fundamental integral rational functions may be taken to be

$$g_1 = y, \quad g_2 = y(y + c)/x,$$

of respective orders 5 and 7, and since, at (∞) ,

$$x^{-2}g_1 = t + \quad, \quad x^{-3}g_2 = t^2 + \quad,$$

we have

$$\sigma_1 + 1 = 2, \quad \sigma_2 + 1 = 3,$$

and the genus 3, which is $\sigma_1 + \sigma_2$, is one less than $\frac{1}{2}(n-1)(r-1)$

The functions $\gamma_0, \gamma_1, \gamma_2$ are found to be given by

$$\gamma_0 = \frac{y^2 + cy + \frac{1}{2}x^2}{f'(y)}, \quad \gamma_1 = \frac{y}{f'(y)}, \quad \gamma_2 = \frac{x}{f'(y)},$$

where $f'(y) = \partial f(x, y)/\partial y$. The everywhere finite integrals are thence given by

$$\int [Ay + (Bx + C)x] dx/f'(y),$$

where A, B, C are arbitrary

The function $P_{x,\infty}^{\alpha}$ is given by

$$P_{x,\infty}^{\alpha} = \int_{(t)}^{(\infty)} \frac{\beta^2 + (\beta + \alpha(x-1))_2 + \beta y + \alpha y(y+c)x^{-1}}{(\alpha-x)f'(\beta)} d\alpha,$$

and writing this as $\int_{(t)}^{(\infty)} (\alpha, x) dx$, we have

$$(\alpha, x) = \frac{\gamma_0(\alpha) + \gamma_1(\alpha)g_1(x) + \gamma_2(\alpha)g_2(x)}{\alpha - x},$$

which can be written in the form

$$\frac{\gamma_0 + \gamma_1 g_1 \frac{(\alpha/x) + \gamma_2 g_2 \frac{(\alpha/x)^2}{x}}{\alpha - x}}{x} = [\gamma_1 g_1 x^{-1} + \gamma_2 g_2 (x^{-1} + \alpha x^{-3})],$$

in which γ_i means $\gamma_i(\alpha)$, and g_i means $g_i(x)$. The former of these two parts is finite when (x) is at (∞) , the latter part, if we write $x = t^{-2}$, and

$$g_1 = y = t^{-6}(1 - \frac{1}{3}mt + \quad), \quad g_2 = \frac{y(y+c)}{x} = t^{-7}(1 - \frac{1}{3}mt + Pt^2 + Qt^3 + \quad),$$

gives

$$- \frac{\beta}{f'(\beta)} t^{-2}(1 - \frac{1}{3}mt + \quad) - \frac{\alpha(1 + \alpha t^2)}{f'(\beta)} t^{-4}[1 - \frac{1}{3}mt + Pt^2 + Qt^3 + \quad],$$

or say

$$t^{-2}\mu_0 \frac{-\beta}{f'(\beta)} + t^{-4}\mu_1 \frac{-\alpha}{f'(\beta)} + t^{-1}\mu_2 \frac{-\alpha^2}{f'(\beta)},$$

where μ_0, μ_1, μ_2 are power series in t , each with 1 as constant term, and the indices 2, 4, 1 of t^{-2}, t^{-4}, t^{-1} are the orders of the non-existing integral rational functions. These indices are equal to $r_1 - \sigma_1\alpha, r_2 - \alpha, r_2 - \sigma_2\alpha$, where $r_1 = 5, r_2 = 7$ are the orders of g_1 and g_2 respectively

The equations for defining the places $(\alpha_1), (\alpha_2), (\alpha_3)$ in terms of u_1 are therefore

$$\sum_{i=1}^3 \int_{(a)}^{(\infty)} \beta d\alpha/f'(\beta) = 0, \quad \sum_{i=1}^3 \int_{(a)}^{(\infty)} \alpha d\alpha/f'(\beta) = 0, \quad \sum_{i=1}^3 \int_{(a)}^{(\infty)} \alpha^2 d\alpha/f'(\beta) = -u_1,$$

and these show that, when (x) is in the neighbourhood of the place (∞) ,

$$(\alpha_1, x) \frac{\partial \alpha_1}{\partial u_1} + (\alpha_2, x) \frac{\partial \alpha_2}{\partial u_1} + (\alpha_3, x) \frac{\partial \alpha_3}{\partial u_1} = t^{-1} + \text{power series in } t$$

The function ψ , of order 6, is of the form

$$x^2 + Mx + N + Hy,$$

where M, N, H are functions of u_1 , determined by the fact that ψ vanishes at $(\alpha_1), (\alpha_2), (\alpha_3)$. The function \mathfrak{S}_1 , of order 7 as an integral rational function of (x) , defined by

$$\mathfrak{S}_1 t = \frac{1}{t-1} x^6 + \frac{\partial}{\partial u_1} \left(\psi t - \frac{1}{2} x^2 \alpha^2 \right),$$

is given by

$$\begin{aligned} \mathfrak{S}_1 &= \frac{\partial \psi}{\partial u_1} - \psi \sum_{i=1}^3 (\alpha_i, x) \frac{\partial \alpha_i}{\partial u_1} \\ &= \frac{\partial \psi}{\partial u_1} - \psi \sum_{i=1}^3 \frac{\beta_i^2 + c\beta_i + \alpha_i(\alpha_i, 1)_2 + \beta_i y + \alpha_i y(y+c)/x}{(\alpha_i - x)f'(\beta)} \frac{\partial \alpha_i}{\partial u_1}, \end{aligned}$$

this is necessarily expressible in the form

$$Lx^2 + Fx + G + Ky - y(y+c)/x,$$

where L, F, G, K are functions of u_1 , but the fact that the function vanishes in $(\alpha_1), (\alpha_2), (\alpha_3)$ does not suffice to determine these coefficients. And the process may be continued to determine $\mathfrak{S}_2, \mathfrak{S}_3$.

§ 4 The function used in the authors' paper for the expression of η'/η , namely, $f(x, \beta)/(x - \alpha)(y - \beta)$, is found on computation, for the example considered in § 3, to lead to

$$\begin{aligned} \frac{f(x, \beta)}{(x - \alpha)(y - \beta)f'(\beta)} \frac{d\alpha}{d\beta} &= (\alpha, x) d\alpha - (mx + h) \frac{\alpha d\alpha}{f'(\beta)} \\ &\quad - m \frac{\alpha^2 d\alpha}{f'(\beta)} - \left[\frac{y(y+c)}{x} + mx^2 + hx + n \right] \frac{d\alpha}{f'(\beta)}, \end{aligned}$$

and the summation of the values of the function on the left for different places (α, β) does not lead to the sum of the values of $(x, x) d\alpha$ at these places unless the sum of the values of $d\alpha/f'(\beta)$ vanishes. The authors, in this case, for which $g = 4$, employ four places $(\alpha_1), (\alpha_2), (\alpha_3), (\alpha_4)$, and four equations of inversion, instead of three, though the integral, $\int d\alpha/f'(\beta)$, used in one of these equations,

has logarithmic infinities at the double point. Such extended equations of inversion are considered in Clebsch and Gordan, 'Abelsche Functionen,' chap XI. Moreover, the function ψ which they employ is of the eighth order. In general, it follows from the authors' paper that an integral rational function of order $2g, = 2p + 2\delta$, is identified, save for a multiplying constant, by its order and by $p + \delta$ of its zeros, if only the terms in the expression of the most general function of this description which are not of integral form in x and y , be omitted: this is in accordance with the Riemann-Roch Theorem, which gives $\delta + 1$ constants in such a function, if we assume that δ of these multiply terms which are not polynomial in x and y (cf. Clebsch and Gordan, *loc cit*, p. 272). On the other hand, in the theory as stated here in § 2, the function ψ , of order $2p$, is not necessarily of polynomial form, this may be shown by taking a particular example. For $p = 4$, there is an equation ('Abel's Theorem,' p. 97)

$$y^3 - \beta_2 y^2 + \alpha_2 \gamma_2 y - \alpha_2^2 \alpha_3 = 0,$$

wherein $\alpha_i, \beta_i, \gamma_i$ are polynomials in x of the degrees indicated by the suffixes, for which all integral functions are expressible in the form

$$(x, 1)^A + (x, 1)^{A_1} y + (x, 1)^{A_2} y^2,$$

in which η , given by

$$\eta = (y^3 - \beta_2 y + \alpha_2 \gamma_2) / \alpha_2,$$

is of order 8. The general integral function of order 8 is thus

$$Ax^8 + Bx + C + Dy + E\eta,$$

and is identified, save for a multiplying constant, by four zeros. But its expression involves η , which is not expressible integrally by x and y .

§ 5. But while it is possible, as in the authors' paper, to deal with a curve of genus $p, = g - \delta$, with a polynomial function ψ , of order $2p + 2\delta$, and an inversion theorem determining $p + \delta$ places $(\alpha_1), (\alpha_2), \dots, (\alpha_p)$, the coefficients in the differential equations obtained will be Abelian-functions belonging to the genus p . For example if we deal with the equation

$$y^2 = (x + 1)^2 x$$

in the authors' manner, with $g = 1$, taking, for $x = t^2, \alpha = \theta^2$, the function $\psi = t^2 - \theta^2$, we shall obtain

$$e^{-\int \frac{\alpha_0}{x} dx} = \frac{e^{t(\tan^{-1} \theta - \tan^{-1} \theta_0)}}{(t - \theta)/(t - \theta_0)},$$

and the differential equation of the second order will be

$$\left[(\theta^2 + 1) \frac{d^2 Z}{d\theta^2} + 2\theta \frac{dZ}{d\theta} - 2 - \frac{t^2}{\theta^2 + 1} \right] Z = 0,$$

where

$$Z = (t + \theta)^{t \tan^{-1} \theta},$$

Or, to take a more crucial example, we may deal with the equation

$$y^2 = x^2(x^2 + mx + n),$$

in the manner suggested above, taking $\psi = \varphi v - \varphi \lambda$, and are then led to the differential equation

$$\frac{\partial^2 Z}{\partial \lambda^2} - [2\varphi \lambda + \varphi v] Z = 0,$$

satisfied by

$$Z = \frac{\sigma(\lambda + v)}{\sigma \lambda} e^{-\lambda \zeta v},$$

as in the authors' paper, 'Proc Lon Math Soc,' vol 21, p 434 (1923). But if we deal with it as in the authors' present paper, the generalised inversion equations require us to consider two arguments λ_1, λ_2 subject to $\lambda_1 + \lambda_2 = u_1$ and

$$(\varphi \lambda_1)^{-1} d\lambda_1 + (\varphi \lambda_2)^{-1} d\lambda_2 = 0,$$

of which the latter leads to,

$$\frac{\sigma(\lambda_1 - \gamma) \sigma(\lambda_2 - \gamma)}{\sigma(\lambda_1 + \gamma) \sigma(\lambda_2 + \gamma)} e^{2u_1 \zeta(\gamma)} = \text{const},$$

where $\varphi \gamma = 0$, and then with $\psi = (\varphi v - \varphi \lambda_1)(\varphi v - \varphi \lambda_2)$ we find, effectively,

$$e^{-\tau} = \frac{\sigma \lambda_1 \sigma \lambda_2}{\sigma(\lambda_1 - v) \sigma(\lambda_2 - v)} e^{-u_1 \zeta v},$$

and the function \mathfrak{S}_1 is given by

$$\mathfrak{S}_1 = A - BP + \frac{1}{2}PP',$$

where $P = \varphi v$, $P' = \varphi' v$, and, with $L_1 = \varphi \lambda_1$, $L_1' = \varphi' \lambda_1$, $L_2 = \varphi \lambda_2$, $L_2' = \varphi' \lambda_2$, we have

$$A = \frac{1}{2} L_1 L_2 \frac{L_1' - L_2'}{L_1 - L_2},$$

$$B = \frac{1}{2} \left(\frac{L_1' - L_2'}{L_1 - L_2} L_2 + L_1' \right),$$

while \mathfrak{S}_2 , which I have formed, is a still less manageable function, but is an aggregate of elliptic functions. The differential equation will thus have elliptic functions in its coefficients (Cf also Hermite's volume, 'Sur quelques applications des Fonctions Elliptiques,' 1885, pp 99, 100, etc.)

The Thermal Conductivities of Oxygen and Nitrogen

By HAMAR GREGORY, Ph D, A R C Sc, D I C, Assistant Prof of Physics, and
SYBIL MARSHALL, M Sc, A R C Sc, D I C

(Communicated by H L Callendar, F R S—Received November 18, 1927)

Introduction

The interest in the determination of the thermal conductivities of oxygen and nitrogen lies partly in their relation to the thermal conductivity of air. The latter is the medium which practically every experimenter on gaseous thermal conduction has investigated, and has therefore become the standard substance in this field of research. Being a mixture chiefly of the gases oxygen and nitrogen, with the latter in the greater proportion, the value of its conductivity should lie between those of oxygen and nitrogen and should be nearer that of nitrogen than that of oxygen. The authors, in common with Weber and Todd, have verified this experimentally, the only observer finding these conductivities in a contrary order being Winkelman, who used a cooling thermometer method. The following is a table of the results hitherto obtained for the absolute thermal conductivities at 0° C of oxygen and nitrogen, together with their authors' results for air. The values marked with an asterisk have been deduced by applying the temperature coefficient, 0.0029 per ° C, to results which were obtained at temperatures above 0° C.

Thermal Conductivity at 0° C in Cal cm⁻¹ sec⁻¹ deg⁻¹

Author	Method	Oxygen	Nitrogen	Air
Stefan (1)	Cooling thermometer	0.0000576*	—	—
Winkelman (2)	"	0.0000551*	0.0000512*	0.0000568
Gunther (3)	"	0.0000569	0.0000569	—
Todd (4)	Plates	0.0000512*	0.0000491	0.0000571
Weber (5)	Hot wire and potentiometer	0.0000577	0.0000596	0.0000568
Gregory and Marshall (6)	Hot wire and bridge	0.0000589	0.0000589	—
Gregory and Archer (7)	"	—	—	0.0000583

(1) 'Wien Ber.', vol 72 (2), p 60 (1875)

(2) 'Pogg Ann.', vol 156, p 407 (1875), 'Wied Ann.', vol 44, pp 177, 429 (1891)

(3) 'Diss Halle a S.' (1906)

(4) 'Roy Soc Proc.', A, vol 83, p 19 (1909)

(5) 'Ann d Physik', vol 54, p 437 (1917)

(6) 'Roy Soc Proc.', A, vol 114, p 354 (1927)

(7) 'Roy Soc Proc.', A, vol 110, p 91 (1926)

Weber has recently published a new result for the thermal conductivity of air, 0.0000574,* which is about 1 per cent higher than his old value. Assuming that, if his results for oxygen and nitrogen were revised, they would be increased in the same proportion, his new values for these gases would be—oxygen 0.0000583, and nitrogen 0.0000572.

A comparative determination was made of the thermal conductivities of oxygen and nitrogen by Eucken † who assumed, as a standard, the value 0.0000566 for the thermal conductivity of air. His results gave oxygen, air and nitrogen in the same order as has been obtained at the Imperial College, but were much lower on account of the value used as a standard.

In deducing the values of the thermal conductivities at 0° C. of oxygen and nitrogen, the authors have plotted the thermal conductivities at five different temperatures, lying between 13° C. and 0° C., against the temperature, the intercept of the straight line drawn through these points with the conductivity axis giving the absolute thermal conductivity at 0° C. These values were not corrected for the discontinuity of temperature at the boundaries of the gas, which is usually calculated from theoretical considerations based on Knudsen's definition of the 'accommodation coefficient' ‡. Such a correction applied to oxygen and nitrogen was found by the authors to be about one sixth of 1 per cent of the absolute conductivity, which is beyond the experimental accuracy in the present research. This correction was also omitted because the authors prefer, in a purely experimental investigation, to apply only such corrections as can be directly determined experimentally, and, as Dr Gregory is at present engaged on an experimental investigation of the conduction of heat through rarefied gases, the correction is omitted in the present paper pending the results of Dr Gregory's research.

In the following experiments, as in those previously carried out in this laboratory, § two systems of main and compensator tubes, in gaseous connection with one another, were used. As each system was made from tubing of a different diameter, a check on the supposed point at which convection vanished, before the mean free path effect set in, was available. When investigating gases for which convection is great, the use of this system is absolutely necessary, and even for oxygen and nitrogen, gases in which the convection losses are negligible over a considerable range of pressures before the conductivity diminishes

* 'Ann d Physik,' vol 82, p 479 (1927)

† 'Phys Z,' vol 12, p 1101 (1911), and vol 14, p 324 (1913)

‡ 'Ann d Physik,' vol 34, p 593 (1911)

§ Gregory and Marshall, Gregory and Archer, *loc cit*

appreciably with pressure, it is advantageous, since each set of tubes gives an independent result for the thermal conductivity at any given temperature. These results should be identical if the apparatus were perfect. In the authors' experiments a maximum discrepancy of a half of 1 per cent was found between the results obtained by the two sets of tubes, and the mean of these was taken to be the absolute thermal conductivity of the gas at the given temperature.

Apparatus

In the following investigations the authors used the apparatus that was employed for their determination of the thermal conductivity of carbon dioxide. This consisted of two main tubes of different diameters and their compensators, along the axes of which were stretched lengths of fine platinum wire which had originally been cut from the same piece. The main and compensator wires were connected, each in series with a standard 1 ohm coil, to the terminals of a Callendar-Griffith's bridge, a separate bridge being used for each system of tubes. Each standard resistance in series with a main wire had its terminals connected to a potentiometer circuit, so that the current flowing in this arm of the bridge could be deduced. The battery circuit of each bridge contained several rheostats arranged so that, once the bridge was set to correspond to a definite temperature, a balance could be obtained by altering the resistance in the battery circuit, and thus the temperature of the wires could be kept constant.

Owing to a defect that developed in one of the Callendar-Griffiths bridges, subsequently to the completion of the determination of the conductivity of CO_2 , this instrument had to be overhauled, and at the same time the connections and contacts in the circuits were renewed. It was found that the introduction of oxygen into the tubes altered the composition of the soldered junctions between the fine platinum wires and the thick platinum leading wires, which resulted in a change in the temperature coefficients of resistance of the systems. This change, however, was final and not progressive as was shown by the fact that, after the initial alteration had taken place, the ice points and fundamental intervals of the systems did not change appreciably during a period of six months, whatever the nature of the gas contained within the tubes. On account of the above changes the bridges were recalibrated and the steam and ice points redetermined for both sets of tubes.

Experimental Procedure

In order to set the bridges so that the temperatures of the wires in the wide and narrow tubes were equal, and also to determine the temperature corresponding to any given bridge setting, the ice points and fundamental intervals of both systems were obtained. Instead of, as before, using a very small indefinite current in the battery circuit, a new procedure was adopted. Three different values of current were used in the determination of each fixed point, and these were larger than the current that would be used had only one value been employed. The advantage of using larger currents lies in the fact that the galvanometer is rendered more sensitive. The determination of the fundamental intervals of this apparatus thus becomes in itself a problem in thermal transmission through the gas, since, for these slightly larger currents, there is bound to be a certain amount of heat generated in the wire.

Now

$$C^2R/l = 2\pi K\theta/\log_e r_2/r_1 + \psi + \phi$$

where ψ is the heat lost by radiation, and ϕ is the heat lost by convection.

The key to the other symbols is given on pp. 598-9.

For small values of θ , the temperature of the wire above that of the tube wall, the heat lost by radiation and convection is negligible.

Therefore

$$C^2R = B\theta$$

where B = a constant, and

$$R = x + C - M$$

where

x = bridge setting corresponding to a temperature difference θ ,

C = resistance of coils unplugged,

M = reading corresponding to the mid-point.

Now

$$\theta = (R - R_0)/R_0\alpha$$

where

R_0 = resistance of the equivalent length of wire at 0°C

α = temperature coefficient of resistance of the wire.

Therefore

$$C^2R = B(x + C - M - R_0)/R_0\alpha = A + Dx,$$

where A and D are constants, i.e., the heat lost by the wire is proportional to the bridge setting.

Therefore, if the heat loss from the wire be plotted against the balance point of the bridge, one should obtain a straight line whose intercept with the balance point axis, corresponding to zero heating effect, gives the true balance point.

The following are two specimen graphs showing how the true ice and steam points were obtained

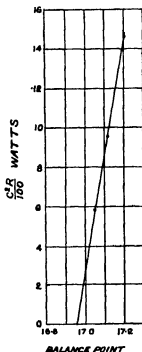


FIG 1 —In Ice = 16.90

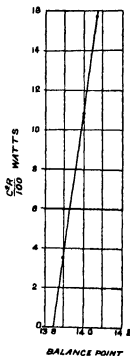


FIG 2 —In Steam = 13.85

True Balance Point for Wide Tube System

The bridges were then set so that the wires in the wide and narrow tubes were at the same temperature, and the ice-cold water in the thermostat surrounding the tubes was started circulating

The gas to be investigated was then admitted into the tubes, which has been previously evacuated and filled with the pure gas several times, and the pressure was lowered in steps, the bridge being rebalanced for each different pressure by altering the current in the battery circuit, and the current flowing through each main wire being measured by means of the potentiometer. Several different settings of the bridges, corresponding to different temperatures of the wire, were used

Key to the Symbols used in the Tabulation of the Results

- P = pressure of gas within the tubes in centimetres mercury
 θ = temperature of wires above 0°C , the bath temperature
 ψ = radiation heat loss per unit length at temperature θ in cals sec^{-1} .

- C = current in amperes in the hot wire
 R/l = resistance per unit length of the wire at temperature θ
 J = mechanical equivalent of heat (= 4.184)
 C^2R/Jl = total heat loss per unit length at temperature θ in cal. sec⁻¹
 θ_1 = temperature drop across tube wall, calculated from the total heat loss, the internal and external radii of the wall, and the thermal conductivity of lead glass (4) and
 for the wide tubes, $\theta_1 = C^2R/Jl \times 3.63$,
 for the narrow tubes, $\theta_1 = C^2R/Jl \times 8.82$
 θ' = $\theta - \theta_1$ = temperature drop across the gas
 K_a = apparent conductivity, in calories, cm⁻¹ sec⁻¹ deg⁻¹
 = $(C^2R/Jl - \psi) \log \exp(r_2/r_1)/2\pi\theta'$
 r_1 = radius of platinum wire in centimetres
 r_2 = internal radius of narrow tubes in centimetres
 r_3 = internal radius of wide tubes in centimetres

Convection ceases for each system at the pressure for which the apparent conductivity is the absolute conductivity, K

C_N = current in narrow system at the above pressure

C_W = current in wide system at the above pressure

Therefore

$$[(C_N^2R/Jl - \psi) \log \exp(r_2/r_1)]/2\pi\theta' = K = [(C_W^2R/Jl - \psi) \log \exp(r_3/r_1)]/2\pi\theta'$$

Therefore

$$\log \exp(r_3/r_1)/\log \exp(r_2/r_1) = (C_N^2R/Jl - \psi)/(C_W^2R/Jl - \psi)$$

$$\alpha_c = \log \exp(r_3/r_1)/\log \exp(r_2/r_1) = 1.183$$

$$\alpha_0 = (C_N^2R/Jl - \psi)/(C_W^2R/Jl - \psi)$$

Thus, when we have two equal values for the apparent conductivity in the two systems corresponding to a different pressure for each system, and the equation $\alpha_c = \alpha_0$ is satisfied, this value of the apparent conductivity is the absolute conductivity of the gas at the mean temperature between the hot wire and the outer wall

θ_m = mean temperature of gas between the wire at 0° C and the wall at θ_1° C

K = mean of the values of the absolute thermal conductivity of the gas calculated for the two widths of tube at a temperature θ_m° C

The absolute conductivity, K, was plotted against the corresponding gas temperature, θ_m° C, and the best straight line was drawn through the points

The intercept of this line with the conductivity axis gave the value of the absolute thermal conductivity of the gas at 0°C

K_0 having been determined, the function f in the equation

$$K_0 = f\eta_0 C_v$$

was calculated for each gas, where

C_v = specific heat at constant volume at 0°C

f = a factor depending on the force operating in molecular collision

Preparation of Oxygen

The oxygen was prepared by heating powdered potassium permanganate. It was purified of carbon dioxide by bubbling through a caustic potash solution and dried by passing first over sticks of caustic potash and then over phosphorus pentoxide. The gas was finally collected in a reservoir, connected to a manometer and to the tubes through a tap, where it was stored at a pressure between 1 and $1\frac{1}{2}$ atmospheres. The whole apparatus as far as a three way tap connected to the flask was evacuated before admitting the oxygen. The three-way tap allowed the gas from the flask to be discharged outside the apparatus until it had swept away all the air remaining in the flask, after which it was turned so that the oxygen passed into the apparatus. The latter was re-evacuated and re-filled with oxygen two or three times before the experiments were carried out.

Results for Oxygen

$I - \theta = 13\ 295^\circ \text{C}$ therefore $\theta_m = 6\ 65^\circ \text{C}$ $\psi = 0\ 000037$ $R/l = 0\ 1314$

P	Wide tubes		Narrow tubes	
	$\theta_1 = 0\ 003^\circ \text{C}$, $\theta' = 13\ 293^\circ \text{C}$		$\theta_1 = 0\ 009^\circ \text{C}$, $\theta' = 13\ 288^\circ \text{C}$	
	C	K_0	C	K_0
80.9	0.1696	0.0000607	0.1837	0.00006015
71.5	1692	8035	1837	801
61.9	1690	8015	1837	801
52.8	1689	801	1837	801
43.3	1688	800	1836	801
33.7	1687	5995*	1836	6008*
24.2	1687	5995	1835	600
15.8	1686	5985	1834	5995
5.8	1682	596	18295	596
1.1	1653	5755	17925	5725

* $\alpha = 1\ 185$

$K = 0\ 0000600$

Results for Oxygen—(continued)

II— $\theta = 17.355^\circ\text{C}$ therefore $\theta_m = 8.68^\circ\text{C}$ $\psi = 0.0000054$ $R/l = 0.1334$

P	Wide tubes		Narrow tubes	
	$\theta_1 = 0.004^\circ\text{C}$, $\theta' = 17.351^\circ\text{C}$		$\theta_1 = 0.012^\circ\text{C}$, $\theta' = 17.343^\circ\text{C}$	
	C	K_a	C	K_a
86.5	0.1970	0.0000615	0.2092	0.0000606
78.1	1933	611	2092	606
67.6	1926	607	20915	606
57.95	1923	605	2091	6055
48.8	1922	604	2091	6055
39.0	1919	603	2090	6055
30.4	1919	603*	2090	6055*
19.95	1918	6025	2089	6045
11.3	1916	601	2087	603
3.5	1905	595	2076	597

* $\alpha = 1.188$ $K = 0.0000604$ III— $\theta = 19.387^\circ\text{C}$ therefore $\theta_m = 9.69^\circ\text{C}$ $\psi = 0.0000063$ $R/l = 0.1343$

P	Wide tubes		Narrow tubes	
	$\theta_1 = 0.005^\circ\text{C}$, $\theta' = 19.382^\circ\text{C}$		$\theta_1 = 0.014^\circ\text{C}$, $\theta' = 19.373^\circ\text{C}$	
	C	K_a	C	K_a
71.9	0.2035	0.00006115	0.2206	0.0000608
63.4	2030	608	2206	608
54.7	2026	606	2205	6075
49.3	2026	606	2205	607
44.9	2024	605	2205	607
39.9	2024	6045	2205	607
35.3	2023	604*	2204	607*
30.0	2022	6035	2204	6065
25.0	2022	603	2203	606
20.4	2021	603	2203	606
15.7	2021	6025	2201	605
10.9	2018	601	2200	604
4.0	2012	595	2191	599

* $\alpha = 1.188$ $K = 0.00006055$

Results for Oxygen—(continued)

IV $-\theta = 21\ 427^\circ\text{C}$ therefore $\theta_m = 10\ 71^\circ\text{C}$ $\psi = 0\ 0000072$ $R/l = 0\ 1353$

P	Wide tubes		Narrow tubes	
	$\theta_1 = 0\ 005^\circ\text{C}$, $\theta' = 21\ 422^\circ\text{C}$		$\theta_1 = 0\ 015^\circ\text{C}$, $\theta' = 21\ 412^\circ\text{C}$	
	C	K_a	C	K_a
73 0	0 2139	0 00006155	0 23145	0 0000610
65 3	2134	6125	23145	610
55 7	2128	6065	23145	610
45 7	2124	607	2314	606
35 2	2123	606*	2314	606*
24 9	2123	606	2313	606
17 3	2121	605	2312	608
12 4	2119	604	2310	607
5 3	2114	601	2303	6035

* $\alpha = 1\ 188$ $k = 0\ 00006075$ V $-\theta = 25\ 513^\circ\text{C}$ therefore $\theta_m = 12\ 75^\circ\text{C}$ $\psi = 0\ 0000089$ $R/l = 0\ 1373$

P	Wide tubes		Narrow tubes	
	$\theta_1 = 0\ 006^\circ\text{C}$ $\theta' = 25\ 507^\circ\text{C}$		$\theta_1 = 0\ 019^\circ\text{C}$, $\theta' = 25\ 494^\circ\text{C}$	
	C	K_a	C	K_a
76 1	0 23385	0 00006265	0 2516	0 0000614
67 1	2323	6185	2515	6135
57 3	2315	614	2515	6135
48 0	2309	611	2515	6135
38 3	2307	610	2514	613
28 3	2305	609*	2513	6125*
23 9	2305	609	2513	6125
19 5	2304	6085	2513	612
15 1	2302	606	2510	611

* $\alpha = 1\ 189$ $k = 0\ 0000611$

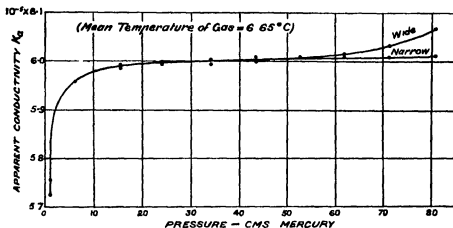


FIG 3 —Variation with Pressure of Apparent Conductivity of Oxygen

Preparation of Nitrogen

A solution of 40 grams of sodium nitrite, 40 grams of potassium bichromate, and 60 grams of sodium sulphate, in a litre of distilled water, was contained in a 2-litre flask. The flask was connected via a three-way tap to chromic acid towers through which the gas was bubbled in order to oxidise any suboxides of nitrogen that might have been formed. These were connected, with a trap between, with towers containing concentrated sulphuric acid as a drying agent and thence to a hard glass tube containing copper turnings, which were heated to a bright redness by means of a gas oven in order to reduce any nitrogen peroxide to nitrogen and absorb any free oxygen in the gas. This was joined to the manometer, phosphorus pentoxide tubes, and reservoirs through a three-way tap, which was used to cut off the apparatus as far as the copper turnings while the reservoirs were being evacuated and the nitrogen was sweeping the fore part of the apparatus clear of air. The tube in the furnace could not be evacuated without collapsing, so, when sufficient gas had passed through to sweep out all the air, the three-way tap was turned so that the gas was admitted into the reservoirs at such a rate that the pressure within the tube containing the copper turnings was maintained at approximately 1 atmosphere. The experiments were carried out after re-evacuating and refilling the reservoirs and tubes with pure nitrogen.

Results for Nitrogen

I— $\theta = 9.188^\circ\text{C}$ therefore $\theta_m = 4.59^\circ\text{C}$ $\psi = 0.0000018$ $R/l = 0.1294$

P	Wide tubes		Narrow tubes	
	$\theta_1 = 0.002^\circ\text{C}$, $\theta' = 9.186^\circ\text{C}$		$\theta_1 = 0.006^\circ\text{C}$, $\theta' = 9.182^\circ\text{C}$	
	C	K_a	C	K_a
85.8	0.14045	0.00005925	0.1521	0.00005875
78.6	14025	591	1521	5875
68.1	14015	590	1521	5875
59.5	1401	5895	15205	5875
50.8	1401	5885	15205	5875
46.3	14005	589	15205	5875
41.4	14005	589	15205	5875
37.5	1400	5885	1520	587
32.9	13995	588*	1520	587*
28.6	13995	588	1520	587
24.8	1399	588	15195	586
19.9	1399	588	1519	586
15.3	13985	5875	15185	5855
10.5	1397	5865	15175	585
4.8	1394	5835	15135	582

* $\alpha = 1.181$ $K = 0.00005875$

II— $\theta = 13.252^\circ\text{C}$ therefore $\theta_m = 6.63^\circ\text{C}$ $\psi = 0.0000036$ $R/l = 0.1314$

P	Wide tubes		Narrow tubes	
	$\theta_1 = 0.003^\circ\text{C}$, $\theta' = 13.249^\circ\text{C}$		$\theta_1 = 0.008^\circ\text{C}$, $\theta' = 13.243^\circ\text{C}$	
	C	K_a	C	K_a
75.5	0.1678	0.0000595	0.1820	0.00005925
66.1	1675	593	1820	5925
56.2	1673	5915	1820	5925
47.0	1672	5905	1820	592
41.1	16715	590	1820	592
35.5	1671	590*	1819	5915*
29.8	1671	590	1819	5915
24.2	16705	5895	1819	5915
18.8	1670	589	1818	5915
12.9	1669	5885	1817	5915
8.5	1662	5835	1808	5795

* $\alpha = 1.186$ $K = 0.0000591$

Results for Nitrogen—(continued)

III.— $\theta = 17\ 316^\circ\text{C}$ therefore $\theta_m = 8\ 66^\circ\text{C}$ $\psi = 0\ 0000054$ $R/l = 0\ 1334$

P	Wide tubes		Narrow tubes	
	$\theta_1 = 0\ 004^\circ\text{C}$, $\theta' = 17\ 312^\circ\text{C}$		$\theta_1 = 0\ 012^\circ\text{C}$, $\theta' = 17\ 304^\circ\text{C}$	
	C	K_a	C	K_a
76 4	0 1916	0 0000602	0 2076	0 0000598
67 4	1911	599	20756	598
57 8	1907	597	20755	598
46 2	1905	595	2075	598
45 4	1904	595	2075	598
41 9	1904	5945	2075	598
38 9	1904	5945	20745	5975
36 4	1903	594	20745	5975
33 2	1903	594*	2074	597*
30 1	1903	594	2074	597
26 8	1903	594	2074	597
23 9	1902	5935	20735	597
20 9	1902	593	2073	5965
19 9	1902	593	20725	596
14 4	1901	593	2072	596
11 0	1900	592	2071	5955
5 1	1896	5895	20655	592

* $\alpha = 1\ 188$ $K = 0\ 00005955$ IV.— $\theta = 21\ 390^\circ\text{C}$ therefore $\theta_m = 10\ 69^\circ\text{C}$ $\psi = 0\ 0000071$ $R/l = 0\ 1353$

P	Wide tubes		Narrow tubes	
	$\theta_1 = 0\ 005^\circ\text{C}$, $\theta' = 21\ 385^\circ\text{C}$		$\theta_1 = 0\ 015^\circ\text{C}$, $\theta' = 21\ 376^\circ\text{C}$	
	C	K_a	C	K_a
78 8	0 2128	0 0000610	0 2296	0 0000601
69 6	2119	606	2295	6005
60 3	2112	601	2295	6005
49 8	2108	5985	2295	6005
45 6	2106	598	2295	6005
43 1	2106	5975	2295	6005
40 6	2105	597	2295	6005
37 8	2105	597	2294	600
36 1	2104	5965*	2294	600*
32 1	2104	5965	2294	600
29 4	2104	5965	2294	600
26 3	2104	596	2293	5995
22 2	2103	596	2293	599
19 6	2103	596	2293	599
16 7	2103	5955	2292	599
13 7	2102	595	2291	5985
7 8	2099	594	2289	597

* $\alpha = 1\ 189$ $K = 0\ 0000598$

Results for Nitrogen—(continued)

V—0 = 25 479° C therefore $\theta_m = 12\ 74^\circ\text{C}$ $\psi = 0\ 0000089$ $R/l = 0\ 1373$.

P	Wide tubes		Narrow tubes	
	$\theta_1 = 0\ 006^\circ\text{C}$, $\theta' = 25\ 473^\circ\text{C}$		$\theta_1 = 0\ 018^\circ\text{C}$, $\theta' = 25\ 461^\circ\text{C}$	
	(ϵ)	K_a	(ϵ)	K_a
80.9	0.2330	0.0000623	0.2492	0.00006045
68.6	2306	610	2492	6045
59.7	2298	603	2492	6045
48.2	2290	602	2492	603
40.4	2287	600*	2491	603*
37.1	2287	600	2491	603
34.2	2286	600	2490	602
31.2	2286	5995	2490	602
27.9	2285	599	2490	602
24.9	2284	599	2489	602
22.0	2284	599	2489	6015
19.1	2284	5985	24885	601
16.1	2283	598	24885	601
12.9	2282	5975	2487	601
9.5	2281	597	2486	600
5.2	2277	595	2480	597

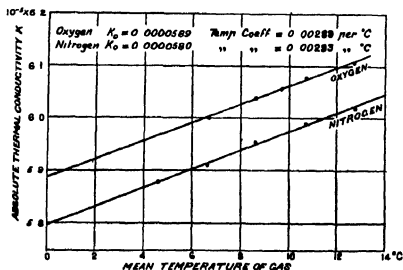
* $a = 1\ 187$ $K = 0\ 00006015$ 

FIG. 4.—Variation with Temperature of Absolute Thermal Conductivities of Oxygen and Nitrogen

From fig 4 the following results were deduced —

Gas	Absolute thermal conductivity at ° C	Temperature coefficient of thermal conductivity
Oxygen	$5.89 \times 10^{-8} \text{ cal cm}^{-1} \text{ sec}^{-1} \text{ deg}^{-1}$	0.00289
Nitrogen	5.80 , , , 	0.00293

"*f*," in the formula $K_0 = f\eta_0 C$, is given for the two gases in the following table, where the values for η_0 and C , are obtained from Landolt and Bornstein's tables

Gas	η_0	C	K_0	f
Oxygen	193×10^{-8}	$0.155 \text{ cal gm}^{-1}$	5.89×10^{-8}	1.97
Nitrogen	187×10^{-8}	0.177 , , 	5.80×10^{-8}	1.96

Studies in Adhesion III—Mixtures of two Lubricants

By MILLICENT NOTTAGE

(A Report to the Lubrication Research Committee of the Department of Scientific and Industrial Research)

(Communicated by Sir William Hardy, F.R.S.—Received February 9, 1928)

[PLATES 14-16]

Three pairs of lubricants were studied, the procedure being that described in the last paper. Briefly the clean cylinder was placed on the clean plate, both being of steel and warmed in clean air to above the melting point of the lubricant. Melted lubricant was then allowed to be drawn in under the cylinder by capillarity and a pool formed. The temperature was kept constant until equilibrium was reached, when the heat was cut off and the lubricant allowed to crystallise. The joint was broken at 18° C.

Of the three pairs the first included substances, namely, palmitic acid and the paraffin $C_{30}H_{62}$, which seemed to be incapable of reacting chemically with each other, the second pair, palmitic acid and cetyl alcohol probably would react chemically, whilst the third pair comprised the paraffin $C_{30}H_{62}$ and the ring compound phenanthrene.

The adhesion of ring compounds is greater than that of chain compounds, and, with few exceptions, too great for measurement by the apparatus employed. Phenanthrene was chosen because it was one of these exceptions.



In its molecule the benzene rings are arranged as shown in the diagram.

The melting-point of each mixture was taken, and in the curves melting-points and adhesion are plotted against molecular composition—that is to say, the percentage of molecules present. The actual values are given in the tables.

The nature of the break is described in certain places as “normal,” and a normal break is one in which there are two surfaces of break each close to a metal face and separating an adsorbed layer from a median plate of crystals and the break occurs at both of these surfaces*.

The structure of the crystalline plates, which varies with composition, is illustrated by photographs.

In describing the structure it was thought better to use the word “constituent” instead of the less ambiguous word “phase.” There were in each case two components present, and they, by solid solution or otherwise, gave rise to distinguishable structural elements. The latter are the constituents.

I—*Palmitic Acid and the Paraffin C₃₀H₆₂*

The adhesion of the admixed substances for all compositions is greater than that of the pure substances. Both the adhesion and the melting-point curves show a well-defined transition-point between 24–25.6 molecules per cent C₃₀H₆₂; i.e., when the mixture contains approximately 3 molecules of palmitic acid to 1 molecule of paraffin, this point is a maximum on the adhesion, and a minimum on the melting-point curve.

The variation in the adhesion and melting-point with molecular composition is accompanied by changes in the structure of the crystalline plate.

Palmitic acid crystallises in long, narrow, plates arranged in a fan-shaped manner (Plate 14, fig. 3). The addition of up to 6.3 molecules per cent C₃₀H₆₂ produces a gradual diminution in the crystal size and a tendency towards a triangular arrangement (see Plate 14, fig. 4, which shows the same type of structure produced by the addition of small quantities of cetyl alcohol to palmitic acid). In the mixture containing 6.3 molecules per cent C₃₀H₆₂, a very small quantity of a second fine-grained constituent is discernible between the needles. The amount of this constituent increases and both constituents become much

* ‘Roy Soc Proc,’ A, vol 118, p 209 (1928)

less coarse until, when the mixture contains 12-25.6 molecules per cent $C_{30}H_{62}$, they are indistinguishable from one another, but they remain immiscible so that the whole plate has a laminated structure, the laminae being traversed by alternate light and dark bands. Near the transition point these laminae are so fine that the broken surface has an iridescent appearance. The crystalline plate, when broken, now forms fragments of angular outline (Plate 14 fig 1). The addition of further quantities of $C_{30}H_{62}$ causes these laminae to disappear altogether and henceforward the crystalline plate appears to be homogeneous. The transition point on the adhesion and melting-point curves is thus accompanied by a change from a system containing two constituents to a system containing only one.

No attempt has been made to work out the constitution of these different crystalline structures. The following suggestions are put forward only tentatively.

Palmitic acid can form solid solutions with the paraffin but the saturation limit is soon reached (at probably less than 6.3 molecules per cent $C_{30}H_{62}$). From this point until the mixture contains approximately 25 molecules per cent $C_{30}H_{62}$, two constituents separate out, viz., a solid solution of the paraffin in palmitic acid (the needles), and a solid solution of palmitic acid in the paraffin (the fine-grained constituent). The immiscibility of these two constituents is the cause of the laminated structure. In mixtures containing more than 25 molecules per cent $C_{30}H_{62}$ (approximately), all the palmitic acid is held in solution by the paraffin. The transition point may therefore be regarded as the point at which the limit of solid solubility of palmitic acid in the paraffin is reached.

The crystalline plates formed from all mixtures which lie on the palmitic acid side of the transition point break quite definitely in the "normal" manner. Those plates which lie on the paraffin side, however, consist of very minute polygonal crystals, and it is difficult to decide where the break really takes place. The broken surfaces are rugged, not plane, and they do not show interference colours. It seems probable that the fracture is of the "normal" type, but, owing possibly to the small amount of cohesion between the individual crystals, the broken crystalline plate is made up of an infinitesimal number of more or less isolated crystals which are so small that the clear spaces in between cannot be easily distinguished. The fracture certainly does not take place at any definite median plane, if it did, both broken surfaces would be plane, not rugged, and one or both would show interference colours owing to the reduction in thickness.

The latent period of this series of mixtures is of interest. Palmitic acid has a latent period of about 60 minutes during which the adhesion increases, the paraffin has no latent period. Mixtures on the palmitic acid side of the transition point have a latent period of increasing, whilst those on the paraffin side have a latent period of decreasing, adhesion.

Table I—Latent Periods for Mixtures of Palmitic Acid and the Paraffin $C_{30}H_{62}$.

Time during which the mixture was kept liquid	Adhesions for mixtures containing					
	1.6 molecules per cent $C_{30}H_{62}$		12.2 molecules per cent $C_{30}H_{62}$		58 molecules per cent $C_{30}H_{62}$	
Minutes	Adhesion measured	Adhesion (gms per sq cm)	Adhesion measured	Adhesion (gms per sq cm)	Adhesion measured	Adhesion (gms per sq cm)
5					19061	24270
10					19874	25320
15						
30	9979	12710	14515	18480	17435	22210
40	{ 12559	{ 15990	{ 18144	{ 23110		
	{ 12078	{ 15390	{ 20512	{ 26130	17378	22120
50	13381	17040	20922	26620		
70	13822	17220	20639	26250	17576	22390

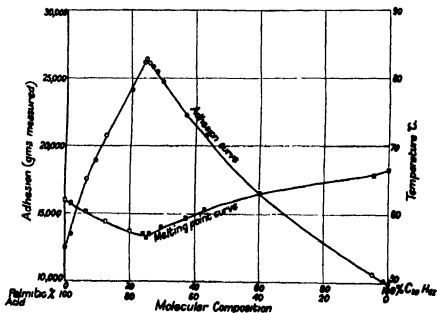


FIG. 1—Palmitic Acid and $C_{30}H_{62}$.

Mixtures containing less than 25 molecules per cent $C_{30}H_{62}$ (approximately) have a latent period of about 50 minutes during which the adhesion increases, whilst those containing more than 25 molecules per cent $C_{30}H_{62}$ have a latent period of not more than 30 minutes during which the adhesion decreases

Table II—I Palmitic Acid and the Paraffin $C_{30}H_{62}$

Weight per cent Palmitic Acid	Weight per cent $C_{30}H_{62}$	Melting point	Adhesion
		" (°)	Grams per square centimetre
100 0	—	62	15853
97 4	2 6	61 6	17130
90 1	9 9	60 2	22340
85 3	14 7	—	24090
81 4	18 6	58 8	26435
70 7	29 3	57 4	30730
65 7	34 3	57 0	33350
65 2	34 8	56 6	33565
63 8	36 2	57 0	33240
62 7	37 3	—	32990
61 1	38 9	—	32440
59 2	40 8	58 0	31420
51 0	49 0	59 4	28350
44 5	55 5	60 6	26490
28 8	71 2	63 0	21075
2 9	97 1	65 8	13585
0 95	99 05	—	12890
—	100 0	66 5	12743

II—Palmitic Acid and Cetyl Alcohol

The adhesion curve shows three well-defined transition points, viz., at 29 8–31 2, 49 3–50 4, and 65 1–67 0 molecules per cent cetyl alcohol. The melting-point curve shows only two such points, viz., at 29 8–31 2 and 65 1–67 0 molecules per cent cetyl alcohol. As the melting-point curve shows no minimum at 49 3–50 4 molecules per cent cetyl alcohol, the maximum on the adhesion curve at this point is probably due to the presence of the compound cetyl palmitate, and not to a mixture or a solid solution of the two substances in equimolecular proportions.

As in the preceding case, the addition of small quantities of cetyl alcohol (up to about 8 molecules per cent) causes a diminution in size and a rearrangement of the palmitic acid crystals (Plate 14, fig 4), no second constituent can be discerned at this stage but the edges of the crystals appear to be slightly roughened. With further addition of cetyl alcohol, a second very fine-grained constituent separates out between the needles which now spread out in a star-

like manner (Plate 15, fig 5) This type of structure persists until the mixture contains 49.3 molecules per cent cetyl alcohol, the proportion of fine-grained constituent gradually increasing until it forms a coherent mass in which are embedded a few very small needles, the crystalline plate now breaks into fragments of irregular outline (Plate 15, fig 6) In the mixture containing 49.3 molecules per cent cetyl alcohol, the needles, although very small, may still be distinguished, in that containing 50.4 molecules per cent they have completely disappeared and henceforth the crystalline plate appears to be homogeneous The maximum on the adhesion curve when the mixture contains 49.3-50.4 molecules per cent cetyl alcohol, therefore coincides with a change in structure from a two-constituent to a one-constituent system

The fine-grained constituent probably consists of cetyl palmitate, the needles of a solid solution of cetyl palmitate in palmitic acid, the solubility of the ester in the acid being low (about 8 molecules per cent cetyl alcohol) The crystalline plate formed from mixtures containing 50.4 molecules per cent and upwards of cetyl alcohol, breaks into small fragments of irregular outline (fig 7) which become slightly coarser as the proportion of cetyl alcohol increases (fig 8) and gradually merge into the structure shown by pure cetyl alcohol (Plate 16, fig 9) All these mixtures containing more than 50 molecules per cent cetyl alcohol probably consist of solid solutions of cetyl palmitate in cetyl alcohol

The break in every case was normal

The mode of freezing is of interest In the case of mixtures containing 20.3-49.3 molecules per cent cetyl alcohol, freezing starts at several points round the edge of the cylinder and gradually spreads from these until the whole has solidified As palmitic acid has the higher freezing-point the needles would probably be deposited first and the fine-grained crystals of cetyl palmitate separate out between them on further cooling The solids so formed are very friable and easily broken up Mixtures containing more than 50 molecules per cent cetyl alcohol solidify slowly, but not in patches, to form translucent, waxy solids which become opaque upon further cooling

Both adhesion and melting-point curves show minima for mixtures containing 29.8-31.2 and 65.1-67.0 molecules per cent cetyl alcohol, these correspond approximately to mixtures containing 1 molecule of cetyl palmitate with 1 molecule of palmitic acid, and 1 molecule of cetyl alcohol respectively The adhesion curve also passes through an extended ill-defined maximum when the mixture contains 76.2-81.1 molecules per cent cetyl alcohol None of these transition points are accompanied by any apparent change in structure

Table III—II Palmitic Acid and Cetyl Alcohol

Weight per cent Palmitic Acid	Weight per cent Cetyl Alcohol	Melting point	Adhesion
		° C	Grams per square centimetres
100 0	—	62	15853
92 4	7 6	60 0	14070
80 6	19 4	57 0	12520
77 2	22 8	55 8	11245
71 4	28 6	54 4	10505
70 0	30 0	54 0	10505
68 3	31 7	54 8	13895
67 2	32 8	54 8	18160
66 8	33 2	54 6	18390
62 0	38 0	54 0	21470
58 1	41 9	53 0	23570
52 1	47 9	50 4	26260
51 0	49 0	48 8	26405
46 0	54 0	48 0	24705
36 2	63 8	44 6	17860
34 3	65 7	44 6	17635
29 0	71 0	45 8	20720
24 8	75 2	46 4	21800
19 8	80 2	47 4	21800
17 8	82 2	47 6	21470
7 9	92 1	48 8	18930
—	100 0	50 0	15840

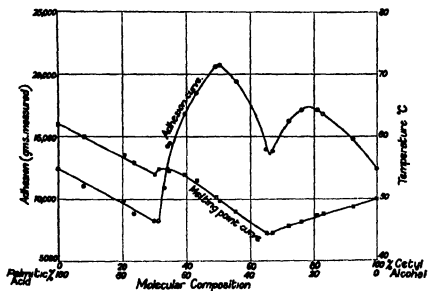


FIG 2 —Palmitic Acid and Cetyl Alcohol

III—Phenanthrene $C_{14}H_{10}$ and the Paraffin $C_{30}H_{62}$

The addition of the paraffin $C_{30}H_{62}$ to phenanthrene causes the adhesion of the latter to decrease at first rapidly and then very gradually. The adhesion remains practically constant for all mixtures containing from 46.6–73.5 molecules per cent $C_{30}H_{62}$. The addition of more than 73.5 molecules per cent causes it to decrease again rapidly. The adhesion curve shows an ill-defined transition point at about 46.6 molecules per cent $C_{30}H_{62}$.

The melting-point of each constituent is lowered by the addition of the other. The melting-point curve is continuous and passes through a minimum extending from approximately 46.6–73.5 molecules per cent $C_{30}H_{62}$, this roughly corresponds with the horizontal part of the adhesion curve. The melting-points of all the mixtures, more especially of those containing 10.2–46.6 molecules per cent $C_{30}H_{62}$ are very indefinite. When heated, the substances gradually become translucent, in some case 15° or 20° below the temperature at which they finally become liquid. Solidification takes place in a similar manner. At a definite temperature, which varies with the composition of the mixture, the excess liquid round the cylinder assumes a crystalline appearance but still remains translucent. At a temperature of about 56° , which is practically the same for all the mixtures, this translucent solid suddenly becomes opaque. This type of fusion and solidification is characteristic of binary mixtures from which on cooling a solid phase separates out of different molecular composition to the liquid phase and *vice versa*.

Phenanthrene crystallises in large, flat square or oblong plates arranged in triangular-shaped masses (Plate 16, fig 10) and the crystalline plate breaks with the normal type of fracture. The addition of up to 10.2 molecules of $C_{30}H_{62}$ produces a diminution in the crystal size and a tendency towards a less definite arrangement. In a mixture containing 22.0 molecules per cent $C_{30}H_{62}$, the phenanthrene structure has practically disappeared and has been replaced by masses of small angular crystals arranged in masses with curved outlines (Plate 16, fig 11). This structure remains practically the same for all mixtures containing more than 22.0 molecules per cent $C_{30}H_{62}$ merging gradually into that of pure $C_{30}H_{62}$ (Plate 16, fig 12). Throughout the whole range of composition only one constituent can be discerned and there is no sharp change in structure anywhere in the series. The two substances are apparently miscible in all proportions in the solid state.

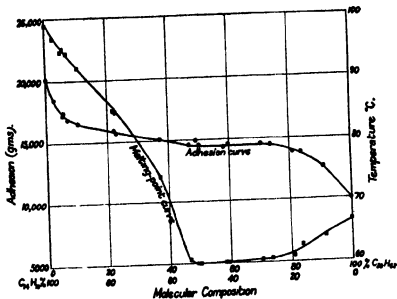
The mode of breaking of the crystalline plates formed from these mixtures is peculiar. If kept liquid for an insufficient length of time, the crystalline plate

breaks to a large extent in the body of the solid but at no definite layer, the fracture often has a conchoidal appearance as though the substance were not definitely crystalline (Plate 16, fig 12) In this state the adhesion is very variable but generally low When equilibrium has been attained by keeping the mixture liquid for at least 60 minutes, the fracture is mainly normal although there is still a tendency for small pieces to be pulled out from the main mass This may be due to the fact that all the mixtures form very hard brittle solids

The latent period of phenanthrene is of interest inasmuch as it is one of decreasing adhesion, a property which it shares with naphthalene, the only other aromatic hydrocarbon examined The latent period of both these substances is about 35 or 40 minutes

Table IV —Latent Period and Adhesion of Phenanthrene and of Naphthalene

Time during which the substance was kept liquid	Phenanthrene		Naphthalene	
	Adhesion (measured)	Adhesion (grams per square centimetre)	Adhesion (measured)	Adhesion (grams per square centimetre)
Minutes				
4	{ 25940 27216	{ 33030 34650		
10			> 27216	> 34650
15	24664	31390		
20			24918	31770
25	22935	29200		
35	{ 20638 20355	{ 26280 25920		
40			21417	27270
45	20469	26060		
55			21319	27140

FIG. 3.—Phenanthrene and C₃₀H₄₂.Table V.—III Phenanthrene and the Paraffin C₃₀H₄₂.

Weight per cent Phenanthrene	Weight per cent C ₃₀ H ₄₂	Melting point ° C	Adhesion Grams per square centimetre
100 0	—	99	26080
94 8	5 2	96 8	23335
88 9	11 1	94 6	21800
88 2	11 8	95 0	22130
85 4	14 6	94 4	21370
78 7	21 3	92 0	21005
60 0	40 0	85 0	20910
59 0	41 0	84 8	19920
41 5	58 5	74 0	19170
37 4	62 6	60 6	18490
30 4	69 6	60 0	19060
29 7	70 3	60 0	18490
23 3	76 7	60 2	18270
22 2	77 8	60 2	18630
15 2	84 8	60 4	18530
13 2	86 8	60 6	18425
9 3	90 7	61 0	17615
7 7	92 3	62 8	17510
4 0	96 0	64 2	16025
—	100 0	66 5	12743



FIG. 1
74.4 mol per cent Palmitic Acid
25.6 mol per cent $C_{10}H_{18}$



FIG. 2
Pure $C_{10}H_{18}$

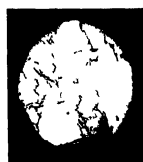


FIG. 3
Pure Palmitic Acid



FIG. 4
92 mol per cent Palmitic Acid,
8 mol per cent Cetyl Alcohol



Magnification 13



FIG 5
76.2 mol per cent Palmitic
Acid, 23.8 mol per cent
Cetyl Alcohol



FIG 6
56.7 mol per cent Palmitic
Acid, 43.3 mol per cent
Cetyl Alcohol



FIG 7
49.6 mol per cent Palmitic
Acid, 50.4 mol per cent
Cetyl Alcohol



FIG 8
33 mol per cent Palmitic Acid,
67 mol per cent Cetyl
Alcohol



Magnification = 13



FIG 9
Pure Cetyl Alcohol



FIG 10
Pure Phenanthrene



FIG 11
62.7 mol per cent Phenanthrene
37.3 mol per cent $C_{16}H_{32}$
(in equilibrium)



FIG 12
62.7 mol per cent Phenanthrene
37.3 mol per cent $C_{16}H_{32}$
(not in equilibrium)



Magnification = 13

A Generalised Spheroidal Wave Equation.

By A. H. WILSON, B.A., Emmanuel College, Cambridge

(Communicated by R. H. Fowler, F.R.S.—Received December 19, 1927)

1. Introduction.

1.1. The differential equation considered in this paper may be written in the form

$$\frac{d}{d\xi} \left\{ (1 - \xi^2) \frac{dX}{d\xi} \right\} + \left\{ \lambda^2 \xi^2 - 2p\lambda\xi - \frac{n_2^2}{1 - \xi^2} + \mu' \right\} X = 0 \quad (1)$$

When $p = 0$ this equation becomes the equation giving the solution of $\nabla^2 X - \lambda^2 X = 0$ in spheroidal co-ordinates. The equation may therefore be called a generalised spheroidal wave equation. In Part I of this paper we shall consider equation (1) when $p \neq 0$, and in Part II, which consists of sections 6 to 10, we shall consider the equation with $p = 0$. The transformation $X = (\xi^2 - 1)^{n_2/2} f$ reduces the equation to one with polynomial coefficients

$$(1 - \xi^2) \frac{d^2 f}{d\xi^2} - 2(n_2 + 1) \xi \frac{df}{d\xi} + \{ \lambda^2 \xi^2 - 2p\lambda\xi + \mu' - n_2(n_2 + 1) \} f = 0. \quad (2)$$

The further transformations $\xi - 1 = x$ and $f = e^{-\lambda x} y$ bring the equation to the following form,

$$x(x+2) \frac{d^2 y}{dx^2} + 2\{n_2 + 1 + (n_2 + 1 - 2\lambda)x - \lambda x^2\} \frac{dy}{dx} + \{(n_2 - 2\lambda)(n_2 + 1) - \mu' - \lambda^2 + 2p\lambda - 2\lambda(n_2 + 1 - p)x\} y = 0, \quad (3)$$

or as we shall write it,

$$x(x+2) \frac{d^2 y}{dx^2} + 2\{n_2 + 1 + (n_2 + 1 - 2\lambda)x - \lambda x^2\} \frac{dy}{dx} + \{\mu + 2p\lambda - 2\lambda(n_2 + 1 - p)x\} y = 0 \quad (3A)$$

We shall take (3A) as our standard form.

1.2. The equation (1) occurs in the important physical problem of determining the possible energies of the ion of molecular hydrogen by means of Schrödinger's wave theory. In this problem n_2 is a positive integer or zero, and in cases where this fact makes any difference to the results we shall assume it. We shall also assume λ to be real. In the physical problem solutions are required which are bounded in the real interval $1 < \xi < \infty$. When $(p - n_2)$ is a positive integer n , there are n values of μ for which equation (3A)

admits of a polynomial solution of degree $(n-1)$. There are also other types of solutions.

1.3 The equation is a confluent form of the general second order linear differential equation with four regular singularities. Such an equation may be represented schematically as

$$y = P \left\{ \begin{array}{cccccc} 0 & b & c & \infty & & \\ 0 & 0 & 0 & n_3 + 1 - p & x & \\ -n_3 & -n_3' & q & n_3' + 1 + p - q & & \end{array} \right\},$$

the notation being an obvious generalisation of Riemann's P-function. Equation (3A) is obtained by taking $b=2$, $n_3=n_3'$ and by making $c \rightarrow \infty$ while $qc \rightarrow -2\lambda$. The point at infinity is therefore an irregular singular point of the equation.

The solution of an equation of this type is probably expressible as a homogeneous integral equation, but we shall obtain our results by means of a solution in series

2 The Solutions in a Finite Form.

We put $p - n_3 = n$ a positive integer and assume a solution

$$y = \sum_0^{n-1} a_n x^n$$

The coefficients are determined by the following relations

$$\left. \begin{aligned} 2(n_3+1)a_1 + (\mu+2p\lambda)a_0 &= 0 \\ 2(m+1)(m+n_3+1)a_{m+1} \\ + \{m(m+2n_3+1-4\lambda) + \mu+2p\lambda\}a_m - 2\lambda(m-n)a_{m-1} &= 0 \\ \text{for } m=1, 2, 3, \dots, n-2 \\ \{(n-1)(n+2n_3-4\lambda) + \mu+2p\lambda\}a_{n-1} + 2\lambda a_{n-2} &= 0 \end{aligned} \right\} \quad (1)$$

These linear equations for the coefficients will have a non-zero solution if and only if the determinant of the system vanishes.

$$\begin{vmatrix} \mu+2p\lambda & 2(n_3+1) & 0 & 0 & 0 & 0 \\ 2\lambda(n-1) & \mu+2p\lambda+2n_3+2-4\lambda & 4(n_3+2) & 0 & 0 & 0 \\ 0 & 2\lambda(n-2) & \mu+2p\lambda+2(2n_3+3-4\lambda) & 6(n_3+2) & 0 & 0 \\ 0 & 0 & 0 & 0 & 2\lambda\mu+2p\lambda+(n-1)(n+2n_3-4\lambda) & 0 \end{vmatrix} = 0 \quad (2)$$

This relation between μ and λ is of the n th degree in μ , and is the necessary and sufficient condition for the existence of a solution of the type assumed. μ can easily be determined for any given values of n . The most interesting values of n are $n = 1, 2$, or 3 . We denote the determinant by $D_n(\mu, \lambda)$.

2.2 Particular Cases

2.21 $n = 1$

The determinant reduces to the single term $\mu + 2p\lambda$, and the corresponding solution is $y = a_0$.

Therefore

$$\left. \begin{aligned} y(x) &= a_0 \\ \mu &= 2\lambda(n_2 - 1) \\ \mu' &= n_2(n_2 + 1) - \lambda^2 \end{aligned} \right\} \quad (3)$$

or

2.22 $n = 2$

$$D_2(\mu\lambda) \equiv (\mu + 2p\lambda)^2 + 2(\mu + 2p\lambda)(n_2 + 1 - 2\lambda) - 4\lambda(n_2 + 1) = 0.$$

Therefore

$$\left. \begin{aligned} \mu &= 2\lambda(n_2 - 1) - (n_2 + 1) \pm \sqrt{(n_2 + 1)^2 + 4\lambda^2} \\ \mu' &= (n_2 + 1)^2 - \lambda^2 \pm \sqrt{(n_2 + 1)^2 + 4\lambda^2} \end{aligned} \right\} \quad (4)$$

To each value of λ there are two polynomial solutions $y(x)$ of the first degree.

2.23 $n = 3$

The expression for μ now becomes more complicated. For simplicity we take $n_2 = 0$, and put $\mu + 6\lambda = \mu_1$.

$$D_3(\mu\lambda) = 32\lambda^3(\mu_1 + 2) - 4\lambda(3\mu_1^2 + 16\mu_1 + 12) + \mu_1^3 + 8\mu_1^2 + 12\mu_1 = 0$$

2.3 All the solutions obtained so far give an expression for $X(\xi)$ which is finite in any interval along the real axis not containing $-\infty$. We shall show that these are the only solutions having this property. There are other solutions expressible in a finite form (when $n_2 \neq 0$), which are bounded in the interval $1 \leq \xi \leq \infty$ but which have a pole of order $n_2/2$ at $\xi = -1$.

We proceed to obtain the most important types of solutions.

3 Solutions which are Finite in the Range $(-2 \leq x \leq 0)$

3.1 If n is a positive integer, the solutions obtained in §2 satisfy the condition. When n is unrestricted such solutions will not be possible, but in either event a non-terminating solution can be found.

We assume a solution of equation (3A) § 1.1 to be of the form

$$y = \sum_0^{\infty} a_n x^n$$

The recurrence relations are

$$\left. \begin{aligned} 2(n_2 + 1)a_1 + (\mu + 2p\lambda)a_0 &= 0 \\ 2(m+1)(m+n_2+1)a_{m+1} \\ + \{m(m+2n_2+1-4\lambda) + \mu + 2p\lambda\}a_m - 2\lambda(m-n)a_{m-1} &= 0 \\ \text{for } m = 1, 2, 3, \end{aligned} \right\} \quad (1)$$

By eliminating the coefficients we obtain an infinite determinantal equation connecting μ , λ and n . This will give a solution whether or not n is an integer. It is necessary to find the radius of convergence of this solution.

Writing (1) in the form

$$\frac{a_{m+1}}{a_m} = - \frac{m(m+2n_2+1-4\lambda) + \mu + 2p\lambda}{2(m+1)(m+n_2+1)} + \frac{2\lambda(m-n)}{2(m+1)(m+n_2+1)} \frac{a_{m-1}}{a_m},$$

we see that $\lim_{m \rightarrow \infty} a_{m-1}/a_m$ is either finite or infinite.

If the limit is finite the radius of convergence is 2 and it is easily seen that the series is divergent at $x = -2$. Choosing the second possibility, the solution becomes an integral function of x .

Let $N_m = a_{m+1}/a_m$ and write the recurrence relation as

$$N_m = -u_m + v_{m-1}N_{m-1}^{-1}$$

The condition that $N_m \rightarrow 0$ can be expressed in the form of the following infinite continued fraction

$$-u_0 = N_0 = \frac{v_0}{u_1 + N_1} = \frac{v_0}{u_1 + \frac{v_1}{u_2 + \frac{v_2}{u_3 + \dots}}} \quad \text{since } N_m \rightarrow 0$$

This continued fraction is convergent* and is the expansion of the infinite determinant obtained by eliminating the coefficients from (1). The series (1), subject to the condition expressed either by the determinant or by the continued fraction, is therefore an integral function of x , and is of course finite in the range $(-2 \leq x \leq 0)$. It is not, however, finite in $(0 \leq x \leq \infty)$. In fact to make $N_m \rightarrow 0$ we must have $N_m \sim \frac{2\lambda}{m}$ and $y(x) \sim e^{2\lambda x}$ for large x . The corresponding function $X(\xi)$ behaves like $e^{\lambda \xi}$ at $+\infty$, and so differs essentially from the solutions discussed in § 2 which tend to zero as $\xi \rightarrow \infty$.

3.2 The other solutions associated with this expansion are of no interest

* Perron, "Die Lehre von den Kettenbrüchen," p. 235

Unless the relation between μ , λ and n is satisfied the solution will only be valid in the circle $|x| = 2$ and the solution is unbounded near $x = -2$. The second root of the indicial equation ($-n_2$) gives a solution unbounded near the origin, and this type of solution is without interest.

4 Solutions in Descending Powers of the Variable

4.1 The chief physical interest lies in the class of solutions $X(\xi)$ which are finite in the range $(1 \leq \xi \leq \infty)$. We have already obtained such solutions in § 2, but it does not follow that these are the only ones satisfying the condition. If $X(\xi)$ is finite in $(1 \leq \xi < \infty)$ then $X(\xi)$ has either no finite singularities or else a singularity at $\xi = -1$. The functions of § 2 are those of the first type, and it remains to determine those of the second type. The obvious expansion is in powers of $(1 + \xi)$. If we expand $y(\xi)$ round $\xi = -1$ the solution will be of the form $y(\xi) = Au \log(\xi + 1) + B(\xi + 1)^{-n_2} v$, if n_2 is an integer, where u and v are infinite series. The solution then has the desired singularity at $\xi = -1$, but the series are not of a simple form, and the conditions at $\xi = 1$ and $\xi = \infty$ will not be easy to satisfy. A more logical method is to expand the solution in descending powers of $(1 + \xi)$. The expansion will then be valid outside the circle $|1 + \xi| = 2$, its infinity condition is satisfied and it only remains to make the solution finite at $\xi = 1$.

4.2 Making the transformation $t = 1/(1 + \xi)$, the equation for y becomes

$$t^2(1 - 2t) \frac{d^2 y}{dt^2} + 2\{(n_2 - 1)t^2 - (n_2 + 2\lambda)t + \lambda\} t \frac{dy}{dt} + \{[(n_2 + 2\lambda)(n_2 + 1) - \mu' - 2\lambda p - \lambda^2]t - 2\lambda(n_2 + 1 - p)\} y = 0 \quad (1)$$

The important range of values is $0 < t \leq \frac{1}{2}$.

We expand y as an ascending series in t

$$y = t^{\rho} \sum_0^{\infty} a_m t^m$$

The indicial equation is $\rho = n_2 + 1 - p$, and so only one integral is regular in this expansion, and even the regular integral is in general divergent.

The recurrence relations giving the coefficients are

$$\left. \begin{aligned} 2\lambda a_1 + \{-(n_2 + 1 - p)(n_2 + 4\lambda + p) \\ + (n_2 + 2\lambda)(n_2 + 1) - \mu' - 2\lambda p - \lambda^2\} a_0 &= 0 \\ 2\lambda m a_m + \{(m + n_2 - p)(m - n_2 - 1 - 4\lambda - p) \\ + (n_2 + 2\lambda)(n_2 + 1) - \mu' - 2\lambda p - \lambda^2\} a_{m-1} \\ - 2 a_{m-2} (m + n_2 - 1 - p)(m - 1 - p) &= 0 \end{aligned} \right\} \quad (2)$$

for $m \geq 2$

These equations give two possibilities. $\lim_{m \rightarrow \infty} a_m/a_{m-1}$ is either infinite or finite. In the first case the series is divergent everywhere, and is the asymptotic expansion of some solution. We must therefore choose the latter alternative

$$\lim_{m \rightarrow \infty} a_m/a_{m-1} = 2$$

The radius of convergence is $\frac{1}{2}$ and we must examine more closely the case $t = \frac{1}{2}$. We can obtain an asymptotic expression for the coefficients by putting $a_m/a_{m-1} = 2(1 - \beta/n)$ and equating powers of m in (2). It is found that $\beta = 1 - n_2$. Therefore for large values of m the coefficients approximate to those in the expansion of $(1 - 2t)^{-n_2}$.

Therefore

$$y \sim t^{n_1+1-p} (1 - 2t)^{-n_2} = (1 + \xi)^{p-1} (1 - \xi)^{-n_2} \quad \text{as } t \rightarrow \frac{1}{2},$$

therefore

$$X(\xi) \sim e^{-\lambda \xi} (1 + \xi)^{n_2/2+p-1} (1 - \xi)^{-n_2/2} \quad \text{near } \xi = 1$$

If $n_2 = 0$ then $y \sim t^{1-p} \log(1 - 2t)$. Therefore $X(\xi)$ has either a pole or a logarithmic singularity at $\xi = 1$, and it is impossible to make $X(\xi)$ bounded as $\xi \rightarrow 1$ by imposing one relation between μ' , λ and p , since $X(\xi)$ is uniformly infinite for all μ' , λ , and p provided the series does not terminate.

It is therefore necessary, and possible, to make the series terminate. It is found that there are two different types of terminating series.

4.31. *The Solutions in a Finite Form*

If the series $y = t^p \sum a_m t^m$ is to terminate, then it is necessary from (2) that

$$(m + n_2 - 1 - p)(m - 1 - p) = 0 \quad \text{for some } m$$

The first factor gives $p - n_2 = n$ a positive integer ≥ 1 . In this case, provided a certain condition between μ' , λ and n is satisfied, the series will be

$$y = t^p \sum_0^{n-1} a_m t^m = t^{1-n} \sum_0^{n-1} a_m t^m \quad n \geq 1$$

y is then a polynomial of degree $(n - 1)$ in ξ , and must be the solution found in § 2. The relation between μ , λ and n is given by § 2.1 equation (2). This solution therefore gives us nothing new.

The second factor gives p to be a positive integer ≥ 1 . The solution then is

$$y = t^{n_1+1-p} \sum_0^{p-1} a_m t^m \quad (p \geq 1)$$

This solution is the product of $(1 + \xi)^{-n_2}$ and a polynomial in ξ of degree

$(p-1)$, and is not included in the previous expansions. It is given by the relations (2) for $m=2, 3$, $(p-1)$, together with

$$\{2\lambda(1-n_2) - \mu' - 2\lambda p - \lambda^2\} a_{p-1} + 2(n_2-1)a_{p-2} = 0$$

Eliminating the coefficients we obtain the following relation between μ , λ and p

$$\left| \begin{array}{ccc} p^2 - p - \mu' + 2\lambda(p - n_2 - 1) - \lambda^2 & 2\lambda & 0 \quad 0 \\ -2(n_2 + 1 - p)(1 - p) & (2 + n_2 - p)(1 - n_2 - 4\lambda - p) & 4\lambda \quad 0 \\ & + (n_2 + 2\lambda)(n_2 + 1) - \mu' - 2\lambda p - \lambda^2 & \\ 0 & -2(n_2 + 2 - p)(2 - p) & \\ 0 & 0 & \end{array} \right| = 0$$

4.32 Special Cases

We can discuss the special cases on exactly similar lines to those employed in § 2.2

1 $p=1$.

$$\mu' = -2n_2\lambda - \lambda^2 \quad (3)$$

2 $p=2$

$$\mu' = 1 - 2n_2 - \lambda^2 \pm \sqrt{1 + 4n_2\lambda + 4\lambda^2} \quad (4)$$

3 If $n_2=1$ we can find an explicit expression for μ'

It is $\mu' = -2p\lambda - \lambda^2$.

4.4 We have yet to prove that there are no further solutions in the range $1 \leq \xi < \infty$

Let the equation for y be written

$$\frac{d^2 y}{dx^2} + P \frac{dy}{dx} + Qy = 0$$

and denote the solution in series given by (2) by y_1

A second solution is given by

$$\begin{aligned} y &= y_1 \int \frac{dx}{y_1^2} e^{-\int P dx} \\ &= y_1 \int \frac{x^{2n_2}}{(1-2x)^{n_2+1}} \frac{e^{2\lambda x}}{y_1^2} dx \end{aligned}$$

Near $t = \frac{1}{2}$

$$y \sim \frac{x^{n_2+1-p}}{(1-2t)^{n_2}} \int \frac{e^{2\lambda x} (1-2x)^{n_2-1}}{x^{2-2p}} dx,$$

and $X(\xi)$ will be finite.

Near $t = 0$

$$y \sim t^{n+1-p} \int \frac{e^{2\lambda x}}{x^{p-2p}} dx,$$

and since $X(\xi) = O(e^{-\lambda\xi} y)$, $X(\xi)$ will be unbounded near $t = 0$. There are therefore no solutions which are not included in the terminating series.

5.1 Relations between the Solutions

We have obtained various types of solutions of the equation and we now summarise our results and state various relations between the solutions.

The fundamental solution is the integral function obtained in § 3.1, subject to a condition expressed by a continued fraction. This solution for $y(x)$ is finite at $x = 0, x = -2$, but behaves like $e^{2\lambda x}$ at infinity. The corresponding function $X(\xi)$ is of the form

$$X_{11}(\xi) = A e^{\lambda\xi} (a_0 + a_1\xi + \dots) + B e^{-\lambda\xi} (b_0 + b_1\xi + \dots),$$

where the infinite series are integral functions of ξ . Neither A nor B can be zero.

From this solution we can obtain a second solution in the usual manner. This second solution $X_{12}(\xi)$ will have the same form at infinity as $X_{11}(\xi)$ but will have singularities at $\xi = \pm 1$. These two associated sets of solutions form a denumerable infinity corresponding to the roots of the infinite continued fraction. There is a third set of solutions which are linear combinations of $X_{11}(\xi)$ and $X_{12}(\xi)$ for the same root of the continued fraction. This type of solution is that obtained in § 4.2 which converges for $|\xi| > 1$. This last type gives a solution finite along the real axis as $\xi \rightarrow \infty$.

$$X(\xi) = e^{-\lambda\xi} \xi^{-n-1+p} \left(c_0 + \frac{c_1}{\xi} + \frac{c_2}{\xi^2} + \dots \right)$$

By changing the sign of λ we obtain another solution

$$X(\xi) = e^{\lambda\xi} \xi^{-n-1-p} \left(d_0 + \frac{d_1}{\xi} + \frac{d_2}{\xi^2} + \dots \right)$$

These last two solutions are normal integrals and are convergent for $|\xi| > 1$. Here again, of course, there is a condition expressed by means of a continued fraction.

None of these solutions is finite in the range $1 \leq \xi \leq \infty$, but by imposing an extra condition we can obtain polynomial solutions for $y(x)$, and hence finite solutions for $X(\xi)$ of the form

$$X(\xi) = e^{-\lambda\xi} (\xi^2 - 1)^{n/2} \sum_{m=0}^{n-1} a_m \xi^m.$$

This completes the specification of the solutions arising from $X_{11}(\xi)$.

The other type of solution arises from the solution mentioned in § 3.2. This solution, which we shall denote by ${}_1X_1(\xi - 1)$, is in ascending powers of $\xi - 1$, has a singularity at $\xi = -1$, and so is only valid inside the circle $|\xi - 1| = 2$. This solution exists for all values of μ except those for which $X_{11}(\xi)$ exists. Also the coefficients in the expansions of ${}_1X_1(\xi - 1)$ and $X_{11}(\xi)$ are the same inside the circle, except that each solution has its appropriate value of μ .

There is a second solution ${}_2X_1(\xi - 1)$ which is finite at $\xi = -1$ and has a singularity at $\xi = 1$. The expansion is therefore valid in the annulus $0 < |\xi - 1| < \infty$. There are corresponding expansions at $\xi = -1$, ${}_1X_2(\xi + 1)$ which is finite at $\xi = 1$ and infinite at $\xi = -1$, and ${}_2X_2(\xi + 1)$ which is infinite at $\xi = 1$ and finite at $\xi = -1$. Only two of these functions are independent. In fact we have

$${}_1X_1(\xi - 1) = {}_1X_2(\xi + 1)$$

$${}_2X_1(\xi - 1) = {}_2X_2(\xi + 1)$$

The only interest we have in these functions is to prove that they are not finite in the real interval $1 \leq \xi \leq \infty$. This is a matter of some difficulty as we cannot obtain explicit expressions for the functions which are valid in the whole of the range in question. We proceed to give the form of the solutions, and then to give a proof of their unsuitability for the physical problem.

With these functions is associated an expansion at infinity. This expansion is the asymptotic one obtained in § 4.2, and is divergent everywhere. There is also another expansion obtained by changing the sign of λ .

The solutions are of the following form

$${}_2X_1(\xi - 1) = A \log(\xi - 1) u_1(\xi - 1) + B(\xi - 1)^{-n_1} v_1(\xi - 1)$$

$${}_1X_2(\xi + 1) = C \log(\xi + 1) u_2(\xi + 1) + D(\xi + 1)^{-n_2} v_2(\xi + 1)$$

When $|\xi|$ is large these two functions must be linear combinations of the asymptotic expansions

$${}_2X_1(\xi - 1) \sim \alpha e^{-\lambda \xi} \xi^{-n_1-1+p} \left(c_0 + \frac{c_1}{\xi} + \dots \right) + \beta e^{\lambda \xi} \xi^{-n_1-1-p} \left(d_0 + \frac{d_1}{\xi} + \dots \right),$$

$${}_1X_2(\xi + 1) \sim \gamma e^{-\lambda \xi} \xi^{-n_2-1+p} \left(c_0 + \frac{c_1}{\xi} + \dots \right) + \delta e^{\lambda \xi} \xi^{-n_2-1-p} \left(d_0 + \frac{d_1}{\xi} + \dots \right).$$

What we have to prove is that none of $\alpha, \beta, \gamma, \delta$ can be zero. We shall only consider the function ${}_1X_1(\xi - 1)$ (or ${}_1X_2(\xi + 1)$) as this is the only function which could give a solution finite in $(1 \leq \xi \leq \infty)$.

The form at infinity of ${}_1X_1(\xi - 1)$ cannot be altered by a change in the value

of μ . Now the two functions ${}_1X_1(\xi - 1)$ and $X_{11}(\xi)$ have the same expansions in the circle $|\xi - 1| = 2$ except that the values of μ are different. By choosing μ suitably ${}_1X_1(\xi - 1)$ becomes $X_{11}(\xi)$ which always involves both exponentials $e^{\lambda\xi}$ and $e^{-\lambda\xi}$. We therefore see that ${}_1X_1(\xi - 1)$ is not finite along the real axis as $\xi \rightarrow \infty$.

We can obtain a solution of the required form by imposing two conditions. This type of solution is obtained in § 4.31 from the asymptotic expansion, it has a pole at $\xi = -1$. In a similar manner we could obtain a solution in a finite form, having a pole at $\xi = 1$.

It may seem at first sight that the solutions in a finite form are incompatible with the fact that ${}_1X_1(\xi - 1)$ and $X_{11}(\xi)$ are unbounded at infinity. This is not so. For definiteness consider $X_{11}(\xi)$. We may write the solution as

$$X_{11}(\xi) = e^{-\lambda\xi} \sum_0^{\infty} a_n \xi^n = e^{-\lambda\xi} y(\xi) \quad \text{if } n_s = 0$$

Our argument shows that if this function is to have no singularities in the finite part of the plane, then $y(\xi) \sim e^{2\lambda\xi}$. If, however, the series for $y(\xi)$ terminates then our argument is invalid, as it depends on the fact that $\frac{a_m}{a_{m-1}}$ exists for all values of $m > 0$.

More precisely, what we have proved is that neither $X_{11}(\xi)$ nor ${}_1X_1(\xi - 1)$ is finite in $1 \leq \xi \leq \infty$ unless it consists of the product of $e^{-\lambda\xi}$ and a terminating series. To make the series terminate requires two conditions.

5.2 Asymptotic Expressions when λ is Large

We can obtain a formal solution of equation (2) § 1 which corresponds to the solution in a finite form found in § 2. Since we have proved that these solutions are finite in the range $-1 \leq \xi \leq 1$ we shall confine ourselves to this range.

For the purpose of obtaining solutions in descending powers of λ , the following transformations are convenient

$$f(\xi) = e^{-\lambda\xi} y(\xi) \quad \text{and} \quad \xi = \cos x$$

The equation for y then is

$$\frac{d^2 y}{dx^2} + \{(2n_s + 1) \cot x + \lambda \sin x\} \frac{dy}{dx} + \{\mu_1 + 2(n_s + 1 - p) \lambda \cos x\} y = 0 \quad (1)$$

where

$$\mu_1 = \mu' + \lambda^2 - n_s(n_s + 1)$$

Owing to the occurrence of the term $\cot x$ this equation is not of Hill's type, and therefore there is no advantage in reducing it to the normal form. The

boundary condition is now replaced by the condition of the solution being periodic

λ is large and positive and we assume solutions of the form

$$y = y_0 + \lambda^{-1} y_1 + \lambda^{-2} y_2 + \\ \mu_1 = \lambda (\mu_1^{(0)} + \mu_1^{(1)} \lambda^{-1} + \mu_1^{(2)} \lambda^{-2} + \dots)$$

If we substitute these expressions in (1) and equate powers of λ we obtain the following set of equations

$$2 \sin x \frac{dy_0}{dx} + \{\mu_1^{(0)} + 2(n_3 + 1 - p) \cos x\} y_0 = 0, \quad (2)$$

$$2 \sin x \frac{dy_1}{dx} + \{\mu_1^{(0)} + 2(n_3 + 1 - p) \cos x\} y_1 + \frac{d^2 y_0}{dx^2} \\ + (2n_3 + 1) \cot x \frac{dy_0}{dx} + \mu_1^{(1)} y_0 = 0, \quad (3)$$

$$2 \sin x \frac{dy_2}{dx} + \{\mu_1^{(0)} + 2(n_3 + 1 - p) \cos x\} y_2 + \frac{d^2 y_1}{dx^2} \\ + (2n_3 + 1) \cot x \frac{dy_1}{dx} + \mu_1^{(1)} y_1 + \mu_1^{(2)} y_0 = 0 \quad (4)$$

The solution of equation (2) is

$$y_0 = (\sin \frac{1}{2} x)^{p-n_3-1-i\mu_1^{(0)}} (\cos \frac{1}{2} x)^{p-n_3-1+i\mu_1^{(0)}}$$

Periodic solutions are then given by

$$\mu_1^{(0)} = 2(p - n_3 - 1 - r), \quad y_0 = (\sin \frac{1}{2} x)^r (\cos \frac{1}{2} x)^{2(p-n_3-1)-r},$$

where $r = 0, 2, 4, \dots, 2(p - n_3 - 1)$, since if r is an even integer the expansions in ξ will be terminating series

Equation (3) then takes the form

$$2 \sin x \frac{dy_1}{dx} + \{\mu_1^{(0)} + 2(n_3 + 1 - p) \cos x\} y_1 \\ + \frac{1}{2} r(r + 2n_3) (\sin \frac{1}{2} x)^{r-2} (\cos \frac{1}{2} x)^{2(p-n_3-1)-r} \\ + \{\mu_1^{(1)} - (p - n_3 - 1)(p + n_3)\} (\sin \frac{1}{2} x)^r (\cos \frac{1}{2} x)^{2(p-n_3-1)-r} \\ + \frac{1}{2} (2p - 2)(2p - 2n_3 - 2 - r) (\sin \frac{1}{2} x)^r (\cos \frac{1}{2} x)^{2(p-n_3-1)-r-2} = 0$$

If y_1 is purely periodic we must have

$$\mu_1^{(1)} = (p + n_3)(p - n_3 - 1)$$

Then

$$y_1 = \frac{1}{2} \left\{ 2 (\operatorname{cosec}^2 \frac{1}{2} x + 2 \log \tan \frac{1}{2} x) (p - 1) (2p - 2n_3 - 2 - r) \right. \\ \left. - (\operatorname{cosec}^2 \frac{1}{2} x + 2 \log \tan \frac{1}{2} x) r (r + 2n_3) \right\} (\sin \frac{1}{2} x)^n (\cos \frac{1}{2} x)^{2(p-n_3-1)-r}$$

To this approximation we have

$$\mu_1 = 2(p - n_3 - 1 - r)\lambda + (p + n_3)(p - n_3 - 1)$$

or

$$\mu' = p(p - 1) + 2(p - n_3 - 1 - r)\lambda - \lambda^2 + O(1/\lambda) \quad (5)$$

If we compare this expression with the explicit values found for particular cases in § 2.2, we see that the constant term in μ' is only correct when $p = n_3 + 1$. The other terms agree in all cases. It is therefore useless to calculate the higher coefficients $\mu_1^{(2)}$, etc.

PART II

6 The Spheroidal Wave Function

If $p = 0$ the equation takes a much simpler form. Many methods are now available for the discussion of the equation which are inapplicable when $p \neq 0$. There will, however, be no solutions in a finite form, and so no solutions which are finite in $1 < \xi < \infty$. All the results of the previous sections which do not depend on $(p - n_3)$ being a positive integer are also true when $p = 0$, but they can usually be obtained more simply. We shall write the equations as

$$\frac{d}{d\xi} \left\{ (1 - \xi^2) \frac{dX}{d\xi} \right\} + \left\{ \lambda^2 \xi^2 - \frac{n_3^2}{1 - \xi^2} + \mu \right\} X = 0, \quad (1A)$$

and $X = (1 - \xi^2)^{n_3/2} f$

$$(1 - \xi^2) \frac{d^2 f}{d\xi^2} - 2(n_3 + 1)\xi \frac{df}{d\xi} + \{\lambda^2 \xi^2 + \mu - n_3(n_3 + 1)\} f = 0 \quad (1B)$$

The equation is similar to Mathieu's equation, and occurs in many physical problems connected with wave motion in spheroids. Solutions are required which are finite for $-1 \leq \xi \leq 1$ or for $1 \leq \xi \leq \alpha$ where α is some finite constant. The equation is well known and has been considered by various writers*. The account which follows is simpler than those referred to, and obtains the results in a more manageable form for physical applications. The methods used subsequently are inapplicable when $p \neq 0$ as they depend on the fact that the expansion proceeds in powers of ξ^2 . The solutions may be either odd or even functions, and can be expanded in powers of ξ or as series of associated Legendre functions. The expansion in Legendre functions has the advantage of rapid convergence when λ is small, but gives rise to complicated expressions. We shall

* NIVEN, 'Phil. Trans.,' A, vol. 171; MACLAURIN, 'Trans. Camb. Phil. Soc.,' vol. 17, ABRAHAM, 'Math. Ann.,' vol. 53; POINCARÉ, 'Quarterly J. Math.,' vol. 49.

be mainly concerned with solutions which are finite in the range $-1 \leq \xi \leq 1$, and this condition determines μ as a function of λ . Unless λ is small this relation is best determined from the series in ξ . Finally we can obtain expansions valid for $|\xi|$ large, and also for λ large. These expansions have not been given before.

7. Expansions in Powers of ξ

There are two different types of series. One an odd series, the other an even series. They refer, however, to different values of μ .

7.1 The Even Series.

If we assume a solution $f = \sum_0^\infty a_{2m} \xi^{2m}$, then we have the recurrence relation

$$(2m+2)(2m+1)a_{2m+2} = \{2m(2m-1) + 4m(n_2+1) - \mu + n_2(n_2+1)\}a_{2m} - \lambda^2 a_{2m-2}$$

Putting $N_m = a_{2m+2}/a_{2m}$ this becomes

$$N_m = \frac{(2m+n_2+1)(2m+n_2) - \mu}{(2m+2)(2m+1)} - \frac{\lambda^2}{(2m+2)(2m+1)} \frac{1}{N_{m-1}} \quad (1)$$

Two cases arise

1 If N_m^{-1} is finite then $\lim_{m \rightarrow \infty} N_m = 1$

The next approximation to N_m is obtained by putting $N_m = 1 - \frac{\alpha}{m}$ in (1)

We find that $\alpha = 1 - n_2$. Therefore for large values of m the coefficients approximate to those in the expansion of $(1 - \xi^2)^{-n_2}$ if $n_2 \neq 0$, and of $\log(1 - \xi^2)$ if $n_2 = 0$. In this case $X(\xi)$ is infinite at $\xi = \pm 1$.

2 If N_m^{-1} is unbounded, then the series represents an integral function, and is therefore finite in the range $-1 \leq \xi \leq 1$. Also $N_m \sim \lambda^2/4m^2$ and $f(\xi) \sim \cosh \lambda \xi$.

The condition that $\lim_{m \rightarrow \infty} N_m = 0$ gives a transcendental equation between μ and λ^2 . We shall obtain this relation in several equivalent forms.

The recurrence relation for the coefficients can be written

$$v_{2m+2} a_{2m+2} + a_{2m} + u_{2m-2} a_{2m-2} = 0$$

where

$$v_{2m+2} = - \frac{(2m+2)(2m+1)}{(2m+n_2+1)(2m+n_2) - \mu}$$

$$u_{2m-2} = - \frac{\lambda^2}{(2m+n_2+1)(2m+n_2) - \mu}$$

Therefore

$$\left. \begin{aligned} v_2 a_2 + a_0 &= 0 \\ v_4 a_4 + a_2 + u_0 a_0 &= 0 \\ v_6 a_6 + a_4 + u_2 a_2 &= 0 \end{aligned} \right\},$$

and so on

The condition $N_m \rightarrow 0$ is equivalent to the vanishing of the following infinite determinant,

$$\begin{vmatrix} 1 & v_2 & 0 & 0 & 0 \\ u_0 & 1 & v_4 & 0 & 0 \\ 0 & u_2 & 1 & v_6 & 0 \\ 0 & 0 & u_4 & 1 & v_8 \\ 0 & 0 & 0 & u_6 & 1 \end{vmatrix} = 0 \quad (2)$$

This determinant is of von Koch's type and is absolutely convergent. The rapidity of convergence is not great enough to enable μ to be calculated easily from the determinant. A more suitable form is obtained by expanding the determinant as a continued fraction, but we can obtain the expansion directly from equation (1)

We have

$$N_{m-1} = \frac{\lambda^2}{(2m + n_2 + 1)(2m + n_2) - \mu - (2m + 2)(2m + 1)N_m},$$

therefore

$$N_0 = \frac{\lambda^2}{(n_2 + 3)(n_2 + 2) - \mu} - \frac{3 \cdot 4 \lambda^2}{(n_2 + 5)(n_2 + 4) - \mu} - \frac{5 \cdot 6 \lambda^2}{(n_2 + 7)(n_2 + 6) - \mu} -$$

since $N_m \rightarrow 0$ as $m \rightarrow \infty$, and since the continued fraction is convergent* for all values of λ and μ . Also $N_0 = a_2/a_0 = \{n_2(n_2 + 1) - \mu\}/2$, and so the equation for μ becomes

$$\begin{aligned} & n_2(n_2 + 1) - \mu \\ &= \frac{1 \cdot 2 \lambda^2}{(n_2 + 3)(n_2 + 2) - \mu} - \frac{3 \cdot 4 \lambda^2}{(n_2 + 5)(n_2 + 4) - \mu} - \frac{5 \cdot 6 \lambda^2}{(n_2 + 7)(n_2 + 6) - \mu} - \end{aligned} \quad (3)$$

* Perron, *loc. cit.*, p. 463.

This is the most symmetrical form of the equation, but we can exhibit its convergence better by dividing by suitable factors

$$\begin{aligned} n_2(n_2+1) - \mu \\ = \frac{1}{1 - \frac{\mu}{(n_2+2)(n_2+3)}} - \frac{2\lambda^2\{(n_2+2)(n_2+3)\}}{1 - \frac{\mu}{(n_2+4)(n_2+5)}} \end{aligned} \quad (4)$$

This is the best form for the relation between μ and λ

The expression which has usually been used for μ is an expansion in ascending powers of λ^2 . The method used by Niven and MacLaurin for obtaining the series is very laborious. The series can be easily obtained from equation (4). The continued fraction has an infinite number of roots and we can approximate to any of these

For simplicity we take $n_2 = 0$

The first root μ_1 for μ is that one for which the zero approximation is $\mu_1 = 0$. If we substitute this value for μ on the right-hand side of (4) we obtain the first approximation $\mu_1 = -\frac{1}{3}\lambda^2$. This can be again substituted on the right and a second approximation obtained. In this way μ_1 can be evaluated to any desired power of λ^2 with very little labour. The result is

$$\mu_1 = -\frac{1}{3}\lambda^2 - \frac{2}{135}\lambda^4 - \frac{4}{3^5}\frac{1}{5}\frac{1}{7}\lambda^6 + \frac{16}{3^7}\frac{1}{5^2}\frac{1}{7^2}\lambda^8 + \dots$$

To find the second root μ_2 we invert the continued fraction into the following form,

$$\begin{aligned} \frac{1}{n_2(n_2+1) - \mu} \\ = 1 - \frac{\mu}{(n_2+2)(n_2+3)} - \frac{2\lambda^2\{(n_2+2)(n_2+3)(n_2+4)(n_2+5)\}}{1 - \frac{\mu}{(n_2+4)(n_2+5)}} \end{aligned}$$

We can then evaluate the root by the same method

When $n_2 = 0$

$$\mu_2 = 6 - \frac{11}{21}\lambda^2 + \frac{94}{(21)^3}\lambda^4 + \dots$$

The roots can be evaluated similarly for any given value of n_2

7.2 The Odd Series

If we assume a solution $f = \sum_0^\infty b_{2m+1} \zeta^{2m+1}$ the recurrence relation for the coefficients is

$$\begin{aligned} (2m+2)(2m+3)b_{2m+3} \\ = \{(2m+n_2+1)(2m+n_2+2) - \mu\}b_{2m+1} - \lambda^2b_{2m-1} \end{aligned} \quad (5)$$

The work is exactly parallel to that in § 7.1, and we shall only give the expression for μ as a continued fraction,

$$(n_2+1)(n_2+2) - \mu = \frac{2 \cdot 3\lambda^2 / \{(n_2+3)(n_2+4)\} \cdot 4 \cdot 5\lambda^2 / \{(n_2+3)(n_2+4)(n_2+5)(n_2+6)\}}{1 - \frac{\mu}{(n_2+3)(n_2+4)} - \frac{\mu}{(n_2+5)(n_2+6)}} \quad (6)$$

By expanding the continued fraction we can obtain the roots $\mu_2, \mu_4, \mu_6, \dots$ as power series in λ^2 .

8. Expansions in Series of Associated Legendre Functions

In this type of expansion we deal directly with $X(\xi)$. The form of the equation suggests the expansion

$$X(\xi) = \sum a_m P_m^{n_2}(\xi)$$

We have the following identity for $\xi^2 P_m^{n_2}(\xi)$

$$\begin{aligned} \xi^2 P_m^{n_2}(\xi) &= \frac{(m-n_2+1)(m-n_2+2)}{(2m+1)(2m+3)} P_{m+2}^{n_2}(\xi) \\ &+ \frac{2m(m+1)-2n_2^2-1}{(2m-1)(2m+3)} P_m^{n_2}(\xi) + \frac{(m+n_2)(m+n_2-1)}{(2m-1)(2m+1)} P_{m-2}^{n_2}(\xi) \end{aligned}$$

There will therefore be two different types of series according as m is even or odd

8.1 The Even Series

$$X(\xi) = \sum_{m=0}^{\infty} a_{2m} P_{2m+n_2}^{n_2}(\xi)$$

By substituting this expression in the differential equation, using the relation for $\xi^2 P_m^{n_2}(\xi)$ and equating to zero the coefficients of the various harmonics, we obtain the following recurrence relation for the coefficients.

$$\begin{aligned} \frac{(2m+2n_2+1)(2m+2n_2+2)}{(4m+2n_2+3)(4m+2n_2+5)} a_{2m+2} \\ + \frac{a_{2m}}{\lambda^2} \left[\mu - (2m+n_2)(2m+n_2+1) + \lambda^2 \frac{(4m+2n_2)(2m+2n_2+1)-2n_2^2-1}{(4m+2n_2-1)(4m+2n_2+3)} \right] \\ + \frac{(2m-1)2m}{(4m+2n_2-3)(4m+2n_2-1)} a_{2m-2} = 0 \quad (1) \end{aligned}$$

There are two possibilities. Either a_{2m+2}/a_{2m} tends to zero or it is unbounded. We must choose the former alternative. As above, this condition is best

expressed by an infinite continued fraction. The expression is very complicated and makes the result of little value except for small values of λ^2 .

We can obtain the series for μ from the continued fraction by successive approximations. The first approximation is obtained by equating to zero the coefficient of a_{2m} in (1). Even for this purpose it is preferable to use the expression found in § 7 as the quantities are less complicated.

8.2 The Odd Series

$$X(\xi) = \sum_{m=0}^{\infty} b_{2m+1} P_{2m+n_1+1}^{n_1}(\xi)$$

Using the same method as in § 8.1 we obtain a recurrence relation for the coefficients. This equation is the same as (1) with $(2m+1)$ written for $2m$. The equation for μ will be given by the corresponding continued fraction.

9 Expansions for Large Values of the Variable

In § 4 we obtained an expansion for $f(\xi)$ round the irregular singularity at infinity. When $p=0$ we can apply the same method. The expansion proceeds in inverse powers of $(\xi+1)$ or $(\xi-1)$, the corresponding solutions being continuations of one another. (Maclaurin has determined an expansion in ξ^{-1} , but this involves four successive coefficients and therefore is not so good as the present one.) We shall only give the expansion in terms of $(1+\xi)$.

Put

$$f(\xi) = e^{\lambda \xi} y_1(\xi)$$

Then as in § 4

$$y_1(\xi) = (1+\xi)^{-n_1-1} \sum_{m=0}^{\infty} a_m (1+\xi)^{-m},$$

where

$$\left. \begin{aligned} 2\lambda a_1 + \{(n_3+1)(n_3-4\lambda) + \mu + \lambda^2 - (n_3+1)(n_3-2\lambda)\} a_0 &= 0 \\ 2\lambda m a_m + \{-(m+n_3)(m-n_3-1+4\lambda) \\ &+ \mu + \lambda^2 - (n_3+1)(n_3-2\lambda)\} a_{m-1} \\ &+ 2(m+n_3-1)(m-1) a_{m-2} &= 0 \end{aligned} \right\} \quad (1)$$

It is usually stated that such an expansion is asymptotic. This is not quite correct. When μ has one of the characteristic values determined in § 7, this series is convergent for $|\xi| > 1$. Otherwise the series is divergent but asymptotic.

By changing the sign of λ we can obtain another expansion

$$f(\xi) = e^{-\lambda \xi} y_2(\xi)$$

10 Asymptotic Expansions for Large Values of λ .

We can obtain two asymptotic expansions by the method used in § 5.2. The work is very similar and will not be given at length.

Putting $f_1(\xi) = e^{\lambda \xi} y_1(\xi)$ and $\xi = \cos x$, and expanding y_1 and μ_1 in powers of λ^{-1} we arrive at the following equations

$$2 \sin x \frac{dy_1^0}{dx} + \{-\mu_1^0 + 2(n_3 + 1) \cos x\} y_1^0 = 0, \quad (1)$$

$$2 \sin x \frac{dy_1^{(1)}}{dx} + \{-\mu_1^{(1)} + 2(n_3 + 1) \cos x\} y_1^{(1)} - \frac{d^2 y_1^0}{dx^2} - (2n_3 + 1) \cot x \frac{dy_1^0}{dx} - \mu_1^{(1)} y_1^0 = 0, \quad (2)$$

and so on

The solution of equation (1) is obtained by taking $\mu_1^0 = 2(r + n_3 + 1)$ where r is an integer, and is

$$y_1^0 = (\sin \frac{1}{2}x)^r / (\cos \frac{1}{2}x)^{2(n_3+1)+r}$$

Since there are terms with negative indices it is not possible to obtain a solution in finite terms. The solution breaks down at $x = \pm \pi$.

Equation (2) now becomes

$$\begin{aligned} 2 \sin x \frac{dy_1^{(1)}}{dx} + \{-\mu_1^{(1)} + 2(n_3 + 1) \cos x\} y_1^{(1)} \\ - \frac{1}{2}r(r + 2n_3) \sin(\frac{1}{2}x)^{r-2} / (\cos \frac{1}{2}x)^{2(n_3+1)+r} \\ - \{\mu_1^{(1)} + n_3(n_3 + 1)\} (\sin \frac{1}{2}x)^r / (\cos \frac{1}{2}x)^{2(n_3+1)+r} \\ - \frac{1}{2}(2n_3 + 2 + r)(\sin \frac{1}{2}x)^r / (\cos \frac{1}{2}x)^{2(n_3+1)+r+2} = 0, \end{aligned}$$

and so $\mu_1^{(1)} = -n_3(n_3 + 1)$

$y_1^{(1)}$ will have the same form as in § 5.2. It is probable that the expansion becomes untrustworthy at this point. For this reason and also because the next approximation is very laborious, we shall not pursue the investigation further.

We have

$$\left. \begin{aligned} \mu &\sim -\lambda^2 + 2\lambda(r + n_3 + 1) + O(1/\lambda) \\ \text{and} \quad f_1(\xi) &= e^{\lambda \xi} y_1 \sim e^{\lambda \cos x} \left\{ (\sin \frac{1}{2}x)^r / (\cos \frac{1}{2}x)^{2(n_3+1)+r} + O(1/\lambda) \right\} \end{aligned} \right\} \quad (3)$$

By assuming a solution $f_2(\xi) = e^{-\lambda \xi} y_2(\xi)$ we can obtain another solution for the same value of μ . This will be obtained by writing $(\pi - x)$ for x in (3).

Therefore

$$f(\xi) = e^{-\lambda \xi} y_2 \sim e^{-\lambda \cos x} \left\{ (\cos \frac{1}{2}x)^r / (\sin \frac{1}{2}x)^{2(n_3+1)+r} + O(1/\lambda) \right\} \quad (4)$$

These solutions fail altogether near certain points, and it is necessary to use the expansion with care. The value for μ is by no means certain, and it is usually necessary to use the continued fraction (4) § 7 to check any results obtained from the asymptotic expansion.

Any solution of the equation can be expressed as a linear combination of these two solutions f_1, f_2 . To obtain the odd and even solutions of § 7 we must satisfy the following relations,

$$f(\xi) = f(\pi - \xi) \text{ for the even functions,}$$

and

$$f(\xi) = -f(\pi - \xi) \text{ for the odd functions}$$

Our approximations do not distinguish between the values for μ corresponding to the even and odd functions, which are

$$f_1(\xi) + f_2(\xi) \text{ an even function,}$$

and

$$f_1(\xi) - f_2(\xi) \text{ an odd function}$$

The Ionised Hydrogen Molecule

By A. H. WILSON, B.A., Emmanuel College, Cambridge

Communicated by R. H. Fowler, F.R.S.—Received December 19, 1927.)

1. Introduction

The model which has been proposed for the ion of the hydrogen molecule H_2^+ , consists of one electron and two protons. Since the mass of the electron is negligible compared with that of the protons, we may, to a first approximation, consider the protons as at rest. The system is then a particular case of the problem of three bodies, and can be solved completely classically. This has been done by Pauli,* and more recently by Niessen†. The value obtained by Pauli for the energy of the normal state is not in agreement with the experimental result inferred from the ionisation potential and heat of dissociation of the molecule. Niessen obtains the experimental result by the introduction of half integer quantum numbers.

* 'Ann d Physik,' vol. 68, p. 177 (1921).

† 'Z f Physik,' vol. 43, p. 604 (1927).

The classical problem is separable in elliptic co-ordinates, and so if we apply Schrödinger's method to the system we shall obtain a wave equation which is separable in the same co-ordinates. The resulting differential equations can be solved exactly. This is the only three-body problem which admits of an exact solution, and it is of interest to obtain an analytical result, and not merely one obtained by a perturbation method, which it may be difficult to justify.

In the present paper the differential equations defining the system are obtained in § 2, and their relevant properties stated in § 3. In § 4 we discuss the relation between the equations, and obtain values for the energies of the various states. Several surprising results appear. In the first place no solution is in general possible. Solutions will only occur for certain distances apart of the nuclei. In the second place it seems probable that these states are illusory, and that there are no positive distances of the nuclei which give states. The difficulties raised are examined in §§ 5 and 6.

2.1 *The Differential Equations of the Problem of Two Fixed Centres*—The ionised hydrogen molecule possesses nine degrees of freedom, and so nine co-ordinates are necessary to specify its configuration. These may be taken as the co-ordinates x, y, z of the electron mass m , and $\xi_1, \eta_1, \zeta_1, \xi_2, \eta_2, \zeta_2$ of the two nuclei both of mass M . If r_1, r_2 are the distances of the electron from the nuclei and r_{12} the distance apart of the nuclei, then the wave equation for the system is

$$\frac{1}{m} \nabla_{xyz}^2 \psi + \frac{1}{M} \nabla_{\xi_1 \eta_1 \zeta_1}^2 \psi + \frac{1}{M} \nabla_{\xi_2 \eta_2 \zeta_2}^2 \psi + \frac{8\pi^2}{h^2} \left(E + \frac{e^2}{r_1} + \frac{e^2}{r_2} - \frac{e^2}{r_{12}} \right) \psi = 0,$$

where E is the energy.

It is not possible to solve this wave equation completely, but it can be split up into successive approximations* since m/M is very small. The zero approximation will be given by

$$\frac{1}{m} \nabla_{xyz}^2 \psi + \frac{8\pi^2}{h^2} \left(E + \frac{e^2}{r_1} + \frac{e^2}{r_2} - \frac{e^2}{r_{12}} \right) \psi = 0$$

To this approximation ψ only contains $\xi_1, \eta_1, \zeta_1, \xi_2, \eta_2, \zeta_2$ as parameters, and for the purpose of solving the equation we can treat these quantities as fixed. When the equation has been solved we obtain E as a function of the above six parameters, and to obtain a stable state of the molecule we must choose them so as to make E a minimum. This is equivalent to quantising the nuclei to a zero approximation, and determines the possible distances apart of the nuclei.

Since r_{12} is supposed fixed for the purposes of the calculation of ψ we need not

* M. Born u. J. Oppenheimer, 'Ann. d. Physik,' vol. 84, p. 457 (1927).

mention explicitly the term e^2/r_{12} . We can take it into account afterwards or consider it absorbed into the term E . In future we shall adopt that convention which seems most suitable for the purpose in hand. The three-body problem has now been reduced to a one-body problem, and we proceed to solve this restricted wave equation.

We consider a slightly more general problem than the ion H_2^+ , and deal with one electron under the action of two nuclei with atomic numbers Z_1, Z_2 , which are at a distance $2c$ apart. The electron is treated as a point charge.

We use elliptic co-ordinates

$$\xi = (r_1 + r_2)/2c, \quad \eta = (r_1 - r_2)/2c,$$

where r_1, r_2 are the distances of the electron from the nuclei. The third co-ordinate is the azimuth ϕ round the line of centres. The ranges of the co-ordinates are

$$\begin{aligned} 1 &< \xi < \infty \\ -1 &\leq \eta \leq 1 \\ 0 &\leq \phi \leq 2\pi \end{aligned}$$

The potential energy of the electron is

$$\begin{aligned} V &= -e^2 (Z_1/r_1 + Z_2/r_2) \\ &= -\frac{e^2}{c(\xi^2 - \eta^2)} [(Z_1 + Z_2)\xi - (Z_1 - Z_2)\eta], \end{aligned}$$

$\nabla^2\psi$ can easily be transformed to these co-ordinates by means of Gauss' theorem, and Schrodinger's equation

$$\nabla^2\psi + \frac{8\pi^2m}{h^2} (E - V)\psi = 0,$$

where E is the energy, becomes

$$\begin{aligned} \frac{\partial}{\partial \xi} \left\{ (\xi^2 - 1) \frac{\partial \psi}{\partial \xi} \right\} + \frac{\partial}{\partial \eta} \left\{ (1 - \eta^2) \frac{\partial \psi}{\partial \eta} \right\} + \left\{ \frac{1}{\xi^2 - 1} + \frac{1}{1 - \eta^2} \right\} \frac{\partial^2 \psi}{\partial \phi^2} \\ + \frac{8\pi^2mc^2}{h^2} \left[E(\xi^2 - \eta^2) + \frac{e^2}{c} \{ (Z_1 + Z_2)\xi - (Z_1 - Z_2)\eta \} \right] \psi = 0 \end{aligned}$$

ψ must be finite, continuous, and single valued in the three-dimensional space ξ, η, ϕ . The equation is separable and so we put

$$\psi = \Phi(\phi) X(\xi) Y(\eta),$$

therefore

$$\Phi(\phi) = \begin{Bmatrix} \cos \\ \sin \end{Bmatrix} n_\phi \phi,$$

where n_2 is a positive integer,

$$\frac{d}{d\xi} \left\{ (1 - \xi^2) \frac{dX}{d\xi} \right\} + \left\{ \lambda^2 \xi^2 - \kappa \xi - \frac{n_2^2}{1 - \xi^2} + \mu \right\} X = 0, \quad (1)$$

$$\frac{d}{d\eta} \left\{ (1 - \eta^2) \frac{dY}{d\eta} \right\} + \left\{ \lambda^2 \eta^2 - \kappa' \eta - \frac{n_2^2}{1 - \eta^2} + \mu \right\} Y = 0, \quad (2)$$

where

$$\left. \begin{aligned} \lambda^2 &= -8\pi^2 mc^2 E / h^2 \quad (\lambda > 0) \\ \kappa &= 8\pi^2 mce^2 (Z_1 + Z_2) / h^2 \\ \kappa' &= 8\pi^2 mce^2 (Z_1 - Z_2) / h^2 \end{aligned} \right\}, \quad (3)$$

μ and λ must be determined so that the equations (1) and (2) have finite and continuous solutions in the ranges $1 \leq \xi \leq \infty$, $-1 \leq \eta \leq 1$

2.2. Before proceeding to the solutions of the equations (1) and (2) we can obtain an insight into their nature by considering some special cases

(1) If $Z_2 = 0$ then $\kappa = \kappa'$ and equations (1) and (2) are identical. The characteristics, or energies, are those of an atom with nuclear charge $Z_1 e$ and one electron $-e$. The solution $X(\xi)$ is bounded for $1 \leq \xi \leq \infty$. If it is also bounded in $-1 \leq \xi \leq 1$, then the same function of η is a solution of equation (2). This is actually the case, and so both μ and λ must be separately determinable from a single differential equation.

(2) If $Z_1 = Z_2 = 1$ we have $\kappa' = 0$. This corresponds to the molecule H_2^+ . Equation (1) is the same as for the helium ion He^+ . The energy E may therefore take values which are included in those of He^+ . For such energies μ and λ will be determined by this equation alone. Equation (2) will give a further condition for μ in terms of λ , and this condition, together with the two derived from (1), should determine both E and c .

The method we adopt is to determine μ so that equation (2) should have a finite solution, and also so that (1) has a finite solution. This will give two distinct expressions for μ , and the common roots ought to determine the possible energies.

In §§ 3 and 4 we apply the ordinary Schrodinger theory, but do not obtain the experimental result. In § 6 we lighten the restrictions on ψ , and then obtain something near the experimental values.

3 Properties of the Functions $X(\xi)$ and $Y(\eta)$

The equations take essentially different forms according as κ (or κ') is or is not zero. If κ is zero then the differential equation is that of the spheroidal wave function, and offers no analytical difficulties. If κ is not zero, solutions of an

entirely different type are possible which are finite in the range $1 < \xi < \infty$. These functions have been studied in detail by the author* with a view to the special applications here. The general properties will be stated here, while particular results will be quoted when they become necessary.

3.1 $\kappa \neq 0, \kappa' \neq 0$

We put $X(\xi) = (\xi^2 - 1)^{n/2} e^{-\lambda \xi} y(\xi)$

The solutions which are finite in $1 < \xi < \infty$ are of two types, and in both $y(\xi)$ consists of a terminating series

Those of the first type are also finite in $-1 < \xi < 1$, and the corresponding solutions are suitable solutions for $Y(\eta)$

$$y(\xi) = \sum_0^{n-1} a_m \xi^m$$

The conditions to be satisfied by λ and μ are that

$$\frac{\kappa}{2\lambda} = n + n_2 \quad (n \geq 1)$$

where n is an integer, and μ is given by a complicated function of λ that can be found for each value of n and which is of the n th degree in μ .

The second type of solution only exists when $n_2 \neq 0$, and $y(\xi)$ has a pole of order n_2 at $\xi = -1$

$$y(\xi) = (1 + \xi)^{-n_2} \sum_0^{p-1} b_m \xi^m$$

In this case

$$\frac{\kappa}{2\lambda} = p \quad (p \geq 1)$$

where p is an integer and μ is a function of λ of the p th degree in μ .

The first type of solution is a possible one for $Y(\eta)$, but there are other types possible. $Y(\eta)$ may be an integral function of η , in which case there is a relation between μ and λ expressed by means of an infinite continued fraction

3.2 $\kappa = 0, \kappa' = 0$

If $\kappa = 0$ there are no functions $X(\xi)$ finite in $1 < \xi < \infty$

If $\kappa' = 0$, $Y(\eta)$ must be an integral function, and μ is given in terms of λ by an infinite continued fraction. When λ^2 is small we can approximate to the roots of the fraction by series in powers of λ^2 .

These results will be found set out in detail in the paper referred to. The explicit forms of the solutions will be given when it is necessary to use them.

* A. H. Wilson, *supra*, p. 617

4 *Special Cases of the Two-Centre Problem.*

We discuss three special cases $Z_1 = 1, Z_2 = 0, Z_1 = 1, Z_2 = 1, Z_1 = 2, Z_2 = 1$. The first is simply the hydrogen atom, while the second is the ionised molecule. The treatment of the atom is given to show the connection between the ion H_2^+ and the ion He^+ .

4.1 $\kappa = \kappa'$

The equations for $X(\xi)$ and $Y(\eta)$ are identical in form

Solutions are given by

$$X(\xi) = (\xi^2 - 1)^{\mu/2} e^{-\lambda\xi} y(\xi), \quad Y(\eta) = (1 - \eta^2)^{\mu/2} e^{-\lambda\eta} y(\eta)$$

where

$$y(\xi) = \sum_0^{n-1} a_m \xi^m$$

The energy is determined by

$$\frac{\kappa}{2\lambda} = n + n_2 \quad (n \geq 1) \quad (1)$$

If $Z_1 = 1, Z_2 = 0$ this gives

$$-E = \frac{R\lambda}{(n + n_2)^2}$$

where n is an integer ≥ 1 , R is the Rydberg constant μ is the same function of λ for both equations, and a knowledge of its exact form is unnecessary. This is just the usual result for the energy.

The other types of solution do not give simultaneously solutions of both equations, and must be disregarded.

4.2 $\kappa \neq 0, \kappa' = 0$

When $Z_1 = Z_2$ this gives the most interesting case, the ion H_2^+ . The equation for $X(\xi)$ will be identical with that corresponding to the helium ion He^+ . Solutions will be given as in § 4.1 by $\kappa/2\lambda = n + n_2$.

The function $Y(\eta)$ will now take a different form. It may be either an even or an odd function. In both cases it must be an integral function. This will give a relation between μ and λ expressed by a continued fraction.

We wish to determine the state with lowest energy, and so we take $n_2 = 0$, and consider the even series for $Y(\eta)$. The relation between μ and λ then is

$$-\mu = \frac{1}{2} \frac{2\lambda^2}{3} - \frac{3}{2} \frac{4\lambda^2}{3 \cdot 4 \cdot 5} + \frac{5}{4} \frac{6\lambda^2}{5 \cdot 6 \cdot 7} - \dots \quad (2)$$

$$1 - \frac{\mu}{2 \cdot 3} - 1 - \frac{\mu}{4 \cdot 5} - 1 - \frac{\mu}{6 \cdot 7} - \dots$$

4.21. The state with the greatest negative energy is given by $n = 1$

The conditions arising out of the ξ equation are

$$\kappa/2\lambda = 1 \quad \text{and} \quad \mu = -\lambda^2$$

If we substitute $\mu = -\lambda^2$ in (2) it seems probable that there is no real solution except $\lambda = 0$. The same is true if we use the odd series for $Y(\eta)$. We can prove this directly from the equation as follows.

Consider the equation

$$\frac{d}{d\eta} \left\{ (1 - \eta^2) \frac{dy}{d\eta} \right\} - \lambda^2 (1 - \eta^2) y = 0,$$

the boundary condition being that y is finite at $\eta = \pm 1$.

Then

$$\begin{aligned} \int_{-1}^1 y \left[\frac{d}{d\eta} (1 - \eta^2) \frac{dy}{d\eta} - \lambda^2 (1 - \eta^2) y \right] d\eta &= 0 \\ &= \left[(1 - \eta^2) y \frac{dy}{d\eta} \right]_{-1}^1 - \int_{-1}^1 (1 - \eta^2) \left[\left(\frac{dy}{d\eta} \right)^2 + \lambda^2 y^2 \right] d\eta, \end{aligned}$$

and this cannot be true with $\lambda^2 > 0$.

Therefore a necessary condition for $Y(\eta)$ to be finite in $-1 \leq \eta \leq 1$ is that $\mu > -\lambda^2$ when $n_2 = 0$.

This solution which ought to lead to the lowest stationary state is therefore ruled out except when $\lambda = 0$. The energy is then $-E = 4R\lambda$, the lowest energy of the helium ion.

4.22. We now consider the state given by $n = 2$.

The conditions arising from the ξ equation are

$$\frac{\kappa}{2\lambda} = 2 \quad \text{and} \quad \mu = 1 - \lambda^2 \pm \sqrt{1 + 4\lambda^2}$$

Since $\mu > -\lambda^2$ is a necessary condition for the existence of $Y(\eta)$ we must take the $+$ sign in μ .

If we attempt to find λ from this condition and from (2), we find that there are no roots when λ is small, but that the two expressions for μ tend to equality for rather large values of λ . It does not seem possible to determine for what values of λ , if any, the two expressions for μ become equal. To do this we should have to tabulate μ for large values of λ , and the work involved in using (2) to a large number of terms would be prohibitive. An alternative method is to use an asymptotic expression for μ . Such an expression can be obtained and is

$$\mu \sim -\lambda^2 + 2\lambda(r + n_2 + 1) + O(1/\lambda) \quad (r \text{ an integer})$$

The term independent of λ in this expansion is doubtful, and so no exact results can be inferred. All that can be said is that the two expressions for μ tend to equality (with $r=0$) as λ becomes large. The corresponding solution may belong either to the molecular ion or to the hydrogen atom.

Two asymptotic solutions for $Y(\eta)$ are given by

$$Y_1(\eta) \sim e^{\lambda \cos x} \{(\sin \frac{1}{2}x)^r/(\cos \frac{1}{2}x)^{r+2} + O(1/\lambda)\}$$

and

$$Y_2(\eta) \sim e^{-\lambda \cos x} \{(\cos \frac{1}{2}x)^r/(\sin \frac{1}{2}x)^{r+2} + O(1/\lambda)\},$$

where $\eta = \cos x$ and we are supposing $n_3 = 0$.

Also $Y_1(\eta) + Y_2(\eta)$ is an even function of η , and $Y_1(\eta) - Y_2(\eta)$ is an odd function. If we use either of the last two functions we shall obtain a state of the molecular ion, as $Y(\eta)$ is then large near $\eta = \pm 1$ and small elsewhere. If we use $Y_1(\eta)$ we then have a wave function which is only apparent near $\eta = -1$, and $Y_2(\eta)$ gives a wave function apparent near $\eta = 1$. These last two solutions correspond to a hydrogen atom perturbed by a very distant nucleus. In these types of stationary states the electron is in an orbit near one nucleus for a long time and then passes over to the other nucleus for the same period. Such orbits are of no interest for the ionised molecule.

We cannot actually decide whether there is a state of the ion corresponding to this solution, but even if there is, it cannot give the experimental result for the lowest energy.

Let us denote the energy of the electron by E_{el} . Then there is also the energy due to the repulsion of the nuclei. This is $e^2/2c$. The total energy $E = E_{el} + e^2/2c$. If I is the ionisation potential of the molecule H_2 , then $-E + I$ is the total work to be done to remove all the components to infinity. This work is also $D + 2R\hbar$, where D is the energy of dissociation of the molecule into atoms. Therefore

$$I - E_{el} - e^2/2c = D + 2R\hbar$$

In the particular case we are considering $-E_{el} = R\hbar$. Therefore

$$I = R\hbar + D + e^2/2c$$

D is known to be about 4.4 volts. This gives I a lower limit of 18 volts however large c may be. There seems to be general agreement that I is just less than 16 volts, and so even if the state exists, it cannot give the experimental result. Also any value of $\kappa/2\lambda > 2$ will give a still higher value of I and deviate still further from the required value.

4.23 The investigation for higher values of n is difficult on account of the complicated relations for μ . It is certain, however, that no solutions exist for small values of λ .

The other types of solution for $X(\xi)$ furnish no values of μ common to the two equations. It therefore seems probable that the system admits of no stationary states

$$4.3 \quad \kappa \neq \kappa' \neq 0$$

We consider the two-centre problem given by $Z_1 = 2$, $Z_2 = 1$. Since the equations connecting μ and λ will be algebraic equations, we ought to be able to decide definitely the existence or non-existence of stationary states

$X(\xi)$ and $Y(\eta)$ will consist of the product of $e^{-\lambda\xi}$ or $e^{-\lambda\eta}$ and a terminating series. To find the lowest state we take $n_3 = 0$ and make $-E$ a maximum

The largest value of $-E$ for which the equation for $Y(\eta)$ admits of a solution is given by $\kappa'/2\lambda = 1$. This necessitates $\kappa/2\lambda = 3$. We then have in addition two relations between λ and μ

From the equation for $X(\xi)$ we have

$$32\lambda^3(\mu_1 + 2) - 4\lambda(3\mu_1^2 + 16\mu_1 + 12) + \mu_1^3 + 8\mu_1^2 + 12\mu_1 = 0,$$

where $\mu_1 = -\mu - \lambda^2 + 4\lambda$

From the η equation we have $\mu = -\lambda^2$ or $\mu_1 = 4\lambda$

Eliminating μ_1 from these equations we have

$$\lambda = 0$$

The common roots are therefore $\lambda = 0$ and $\lambda = \infty$. Neither of these values gives a solution of the two-centre problem. It is not possible to treat the general case in this manner, but it seems probable that no solutions exist

5. From the results of the previous sections it is only possible to draw the conclusion that it is not correct to treat the problem of two centres in this manner. The question then arises what attitude we are to take towards the difficulty. Several attempts have been made to determine the states, and we shall examine these

Burrau* used the equations of § 2.1 and obtained their characteristic numbers by numerical integration. Equation (2) presents no difficulties either in the numerical method or in the exact analytical investigation. Equation (1) presents many difficulties from the analytical side, and is not satisfactorily solved in Burrau's paper. His method is to transform the equation into a Riccati equation and then to solve this numerically. In his treatment of equation (1) he expands the Riccati equation round the irregular singularity at infinity. This expansion will in general be divergent, but nevertheless asymptotic. To make it convergent will require an extra condition to be imposed on μ . Burrau

* 'K. Danske Vid. Selskab,' vol. 7, No. 14 (1927)

does not justify the use of the asymptotic series, and it is probable that this invalidates his solution. He obtains the experimental result for the lowest energy, but his equations are equivalent to those used here, and the analytical solutions show no results corresponding to his.

Hund* attempted to obtain qualitative information about the term spectrum of the two centre problem by considering the transition from infinitely distant nuclei to coincident nuclei. To do this he considers a one-dimensional problem, and then generalises it to separable systems. The equations of the two-centre problem are not of the type he considers. However, he only uses these results to prove that, during the passage from infinitely distant nuclei to proximate nuclei, no terms are lost. We can prove this for each of the equations (1) and (2) by means of their asymptotic expansions for large λ . The form of the solution of (1) is independent of the value of λ , and cannot be affected by the transition. The corresponding result for equation (2) has already been proved in § 4.22. When λ is large the electron may be in the neighbourhood of either nucleus. The argument in § 4.22 shows that when λ is small we shall have two characteristic functions, one even and one odd, corresponding to each state when λ is large. The states which exist for large λ must be given weight 2, as the electron has two possible orbits of equal energy round the two nuclei. The number of states, therefore, remains the same.

Unsold† has obtained the energy of the normal state by a perturbation method. He considers a hydrogen atom perturbed by a proton and calculates the additional energy by successive approximations. The difficulty about this method lies in the convergence. Unsold finds that the second approximation is nearly twice as large as the first, and has the opposite sign. Nevertheless he obtains the experimental result, but does not discuss the third approximation.

In the previous sections we have seen that the solutions $X(\xi)$ which are finite in $1 \leq \xi < \infty$ do not give any states of the system. This is due to the fact that two conditions are necessary to make $X(\xi)$ finite, whereas we should expect that only one condition is necessary. We should expect the electronic motion to contribute two restrictions, one from each of the equations $X(\xi)$ and $Y(\eta)$. We would then be able to quantise the nuclei by making the total energy a minimum. But since the electronic motion furnishes three restrictions, there are no parameters available for quantising the nuclei. It is also suggestive that Burrau has obtained good agreement with experiment by imposing only two conditions.

* 'Z f Physik,' vol. 40, p. 743 (1927).

† 'Z f Physik,' vol. 43, p. 563 (1927).

If we allow such a procedure we must abandon our restriction that ψ must be finite throughout the whole space

In the next section we deal with wave functions which are not finite everywhere

6 The Energy of the Normal State

If we allow ψ to become infinite, we have a much larger class of functions to deal with. If ψ is to have any physical significance it seems necessary that it should vanish at infinity. We do not, however, demand that ψ should be finite at $\xi = 1$.

Such solutions are best obtained in descending powers of the variable. If we put

$$X(\xi) = (\xi^2 - 1)^{n/2} e^{-\lambda \xi} y(\xi)$$

and

$$t = (1 + \xi)^{-1},$$

then

$$y(t) = t^{n+1-\kappa/2\lambda} \sum_0^{\infty} a_m t^m,$$

where

$$\begin{aligned} 2\lambda m a_m + \left\{ \left(m + n_3 - \frac{\kappa}{2\lambda} \right) \left(m - n_3 - 1 - 4\lambda - \frac{\kappa}{2\lambda} \right) \right. \\ \left. + (n_3 + 2\lambda)(n_3 + 1) - \mu - \kappa - \lambda^2 \right\} a_{m-1} \\ - 2a_{m-2} \left(m + n_3 - 1 - \frac{\kappa}{2\lambda} \right) \left(m - 1 - \frac{\kappa}{2\lambda} \right) = 0 \quad (1) \end{aligned}$$

We can write this in the form

$$N_{m-1} + u_{m-1} - v_{m-2} N_{m-2}^{-1} = 0$$

where

$$N_{m-1} = \frac{a_m}{a_{m-1}}$$

If the series is to have a non-zero radius of convergence we must choose μ so as to make $\lim_{m \rightarrow \infty} N_m = 2$. This condition can be expressed in the form of a continued fraction

$$N_1 = a_1/a_0 = -u_0 = v_0/(u_1 + N_1) = \frac{v_0}{u_1 + u_2 + u_3 + \dots} \quad (2)$$

This infinite continued fraction is convergent, and so we can use it to determine the values of μ which give a solution of the required type. Although this solution is finite as $\xi \rightarrow \infty$ along the real axis, it is not finite at $\xi = 1$. The second approximation to N_m is

$$N_m = 2 \{ 1 - (1 - n_3)/m \}$$

Near $\xi = 1$, $X(\xi)$ behaves like $(\xi - 1)^{-1/2}$ or like $\log(\xi - 1)$ and so does not fulfil the condition of being bounded. In spite of this lack of boundedness we shall use this type of solution, and calculate the energy it gives for the normal state.

The continued fraction (2) is in the form adapted for the calculation of the smallest characteristic number, and on putting $n_3 = 0$ it becomes

$$\frac{\mu + 2p\lambda + \lambda^3 - 2\lambda + (1-p)(4\lambda + p)}{2\lambda} = \frac{2(1-p)^2}{(2-p)(1-4\lambda-p) + 2\lambda - \mu - 2p\lambda - \lambda^3 +} \frac{8\lambda(2-p)^2}{(3-p)(2-4\lambda-p) + 2\lambda - \mu - 2p\lambda - \lambda^3 +} \quad (3)$$

where $p = \kappa/2\lambda$.

We can obtain another relation for μ from § 4.2 equation (2), arising out of the equation for $Y(\eta)$. This second relation is also in the form of an infinite continued fraction. In this case, however, we can easily approximate to the roots by expressing μ as a series in powers of λ^2 . The lowest root is given by

$$\mu = -\frac{1}{3}\lambda^2 - \frac{2}{135}\lambda^4 - \frac{4}{3^5 5 \cdot 7}\lambda^6 + \frac{16}{3^7 5^3 7^2}\lambda^8 + \quad (4)$$

These two expressions (3) and (4) determine p as a function of λ . It is possible to approximate to (3) by a series, but the expansion is of little value, as the convergence is slow owing to the presence of the terms involving p . At this stage it is best to adopt a numerical method. If λ is not too large we can obtain an accurate value of μ from (4) and substitute this in (3). For any given value of λ an approximate value of p can be obtained by inspection, and then the successive convergents of the fraction can be calculated, and the error can be roughly determined. By several trials p can be calculated accurately. Using this method a few values of p have been rather roughly computed, and the values obtained lie quite close to those obtained by Burrau. Although these results do not agree entirely with Burrau's, the agreement is sufficient to make it fairly certain that it is the present type of function that Burrau has used. Burrau obtains values of E_n for various values of c . He then adds the nuclear energy $e^2/2c$ and then determines c by making this total energy a minimum. Burrau's method gives a value for the energy which, considering the complicated motion of the nuclei, is in good agreement with the experimental result. We may therefore safely assume that the present method leads to the correct result. The actual calculation has not been carried out, as it would not lead to a result materially different from Burrau's, and also because ψ does not satisfy the condition of being bounded.

It is difficult to see what the physical significance can be of a wave function which becomes logarithmically infinite. The infinity is certainly not a very large one, but for states in which the rotational quantum number is not zero the wave function has a pole of order $n_2/2$. A similar difficulty arises in the theory of the relativistic hydrogen atom. In this problem ψ involves a factor $r^{-\lambda}$ where λ is a small positive constant, and ψ is infinite at the nucleus. In neither problem is there any obvious interpretation of the infinity.

In conclusion I should like to thank Mr R. H. Fowler very much for many helpful discussions and criticisms.

The Band Spectrum of Water Vapour—II

By DAVID JACK, M.A., B.Sc., Assistant and Carnegie Teaching Fellow, The University, St. Andrews

(Communicated by O. W. Richardson, F.R.S.—Received February 17, 1928)

1 *New Measurements of the Band λ 3428*

In a previous communication* on the band spectrum of water vapour reference was made to some measurements by Tanaka† on the band 3428. The author has since measured and analysed this band. The experimental arrangements were the same as for the work on the band 2608. Two plates exposed for about one hour were measured, and the results showed close agreement. The dispersion obtained, 8.0 Å per millimetre, was inferior to that in the band 2608, but the consistency of the measurements indicates that errors are unlikely to exceed 0.05 Å, while the probable error is considerably less. Overlapping of lines is somewhat more troublesome in the band 3428, and consequently there is a slightly increased tendency to irregularities in the results.

Details of the band are given in Table I, arranged as for the band 2608. Some fairly strong lines present on the plates are not accounted for in the table.

Comparison of the term differences in this band with those in the bands previously analysed shows that the initial terms are the same for the two bands 3428 and 3064, and the final terms are the same for the three bands 3428, 3122 and 2875. This is in agreement with the scheme already given‡. The following

* 'Roy. Soc. Proc.,' A, vol. 115, p. 373 (1927).

† 'Roy. Soc. Proc.,' A, vol. 108, p. 594 (1925).

‡ *Loc. cit.*

assignment of vibrational quantum numbers may be made,* where n' denotes the initial, and n'' the final quantum number

$n' \backslash n''$	0	1
0	3064	3428
1	2811	3122
2	2608	2875

The bands in any column form an n' progression, i.e., a collection of bands in which n'' is constant and n' has different values for different bands of the progression, the bands in any row form an n'' progression

Table I -- Band λ 3428

m	$P_1(m)$					$P_2(m)$				
	I	$\lambda(\text{air})$	$\eta(\text{vac})$	Δ	Δ^2	I	$\lambda(\text{air})$	$\eta(\text{vac})$	Δ	Δ^2
2	5	3477.29	28749.8	-29.4		1	3462.54	28872.3	-48.5	
3	5	3480.86	28790.4	29.0	+0.4	9	3468.13	28825.8	48.2	+0.3
4	8	3484.38	28691.4	33.2	-4.2	5	3473.69	28779.6	45.9	0.3
5	8	3488.41	28658.2	37.3	4.1	5	3479.25	28733.7	46.1	-0.2
6	5	3492.95	28620.9	37.6	0.3	6	3484.84	28687.6	45.9	+0.2
7	6m	3497.55	28583.3	41.9	4.3	5	3490.41	28641.7	48.9	-3.0
8	4m	3502.68	28541.4	45.7	3.8	2	3496.38	28592.8	47.1	+1.8
9	3	3508.30	28495.7	45.5	+0.2	1	3502.15	28545.7	50.0	-2.9
10	5	3513.92	28450.2	47.4	-1.9	3	3508.30	28495.7	50.6	0.6
11	4	3519.78	28402.8	52.9	5.5	0	3514.54	28445.1	52.8	2.2
12	1	3526.35	28349.9	49.7	+3.2	5	3521.08	28392.3	51.6	+1.2
13	1m	3532.53	28300.2	51.1	-1.4	2	3527.50	28340.7	55.5	-3.9
14	0	3538.93	28249.1	53.5	2.4	0	3534.41	28285.2	55.8	0.3
15	2m	3545.64	28195.6	58.0	4.6	3	3541.40	28229.4	59.1	3.3
16	0	3552.96	28137.6			0	3548.63	28170.3		

* This is an extension of the values given on p 188 of "Molecular Spectra in Gases," (National Research Council)

Table I—(continued)

m	Q ₁ (m)					Q ₂ (m)				
	I	$\lambda(\text{air})$	$\nu(\text{vac})$	Δ	Δ^2	I	$\lambda(\text{air})$	$\nu(\text{vac})$	Δ	Δ^2
2	5	3473.25	28783.3			7	3458.48	28906.2		
3	8	3472.53	28789.2	+5.9		6	3460.05	28893.1	-13.1	+0.9
4	9	3472.14	28792.5	3.3	-2.6	7	3461.51	28880.9	12.2	-0.3
5	9	3472.14	28792.5	0.0	3.3	7	3463.01	28868.4	12.5	0.8
6	8	3472.53	28789.2	-3.3	2.6	7	3464.60	28855.1	13.3	0.6
7	5	3473.25	28783.3	5.9	3.6	7	3466.27	28841.2	13.9	1.5
8	5	3474.39	28773.8	9.5	2.1	9	3468.13	28825.8	15.4	0.8
9	5	3475.90	28762.2	11.6	0.8	7	3470.07	28809.6	16.2	0.9
10	5	3477.20	28749.8	12.4	3.7	9	3472.14	28792.5	17.1	3.5
11	5	3479.25	28733.7	16.1	5.0	5	3474.02	28771.9	20.6	1.5
12	5	3481.80	28712.6	21.1	0.1	5	3477.29	28749.8	22.1	0.9
13	8	3484.38	28691.4	21.2	2.1	5	3480.08	28726.8	23.0	2.7
14	1	3487.21	28668.1	23.3	3.1	5	3483.20	28701.1	25.7	1.6
15	5	3490.41	28641.7	26.4	2.3	1	3486.52	28673.8	27.3	2.2
16	6m	3493.92	28613.0	28.7	1.0	7	3490.10	28644.3	29.5	1.8
17	6m	3497.55	28583.3	29.7	3.0	6m	3493.92	28613.0	31.3	3.4
18	4	3501.56	28550.6	32.7	2.8	4	3498.16	28578.3	34.7	2.2
19	3	3505.92	28515.1	35.5	2.9	4m	3502.88	28541.4	36.9	1.7
20	8	3510.64	28476.7	38.4		4	3507.43	28502.8	38.6	

Table I—(continued)

m	R ₁ (m)					R ₂ (m)				
	I	$\lambda(\text{air})$	$\nu(\text{vac})$	Δ	Δ^2	I	$\lambda(\text{air})$	$\nu(\text{vac})$	Δ	Δ^2
2	0	3465 66	28846 3			6	3450 37	28974 1		
3	0m	3460 62	28888 3	+42 0		2	3447 00	28994 9	+20 8	+0 8
4	1	3455 97	28927 2	38 9	-3 1	5	3445 34	29016 5	21 6	-0 2
5	2	3451 95	28960 8	33 6	5 3	3	3442 79	29037 9	21 4	1 3
6	2	3448 36	28991 1	30 3	3 3	2	3440 41	29058 0	20 1	0 6
7	5	3445 34	29016 5	25 4	4 9	0	3438 10	29077 5	19 5	2 0
8	10	3442 33	29041 8	25 3	0 1	10	3436 04	29095 0	17 5	0 1
9	1	3439 87	29062 6	20 8	4 5	6	3433 98	29112 4	17 4	3 5
10	0	3437 75	29080 5	17 9	2 9	7m	3432 34	29128 3	13 9	1 8
11	10	3436 04	29095 0	14 5	3 4	2	3430 82	29138 4	12 1	2 3
12	2	3434 47	29108 3	13 3	1 2	3	3429 77	29148 2	9 8	2 4
13	2	3433 15	29119 5	11 2	2 1	2	3428 89	29155 6	7 4	2 7
14	7m	3432 34	29126 3	6 8	4 4	5	3428 34	29160 3	4 7	2 2
15	7m	3432 11	29128 3	2 0	4 8	7	3428 05	29162 8	2 5	2 5
16	7m	3432 34	29126 3	-2 0	4 0	7	3428 05	29162 8	0 0	2 5
17						5	3428 34	29160 3	-2 5	

2 Moments of Inertia

It is important to determine as accurately as possible the moments of inertia of the molecular systems concerned in the emission of band spectra. The values in the previous communication (p 383) were only *relative* values which were given to provide ready means of comparing the initial and final moments of inertia in all the bands. These relative values were determined from term differences involving data on the P and Q branches, since the data on the R branches of the bands 3122 and 2875 are very limited and somewhat irregular. It was pointed out, however, that the choice of P and R branches is to be preferred since the final Q terms differ from the final P and R terms.

There is now no doubt as to the correct assignment of the bands to form a band system, and since all the bands in any one progression have one moment of

inertia in common, it is only necessary to calculate that moment of inertia directly for the most intense band in the progression

The author has decided to employ the notation of the recent report of the National Research Council, on "Molecular Spectra in Gases," which differs slightly from the notation formerly used. Symbols referring to the initial and final states are now distinguished by one dash and two dashes respectively, so that equations (1) and (2) of the previous paper must be replaced by the following —

$$\left. \begin{aligned} P(m) &= v_0 + F'(m-1) - F''(m), & m-1 \rightarrow m, \\ Q(m) &= v_0 + F'(m) - F''(m), & m \rightarrow m, \\ R(m) &= v_0 + F'(m+1) - F''(m), & m+1 \rightarrow m, \end{aligned} \right\}, \quad (1)$$

and

$$\left. \begin{aligned} P(m) &= v_0 + (B' - B'') m^2 - 2B'm + B', \\ Q(m) &= v_0 + (B' - B'') m^2, \\ R(m) &= v_0 + (B' - B'') m^2 + 2B'm + B' \end{aligned} \right\} \quad (2)$$

In particular B, B', I and I' are replaced by B', B'', I' and I''

It appears that the terms may be more accurately represented by an expression of the form,

$$F(m) = Bm^2 + Dm^4,$$

than by the simple expression, $F(m) = Bm^2$. Further, the author has shown* that, in order to make the theoretical expressions fit the values of m usually associated with the water-vapour bands, m must be replaced by $m - \frac{1}{2}$. The terms will therefore be defined by

$$F(m) = B(m - \frac{1}{2})^2 + D(m - \frac{1}{2})^4 \quad (3)$$

The corresponding expression for the term differences is

$$F(m+1) - F(m-1) = (4B + 8D)(m - \frac{1}{2}) + 8D(m - \frac{1}{2})^3 \quad (4)$$

Following Birge, these differences will be denoted $2\Delta F(m)$. The quantities $2\Delta F(m)$ are easily obtained from data on the P and R branches since, from equations (1),

$$\left. \begin{aligned} R(m) - P(m) &= F'(m+1) - F'(m-1) = 2\Delta F'(m), \\ R(m-1) - P(m+1) &= F''(m+1) - F''(m-1) = 2\Delta F''(m) \end{aligned} \right\} \quad (5)$$

* *Loc. cit.*

It appears from a recent paper by Kemble* that it is justifiable to use the mean values of $2\Delta F(m)$, in conjunction with equation (4), for the determination of the values of B . In the paper referred to, Kemble gives an explanation of the doublets in the spectrum of water vapour in terms of Hund's theory of spinning electrons.

The components of a doublet are supposed to arise from different orientations of the axis of electron spin with respect to the axis of nuclear rotation. Kemble considers two cases. In case I the axis of electron spin, s , tends, for low speeds of nuclear rotation, to set itself antiparallel to σ , the component of the orbital angular momentum parallel to the nuclear axis, at high speeds it tends to set parallel to j , the resultant of the nuclear and electronic orbital angular momenta. In case II, s tends to become oriented parallel to σ for low speeds, and antiparallel to j for high speeds. These two cases together give rise to "normal doublets." Another type of doublet, known as an "inverted doublet," is obtained when the parallel arrangement of s and σ passes over to a parallel arrangement of s and j .

In the water-vapour doublets which are of the inverted type, Kemble obtains the following expression for the terms —

$$F(j) = B[(j \pm s)^2 - \sigma^2 - D(j \pm s)^4/B \pm P(P + 2\alpha)s^2/(j \pm s) + \quad]$$

Here P denotes the constant, $A/2Bs^2$, A being a constant depending on the mutual magnetic energy of s and σ , and α denotes σ/s . The expression represents two sets of energy levels. A pair of levels, so chosen that

$$j_1 + s = j_2 - s = T$$

will form a natural doublet. The connection between T and m is given by $T = m - \frac{1}{2}$. It should be pointed out that, here, the suffixes 1 and 2 have their usual significance as applied to the water-vapour doublets, whereas in Kemble's paper they have been interchanged, owing to the fact that quantities relating to the parallel and antiparallel arrangements of s and j are distinguished by the suffixes 1 and 2 respectively.

In the initial state the two values of $2\Delta F'_i(m)$, ($i = 1, 2$), are approximately equal so that either of these quantities or their mean may be represented by

$$2\Delta F'(m) = (4B' + 8D')T + 8D'T^2$$

* 'Phys. Rev.', vol 30, p 387 (1927)

The mean values of the final term differences are given by a similar expression, namely,

$$2\Delta F''(m) = (4B'' + 8D'')T + 8D''T^3,$$

and, since $T = m - \frac{1}{2}$, these expressions are precisely the same as equation (4)

The writer calculated the values of B and D in equation (4) by the method of least squares. This was done for the leading band of each progression, using all the available data on the band in question. The results, which have been checked by a graphical method are given in Table II in wave-number units. The quantities in brackets have been obtained indirectly from the data on other bands. The table also includes the values of the moments of inertia, I, in units 10^{-40} gm cm² obtained from the values of B, taking

$$h = 6.557 \times 10^{-27} \text{ erg sec. and } c = 2.9986 \times 10^{10} \text{ cm/sec}$$

Table II

Band	B'	D'	I	B''	D''	I'
3064	16 954	-0 0020	1 633	18 479	-0 0018	1 498
2811	16 101	-0 0018	1 720	(18 479)		(1 498)
2608	15 233	-0 0018	1 818	(18 479)		(1 498)
3428	(16 954)		(1 633)	17 775	-0 0017	1 558
3122	(16 101)		(1 720)	(17 775)		(1 558)
2875	(15 233)		(1 818)	(17 775)		(1 558)

Kemble gives values of B and D calculated from data for the lines of the band 2811 from $m = 16$ to 20, as follows —

$$B' = 16.12(5), \quad D' = -0.0020,$$

$$B'' = 18.47, \quad D'' = -0.00177$$

The results in Table II, for the band 2811, are in good agreement with Kemble's

The values of I for the state of no vibration are of special interest in connection with the structure of the emitter. These values which are denoted I'_0 and I''_0 , are the values of I' and I'' for the band 3064, viz, $I'_0 = 1.633$, $I''_0 = 1.498$. The result for I''_0 differs appreciably from that given by Birge in the report on "Molecular Spectra in Gases," p. 232. In a private communication Prof. Birge has requested the writer to state that the value given by him is incorrect owing to an accidental error, and that he now accepts $I''_0 = 1.50$. The author's values of the moments of inertia give for r_0 , the nuclear separation, $r'_0 = 1.022 \times 10^{-8}$ cm, and $r''_0 = 0.979 \times 10^{-8}$ cm in the case of the OH ion.

Summary

New measurements have been made of the band 3428 and the results of the analysis of the band are given in Table I. The band corresponds to the transition $0 \rightarrow 1$ of the vibrational quantum number.

Moments of inertia which are believed to be accurate are given for all the bands, to replace the relative values in a previous communication. The values for the vibrationless state are, $I'_0 = 1.633$, $I''_0 = 1.498$, in units 10^{-40} gm cm². The corresponding nuclear separations are, $r'_0 = 1.022 \times 10^{-8}$ cm, and $r''_0 = 0.979 \times 10^{-8}$ cm in the case of the OH ion.

The author wishes to express his thanks to Prof. H. Stanley Allen for the interest he has shown in the work, and for his many helpful suggestions, and also to Prof. Birge for his kindly criticisms.

The Wave Equations of the Electron

By Prof. C. G. DARWIN, F.R.S.

(Received March 6, 1928.)

1. In a recent paper Dirac* has brilliantly removed the defects before existing in the mechanics of the electron, and has shown how the phenomena usually called the "spinning electron" fit into place in the complete theory. He applies to the problem the method of q -numbers and, using non-commutative algebra, exhibits the properties of a free electron, and of an electron in a central field of electric force. In a second paper† he also discusses the rules of combination and the Zeeman effect. There are probably readers who will share the present writer's feeling that the methods of non-commutative algebra are harder to follow, and certainly much more difficult to invent, than are operations of types long familiar to analysis. Wherever it is possible to do so, it is surely better to present the theory in a mathematical form that dates from the time of Laplace and Legendre, if only because the details of the calculus have been so much more thoroughly explored. So the object of the present work is to take Dirac's system and treat it by the ordinary methods of wave calculus. The chief

* 'Roy Soc. Proc.' A, vol. 117, p. 610 (1928).

† 'Roy Soc. Proc.' A, vol. 118, p. 351 (1928).

point of interest is perhaps the solution of the problem of the central field, which can be carried out exactly and leads to Sommerfeld's original formula for the hydrogen levels. But it is also of some interest to exhibit the relationship of the new theory to the previous equations which were derived empirically by the present writer*. It appears that those equations were an approximation to the new ones, derived by an approximate elimination of two of Dirac's four wave functions. We shall also review a few other points connected with the free electron, the emission of radiation from an atom and its magnetic moment, and shall outline a discussion of the Zeeman effect.

2 Dirac's guiding principle is that the "Hamiltonian equation" must be linear, and he adopts the form

$$p_0 + \alpha_1 p_1 + \alpha_2 p_2 + \alpha_3 p_3 + \alpha_4 mc = 0,$$

where

$$\left. \begin{aligned} p_0 &= -\frac{\hbar}{2\pi i} \frac{1}{c} \frac{\partial}{\partial t} + \frac{e}{c} V \\ p_1 &= \frac{\hbar}{2\pi i} \frac{\partial}{\partial x} + \frac{e}{c} A_1, \text{ etc} \end{aligned} \right\}, \quad (2.1)$$

V and A being scalar and vector potentials, while $\alpha_1, \alpha_2, \alpha_3, \alpha_4$ are four four-rowed matrices obeying the rules

$$\alpha_s^2 = 1, \quad \alpha_s \alpha_t + \alpha_t \alpha_s = 0.$$

The α 's are capable of an indefinite number of forms, and he gives rules for forming one set (though he does not write them out). The four-rowed matrices imply four wave functions which satisfy the simultaneous equations

$$\left. \begin{aligned} (p_0 + mc) \psi_1 + (p_1 - ip_2) \psi_4 + p_3 \psi_3 &= 0 \\ (p_0 + mc) \psi_2 + (p_1 + ip_2) \psi_3 - p_3 \psi_4 &= 0 \\ (p_0 - mc) \psi_3 + (p_1 - ip_2) \psi_2 + p_3 \psi_1 &= 0 \\ (p_0 - mc) \psi_4 + (p_1 + ip_2) \psi_1 - p_3 \psi_2 &= 0 \end{aligned} \right\}. \quad (2.2)$$

We shall take these, then, as our fundamental equations and discuss their solution, employing only the ordinary methods of differential equations.

The equations are very unsymmetrical, and it is, of course, necessary first to show that they can be restored to their original form when axes are changed or a relativity transformation is applied. The general formulæ are complicated (being best expressed by four-dimensional Cayley parameters), but it is sufficient to verify the result for certain simpler transformations which can be imagined

* 'Nature,' vol 119, p 282 (1927), 'Roy Soc Proc,' A, vol 116, p 227 (1927)

applied successively This is so straightforward that we need merely give the results

(1) Relativity transformation

$$\begin{aligned}x &= x', & y &= y', \\z &= z' \cosh \beta + \alpha' \sinh \beta, \\ \alpha &= \alpha' \cosh \beta + z' \sinh \beta\end{aligned}$$

The equations are restored to their original form by

$$\begin{aligned}\psi_1' &= \psi_1 \cosh \frac{\beta}{2} + \psi_3 \sinh \frac{\beta}{2}, \\ \psi_2' &= \psi_2 \cosh \frac{\beta}{2} - \psi_4 \sinh \frac{\beta}{2}, \\ \psi_3' &= \psi_3 \cosh \frac{\beta}{2} + \psi_1 \sinh \frac{\beta}{2}, \\ \psi_4' &= \psi_4 \cosh \frac{\beta}{2} - \psi_2 \sinh \frac{\beta}{2}\end{aligned}$$

(2) Rotation about z

$$\begin{aligned}x &= x' \cos \alpha - y' \sin \alpha, \\ y &= y' \cos \alpha + x' \sin \alpha, \\ z &= z', & t &= t'\end{aligned}$$

Then

$$\psi_1' = \psi_1 e^{i\alpha/2}, \quad \psi_2' = \psi_2 e^{-i\alpha/2}, \quad \psi_3' = \psi_3 e^{i\alpha/2}, \quad \psi_4' = \psi_4 e^{-i\alpha/2}$$

(3) Rotation about y

$$\begin{aligned}z &= z' \cos \alpha - x' \sin \alpha, \\ x &= x' \cos \alpha + z' \sin \alpha, \\ y &= y', & t &= t', \\ \psi_1' &= \psi_1 \cos \frac{\alpha}{2} + \psi_3 \sin \frac{\alpha}{2}, \\ \psi_2' &= \psi_2 \cos \frac{\alpha}{2} - \psi_1 \sin \frac{\alpha}{2}, \\ \psi_3' &= \psi_3 \cos \frac{\alpha}{2} + \psi_4 \sin \frac{\alpha}{2}, \\ \psi_4' &= \psi_4 \cos \frac{\alpha}{2} - \psi_3 \sin \frac{\alpha}{2}\end{aligned}$$

These three transformations can build a group which represents any relativity transformation, and so the invariance is proved

It is of some interest to consider this invariance a little further. The whole theory of general relativity is based on the idea of invariance of form, and here we have a system invariant in fact but not in form. Should it not be possible to give it formal invariance as well, and would not that be the right way to express our equations? It is so possible, but it is not hard to show that it requires no less than 16 quantities to do it,* viz., two scalars, two four-vectors and one six-vector, and even so each will have a real and imaginary part, so that we may say that 32 quantities are required†. It seems quite preposterous to think that a single electron should require 32 equations to express its behaviour, and, moreover, these 32 will involve a large number of arbitrary inter-relations of no influence on the four quantities which are actually sufficient to describe it. Now the relativity theory is based on nothing but the idea of invariance, and develops from it the conception of tensors as a matter of necessity, and it is rather disconcerting to find that apparently something has slipped through the net‡ so that physical quantities exist which it would be, to say the least, very artificial and inconvenient to express as tensors. It does not seem possible to make anything further out of the matter until it has developed more, and we shall be content with one observation. Unlike the electromagnetic equations, our wave equations are homogeneous, so that there is no external quantity, like the electric current, etc., which could, so to speak, anchor them down in form to a definite set of directions. Now, there ought to be something of the kind because of the electromagnetic field of the electron, which in classical theory is made responsible for its mass. So we may perhaps conclude that it is not to be expected that our equations will attain a final form until the terms in m_0 are eliminated, that is, until we know how to do in the quantum theory a calculation like that which gives electromagnetic mass in the classical

In my earlier paper a similar question arose and was much more easily resolved. In that work there were only two functions instead of the four here, and it was an easy matter to throw them into space-vector form, though it involved having four equations instead of two with a corresponding arbitrariness

* We can express the equations as a group of 16 in

$$\alpha\psi_1 + \beta\psi_2 + \gamma\psi_3 + \delta\psi_4, \quad \alpha\psi_1 + \beta\psi_2 + \gamma\psi_3 + \delta\psi_4, \text{ etc.},$$

with $\alpha\beta\gamma\delta$ arbitrary constants and can throw these into tensor form

† Our equations (2.2) do not, of course, include gravitation, and this may be the hole in the net. But if gravitation were included, we should presumably be forced to introduce the tensor form, involving 16 complex or 32 real quantities, and this does not seem physically very plausible.

in the solution. It appeared reasonable to make the step from two to four, and so to gain the advantage of vector notation, but to expand from four to sixteen is a different matter, and suggests that even in the simpler case the expansion is rather artificial. Nevertheless, it is not without interest to exhibit Dirac's equations in the form of space-vectors, without bringing in the time as part of the vectorial system. This can be done by a method similar to the substitution (5.1) of my paper. Take two vectors X, Y and two scalars X_0, Y_0 , and write p_1, p_2, p_3 as a vector p . The equations

$$\left. \begin{aligned} (p_0 + mc) Y_0 &= (p, X) \\ (p_0 + mc) Y - p X_0 &= [p, X] \\ (p_0 - mc) X_0 &= (p, Y) \\ (p_0 - mc) X - p Y_0 &= -[p, Y] \end{aligned} \right\} \quad (2.3)$$

can be combined together in pairs according to either of the following alternative schemes so as to give Dirac's equations —

$$\left. \begin{aligned} \psi_1 &= Y_0 - iY_3 \\ \psi_2 &= Y_1 + iY_2 \\ \psi_3 &= iX_3 - X_0 \\ \psi_4 &= iX_1 - X_2 \end{aligned} \right\}, \quad \left. \begin{aligned} \psi_1 &= -Y_1 + iY_2 \\ \psi_2 &= Y_3 + iY_0 \\ \psi_3 &= -iX_1 - X_2 \\ \psi_4 &= iX_3 + X_0 \end{aligned} \right\}$$

So we might regard (2.3) as the primitive equations giving Dirac's twice over

Now the operation $p_1 = \frac{\hbar}{2\pi i} \frac{\partial}{\partial x} + \frac{e}{c} A_1$ may be likened to a "covariant differentiation" (say, by the introduction of a fifth dimension in the manner of Klein*), and in this sense $[p, X]$ may be called *curl* X and (p, X) , *div* X . In the same sense p_0 is a time differentiation, and we see that (2.3) bear a rather striking resemblance to the electromagnetic equations with X and Y for E and H , and X_0, Y_0 playing a role akin to electric and magnetic density. It does not seem possible to push this rather loose analogy farther at present, and again we have a hint as to the reason, because there is no electromagnetic analogue to the terms in mc , and this will only be supplied when we know how to calculate electromagnetic mass in the quantum theory.

3 The equations (2.2) are sufficient to determine the levels of any system, but that is not enough, for we also require to know the rules of combination, and for this we must have the extension of the "electric density" of Schrödinger's theory to the present case. In order to find the radiation of an atom

* Klein, 'Z f Physik,' vol 37, p 895 (1926)

we combine atom and radiation field into a single system, expressing the equations all together most conveniently by means of a variational principle

The variational function is easy to construct. Multiply the equations (2.2) by $\delta\psi_1^*$, $\delta\psi_2^*$, $\delta\psi_3^*$, $\delta\psi_4^*$ respectively and add them together. Add on their conjugates and integrate over all space and time. Integrating by parts, this can be written as the variation of a single function. To this we must add $\frac{1}{8\pi} (H^2 - E^2)$, integrated over space and time, in order to give the dynamical effect of the radiation. Then, if we express H and E in terms of the potentials, and vary V and the A 's as well as the ψ 's and ψ^* 's, we shall obtain equations for V and the A 's as well as (2.2) and their conjugates, and shall thus have the radiation completely linked with the material motion. In carrying out this process one point is to be noticed. The equations (2.2) are homogeneous and so do not fix the magnitudes of the ψ 's. The equation for V is not so, but determines V as proportional to a quadratic expression in the ψ 's. We naturally adjust this by normalising the ψ 's so that the total charge shall be $-e$, the charge of an electron. It is more convenient to normalise the ψ 's to unity, and therefore the terms $\frac{1}{8\pi} (H^2 - E^2)$ must be multiplied by a suitable constant. To save writing out many formulæ twice, we shall anticipate the knowledge of this constant, it is $-1/c$. Proceeding in this way we arrive at the variational function

$$\begin{aligned}
 S = \iiint dx dy dz dt \left\{ \frac{1}{2} \frac{\hbar}{2\pi c} \left[\psi_1^* \left(-\frac{1}{c} \frac{\partial \psi_1}{\partial t} + \left(\frac{\partial}{\partial x} - i \frac{\partial}{\partial y} \right) \psi_4 + \frac{\partial}{\partial z} \psi_2 \right) \right. \right. \\
 + \psi_2^* \left(-\frac{1}{c} \frac{\partial \psi_2}{\partial t} + \left(\frac{\partial}{\partial x} + i \frac{\partial}{\partial y} \right) \psi_3 - \frac{\partial}{\partial z} \psi_4 \right) \\
 + \psi_3^* \left(-\frac{1}{c} \frac{\partial \psi_3}{\partial t} + \left(\frac{\partial}{\partial x} - i \frac{\partial}{\partial y} \right) \psi_2 + \frac{\partial}{\partial z} \psi_1 \right) \\
 \left. \left. + \psi_4^* \left(-\frac{1}{c} \frac{\partial \psi_4}{\partial t} + \left(\frac{\partial}{\partial x} + i \frac{\partial}{\partial y} \right) \psi_1 - \frac{\partial}{\partial z} \psi_2 \right) \right] + \text{the conjugate of} \right. \\
 \left. \text{the preceding} \right. \\
 + mc(\psi_1\psi_1^* + \psi_2\psi_2^* - \psi_3\psi_3^* - \psi_4\psi_4^*) + \frac{eV}{c} \sum_1^4 \psi_\lambda \psi_\lambda^* \\
 + \frac{eA_1}{c} (\psi_1^*\psi_4 + \psi_2^*\psi_3 + \psi_3^*\psi_2 + \psi_4^*\psi_1) \\
 + \frac{eA_2}{c} (-i\psi_1^*\psi_4 + i\psi_2^*\psi_3 - i\psi_3^*\psi_2 + i\psi_4^*\psi_1) \\
 + \frac{eA_3}{c} (\psi_1^*\psi_3 - \psi_2^*\psi_4 + \psi_3^*\psi_1 - \psi_4^*\psi_2) \\
 \left. \left. - \frac{1}{8\pi c} \left[(\text{curl } \mathbf{A})^2 - \left(\frac{1}{c} \frac{\partial \mathbf{A}}{\partial t} + \text{grad } V \right)^2 \right] \right\} \quad (3.1)
 \end{aligned}$$

If we vary this function it is easy to see that we obtain (2.2) and their conjugates and also

$$\left. \begin{aligned} \frac{1}{4\pi} \square V &= e \sum_1^4 \psi_\lambda^* \psi_\lambda \\ \frac{1}{4\pi} \square A_1 &= -e \{ \psi_1^* \psi_4 + \psi_2^* \psi_3 + \psi_3^* \psi_2 + \psi_4^* \psi_1 \} \end{aligned} \right\}, \quad (3.2)$$

etc, where \square signifies $\frac{\partial^2}{\partial x^2} + \frac{\partial^2}{\partial y^2} + \frac{\partial^2}{\partial z^2} - \frac{1}{c^2} \frac{\partial^2}{\partial t^2}$. We conclude that the electro-

magnetic effect of the electron can be represented by taking density ρ and current densities j_1, j_2, j_3 , where

$$\left. \begin{aligned} \rho &= -e (\psi_1^* \psi_1 + \psi_2^* \psi_2 + \psi_3^* \psi_3 + \psi_4^* \psi_4) \\ j_1 &= ec (\psi_1^* \psi_4 + \psi_2^* \psi_3 + \psi_3^* \psi_2 + \psi_4^* \psi_1) \\ j_2 &= ec (-i \psi_1^* \psi_4 + i \psi_2^* \psi_3 - i \psi_3^* \psi_2 + i \psi_4^* \psi_1) \\ j_3 &= ec (\psi_1^* \psi_3 - \psi_2^* \psi_4 + \psi_3^* \psi_1 - \psi_4^* \psi_2) \end{aligned} \right\}, \quad (3.3)$$

provided that the ψ 's are normalised by the rule

$$\iiint \sum_{\lambda=1}^4 \psi_\lambda \psi_\lambda^* dx dy dz = 1 \quad (3.4)$$

Since S is invariant for relativity transformations, ρ and j will be covariant for such transformations, and this can also be easily verified by applying the transformations of § 2 in turn.

It should be observed that ρ and j satisfy the equation of continuity

$$\frac{\partial \rho}{\partial t} + \text{div } j = 0, \quad (3.5)$$

as may be directly verified with the use of (2.2). That (3.5) should be verified is in a sense the starting point of Dirac's argument. For if it had not been so spontaneously, we should have been compelled to force it by introducing

into S a term $\left(\frac{1}{c} \frac{\partial V}{\partial t} + \text{grad } A \right) F$ with F undetermined. The result would give extra terms in ρ and j involving $\frac{\partial F}{\partial t}$ and $\text{grad } F$, and the condition

$\frac{1}{c} \frac{\partial V}{\partial t} + \text{grad } A = 0$ would then fix F . In general it would involve Y and A , and

therefore ρ and j would do so too. It was the presence of such terms in Klein's†

† 'Z f Physik,' vol. 41, p. 407 (1927)

evaluation of density and current that was objectionable and that led Dirac to his new equations

To complete the rules for calculating intensities we have to break up ρ and j into terms corresponding to pairs of states. This can be done in the manner of Klein, but perhaps the following picture, though very incomplete,† may make the process clearer, and may show under what conditions we expect to get line spectra with definite intensities, it is applicable to any system. Imagine that we have an assembly of atoms in an enclosure. The equations (2.2) and (3.2), together with appropriate boundary conditions, will describe the state of affairs. Thermal equilibrium will be produced, with the accompanying black radiation, and the equations will be quite insoluble, because in solving (2.2) the electromagnetic fields, themselves determined by (2.2), will not be small. At any instant of time we can imagine the state expressed by an expansion in proper functions, and the average values of the coefficients will be determined by the appropriate statistics—in particular, states of nearly equal energy will have equal average coefficients. Now if the enclosing barrier is suddenly removed, the radiation before present will spread away with the speed of light and the matter will be left only under the influence of any existing permanent electromagnetic forces. The problem is now soluble by approximations, first solving (2.2) for the ψ 's, neglecting the radiation, and then substituting the values found in (3.2) to give the radiation. If ψ_λ is initially $\sum_p a_p \psi_\lambda^p$, the first process gives $\psi_\lambda = \sum_p a_p \psi_\lambda^p e^{i \frac{2\pi}{h} W_p t}$. Next we form

$$\rho = \sum_p \sum_q \sum_{\lambda=1}^4 a_p a_q^* \psi_\lambda^p \psi_\lambda^{q*} e^{i \frac{2\pi}{h} (W_p - W_q) t},$$

and similar values for the j 's. Substituting these in (3.2) we can evaluate the electric force at a distant point, and it will evidently consist of a sum of periodic terms corresponding to the spectrum lines given by $W_p \rightarrow W_q$. The process is exactly that introduced by Klein, only a little more definite in that no appeal is made to the correspondence principle.

4 We shall next exhibit the relationship of Dirac's equations to previous theories, and shall show that the latter are successive approximations to (2.2). The guiding principle in this is the fact that of the four ψ 's, ψ_3 and ψ_4 are very much larger than ψ_1 , ψ_2 , since this leads to a method of approximation. We shall treat of the case of the stationary states of an electron in an atom.

The first approximation leads to Schrödinger's equation in both ψ_3 and ψ_4 .

† The incompleteness lies chiefly in the fact that no distinction is made between one atom and many atoms.

independently, but in doing this it must not be forgotten that that equation is not even approximately right as far as concerns the effects of magnetic fields

We must therefore restrict ourselves to equations in which $p_1 = \frac{\hbar}{2\pi i} \frac{\partial}{\partial x}$ without a vector potential, so that $p_1 p_2 = p_2 p_1$, etc. Starting with complete neglect of ψ_1, ψ_2 we see that ψ_3, ψ_4 , and therefore ψ_1, ψ_2 also, are proportional to $e^{-i \frac{2\pi}{\hbar} m c t}$. Hence $(p_0 + mc) \psi_1$ is nearly equal to $2mc\psi_1$, and so we take

$$\left. \begin{aligned} \psi_1 &= -\frac{\hbar}{2\pi i} \frac{1}{2mc} \left[\left(\frac{\partial}{\partial x} - i \frac{\partial}{\partial y} \right) \psi_4 + \frac{\partial}{\partial z} \psi_3 \right] \\ \psi_2 &= -\frac{\hbar}{2\pi i} \frac{1}{2mc} \left[\left(\frac{\partial}{\partial x} + i \frac{\partial}{\partial y} \right) \psi_3 - \frac{\partial}{\partial z} \psi_4 \right] \end{aligned} \right\} \quad (4.1)$$

Substituting in the third equation we get

$$\left(-mc + \frac{eV}{c} - \frac{\hbar}{2\pi i} \frac{1}{c} \frac{\partial}{\partial t} \right) \psi_3 = \left(\frac{\hbar}{2\pi i} \right)^2 \frac{1}{2mc} \Delta \psi_3$$

The same equation holds for ψ_4 , so that we simply have Schrödinger's equation twice over

In the second approximation, following Dirac's § 4, we form exact second order equations in ψ_3, ψ_4 , and from these we eliminate ψ_1, ψ_2 by means of (4.1). In (2.2) operate the third equation by $(mc + p_0)$, the second by $-(p_1 - ip_2)$, the first by $-p_2$ and add. We have

$$\begin{aligned} p_0 p_1 - p_1 p_0 &= -\frac{\hbar}{2\pi i} \frac{1}{c} \frac{\partial}{\partial t} \frac{eA_1}{c} - \frac{\hbar}{2\pi i} \frac{\partial}{\partial x} \frac{eV}{c} = \frac{e}{c} \frac{\hbar}{2\pi i} E_1, \\ p_1 p_2 - p_2 p_1 &= \frac{\hbar}{2\pi i} \frac{\partial}{\partial x} \frac{eA_2}{c} - \frac{\hbar}{2\pi i} \frac{\partial}{\partial y} \frac{eA_1}{c} = \frac{e}{c} \frac{\hbar}{2\pi i} H_3, \end{aligned}$$

and using these and similar relations we get

$$\begin{aligned} \left[-m^2 c^2 + p_0^2 - p_1^2 - p_2^2 - p_3^2 - \frac{e}{c} \frac{\hbar}{2\pi} H_3 \right] \psi_3 - \frac{e}{c} \frac{\hbar}{2\pi} (H_1 - iH_2) \psi_4 \\ - \frac{e}{c} \frac{\hbar}{2\pi} i [(E_1 - iE_2) \psi_4 + E_3 \psi_1] = 0 \end{aligned}$$

Now substitute for ψ_1, ψ_2 from (4.1). Those equations ought now to contain terms involving the A 's, but, as they are to be multiplied by E 's, these may be neglected. We have

$$\begin{aligned} \left(D - \frac{2\pi e}{ch} H_3 \right) \psi_3 - \frac{2\pi e}{ch} (H_1 - iH_2) \psi_4 + \frac{e}{2mc^2} \left\{ \left(E_1 \frac{\partial}{\partial x} + E_2 \frac{\partial}{\partial y} + E_3 \frac{\partial}{\partial z} \right) \psi_3 \right. \\ \left. + i \left(E_2 \frac{\partial}{\partial z} - E_3 \frac{\partial}{\partial y} \right) \psi_4 + \left(E_3 \frac{\partial}{\partial x} - E_1 \frac{\partial}{\partial z} \right) \psi_4 + i \left(E_1 \frac{\partial}{\partial y} - E_2 \frac{\partial}{\partial x} \right) \psi_3 \right\} = 0, \end{aligned} \quad (4.2)$$

where $D = \left(\frac{2\pi}{h}\right)^2 (-m^2c^2 + p_0^2 - p_1^2 - p_2^2 - p_3^2)$ is the same quantity as in my paper. Similarly

$$\begin{aligned} \left(D + \frac{2\pi e}{ch} H_3 \right) \psi_4 - \frac{2\pi e}{ch} (H_1 + iH_2) \psi_3 + \frac{e}{2mc^2} \left\{ (E_1 \frac{\partial}{\partial x} + E_2 \frac{\partial}{\partial y} + E_3 \frac{\partial}{\partial z}) \psi_4 \right. \\ \left. + i(E_3 \frac{\partial}{\partial z} - E_2 \frac{\partial}{\partial y}) \psi_3 - (E_3 \frac{\partial}{\partial x} - E_1 \frac{\partial}{\partial z}) \psi_2 - i(E_1 \frac{\partial}{\partial y} - E_2 \frac{\partial}{\partial x}) \psi_1 \right\} = 0 \end{aligned} \quad (4.3)$$

Apart from the terms in

$$P \equiv E_1 \frac{\partial}{\partial x} + E_2 \frac{\partial}{\partial y} + E_3 \frac{\partial}{\partial z}, \quad (4.4)$$

these are identical with the equations of my paper, provided that we identify ψ_3 with f , ψ_4 with $-g$. The extra terms in P rectify one of the earlier defects, for with my equations the s -levels of hydrogen fell in the wrong place though all others were correct. Now when the approximative method is used, the new terms affect the levels by an amount depending on $\int_0^\infty f(r) [P f(r)] r^2 dr$ and for

hydrogen $E_1 = ex/r^3$ so that $P = \frac{e}{r^3} \frac{d}{dr}$ and the integral depends on $[f(0)]^2$

Since $f(0)$ vanishes unless $k=0$, all levels other than s -levels are unaffected, and a more detailed calculation shows that the s -levels now fall in the right place.

The formulæ for intensities are also the same to a first approximation, because to this degree $ff^* + gg^*$ is the same as $\sum_1^4 \psi_\lambda \psi_\lambda^*$. It is of more interest to consider the formulæ for magnetic moment. For this we take all the ψ 's in (3.3) as belonging to a single state, so that the time disappears and we have $d\psi/dt = 0$. With this condition and the condition $\iiint j \, dx \, dy \, dz = 0$ (which holds because there is no progressive current in a stationary atom) the magnetic moment can be seen to have as first component

$$\mu_1 = \frac{1}{2e} \iiint (y j_3 - z j_2) \, dx \, dy \, dz$$

Substitute (4.1) in (3.3) so as to obtain the approximations for j_1, j_2 . After some partial integrations we find

$$\begin{aligned} \mu_1 = \frac{eh}{4\pi mc} \iiint \left[\frac{1}{2i} (\psi_2 R_1 \psi_3^* + \psi_4 R_1 \psi_4^* - \psi_2^* R_1 \psi_3 - \psi_4^* R_1 \psi_4) \right. \\ \left. - (\psi_3 \psi_4^* + \psi_3^* \psi_4) \right] dx \, dy \, dz, \quad (4.5) \end{aligned}$$

where $R_1 = y \frac{\partial}{\partial z} - z \frac{\partial}{\partial y}$. This is the value† given before, when we replace ψ_3, ψ_4 by f and $-g$. Similar methods apply for the other components. A cyclic change gives the first terms, and the last are

$$-i(\psi_3\psi_4^* - \psi_3^*\psi_4) \quad \text{and} \quad +(\psi_4\psi_3^* - \psi_3\psi_4^*) \quad (4.6)$$

respectively for μ_2 and μ_3 .

Dirac's success in finding the accurate equations shows the great superiority of principle over the previous empirical method, but it is perhaps not without interest (at any rate to the present writer, who had projected but not begun such work) to consider whether the empirical method could have led by way of improved approximations to the accurate result. The most critical step in doing so had been made, though not quite rightly and for a wrong reason, in the replacement of $2mc$ by a time differential (it had been replaced by

$$2\left(-\frac{h}{2\pi i} \frac{1}{c} \frac{\partial}{\partial t} + \frac{eV}{c}\right),$$

whereas only half should have been treated in this way). There also seemed nothing to prevent carrying out a higher approximation so as to make the hydrogen levels fall more exactly together. A further guide lay in the fact that the electric current *must* be a more primitive thing than the magnetic moment, and when the current is deduced from (4.5), (4.6), it has certain complicated small terms admitting of modification. On the other hand, the absence of the terms (4.4) would have caused trouble. On the whole, it seems not impossible that one might with much labour have arrived at some sort of eliminant of Dirac's equations. Fortunately, he has made such work unnecessary.

5. The free motion of an electron calls for comment. In the equations (2.2) we now omit V and A altogether. Assume as solution

$$\psi_A = a_A \exp i \frac{2\pi}{h} (px + qy + rz - Wt),$$

and on substituting we have a determinant which reduces to

$$(W^2 - m^2c^2 - p^2 - q^2 - r^2)^2 = 0$$

† In § 6 of my paper, by a blunder I took the magnetic moment as $\frac{W}{\partial H}$ instead of $-\frac{\partial W}{\partial H}$. The expressions (6.7) there for the components of μ should have their signs changed. Those expressions can be written in terms of f, g by substituting $X_1 = f, X_2 = g, X_3 = g, X_4 = -f$.

We must therefore take $W = \sqrt{(m^2c^2 + p^2 + q^2 + r^2)}$, which we shall call W_{per} for short. We can take a_3, a_4 as arbitrary, say, A, B , and then have

$$a_1 = -\frac{Ar + B(p - iq)}{mc + W_{per}}, \quad a_2 = -\frac{A(p + iq) - Br}{mc + W_{per}}$$

From these we find that p and q are proportional to $|A|^2 + |B|^2$, and that j is a vector along $p \ q \ r$.

An important point now arises if we consider the problem from the point of view raised in a recent paper †. The motion of the electron is there regarded as a pure wave problem, the solution consisting in finding the way in which given *arbitrary* initial conditions are propagated. Suppose that we have arbitrary initial values of all four ψ 's at every point of space. We can submit them to Fourier analysis and have

$$\psi_\lambda = \int a_\lambda(p, q, r) \exp i \frac{2\pi}{h} (px + qy + rz) dp dq dr.$$

The a_λ 's will have arbitrary values, but this is impossible since we have just seen that a_1, a_2 are determinate in terms of a_3, a_4 . There can hardly be a question that a complete theory will overcome this difficulty by admitting negative values of W , but we are evidently in contact with the question raised by Dirac in his § 1, connected with the possible changes of e into $-e$. At present this is unsolved, so we must be content to say that we are not entitled to assume completely arbitrary initial conditions, but may only take two of the four functions arbitrary.

To understand the physical meaning of the equations in free space, we want to be able to associate a given solution with the rectilinear motion of an electron with magnetic moment in a given direction. As long as we only deal with solutions of type (5.1) nothing can be said about the magnetic moment, because the waves fill all space uniformly and there is, therefore, no distant point left from which to observe it. In order to get a magnetic moment we must construct a wave packet. We may, for instance, assume that initially ψ_3 and ψ_4 contain a factor $\exp -\frac{1}{2\sigma^2}(x^2 + y^2 + z^2)$. These will fix ψ_1, ψ_2 , and it is impor-

tant to observe that in consequence of the differential inter-relation between them, the ratio of ψ_1, ψ_2 will vary in the different parts of the packet, so that the current j will no longer be everywhere straight along the main direction of wave motion, and a magnetic moment becomes possible. The complete solution can be set down in Fourier integrals, but it does not seem possible to

† 'Roy. Soc. Proc. A, vol. 117, p. 258 (1927)

work them out. It is therefore simpler to recur to the approximation of § 4, which shows that coefficients A and B for ψ_3, ψ_4 will be associated with various moments. By consideration of the last term in (4.5), (4.6), we see that if A, B are respectively proportional to $(1-n)$ and $(-l-m)$ we shall have magnetic moment along the direction l, m, n . For high speeds of motion the approximation would fail, but so would the idea of magnetic moment.

The same approximate method is adequate for the case of motion in a magnetic field and for the Stern Gerlach effect. For the case of a uniform field it is possible to find accurate solutions of the equations, but they correspond to a quantised circular motion, and are not of much interest, as they need to be combined into wave packets if any close relationship is to be seen with the velocity of the electron.

6. We now consider the energy levels for an electron in a central field, and in particular for hydrogen. Before proceeding to the solution, it will be well to discuss the question of the nomenclature of the various quantum states. Dirac points out that angular momentum is no longer an integral of the motion, but finds a modified integral of a similar type. He thus suppresses the use of k and uses a quantum number j . With the method of solution which we shall be using the dynamical meaning of quantum numbers goes very much into the background, and we are left only with integers defining the orders of spherical harmonics and other functions entering the solution. From this point of view the quantum number is only a convenient name associated with those functions—for example the quantum number m was adopted as $u + \frac{1}{2}$ in the earlier theory because a certain solution involved P_u^m and P_u^{m+1} . The fact that there exists a dynamical integral is then largely irrelevant—under special circumstances it might help in guessing a solution, but usually it merely reduces to an identity in the properties of a function found in some other way.

In view of these considerations, I have concluded, with some hesitation, that it is more convenient not to alter the notation in the way done by Dirac. The quantum numbers k, j, m retain their old classificatory, but not their dynamical significance, in this way any line of a spectrum can be described by the same numbers as were used before and doublets are classified like other multiplets. To define them more precisely we take m as given by Landé's g -formula, and j as the maximum positive value of m . For doublets it is therefore a half-number, and k may be either of the adjacent integers. We shall, in fact, see that every solution involves four different spherical harmonics, $P_m^j, P_{m+1}^j, P_{m+1}^{j+1}$ and P_m^{j+1} and j and m are simply the averages of subscripts and of superscripts respectively. k , which is the subscript of ψ_3 , has not the same symmetrical property as j .

and m , but is called a quantum number because it defines the rule of combination of levels and of the Zeeman effect. We adopt for it the numeration 0, 1, 2, ..., not 1, 2, 3, ..., as this has proved most convenient in spectroscopy.

In Dirac's new notation j can take on negative values, and it is at first sight tempting to follow this change. It would not be hard to invent negative spherical harmonics P_{-j}^m , which would make it possible to write all the solutions in a single form, but it would lead to little simplification. For his j values do not run right through from positive to negative, they miss the value zero and it would be necessary to study combinations of like and of unlike signs separately, and this can be done just as well with only positive values and a second number k acting as a sort of plus or minus sign. Moreover, as we shall see, we can take full advantage of Dirac's method in discussing the radial functions. The following scheme shows the relationship between the values used here and by Dirac —

		s	p	d
Here	k j	0 $\frac{1}{2}$	$\frac{1}{2}$ $\frac{1}{2}$ $\frac{1}{2}$ $\frac{1}{2}$	$\frac{2}{2}$ $\frac{2}{2}$ $\frac{3}{2}$ $\frac{5}{2}$
Dirac	j	-1	1 -2	2 -3

7 In order to solve for the levels in a radial field of force, we put $p_0 = \frac{W}{c} + \frac{eV}{c}$

where V depends only on the radius, and we omit the vector potentials. The equations (2.2) now become —

$$\left. \begin{aligned} \frac{2\pi\epsilon}{\hbar} \left(\frac{W+eV}{c} + mc \right) \psi_1 + \left(\frac{\partial}{\partial x} - i \frac{\partial}{\partial y} \right) \psi_4 + \frac{\partial}{\partial z} \psi_3 &= 0 \\ \frac{2\pi\epsilon}{\hbar} \left(\frac{W+eV}{c} + mc \right) \psi_2 + \left(\frac{\partial}{\partial x} + i \frac{\partial}{\partial y} \right) \psi_3 - \frac{\partial}{\partial z} \psi_4 &= 0 \\ \frac{2\pi\epsilon}{\hbar} \left(\frac{W+eV}{c} - mc \right) \psi_3 + \left(\frac{\partial}{\partial x} - i \frac{\partial}{\partial y} \right) \psi_2 + \frac{\partial}{\partial z} \psi_1 &= 0 \\ \frac{2\pi\epsilon}{\hbar} \left(\frac{W+eV}{c} - mc \right) \psi_4 + \left(\frac{\partial}{\partial x} + i \frac{\partial}{\partial y} \right) \psi_1 - \frac{\partial}{\partial z} \psi_2 &= 0 \end{aligned} \right\} \quad (7.1)$$

Following previous methods we try to express the four functions as spherical harmonics multiplied by radial functions.

We may first conveniently give certain formulae for spherical harmonics

that are easily proved. We abbreviate the notation by writing P_k^* for the whole harmonic, thus

$$P_k^* = (k-u)! \sin^u \theta \left(\frac{d}{d \cos \theta} \right)^{k+u} \frac{(\cos^2 \theta - 1)^k}{2^k k!} e^{ku},$$

which exists for any positive integral value of k and for any integral value of u between $\pm k$ inclusive. Then, if f is any function of the radius we have —

$$\left. \begin{aligned} \left(\frac{\partial}{\partial x} + \frac{\partial}{\partial y} \right) f P_k^* &= \frac{1}{2k+1} \left\{ \left(\frac{df}{dr} - \frac{k}{r} f \right) P_{k+1}^* \right. \\ &\quad \left. - (k-u)(k-u-1) \left(\frac{df}{dr} + \frac{k+1}{r} f \right) P_{k-1}^* \right\} \\ \left(\frac{\partial}{\partial x} - \frac{\partial}{\partial y} \right) f P_k^* &= \frac{1}{2k+1} \left\{ - \left(\frac{df}{dr} - \frac{k}{r} f \right) P_{k+1}^* \right. \\ &\quad \left. + (k+u)(k+u-1) \left(\frac{df}{dr} + \frac{k+1}{r} f \right) P_{k-1}^* \right\} \\ \frac{\partial}{\partial z} f P_k^* &= \frac{1}{2k+1} \left\{ \left(\frac{df}{dr} - \frac{k}{r} f \right) P_{k+1}^* \right. \\ &\quad \left. + (k+u)(k-u) \left(\frac{df}{dr} + \frac{k+1}{r} f \right) P_{k-1}^* \right\} \end{aligned} \right\} \quad (7.2)$$

We may note that these formulæ automatically look after "end effects", thus, if we apply the first or third to P_k^* the factor $(k-u)$ in the second term cuts out the terms in P_{k-1}^* , P_{k+1}^* , functions which do not exist.

Consider how these relations will work in (7.1). We try to get a solution in which at least one of the ψ 's only involves a single spherical harmonic. Suppose that ψ_2 is proportional to P_k^* . Then the third equation of (7.1) tells us that terms from $\frac{\partial}{\partial z} \psi_1$ and $\left(\frac{\partial}{\partial x} - \frac{\partial}{\partial y} \right) \psi_2$ must cancel out with this, and any other terms they give must cancel out together. It follows that ψ_1 , ψ_2 must involve the same function of r , and must either be of the forms P_{k+1}^* , P_{k+1}^{*+1} , or P_{k-1}^* , P_{k-1}^{*+1} . A similar argument then shows that ψ_4 must involve r in the same way as ψ_2 and must have spherical function P_k^{*+1} . We therefore take as trial solution

$$\begin{aligned} \psi_1 &= -\alpha_1 F(r) P_{k+1}^*, & \psi_2 &= -\alpha_2 F(r) P_{k+1}^{*+1}, \\ \psi_3 &= \alpha_3 G(r) P_k^*, & \psi_4 &= \alpha_4 G(r) P_k^{*+1} \end{aligned}$$

(the factor $-i$ is introduced in ψ_1 , ψ_2 to make F real). We then find that the

α 's can be adjusted so that all four equations are satisfied. For example, the first equation gives

$$\begin{aligned} \frac{2\pi}{h} \left(\frac{W + eV}{c} + mc \right) a_1 F P_{k+1}^u & \\ + \frac{a_4}{2k+1} \left\{ - \left(\frac{dG}{dr} - \frac{k}{r} G \right) P_{k+1}^u + (k+u+1)(k+u) \left(\frac{dG}{dr} + \frac{k+1}{r} G \right) P_{k-1}^u \right\} & \\ + \frac{a_3}{2k+1} \left\{ \left(\frac{dG}{dr} - \frac{k}{r} G \right) P_{k+1}^u + (k+u)(k-u) \left(\frac{dG}{dr} + \frac{k+1}{r} G \right) P_{k-1}^u \right\} = 0 \quad (7.3) \end{aligned}$$

If, then, we take $a_4(k+u+1) + a_3(k-u) = 0$, the terms in P_{k-1}^u cancel. In the second equation, the same ratio makes the coefficient of P_{k-1}^{u+1} disappear. From the other two equations we find similarly $a_1 = a_2$, the ratio $a_1 : a_2$ is immaterial as it may be incorporated in F or G . We thus find as the complete solution

$$\left. \begin{aligned} \psi_1 &= -i F_k P_{k+1}^u, & \psi_2 &= -i F_k P_{k+1}^{u+1} \\ \psi_3 &= (k+u+1) G_k P_k^u, & \psi_4 &= (-k+u) G_k P_k^{u+1} \end{aligned} \right\} \quad (7.4)$$

where F_k, G_k satisfy the relations

$$\left. \begin{aligned} \frac{2\pi}{h} \left(\frac{W + eV}{c} + mc \right) F + \frac{dG}{dr} - \frac{k}{r} G &= 0 \\ - \frac{2\pi}{h} \left(\frac{W + eV}{c} - mc \right) G + \frac{dF}{dr} + \frac{k+2}{r} F &= 0 \end{aligned} \right\} \quad (7.5)$$

This solution we name $(k, j = k + \frac{1}{2}, m = u + \frac{1}{2})$

A similar process gives a different solution if we make the first instead of the second terms in (7.3) cut out. We now have ψ_1 involving P_{k-1}^u instead of P_{k+1}^u . F and G must then satisfy

$$\left. \begin{aligned} \frac{2\pi}{h} \left(\frac{W + eV}{c} + mc \right) F + \frac{dG}{dr} + \frac{k+1}{r} G &= 0 \\ - \frac{2\pi}{h} \left(\frac{W + eV}{c} - mc \right) G + \frac{dF}{dr} - \frac{k-1}{r} F &= 0 \end{aligned} \right\} \quad (7.6)$$

We can regard these equations as the same as (7.5) by changing k into $k-1$, so we write the solution F_{-k-1}, G_{-k-1} . Then we have

$$\left. \begin{aligned} \psi_1 &= -i (k+u) F_{-k-1} P_{k-1}^u, & \psi_2 &= -i (-k+u+1) F_{-k-1} P_{k-1}^{u+1} \\ \psi_3 &= G_{-k-1} P_k^u, & \psi_4 &= G_{-k-1} P_k^{u+1} \end{aligned} \right\} \quad (7.7)$$

This solution we name $(k, j = k - \frac{1}{2}, m = u + \frac{1}{2})$. We see in the subscripts of F and G the point of Dirac's method of allowing j to be negative. The equations (7.5) and (7.6) are substantially his equations at the foot of p. 622.

We have not justified the use of k as a quantum number, and this cannot be done until we study intercombinations, but anticipating this we may now count up the number of solutions and see that it is right for doublet spectra. In order to do this we must see what end cases are admissible. Take the first type of solution (7.4). If $u = k$, $\psi_4 = 0$ on account of the factor $(-k + u)$, and so in substituting in (7.1) we shall not be led astray by applying (7.2) to the impermissible function P_k^{k+1} . On the other hand, if we take $u = k + 1$, we get a function ψ_4 , but none of the others, and so evidently no solution. Similarly, at the other end we may take $u = -k - 1$ (involving $\psi_2 = 0$) but not $u = -k - 2$. In all there will be $2k + 2$ solutions. In the second type (7.7) we see in the same way that we may take u between $-k$ and $k - 1$ inclusive and so get $2k$ solutions. In both cases there are therefore $2k + 1$ solutions, as there should be. In the special case $k = 0$ there are only two solutions of the first type, and none of the second.

We have thus found by trial a system of solutions of our equations, and the important question arises as to whether it is a *complete* set. Can we simultaneously expand four arbitrary functions $\psi_1, \psi_2, \psi_3, \psi_4$ in terms of the solutions (7.4) and (7.7)? The full consideration would require a discussion of the radial functions including the quasi-hyperbolic case, which we shall not attempt, for even without it we can see that we have only half as many proper functions as are required. Taking an arbitrary radius we may expand the four given functions in spherical harmonics over the sphere. The k th harmonic will thus have $4(2k + 1)$ coefficients, all arbitrary, whereas we have seen that there are only $2k + 2 + 2k$ proper functions with ψ_2 and ψ_4 of order $\leq k$. The incompleteness is evidently the same thing as was pointed out in § 5. To get a complete set we must double the number of solutions by admitting negative values of the energy, and we have at present little idea of what this means.

8. We now discuss the radial functions (7.5). In the case where the radial force is arbitrary we can proceed by approximation based on the fact that F is much smaller than G . But the process would run very closely parallel to that of Dirac (p. 623) and we need not give it. We may only note that the null approximation gives Schrödinger's equation for G , and the next breaks it into

† If we start at the zero order and work up, determining each term as we go, the counting is a little different. For example, say that the expansion of the ψ 's only contains zero and first order harmonics. Then we have $2 + 2 = 4$ relations to fit to $4(1 + 3) = 16$ arbitrary quantities. If the second order is included as well, we have $2 + 2 + 4 + 4 = 12$ relations for $4(1 + 3 + 5) = 36$ quantities. In an infinite series, of course, the exact counting does not matter; the two sequences approximate to the ratio 1 : 2.

two terms depending on parameters k and $-k-1$, in fact, the ordinary doublet spectrum

We shall therefore proceed to find the accurate solution for the case of hydrogen. We take $V = e/r$ and it is convenient to introduce certain auxiliary symbols. Take

$$\frac{2\pi}{\hbar} \left(mc + \frac{W}{c} \right) = A^2, \quad \frac{2\pi}{\hbar} \left(mc - \frac{W}{c} \right) = B^2, \quad (8.1)$$

with A and B both positive, and write as usual for the "fine structure constant"

$$\gamma = \frac{2\pi e^2}{c\hbar} \quad (8.2)$$

and the equations (7.5) become

$$\left. \begin{aligned} \left(A^2 + \frac{\gamma}{r} \right) F + \frac{dG}{dr} - \frac{k}{r} G &= 0 \\ \left(B^2 - \frac{\gamma}{r} \right) G + \frac{dF}{dr} + \frac{k+2}{r} F &= 0 \end{aligned} \right\} \quad (8.3)$$

We solve these in series of the form

$$\left. \begin{aligned} F &= e^{-\lambda r} \{ a_0 r^s + a_1 r^{s-1} + a_2 r^{s-2} + \dots \} \\ G &= e^{-\lambda r} \{ b_0 r^s + b_1 r^{s-1} + b_2 r^{s-2} + \dots \} \end{aligned} \right\} \quad (8.4)$$

Substitute and equate to zero the various terms. We have

$$A^2 a_0 - \lambda b_0 = 0, \quad B^2 b_0 - \lambda a_0 = 0,$$

$$A^2 a_1 + \gamma a_0 - \lambda b_1 + (\beta - k) b_0 = 0, \quad B^2 b_1 - \gamma b_0 - \lambda a_1 + (\beta + k + 2) a_0 = 0,$$

$$A^2 a_{s+1} + \gamma a_s - \lambda b_{s+1} + (\beta - k - s) b_s = 0, \quad B^2 b_{s+1} - \gamma b_s - \lambda a_{s+1} + (\beta + k + 2 - s) a_s = 0$$

The first pair determine $\lambda = AB$, we must take the positive solution to make F, G finite at infinity. We also have $b_0/a_0 = A/B$. Substituting in the next pair, we find that both a_1, b_1 can be eliminated simultaneously. We get the indicial equation

$$\beta = -1 + \gamma \frac{A^2 - B^2}{2AB} \quad (8.5)$$

A similar elimination of a_{s+1}, b_{s+1} can be carried out and we have

$$A a_s \left(\beta + k + 2 - s + \gamma \frac{B}{A} \right) + B b_s \left(\beta - k - s - \gamma \frac{A}{B} \right) = 0,$$

from which we may substitute

$$\left. \begin{aligned} b_s &= c_s \left[\gamma \frac{B}{A} + \beta + k + 2 - s \right] \\ c_s &= c_s \frac{B}{A} \left[\gamma \frac{A}{B} - \beta + k + s \right] \end{aligned} \right\} \quad (8.6)$$

and can now form a difference equation for c_s . This reduces to

$$AB(2s+2)c_{s+1} = -c_s \{ (s-\beta-1)^2 - [(k+1)^2 - \gamma^2] \}$$

Writing $\sqrt{(k+1)^2 - \gamma^2} = k'$ (supposed positive) we have

$$2AB(s+1)c_{s+1} = -c_s(\beta+1-s-k')(\beta+1-s+k'),$$

and so

$$c_s = (-)^s \frac{(\beta-k'+1)(\beta-k')}{2^s s! (AB)^s} \frac{(\beta-k'-s+2)(\beta+k'+1)(\beta+k')}{s! (AB)^s} \frac{(\beta+k'-s+2)}{s! (AB)^s} \quad (8.7)$$

The series for F and G are composed of terms of this type each multiplied by a factor given by (8.6). If the solution is to be finite throughout space it is necessary that these series should terminate for some value of s such that $\beta-s \geq 0$. It is therefore necessary that $\beta = k' + n' - 1$, where n' is zero or a positive integer. This condition determines the energy levels. For we have

$$k' + n' = \gamma \frac{A^2 - B^2}{2AB} = \gamma \frac{W}{\sqrt{m^2 c^4 - W^2}},$$

and so

$$W = mc^2 \left\{ 1 + \frac{\gamma^2}{(k' + n')^2} \right\}^{-1} \quad (8.8)$$

This is exactly the original Sommerfeld expression for the energy levels of hydrogen. The only difference is that our k may take the value zero, so that the formula now involves $\sqrt{(k+1)^2 - \gamma^2}$.

The process of solution has at no stage made use of the fact that k is positive, and we conclude that the same solution will hold for (7.6) provided that we write $-k-1$ for k . In this case then $k' = \sqrt{(k^2 - \gamma^2)}$, and we see how the two k levels split. If we compare j 's instead of k 's we must take $k+1$ for the second solution, and the levels fall exactly together. In the case $k=0$ there is no second solution and no corresponding radial function for $k=-1$, as (8.7) will not then factorise into real factorials, so that the series cannot terminate.

We may now express the proper functions in terms of the quantum numbers. We make use of the auxiliary quantities

$$k' = \sqrt{((k+1)^2 - \gamma^2)}, \quad N = \sqrt{((k' + n')^2 + \gamma^2)}$$

and

$$\frac{2\pi m c \gamma}{h} = \frac{4\pi^2 m c^2}{h^2} = \frac{1}{a}$$

Then a is the "radius of the first hydrogen orbit" and N is approximately the total quantum number, counting 1, 2, 3, for the hydrogen levels. We then have

$$W = m c^2 (k' + n')/N$$

$$\begin{aligned} G_k &= e^{-r/aN} \left\{ r^{k+n-1} (N+k+1) - r^{k'+n'-2} a N (N+k) \frac{n' (n'+2k')}{2} \right. \\ &\quad \left. + r^{k'+n-3} a^2 N^2 (N+k-1) \frac{n' (n'-1) (n'+2k') (n'+2k'-1)}{2 \cdot 4} - \dots \right\} \\ F_k &= \frac{\gamma}{N+k'+n'} e^{-r/aN} \left\{ r^{k'+n'-1} (N+k+1) - r^{k'+n'-2} a N (N+k+2) \frac{n' (n'+2k')}{2} \right. \\ &\quad \left. + r^{k'+n-3} a^2 N^2 (N+k+3) \frac{n' (n'-1) (n'+2k') (n'+2k'-1)}{2 \cdot 4} - \dots \right\} \end{aligned}$$

(89)

We may observe that if we approximate by neglecting γ , we find that G_k and G_{-k-1} are respectively $(N+k+1)$ and $(N-k)$ times the ordinary radial function of Schrödinger.

The solution reveals a small blemish in the equations, for we have to admit the existence of proper functions which become infinite. The last term in the series for G has power $r^{k'-1}$, and if $k=0$, k' is very slightly less than 1, so that there will be a term with a small negative power of r . Of course all integrals connected with the spectrum are amply convergent. We do not perhaps know enough about the essential rules for proper functions to pay much attention to this defect. Moreover, it may well be that it would disappear if we could solve the problem of two bodies properly instead of treating the nucleus as an abstract centre of force.

As an example of these apparently complicated functions, we may set down the solutions corresponding to $N=1$ (exactly), the lowest hydrogen state

We shall replace the spherical harmonic symbols by the corresponding solid harmonics. Then the two solutions are ($k = 0$, $n' = 0$, $N = 1$, $u = 0$ and -1)

$$W = mc^2 \sqrt{1 - \gamma^2}, \quad \beta = \sqrt{1 - \gamma^2} - 1,$$

$$\psi_1 = -\frac{\gamma y}{1 + \sqrt{1 - \gamma^2}} x r^{s-1} e^{-r/a},$$

$$\psi_2 = -\frac{\gamma y}{1 + \sqrt{1 - \gamma^2}} (x + iy) r^{s-1} e^{-r/a},$$

$$\psi_3 = r^s e^{-r/a}, \quad \psi_4 = 0,$$

and

$$\psi_1 = \frac{\gamma y}{1 + \sqrt{1 - \gamma^2}} (x - iy) r^{s-1} e^{-r/a},$$

$$\psi_2 = -\frac{\gamma y}{1 + \sqrt{1 - \gamma^2}} x r^{s-1} e^{-r/a},$$

$$\psi_3 = 0, \quad \psi_4 = -r^s e^{-r/a}.$$

This will suffice as an illustration of the accurate solution.

9 We now consider the rules of combination. The emission can be calculated from (3.2) by setting down the values of V and A at a distant point. They depend on the retarded potentials and the work follows that of Klein very closely, so that we need not give details. We omit discussion of the very weak radiations of quadrupole and higher types. In calculating the chief radiation we shall have contributions from V and also from A . Taking the transition $p \rightarrow q$ we write $W_p - W_q = h\nu$ and find

$$V(x', y', z') = \frac{e^{i2\pi\nu(t-r'/c)}}{r'} \iiint \rho_{pq} \frac{(\mathbf{r}, \mathbf{r}')}{r'} + \frac{2\pi\nu}{c} dx dy dz,$$

where \mathbf{r} , \mathbf{r}' are the vectors from the origin to x, y, z and to the distant point of observation x', y', z' respectively, and r' is the absolute value of \mathbf{r}' . Similarly,

$$A_1(x', y', z') = \frac{e^{i2\pi\nu(t-r'/c)}}{r'} \iiint \frac{(\mathbf{j}_1)_{pq}}{c} dx dy dz$$

V involves the electric moment, and it should be noticed that, in spite of its different appearance, A does so too. For

$$\iiint j_1 dx dy dz = \iiint -x \left(\frac{\partial j_1}{\partial x} + \frac{\partial j_2}{\partial y} + \frac{\partial j_3}{\partial z} \right) dx dy dz,$$

since on partial integration the last two terms vanish. Hence by (3.5)

$$\iiint j_1 dx dy dz = \iiint x \frac{\partial \rho}{\partial t} dx dy dz = i2\pi\nu \iiint x \rho dx dy dz$$

Thus it will suffice to discuss the electric moment.

When our proper functions are written as the tesseral spherical harmonics, the three appropriate types of moment are $x + iy$, z , $x - iy$. For determining what combinations occur we require the following easily proved relations —

$$\begin{aligned} \iint P_k^u P_{k-1}^{u-1*} \sin \theta e^{-i\phi} \sin \theta d\theta d\phi &= - \iint P_k^u P_{k-1}^{u+1*} \sin \theta e^{i\phi} \sin \theta d\theta d\phi \\ &= \iint P_k^u P_{k-1}^{u*} \cos \theta \sin \theta d\theta d\phi = \frac{4\pi}{(2k+1)(2k-1)} (k+u)! (k-u)! \end{aligned} \quad (91)$$

For all other products of these types the integral vanishes. We may here note also the normalising relation

$$\iint P_k^u P_k^{u*} \sin \theta d\theta d\phi = \frac{4\pi}{2k+1} (k+u+1)! (k-u)! \quad (92)$$

With the help of (91) we can see what combinations might occur. It will evidently suffice to treat of only one type of polarisation and we shall take that corresponding to z . The following scheme then shows the only solutions which might, according to (91), combine with the first. We only mark the harmonic coefficients

k	j	ψ_1	ψ_2	ψ_3	ψ_4
k	$k + \frac{1}{2}$	P_{k+1}^u	P_{k+1}^{u+1}	P_k^u	P_k^{u+1}
$k-1$	$k - \frac{1}{2}$	P_k^u	P_k^{u+1}	P_{k-1}^u	P_{k-1}^{u+1}
$k+1$	$k + \frac{1}{2}$	P_k^u	P_k^{u+1}	P_{k+1}^u	P_{k+1}^{u+1}
$k+1$	$k + \frac{3}{2}$	P_{k+2}^u	P_{k+2}^{u+1}	P_{k+1}^u	P_{k+1}^{u+1}
$k+3$	$k + \frac{5}{2}$	P_{k+2}^u	P_{k+2}^{u+1}	P_{k+3}^u	P_{k+3}^{u+1}
$k-1$	$k - \frac{3}{2}$	P_{k-2}^u	P_{k-2}^{u+1}	P_{k-1}^u	P_{k-1}^{u+1}

When we examine these, actually putting in the coefficients, we find that the last two vanish identically. This verifies the j rule, that only $j \rightarrow j \pm 1$ or $j \rightarrow j$ are possible combinations.† A similar result follows, of course, if we examine the other polarisations or the combinations of the second type of solution. We shall not give the numerical values here as these are well known, but one more point deserves remark. The radial integrations are, speaking

† Of course the k rule is required as well, for there are levels k , $k - \frac{1}{2}$ and $k + 2$, $k + \frac{3}{2}$ which do not combine with k , $k + \frac{1}{2}$. Dirac's use of negative j does make the statement simpler.

accurately, different for the three lines arising from a given $k \rightarrow (k-1)$. They are, in fact,

$$\int (F_k F_{k-1} + G_k G_{k-1}) r^2 dr, \quad \int (F_{-k-1} F_{-k} + G_{-k-1} G_{-k}) r^2 dr$$

and

$$\int (F_{-k-1} F_{k-1} + G_{-k-1} G_{k-1}) r^2 dr$$

But to a first approximation we saw that F could be neglected beside G , while $G_{-k-1} = G_k$, so that to this approximation the three radial integrations are the same. This explains why the intensities bear simple numerical ratios to one another in doublet spectra

10. When a uniform magnetic field is imposed on a doublet atom it is not possible to get an accurate solution, and we have to fall back on the method of perturbations. The simplest way of working out the Zeeman effect is to use the approximation of § 4, which reduces it to the work done in my earlier paper. That this is a sufficient approximation may be seen from the fact that it gives the doublet fine structure and treats the magnetic structure as of the same order of magnitude, which is just the degree of accuracy required to explain the observed effects. But a direct attack, starting from the accurate solution of (7.1) and superposing on it the magnetic field, is also interesting, it throws the solution into rather a different form because the levels of the fine structure are already separated, whereas in the earlier process they were attributed to a perturbation acting together with the magnetic field.

We must first see how the method of perturbations will go. The solutions of (2.2), when p_0 is replaced by W so that they give the levels, obey an orthogonal relation, as is easily proved directly, thus for any two solutions p, q either

$$W_p - W_q = 0, \quad \text{or} \quad \iiint \sum_{\lambda=1}^4 \psi_\lambda^p \psi_\lambda^{q*} dx dy dz = 0 \quad (10.1)$$

In the case of degeneracy, where $W_p = W_q$, the partly arbitrary ψ_λ^q can be chosen so that (10.1) will still be true. This has already been done in our case. Let us suppose that on account of small changes in V and A the four equations (2.2) are affected by small extra terms which we may write as $P_1 \psi \quad P_4 \psi$, each symbol signifying that any of the ψ 's may enter into each equation. We require a solution near W_p and assume that it is of the form

$$\psi_\lambda = \sum a_\lambda \psi_\lambda^q,$$

where the a_s 's are small for all cases where W_s is not nearly equal to W_p . Notice the slight difference that we must make from the theory of perturbations of a degenerate system, on account of the fact that we have to allow for the interaction of solutions that initially are not quite coincident. Substituting in (2.2) we have

$$\sum_s \frac{1}{c} (W - W_s) a_s \psi_s^* + \sum_s a_s P_1 \psi_s^* = 0, \text{ etc}$$

We multiply these by ψ_1^{**} , etc., add the four equations together and integrate over space. We thus find

$$\frac{1}{c} (W - W_0) a_0 \int \sum_{\lambda=1}^4 \psi_\lambda^* \psi_\lambda^{**} dx dy dz + \sum_s a_s \int \sum_{\lambda=1}^4 \psi_\lambda^* P_\lambda \psi_s^* dx dy dz = 0$$

If there are a number of states q near p , even though not coincident with it, the associated a_q 's need not be small and must be retained. We then form the determinant in the usual way, giving an algebraic equation for W , and afterwards we can determine the various ratios for a_q .

For a magnetic field along z we take $A_1 = -\frac{1}{2}Hy$, $A_2 = \frac{1}{2}Hx$ and so must add on to (2.2) terms

$$P_1 \psi = -i \frac{eH}{2c} (x - iy) \psi_4, \quad P_2 \psi = i \frac{eH}{2c} (x + iy) \psi_3,$$

$$P_3 \psi = -i \frac{eH}{2c} (x - iy) \psi_2, \quad P_4 \psi = i \frac{eH}{2c} (x + iy) \psi_1$$

We hence get

$$\frac{1}{c} (W - W_0) a_0 \int \sum_{\lambda=1}^4 \psi_\lambda^* \psi_\lambda^{**} dx dy dz + \frac{eH}{2c} \sum_s a_s [q, s] = 0, \quad (10.2)$$

where

$$[q; s] = \int \{ -i \psi_1^{**} (x - iy) \psi_4^* + i \psi_2^{**} (x + iy) \psi_3^* - i \psi_3^{**} (x - iy) \psi_2^* + i \psi_4^{**} (x + iy) \psi_1^* \} dx dy dz \quad (10.3)$$

This expression determines whether two levels q, s can interfere with one another in producing the Zeeman effect. If we apply the formulae of (9.1) to any of the solutions (7.4) or (7.7), we at once see that unless the number u is the same for both q and s , the integral must vanish. Hence only levels with the same quantum number $m (= u + \frac{1}{2})$ can interfere. Further, we can build a table, of the same kind as was made in § 9 for combinations, to show what possible k, j values might give non-vanishing integrals, and, just as there, we find that some of the possibilities disappear on closer examination. We are left to consider interferences of $(k, k + \frac{1}{2})$ and $(k, k - \frac{1}{2})$ with themselves and one

another and also of $(k, k + \frac{1}{2})$ with $(k + 2, k + \frac{3}{2})$ (the case $(k, k - \frac{1}{2})$ with $(k - 2, k - \frac{3}{2})$, which also occurs, is essentially the same as this last) The first set are what we are familiar with, but the last is rather unexpected. We shall prove that it is small of an order to be neglected, because it corresponds to the terms we should have by a second approximation

Substituting out of (7.4), (7.7) and applying (9.1) we find

$$[k, k + \frac{1}{2}, k + 2, k + \frac{3}{2}] = \frac{4\pi}{2k+3} (l+u+2)! (k-u+1)! \int (F_k G_{k-3} + G_k F_{k-3}) r^3 dr$$

In order to reduce the radial integration, we proceed as follows. Take the equations (7.5) and a similar pair in which k is replaced by another number l . Multiply the first of (7.5) by G_l , the second by F_l and add. This removes the terms in W and eV . Then interchange k and l and add the two expressions together. The result is

$$\frac{2\pi}{h} 2mc (F_k G_l + F_l G_k) + \frac{d}{dr} (F_k F_l + G_k G_l) - \frac{k+l}{r} G_k G_l + \frac{k+l+4}{r} F_k F_l = 0$$

Hence making a partial integration we find

$$\int (F_k G_l + F_l G_k) r^3 dr = \frac{h}{4\pi mc} \int [G_k G_l (k+l+3) - F_k F_l (k+l+1)] r^3 dr \quad (10.4)$$

For the case $l = -k - 3$, the term in G therefore vanishes. We know that F is smaller than G in a ratio of order γ^{-1} , hence this integral bears to one where the coefficient of G does not vanish a ratio γ^3 , which is the order of a term of the second, not the first approximation.

We are thus left with the result that only the two k levels interfere. Let us call $(k, k + \frac{1}{2})$, p and $(k, k - \frac{1}{2})$, q . Then our solution may be written as

$$\psi_\lambda = a\psi_\lambda^p + b\psi_\lambda^q,$$

and we find by the application of (9.1) and (10.4) that

$$[p, p] = -4\pi \frac{2k+2}{2k+1} (2u+1)(k+u+1)(k-u)! \frac{h}{4\pi mc} \int \left(G_k^2 - \frac{2k+1}{2k+3} F_k^2 \right) r^3 dr,$$

$$[q, q] = -4\pi \frac{2k}{2k+1} (2u+1)(k+u)(k-u-1)! \frac{h}{4\pi mc} \int \left(G_{-k-1}^2 - \frac{2k+1}{2k-1} F_{-k-1}^2 \right) r^3 dr$$

$$[p, q] = [q, p] = -\frac{4\pi}{2k+1} 2(k+u+1)(k-u)! \frac{h}{4\pi mc} \int G_k G_{-k-1} r^3 dr$$

We also require the normalisations. Using (9.2) these are

$$\int \sum_{\lambda} |\psi_{\lambda}^{\pm}|^2 dx dy dz = 4\pi (k+u+1)! (k-u)! \int (F_k^2 + G_k^2) r^2 dr,$$

$$\int \sum_{\lambda} |\psi_{\lambda}^{\pm}|^2 dx dy dz = 4\pi (k+u)! (k-u-1)! \int (F_{k-1}^2 + G_{k-1}^2) r^2 dr$$

Now we have seen that in all these the terms in F_k, F_{k-1} are small compared to those in G . Furthermore, we know that to the same approximation G_{k-1} is proportional to G_k , and may be taken equal to it by a suitable definition. Hence all the radial integrations are the same, and they may therefore be omitted. The equation (10.2) thus becomes

$$\frac{a}{c} (W - W_0) - \frac{eH}{2c} \frac{\hbar}{4\pi mc} \frac{2k+2}{2k+1} (2u+1) a - \frac{eH}{2c} \frac{\hbar}{4\pi mc} \frac{2b}{2k+1} = 0$$

$$\frac{b}{c} (W - W_0) - \frac{eH}{2c} \frac{\hbar}{4\pi mc} \frac{2k}{2k+1} (2u+1) b - \frac{eH}{2c} \frac{\hbar}{4\pi mc} \frac{(k+u+1)(k-u)}{2k+1} 2a = 0$$

To reduce this to the familiar form we write W_0 as the mean centre of the two lines, so that

$$W_+ = W_0 + k\beta, \quad W_- = W_0 - (k+1)\beta,$$

and $W = W_0 + \bar{W}$. Also take $\omega = \frac{eH}{2mc} \frac{\hbar}{2\pi}$. Then we have

$$a \left\{ \bar{W} - k\beta - \omega \frac{k+1}{2k+1} (2u+1) \right\} - b\omega \frac{1}{2k+1} = 0,$$

$$-a\omega \frac{(k+u+1)(k-u)}{2k+1} + b \left\{ \bar{W} + (k+1)\beta - \omega \frac{k}{2k+1} (2u+1) \right\} = 0,$$

and from this we derive

$$\bar{W}^2 + \beta \bar{W} - k(k+1)\beta^2 + \omega(2u+1)(\bar{W} + \beta) + \omega^2 u(u+1) = 0,$$

which is the standard equation for the Zeeman effect in doublets. It will be seen that the algebra is a little more complicated than that which comes from forming the approximate equations in ψ_2, ψ_4 , as was done before. We shall not work out intensities as nothing new would be found.

Summary

Dirac's recent papers on the Quantum Theory of the Electron are discussed making use of the ordinary methods of differential equations instead of the non-commutative algebra used by him.

The equations are formed and proved invariant for relativistic transformations.

The emission of radiation from an atom containing Dirac's electron is discussed

It is shown how Schrödinger's equation, and the pair of equations recently given by the present writer, are successive approximations to Dirac's.

A few points in the free motion of an electron are reviewed

The equations are solved for the motion of an electron in a central field of force They are shown to be expressible in terms of spherical harmonics and to lead to a doublet structure for the spectrum

The discussion of the radial functions in the case of hydrogen is shown to lead exactly to Sommerfeld's original formula for the levels

The rules of combination are considered in outline, and the Zeeman effect is worked out

Fluid Resistance to Moving Spheres.

By R. G. LUNNON, M A, M Sc

(Communicated by T. H. Havelock, F.R.S.—Received January 31, 1928)

In a previous paper on the resistance of air to falling spheres,* attention was drawn to the value of supplementing that work by observations on the fall of solid spheres in liquids, and the present paper gives the results of such experiments They confirm our previous conclusions as to the increased resistance to accelerated motion and they give more precise values for the resistance to uniform motion, a problem which can now be regarded as fairly solved on its experimental side

In these experiments, spheres of steel, bronze and lead, up to 5 cm. in diameter, were allowed to fall freely in water through distances up to 200 cm. The water was contained in a special steel tank, with two opposite faces of plate glass, its cross section was square, 45 cm in breadth Each ball was released from supporting rings beneath the surface of the water, and the measured fall ceased when it struck a small platform which could be set at any desired depth. At the instants of release and striking, a phonic chronograph (as previously described) was started and stopped by appropriate electrical

* Lunnnon, 'Roy. Soc. Proc.,' A, vol. 110, p. 304 (1926).

devices, and the time of fall for a series of distances was then recorded for each ball

The release apparatus was designed to give the minimum disturbance to the liquid, and to avoid any initial rotation of the falling sphere. It consisted, as shown in fig 1 (A), of a pair of tongs carrying two wire rings for holding the ball, and controlled by two springs and an electromagnet

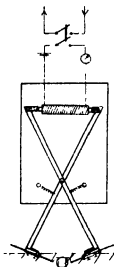


FIG 1A

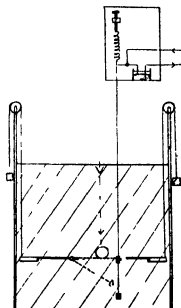


FIG 1B

When the current through the magnet winding was switched off, the springs opened the tongs, and the small time-lag between these two events was found to be constant for a single value of the current, provided that the ends of the magnet and of the soft iron pole-pieces were carefully planed and separated by thin paper

The striking device, shown in fig 1B, was a hinged perforated plate, carried on an iron frame. A light wire of constant length, held taut by a small weight, was fastened to the plate and its upper end was carried by a spring above the water, its sudden movement when the plate was struck, operated through a light lever to break a mercury contact and arrest the chronograph. The adjustment of this apparatus for each depth of fall was simple, and the action was satisfactory. Sometimes six similar balls could be dropped in succession through the same distance, without the readings of the time interval differing by more than 0.002 second.

Two independent measurements of the time-lag in the apparatus showed that it was a constant, 0.023 second, under the standard conditions. In the first, the distance of fall of a sphere was reduced in successive readings until it was only 5 mm, and a distance-time (s, t) graph was drawn. This was a smooth curve, and could be extrapolated to the s -axis with an error less than 0.001 second. In the second, the level of the water was lowered down to the plate, and the known time of fall in free air was subtracted from the time recorded. A possible variation of the lag with the weight of the ball was suspected and carefully examined, but for all spheres heavier than the 0.87 cm steel ball, the lag was constant. No smaller balls were used in the detailed work, but a few readings were taken with very small balls with a stop-watch. The watch was also used for some readings with a 2-inch ball of phosphor-bronze which was too heavy to be held by the tongs.

Sources of Error

The times with which we were concerned were between 0.1 and 1.5 seconds and a possible error of ± 0.001 second was imposed by the instruments. The recorded times differed among themselves by more than this in the long falls. For instance, the times for four successive falls through 193.3 cm by an "L" steel ball were registered as 1.273, 1.278, 1.266 and 1.270 seconds. An obvious reason was that the falls were not straight. There is always some swerving in the path of falling spheres. It is easily visible with a light ball, e.g., large rubber ball falling 100 metres in air, or with a stone falling in water. It was just visible with a steel ball of diameter of 1.27 cm falling in water through 150 cm. Apart from being visible during the falls, a departure from a straight path was usually shown by the sphere striking the plate at some distance from the point vertically beneath the point of release. When this distance exceeded 2 cm the reading was rejected, the results were then more consistent, and the lowest reading was taken.

Measurements were made on different days, often at widely separated intervals. They were compared by plotting graphs of two kinds. In the first place, the times for a single fall-distance were plotted against the diameter of the falling spheres, usually six or seven sizes, all of steel spheres, would be dropped through the same distance, consecutively, at least four spheres of each size being used. In the second graphs, the times for different distances for a single ball were compared. On graphs of the first kind, there were hardly any points more than 0.003 second off a smooth curve, these graphs were used as a check, to

avoid obvious errors in the readings. On those of the second kind (s, t graphs) there were sometimes discrepancies of 0.005 second.

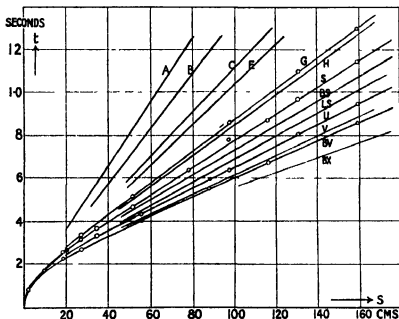


FIG. 2.—Times of Fall for Spheres in Water

Temperature

The effect of temperature was considered. Readings were always taken from thermometers at the top and the bottom of the tank, and these differed sometimes by more than 0.5°C . The temperature of the water was as low as 8.5°C on certain cold days, and its highest temperature during the experiments was 18°C . This corresponds to a difference of 25 per cent in the viscosity of water, but we failed to detect any variation in the speed of a falling sphere to within 1 per cent. This is in agreement with the known relation between resistance and speed. For although the graph of ψ , the resistance coefficient with R , the Reynolds number, is not a horizontal line (in which case the viscosity would have no effect), yet its gradient is very slight in this range of speeds. We have calculated the effect for one of the steel balls ($d = 1.27\text{ cm}$) by taking each of a series of values of the velocity, V , calculating ψ , then using the ψ, R graph to find R , and from this calculating the kinematic viscosity, ν . For instance, if V is 166 cm per second, ψ must be 0.159, R is then 1.24×10^4 , and hence $\nu = 0.17$. (The density of water enters into R , and its variation is inappreciable.) When the velocity is 161, 163, or 166 cm per second, the

value of ν is 0 10, 0 13, 0 17 For the range of temperature during our experiments (8° to 18° C), the variation in ν is less than this, and the change in velocity should therefore be inappreciable, as we found it to be No observation of a decrease of resistance with an increase of viscosity has yet been made, it should be possible to observe it by finding that a $\frac{1}{2}$ -inch steel ball in water at 2° C falls at 166 cm per second, whereas the same ball finds greater resistance in very much less viscous water at 20° C, and falls at 161 cm per second

Results

The final results for steel spheres of 12 different sizes, and for bronze and lead spheres of five and two sizes respectively, are shown in Table I The times given have been corrected for lag and for chronoscope rating error in the manner already described Some of the displacement curves are shown in fig 2 The final velocities, c , range from 135 to 280 cm per second, and they are attained in the first 80 cm of fall The values can be obtained accurately from the curves (drawn on a large scale), for the many points for $s > 80$ lie very closely on straight lines Further, by drawing these lines backwards to cut the axis $s = 0$, the intercepts t_0 can be measured These are of value because the initial parts of the curves can be fairly well fitted by an equation of the form $gs = c \log \cosh qt$, and for large values of s , this equation is equivalent to $gs = c(qt - \log 2)$ This is the equation of the straight lines, and the intercept t_0 is evidently related to q by the formula $qt_0 = \log 2$

Table I—Times of Fall (in seconds) through Heights s (in centimetres)

s	Steel								Bronze				Lead	
	G	H	K	S	P	L	U	V	BS	BU	BV	BW	LS	LU
2 5				0 085			0 082							
9 8		0 181	0 179	0 177	0 175	0 175		0 165	0 176				0 174	
18 8				0 258			0 226			0 218				0 212
27 0	0 339		0 325	0 316		0 308		0 281			0 270			
34 6		0 392	0 376	0 368	0 360	0 354	0 335	0 358	0 328				0 349	
51 1	0 518	0 510	0 486	0 472	0 461	0 444		0 403	0 462				0 436	
55 7							0 435	0 426		0 420	0 405	0 400		0 405
77 9		0 695	0 661	0 640	0 624	0 607		0 598	0 567		0 560	0 555	0 546	0 580
87 5							0 598	0 567						0 547
97 3	0 860	0 836	0 786	0 761	0 733	0 712	0 640	0 722		0 704	0 682	0 684	0 675	0 687
116 0		0 964	0 908	0 877	0 839	0 815		0 807					0 783	0 659
130 7	1 100			0 970			0 807							
159 7	1 305	1 268	1 188	1 146	1 094	1 054	0 948	0 896	1 076	0 886	0 860	0 802	1 019	0 820
192 9	1 57	1 514	1 418	1 351	1 297	1 241	1 100	1 050	1 256	1 02	0 978	0 83	1 180	0 971

(a) *Resistance to Accelerated Motion*—The extent to which the formula is in agreement with the experimental results, may be first shown by reference to the $\frac{1}{2}$ -inch steel ball ($d = 1.27$ cm). The values of c and q , as given by the graph, are 162 and 4.33 respectively, and Table II shows the times calculated from the

Table II Test of Formula for Acceleration Period for S Ball

s	2.5	6.8	9.8	12.5	18.8	20.2	27.0	34.6	42.0	51.1	centi- metres
t (observed)	0.085	0.143	0.177	0.203	0.258	0.268	0.316	0.368	0.412	0.472	seconds
t (calculated)	0.085	0.142	0.175	0.200	0.252	0.262	0.315	0.364	0.409	0.472	seconds
$t_o - t_c$	0	0.001	0.002	0.003	0.006	0.006	0.001	0.004	0.003	0	seconds

formula $qs = c \log \cosh qt$. There is a small regular discrepancy between these and the experimental values, so that the resistance is first a little greater than the formula implies, and afterward a little less. In the experiments on air resistance, a similar effect was noticed. In that case, we were able to deduce the actual resistance from the displacement curves, but in the present measurements the times are smaller and the experimental errors of 0.001 second are too large in comparison for this deduction to be made. We can be sure, however, that the general shape of the acceleration-velocity curve is that of fig. 3 resembling the curves of fig. 5 in our previous paper. The broken straight line corresponds to the equation given above.

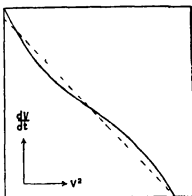


FIG. 3

The discrepancies for other spheres are all similar in their variation. Table III gives their values in thousandths of a second at four different distances.

Table III—Test of Formula for Acceleration Period for 7 Balls

Distance	Values of t (observed) — t (calculated) in thousandths of a second						
s	H	K	S	P	L	BS	LS
9.8	2	4	2	3	1	6	6
20.2	8	9	6	5	9	7	11
34.6	8	7	4	4	6	6	7
51.1	6	4	0	2	-3	9	-1

If these small amounts are neglected, the motion can be described in terms of a constant "carried mass" For a resistance formula which leads to the above displacement equation is

$$F = av^2 + b(dv/dt) \quad (1)$$

where b is the carried mass Here b is connected with q by the relation

$$cq(m + b) = mg(1 - \sigma/\rho), \quad (2)$$

where m is the mass of the sphere, ρ its density and σ the density of the liquid The calculated values of b are given in Table IV

Table IV—Acceleration Constants

Sphere	t_0	q	b	Sphere	t_0	q	b
	second		gramme		second		gramme
Steel H	0 143	4 85	0 86	Bronze BS	0 17	4 08	2 0
" K	0 15	4 62	1 2	" BU	0 20	3 46	4 1
" b	0 16	4 33	1 4	" BV	0 21	3 30	6 6
" P	0 165	4 20	2 2	" BW	0 23	3 01	9 2
" L	0 17	4 08	2 9	" BV	0 24	2 83	12 2
" U	0 195	3 56	4 3	Lead LS	0 18	3 86	2 6
" V	0 20	3 46	7 3	LU	0 21	3 30	5 4

It appears that b is larger for the larger spheres, but it does not bear a constant ratio to the mass of water displaced For small spheres, b is twice the displaced mass, and for $1\frac{1}{4}$ -inch spheres, the ratio is one-half There is a close proportionality for all three kinds of spheres between b and the square of the sphere diameter, with a factor of about one, the same proportional relation held for motion in air, with a factor of one-half, but the ratio of the carried mass to the displaced mass of air was very large Cook* noticed that for a very large sphere, the carried mass appeared to be about one-half of the displaced mass of water, and the corresponding fraction was 0 83 in some experiments by Relf and Jones,† using the spherical bob of a pendulum No other estimates of its value have been made A similar ratio is commonly used in the calculation of the resistance of ships, the carried mass being taken as one-fifth of the weight of the ship The extent to which this ratio affects the motion may be illustrated by the fact that if the ratio were also one-fifth in our own case, the values of t_0 would range from 0 11 to 0 15 second for the steel balls, whereas the actual values are from 0 14 to 0 18 second, with an error less than 0 005 second

* 'Phil Mag,' vol. 39, p 350 (1920)

† Quoted by Cowley and Levy, "Adv Ctce Aero, R & M," No 612 (1918)

[*Added February 29, 1928* —The carried mass can be expressed in terms of non-dimensional quantities. For the case of a falling sphere, it is easily shown by the method of dimensions that $6b/\pi\rho d^3$ (i.e., the ratio of the carried mass of fluid to the displaced mass) is a function of cd/v (i.e., the Reynolds number for the final speed) and qd/c . Values of these quantities can be calculated from the results of this paper, and also from those of the earlier measurements in air. We find that the mass-ratio decreases when either cd/v or qd/c increases, and that the data for water and for air experiments are in accord with each other, although they relate to widely separated ranges of qd/c . They are too few for accurate general conclusions to be drawn, but their variation can be shown by the following approximate figures.

$qd/c \times 10^4$		0.3	1	4	25	30	45
$\frac{v}{10^4}$ \times $\frac{cd}{\rho}$	2	1200	500	100	1	0.80	0.20
	6	600	100	95	0.90	0.25	0.18
	10	300	250	95	—	0.18	0.11

Values of the Carried-mass Ratio

When these values are plotted on a logarithmic scale, against qd/c , for constant values of R , the air and water figures give points lying on the same curves. The only other figure available for comparison is deduced from Cook's readings, for $cd/v = 14 \times 10^4$, $qd/c = 1560 \times 10^{-4}$, the carried mass ratio may be 0.46, with a large possible error. This is outside the range of values given above.]

It may be remarked that the approximate law of resistance (1) is analytically equivalent for a falling sphere to a law containing only the velocity, namely,

$$F = A + Bv^2,$$

the connection between these constants and the previous ones being

$$A = gbm(1 - \sigma/\rho)/(m + b), \quad B = am/(m + b)$$

Although this simpler hypothesis affords an equal fit with the experimental results, it has two serious disadvantages, it suggests a definite resistance when both velocity and acceleration are zero, and its constants, A , B , are found to depend upon the mass or density of the sphere. On the other hand, our previous results with falls in air, using spheres of widely differing densities, are in agreement with the present ones in showing that the new factor b is nearly independent of the density. This suggests that the form (1) may have a wider

application as an approximate formula than merely to the case of spheres falling in a fluid

(b) *Resistance to Uniform Motion*—The resistance to uniform motion is best expressed in terms of the resistance coefficient ($\psi = F/\rho v^2 d^2$) and the Reynolds number, and their values in our experiments are given in Table V. In this list

Table V

Sphere	<i>d</i>	<i>m</i>	ρ	<i>c</i>	ψ	<i>R</i> + 100
	(cm.)	(gm.)	(gm./c.c.)	(cm./sec.)		
Steel A	0.238	0.054	7.75	67	0.175	14.1
" B	0.317	0.129	7.75	82	0.159	23.1
" C	0.476	0.432	7.75	104	0.150	44.2
" F	0.635	1.030	7.75	120	0.150	87.5
" G	0.878	2.695	7.75	140	0.155	109
" H	0.952	3.48	7.69	144	0.164	120
" K	1.111	5.67	7.75	153	0.165	152
" S	1.270	8.27	7.69	162	0.167	184
" P	1.429	11.86	7.75	171	0.170	219
" L	1.650	18.25	7.75	180	0.174	265
" U	2.540	66.12	7.69	214	0.191	486
" V	3.175	129.14	7.69	233	0.202	661
Bronze B8	1.27	9.56	8.90	177	0.165	159
" BU	2.54	76.50	8.90	239	0.194	542
" BV	3.17	149.2	8.90	253	0.201	717
" BW	3.81	258.4	8.90	278	0.201	940
" BX	5.08	612.0	8.90	(302)	(0.197)	(1370)
Lead LS	1.27	11.28	10.50	192	0.171	217
" LU	2.54	90.48	10.50	254	0.197	578

there are included the figures of several very small spheres, and for one large one, which depend upon stop-watch observations and are less accurate. The ψ , *R* graph is given in fig. 4. The points for the three different metals lie on a single smooth curve, which supports their value. They are in almost complete accord with the points recorded by Wieselsberger,* whose results obtained from the Göttingen wind tunnel are the most extensive set of sphere resistance measurements. This agreement between air and water results extends over a hundred-fold range of velocities (from $R = 10^3$ to $R = 10^5$), and thus verifies the principle of dynamical similitude for turbulent fluid motion. Liebster's† low speed results are in similar agreement, but Allen's‡ figures in the region of $R = 3 \times 10^3$, give lower values of ψ , probably because the wall effects could

* 'Phys. Z.', vol. 22, p. 322, and vol. 23, p. 222 (1922)

† 'Ann. d. Physik,' vol. 25, p. 670 (1924), and vol. 82, p. 541 (1927)

‡ 'Phil. Mag.', vol. 50, pp. 323, 519 (1900)

not be allowed for in his small vessel Shakespear's* results are also low, in comparison, by about 6 per cent, and our own experiments in mines gave still

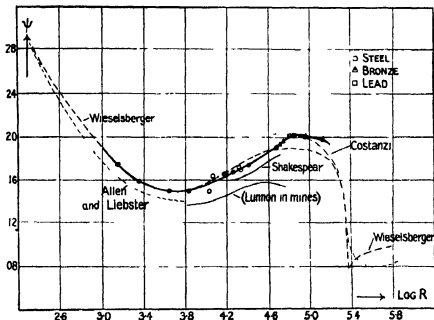


FIG. 4.—Variation of Resistance Coefficient with Reynolds Number

lower values. These differences must be attributed to different degrees of initial turbulence in the fluid. The water in our tank was quite still, the air in Shakespear's tower was only comparatively quiet, and the air in mine-shafts was probably least quiet (although the vane anemometer registered no currents), because of the gradient of temperature within it, and the presence of inlet passages near the base of the shafts.

The course of the ψ, R curve being now well determined, emphasis may be given to the fact that the resistance is never proportional to a simple power of the velocity over any extended range of speed. In illustration of this, we have calculated the constants in a simple power law for the case of a sphere of 2 cm diameter, in water at 12° C, and the following formulæ are the result. They are based on the experimental ψ, R curve.

* * Phil. Mag., vol. 28, p. 728 (1914)

$V = 0.005$ cm per second	$F = 0.24 V$
$V = 0.008$ „	$F = 0.47 V^{1.12}$
$V = 0.014$ „	$F = 0.65 V^{1.16}$
$V = 0.042$ „	$F = 0.91 V^{1.28}$
$V = 0.18$ „	$F = 1.12 V^{1.36}$
$V = 0.74$ „	$F = 1.26 V^{1.52}$
$V = 3.8$ „	$F = 1.15 V^{1.74}$
$V = 21$ „	$F = 0.73 V^{1.94}$
$V = 89$ „	$F = 0.52 V^{2.05}$
$V = 400$ „	$F = 0.72 V^2$

The first and last of these correspond to the laws of Stokes and Newton, for higher speeds, the resistance changes rapidly, and in a more complex manner.

Our previous note on Sir Isaac Newton's results, with spheres falling in air and water, can now be extended. A complete analysis of them shows that his good agreement between experiment and theory, in the case of spheres falling in air, is mainly a result of the cancelling of two opposite errors.

He over-estimated the resistance coefficient, and omitted the "carried mass" effect for the acceleration period. In the water experiments, where the range of R was different, his value of the resistance coefficient was nearly correct, but by omitting the acceleration term he failed to show so good an accord between theory and experiment. Also, his weighted wax spheres fell in the water with considerable swerving, and the experimental results are not in good agreement with each other. It is no mean tribute to his care and skill as an experimenter that most of the results should still be worthy of this complete analysis.

Wall Effect

The well-known Ladenburg correction for the influence of cylindrical walls upon the resistance, is not applicable if the Reynolds number exceeds 1000. We have performed some experiments to examine this influence at higher speeds. Spheres were allowed to fall freely in the tank already described, and glass tubes of different diameters and lengths were held vertically in the water in turn, so that the spheres fell centrally through them. By timing the fall of the same sphere through tubes of equal diameters and different lengths, the terminal velocity for each sphere was deduced. The results for a series of steel balls, and for four sizes of tube, are shown in fig. 5, the temperature of the water was 13.5°C . The reduction in velocity becomes very marked as the ratio of the diameters of sphere and tube increases. It is to be remembered

that for all these speeds, the resistance is roughly proportional to the square of the speed, and the uppermost curve would be a parabola if this proportionality were exact

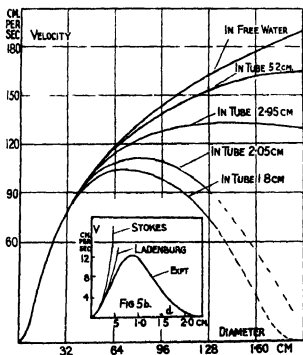


FIG 5—Rates of Fall for Steel Balls in Water in Tubes

Inset—Rate of Fall for Balls in Glycerine in Tube

It is of interest to contrast the shape of these curves with those which describe the similar effect in a more viscous liquid, where the velocities are small Fig 5b (inset) shows the velocities obtained by dropping steel balls through glycerine in a tube of 2.25 cm diameter

In Ladenburg's formula, the ratio of the reduced velocity to the velocity in unbounded fluid, is expressed as a linear function of the ratio of the sphere and tube diameters, for small spheres The corresponding function for the present results is less simple, and is shown by the curve of fig 6 The reduction in velocity is proportionately less than would be given by the earlier formula A linear relation may be given for the range $0 < d < 0.3 D$, viz, $V = V_0(1 - 0.23 d/D)$

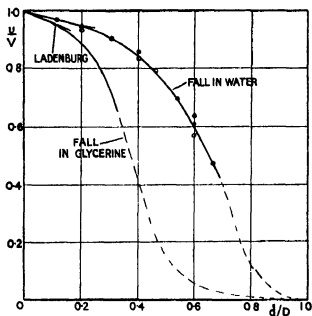


FIG. 6—Ratio of Falls of Spheres in Tubes

Character of the Fluid Motion

The explanation of the resistance law must be based upon a knowledge of the lines of flow in the fluid. Although little progress has been made in this direction, it may be convenient to summarise such observations as have been made.

The regular stream-line pattern of the Stokes solution becomes deformed at moderate speeds, and at the first critical speed a vortex ring is formed close behind the sphere, appearing as two eddies when cut by a plane through the axis of motion.

In air, this appears at the velocity corresponding to $R = 8$, and it has been carefully studied by Nisi and Porter* for speeds up to $R = 50$, and for higher values in narrow channels. (Reference has already been made to the experiments of Williams,† where no eddies appeared behind the sphere even up to $R = 720$, in water in a vessel whose breadth was more than eight times the diameter of the sphere.) The ring becomes larger and moves further from the sphere as the velocity increases, and it is eventually thrown off from the sphere altogether. This was observed by Schmidt‡ behind a wax ball dropping in

* 'Phil. Mag.' vol 46, p 754 (1923)

† 'Phil. Mag.' vol. 29, p 526 (1915)

‡ 'Ann. d. Physik,' vol 61, p 633 (1920)

water, at a velocity corresponding to $R > 1000$. The change is accompanied by a change in the resistance. A sphere in falling first gathers speed, then travels more slowly as the vortex ring grows in strength, and then gains speed again immediately the ring has slipped away. These changes have been noticed also in the rising of a balloon soon after it has been loosed.

It is probable that a succession of rings form and slip away behind a sphere in this way, and that they do so with a definite periodicity which depends upon the velocity. They have not been observed, though Schmidt records a case when a second ring appeared to form. It is well known that when a fluid flows past a cylinder, eddies are formed regularly to them is due the note produced when a thin stick is moved quickly through the air. No similar periodicity has been measured in the vortex rings behind a sphere, though it might be sought by a modification of Relf's method for a cylinder, using a circular wire.

The only direct record of the motion behind the sphere for higher values of R is one made by Ermisch*. His photographs appear to confirm a suggestion of v. Karman's, that two eddies form with their axes parallel to the line of relative motion of the sphere and fluid, and equidistant from the central line. These two eddies trail behind the sphere as two vortex lines, which are not parallel, but twist round each other as interlaced spirals. This is for $R = 8400$ when a sphere is held in flowing water. If a periodicity exists in this motion, it will be difficult to detect. It is to be noted that if two such spiral threads are formed, and the sphere is free to move, their reaction on the sphere must tend to displace it, and this may be the cause of the slightly curved and spiral path which is always followed by a sphere falling through liquid. The lateral movements of the sphere are accompanied by periodic changes in the vertical velocity, as is shown by Liebster's measurements from cinematograph records.

If, however, this second kind of vortex motion behind the sphere is possible, the transition to it from the first kind, as speed increased, would be abrupt, for the two are quite different. This transition would almost certainly be accompanied by a change of resistance. Yet the resistance curve is actually a smooth one. Moreover, it does not seem possible that these are two alternative stable types of wake structure, for there is no evidence of two different values of the resistance for the same speed. (In the case of a cylinder, evidence of this kind has been recorded by Relf†)

The width of the disturbed wake behind the sphere, and the position, on the sphere, of the circle at which the wake envelope leaves it, are factors which

* 'Abh. Aero. Inst. Aachen,' vol 8, p 49 (1927)

† "Adv. Ctee. Aero., R. & M.," No 102 (1914)

determine the resistance at higher speeds. Ermisch has measured the pressure at points on the surface of the sphere, and we deduce from his measurements that this circle moves forward on the sphere as R rises from 800 to 26,000. This is accompanied by a broadening of the wake, and the rising portion of the ψ, R curve may here find its explanation. At speeds just beyond those reached in our experiments, the circle moves suddenly behind the sphere, and the wake is much reduced in width, the resistance coefficient here falls very suddenly and remains low until speeds are attained which approach the velocity of sound in the fluid.

My thanks are due to the Armstrong College Research Committee for a grant towards the cost of the apparatus used.

Summary

By timing the falls of metal spheres in water, through distances up to 2 metres, the resistance of a fluid at high speeds has been measured both for accelerated and for uniform motion.

(1) The variation of resistance with speed is shown on a graph of the resistance coefficient ($\psi = F/\rho v^2 d^2$) with the Reynolds number ($R = vd/\nu$). The results are in good agreement with previous measurements in which air was the fluid concerned.

(2) During accelerated motion, the resistance is increased in a regular way, which can be described approximately in terms of a carried mass, varying from one-half to twice the mass of the displaced fluid.

(3) The effect of cylindrical walls has been measured.

(4) The motion of the fluid behind the sphere is described.

*Studies in the Behaviour of Hydrogen and Mercury at the
Electrode Surfaces of Spectrum Tubes*

By M C JOHNSON, M A , M Sc , Lecturer in Physics, Birmingham University

(Communicated by S W J Smith, F R S —Received February 8, 1928)

Introduction —The apparently capricious control exercised over the spectrum of one gas by the presence of small quantities of another gas is known to involve a great many different processes. The rate at which ions of the one gas are neutralised may be profoundly modified if the other gas has a very different ionisation potential. Both intensities of lines and their broadening in interionic fields will be altered in this way.

The work of Merton and his followers on changes in intensity grouping of lines in mixed gases, and of Fulcher, Dempster, Hulburt and others on changes in line broadening in mixed gases, suggests that in most experiments the combination of the above processes is too complex for quantitative measurement of any one variable to be isolated.

We can, however, select particular pairs of gases and examine details of their behaviour with respect to any one known spectral mechanism. The mechanism selected in the present paper is the emission of a Balmer line by neutralisation of positive rays in hydrogen. The foreign gas is mercury. These two substances are among the commonest intruders in spectroscopic apparatus, and all workers in high vacua are familiar with some of the electrode phenomena of the adsorption of the one and the amalgamation by the other. In order to form hypotheses connecting the effect of Hg on the positive rays of H with previously known facts, a series of experiments is designed, on Doppler effects, on current and potential relations, and on cathode disintegration.

PART I —EXPERIMENTAL

1 *Effect of Mercury on the Doppler Spectrum of Hydrogen Positive Rays* — A Balmer spectral line photographed longitudinally through a perforated cathode supplies information which is absent from capillary spectrograms. The photometry of the "moving" and "resting" components of the line enables us to observe changes in the proportion of the spectrum which is carried by moving protons on neutralisation, and the proportion which is excited in stationary gas by positive ion bombardment. In a tube designed after Wien's

manner for the extension of some work previously published,* it was noticed that considerable change in the H spectrum came about after an accidental admission of Hg vapour from a large diffusion pump through inefficient trapping. The precise nature of the change was elucidated by the following experiments.

The pumping system was changed from diffusion to an ordinary Gaede rotary pump and an efficient trap inserted to avoid future contamination. After preliminary experiments on the efficiency of various traps in removing Hg from a Geissler tube, an absorption tube lined with sodium film was found to be capable of removing Hg lines entirely from a tube which had moderate glass and metal surface areas. The positive ray tube was connected to a system previously described,† whereby large quantities of H could be pumped through without air contamination.

After about fifty hours' discharge and constant refilling and pumping without any further contamination by Hg, the amount of free Hg vapour relative to the amount of H must have been negligible from the point of view of partial pressures.

The H_β spectral region was then photographed at an inclination of about 5° to the axis of flight of the positive rays, to avoid illumination from the anode end of the tube. Exposures up to $11\frac{1}{2}$ hours were given on Imperial Eclipse plates through a Merton photometric wedge. Two successful exposures were secured and the tube then collapsed from the increased sputtering which resulted from the original contamination. During these experiments the spectroscopic appearance was as follows —

	<i>Anode</i>	<i>Cathode face</i>	<i>Behind cathode</i>
Before contamination	H_2 stronger than H_1	H_1 stronger than H_2	H_2 invisible
After contamination	Hg strongest H_2 strong H_1 absent	H_2 faint H_1 nearly equal to Hg	H_2 invisible. H_1 stronger than Hg

The plates were compared with similar plates taken before contamination by the Hg. These had been obtained using the same source of potential, cathode, dispersion system, and source of H, and had shown no trace of impurity among a large group of lines measured in the "many-lined" or H_2 spectrum near H_β . Both sets of images were enlarged together through a process screen by Merton's

* Johnson, 'Roy Soc Proc,' A, vol 114, p 697 (1927)

† Johnson, 'Proc Phys Soc,' vol. 38, p 325 (1926)

well-known method, but after various experiments with printing it was found more accurate to measure the original negatives on a Hulger comparator. This is due to the different degrees of faintness of different parts of the moving and resting lines, which made magnifications suitable to one region of each image impracticable for other regions.

Intensities of resting component (H_R) and moving component (H_M) of spectral line H_β , in terms of heights of Merton wedge images measured in arbitrary units

Plate 1 2100 volts *Before contamination.* $H_R = 246, 259, 257$
 $H_M = 203, 201, 205$

Mean intensity ratio $H_R/H_M = 1.25 \pm 0.04$

Plate 2 2400 volts *Before contamination* $H_R = 159, 166,* 156$
 $H_M = 123, 135,* 127$

Mean intensity ratio $H_R/H_M = 1.25 \pm 0.04$

Plate 3 2600 volts *After contamination* $H_R = 115, 130,* 112, 116, 118$
 $H_M = 67, 81,* 66, 68, 67$

Mean intensity ratio $H_R/H_M = 1.69 \pm 0.12$

Plate 4 2200 volts *After contamination* $H_R = 138, 137, 159,* 140, 119\dagger$
 $H_M = 80, 78, 90,* 80, 64\dagger$

Mean intensity ratio $H_R/H_M = 1.77 \pm 0.08$

All positive ray illumination is faint compared with most sources used in spectroscopy, and with the contaminated tube the length of exposure had to be limited only by the length of life of the tube. Hence the error is greater than with the denser images for which Merton's method of spectrophotometry was originally designed. The conclusion, however, is established beyond the margin of error indicated, that Hg at a partial pressure of the order implied by several days of washing with H, increases to the above recorded extent the ratio H_R/H_M . This measures—as discussed in the papers quoted above—the decrease in the proportion of the H spectrum excited by neutralisation of protons at the cathode, relative to the proportion excited by impact.

2 *Effect of Cathode Material on the Behaviour of Mercury*—With any other metal than aluminium as electrode material, the life of the positive ray tube would have been less than the required duration of a photographic exposure. Accordingly, in testing the connection of cathode material with the facts of the preceding paragraph, the Doppler effect could not be employed, and was

* These images estimated to extreme of visibility

† These images estimated to end of apparent sharp boundary

replaced by the accompanying phenomenon, namely, the domination of the spectrum by mercury at a low partial pressure

Comparison experiments were made between tubes with electrodes of aluminum and of nickel, fed with hydrogen from palladium valves and evacuated over silver film for absorbing Hg vapour. The silver tubes could be replaced by reservoirs of Hg without admitting air to the system. For all experiments the spectra were produced in the "black" stage, in order to facilitate recognition of any impurity lines, and of the first appearance of Hg lines on admitting Hg vapour. Current and potential relations were observed to be constant for several days preceding each experiment, so that changes due to the admission of vapour could be isolated when they occurred.

It was found that with Al electrodes the Hg spectrum appears instantaneously with Hg contamination, and persists at great strength, while the partial pressure of free Hg vapour is reduced to negligible amount, as in the positive ray case. With Ni electrodes a partial pressure of Hg vapour larger by 100 per cent is required before Hg lines appear, comparatively faintly and after a lapse of the order of ten minutes after admission.

3 Current and Potential Relations with Electrodes of Different Sensitivities to Mercury—It is necessary to know whether the different behaviour of Hg in Al and Ni tubes involves a corresponding difference in the ease of maintaining a discharge between pure and contaminated electrodes of these metals. Accordingly, two Geissler tubes were constructed with electrodes of Al and Ni rod respectively. In all other ways they were made closely alike, e.g., the glass shields against sputtering required for the Ni tube were also provided in the Al tube. The tubes were connected together in parallel, both with respect to the dividing of the high-tension current and to the gas connections. These latter included the Hg reservoir and Ag absorber used in the previous experiments.

A pressure range was selected for observation, over which an appreciable current flowed through both parallel tubes simultaneously. Curves of fall of potential across the system plotted against current in each tube were constructed for the following conditions of experiment, and were found to be repeatable to the accuracy of reading the instruments —

Curve 1 —Air pressure decreasing by absorption at solid surfaces within tube, i.e., when outgassing was complete and the subsequent process of hardening had set in

Curve 2 —Air pressure decreasing by pumping out

Curve 3 —Repetition of 2 for check

Curve 4 —Hydrogen pressure decreasing by pumping out.

Curve 5 —Repetition of 4 for check

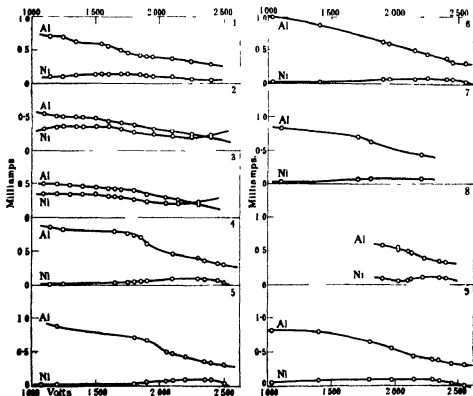
Curve 6 —Repetition of 4 after prolonged washing with H

Curve 7 —Repetition of 4 in reverse order, i.e., readings taken during increase of pressure by admission of H from Pd valve, instead of during decrease of pressure

Curve 8 —Gas pressure increasing by evaporation of Hg from reservoir

Curve 9 —Repetition of 4 after the Hg admitted in 8 had been pumped off and the system washed with H

During 1, 2, 3 both tubes showed the nitrogen bands of air. During 4, 5, 6, 7 a pure H spectrum was shown. In the course of 8 Hg lines appeared in both tubes. In 9 the Hg spectrum was stronger than that of H.



From the graphs it is clear that the method is sufficiently sensitive to detect changes in the ratio of resistances of the tubes due to different behaviour of gases at the solid surfaces. These solid surfaces only differed in the two tubes at the electrodes of Ni in the one and Al in the other. For instance, separate

curves with air agree fairly well among themselves when the air is being pumped out, but are distinct from a curve in which air is being lost to the discharge by absorption within the tube. All the curves in air are again distinct from the remarkably constant curves in H which agree among themselves whether the tubes are new to H or have been much washed out, and whether the readings are taken on decreasing or increasing the pressure.

For the interpretation of the previous experiments on the spectroscopic effects of Hg on H, it is important to note that both the relative and total changes in resistance of the Ni and Al tubes are still the same as for pure H, both when Hg is being admitted and when H is being pumped over surfaces contaminated enough to show the Hg spectrum dominant.

4 *Spectra in the Parallel Nickel and Aluminum Tubes and in the Isolated Nickel Tube* --There is a difference between the development of the Hg spectrum in the parallel tubes during the process represented in graph 8 and its development with the Ni tube alone in the previous experiments. In the present case the Hg lines appeared in the Ni tube within half a minute of their instantaneous appearance in the Al tube. Thus, when the Ni tube is in gaseous connection with Al, its spectrum becomes contaminated almost as rapidly as that of the Al tube, but if no Al is in the connected system, the time taken for even a weaker Hg spectrum to be excited by the same experimental procedure is multiplied twenty-fold.

5 *Differences between Thermal and Electrical Disintegration of Mercury and Aluminum Cathodes* --The greatly increased sputtering from the positive ray cathode after contamination by Hg might simply be due to the very much greater vapour pressure of Hg compared with that of Al at the same temperature, i. e., to a purely thermal evaporation of the Hg attached to the Al surface.

Again, it might be a true electrical sputtering, due to positive ion bombardment rather than thermal evaporation, but in composition a sputtering of Hg, not of Al.

To distinguish between these a discharge was passed through a hydrogen tube with a cathode of Hg frozen in liquid air. Simultaneously, in a tube in gaseous connection with this, a thermal deposit of Hg was produced by heating in an asbestos jacket. The texture of the thermal deposit was coarse and structureless, while the deposit from the solid Hg was fine and arranged in rings similar to the succession seen along the glass near the cathode of the positive ray tube.

The film due to thermal evaporation of Hg was seen at once to have nothing

in common with the disintegration product of the Al cathode in the positive ray tube after contamination by Hg

But the film on the cold tube, distinguished by its banded structure and fine grain from the thermal deposit, had to be compared carefully with the film from the contaminated Al. The tubes were accordingly cut up and specimens taken of glass covered with (a) the true electrically sputtered layer from solid Hg, (b) the sputtered layer of an old positive ray tube with Al electrodes which had never been contaminated with Hg, (c) the layer of increased sputtering of the positive ray tube after its Al had been contaminated with Hg.

In spite of the similarity of the sequence in the banded structures common to (a) and (c) and even faintly discernible in (b), it became clear for the following reasons that the increased sputtering from Al after contamination is not an electrical sputtering of Hg, but of Al itself.

Firstly, comparing regions of similar density on each specimen, the dull whitish colour of (c) alone betrayed the Al oxide, and had the same appearance as the face of the cathode from this tube itself. This oxide is well known to appear on an Al surface when exposed to air after contamination by Hg.

Secondly, when the three specimens were heated in a sand bath, the Hg from (a) evaporated, leaving clear glass at quite a low temperature, while the pure Al of (b) remained unchanged. The unknown film (c) from the contaminated tube remained with (b), indicating that it is mainly of Al, not of Hg.

6 *Summary of Experimental Results*—The facts elicited by the above experiments may be classified as follows for the purpose of relation to what is otherwise known of the behaviour of H, Hg, and Al.

Positive Ray Phenomena—Once an Al cathode has been exposed to Hg vapour, and thereafter washed for a long time in streams of H without further admission of Hg, the resulting domination of Hg lines over the H spectra, and the increase in rate of cathode disintegration, is accompanied by a decrease in the proportion of the spectrum of H due to neutralisation of protons, as deduced from the Doppler effect.

Spectroscopic Phenomena—The domination by the Hg spectrum is instantaneous with an Al cathode. It is almost instantaneous with an Ni cathode so long as there is gas connection with another tube containing Al. But with an isolated Ni cathode the Hg spectrum is weaker and requires greater pressure of Hg and longer time to make it appear.

Resistance Phenomena—The admission of Hg to H tubes with Ni and Al electrodes, and the above subsequent spectroscopic behaviour of the tubes, is accompanied by no alteration of the relative resistances at Ni and Al electrodes,

although with air instead of H the relative resistance changes are measurable

Time Phenomena—In badly contaminated tubes the gradual saturation of the absorbing Na or Ag, and the gradual weakening of the Hg spectrum at the electrodes, were found to be functions of the time during discharge, not of the intervals of time between Admission of Hg to all tubes continues to decrease the resistance of the tube after admission has ceased, for as long as ten minutes

Disintegration Phenomena—When solid, an Hg cathode can be made to disintegrate electrically in a way distinct from its thermal evaporation. But the disintegration layer from the Al cathode after Hg contamination is of Al and is neither due to thermal nor electrical disintegration of Hg

PART II -- THEORETICAL

1 The result of the positive ray experiments, namely, the decrease in the proportion of the spectrum excited by proton neutralisation, at an Al cathode after contamination by Hg, would find a ready explanation in any tendency of the Hg to decrease the liberation of electrons from the Al surface

Ratner* has shown that liberation of electrons by positive ion bombardment of a cathode can no longer be regarded as the principal means by which a discharge is maintained. Photo-electric liberation from the cathode is the alternative pointed to by J J Thomson's studies of the frequency of radiations in the neighbourhood of electrodes This mechanism is now accepted as controlling the normal working of discharge † Now, it is well known that some gas films do alter photo-electric emission profoundly, but there is no direct evidence that an Hg surface on Al hinders emission, as would be required for an explanation of the present phenomena on these lines The existing data mainly concern photo-electric fatigue, e.g., Allen‡ states that the fatigue of zinc is much the same whether its surface is polished or amalgamated Millikan and Wright§ state that the increase of photo-electric sensitivity with time of illumination is the same for many metals, including Al, whether they have or have not been exposed to Hg vapour That surface conditions at a cathode may entirely alter the photo-electric control of a discharge is, however, put forward by Ratner|| on experimental evidence, from the study of the gradual polarisation of an X-ray bulb at constant gas pressure

* 'Phil Mag,' vol 40, p 792 (1920)

† Taylor, 'Roy Soc Proc,' A, vol 114, p 73 (1927)

‡ 'Roy Soc Proc,' A, vol 78, p 485 (1907)

§ 'Phys Rev,' vol 34, p 68 (1912)

|| 'Phil Mag,' vol 43, p 193 (1922)

But if we consider the positive ray experiment in the light of the subsequent measurements of the constant resistance of tubes with different capacities for absorbing Hg, we have to abandon any such explanation involving inhibition of photo-electric liberation at the contaminated surface. For such inhibition would show itself in an increase of electrode resistance such as found by Ratner in X-ray tubes. Not only does the emergence of the Hg spectrum take place without altering the relative resistance at Al and Ni cathodes, but the total resistance of the whole system remains unaltered by Hg, in spite of the sensitivity of the method of measurement to the change from air to hydrogen. Hence, the decrease of electron capture by protons does not mean that fewer electrons are available by photo-electric liberation at the place where the decrease is seen.

2 Since the action of Hg at the Al cathode cannot be regarded as altering its power of emitting electrons, the explanation of the decrease of electron capture by protons can be connected with the phenomenon of the domination of the spectrum by Hg lines. This occurs, as was shown, at a partial pressure of free Hg vapour which is extremely small, and is typical of a large class of phenomena in the spectroscopy of mixed gases, when often the spectrum of the component greatly in excess is the weaker. In the present case Hg atoms are numerically rare compared with H atoms and H molecules, but the resonance and ionisation potentials of Hg are 4.8, 6.5 and 10.2 volts respectively. Those of the H atoms are 10.2 and 13.5 volts. The ionisation potential of the H molecule is not agreed upon. Horton and Davies* suggest 22.8 volts. It is probable, therefore, that ease of ionisation and excitation to some extent tends to make up for the numerical inferiority of Hg. Further, the slower motion of the massive singly charged Hg ions compared with H_1^+ and H_2^+ allows readier re-combination with free electrons met. It is reasonable to expect that this easier ionisation and re-combination would allow to the few Hg atoms the abnormally large share they seem to take in the spectroscopic phenomena of the tube. The same properties will ensure that, for the same total current density of the tube, Hg ions can seize the electrons which in the pure tube would, after longer free path, fall to the faster H ions. This would decrease, as observed, the part of the positive ray hydrogen spectrum denoting the neutralisation of protons.

3 The long pumping and washing with H, which was unable to destroy the above phenomena, together with the fact that Hg is only freed during discharge, shows that the Hg is derived from the Al cathode surface. But it is able to migrate, probably through its frequent exchange of charge, this is shown by

* 'Phil. Mag.', vol. 46, p. 896 (1923).

its rapid appearance in the connected Ni tube which, when isolated from Al, could only make use of Hg much more slowly. It is important to enquire whether the present experiments make any discrimination between the several processes covered by the term "occlusion" of vapour at the solid surface. Porter* has classified several of these, of which the most important are adsorption, formation of charged double layers, solution, formation of definite chemical compounds. The evidence from the chemical point of view is not agreed as to the precise nature of the relation of Hg to Al. Though some suggest† a compound Al_2Hg_3 , but an amalgam of varying composition for Ni, a recent reference‡ states that the constitution of the Al-Hg system is unknown, but results in a solid brittle amalgam.

The study of cathode disintegration allows us, independently of any decision as to the chemical constitution of the amalgam, to form a hypothesis as to some physical aspects of the behaviour of the Hg, H and Al. The experimental facts show that the much-increased disintegration product after contamination of the Al cathode by Hg was neither due to thermal evaporation of Hg nor to true electrical sputtering of Hg, theories of the action of the Hg on the Al must accordingly assume that it facilitates the detachment of the Al itself.

It is well known§ that the sputtering in tubes with Al electrodes, usually very slight, is increased if the atmosphere of the tube is of one of the inert gases Ne, Xe, Kr, and Hg has already been classed with these, both as to its increase in sputtering|| and in the fact that it behaves as a monatomic gas. Kohl-schütter has shown¶ that sputtering of any metal increases with increase in atomic weight of the gas in the tube. Assuming that these two groups of phenomena are of one origin, J J Thomson points out that the rare gases and *a fortiori* Hg vapour show peculiar liability to multiple ionisation**. Accordingly, he suggests†† that it is the increased energy in the dark space of multiply charged particles which leads to the encouragement that these elements give to the break-up of Al cathodes.

But in the present case the cathode disintegration goes on when all the Hg free vapour has been pumped off, and is mainly a delayed effect of the temporary

* 'Trans Faraday Soc,' vol 14, p 192 (1919)

† Friend, 'Inorganic Chemistry,' vol 3, part 2, pp 218, 221

‡ Anderson, 'Metallurgy of Aluminium,' p 728 (1925)

§ Campbell, 'Phil. Mag,' vol 28, p 347 (1914)

|| Kaye, 'Proc Phys Soc,' vol 25, p 199 (1913)

¶ 'Z Electrochem,' vol 15, p. 316 (1909)

** 'Positive Rays,' 2nd ed, p 83

†† *Ibid*, p 174

intrusion of Hg. The Hg present during the greater part of the disintegration is only that derived from the cathode itself, and in that extremely small partial pressure the occurrence of multiple ionisation must be of a very small order of probability compared with the main bombardment by protons and H molecules. We cannot here invoke the ionisation properties which allow the Hg atoms to contribute abnormally to the spectrum and electron capture, since those only concern the first ionisation potential compared with that of H. Accordingly, the explanation which would fit the facts when the monatomic gases are the main constituent of the tube is not to be relied upon when, as at present, the disintegration outlasts their introduction as temporary impurity.

4 Hence it is probable that the action of Hg in loosening the Al is not the primary result of bombardment but a secondary result, the primary result ceasing when the partial pressure of Hg vapour is reduced very low. We are led to a hypothesis of the nature of the primary effect of the bombardment by multiply charged ions, from the well known phenomena of the oxidation of Al. Pure Al is very readily oxidised, but in practice most Al appears to resist corrosion because of a protecting layer on the surface, which, when once formed, prevents gas from passing from outside to the layers of Al beneath. According as we try to explain this layer chemically or physically it can be looked upon as an Al oxide or as a layer of oxygen behaving in the manner studied by Langmuir. In either case it probably inhibits the passage of gas from inside to outside as it does from outside to inside, as in the phenomenon of the "passivity" of metals due to a film mechanically hindering metallic ions from entering solution. Under certain circumstances Al can liberate much of the gas, mostly H, which it contains in its bulk, and it is natural to suppose that liberation as a diffusion process would in a vacuum discharge be greatly facilitated if the protecting layer were removed. But if the gases in the structure of the Al were thus allowed to diffuse out, their removal from whatever place their atoms occupied in the Al structure, or between the crystal cells of Al, would leave some interstices unoccupied and the Al permanently more open to penetration by the further bombardment by protons. A similar case is the opening of a metallic lattice by oxidation and reduction.*

Accordingly, we suppose that when a monatomic gas is suddenly let into the tube, the increased energy of its multiply charged ions effects what the steady proton bombardment had not been able to, namely, some break-up of the protective film over the Al cathode. This allows the gases in the Al structure to diffuse out, which they would have done before if not locked in by the oxygen.

-or oxide film For under the conditions of the discharge in the surrounding vacuum, the metal is supersaturated with gas which, when the film was formed in air, had been its normal complement. This breaking of the films will occur when the first rush of multiple ions of Hg occurs, but the consequent slow diffusion outwards of the gas will leave a permanently and increasingly weakened Al structure This will hence continue an increasing sputtering now that the protecting layer has gone, even though all possible efforts are made to remove the Hg, which has fulfilled its function

5 The above hypothesis would account for the continued sputtering in the above experiments, but for confidence it would require some evidence of the intermediate link in the sequence, i.e., the liberation of gas from inside the Al

The existence of this link is suggested by Baly's observation* that the admission of a trace of Ne, Kr, Xe into a discharge tube whose outgassing of Al electrodes was apparently complete causes a further evolution of H In the present experiments it is also supported by the following interpretation of the time phenomena observed Consider the possible meaning of the increase of gas pressure in the tubes after flooding by Hg vapour had been completed In other experiments, in addition to the above, the admission of Hg continued to lower the tube resistance after the Hg reservoir had cooled Now, after flooding from the hot reservoir, the re-condensation of what does not cling to the electrodes takes the form of a multitude of very small drops, over whose curved surfaces the vapour pressure will be greater than over the initial single pool This is, however, not enough to account for the 100 per cent increase in total gas pressure after cooling, in a system whose history was a guarantee against leak and normal degassing It is, moreover, partly counteracted by the fact that Hg vapour pressure over amalgams is less than over pure Hg at the same temperature † Since the heating of the Hg reservoir was so localised as not to liberate gas from the glass walls, and since the liberation was maintained, it seems probable that the increase in gas pressure after cooling of the Hg represents a liberation from the electrodes, as would be expected on our hypothesis of the preceding paragraph In the present case no spectral trace of anything but H and Hg were seen, so the liberated gas is probably H.

6 The protective layer on the Al, the H in the Al structure, and the final amalgam of the Hg on the Al after the protecting layer is broken and the H liberated, could all be described in chemical or in purely physical terms according as we regarded the several surface phenomena as chemical or physical We

* 'Phil. Trans,' vol 202, p. 185 (1904)

† Foster and Beebe, 'J Am. Chem. Soc,' vol. 42, p 545 (1920)

have accordingly pairs of alternatives such as true oxide or Langmuir layer of orientated oxygen molecules, the trapping of molecules between lattice cells or the existence of unstable hydrides, the formation of Al_2Hg_3 or solid solution. But between such pairs of terms it is nowadays recognised to be hard to distinguish in a border region where even in adsorbed layers of monomolecular thickness chemical bonds may have to be assumed *

The Langmuir type of layer is suggested for the present case rather than an oxide, because of its stability under a proton bombardment which disintegrates metals and most compounds † Mechanical trapping rather than a chemical composition is more probable as the behaviour of H, since it diffuses out *in vacuo* Solid solution, or at least a series of varying composition rather than Al_2Hg_3 , is suggested for the amalgam for the following reason Metallic sputtering is known to be of particles of colloidal size, ‡ and the Hg and not the Al is shown by the spectra to be atomic in the present experiments Hence, some system of Hg and Al allowing differential evaporation is required, such as Crookes§ found in the sputtering of gold-aluminium The latter is now known|| to cover a varying composition Al_2Hg_3 , on the other hand, would probably dissociate and show an Al as well as an Hg spectrum at the cathode

7 Comparison may be made between the foregoing theory of the rupture of a surface layer by bombardment and the well-known phenomenon of the oxidation of aluminium when amalgamated in air In the latter case it is open to chemistry to suggest that the mercury removes the surface film of oxygen by entering with it into some transitory combination Such an explanation would be difficult to trace because of the several variables involved by the presence of air Actually, however, the writer has, after wide enquiry, failed to hear of any case where the amalgamation took place without (a) scouring the aluminium or (b) rubbing in the mercury, either of these would destroy the surface film mechanically, as it is here suggested that the Mercury bombardment does *in vacuo* If it were shown that the opening of the inner surface to oxidation could occur without (a) or (b), it would be necessary to invoke the more complex chemical explanation When found, that explanation would also serve as alternative to the present physical explanation of the phenomena *in vacuo*

* Iredale, 'Phil Mag,' vol 49, p 627 (1925)

† Wien, 'Kanalstrahlen,' p 26 (1923)

‡ Kaye, 'Proc Phys. Soc,' vol 25, p 198 (1913)

§ 'Roy Soc Proc,' A, vol 50, p 88 (1891)

|| Whetham, 'Theory of Solution,' p 62

8 Conclusion—The experiments described in Part I, together with certain previously known facts, would be accounted for on the following hypothesis —

The admission of a gas known to be liable to multiple ionisation leads to a more violent bombardment of the cathode. This, however, causes an increased cathode disintegration long after the gas is pumped off, which cannot, therefore, be the direct result of the bombardment as on Thomson's theory. It would be in accord with the other phenomena here described that the direct effect should be to break the protective layer of oxygen on the Al and thus allow diffusion of gas out from the metal structure. Such diffusion out is observed in the present experiment. The resultant weakening of the Al structure is the actual cause of the increased sputtering. The Hg in combination or in solution on the cathode is evaporated and contributes to the spectrum, but not to sputtering. This contribution, owing to its favourable ionisation potential, is much greater than expected from the very low partial pressure compared with H. Its ability to capture electrons, due to its mass and critical potentials, results in the decrease of the H Doppler effect observed in the positive ray experiments. The experiments on the resistance of the tubes show that an alternative explanation in terms of inhibition of photo-electric liberation at the cathode is both unnecessary and unlikely.

I owe my best thanks to Prof S W J Smith, F R S, for generously giving me both time and equipment for these experiments. To Mr G O Harrison, of the Physics Workshop, I owe not only the instrument construction acknowledged in previous papers, but in several instances the carrying out of tests and experiments suggested by his long experience in vacuum and surface research

An X-Ray Investigation of the Structure of some Naphthalene Derivatives

By J MONTEATH ROBERTSON, M A , B Sc , Ph D , Carnegie Research Fellow

(Communicated by Sir William Bragg, F R S —Received March 5, 1928)

[PLATE 17]

The crystal structure of naphthalene tetrachloride has been investigated by Sir William Bragg,* who finds it to consist of a monoclinic body-centred lattice containing four molecules of $C_{10}H_8Cl_4$ per unit cell, the space group being apparently C_2^4 . The orientation and the structure of the molecules suggested (*loc cit*) is in harmony with the dimensions of the unit cell, and explains the chief features of the intensities in the most prominent spectra. In the present paper this structure is further examined by the rotating crystal method and, by means of a comparison with 1 2 3 4 5 8-hexachloronaphthalene-1 2 3 4-tetrahydride (referred to hereafter as dichloronaphthalene tetrachloride), an attempt is made to locate the halogen atoms. Several naphthalene derivatives were investigated, and the dichlor-tetrachloride was finally selected for a detailed examination because the crystal structure is very closely similar to that of naphthalene tetrachloride, and hence a direct comparison of intensities, etc., becomes possible.

The dimensions of the unit cells of these chlorides compared with naphthalene are given below —

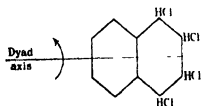
Compound	a	b	c	β	Space group	Mols per unit cell	Density
Naphthalene	8.34	6.0	8.7	$122^\circ 49'$	C_{2h}^4	2	1.152
Naphthalene tetrachloride	7.9	10.3	14.2	$112^\circ 40'$	C_2^4 or C_{2h}^4	4	1.67
Dichloronaphthalene tetrachloride	7.8	12.3	13.9	$116^\circ 14'$	C_2^4 or C_{2h}^4	4	1.87

These data agree reasonably well with the axial ratios recorded in Groth,† except that in the case of naphthalene tetrachloride the length of the c axis is now found to be doubled, and in the case of the dichlor-tetrachloride we have interchanged the a and the c of Groth.

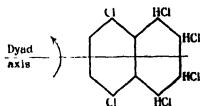
* 'X-Rays and Crystal Structure,' p 263 (1923), 'Z für Krist,' vol 66, p 22 (1927)

† 'Chem. Kristallographie,' vol 5 pp 368, 369

The X-ray results (see below) show that in the case of these two chlorides the general plane $\{h k l\}$ is halved when $h + k + l$ is odd, and that all the $\{h 0 l\}$ planes are halved. The lattice is therefore body centred (Γ') and the space group must be either C_{2h}^6 (monoclinic prismatic) or C_2^4 (monoclinic domatic) *. It is not possible to distinguish between these two cases by any known X-ray method. There is, however, certain other evidence which is strongly in favour of the latter space group, and which therefore leads us to infer, as Bragg has pointed out (*loc cit*), a hitherto unsuspected polarity in the crystal. First let us consider the requirements of the monoclinic prismatic group C_{2h}^6 . The elements of symmetry are a glide plane and a dyad rotation axis, and eight asymmetric molecules are required to form the unit cell. As only four molecules are actually present in these crystals, each molecule must possess either a centre or a dyad axis of symmetry along the b axis of the crystal. It is certain that if the crystal molecule bears any resemblance to the structural formula advanced from chemical considerations, then a centre of symmetry is impossible, and a dyad axis could only lie along the long axis of the molecule as indicated below.



Naphthalene tetrachloride



Dichloronaphthalene tetrachloride

In other words, we must place this axis of the molecule along the b axis of the crystal. We cannot disprove this possibility directly, but we shall see that all the evidence points to the axis of the molecule being nearly coincident with the c axis of the crystal, as in the case of naphthalene and anthracene. It is in view of this evidence that we are led to reject the monoclinic prismatic space group and adopt the lower symmetry of the domatic class. The space group C_2^4 , containing only a glide plane of symmetry, requires only four asymmetric molecules per unit cell. No molecular symmetry is possible. It will be adopted in the following discussion as being the most reasonable working hypothesis.

In this space group we now require to determine as far as possible the relative position of the original and the reflected molecule. Bragg has made use of the fact (*loc cit*) that if this approximates to certain values, then certain sets

* Cf. Astbury and Yardley, 'Phil. Trans.' A, vol. 224, p. 229 (1924).

of planes tend to give weak reflections, and hence from a study of these the approximate position of the reflected molecule may be determined, provided that the molecules (the standard molecule and the reflected molecule) present approximately the same appearance when viewed from all points

In his investigation of the tervalent metallic acetylacetonates W T Astbury* has discussed this method of locating the position of molecules, and has pointed out that, for example, when the odd hyperbolæ are almost completely obliterated in a rotation photograph, then the molecule which subdivides the primitive translation parallel to the rotation axis must possess "*approximately that element of symmetry which is involved in deriving it from the molecules at the ends of the primitive translation*"

This method of locating molecules therefore appears to have a wide application, and if applied carefully it may in certain cases give information regarding the position of important groups of atoms, leading to the correct orientation of the molecule. The effects, however, may be small, and we may not be able to distinguish them by simple inspection of a rotation photograph, because the operation of the space group halvings will in general cause the absence of many strong reflections from certain layer lines, and this effect may be mistaken for a weakening of the reflections from the general plane

We can proceed by making a classification of all the reflections in such a way that the different effects can be clearly distinguished. By means of Bernal's method of interpretation,† which has been followed in all the work described here, indices can be assigned with certainty to all the reflections. In arranging the results so as to obtain the information required, several points must be noted

(1) We must interpret all the reflections occurring in rotations about any axis within a certain range. In the present example, all reflections up to $\xi = 1.50$ have been interpreted on five layer lines in photographs taken about the b axis. With the $K\alpha$ rays from a copper anticathode this gives about three hundred planes in each crystal, which is enough to give good averages of intensities for certain sets. In more complicated crystals with larger unit cells a smaller ξ value would doubtless give sufficient planes for classification. But it is important to classify all planes up to a selected ξ value.

(2) Before recording a plane absent we must make sure that it has been in a reflecting position. In other words, the instrumental limits must be clearly indicated in the classification.

* 'Roy Soc Proc,' A, vol 112, p 457 (1926)

† 'Roy Soc Proc,' A, vol. 113, p 117 (1926).

(3) Planes absent owing to the operation of space group halvings must be distinguished from those whose absence is due to other causes, and allowance made in comparing the intensities of certain sets

These points can be most clearly set forth by arranging the results in the form of a series of tables based on the reciprocal lattice of the crystal. Each table contains an account of the reflections observed along one layer line in the crystals. The limits of the region interpreted ($\xi = 1.50$ for naphthalene tetrachloride) and the instrumental limits are indicated by a full line across the column ———. Planes which have been in a reflecting position and found to be absent are marked Abs. Reflections which are absent on account of space group halvings are simply omitted. The regularity of the resulting pattern on the tables at once indicates the type of lattice. The body-centred lattice in these crystals is the cause of the staggered effect, analogous to the appearance of an oscillation photograph taken about the b axis.

The intensities of reflection have in most cases been estimated by eye from overlapping oscillation photographs. No great accuracy is claimed for the results, but by comparing the $K\alpha$ (copper) reflections with the $K\beta$ reflections, an approximate idea of the intensities is obtained. The following table indicates the standard adopted —

———		Intensity, I	n
vs	= very strong	100	7
s	= strong	42	6
ms	= medium strong = β of vs	18	5
m	= medium = β of s	7	4
wm	= weak medium = β of ms	3	3
w	= weak = β of m	1.3	2
vw	= very weak = β of wm	0.5	1

The ratio of the intensity of the $K\alpha$ to the $K\beta$ line of copper is about 5.7 to 1 on the photographic plate, *i.e.*, after passing through the aluminium window (1/1000 in.) of the X-ray tube,* so that, putting $vs = 100$ we find the approximate values of the other standards as given above. If, however, the crystal absorbs the X-ray beam considerably, as is the case with these chlorides, it is likely that the observed ratio of α to β will be still further reduced by differential absorption. The number n , which simply indicates the order of intensity, has been used in comparing the intensities of sets of planes. The number n is not proportional to the intensity I , but is a linear function of the logarithm of the intensity.

* 'Roy Soc. Proc.' A, vol. 115, p. 645 (1927)

Taking the ratio of the intensity of the α to the β reflection as 5.7 and using common logarithms,

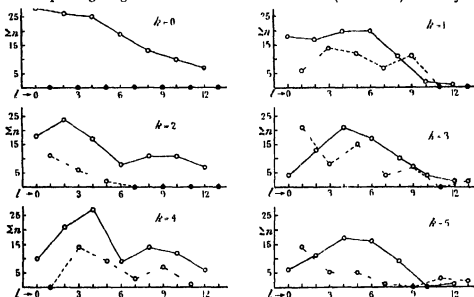
$$u = A \log I + B,$$

where

$$A = 2.64 \text{ and } B = 1.71$$

Tables I-V show the reflections observed in photographs taken about the b axis of the two crystals investigated. Other important planes like the (010) series, which require to be measured in photographs about other axes, are given later.

Figs 1-6 show the distribution of intensities in naphthalene tetrachloride plotted as Σn against the l index (horizontal columns in the tables). The corresponding diagrams for the dichloro-tetrachloride (not shown) are very



FIGS 1-6—Naphthalene Tetrachloride

similar, though somewhat more confused. The general weakness of the reflections from planes with the l index odd is at once obvious. There is, however, another effect. We see that the diagrams for $k=1, 3$ and 5 are much more confused, especially at the ends, than the $k=0, 2$ and 4 diagrams. The explanation of this is to be found in another tendency for weak planes when k is odd. Bearing in mind the general halving when $k+l$ is odd, we have

k odd	$k=0$	l odd	Space group halving
k even	$k=1$	l odd	Opposing effects
k odd	$k=2$	l odd	Double weakening effect
k even	$k=3$	l odd	Opposing effects
k odd	$k=4$	l odd	Double weakening effects
k even	$k=5$	l odd	Opposing effects.

TABLE I—Planes $\{hkl\}$
 B = Intensity of reflection in naphthalene tetrachloride
 C = Intensity of reflection in dichlor-naphthalene tetrachloride

l	A	B	C	A	B	C	A	B	C	A	B	C	A	B	C
12	0012	m	v w												
11															
10	0010	m	w												
9				2010	v w	w									
8	0008	w	w				2008	w m	Abc						
7										4008	w	v w			
6	0006	w m	w				2006	m s	w m						
5										4006	Abc	w			
4	0004	m s	s				2004	m	w m						
3										4004	v w	v w			
2	0002	s	v w				2002	v s	Abc						
1										4002	v w	trace			
0							2000	s	m s						
1										4000	v s	s			
2							2002	v s	Abc						
3										4002	w	v w			
4															
5							2004	v s	m s						
6							2006	s	m						
7										4006	w m	m			
8							2008	m	w m						
9										4008	m	Abc			
10							2010	w	m						
11										4010	v w	v w			
12							2012	s	w						
13										4012	Abc	v w			

TABLE V—Planes $\{h k l\}$
 A = Indices $\{h k l\}$ B = Intensity of reflection in naphthalene tetrachloride
 C = Intensity of reflection in dichloronaphthalene tetrachloride

<i>l</i>	A	B	C	A	B	C	A	B	C	A	B	C	A	B	C	A	B	C	A	B	C	A	B	C
12	0412	v w	w	1411	Abs	v w	2410	Abs	Abs	3409	Abs	Abs	448	v w	w	545	v w	Abs	644	Abs	Abs	741	Abs	Abs
11	0410	s	v w	149	w	Abs	248	m	w m	347	Abs	v w	446	Abs	w	543	Abs	v w	642	v w	Abs	743	Abs	Abs
10	048	Abs	Abs	147	Abs	w	246	m	Abs	345	v w	v w	444	w m	v w	541	Abs	v w	640	Abs	Abs	745	Abs	Abs
9	046	w	m	145	w m	v w	244	m, s	Abs	343	w	w	442	v w	m s	541	Abs	v w	648	Abs	Abs	747	Abs	Abs
8	044	s	Abs	143	w m	w m	242	m	w	341	Abs	Abs	440	m s	w	541	Abs	v w	645	w	v w	749	Abs	Abs
7	042	v, s	s	141	Abs	Abs	240	Abs	w	341	Abs	w m	442	m	m	543	w	w	642	v w	Abs	741	Abs	Abs
6							242	w m	m	343	w m	v w	444	w m	v w	543	w m	v w	644	m	Abs	745	Abs	Abs
5							244	s	v w	345	v w	w	446	v w	w	547	v w	w	645	Abs	Abs	747	Abs	Abs
4							246	w	w	347	v w	v w	448	w	v w	549	v w	Abs	648	w	v w	749	Abs	Abs
3							248	m, s	m	349	w	w	449	m	w	541	Abs	v w	649	v w	v w	741	Abs	Abs
2							249	v w	w	341	Abs	Abs	441	v w	w	543	v w	Abs	641	v w	v w	743	Abs	Abs
1							241	v w	w	343	v w	w	443	v w	w	545	v w	Abs	643	v w	v w	745	Abs	Abs
0							243	v w	w	345	v w	w	445	v w	w	547	v w	Abs	645	v w	v w	747	Abs	Abs
1							245	v w	w	347	v w	w	447	v w	w	549	v w	Abs	647	v w	v w	749	Abs	Abs
2							247	v w	w	349	v w	w	449	v w	w	541	Abs	v w	649	v w	v w	741	Abs	Abs
3							249	v w	w	341	Abs	Abs	441	v w	w	543	v w	Abs	641	v w	v w	743	Abs	Abs
4							241	v w	w	343	v w	w	443	v w	w	545	v w	Abs	643	v w	v w	745	Abs	Abs
5							243	v w	w	345	v w	w	445	v w	w	547	v w	Abs	645	v w	v w	747	Abs	Abs
6							245	v w	w	347	v w	w	447	v w	w	549	v w	Abs	647	v w	v w	749	Abs	Abs
7							247	v w	w	349	v w	w	449	v w	w	541	Abs	v w	649	v w	v w	741	Abs	Abs
8							249	v w	w	341	Abs	Abs	441	v w	w	543	v w	Abs	641	v w	v w	743	Abs	Abs
9							241	v w	w	343	v w	w	443	v w	w	545	v w	Abs	643	v w	v w	745	Abs	Abs
10							243	v w	w	345	v w	w	445	v w	w	547	v w	Abs	645	v w	v w	747	Abs	Abs
11							245	v w	w	347	v w	w	447	v w	w	549	v w	Abs	647	v w	v w	749	Abs	Abs
12							247	v w	w	349	v w	w	449	v w	w	541	Abs	v w	649	v w	v w	741	Abs	Abs
13							249	v w	w	341	Abs	Abs	441	v w	w	543	v w	Abs	641	v w	v w	743	Abs	Abs

We may summarise these effects by adding up the intensity numbers for all the planes. Fig. 7 shows these numbers plotted against the index h (vertical columns in the tables)

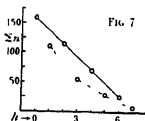


FIG. 7

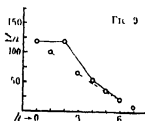


FIG. 9

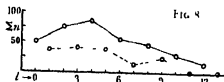


FIG. 8

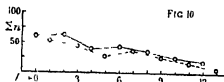


FIG. 10

Figs. 7, 8—Naphthalene Tetrachloride

Σn summed from $k = 1$ to $k = 4$ only

Figs. 9, 10—Dichloronaphthalene Tetrachloride

Σn summed from $k = 1$ to $k = 4$ only

The intensity numbers are summed from $k = 1$ to $k = 4$ only in order to eliminate the effect due to the general halving of the $(h\ 0\ l)$ planes when h is odd. $k = 5$ is not included because we must have an equal number of k odd planes and k even planes in order to eliminate the alternating effect due to the tendency for weak planes when l is odd. The tendency for weak planes when h is odd is now obvious. Fig. 8 summarises in the same way the tendency for weak planes when l is odd.

Figs. 9 and 10 are prepared in exactly the same way from the data for dichloronaphthalene tetrachloride, and show that the same effects to a less extent are operating. We may note that in this case the tendency for weak planes when h is odd is at least as strong as the tendency when l is odd. Reference to this fact will be made later.

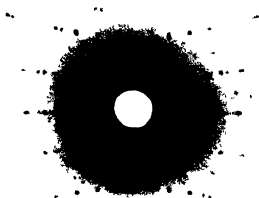
The weakening effects which are most pronounced, viz., when l is odd in naphthalene tetrachloride, and when h is odd in dichloronaphthalene tetrachloride, are readily seen on the rotation photographs about the c and the a axes respectively in these crystals (Plate 17). In naphthalene tetrachloride the intermediate hyperbolae, which contain all the reflections when l is odd, are very faint. The great strength of the fourth hyperbola is interesting (cf fig 8). This photograph was taken with a very minute crystal, measuring about half a cubic mm. With larger crystals the absorption is very

great, and the intensity of the resulting broken reflections is hard to estimate. In dichloronaphthalene tetrachloride the intermediate hyperbolæ contain all the h odd reflections, which are seen to be relatively weak. The crystal in this case was a small needle whose axis was the a axis. This form is typical of dichloronaphthalene tetrachloride. One advantage of the diagrams over the photographs is shown in the much larger range recorded. For instance, in fig 9 we can compare the intensities of planes up to $l = 13$, whereas in the photograph about the c axis only about five hyperbolæ ($l = 5$) are visible. The planes with higher indices are recorded in oscillation photographs about the b axis (using a circular camera).

In seeking an explanation for the above facts we must consider the position of the reflected molecule in the unit cell. If A represents a standard molecule, then an exactly similar molecule A' is situated at the centre of the cell. The reflected molecule B is derived from A by a reflection in the ac plane plus a translation of $\frac{1}{2}c$ along the c axis and may be anywhere along B_1B_2 (fig. 11 (a)). We have to determine a parameter which as far as possible expresses its position along this line*. The molecule B' is derived from A' in the same way as B is derived from A . Suppose that the reflected molecule bears some resemblance to the original molecule from all points of view and that we can therefore place it at a more or less definite position with respect to the original molecule. Consider first the arrangement shown in fig. 11 (a), where the reflected molecule B_1 subdivides the primitive translation A_1A_3 . The length of the c axis is approximately halved and we shall get weak planes when the corresponding index l is odd, because all such planes are interleaved with reflected molecules. If the reflected molecule were exactly like the standard molecule, and were situated exactly at B_1 , then $B_1B_2B_3B_4A_5A_6A_7A_8$ would become the unit cell,† and the l odd planes would entirely disappear. We see that, generally, given the necessary similarity between the standard molecule and the one derived from it by a symmetry operation (cf p 711, and Astbury, *loc cit*), then those planes

* If A is a point representing the position of a standard molecule, we cannot in general define the position of the reflected molecule by another point such as B . Let the co-ordinates of A be x, y, z , with the a, b , and c directions as axes. Then the co-ordinates of the equivalent point on the reflected molecule are $x, -y + \beta, z + \frac{1}{2}c$, where β has to be determined. If, however, we can infer an approximate plane of symmetry in the molecule, as is probable in this case, then any point situated on this plane can be thought of as representing approximately the position of the molecule in question.

† It is convenient in this work to refer the indices to the body-centred cell containing four molecules. The true unit cell, of course, is only half this size and contains two molecules.



Naphthalene Tetrachloride (Rotation about c axis)



Dichloronaphthalene Tetrachloride (Rotation about a axis)

will tend to be weak which have the index corresponding to the direction which is subdivided by the symmetry molecule as an odd number. The extension to more than one subdividing molecule is obvious.

For example, in fig 11 (a) the second reflected molecule B' subdivides the primitive translation A_1A_2 . Change the unit cell so that this direction a' is the new a direction. Then the indices $h'k'l'$ referred to the new cell are given by $h' = h + k$, $k' = k$, $l' = l$, and we get weak planes when h' is odd, i.e., when $h + k$ is odd, and therefore when l is odd, because $h + k + l$ is even. Hence the effect of both reflected molecules is to give weak planes when l is odd and there is no other effect.

It can be seen in the same way that in the structure shown in fig 11 (b) the effect of both reflected molecules is to produce weak planes when h is odd.

But the results show that in the case of naphthalene tetrachloride and dichloronaphthalene tetrachloride both these effects are present, the l odd effect being predominant in the former crystal and the h odd effect in the latter.

If the reflection molecule were in some intermediate position between that shown in fig 11 (a) and fig 11 (b), there would be no tendency to either effect.

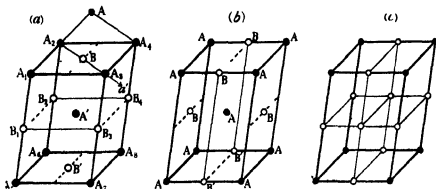


FIG 11

A structure such as that shown in fig. 11 (c), where the lattice is no longer body centred, would give rise to both effects, the unit cell being effectively quartered, but such a structure is impossible within the space group we are considering (C_{2v}). Under these circumstances we can only conclude that the molecule functions as if it were effectively in both the positions required by figs 11 (a) and 11 (b). A simple explanation of this anomaly presents itself when we consider the probable structure of the molecule as built into the crystal. The chemical structure indicates that the four chlorine atoms were attached to one carbon ring, and the approximate plane of symmetry which is required in the

molecule to account for the tendency to give sets of weak planes indicates that the chlorine atoms must be approximately symmetrically placed on either side of the ring. If now we place the molecule along the c axis of the crystal, the appearance when viewed along that axis can be roughly indicated by fig 12, where the ovals are taken to represent an end-on view of the region occupied

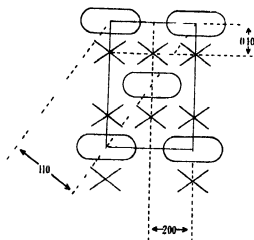


FIG 12 — Projection of Unit Cell on ab plane (001)

by the carbon rings, and the crosses indicate the approximate location of the halogen atoms on either side of the molecule. We do not require at present to discuss the exact position of these atoms. We now see that whereas the molecule as a whole, and the carbon rings considered by themselves, conform to the structure of fig 11 (a), yet the groups of halogen atoms, considered by themselves, conform to the other type of structure shown in fig 11 (c). We may therefore conclude that the tendency for weak planes when h is odd is due to the effect of these groups of atoms which virtually lie on a different type of lattice. Confirmation is obtained from dichloronaphthalene tetrachloride. We have now six chlorine atoms instead of four, and the latter effect predominates. In the case of this crystal, however, the increase in the length of the b axis (12.3 instead of 10.3) must affect the structure shown in fig 12, probably in disturbing the alignment of the halogen atoms. It is not surprising, therefore, that we get more confusing relations in the diagrams (figs 9, 10).

Having found the most probable arrangement and orientation of the molecules in these crystals, we can now proceed to a qualitative examination and comparison of the intensities of the most important reflections, as preliminary to the development of an exact structure factor. Take first the case of the $\{010\}$,

planes The observed results are as follow, measured on rotations and oscillations about the *a* and *c* axis —

	Naphthalene tetrachloride	Dichloronaphthalene tetrachloride
020	trace	w m
040	v s	m
060	trace	v w
080	m +	w m +
0, 10, 0	Abs	w m +
0, 12, 0	w	Abs

The almost exact quartering in the case of naphthalene tetrachloride is explained by fig 12 Summing atomic numbers, $C_{10}H_8 = 68$ and $Cl_4 = 68$, so that the chlorine atoms should be equal in reflecting power to the carbon rings The distance from the centres of the chlorine atoms to the centres of the carbon atoms must be almost exactly $\frac{1}{4}b = 2.58$ We may note here that, in order to explain the very perfect quartering observed in the higher orders, calculation shows that we require to assume almost flat carbon rings in the naphthalene tetrachloride molecules If the rings were like those in the diamond structure, built in strictly tetrahedral manner, then the tenth order should be stronger than the twelfth, whereas we find a distinct twelfth order and no trace of the tenth It is hoped to discuss this point in more detail later In the case of dichloronaphthalene tetrachloride we have $C_{10}H_8 = 66$ and $Cl_4 = 102$, so that we should now expect the 020, 060, to appear, which is in agreement with the facts These orders, however, are somewhat stronger than we should expect by simply increasing the weight of the halogens The increase in the length of the *b* axis indicates, as we have seen, that some displacement across the plane has most likely occurred as well Although this must have a very marked effect on the intensities of all the higher orders, we can neglect it in the general discussion of the simple planes given below

Consider next the following planes —

	Naphthalene tetrachloride	Dichloronaphthalene tetrachloride
200	s	m s
400	v s	s
600	v w	Abs
110	m s	s
220	v s	v s
330	v w	Abs
440	m s	w

Reference to fig 12 will show that in these sets of planes we should not expect much change in the relative intensities of the reflections between the two compounds provided that the two additional substituted chlorine atoms in dichloronaphthalene tetrachloride are situated somewhere *beneath* the other halogens. Such a substitution would increase the weight of some of the scattering centres without materially affecting their distribution across the plane. This inference is again in accordance with the results.

Let us now make a projection on the bc plane (parallel to the a axis) of the structure thus far obtained. The appearance is shown in fig 13, where the crosses as before indicate the region occupied by the halogen atoms, and the

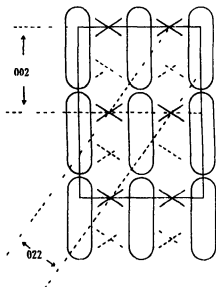


FIG 13 —Projection of Unit Cell on bc plane (100)

oblongs a side view of the carbon rings. The dotted crosses represent the region of the substituted chlorine atoms, situated *beneath* the others. We now see that these substituted atoms will greatly alter the distribution of the scattering centres across the (011) and the (002) planes, and hence we should expect pronounced changes in the relative intensities of the orders of these planes when the two compounds are compared, and the following observed results show that this is the case —

	Naphthalene tetrachloride	Dichloronaphthalene tetrachloride
011	w	w
022	v s	v w
033	m	m
044	s	Abc
002	s	v w
004	m s	s
006	w m	w
008	w	w

We can see at once from fig 13 why the strong (002) of the naphthalene tetrachloride nearly disappears in dichloronaphthalene tetrachloride, and is replaced by a strong (004)

Other striking confirmations of this view of these structures are obtained from a study of some $\{h0l\}$ planes. As all these planes are halved by space-group considerations, we now only require to take account of the configuration of one molecule. Fig 14 shows the projection of one quarter of the unit cell on the ac plane. The molecule now lies in the plane of the paper. If we adopt

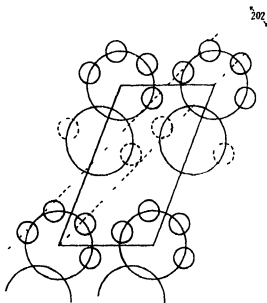


FIG 14 —Projection of Quarter of a Unit Cell on ac plane (010)

the flat ring in graphite, the distance from centre to centre of the carbon atoms = 1.41 Å U, and this is the radius of the atom centres which lie on the large

rings in the diagram. If we adopt the tetrahedral ring, as in the diamond,* and place it as is required to account for the position of the chlorine atoms, *i.e.*, with a minimum extension along the *b* axis, then it will project into exactly the same diagram on this plane, when *r* the radius of the atom centres, and the distance from centre to centre in the projection, is given by

$$r = \frac{1}{2} \sqrt{2} D = 1.41 \text{ \AA U},$$

when *D* the diameter of the carbon atom is now taken as 1.50 \AA U. It is therefore obvious that the $\{h0l\}$ planes contain no information as to whether the graphite or diamond structure is present in this case.

The positions of the centres of the chlorine atoms to be expected from chemical considerations are indicated by small rings, the two substituted atoms being shown by a broken line. The carbon atoms are not shown.

Consider the following $\{h0l\}$ planes --

	Naphthalene tetrachloride	Dichloronaphthalene tetrachloride
202	v s	Ab s
404	v w	v w
20 $\bar{2}$	v s	Ab s
40 $\bar{4}$	w m	m

The diagram shows the effect of the chlorine atoms in making the (202) strong in naphthalene tetrachloride and absent in dichloronaphthalene tetrachloride.

Based upon the dimensions and orientation discussed above, an exact structure factor can be developed which explains most of the prominent features in the intensities of the $\{h0l\}$ planes. Its discussion, however, is postponed for the present, owing to some uncertainties which enter into the exact treatment of so complicated a molecule.

Summary

The structures of naphthalene tetrachloride and 1,2,3,4,5,8-hexachloronaphthalene-1,2,3,4-tetrahydride have been examined by the rotating crystal method, and are found to be closely similar. The lattices are body centred, and the most probable space group is C_4^1 , with four asymmetric molecules per unit cell. This involves a polar crystal.

The parameter of the reflected molecule is determined by a statistical investigation of the intensities of the general plane, based upon Bernal's method

* Cf. Bragg, 'X-rays and Crystal Structure,' p. 237 (1923).

of interpretation. This also leads to an approximate location of the halogen atoms, which are found to lie on what is virtually a different type of lattice.

A comparison of the intensities of the simple axial planes, and some others, in the two crystals shows that the two additional substituted chlorine atoms in dichloronaphthalene tetrachloride must lie somewhere beneath the added chlorine atoms when we view the structure along the *c* axis. In view of the chemical structure this can only mean that the long axis of the molecule is approximately coincident with the *c* of the crystal, with the chlorine atoms on either side of the molecule interleaving the carbon rings. The intensity distribution in the higher orders of certain planes requires an almost flat carbon ring as in the graphite structure.

In conclusion, I wish to express my sincere thanks to Sir William Bragg for his invaluable suggestions and encouragement throughout the course of this work. To Dr Muller, Mr Astbury and other workers in the Davy Faraday Laboratory, and to Mr Bernal I am also indebted for much valuable advice. The dichloronaphthalene tetrachloride was synthesised and prepared as single crystals by Dr Gilchrist in this laboratory. To the Carnegie Trust I am indebted for a Research Fellowship, and to the Chemical Society for a grant.

OBITUARY NOTICES
OF
FELLOWS DECEASED.

CONTENTS

	PAGE
ALBIN HALLER	i
FRANCIS ROBERT JAFF (with portrait)	iii

ALBIN HALLER--1849-1925

THE earlier years of ALBIN HALLER were spent in his native village of Feller-ingen, not far from Mulhouse, where he was born on March 7th, 1849. He was the eldest son of a family of eleven, and at the age of 14, after he had attended the primary school at Weeserling, he was apprenticed as a carpenter in his father's workshop. However, by a lucky chance, he happened, two years later, to make the acquaintance of a pharmacist, M. Achille Gault, who took him into his laboratory and gave him his first lessons in chemistry. For three years M. Gault, who was quick to recognize the marked ability of his pupil, devoted his leisure time to the training of Haller, and ultimately sent him to his brother M. Leon Gault, of Colmar, to whom he became assistant.

Early in the Franco-Prussian war Haller volunteered for service, joining at Belfort in 1870, but after the disastrous year of 1871 he elected to remain in France and rejoined M. Gault at Nancy, where he assisted in the establishment of a pharmacy, and continued to study for his pharmaceutical examinations under the direction of his master. In 1872 the University of Strasbourg was established at Nancy, and Haller became in rapid succession "aide-préparateur," "préparateur" and "chef de travaux" in the Ecole Supérieure de Pharmacie. In 1879 he obtained the "doctorat ès sciences," and in 1885 was appointed a professor in the Faculty of Science of the University. By this time his keen insight and great manipulative skill as a research worker, and his marked ability as an administrator and inspiring lecturer, had become generally recognized, so that in 1899 he was called to Paris as successor to Friedel and Wurtz at the Sorbonne. From this time onward, up to within a very short period of his death, at the age of 76, Haller continued to publish at frequent intervals a great number of original memoirs, amounting in all to 250, covering a wide range of chemical research. His great organizing ability enabled him to establish the Institut Chimique of the University of Nancy in 1890, and subsequently a similar organization devoted to the study of physical and electro chemistry. He was chiefly responsible for the development of the teaching of applied chemistry in France, and in 1908 succeeded Berthelot as President of the Commission on Explosives.

The scientific work of Albin Haller was chiefly on the organic side of chemistry, and was carried out during a period of more than fifty years of a long and active life. Perhaps his most striking work is embodied in his contributions to the chemistry of camphor, that elusive ketone which baffled the efforts of several of the leading organic chemists of the world to determine its structure for upwards of thirty years. A substance of obvious homogeneity, markedly crystalline, and of ample molecular complexity, camphor possesses that

peculiar form of structure, of which we still know so little, which causes it to yield, in accordance with the character of the reagent used, derivatives and degradation products which may belong either to the aromatic or aliphatic series. It is, in fact, an aromatic-aliphatic compound, and although, at the present time, we know its structure, we are, nevertheless, able to appreciate the great difficulties which confronted the pioneers in this field, and to sympathise with those who made false deductions from the experimental facts they obtained. It is a remarkable tribute to the intuition possessed by Haller that amid the mass of conflicting and apparently unrelated facts, and the persistence of many contending hypotheses, he was able to steer the right course and to place the chemistry of camphor on a basis which ultimately led to the elaboration of its true formula by Bredt and to its final preparation by synthesis. Haller showed, for example, that camphoric acid was a dibasic (dicarboxylic) acid, and he was able to regenerate camphor from it by working through camphoric anhydride and campholide, a process used later by Komppa in his classical synthesis of the ketone. Moreover, Haller showed conclusively that camphor

possessed the formula $C_9H_{14} \begin{array}{c} \diagup CH_2 \\ | \\ CO \end{array}$ a fact which he established by preparing

arylidene and alkylidene camphors and by the production of cyanocamphor

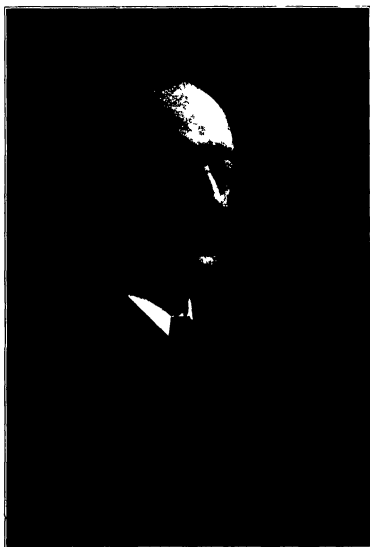
$C_9H_{14} \begin{array}{c} \diagup CH \quad CN \\ | \\ CO \end{array}$ from sodio-camphor and cyanogen chloride. In his experi-

ments with sodio-camphor he noticed that the hydrogen generated in the reaction between sodium and the ketone led to a partial reduction of the products formed, and he therefore introduced the use of sodamide, a substance which yields the sodio derivative smoothly and without the formation of a deleterious by-product



If it be true that the definition of a great chemist is one who introduces a new reagent, then undoubtedly Haller falls within the definition, for sodamide proved to be a substance of very considerable value for research purposes, not only in his hands, but also to many other organic chemists who have had to deal with the formation of derivatives through the sodio derivatives of ketones and ketonic esters.

Haller used the reagent in a variety of ways with very fruitful results, and technically it has been applied in the Heumann synthesis of indigo, thus enabling this method to become a real economic competitor with other synthetic processes. It is impossible in a memoir such as this to give more than a very brief account of the matters dealt with in Haller's many publications. His researches on pseudo-acids, on alcoholysis, on optical rotatory power are



F. R. Japp.

[By permission from the Journal of the Chemical Society.]

all deserving of detailed treatment, as are also his many discoveries in branches of organic chemistry other than those mentioned above

It is sufficient to say that all the sections of organic chemical science in which he worked he enriched by his discoveries, and the literature he created stands as a permanent record to his memory. Many students passed through his hands, and many still live to bear witness to his inspiring personality and lucid power as a teacher.

He was elected a Foreign Member of the Society in 1921, and was awarded the Davy Medal in 1917

J. F. T.

FRANCIS ROBERT JAPP 1848 1925

FRANCIS ROBERT JAPP, who died on August 1, 1925, at the advanced age of 77, was born at Dundee on February 8, 1848. He was the youngest son of James Japp, minister of the Catholic Apostolic Church in that city, and received his earlier education in the High School there. At the age of sixteen he went to the Madras College at St Andrews, and three years later entered the University as an Arts Student. Japp graduated M.A. at St Andrews in 1868, and then went to the University of Edinburgh to study law, but had to relinquish his studies in the summer of 1869 on account of failing health. Without question, had Japp been able to continue his studies at Edinburgh he would have become a distinguished lawyer and would have been lost to chemistry, because the state of his health rendered it necessary for him to reside abroad, during 1871-1873 he spent his time at Göttingen, Berlin and Heidelberg, places which were centres of chemical activity in those days as they are now. The record of the following two years may be told in Japp's own words, communicated to Dr Alexander Findlay, author of the obituary notice in the *Journal of the Chemical Society*, which he has been good enough to allow the writer to use for the purposes of this memoir.

"In the spring of 1873 I returned to England and spent the time partly in London, partly in Scotland. I had by this time taken up the subject of chemistry, in which I had always been interested. In the autumn of 1873 I returned to Heidelberg and began the study of that subject under Bunsen. I was then twenty-five years of age, and my friends, who had long despaired of my ever taking up anything seriously, regarded this last step as the crowning folly of a

hopeless career " In 1875 Japp graduated Ph D at Heidelberg, and then went to Bonn to work in the laboratory of August Kekulé Here he remained for three years, and the admiration and affection he felt for his great teacher is clearly expressed in the Memorial Lecture he gave before the Chemical Society in 1897 (" J Chem. Soc.," vol 73, p 97, 1898)

Japp returned to Scotland in 1878 and continued his research work in the laboratory of Professor Crum Brown at Edinburgh, but was appointed in the same year by Professor (later Sir) Edward Frankland to take charge of the research laboratory which had been established at the Normal School of Science, South Kensington When the Science and Art Department took over the Science Schools in 1881, Japp was appointed Assistant-Professor in the reorganised Normal School of Science and Royal School of Mines, working, first, under E Frankland, and subsequently, under T E Thorpe, who succeeded Frankland in the Chair of Chemistry in 1885 It is evident that at this period Japp's power and ability as a research worker was generally recognised, for in this year he was elected a Fellow of the Society at the age of 37 In 1889 Japp was appointed to the Chair of Chemistry in the University of Aberdeen, in succession to Thomas Carnelley, a post which he held until his retirement in 1914

During the twelve years Japp remained in London, he took an active part in all chemical matters which centred in the activities of the Chemical Society, and was a prominent member of Council and of the Publication Committee He attended most of the scientific meetings and joined in the discussions on the papers read On these occasions it is said that " opportunity arose for his revealing, not only his dry humour, but also his profound knowledge of chemical literature and a width of classical and philosophical reading altogether beyond the range of the attainments of the great majority of his contemporary chemical colleagues " After his departure, Japp seldom revisited London, and but few of the rising generations of chemists, from 1890 onward, ever saw him About half of his published papers appeared during the London period, and the number of his collaborators shows that he was always able to gather round him a large and enthusiastic band of workers During this period he also published (with E Frankland) a text-book on Inorganic Chemistry, and later he collaborated with the same author in the preparation of a new edition of Frankland's " Lecture Notes on Organic Chemistry "

The Chemistry Department of the University of Aberdeen was, when Japp took over the duties of Professor, housed in a series of four or five rooms, badly lit and ventilated, and it was clear to him that he could not build up a school of research under the conditions that existed He therefore set to work to arouse public opinion, and succeeded so well that when the new buildings were erected in 1896 Japp found himself in possession of new laboratories, which at that time must have been regarded as ample At the same period developments took place in the University curriculum, and it

fell to Japp's lot to establish a school of advanced chemical study. This he did so efficiently that he was able to raise the University standard in chemistry from one which dealt mainly with the requirements of medical and elementary students, to one which embodied a school of advanced study and research, from which emerged a steady succession of able chemists, many of whom occupy at the present time important academical and industrial posts in various parts of the world.

During the tenure of the chair at Aberdeen Japp published some 40 papers, mainly with the help of his research assistants and his graduate pupils. His last paper—that is to say, the last to which he put his name—appeared in 1905, but for the ensuing 19 years, until his retirement, many important communications issued from his laboratory, and although his name does not appear on them, they were nevertheless mostly inspired and directed by him. It was characteristic of his self-effacing modesty that he should wish to let his younger co-workers have all the credit for the work they carried out with him.

Although a man of wide knowledge and broad views, Japp's actual research work was restricted to a comparatively narrow field, and practically the whole of it was conducted with phenanthraquinone, benzil and benzoin as raw materials. His object, as he himself has stated, was the synthesis of cycloids containing not only carbon but also oxygen and nitrogen as members of the ring. By doing this he hoped not only to throw light on the ease of formation and reactions of such cyclic compounds, but also by comparing like with like to gain some insight regarding the structure of benzene and allied substances. With those objects in view he prepared a number of oxazoles, iminazoles, furfurans, indoles, azines, pyrrolones and pyrroles, and in the homocyclic series, anhydrazetone benzil and its carboxylic acid, using, for the most part, a new reaction he had discovered, namely, the condensation of ketones with aldehydes in the presence of ammonia or caustic potash. Indeed, he applied this reaction in many directions, and was able to prepare a number of compounds which served to elucidate the structures of several organic substances prepared by others, the constitutions of which were in doubt.

Japp was Foreign Secretary of the Chemical Society from 1885 to 1891, and Vice-President from 1895 to 1899. In 1891 he was awarded the Longstaff Medal of the Society, the highest mark of appreciation which British chemists can show. In 1898 he was President of Section B of the British Association, and delivered a striking address which was an argument, based on the results of stereochemical investigation, in favour of the doctrine of vitalism. Apart from his distinction as a chemist Japp was a linguist of considerable attainments, and the literatures of Germany, France and Italy were open to him in the languages of their authors. He was, moreover, a musician of no mean skill. After his retirement from the chair at Aberdeen in 1914, he resided first at

Acton and later at Richmond, where he died. The closing years of his life were saddened by the death of his only son, who died in 1920 from an illness contracted while on military service. In 1921 Japp had to undergo an operation from the effect of which he never completely recovered. In his last years failure of eyesight deprived him of the companionship of books. In 1879 he married Elizabeth Tegetmeyer, of Kelbra-Kyffhäuser, a small town near Nordhausen, by whom and by two daughters he is survived.

J F T

INDEX to VOL CXVIII (A)

- Adam (N K) Note on the Explanation of a so called "Intertraction" Phenomenon, 202
- Adhesion, studies in, II (Hardy and Nottage), 209, III (Nottage), 607
- Aerofoil, effect of compressibility on lift (Glauert), 113
- Alkaline earth halide spectra, and their origin (Walters and Barratt), 120
- Alpha particles from radium and thorium, velocities (Briggs), 549
- Aniline, variation of the specific heat (Lang), 138
- Baker (H F) Note on the paper 'Commutative Ordinary Differential Operators by Burchall and Chaundy,' 584
- Barratt (H) See Walters and Barratt
- Bending of a supported rectangular plate (Lovc), 427
- Bridge, oscillations caused by the passage of a locomotive (Inghis), 60
- Briggs (G H) A Redetermination of the Velocities of α -Particles from Radium C, Thorium C and C', 549
- Brode (W R) The Analysis of the Absorption Spectrum of Cobalt Chloride in Concentrated Hydrochloric Acid, 286
- Burchall (J L) and Chaundy (T W) Commutative Ordinary Differential Operators, 557
- Carbon, the arc spectrum of (Fowler and Selwyn), 34
- Chaundy (T W) See Burchall and Chaundy
- Childs (W H J) The Distribution of Intensity in the Band Spectrum of Helium 296
- Cobalt chloride, absorption spectrum (Brode), 286
- Commutative ordinary differential operators, note on (Baker), 584
- Commutative ordinary differential operators (Burchall and Chaundy), 557
- Copeson (E T) On Electrostatics in a Gravitational Field, 184
- Coulombian centre of force, wave equation for scattering (Mott), 542
- Crystal of a iron under torsion (Gough), 498
- Crystals of β -brass, deformation of (Taylor), 1
- Crystals of ethane derivatives (Yardley), 449, 485
- Crystals of sulphates and selenates containing thallium (Tutton), 367, 393
- Curtis (W E.) The Structure of the Band Spectrum of Helium, IV, 157
- Darwin (C G) The Wave Equations of the Electron, 654
- (K) Examples of the Zeeman Effect at Intermediate Strengths of Magnetic Field, 264
- Dirac (P A M.) The Quantum Theory of the Electron, II, 351
- Electrode surfaces of spectrum tubes, behaviour of hydrogen and mercury (Johnson), 695
- Electron, quantum theory, II (Dirac), 351
- Electron, wave equations (Darwin), 654
- Electrostatics in a gravitational field (Copeson), 184
- Ethane derivatives, X-ray study (Yardley), 449, 485

- Farr (C C) and Macleod (D B) Some Physical Properties of Gas freed Sulphur, 534
- Fluid motion, some cases of instability (Jeffreys), 195
- Fluid resistance to moving spheres (Lunnion), 680
- Fowler (A) and Selwyn (E W H) The Arc Spectrum of Carbon, 34
- (R H) The Chemical Constant of Hydrogen Vapour and the Failure of Nernst's Heat Theorem, 52, The Photo electric Threshold Frequency and the Thermionic Work Function, 229
- Glauert (H) The Effect of Compressibility on the Lift of an Aerofoil, 113
- Gough (H) The Behaviour of a Single Crystal of α Iron subjected to Alternating Torsional Stresses, 498
- Gravitational field, electrostatics in (Copson), 184
- Gregory (H) and Marshall (S) The Thermal Conductivities of Oxygen and Nitrogen, 594
- Haller (A), obituary notice of, 1
- Hardy (Sir William) and Nottage (M) Studies in Adhesion, II, 200
- Hartree (D R) See James, Waller and Hartree
- Havelock (T H) Wave Resistance, 24
- Helium, intensity of band spectrum (Childs), 296
- Helium, structure of band spectrum (Curtis), 157
- Henderson (M C) See Watson and Henderson
- Hinshelwood (C N) and Thompson (H W) The Kinetics of the Combination of Hydrogen and Oxygen, 170
- Hydrogen and oxygen, kinetics of combination (Hinshelwood and Thompson), 170
- Hydrogen molecule, ionised (Wilson), 635
- Hydrogen vapour, the chemical constant of, and Nernst's heat theorem (Fowler), 52
- Inglis (O E) Oscillations in a Bridge caused by the Passage of a Locomotive, 80
- Interaction phenomenon, note (Adam), 262
- Jack (D) The Band Spectrum of Water Vapour, II, 647
- James (R W), Waller (I) and Hartree (D R) An Investigation into the Existence of Zero-Point Energy in the Rock-Salt Lattice by an X-Ray Diffraction Method, 334
- Japp (F R), obituary notice of, 111
- Jeffreys (H) Some Cases of Instability in Fluid Motion, 195.
- Jex (C S) See Shaw and Jex
- Johnson (M. C) Studies in the Behaviour of Hydrogen and Mercury at the Electrode Surfaces of Spectrum Tubes, 685.
- Kinetics of the combination of hydrogen and oxygen (Hinshelwood and Thompson), 170
- Lang (H R.) On the Measurement of the Variation of the Specific Heat of Aniline with Temperature, using the Continuous Flow Electric Method, 138
- Light, emission by sodium flames and absorption by mercury vapour (Wilson), 362
- Lonsdale (Mrs.) See Yardley
- Love (A. F H) The Bending of a Centrally-Loaded Isotropic Rectangular Plate, Supported at two opposite Edges, 427
- Lunnion (R. G) Fluid Resistance to Moving Spheres, 680
- Macleod (D B) See Farr and Macleod.
- Magnetic field, examples of Zeeman effect (Darwin), 264

- Marshall (S) *See* Gregory and Marshall
- Mercury vapour, absorption of light (Wilson), 362
- Mott (N F) The Solution of the Wave Equation for the Scattering of Particles by a Coulombian Centre of Force, 542
- Naphthalene derivatives, structure (Robertson) 709
- Nernst's heat theorem and the chemical constant of hydrogen (Fowler), 52
- Nitrogen and oxygen, thermal conductivities (Gregory and Marshall) 594
- Nottage (M) Studies in Adhesion, III, 607
- Nottage (M) *See also* Hardy and Nottage
- Obituary Notices —
- Haller (A) 1 Japp, E R , III
- Oscillations in a bridge caused by the passage of a locomotive (Ingles), 60
- Oxygen and hydrogen kinetics of combination (Hinshelwood and Thompson) 170
- Oxygen and nitrogen, thermal conductivities (Gregory and Marshall), 594
- Photo electric threshold frequency and thermionic work function (Fowler), 229
- Quantum theory of the electron (Dirac), 351
- Radium and thorium products, heating effects (Watson and Henderson), 318
- Radium and thorium, velocity of α -particles (Briggs), 549
- Relativity and wave mechanics (Wilson) 441
- Robertson (J M) An X Ray Investigation of the Structure of some Naphthalene Derivatives, 709
- Rock salt lattice, zero-point energy (James Waller and Hartree), 334
- Scattering of particles, wave equation (Mott), 542
- Schonland (B F J) The Polarity of Thunderclouds, 233, the Interchange of Electricity between Thunderclouds and the Earth, 252
- Selwyn (E. W H) *See* Fowler and Selwyn
- Shaw (P E.) and Iex (C S) Tribo-electricity and Friction II 97, III, 108
- Sodium, emission of light by flames containing (Wilson), 362
- Specific heat of aniline, measurement of variation (Lang) 138
- Spectra, alkaline earth halide (Walters and Barratt), 120
- Spectrum, absorption, of cobalt chloride (Brode), 286
- Spectrum, arc, of carbon (Fowler and Selwyn), 34
- Spectrum, band, of helium, intensity (Chikla), 296
- Spectrum, band, of helium, structure (Curtis), 157
- Spectrum, band, of water vapour (Jack), 647
- Sulphur, gas-free, physical properties (Farr and Macleod), 534
- Taylor (G I) The Deformation of Crystals of β -Brass, 1
- Thallium, hexahydrated double selenates containing (Tutton), 393
- Thallium, hexahydrated double sulphates containing (Tutton), 397
- Thermal conductivities of oxygen and nitrogen (Gregory and Marshall), 594
- Thermionic work function and photo-electric threshold frequency (Fowler), 229
- Thompson (H W) *See* Hinshelwood and Thompson
- Thorium and radium products, heating effects (Watson and Henderson), 318
- Thunderclouds and the earth, interchange of electricity (Schonland), 252

Thunderclouds polarity (Schonland) 233

Trio electricity and friction (Shaw and Jex) II 97 III 108

Tutton (A E H) The Hexahydrated Double Sulphates and Selenates containing Thallium
367 393

Waller (I) See James Waller and Hartree

Walters (O H) and Barratt (H) The Alkaline Earth Halide Spectra and their Origin 120

Water vapour band spectrum (Juck) 647

Watson (S W) and Henderson (M C) The Heating Effects of Thorium and Radium
Products 318

Wave equation generalised spheroidal (Wilson) 617

Wave equations of the electron (Darwin) 654

Wave mechanics and relativity (Wilson) 441

Wave resistance (Havelock) 24

Wilson (A H) A Generalised Spheroidal Wave Equation 617 The Ionised Hydrogen
Molecule 635

——— (H A) The Emission of Light by Fluorescent Sodium and the Absorption
of Light by Mercury Vapour 362

——— (W) Relativity and Wave Mechanics 441

Yardley (K) An X-Ray Study of some Simple Derivatives of Ethane Part I 441
Part II 485

Zeeman effect at intermediate strengths of magnetic field (Darwin) 264

END OF THE ONE HUNDRED AND EIGHTH VOLUME (SERIES A)

INFORMATIONAL

[illegible]